

UPGRADES AND DEVELOPMENTS AT THE ISIS LINAC

A. Letchford, STFC Rutherford Appleton Laboratory, Didcot, UK

Abstract

The ISIS Spallation Neutron Source at the Rutherford Appleton Laboratory (RAL) in the UK has a 70 MeV H⁻ linac operating at 202.5 MHz. The linac consists of a 665 keV Radio Frequency Quadrupole (RFQ) and a 4-tank Drift Tube Linac (DTL). In order to ensure continued reliability, increase performance and lay the groundwork for possible facility upgrades in the future, a programme of R&D has been taking place in recent years. This paper will discuss three elements of that programme: the complete replacement of DTL Tank 4; the design of a Medium Energy beam Transport (MEBT) to go between the RFQ and DTL; and the Front End Test Stand (FETS), a demonstrator for the front end of a possible future high current, higher energy linac.

REPLACEMENT OF DTL TANK 4

Background

ISIS is the UK's venerable Spallation Neutron and Muon Source having produced first neutrons in December 1984 with routine operations beginning in June 1985. Originally simply called the 'Spallation Neutron Source' (SNS) it was officially inaugurated and named ISIS in October 1985 [1]. In order to minimise the cost, ISIS was largely constructed in buildings previously built for the Nimrod 7 GeV proton synchrotron (which operated between 1964 and 1978) [2] and also recycled some Nimrod accelerator components.

The 202.5 MHz, 70 MeV linac was originally designed as an upgrade for Nimrod operating at 1 pps but was repurposed for ISIS operating at 50 pps when Nimrod ceased operations. Tank 2 (10 – 30 MeV) and Tank 3 (30 – 50 MeV) had themselves already been recycled from the Proton Linear Accelerator (PLA) [3], which operated between 1959 and 1969. Tank 1 (0.665 – 10 MeV) and Tank 4 (50 – 70 MeV) were newly constructed in the late 1970s and were essentially copies of the Fermilab design.

The construction method of Tanks 2 and 3 (known as the 'old tanks')¹, with a thin-walled copper resonator inside a separate, split, steel vacuum vessel makes them eminently maintainable as evidenced by their continued operation at 50 times the original rep. rate despite being over 60 years old. Tanks 1 and 4 (known as the 'new tanks') were constructed with the then more modern method of sections of steel tube with an explosively bonded copper lining, bolted together and internally welded. Although cheaper to manufacture, this construction style does present some challenges should internal repairs to or maintenance of the tank become necessary.

Early in its life vacuum leaks due to cracks in the internal welds were detected in Tank 4. The solution was to

fit copper patches with RF contacts and polymer o-rings, blind bolted to the inside of the tank which required craftsmen to work inside the tank with the drift tubes present. Although this was initially effective the vacuum pressure slowly deteriorated over time. This was addressed by the addition of more and higher capacity vacuum pumps and a variety of other ad hoc remedies. With knowledge that it would now be virtually impossible for anyone to work inside the tank due to beam loss induced activity (exacerbated by stripping of the H⁻ in the deteriorating vacuum) and somewhat different attitudes to staff duty of care, coupled with a growing fear of the consequences of a sudden, catastrophic failure of the tank, replacing Tank 4 eventually became the highest priority accelerator engineering project at ISIS.

As well as being operationally vital for ISIS, designing and building a new DTL tank also helps to develop essential skills which will be necessary for any future large scale facility upgrade.

Design of the New Tank

An early decision was that the new tank should be a direct plug-in replacement for the old tank with the same length and beam dynamics. Although dated by today's standards and not the design anyone would produce if designing it today, the primary objective was to secure reliable operation of the facility for future decades rather than specifically to improve its performance.

Due to the irreparable nature of the original tank being a major factor in requiring a replacement, one design goal was to build a tank which would not have this drawback. Early 3D RF modelling showed that it was possible to add shallow hatches along the tank with negligible impact on the calculated quality factor but which give relatively easy access to much of the inside.

As the tank is fitted with a bulk tuner², compensating for the small frequency shift produced by the hatches simply required a resizing of the bulk tuner. Figure 1 shows the tank during assembly with 3 of the hatches visible.

The new tank is made from 6, approx. 2 m long steel sections electroplated with copper. Unlike the welded original the sections are bolted together using Helicoflex seals [4, 5]. Each section has 2 hatches and for the section containing the RF feed the window housing is mounted on one of the hatches. Each hatch has a double seal formed by an RF contact and o-ring.

The drift tubes were internally redesigned with an improved cooling circuit and stem design. In some areas a lack of precise details about the original manufacturing methods also necessitated a redesign. Where vacuum brazing had been used in the original it was replaced by electron beam (EB) welding.

¹ 'Type 850' manufactured by the Metropolitan Vickers Electrical Co. Ltd in Manchester, UK.

² A T-shaped bar in the bottom of the tank to shift the frequency from 201.25 MHz used at Fermilab to 202.50 MHz used at ISIS.

ELECTRON ION COLLIDER STRONG HADRON COOLING INJECTOR AND ERL

E. Wang*, W. Bergan, F. Willeke

Brookhaven National Laboratory, Upton, NY, USA

S. Benson, K. Deitrick, Thomas Jefferson National Accelerator Facility, Newport News, VA, USA

C. Mayes, D. Douglas, C. Gulliford, N. Taylor, Xelera Research LLC, Ithaca, NY, USA

J. Qiang, Lawrence Berkeley National Laboratory, Berkeley, CA, USA

Abstract

Intra-beam Scattering (IBS) and other diffusion mechanisms in the EIC Hadron Storage Ring (HSR) degrade the beam emittances during a store, with growth times of about 2 hours at the nominal proton energies of 275 GeV, 100 GeV, and 41 GeV. Strong Hadron Cooling (SHC) can maintain good hadron beam quality and high luminosity during long collision stores. A novel cooling method – Coherent electron Cooling (CeC) – is chosen as the baseline SHC method, due to its high cooling rates. An Energy Recovery Linac (ERL) is used to deliver an intense high-quality electron beam for cooling. In this paper, we discuss the beam requirements for SHC-CeC and describe the current status of the injector and ERL designs. Two designs of injector and ERL will be presented: one for dedicated SHC and another one for SHC with pre-cooler.

INTRODUCTION

The Electron-Ion collider(EIC) is the next nuclear facility in the US to be constructed at Brookhaven National Laboratory, collaborating with Thomas Jefferson Laboratory. It aims to deliver high current, high polarization electron, and polarized proton beams for a high luminosity collision to study nucleon structures. In the Hadron Storage Ring (HSR), the intra-beam scattering and other diffusion mechanisms such as the beam-beam effect can degrade the hadron beam emittance during a collision. To maintain the hadron beam quality for long collision runs, we need to cool the hadron beam. SHC will boost EIC luminosity by a factor of 3–10. The requirements for the EIC cooler is following:

1. Cool the proton beam at 275 GeV, 100 GeV, and 41 GeV.
2. The cooling time shall be equal to or less than the diffusion growth time from all sources.
3. Must cool the hadron beam normalized RMS vertical emittance from 2.5 μm (from injector) to 0.3 μm in 2 hours.
4. The cooling section must fit in the available IR space

The current baseline of the EIC project is using a novel cooling method -Coherent electron Cooling(CeC) to cool the 275 GeV and 100 GeV hadron beam [1]. We name a cooling technique that provides a strong cooling rate at high energies as strong hadron cooling (SHC). We also plan to use electron cooling to cool the initial hadron emittance at 24 GeV and

possibly extend to cool the hadron beam at 41 GeV of collision energy. The SHC-CeC was proposed in reference [2] and several amplifier mechanisms are developed later [3]. It can be considered as a variant of stochastic cooling with the bandwidth raised from GHz RF frequency to tens THz optical frequency since we use electron beam as a signal instead of using cables and amplifiers. We choose one using a combination of drift with one-quarter of plasma oscillation length and a chicane micro-bunching amplifier as our EIC SHC baseline design as shown in Fig. 1.

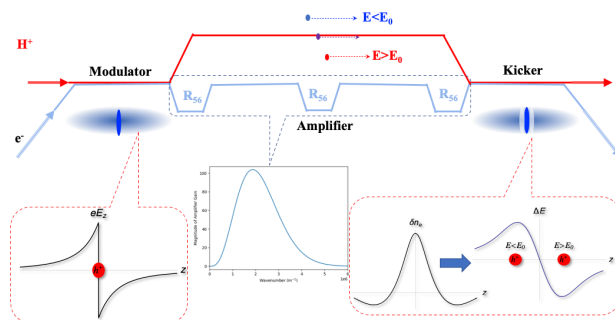


Figure 1: Schematic layout of SHC-CeC. It consists of a modulator, amplifier, and kicker section. The detailed explanations of the three sections can be found in [3]. The bottom figures show the hadron particle wake, amplification section gain, and micro-bunching electron wake.

A 1-D cooling code based on quasi-1D theory has been developed. Simulation results provide information on the saturation of the amplified cooling signal [4]. We simulate turn-by-turn hadron performance, and the interplay between cooling, diffusion, and IBS in longitudinal and transverse directions [5]. Currently, we use this code to optimize the cooling parameters. Table 1 shows the optimal electron parameters in the cooling section.

SHC needs a high-quality electron beam with a high current, small energy spread, and small noise in the beam. The noise of the electron beam shall be less than a factor of 2 of the Poisson noise at around the electron wake frequency. The cooling section lattice design and ERL considerations are discussed in Ref [6]. In this paper, we mainly discuss the injector and ERL designs.

* wange@bnl.gov

BEAM COMMISSIONING AND INTEGRATED TEST OF THE PIP-II INJECTOR TEST FACILITY*

E. Pozdeyev[†], R. A. Andrews, C. M. Baffes, C. Boffo, D. M. Ball, R. Campos, J.-P. Carneiro, B. E. Chase, Z. Chen, D. J. Crawford, J. Czajkowski, N. Eddy, M. El Baz, M. I. Geelhoed, V. Grzelak, P. M. Hanlet, B. M. Hanna, B. J. Hansen, E. R. Harms Jr, B. F. Harrison, M. A. Ibrahim, K. R. Kendziora, M. J. Kucera, D. Lambert, J. R. Leibfritz, P. Lyalyutskyy, J. N. Makara, H. P. Maniar, L. Merminga, R. M. Neswold, D. J. Nicklaus, J. P. Ozelis, D. Passarelli, N. H. Patel, D. W. Peterson, L. R. Prost, G. W. Saewert, A. Saini, V. E. Scarpine, A. V. Shemyakin, J. M. Steimel, A. Sukhanov, P. Varghese, R. Wang, A. A. Warner, G. Wu, R. M. Zifko
Fermi National Laboratory, Batavia, IL, USA
V. Mishra, M. Pande, K. Singh, V. Teotia, Bhabha Atomic Research Centre, Mumbai, India

Abstract

The PIP-II Injector Test (PIP2IT) facility is a near-complete low energy portion of the Superconducting PIP-II linac driver. PIP2IT comprises the warm front end and the first two PIP-II superconducting cryomodels. PIP2IT is designed to accelerate a 2 mA H- beam to an energy of 20 MeV. The facility serves as a testbed for a number of advanced technologies required to operate PIP-II and provides an opportunity to gain experience with commissioning of the superconducting linac, significantly reducing project technical risks. Some PIP2IT components are contributions from international partners, who also lend their expertise to the accelerator project. The project has been successfully commissioned with the beam in 2021, demonstrating the performance required for the LBNF/DUNE. In this paper, we describe the facility and its critical systems. We discuss our experience with the integrated testing and beam commissioning of PIP2IT, and present commissioning results. This important milestone ushers in a new era at Fermilab of proton beam delivery using superconducting radio-frequency accelerators.

INTRODUCTION

The Proton Improvement Plan II (PIP-II) is an essential enhancement to the Fermilab accelerator complex [1] that will provide the world's most intense high-energy neutrino beam to the Deep Underground Neutrino Experiment (DUNE) in South Dakota [2]. PIP-II high-level goals are to 1) reduce the time required for DUNE to achieve its goals by delivering the proton beam power to the LBNF target in excess of 1 MW in the energy range between 60 GeV to 120 GeV, and 2) sustain high reliability, multi-user operations of the Fermilab complex.

PIP-II consists of 1) a Superconducting (SC) 800 MeV H- linac, 2) an approximately 300-meter-long beam transfer line that takes the beam to the Fermilab Booster, and 3) accelerator upgrades required to deliver 1.2 MW of the beam power on the LBNF target at 120 GeV.

* This manuscript has been authored by Fermi Research Alliance, LLC under Contract No. DE-AC02-07CH11359 with the US Department of Energy, office of Science, Office of High Energy Physics

[†] pozdeyev@fnal.gov

The front end of the linac plays a critical role in the accelerator. It generates the beam, defines beam parameters, accelerates the beam to an energy compatible with downstream accelerating structures, and generates a required bunch pattern.

Fermilab and the PIP-II project constructed the PIP-II Injector Test Facility (PIP2IT) as a testbed for PIP-II technologies to test critical PIP-II front end systems, validate the design of SC cryomodels, and demonstrate feasibility of bunch-by-bunch chopping.

PIP2IT included a nearly complete copy of the PIP-II front end and the first two PIP-II cryomodels. Figure 1 shows the layout of PIP2IT with its main components. PIP2IT was commissioned in two phases. Phase 1 up to the end of the 2.1 MeV MEBT was commissioned with beam from 2015 to 2018 [3]. The HWR and SSR1 cryomodels were added in 2019-2020, leading to the second phase of commissioning of the whole accelerator between June 2020 and April 2021. In April 2021 the PIP2IT beam commissioning was stopped. The PIP2IT hardware was disassembled and moved to storage to be installed later in the PIP-II tunnel. The area used by PIP2IT was reconfigured for PIP-II cryomodel testing.

This paper focuses on the second phase of PIP2IT commissioning.

GOALS OF PHASE 2 COMMISSIONING

The main goals of the PIP2IT test were:

- Conduct integrated commissioning of PIP2IT
- Demonstrate beam with LBNF/DUNE parameters at the end of SSR1 CM
- Validate beam optics and measure beam parameters. Test beam tuning procedures
- Test PIP-II technical systems to inform design decisions
- Gain experience with installation, testing, and operation of PIP2IT equipment
- Integrate in-kind contributions
- Include lessons learned in the design of technical systems and operational procedures

Note that equipment testing was a critical part of PIP2IT, having same priority as the beam commissioning.

BEAM COMMISSIONING OF NORMAL CONDUCTING PART AND STATUS OF ESS PROJECT

R. Miyamoto*, C. Amstutz, S. Armanet, R. Baron, E. Bergman, A. Bhattacharyya, B. Bolling, W. Borg, S. Calic, M. Carroll, J. Cereijo Garcia, J. Christensson, J. Christie, H. Danared, C. Derrez, I. Kittelmann, E. Donegani, S. Ekström, M. Eriksson, M. Eshraqi, J. Esteban Müller, K. Falkland, A. Forsat, S. Gabourin, A. Garcia Sosa, A. Gorzawski, S. Grishin, P. Gustavsson, W. Hees, M. Jensen, B. Jones, S. Haghtalab, V. A. Harahap, H. Hassanzadegan, J. Jamroz, A. Jansson, M. Juni Ferreira, M. Kalafatic, H. Kocevar, S. Kövecses, E. Laface, B. Lagoguez, Y. Levinsen, M. Lindroos, A. Lundmark, M. Mansouri, C. Marrelli, C. Martins, J. Martins, S. Micic, N. Milas, M. Mohammednezhad, R. Montano, M. Munoz, G. Mörk, D. Nicosia, B. Nilsson, D. Noll, A. Nordt, T. Olsson, N. Öst, L. Page, D. Paulic, S. Pavinato, A. Petrushenko, C. Plostinar, J. Riegert, A. Rizzo, K. Rosengren, K. Rosquist, M. Serluca, T. Shea, A. Simelio, S. Slettebak, H. Spoelstra, A. Svensson, L. Svensson, R. Tarkeshian, L. Tchelidze, C. Thomas, E. Trachanas, P. van Velze, K. Vestin, R. Zeng, ESS, Lund, Sweden
A. C. Chauveau, P. Hamel, O. Piquet, CEA, Saclay, France
I. Bustinduy, A. Conde, D. Fernandez-Cañoto, N. Garmendia, P. J. Gonzalez, G. Harper, A. Kaftoosian, J. Martin, I. Mazkarian, J. L. Munoz, A. R. Páramo, S. Varnasseri, A. Zugazaga, ESS-Bilbao, Bilbao, Spain
C. Baltador, L. Bellan, M. Comunian, F. Grespan, A. Pisent, INFN, Italy

Abstract

The European Spallation Source, currently under construction in Lund Sweden, will be a spallation neutron source driven by a superconducting proton linac with a design power of 5 MW. The linac features a high peak current of 62.5 mA and long pulse length of 2.86 ms with a repetition rate of 14 Hz. The normal conducting part of the linac has been undergoing beam commissioning in multiple steps, and the main focus of the beam commissioning has been on bringing systems into operation, including auxiliary ones. In 2022, beam was transported to the end of the first tank of the five-tank drift tube linac. This paper provides a summary of the beam commissioning activities at ESS and the current status of the linac.

INTRODUCTION

European Spallation Source (ESS) [1], currently under construction in Lund, Sweden, is a neutron source driven by a superconducting (SC) proton linac with a design beam power of 5 MW. When the beam power exceeds 2 MW, the ESS will be the brightest neutron source in the world. The linac has a normal-conducting injector, consisting of an ion source (IS), low energy beam transport (LEBT), radio-frequency quadrupole (RFQ), medium energy beam transport (MEBT), and drift-tube linac (DTL) with five tanks. The SC part uses three types of cavities: spoke cavities, medium- β elliptical cavities, and high- β elliptical cavities. Following the SC part is the high energy beam transport (HEBT), which has rooms for additional cryomodules (up to 16) as contingency or for potential upgrades. After the HEBT, the linac is split

Table 1: ESS Linac High Level Parameters for the Design and Initial Operations (Ops.)

| Parameter | Unit | Value |
|----------------------------|------|---------------|
| Beam power (design) | MW | 5 |
| Beam energy (design) | GeV | 2 |
| Beam power (initial Ops.) | MW | 5 |
| Beam energy (initial Ops.) | GeV | 0.8 |
| Peak beam current | mA | 62.5 |
| Beam pulse length | ms | 2.86 |
| Beam pulse repetition rate | Hz | 14 |
| Duty factor | % | 4 |
| RF frequency | MHz | 352.21/704.42 |
| Availability | % | 95 |

into two: a straight transport line to the tuning beam dump and a dogleg with a 4 degrees bend and 4.5 m elevation. The section after the dogleg is referred to as Accelerator-to-Target (A2T), where each beam pulse is painted over the spallation target with a cross-check pattern and rectangular border by using the rastering system [2, 3]. In the following, the part from the IS to DTL is referred to as the normal-conducting linac (NCL), and the rest is referred to as the superconducting linac (SCL). Figure 1 shows a schematics layout of the linac, and Table 1 lists the high-level parameters for the design [1] and during the initial operations [4]. The design energy of 2 GeV, with a 62.5 mA current and 4% duty factor, makes a 5 MW beam power. The beam energy will be limited to 800 MeV during the initial operations due to a budget issue, and this reduces the beam power to 2 MW.

* ryoichi.miyamoto@ess.eu

FIRST YEARS OF LINAC4 RF OPERATION

S. Ramberger*, R. Wegner, CERN, Geneva, Switzerland

Abstract

Following the construction, commissioning, run-in, and connection, in 2021 Linac4 at CERN saw its successful start-up to full operation. Being composed primarily of RF systems, occupying most of the tunnel and the equipment hall, a coordinated effort has been put in place by four RF teams providing cavities, amplifier chains, low-level RF and general control systems. While all parts came together with impressive performance from day one, many details required a considerable debugging effort to achieve the requested availability of at least 95% from first operation in the synchrotron complex. This contribution focuses on issues in equipment reliability, radiation to electronics, thermal stability, systems interaction, as well as a few aspects of complex low-level RF setup. It will also discuss decisions taken with respect to spare policies and upgrades for the coming years.

INTRODUCTION

Linac4, the new H^- accelerator at CERN has been constructed as a replacement for Linac2, a proton machine, which was close to its end of lifetime [1]. While the design efforts for Linac4 began in 2004, the actual project was started in 2008. The ground-breaking took place on 16 October 2008, and the inauguration was celebrated on 9 May 2017, following the first beam commissioning of the machine. Linac4 has been designed as part of the LHC injector upgrade with the aim to be able to reach up to twice the beam intensity out of the PS Booster, which is a 4-ring synchrotron following Linac4 and which accelerates the beam from 160 MeV to 2 GeV.

Supporting a rich physics program at the LHC as well as at ISOLDE, AD, and several fixed target experiments, the injector complex is required to almost continuously supply all customers reliably with the requested beam types and beam quality throughout the year. Beam production is based on a complex operation with pulse to pulse modulation (PPM) that must make sure that all facilities are served in parallel with individually tailored beams.

In this context, the performance of the accelerators is primarily monitored in terms of machine availability of non-degraded beam quality. Equipment faults are registered by the operation team in the accelerator fault tracking (AFT) system, analysed by equipment experts, and discussed in weekly meetings [2].

The decision to delay the connection of Linac4 from the long LHC shutdown LS1 (2013–2015) to LS2 (2019–2021), in order to reduce interference with LHC activities, was extremely beneficial for the reliability of the machine. Having been run for almost 40 years, Linac2 was still at an average of 98% of overall availability in the final years. Having the

very reliable Linac2 as its predecessor, the challenge for Linac4 was set high, to deliver at its start-up all the previously defined beams at 95% availability despite its about three times higher beam energy and number of RF systems.

In the following sections, a brief introduction to the Linac4 machine and the start-up phase is given. A number of exemplary RF issues that were encountered in the commissioning and early RF operation are described. Operational strategies and spare policies are discussed with an outlook on future RF activities.

THE MACHINE

As is the case for linear accelerators in general, Linac4 consists primarily of RF systems and equipment required to run these. Linac4 operates at an RF frequency of 352.2 MHz and at about 0.1% duty cycle with a beam-pulse length of up to 600 μ s and a 1.2 s repetition time. The machine has a length of about 80 m. The average operational beam current is up to 23 mA after beam chopping with an emittance of 0.3π mm mrad at 160 MeV.

Cavities in the beamline tunnel are 12 m below the equipment hall where klystrons are located. The equipment hall is about 100 m long and 12 m wide. Connection of RF equipment from the hall to the tunnel passes via shafts with rectangular half-height WR2300 waveguides, and coaxial cables close-by, to keep line-lengths short and at the same environmental conditions. High-voltage (HV) modulators placed next to klystrons, generating the high voltage pulses of up to 110 kV for the klystrons, are taken care of by the power converter group.

The RF structures on the beam line accelerate beam out of the source at 45 keV consecutively with a Radio-Frequency Quadrupole (RFQ) to 3 MeV, 3 Bunchers, 3 Drift-Tube Linacs (DTL) to 50 MeV, 7 Cavity Coupled DTLs (CCDTL) to 102 MeV, and 12 PI-Mode Structures (PIMS) to 160 MeV in the main tunnel, and 1 PIMS-type Debuncher cavity is located in the transfer line tunnel. The RF teams are also in charge of the two chopper structures located in the MEBT line between the first two Buncher cavities and the 2 MHz source amplifier providing about 30 kW RF power to the plasma chamber.

THE ORGANISATION

The key to the success of Linac4 is the dedication of all teams. Within the RF group at CERN, four of the hierarchical sections are contributing to the operation of the accelerator with each section being responsible for certain parts of the systems, divided into klystrons, controls, feedback, and other linac RF systems. A tight collaboration is also established with other groups at CERN, in particular for power converters, cooling, mains electricity, vacuum, general control, beam physics, and operation group. The effort within

* Suitbert.Ramberger@cern.ch

HELEN: A LINEAR COLLIDER BASED ON ADVANCED SRF TECHNOLOGY*

S. Belomestnykh^{†,1}, P. C. Bhat, M. Checchin[‡], A. Grassellino, M. Martinello[‡], S. Nagaitsev²,
 H. Padamsee³, S. Posen, A. Romanenko, V. Shiltsev, A. Valishev, V. Yakovlev,

Fermi National Accelerator Laboratory, Batavia, IL, USA

¹also at Stony Brook University, Stony Brook, NY, USA

²also at University of Chicago, Chicago, IL, USA

³also at Cornell University, Ithaca, NY, USA

Abstract

This paper discusses recently proposed Higgs-Energy LEptoN (HELEN) e^+e^- linear collider based on advances in superconducting radio frequency technology. The collider offers cost and AC power savings, smaller footprint (relative to the ILC), and could be built at Fermilab with an interaction region within the site boundaries. After the initial physics run at 250 GeV, the collider could be upgraded either to higher luminosity or to higher (up to 500 GeV) energies.

INTRODUCTION

One of the highest priorities for the particle physics community is to make precision measurements of the Higgs boson properties and look for any deviations from the Standard Model using an e^+e^- collider at the center-of-mass energy of 250 to 360 GeV (Higgs factory). For many years, the International Linear Collider (ILC) has been the prime candidate for such a machine. Its mature superconducting radio frequency (SRF) technology has been “shovel ready” and has been used already to build such linacs as European XFEL in Hamburg, Germany, and LCLS-II at SLAC in the USA. Meanwhile, the SRF community continues to make progress improving the performance of SRF cavities.

In this paper we discuss how recent advances in the SRF technology can be applied for a more compact and cost-effective e^+e^- linear collider. This recently proposed machine is named Higgs-Energy LEptoN (HELEN) collider [1]. If the ILC cannot be realized in Japan in a timely manner, HELEN could be built after relatively short period of dedicated R&D efforts. At the core of this collider is the traveling wave (TW) SRF technology. The paper describes the machine in some detail including tentative list of parameters, layout and possible siting, and potentials for luminosity and energy upgrades. Finally, we provide summary and conclusions.

PROMISE OF TRAVELING WAVE SRF

Travelling wave structures offer several advantages over the traditional standing wave SRF structures: substantially

lower H_{pk}/E_{acc} and lower E_{pk}/E_{acc} , ratios of peak magnetic field and peak electric field to the accelerating gradient, respectively, together with substantially higher R/Q . To reach the maximal gradient, the optimal TW cavity design must have the lowest possible H_{pk}/E_{acc} , since H_{pk} presents the hard ultimate limit to the performance of Nb cavities via RF superheating field.

On the other hand, as Fig. 1 shows, the TW structure requires almost twice the number of cells per meter compared to the SW structure to provide the proper phase advance (105° in Fig. 1), as well as a feedback waveguide for redirecting power from the end to the front of the accelerating structure. The feedback waveguide requires careful tuning to compensate reflections along the TW ring and thus obtain a pure traveling wave regime at the desired frequency.

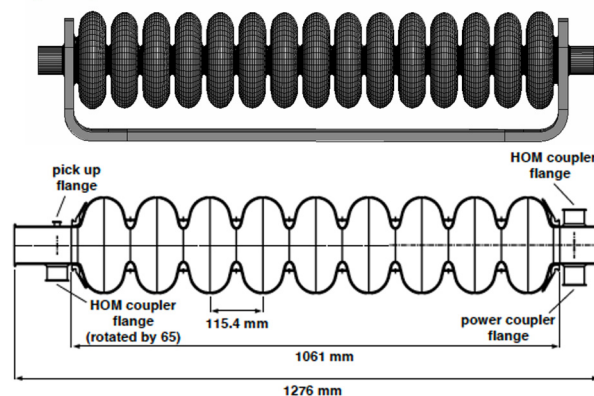


Figure 1: A one-meter-long TW structure with a 105° phase advance per cell compared to the one-meter standing-wave TESLA structure [2]. Note that a TW structure for HELEN will be longer, perhaps 2-meter long.

Recent TW cavity geometry optimization study [3] demonstrated that for an aperture radius $R_a = 25$ mm and phase advance of 90° , one can achieve $H_{pk}/E_{acc} = 28.8$ Oe/(MV/m) with $E_{pk}/E_{acc} = 1.73$. Since H_{pk}/E_{acc} is 42.6 Oe/(MV/m) for the TESLA structure, the TW structure has reduced the critical parameter H_{pk}/E_{acc} by almost a factor of 1.5. At the same time, the peak electric field ratio is smaller than TESLA cavity value of 2.0 and we gain a factor of 2.1 in R/Q although losing in the geometry factor by 1.45 (186 Ohm vs. 270 Ohm). Thus, for the same accelerating gradient the TW cavity is more cryogenically efficient than TESLA cavity. The high group

* Work supported by the Fermi National Accelerator Laboratory, managed and operated by Fermi Research Alliance, LLC under Contract No. DE-AC02-07CH11359 with the U.S. Department of Energy.

[†] sbelomes@fnal.gov

[‡] present affiliation: SLAC, Menlo Park, CA, USA

LIGHTHOUSE - A SUPERCONDUCTING LINAC FOR PRODUCING MEDICAL ISOTOPES

J. M. Krämer, G. Blokesch, M. Grewe, B. Keune, V. Kümper, M. Pekeler, C. Piel, P. v. Stein, T. T. Trinh, C. Quitmann†
RI Research Instruments GmbH, Bergisch Gladbach, Germany

Abstract

The medical isotope ^{99}Mo is used for diagnosing several 10 million patients every year. Up to now, it is produced from highly enriched Uranium (HEU) using high-flux neutron reactors. The Institute for Radio Elements (IRE), Belgium has projected the design of a high-power superconducting linac for producing ^{99}Mo without use of nuclear fission as part of their SMART project. The LightHouse accelerator consists of a photo gun and seven superconducting radiofrequency (SRF) modules, a beam splitter, and target illumination optics. It will deliver two electron beams of 75 MeV and 1.5 MW each.

The photo gun and the SRF modules are based on the CBETA design of Cornell University. Photocathodes are prepared and transferred in situ. We report on the design principles and the Beam Test Facility operating since April 2022.

DESCRIPTION OF PROJECT

Radioisotopes are used in nuclear medicine to detect numerous diseases for example by spectroscopic imaging. In case of cancer, it is predominantly used to determine how much the disease has spread to identify to best possible treatment. The metastable isotope $^{99\text{m}}\text{Tc}$ is applied to patients in more than 80% of the diagnostic treatments. IRE [1] is one of the world's leading suppliers of its parent isotope ^{99}Mo .

The large majority of ^{99}Mo production is based on purification of fission products produced in nuclear research reactors from enriched Uranium. The risk of proliferation, aging reactors, and long-lived nuclear waste are reasons to switch to an alternative production process. Within the SMART project (Source of Medical Radioisotopes) [2], IRE is developing a ^{99}Mo production facility based on accelerator technology in partnership with ASML [3]. In this approach, a ^{100}Mo target is illuminated with an electron beam. The electrons are stopped in the ^{100}Mo target, producing bremsstrahlung. A (γ, n) reaction will then knock out one neutron from the Mo-nucleus, yielding the radioisotope ^{99}Mo .

Currently, the project is in the design and prototyping phase, which is going to be completed in 2024 with a decision of IRE's board on the realization of the project. Manufacturing and construction are scheduled to be completed by 2026, to be followed by installation and commissioning until 2029. After one year of pilot production, the high-volume production is envisioned to start in 2030.

Within this project, RI Research Instruments (RI) [4] takes the responsibility for the design, fabrication, installation, and commissioning of the full accelerator. This includes the photocathode production and laser systems, the cryogenic plant and RF amplifiers, the machine protection system, the accelerator control system, and the beam transport and beam scanning onto the target.

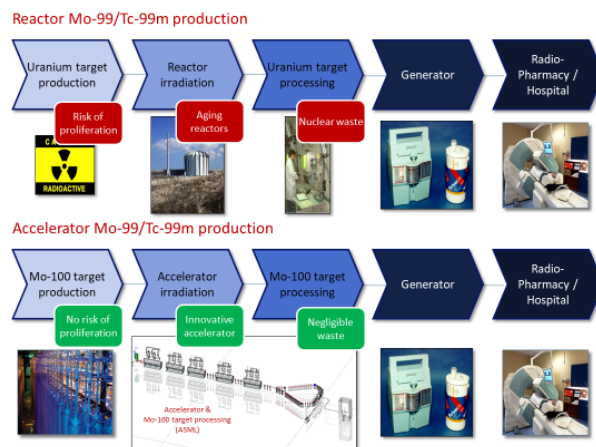


Figure 1: Innovative production of Mo-99 from accelerator irradiation compared to traditional production in a nuclear reactor from Uranium targets. Courtesy of IRE.

DESIGN PRINCIPLES

The new production site is planned to take over the full volume of ^{99}Mo production for IRE. The required beam power is 3 MW, with an electron beam energy of 75 MeV and a beam current of 40 mA at 1.3 GHz continuous wave (CW). The large average beam power calls for the use of SRF technology.

To reach the desired specific activity of ^{99}Mo , a two-sided irradiation is mandatory. This results in a superior depth profile of heat load and specific activity inside the target. The two-sided irradiation is realized by splitting the electron beam in two after acceleration to full energy.

Injectors

Relying on a single production facility also puts high demands on the uptime of the accelerator. This is implemented by providing two fully equipped parallel injectors allowing for rapid switching. As they will be placed in separate rooms, it will also be possible to maintain one injector while the rest of the accelerator is running in full production mode with the other injector.

A 3D model of the LightHouse accelerator is shown in Fig. 2. The photo-gun operates at 350 keV and the SRF module with five two-cell cavities accelerates the beam to

† christoph.quitmann@research-instruments.de

EXPERIMENTAL STUDY TO OPTIMIZE THE TREATMENT EFFICACY OF PHARMACEUTICAL EFFLUENTS BY COMBINING ELECTRON BEAM IRRADIATION

P. Kumar*, M. Meena, A. B. Kavar, P. Nama, A. Pathak, R. Varma
 Indian Institute of Technology Bombay, 400076, Mumbai, India

A. Deshpande, T. Dixit, R. Krishnan, Society for Applied Microwave Electronics
 Engineering & Research (SAMEER) Medical Electronic Division, 40007, Mumbai India

Abstract

Here, we report our first step towards tackling this issue at the roots by irradiating the pharmaceutical effluents from a stages of their existing treatment plant with an Electron Beam (EB) with doses varying from 25 kGy to 200 kGy. We have used a normal conducting pulsed wave linear accelerator developed by SAMEER. It produced a pencil beam of electrons of energy 6 MeV with an average current of 16 μ A. To ensure optimum dose delivery, Fluka-Flair Simulations have been used. We have successfully demonstrated that electron beam irradiation along with the use of conventional techniques like coagulation after the irradiation can further increase the efficacy of the process with a final reduction in Chemical Oxygen Demand (COD) to be as large as 65% in some of the cases.

INTRODUCTION

Every day, the global demand for fresh water rises, putting additional strain on available water resources such as rivers and lakes. Furthermore, human activities have resulted in the release of new pollutants known as Contaminants of Emerging Concern (CECs) into these resources, which include micropollutants, endocrine disruptors (EDs), pesticides, pharmaceuticals, hormones, toxins, and synthetic dyes [1]. Pharmaceutical effluents are the most difficult to treat conventionally due to the presence of ammonium nitrogen, toxic and complex compounds produced as byproducts in drug manufacturing. The conventional treatments primarily aim to convert pollutants from one phase to another, pollutants can still contaminate groundwater after purification because the residue is disposed of in a landfill. As a result, we need a treatment process that can breakdown and degrade these complex compounds into smaller, less harmful byproducts such as salts or water.

According to the research, electron beam irradiation is an efficient method for degrading complex compounds [2], which also improves the efficiency of conventional wastewater treatment plants. This inspired us to develop a compact, high intensity superconducting electron accelerator that can be easily integrated into existing industrial effluent treatment systems as shown in the Fig. 1.

In this paper, We reported our first step toward this technology by using an Electron Beam (EB) to irradiate pharmaceutical effluent collected from existing industrial treatment

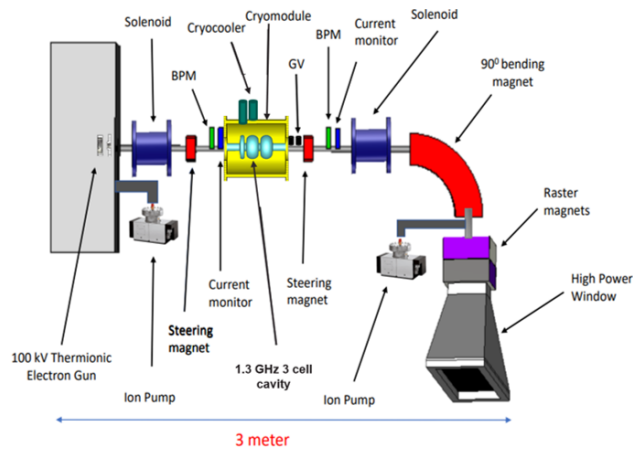


Figure 1: A Schematic figure of proposed accelerator structure.

plant. Furthermore, the EB process has been investigated in combination with a number of enhancement processes, including chemical coagulation and scavengers such as titanium dioxide (TiO_2), air, and ozone flow.

MATERIAL AND METHODS

The industry from which samples are collected has wastewater purification scheme from which sample S is collected after the stage soil biotreatment (SBT) as shown in the Fig. 2. The initial chemical oxygen demand (COD), pH, and total dissolved solids (TDS) values for this sample are 704 ppm, 7.74, and 1421 ppm, respectively. The Titrimetric

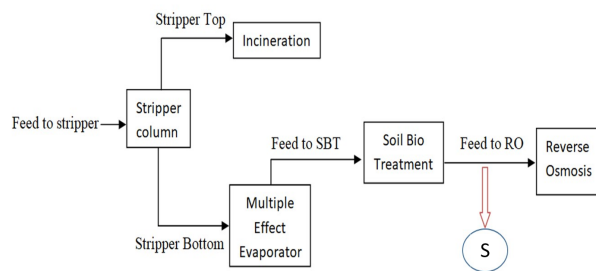


Figure 2: Stage of sample S collection from the industrial wastewater treatment plant.

Method is used for quantitative COD analysis and is used to determine the quality of irradiated water sample S. For

* panku.r.k@gmail.com

RF DESIGN, OPTIMIZATION AND MULTIPHYSICS STUDY OF A $\beta = 1$, 1.3 GHz SINGLE CELL ACCELERATING CAVITY FOR HIGH-INTENSITY COMPACT SUPERCONDUCTING ELECTRON ACCELERATOR (HICSEA)

Manisha Meena, Abhishek Pathak, Raghava Varma,
 Indian Institute of Technology Bombay, Mumbai, India

Abstract

High-energy electron accelerators have been used in water purification for several years. They are very effective for the removal of complex impurities. This study aims to design a superconducting electron beam accelerator with an output energy of 1 MeV and beam power of 40 kW for wastewater treatment. A 1.3 GHz single cell elliptic cavity with $\beta = 1$ was designed and optimized for TM_{010} mode and an accelerating gradient of 15 MV/m. For the optimized cavity, the RF parameters, namely, R/Q, transit time factor and geometry factor (G) were found to be 174.93 Ω , 0.67 and 276 Ω , respectively. Multiphysics studies showed that the value of R/Q for fundamental accelerating mode was 174.93 Ω . It was much higher than that of other modes, thus, HOM coupler is not required for the system. The Lorentz force detuning coefficient after stiffening the cavity iris, and the temperature rise due to the RF surface losses were found to be 0.20 Hz/(MV/m)² and 0.085 K, respectively. It is also observed that there is no occurrence of multipacting for the designed accelerating gradient.

INTRODUCTION

Accelerator technology has been proven to be an efficient and sustainable resource for wastewater treatment [1]. Therefore, IIT Bombay proposed to develop a 40 kW superconducting electron accelerator system as shown in Fig. 1 in collaboration with Japanese Universities and Institutes. The proposed accelerator consists of a 1.3 GHz superconducting single cell elliptic cavity to achieve desired beam energy of 1 MeV.

This paper presents detailed RF design and multiphysics optimization studies to maximize RF efficiency, and to obtain an acceptable beam quality at the exit of cavity. The RF design and optimization studies are performed using CST Microwave Studio and Poisson Superfish.

The RF design includes optimization of peak surface electric and magnetic fields since these are the limiting criteria to obtain high accelerating gradient (E_{acc}) and low power loss for SRF cavities. The magnetic field is smoothed out by the appropriate arc at the equator, which lowers the peak surface magnetic field. As with the iris region, smooth curvature lowers the peak surface electric field and solves the issue of field emission. The RF design and optimization have been followed up with multiphysics studies in order to ensure a stable and reliable operation of the cavity. The multipacting studies includes higher order modes (HOMs) analysis, Lorentz force detuning study, multipacting study, and thermal analysis.

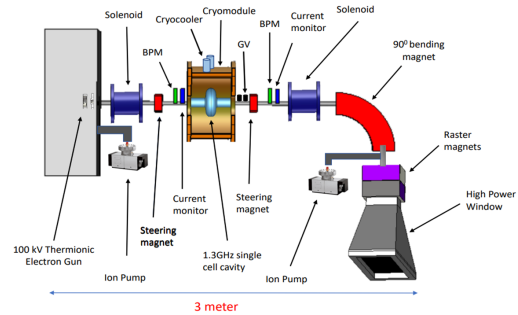


Figure 1: Prototype of the proposed electron accelerator system and its components.

RF CAVITY DESIGN AND OPTIMIZATION

The RF design and simulations are performed with cavity symmetry in YZ plane as shown in Fig. 2, where Z is along the cavity length and Y is along the cavity radius. The seven geometry parameters that determine the cavity design include half-cell length (L), iris radius (R_{iris}), iris ellipse radii a and b, equator ellipse radii A and B, and cavity radius (R_{eq}). The wall angle (α) can be derived from these seven parameters. The half-cell length of the cavity for $TM_{010} - \pi$ mode operation is chosen as $\beta\lambda/4$ to ensure synchronization of the bunch with RF field. The iris radius is chosen to be 3.2 cm, while the cavity radius (R_{eq}) is tuned to achieve the resonant frequency of 1.3 GHz. The wall angle is chosen to be 90° because the product of geometry factor (G) and ratio of shunt impedance to quality factor (R/Q) of the cavity increases with wall angle which in turn is inversely proportional to the power loss. However, the upper limit for α is limited by manufacturing and cleaning constraints.

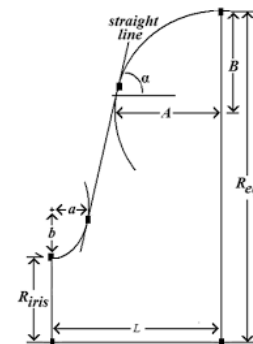


Figure 2: Schematic design and geometry parameters of the half-cell cavity [2].

A COMPACT INVERSE COMPTON SCATTERING SOURCE BASED ON X-BAND TECHNOLOGY AND CAVITY-ENHANCED HIGH-AVERAGE-POWER ULTRAFast LASERS

A. Latina, V. Muşat, R. Corsini, L. A. Dyks, E. Granados, A. Grudiev, S. Stapnes,
W. Wuensch, CERN, Geneva, Switzerland
E. Cormier, CELIA, Talence, France
G. Santarelli, ILE, Palaiseau CEDEX, France

Abstract

A high-pulse-current injector followed by a short high-gradient X-band linac is considered as a driver for a compact Inverse Compton Scattering source. We show that using a high-power ultrashort pulse laser operating in burst mode and a Fabry-Pérot enhancement cavity, X-rays with flux values over 10^{13} ph/s and photon energies up to MeV are achievable. The resulting high-intensity and high-energy X-rays allow for various applications, including cancer therapy, tomography, and nuclear waste management. A preliminary conceptual design of such a compact ICS source is presented, together with simulations of the expected performance.

INTRODUCTION

The number of Inverse-Compton Scattering (ICS) sources has steadily increased over the last few years. Most ICS designs are based on storage rings due to a circular layout, which maximises the repetition rate and flux. However, the latter comes at the cost of increasingly large facilities. In the 2000's, Energy Recovery Linacs (ERLs) have garnered interest as potential drivers for ICS, and several designs based on ERLs exist [1]. However, these machines are typically based on super-conducting technology, which is not readily available in hospitals or small laboratories. Normal-conducting, low-emittance linacs can also be adapted for compact ICS designs. Linac-based ICS sources tend to offer higher brilliance due to the lower emittance obtained from the photoinjector but exhibit lower fluxes since the electron bunches are used only once.

Stemming from the R&D made at CERN in the context of X-band high-gradient multi-bunch acceleration for the Compact Linear Collider [2], this paper proposes a high pulse-current accelerator based on a photoinjector and a short X-band linac, which can deliver high-charge electron pulses and ultimately high-flux photons. Given the compactness of the linac, electron beam energies up to hundreds of MeV are achievable within a few metres, allowing for the generation of MeV photons.

Inverse-Compton Scattering

ICS is defined as the scattering of a low-energy photon from a relativistic electron resulting in a high-energy photon. Figures of merit for ICS photons are energy, bandwidth, flux, and brilliance. The following equations are derived in the Thomson regime, where the electron recoil is negligible.

Table 1: Electron Beam Parameters From the HPCI Injector at the Interaction Point

| Parameter | Value | Unit |
|--------------------------------------------|-------|---------------|
| Energy | 140 | MeV |
| Bunch charge, Q | 300 | pC |
| Bunch repetition frequency, f | 10 | Hz |
| Nb of bunches per train | 1000 | |
| <i>rms</i> spot size at the IP, σ^* | 30 | μm |
| Bunch length, σ_z | 300 | μm |
| Bunch spacing | 1/3 | ns |
| Normalised | | |
| Transverse emittance, $\epsilon_{x,y}^N$ | 5 | mm mrad |

For an ultra-relativistic electron, the maximum achievable energy in an ICS interaction is given in a head-on collision by

$$E_X = 4\gamma^2 E_{\text{laser}}, \quad (1)$$

where γ is the relativistic factor of the electron beam and E_{laser} is the laser photon energy [3]. Assuming a round Gaussian transverse distribution for the electron and laser beams [4], the total flux of the ICS photon beam \mathcal{F} can be derived by taking the time derivative of the number of the scattered photons,

$$N_\gamma = \sigma_T \frac{N_e N_{\text{laser}} \cos(\phi/2)}{2\pi\sigma_{\gamma,y} \sqrt{\sigma_{\gamma,x}^2 \cos^2(\phi/2) + \sigma_{\gamma,z}^2 \sin^2(\phi/2)}}, \quad (2)$$

where σ_T is the Thomson cross section, N_e the number of electrons in a bunch, N_{laser} , the number of photons in the laser macropulse, ϕ the crossing angle between the electron and laser beam in the $x-z$ plane, and σ_γ the source *rms* spot size at the interaction point (IP). For a high repetition rate f , the average flux is $N_\gamma f$. The average brilliance \mathcal{B} , given a non-diffraction limited beam, is [3]

$$\mathcal{B} = \frac{\mathcal{F}_{0.1\%}}{4\pi^2 \sigma_{\gamma,x} \sqrt{\epsilon_x / \beta_x^*} \sigma_{\gamma,y} \sqrt{\epsilon_y / \beta_y^*}}, \quad (3)$$

where $\mathcal{F}_{0.1\%}$ is the flux in a 0.1% bandwidth at the Compton edge, $\epsilon_{x,y}$ are the normalised emittances, and $\beta_{x,y}^*$ is the Twiss parameters at the IP. Peak brilliance, $\hat{\mathcal{B}}$, is the average brilliance normalised by $(\sigma_{\gamma,t} \cdot f)$, with $\sigma_{\gamma,t} = \sigma_{\gamma,z}/c$.

THE LINAC TEST FACILITY AT DARESBUARY LABORATORY

R. Schnuerer, A. Wheelhouse[†], STFC, Daresbury, UK
N. Patel, H. Gasson, D. Rowlands, I. Tahir, Teledyne UK Ltd, Chelmsford, UK

Abstract

The LINAC Test Facility (LTF) based at Daresbury Laboratory supports research and development of applications in medical, security, and environmental technologies through the operation of a Compact LINAC. This facility has been operated and upgraded over several years and this work has been performed in a collaboration between STFC and Teledyne e2v, enabling the facility to deliver an increased accelerating gradient of 6 MeV, which has broadened the capability to provide testing of radiotherapy and security scanning technologies. This paper describes the developments undertaken, the benefits gained by both parties, and future planned improvements.

INTRODUCTION

For decades the Accelerator Science and Technology Centre (ASTeC) at STFC Daresbury Laboratory has been home to advanced particle accelerator research. Working on a wide range of projects, carrying out research, developing and building the next generation of accelerators, one aim is to support industrial applications of particle accelerator technology. The LINAC Test Facility (LTF) is dedicated to facilitating research and development of applications in medical, security, and environmental technologies through the operation of a Compact LINAC. To advance the world's next generation of particle accelerator technologies and attract exciting new opportunities for UK industry, STFC and Teledyne e2v established a collaboration and strategic relationship in 2018 and share a positive, impactful relationship continuing through to 2022 and beyond. Teledyne e2v [1] is a leading supplier of RF technologies and components in many industries, including radiotherapy, security, and high-energy physics. The company required access to an accelerator and radiation test facility. Gaining access to STFC's unique facilities allowed Teledyne e2v to assist with the development of their integrated RF sub-systems.

An important part of the collaboration between STFC and Teledyne e2v is the Compact LINAC, an innovative and highly compact electron beam accelerator, used by both industry and the research community for testing x-ray and electron beam technologies. The Compact LINAC has undergone important upgrades enabling the facility to deliver an increased accelerating gradient and beam energy of 6 MeV [2].

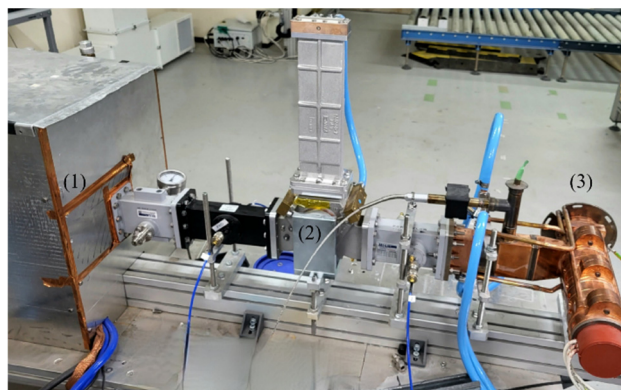


Figure 1: The Compact LINAC in the LTF. The main components are (1) 3.1 MW S-Band Magnetron, (2) 3-Port Circulator and (3) the 6 MeV Linear Accelerator.

The Compact LINAC uses a commercially available 6 MeV linear particle accelerator manufactured by AccelRAD Technologies, Belmont, USA. The S-Band LINAC produces electrons and X-rays and is powered by a tuneable S-Band Magnetron, see Figure 1. The pulsed RF frequency is 2.998 GHz, and the peak output power is 3.1 MW. The Compact LINAC's RF repetition rate is from a single pulse up to 400 Hz with a pulse width from 0.5 to 4 μ s [3].

In this paper, the Compact LINAC system is described, and operating conditions specified. Further, a few examples of work are listed to show the wide range of application possibilities with the system.

OPERATING CONDITIONS

The system comprises a Teledyne e2v AMM1 modulator [4] and MG7095 magnetron [5] paired with a Teledyne e2v electromagnet* an AFT three-port circulator, AccelRAD 6 MeV LINAC, and bespoke Electron gun driver. The combination of the AMM1 modulator and magnetron with electromagnet allows for a wide range of operating points, see Table 1 and Figure 2. The pulse width and repetition frequency can be changed quickly and easily allowing for the output dose rate to be controlled.

[†] alan.wheelhouse@stfc.ac.uk

*MG6062

CHALLENGES FOR HIGH-ENERGY X-RAY SECURITY SCREENING LINACS

M. J. Jenkins*, J. Ollier, M. G. Procter, Rapiscan Systems Ltd, Stoke-on-Trent, UK

Abstract

X-ray based Cargo and Vehicle Inspection (CVI) systems are used for security and customs inspections at a variety of locations. To provide the maximum flexibility many users require mobile CVI systems to allow vehicles to be screened efficiently for threats and contraband. The need for mobile systems means that the linear accelerator, and ancillary systems, used to generate the x-rays must be compact, rugged, and reliable. These systems must meet image performance tests specified by American National Standards Institute (ANSI) and the International Electrotechnical Commission (IEC). The IEC also defines a standard for material discrimination. The requirements of these standards mean that the x-ray output produced by the linac needs to be consistent during and between scans, with the stability and repeatability of the output being critical. The tolerances on the linac output to meet the performance standards combined with the need for a compact system gives an unusual challenge for the linac design. A review of how different stability measures impact the performance tests is presented. This is compared to current technologies and possible future linacs used for mobile CVI systems.

MOBILE CARGO AND VEHICLE INSPECTION SYSTEMS

Mobile Cargo and Vehicle Inspection (CVI) systems are an important tool for customs agencies, security services and military organisations. Mobile CVI systems allow for inspection points to be set up where needed. This allows the user to react to any intelligence they receive or to changes in traffic flow across borders and other inspection points. The typical design of linac based mobile CVI systems includes: an electron linac with a nominal energy of 3 to 7 MeV, a conversion target, slit collimator, detector array and x-ray beam stop. These are all mounted to a truck or trailer to allow the system to be moved as required. Figure 1 shows a Rapiscan Eagle M60 which is a mobile CVI system.

This system uses a 6 MeV electron linac to produce x-ray pulses with a bremsstrahlung spectrum with an end point energy of up to 6 MeV. Figure 2 shows a typical x-ray spectrum from a 6 MeV linac used on a transmission imaging CVI system. The spectra is not ideal for transmission imaging as the majority of photons emitted have an energy of less than 1 MeV. Low energy x-rays contribute to some performance metrics however, they also cause a lot of scatter which adds noise to the final image. For transmission imaging a more uniform spectral distribution would be preferred.

The x-ray beam is then collimated into a fan beam which is used with an L-shaped detector array to image the cargo or

* mjenkins@rapiscansystems.com



Figure 1: Rapiscan Eagle M60 in the deployed position ready for scanning.

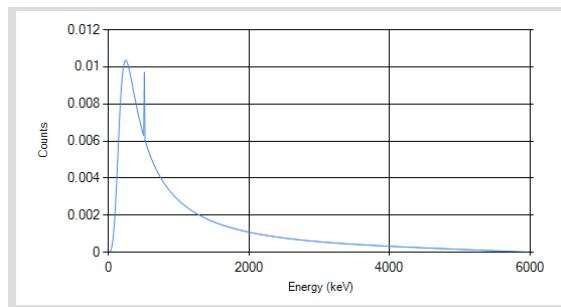


Figure 2: Typically 6 MeV x-ray spectrum used in transmission imaging systems.

vehicle under inspection. Figure 3 shows an outline drawing of the rear of the Eagle M60 with the linac, slit collimator and L-shaped detector array indicated.

The imaging methodology used by mobile CVI systems like the Eagle M60 require either the CVI system or the object under inspection to move through the scan tunnel between the linac and detector array. As the object under inspection passes through the imaging plane the linac is pulsed generating a series of x-ray pulses. The signal from each pulse is captured individually as a line, these lines are then stitched together to create an image of the object under inspection. Figure 4 shows a typical x-ray image of cargo imaged by a mobile CVI system. The pulse rate of the linac is determined by the geometry of the system and the speed at which the object passes through the imaging plane. For mobile CVI systems this is typically between 80 and 400 Hz.

IMAGE PERFORMANCE STANDARDS

The American National Standards Institute (ANSI) and the International Electrotechnical Commission (IEC) have

DESIGN OF A COMPACT LINAC FOR HIGH AVERAGE POWER RADIOTHERAPY*

C. D. Nantista^{†,1}, G.B. Bowden¹, Z. Li¹, M. Shumail¹, S.G. Tantawi¹ and B.W. Loo^{2,3}

¹SLAC National Accelerator Laboratory, Menlo Park, USA

²Department of Radiation Oncology, Stanford University School of Medicine, USA

³Stanford Cancer Institute, Stanford University School of Medicine, USA

Abstract

We present the design of a compact, 10 MeV, 300 mA pulsed X-band linac developed for medical application. The layout, <1 m including gun, buncher, capture section and current monitor, is of a recent configuration in which the 36 main linac cavities are individually fed in parallel through side waveguide manifolds, allowing for split fabrication. Initially destined for experimental study of FLASH irradiation of mouse tumors, the design was developed as a prototype for realization of a PHASER cancer treatment machine, in which multiple linacs, powered sequentially from a common RF source, are to provide rapid treatment to patients from multiple directions without mechanical movement, delivering dosage on a time scale that essentially freezes the patient. In this paper, we focus on the RF design, beam capture optimization, mechanical design and fabrication of the linac itself, deferring discussion of other important aspects such as window and target design, experimental specification setting, radiation shielding and operations.

INTRODUCTION

A fundamental goal for improving the effectiveness of radiation therapy for curing cancer is maximizing the differential damage done to cancerous tumors and normal tissue. To this end, so-called FLASH radiotherapy, with greatly enhanced dose rates (>50 Gy/s), promises significant advantages, used in conjunction with modern imaging and localization techniques. Rapid dose delivery effectively addresses the problem of “motion management”.

A revolutionary platform for implementing multidirectional FLASH treatment has been proposed [1]. Dubbed PHASER (Pluridirectional High-energy Agile Scanning Electronic Radiotherapy), it employs multiple (16) electron linacs, arrayed to target a common point and fired in sequence, thus eliminating the need for gantry motion.

The linacs for this scheme are required to compactly produce pulsed 300 mA, 10 MeV electron beams. We briefly describe here the effort toward developing such a linac at X-band using a distributed coupling approach [2], in which the cavities are individually powered from side manifolds.

LINAC ANATOMY

The overall RF layout of the PHASER linac vacuum space between the 30 kV electron gun and the target (neither shown) is illustrated in Fig. 1. It consists of a buncher cavity, a 5-cell single-feed capture section and a 36-cavity distributed-coupling main linac with two side manifolds,

followed by a current monitor cavity. On either side of the capture section is a drift space where the beam tube is surrounded by a solenoidal permanent magnet for focusing. The operating frequency is 11.424 GHz, and the beam is bunched and accelerated from a 30 kV gun up to 10 MeV in 26 inches (0.66 m), an effective gradient of ~15 MV/m.

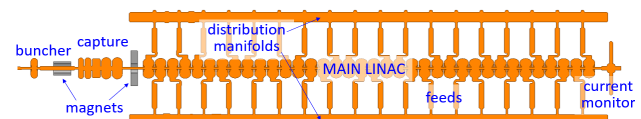


Figure 1: Linac RF design vacuum space.

CAVITY DESIGN

Main Linac Cavities

By eliminating the need for cell-to-cell coupling through the beam iris, the distributed coupling paradigm, like off-axis coupling schemes, allows greater freedom in cavity shape design, in particular allowing nose cones and a small beam aperture. For the main linac, cavity shapes were designed using an organic optimization code that maximizes shunt impedance while limiting peak surface fields related to RF breakdown, thus providing both good acceleration efficiency and high-gradient capability.

While ideally cavity spacing would track beam velocity, an acceptable solution was found to utilizing only two cell types, simplifying the RF design of the linac without losing much efficiency. The cavity shapes, optimized around different beam betas, are illustrated in Fig. 2. With a beampipe radius of 1 mm, effective shunt impedances of ~200 MΩ/m are achieved. Of the 36 cavities, the first 6 are of type A and rest of type B. To further maintain the beam phasing through the π-mode structure, the spacing after each A cavity was allowed to gradually increase from 1.249 cm to a constant 1.307 cm for the B cavities.

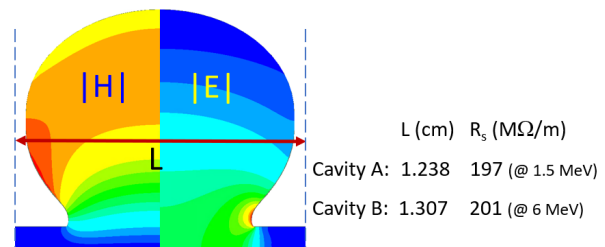


Figure 2: Main linac cavity profiles (dimensions in cm).

Capture Section/Injector

The capture section has five iris-coupled cells, with input coupler in the center cell. The outer walls are fully rounded, except for the coupler cell. The cell lengths increase with

*Work supported by a grant from Stanford University School of Medicine.
[†]nantista@slac.stanford.edu

NEW X-BAND AND S-BAND LINEAR ACCELERATORS AT VAREX IMAGING

Andrey V. Mishin, Brian C. Howe, Varex Imaging Corporation, Salt Lake City, UT, USA
 John Stammetti, Varex Imaging Corporation, Las Vegas, NV, USA

Abstract

We have designed, built, and high-power tested the advanced linear accelerators equipped with our new 3 MeV X-Band Accelerator Beam Centerline ABC-3-X-T-X and a reduced spot (RS) S-Band ABC-7ER-S-T-RS-X with broad 3 MeV to 8 MeV energy regulation, which demonstrated excellent performance and superior beam quality. We are immensely proud of these recent accomplishments and would like to share the news with the community.

LINACS FOR SECURITY, NDT, MEDICAL APPLICATIONS

Our new Varex High Energy Sources (HES) R&D group has been expanded and it now includes both (1) the Accelerator Beam Centerline (ABC) group in Salt Lake City, which is engaged in design and production of the Accelerator Beam Centerlines and (2) our Linear accelerator (LINAC) Subsystem Design and Engineering group in Las Vegas. The LINACs we produce are used by the customers worldwide in various Security Screening, Non-Destructive Testing (NDT), and Medical Radiation Therapy systems.



Figure 1: 3 MeV S-Band and 3 MeV X-Band ABC (at the correlated RF power settings). Note difference in radial dimensions for the two ABCs.

Our primary objective after separation of Varex Imaging from its mother company Varian Medical in 2017 has been to design the replacements for the guides supplied by Varian in Palo Alto as well as new models, and establish production of such guides, which we call Accelerator Beam Centerlines (ABC) (Fig. 1). We previously reported on the progress of our guides design and test [1-4]. Currently, we have created a triode e-gun based ABC series that we intend to use for new products, which often exceed their predecessors' parameters. In this paper, we would like to

summarize the results on the latter and report experimental results. The key models of our triode e-gun based ABCs are presented in Table 1. We are concluding our work on the new linac subsystem designs, which should be available for commercial supply in the next calendar year. This includes but is not limited to S-Band linac subsystems: improved Mi6SSM (the base system is already on the offering list), Mi7SSM; and an X-Band linac Subsystem: M3X. In addition, we are offering our ABCs and, potentially, systems, for medical applications. We have designed and fully qualified all three ABCs – all of which meet or exceed the specification requirements. In Fig. 2, a traditional 6 MeV ABC is shown next to an X-Band ABC-3-X-O-T-X, which was originally designed for a small, 350 kW magnetron, and then employed in a system M3X with a more powerful magnetron.

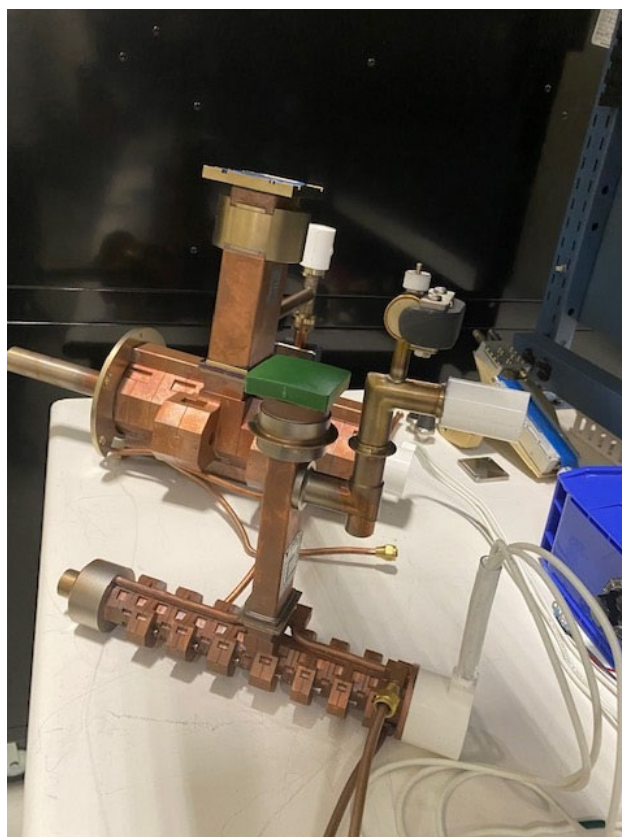


Figure 2: X-band ABC-3-X-O-T-X and S-Band ABC-6-S-O-T-X.

LOW ENERGY LINAC FOR ELECTRONIC BRACHYTHERAPY*

Chunguang Jing[†], Wade Rush, Pavel Avrakhov, Ben Freemire, Ao Liu, Edgar Gomez, Weinan Si, Sean Miller, John Callahan, Yubin Zhao, Roman Kostin, Euclid Techlabs LLC, Solon, OH, USA
James Welsh, Edward Hines Jr VA Hospital, Hines, IL USA

Chenguang Liu, Mark.Pankuch, Northwestern Medicine Chicago Proton Center,
Warrenville, IL, USA

Daniel Mihalcea, Philippe Piot, Northern Illinois University, DeKalb, IL, USA

John Power, Wanming Liu, Scott Doran, Argonne National Laboratory, Lemont, IL, USA

Abstract

The use of electronic brachytherapy (EB) has grown rapidly over the past decade. It is gaining significant interest from the global medical community as an improved user-friendly technology to reduce the usage of Ir-192. However, the present EB machines all use electron beams at energies of 100 kV or less to generate the X-ray photons, which limits their use to low dose-rate brachytherapy. We focus on the development of a compact and light weight 1 MeV linac to generate and deliver >250 kV X-ray photons to the patient. The device is intended to retrofit to existing brachytherapy applicators. In this paper we will report progress on this project.

MOTIVATION

The purpose of this effort is to deliver a prototype High Dose Rate (HDR) Electronic Brachytherapy (EB) machine to replace the radioactive sources, e.g. Ir-192, that are commonly used in brachytherapy. Permanent implant brachytherapy generally makes use of radioactive “seeds.” These tiny seeds are about the size of a rice grain (~5 mm long) and are implanted using ultrasound or another form of imaging guidance. Take, for example, Ir-192, which has a short half-life of only 74 days. The short half-life means it has a higher specific activity, and it is exclusively used for HDR brachytherapy. On the other hand, the short half-life of a material like Ir-192 means frequent replacement of the sources, and the increased possibility of interception by criminals during shipment and replacement. In contrast, particle accelerators have been successfully employed as a replacement technology for radionuclide radiation sources in many applications. X-ray generators have been broadly used for clinical radiation therapy [1]. However, their design is complicated and too bulky for some space-limited applications like EB. Miniature DC high-voltage X-ray generators can be made to the size of centimeters, and have been evolving over the last decade, with Xoft being the primary example [2]. However, with only 50 kVp bremsstrahlung, they are not a suitable substitute for the main thrust of HDR (high-dose-rate) brachytherapy, which currently uses Ir-192.

Euclid Techlabs proposed a novel design of an electron accelerating structure with two important features that are necessary for use in EB, particularly aiming for the retrofitting of existing EB applicators: a very small transverse

size and very high dose delivery stability. In this project, we leverage this with a cost effective 1 MeV metallic brazeless accelerator, which was successfully tested before [3]. The design has been further improved since then. The enabling factor for the proposed approach is that for the case of a minimum weight accelerator, the beam current is a miniscule ~1 μ A at the target, which can deliver enough dose (1Gy/min @ 1cm) for EB treatment management plan (TMP). Using Bremsstrahlung radiation, the proposed 1 MeV electron beam will generate broad energy spectrum photons up to 1 MeV with a mean energy of 250~450 keV (depending on the applied target material), compared to the 380 keV narrow spectrum line of Ir-192. This is far more energetic than the current EB source. In order to generate such a powerful radiation dose, in comparison with the state-of-the-art 50 kV DC accelerator-based EB system, this proposed RF accelerator-based EB system has a much larger size. However, one can imagine that the size and weight can easily be managed using modern robotic technology. Figure 1 illustrates this concept. A higher energy electron beam can be focused to a pencil beam to retrofit to the existing applicators.

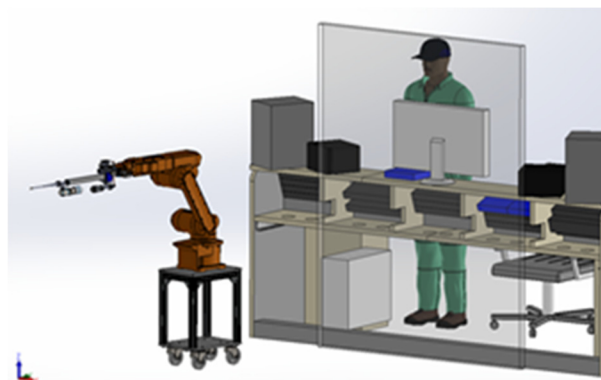


Figure 1: Artist's view of an RF accelerator-based EB system.

ACCELERATOR DESIGN

To achieve the compactness, the electrons are produced by a field emission cathode, which can generate high quality bunch electrons with proper designed bunching cavities. Figure 2 shows the profile of accelerating field along the axis. The significant high field at the cathode location help improve beam quality of the emitted electrons and prompt acceleration. With optimization, it can achieve nearly 90% of beam transmission passed through the 8-cell accelerating structure without an external focusing

* Work supported by NNSA Identification No. 89233121CNA000209.

[†] c.jing@euclidtechlabs.com

CRYOGENIC ACCELERATOR DESIGN FOR COMPACT VERY HIGH ENERGY ELECTRON THERAPY*

E. C. Snively[†], M. Shumail, C. Nantista, Z. Li, M. Oriunno, G. Bowden, V. Borzenets, A. Krasnykh,
S.G. Tantawi, SLAC National Accelerator Laboratory, Menlo Park, CA, USA
B.W. Loo, Dept. of Radiation Oncology, Stanford School of Medicine, Stanford, CA, USA

Abstract

We report on the development of a cryogenic X-band (11.424 GHz) accelerator to provide electron beams for Very High Energy Electron therapy. The distributed coupling linac is designed with a 135° phase advance, optimized to produce a 100 MeV/m accelerating gradient in a one-meter structure using only 19 MW when operating around 77 K. This peak power will be achieved through pulse compression of a 5-8 MW few- μ s pulse, ensuring compatibility with a commercial power source. We present designs of the cryogenic linac and power distribution system, as well as a room temperature pulse compressor using the HE_{11} mode in a corrugated cavity. We discuss scaling this compact and economical design into a 16 linac array that can achieve FLASH dose rates (> 40 Gy/s) while eliminating the downtime associated with gantry motion.

INTRODUCTION

The linear accelerator (linac) design presented here aims to demonstrate a Very High Energy Electron (VHEE) therapy system that is compact enough to fit within a conventional clinical radiation treatment room. Because VHEE therapy eliminates the process of using the electron beam to produce X-rays, relying instead on the therapeutic dose provided by the electrons themselves, this treatment scheme inherently allows for higher dose rates, making it an attractive approach to deliver FLASH treatments exceeding 40 Gy/s.

Electron beam energies on the order of 100 MeV are needed to reach deep-seated tumors throughout the body. Designing a linac capable of accelerating electrons up to 100 MeV within a meter is well within the known state of the art. However, the typical amount of RF power needed to power the linac to achieve this high gradient requires sources that are incompatible with existing medical treatment facility infrastructure. Typically, the required RF power is on the order of 150 to 200 MW at X-band. The sources that can generate this type of power typically occupy the space of several treatment rooms. Furthermore, the cost of such a source would be highly prohibitive; a VHEE device with these power requirements would not be competitive with other radiotherapy modalities.

SYSTEM DESIGN

The accelerator design presented here requires only 5-8 MW of RF power at 11.4 GHz to generate a 100 MeV beam, compared with the typical 150-200 MW required for

conventional linacs. This breakthrough in power efficiency is accomplished through the development of a novel high efficiency linac operated at cryogenic temperatures and a novel ultra-compact RF pulse compression scheme.

135 Degree Phase Advance Linac

The phase advance of this standing wave linac design, 135° per cell, provides the highest possible geometric shunt impedance, reaching 192 M Ω /m at room temperature. A narrow beam pipe radius of 1 mm reduces coupling between cells to the point where the relative phase can be arbitrarily chosen to maximize shunt impedance. The cavity geometry, shown in Fig. 1, features a re-entrant nose cone to maximize the ratio of on-axis accelerating gradient to surface field using a geometric optimization approach [1]. The Q_0 of the cavity is 8100 at room temperature. By reducing the operating temperature to 77 K, we expect to gain a factor of 2.7 in Q_0 , with a corresponding increase in the shunt impedance by the same factor [2].

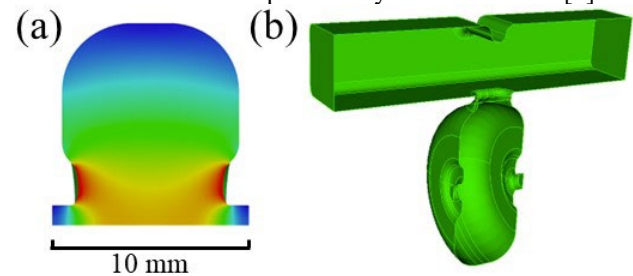


Figure 1: (a) Cross-section of the electric field profile simulated in one half of the 135° phase advance linac cavity. (b) 3D model showing one half of the power distribution waveguide with coupling iris for a single cavity.

Power is coupled to each cell through a distributed power coupling manifold. To accommodate the 135° phase advance, four parallel manifolds are used. The phase advance between the feeding junctions on each waveguide is 180° which allows feeding every fourth cavity as the phase advance to every fourth cavity is $135^\circ \times 4 \equiv 180^\circ$. The full one-meter structure is composed of 104 cells. Power couples to the cell through an iris at the cell equator, as shown in Fig. 1 b. The parameters of the iris, along with the inverted feature opposite the cell in the waveguide, have been optimized using the parallel ACE3P solvers developed at SLAC to produce the correct transfer S-matrix and coupling for a beam-loaded cavity.

RF Pulse Compressor

The VHEE system presented here is intended to be compatible with a commercial 11.424 GHz RF power source, taking a 6 MW peak power input in a ~ 4 μ s pulse length

* Work supported by U.S. D.O.E. Contract No. DE-C02-76SF00515 and D.O.E. solicitation LAB 20-2262 under FWP 100623.

[†] esnively@slac.stanford.edu

DESIGN AND OPTIMIZATION OF A 100 kV DC THERMIONIC ELECTRON GUN AND TRANSPORT CHANNEL FOR A 1.3 GHz HIGH INTENSITY COMPACT SUPERCONDUCTING ELECTRON ACCELERATOR (HICSEA) *

Pragya Nama[†], Abhishek Pathak, Raghava Varma
 Indian Institute of Technology Bombay, Mumbai, India

Abstract

Here we present the design and optimization of a 100 kV DC thermionic electron gun and a transport channel that provides transverse focusing through a normal conducting solenoid and longitudinal bunching with the help of a single gap buncher for a 1.3 GHz, 40 kW, 1 MeV superconducting electron accelerator. The accelerator is proposed to treat various contaminants present in potable water resources. A 100 kV thermionic electron gun with LaB₆ as its cathode material was intended to extract a maximum beam current of 500 mA. To minimize beam emittance, gun geometry, i.e., cathode radius and height and radius of the focusing electrode, is optimized. The minimal obtained emittance at the gun exit is 0.3 mm.mrad. A normal conducting focusing solenoid with an iron encasing is designed and optimized to match and transport the beam from the gun exit to the superconducting cavity. Finally, a 1.3 GHz ELBE type buncher is designed and optimized to bunch the electron beam for further acceleration.

INTRODUCTION

Accelerator technology is proven very efficient for treating harmful pollutants in water resources [1,2]. A 1.3 GHz, 1 MeV, 40 kW high intensity compact superconducting electron accelerator (HICSEA) is proposed by IIT Bombay and Japanese institutions (KEK, Tohoku etc.) to treat various pollutants present in the limited usable water resources. The proposed accelerator will be a 3 m long with an industrial-grade thermionic electron gun followed by a transport channel for transverse and longitudinal focusing, a single-cell Nb₃Sn accelerating cavity, a bending magnet, and finally a raster magnet. A schematic of the proposed accelerator is shown in Fig. 1. In this paper, we discuss the design and optimization studies for a dedicated electron source, i.e., a 100 kV thermionic diode electron gun followed by a transport line that constitutes a normal conducting solenoid and a buncher cavity.

The electron gun is based on a DC thermionic cathode and operates at 100 kV in the intensity range of 100 mA to 500 mA. Thermionic electron emission sources (W, CeB₆, and LaB₆) are cheaper, compact, can operate under lower vacuum conditions, and provide greater brightness for large-area illumination [3]. There are several other advantages

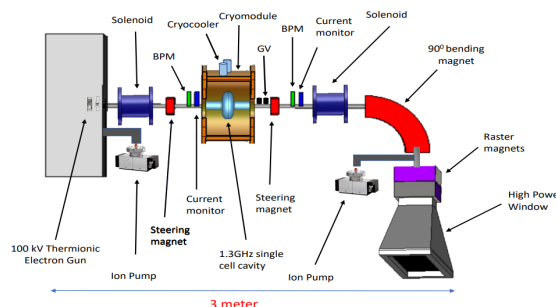


Figure 1: Schematic of proposed accelerator.

of using thermionic cathodes, such as emission capability, ease of maintenance, and ease of finding supplies. The thermionic cathode is also cost-effective, compact, simple in operation, and can produce large current densities of 10-100 A/cm². As the proposed accelerator operates with a beam current of 500 mA, space-charge forces will play a significant role and may lead to emittance growth. Therefore, the design of an optimized transport channel constituting a buncher for efficient bunching of the DC beam produced by the thermionic electron gun and a solenoid for transport confinement is an essential part of the linac design. Followed by the thermionic gun optimization, we performed modeling and optimization studies for a normal conducting solenoid and a single-gap buncher cavity to bunch, transport, and match the beam from the electron gun to the single-cell accelerating cavity while keeping a minimum emittance growth throughout the accelerator.

GUN DESIGN

The gun design comprises a planar cathode with a focusing electrode, and an anode. A flat symmetric cathode of circular cross section was chosen for this study. The cathode material used for this study was LaB₆ (work function = 2.67 eV) because of its better emission properties such as uniform emission density, smooth surface and high resistance against contamination [4]. Here, cathode along with the focusing electrode is held at -100 kV and anode was grounded. The design of the electron gun is such that the maximum current up to 500 mA can be extracted efficiently from it. For the current of 1 A, further optimizations or more geometry modification such as inclusion of an extra electrode might be needed.

A cross sectional view of cathode is shown in Fig. 2. To minimize the beam emittance, various geometry parameters

* Work supported by SERB's Prime Minister Fellowship for Doctoral Research managed by FICCI

[†] pragya2595@gmail.com

MUNIPULATION AND MEASUREMENT OF POLARIZATION STATES FOR THz COHRENET UNDULATOR RADIATION

S. Kashiwagi[†], H. Saito, F. Hinode, T. Muto, K. Nanbu, I. Nagasawa and H. Hama,
Research Center for Electron Photon Science (ELPH), Tohoku University, Sendai, Japan
H. Zen, Institute of Advanced Energy (IAE), Kyoto University, Uji, Japan
A. Irizawa, Research Organization of Science and Technology, Ritsumeikan University, Japan

Abstract

We are conducting research an accelerator-based terahertz source that can produce arbitrary polarization states from linearly polarized coherent undulator radiation (CUR). The polarization manipulation of the CUR can be realized using the Martin Puplett interferometer employed as an optical phase shifter. Variable polarization manipulator (VPM) was demonstrated using the terahertz CUR source based on an extremely short electron bunch at Research Center for Electron Photon Science (ELPH), Tohoku University. The horizontally polarized CUR with a frequency of 1.9 THz was manipulated into variable polarization state, and Stokes parameters were measured to derive the degree of polarization states. Experimental results will be presented in this conference.

INTRODUCTION

A test accelerator as a coherent terahertz source (t-ACTS) is currently under development at ELPH in Tohoku University [1-3], wherein extremely short electron bunches are used to generate intense coherent THz radiation. THz radiation sources have attracted considerable interests because of their potential applications in fields such as material science, medical imaging, and high-speed communication. The coherent THz radiation having polarization control ability can be used for various types of scientific investigation and applications. Vibrational circular dichroism (VCD) measurements in the THz region are extremely sensitive to conformational changes in proteins [4, 5]. A THz source capable of switching left and right circular polarizations with high speed is very useful for biological analysis and is in great demand. Because although a quarter waveplate (QWP) is used to change linearly polarized light into circularly polarized light, no QWP can be used in a wide THz wavelength range. We developed a system that manipulates linearly polarized CUR in the THz region into arbitrary polarization states and measured the degree of polarization.

MANIPULATION AND MEASUREMENT OF POLARIZATION STATE

Polarization Manipulation

As a relativistic electron beam propagates through an undulator, under the condition that the pulse length of the electron beam is sufficiently shorter than the resonance wavelength of the undulator radiation, the radiation will

have temporal coherence. The temporal profile of the electric field of the undulator radiation shows an almost sinusoidal wave with a cycle of the number of undulator periods [6].

The polarization state of the CUR is manipulated by exploiting the property of temporal coherence. The variable polarization manipulator (VPM) consists of a wire-grid as beam-splitter and two rooftop mirrors, with one rooftop mirror mounted on a movable stage [7]. The radiation from a planar undulator is linearly polarized, therefore the input polarizer is not necessary. An incident beam of the CUR is split into two orthogonal linear polarizations by the wire-grid splitter, and the reflected and transmitted beams travel to the rooftop mirrors. Polarization of two beams are flipped by 90° using the rooftop mirrors and the round-trip beams are superimposed at the splitter wire-grid. The relative phase (δ) between the two orthogonal linearly polarized beams is adjusted using the movable stage. By using the VPM, it is possible to produce various polarization states by simply adjusting the relative phase. All polarization states can be realized simply by moving the interferometer stage. In other words, the left and right circular polarization can be switched by simply shifting the movable stage by half a wavelength ($\sim 150 \mu\text{m}$ at 1 THz). The VPM can realize high-speed switching the left and right circular polarization at several-hundred-Hz using a piezoelectric actuator stage. In addition, it has the advantage of high transmission efficiency in the interferometer.

Polarization Measurements

The polarization state of light can be expressed by measuring the Stokes parameters (S_0, S_1, S_2, S_3), which are four elements of the Stokes vector. The partial polarization in which polarized and unpolarized lights are mixed can be expressed using polarization degree P ($0 \leq P \leq 1$) as follows:

$$S = \begin{pmatrix} S_0 \\ S_1 \\ S_2 \\ S_3 \end{pmatrix} = (1 - P) \begin{pmatrix} S_0 \\ 0 \\ 0 \\ 0 \end{pmatrix} + P \begin{pmatrix} S_0 \\ S_1 \\ S_2 \\ S_3 \end{pmatrix}. \quad (1)$$

In the case of complete polarization, $P = 1$, and the degree of polarization P can be defined as:

$$P = \frac{I_{\text{POL}}}{I_{\text{TOT}}} = \frac{\sqrt{S_1^2 + S_2^2 + S_3^2}}{S_0}, \quad (2)$$

where I_{TOT} is the total intensity and I_{POL} is the intensity of the partial polarization. The four Stokes parameters can be

[†] kashiwagi@ins.tohoku.ac.jp.

PROGRAMMABLE SLED SYSTEM FOR SINGLE BUNCH AND MULTIBUNCH LINAC OPERATION

C. Christou, P. Gu, A. Tropp
 Diamond Light Source, Didcot, Oxfordshire, UK

Abstract

The Diamond Light Source pre-injector linac generates single bunch and multibunch 100 MeV electron beams for top-up and fill of the storage ring. Two high-power 3 GHz klystrons are required for reliable injection into the booster. In order to introduce redundancy, a SLED pulse compressor is being installed so that the linac can operate from just one klystron, with the second klystron held as a standby. A phase flip can be used to generate a transient RF spike, suitable for single bunch operation, and a programmable amplitude and phase drive profile can be specified to generate a constant-power output suitable for multibunch operation. Details are presented of design, installation and high-power operation of the SLED system, and the ability to generate a long pulse, including corrections for klystron nonlinearity and deviations from modulator flat-top, is demonstrated.

LINAC DESIGN AND OPERATION

A schematic diagram of the present Diamond linac power distribution is shown on the left side of Fig. 1. Klystrons K1 and K2 power primary and final bunching units (PBU and FBU) and two accelerating structures (AS1 and AS2). One klystron powers PBU, FBU and AS1 and the other powers AS2. Beam from AS1 can drift through AS2 and so two waveguide switches (SW1 and SW2) allow either klystron to power the bunchers and AS1 to deliver low-energy beam to the booster in the event of a klystron or modulator failure [1].

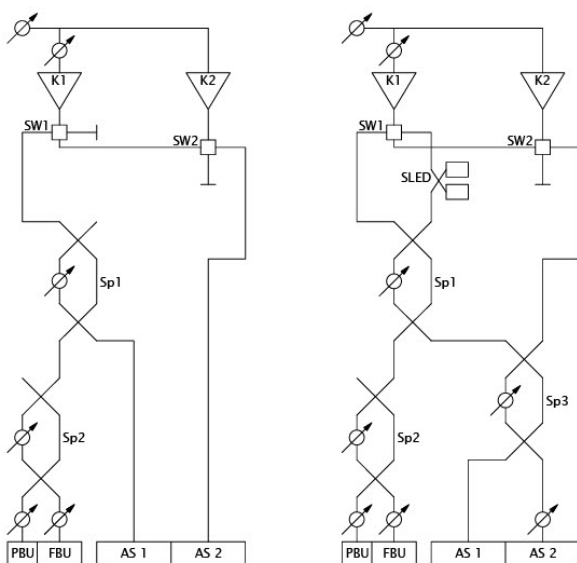


Figure 1: Linac configuration without (left) and with (right) SLED cavity.

Injection efficiency into the booster is poor at low energy, and so a SLED is being installed to enable full energy operation with one klystron. The right side of Fig. 1 shows the network with the SLED. Power from either klystron is compressed in the SLED and then split to the linac structures by power splitters Sp1, Sp2 and the new Sp3, which controls relative powers in AS1 and AS2.

SLED CAVITY PARAMETERS

Pulse compression is achieved by using the first part of a high-power RF pulse to charge the SLED cavities and then adding the second part of the pulse to the SLED cavity discharge [2]. Figure 2 shows an analytic solution for the fields ($= \sqrt{\text{power}}$) in the cavity charge and discharge process, with the bold blue line representing the summed pulse delivered to the linac. The RF pulse is divided in two by a 180° flip of the input phase, shown as a change of direct output from +1 to -1.

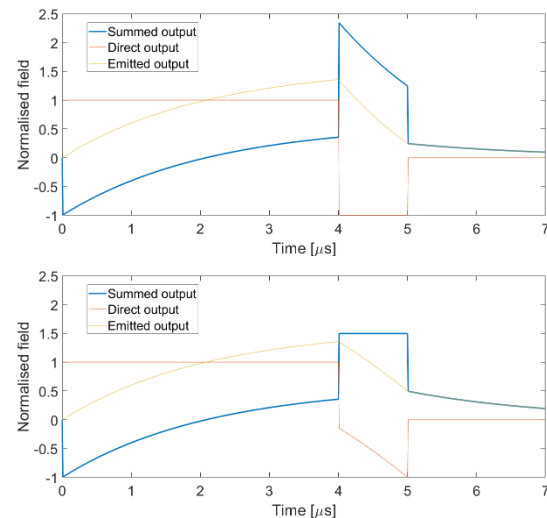


Figure 2: Calculated SLED performance with phase flip (above) and additional amplitude shaping (below).

The upper plot in Fig. 2 shows the sharp spike generated by a simple phase flip. This pulse shape can be used for single-pulse operation, but multibunch operation requires equal acceleration of every bunch in a 500 MHz 120-bunch train, duration 240 ns. The accelerating structure filling time is 740 ns and so the SLED must deliver a flat high-power pulse of duration 1 μ s. The lower plot shows a 5 μ s RF pulse with a flip at 4 μ s and a post-flip pulse amplitude modulated to generate this 1 μ s flat output pulse.

SLED parameters were chosen to generate a long flat pulse: cavity Q_0 was slightly above 100,000 and coupling β was 4.0, suitable for a 1 μ s double-power pulse.

IDENTIFICATION OF THE MECHANICAL DYNAMICS OF THE SUPERCONDUCTING RADIO-FREQUENCY CAVITIES FOR THE EUROPEAN XFEL CW UPGRADE

W. H. Syed*, A. Bellandi†, A. Eichler, J. Branlard,
Deutsches Elektronen-Synchrotron DESY, Germany

Abstract

The European X-Ray Free-Electron Laser (EuXFEL) is to-date the largest X-ray research facility around the world which spans over 3.4 km. EuXFEL is currently being operated in a pulsed mode with a repetition rate of 10 Hz. One upgrade scenario consists of operating the EuXFEL also in a Continuous-Wave (CW) mode of operation to improve the quality of experiments. This upgrade brings new challenges and requires new algorithms to deal with controlling a stable accelerating field inside the Superconducting Radio-frequency (SRF) accelerating cavities and keeping them on resonance in this new mode of operation. The purpose of this research work is to identify the mechanical dynamics of the cavities which will facilitate the development of the resonance controller for the CW upgrade. To this extent, experiments were conducted at a test bench. For the first time, in this work, two different types of spectrally rich excitation signals: multi-sine and stepped-sine are used to excite the mechanical dynamics of the cavities using the piezo actuator. After the analysis of experimental data, mechanical modes are successfully identified and will be used to design the controller.

INTRODUCTION

The European X-Ray Free-Electron Laser (EuXFEL) is used to generate ultrashort X-ray flashes with a very high brilliance in the femtosecond range for various scientific and industrial research purposes. Currently, EuXFEL is being operated in a pulsed mode with a repetition rate of 10 Hz and a duty factor of 1.4% and can produce a maximum of 27000 electron bunches per second with a temporal separation of 220 ns. The possibility a Continuous-Wave (CW)-upgrade for EuXFEL is currently being investigated as CW allows a high average beam current and a flexible bunch pattern of the beam, which will be of great importance for the quality of experiments at the EuXFEL. To investigate the possibility a CW-upgrade, experiments are being conducted on a facility called Cryo-Module Test Bench (CMTB) at DESY, containing 8 TESLA-type SRF cavities, same as in EuXFEL. To upgrade EuXFEL to CW mode of operation, the Superconducting Radio-frequency (SRF) cavities must be operated at a very high-quality factor, in the order of 10^7 , due to power limitations. But this very high-quality factor would result in an extremely narrow half-bandwidth, of less than 20 Hz [1], when operating cavities at 1.3 GHz. This will make the

cavities more sensitive to external mechanical disturbances or microphonics, which would cause detuning effects. Detuning is the difference between the operating frequency of the SRF cavity and the resonance frequency of the cavity. So to keep the SRF cavity at resonance with the required field stability and as well as to limit the required power, a control solution must be developed to suppress the effect of these microphonics using fast piezoelectric tuners. Various filter-based model-less algorithms have been investigated for microphonics suppression as in [2], but these solutions show limitations when combined with RF field control and are only able to suppress narrow bandwidth microphonics. To overcome this problem, a model-based control strategy can be used for microphonics suppression. However, before developing a model-based control strategy, the mechanical dynamics of the cavity (from piezo actuation to the detuning) in the form of a model (transfer function or state-space) must be identified with reasonable accuracy. So far extensive research has been done to investigate the mechanical dynamics of the cavity as in [3–6]. The commonly used excitation signal are either the stepped sine or chirp. However, a comparison between different excitation signals was never done, with the exception of [7], where stepped-sine and step signal are compared for identifying the cavity's mechanical modes. Still, in [7], spectrally rich signals like stepped-sine, chirp, multi-sine, etc. are not compared. For the first time, in this work, two different spectrally rich excitation signals: multi-sine and stepped-sine are used to investigate the mechanical dynamics of the cavity. The reason for using multi-sine is that on one hand it is very time efficient compared to stepped-sine and on the other hand it is a much more reliable signal compared to a simple step signal when it comes to system identification. We could have used chirp as well along with stepped-sine and multi-sine but due to technical limitations of our measurement setup we are only able to collect one second of measurements at a time. So if we cover the desired frequency region using one second of a chirp signal, we might not get the steady-state measurement for the desired frequency region.

If we can identify the mechanical dynamics of the cavity using multi-sine with reasonable accuracy then it would significantly reduce the time during the online implementation routine and will be preferred over stepped-sine especially when re-characterization of the system is required often.

EXPERIMENT

Choice of excitation signal plays a key role when it comes to identify a dynamical system whether for control purpose

* Main Author. W.H.Syed. wasif.haider.syed@desy.de

† Presenter. A.Bellandi. andrea.bellandi@desy.de

BEAM-TRANSIENT-BASED LLRF VOLTAGE SIGNAL CALIBRATION FOR THE EUROPEAN XFEL

N. Walker, V. Ayvazyan, J. Branlard, S. Pfeiffer, C. Schmidt, DESY, Hamburg, Germany.

Abstract

The European XFEL linac consists of 25 superconducting RF (SRF) stations. With the exception of the first station which is part of the injector, each station comprises 32 1.3-GHz SRF TESLA cavities, driven by a single 10-MW klystron. A sophisticated state-of-the-art low-level RF (LLRF) system maintains the complex vector sum of each RF station. Monitoring and maintaining the calibration of the cavity electric field (gradient) probe signals has proven critical in achieving the maximum energy performance and availability of the SRF linac. Since there are no dedicated diagnostics for cross-checking calibration of the LLRF system, a procedure has been implemented based on simultaneously measuring the beam transient in open-loop operation of all cavities. Based on methods originally developed at FLASH, the European XFEL procedure makes use of automation and the XFEL LLRF DAQ system to provide a robust and relatively fast (minutes) way of extracting the transient data, and is now routinely scheduled once per week. In this paper, we will report on the background, implementation, analysis methods, typical results, and their subsequent application for machine operation.

BEAM TRANSIENT

The beam transient voltage V_t as a function of beam-on time t for an on-resonance cavity can be expressed as

$$V_t(t) = -\frac{Q_b}{\Delta t_b} R_L (1 - e^{-t/\tau})$$

$$\approx -\frac{1}{2} Q_b \left(\frac{r}{Q}\right) \omega_0 \frac{t}{\Delta t_b} \text{ for } t \ll \tau, \quad (1)$$

where Q_b is the single bunch charge; Δt_b is the bunch spacing; R_L is the loaded shunt impedance; and ω_0 and τ are the cavity frequency and time constant respectively. The basic assumption is that all cavities generate the identical transient response (for the same beam pulse). For short beam pulses of $\sim 50 \mu\text{s}$ ($\ll \tau = 1130 \mu\text{s}$) the only variations arise from differences in (r/Q) ($=1030 \Omega$) or cavity frequency ($f_0 = 1.3 \text{ GHz}$) which are considered negligible. Taking typical beam values of $Q_b = 250 \text{ pC}$ and $\Delta t_b = 0.45 \mu\text{s}$ (2.25 MHz repetition rate), equation (1) gives $\sim 1 \text{ kV}$ transient amplitude per bunch, or $\sim 100 \text{ kV}$ for a one-hundred-bunch beam pulse, which represents a $\sim 0.5\%$ of the typical accelerating gradient in a cavity ($\sim 20 \text{ MV}$). Although the RF stability is in general better than this at XFEL [1-3], resolving the transient generally requires averaging over many pulses.

ALGORITHM

The approach dates back to a similar method developed for FLASH [4]. The beam transient is measured with the

nominal accelerating RF field present, which provides a calibration point at the typical working values. Furthermore, since no changes are need to the operational state of the accelerator taking the measurements becomes very quick and can be done within a few minutes during nominal operations. The transient itself is measured using the difference between beam-on and beam-off measurements. Figure 1 shows an example of the typical raw data.

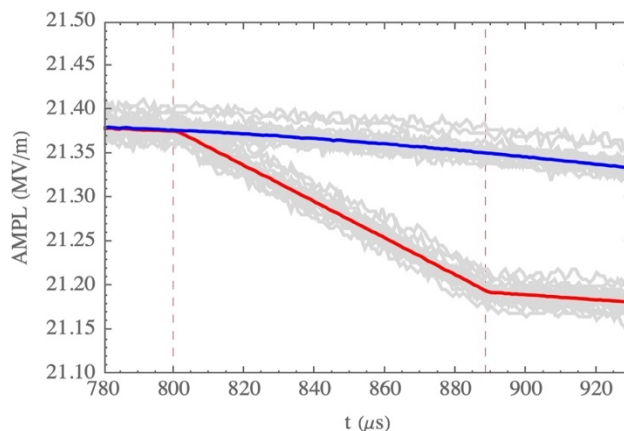


Figure 1: Example of cavity voltage amplitude data used to calculate the transient. Blue: averaged beam off. Red: averaged beam on. Grey: individual single-pulse measurements. The dashed lines indicate the period of the beam pulse, which in XFEL starts at $t = 800 \mu\text{s}$.

All the measurements are taken open-loop (i.e. no feedback control). The beam is turned on and off with a period of ~ 5 seconds (50 pulses) for total time of approximately one minute (see Fig. 2). The on and off data are interleaved to reduce the influence of slow drifts in the applied RF which could influence the difference calculation. During the beam-on data, the beam energy at the end of the accelerator is also recorded; this additional data can be used for absolute calibration. The RF signals are automatically recorded by the XFEL DAQ system, which runs continuously.

The analysis of the data is performed entirely in the complex plane. The raw cavity voltage waveforms are extracted from the DAQ system as amplitude and phase and converted into complex numbers. The beam-on and beam-off data are first averaged and then subtracted to provide the required beam transient. The transient is reported after 100 bunches ($t = 845 \mu\text{s}$). Despite the care taken to avoid the influence of drifts in the RF, experience has shown that some offset between the on and off datasets is inevitable. Hence a small correction is applied to the transient measurement based on the difference between the signals at the start of the beam pulse ($t = 800 \mu\text{s}$, see Fig. 3). Care has been taken to make sure that the correlation between the real and imaginary parts is taken into account in

SIMULATION STUDY OF AN ACCELERATOR-BASED THz FEL FOR PUMP-PROBE EXPERIMENTS AT THE EUROPEAN XFEL*

P. Boonpornprasert[†], G. Georgiev, M. Krasilnikov, X. Li, A. Lueangaramwong,
Deutsches Elektronen-Synchrotron DESY, Platanenallee 6, 15738 Zeuthen, Germany

Abstract

The European XFEL considers to perform THz-pump and X-ray-probe experiments. A promising concept to provide the THz pulses with satisfactory properties for the experiments is to generate them using a linear accelerator-based free-electron laser (FEL). A simulation study of a THz FEL facility capable of generating powerful tunable coherent THz radiation that covers the wavelength range of 25 μm to 100 μm was performed. An accelerator beamline layout based on the Photo Injector Test Facility at DESY in Zeuthen (PITZ) and an APPLE-II undulator with a period length of 40 mm were used in the simulation study. Results of the study are presented and discussed in this paper.

INTRODUCTION

The European XFEL has planned to perform THz pump-X-ray probe experiments at the full bunch repetition rate for users. A promising concept to provide the THz pulses with a pulse repetition rate identical to that of the X-ray pulses is to generate them using a linear accelerator-based THz source [1, 2]. The Photo Injector Test Facility at DESY in Zeuthen (PITZ) is an ideal machine as a prototype for developments of the THz source [3].

Research and development (R&D) of the prototype linear accelerator-based THz source are ongoing at PITZ. The R&D has been conducted in two parts. The first part is a proof-of-principle experiment to generate THz Self-Amplified Spontaneous Emission (SASE) FEL using an LCLS-I undulator (on loan from SLAC) driven by an electron bunch from the PITZ accelerator [4–6]. The second part is a conceptual design study of an ideal accelerator-based THz source facility that can be established at the European XFEL site and used for the pump-probe experiments.

Recently, the installation of the first THz beamline setup at PITZ was finished [7] and the first commissioning of the proof-of-principle experiment has been performed with a bunch charge of up to 3 nC. Measurements of the THz generation have been taken using pyrodetectors and the statistics properties analysis reflects the expected SASE performance [8, 9].

As the proof-of-principle experiments are ongoing at the PITZ facility, we also have worked on a conceptual design of the ideal THz source that can produce intense, tunable, and narrow-band THz radiation using a SASE FEL, a seeded FEL, and superradiant undulator radiation (SUR). A basic concept layout of the ideal THz source for simulation studies

is shown in Fig. 1. The layout consists of an RF electron gun, two identical RF linacs, a bunch compressor, and a THz FEL undulator. Models and locations of the RF gun and the first linac in the layout are identical to those at the PITZ facility, with an additional linac downstream from the first one. Descriptions of the gun and the linac are presented in [10]. Description and preliminary simulation studies of the bunch compressor are presented in [11]. The THz FEL undulator used in this study is an APPLE-II type undulator in a circular polarization mode with a period length of 40 mm [12].

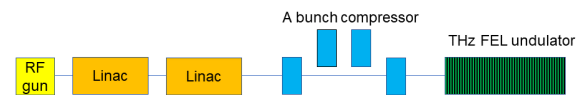


Figure 1: The basic concept layout of the ideal THz source.

In this paper, we focus on simulations of the SASE FEL. We also perform an example simulation of the seeding FEL for comparison with the SASE. We left SUR simulation for future study. First, we performed beam dynamics simulations using The ASTRA program package [13]. Next, we conducted FEL process simulations using the Genesis 1.3 code [14]. Then, we performed an example simulation of the seeded FEL with a center wavelength of 100 μm to demonstrate an improvement of THz pulse properties compared to the SASE case. Finally, a conclusion and outlook are given.

BEAM DYNAMICS SIMULATIONS

Beam dynamics simulations using the ASTRA program package were performed in order to deliver an uncompressed 4 nC electron beam from the cathode to the undulator entrance. Space-charge calculations were included in the simulations. The beam transport line layout used in these simulations follows the schematic diagram in Fig. 1. Some important machine and beam parameters used in the simulations are listed in Table 1.

The main solenoid current at the gun was optimized for minimum beam emittance values at the undulator entrance, 18 m downstream from the cathode. The accelerating gradient of the second linac was scanned from 0 to 18 MeV/m to achieve various beam momenta. Figure 2 shows simulated normalized transverse emittance at the undulator entrance as a function of the main solenoid current and the beam momentum. The emittance for each beam momentum is minimized in a main solenoid current range of 360 A to 365 A. We selected the beam with minimum emittance for each beam momentum and used it for FEL simulations in the next step.

* This work was supported by the European XFEL research and development program.

[†] prach.boonpornprasert@desy.de

LASER-TO-RF SYNCHRONISATION DRIFT COMPENSATION FOR THE CLARA TEST FACILITY

J. R. Henderson, A. J. Moss, and E. W. Snedden
ASTeC, STFC Daresbury Laboratory, Warrington, U.K.
A. C. Dexter, Lancaster University, Lancaster, U.K.

Abstract

Femtosecond synchronisation between charged particle beams and external laser systems is a significant challenge for modern particle accelerators. To achieve femtosecond synchronisation of the CLARA electron beam and end user laser systems will require tight synchronisation of several accelerator subsystems. This paper reports on a method to compensate for environmentally driven long-term drift in Laser-RF phase detection systems.

INTRODUCTION

The Compact Linear Accelerator for Research and Applications (CLARA) facility [1] is a test bed for accelerator and Free Electron Laser technology. CLARA will deliver a 250 MeV electron beam to the Full Energy Beam Exploitation (FEBE) [2] experimental hutch, and femtosecond synchronization of particle beams to an external laser is a foreseen requirement for future exploitation. To recover femtosecond dynamics from pump-probe experiments on CLARA will require femtosecond synchronisation between end station laser systems and several RF accelerator components.

LASER-RF PHASE DETECTOR CONCEPT

CLARA is a normal-conducting linear accelerator where an electron beam is generated by a UV photo-injector laser system in an s-band electron gun and then accelerated to full energy by four traveling wave linacs. The CLARA photo-injector (PI) laser system and high power RF systems are seeded by pulsed laser and RF master oscillators respectively. The PI (mode-locked) laser master oscillator, is currently locked to the RF master oscillator using a direct photodetection Phase Locked Loop (PLL) based on analogue electronics. The noise performance and long term stability of the laser-RF Phase Locked Loop has a significant impact of the quality of CLARA electron beam.

Direct photodetection Laser-RF phase locked loops use a fast photodetector and analogue electronics to determine the laser-RF phase error and a control loop to reduce this phase error to zero. This approach is very robust, well understood and has been widely used. However non-linearities in the standard photodetectors result in unwanted amplitude-to-phase (AM-PM) noise conversion [3] which limits the synchronisation between mode-locked laser systems and RF master oscillators. Laser-RF synchronisation on the order of several tens of femtoseconds would be acceptable for most applications,

however to resolve femtoseconds level dynamics with pump-probe experiments, such X-ray FEL pump-probes schemes, requires sub 10 femtoseconds synchronisation. Several approaches to resolve AM-PM noise conversion have been proposed in the literature [3].

To resolve limitations related to direct detection Laser-RF PLL, a Laser-RF PLL system was developed that is immune to AM-PM conversion noise and is able to compensate for the inherent system drift that results from using Mach Zehnder Modulators (Fig. 1). The method of Mach Zehnder Phase Detector Reverse Bias Detection (MZPD-RBD) (Fig. 2) developed in this paper follows the work of [4-6]. Here an emphasis was placed on developing a system that could be easily constructed within limited space, which used commercially available optical components and required a minimal number of free-space optical components.

Short term locking performance is achieved by imprinting the phase error information between mode-locked laser pulse train and radio-frequency wave as an amplitude modulation of the laser pulse train itself (at half the laser repetition rate) using a Mach Zehnder (Intensity) Modulator. The amplitude modulation is enabled by simultaneously applying an alternating bias signal to the MZM. The alternating bias signal flips the MZM total phase advance by π at rate of half laser repetition rate. At the output of the MZM the laser pulse train has the following pulse pattern,

$$I_n = 0.5 * I_0 [1 + (-1)^n \sin(\phi_{RF} \sin(\phi_e + \phi_b))] \quad (1)$$

where I_0 is the input laser pulse intensity, ϕ_e laser-RF phase error, bias drift term ϕ_b , and ϕ_{RF} is related to the electro-optic conversion efficiency of the MZM. Note the sign flip in equation (1) between each adjacent laser pulses from the MZM, this allows one to retrieve laser-RF ϕ_e phase error by simply subtracting the optical intensity (or heights) of adjacent optical pulses, assuming that the bias drift term ϕ_b is set to zero. In this paper Laser-RF phase error information is extracted using a fast photodetector and traditional RF frequency down-conversion techniques. The alternating bias signal is triggered by laser pulse train itself and is therefore intrinsically synchronous to the laser pulse train at a fixed rate of $f_{rep}/2$. This method is effectively immune to laser amplitude noise and AM-PM conversion noise. This technique is similar to that developed in [4, 5], the main advantages here are; interleaving the optical pulse train is not required for bias drift detection and each optical pulse we always 'see' the correct bias voltage regardless of relative phase.

PRESERVING BRIGHT ELECTRON BEAMS: DISTORTED CSR KICKS

A. Dixon^{*1}, University of Liverpool, Liverpool, United Kingdom
 S. Thorin, MAX IV Laboratory, Lund, Sweden
 P. H. Williams^{1,2}, ASTeC, Warrington, United Kingdom
 T. K. Charles¹, University of Liverpool, Liverpool, United Kingdom
¹ also at Cockcroft Institution, Warrington, United Kingdom
² also at STFC Daresbury Laboratory, Warrington, United Kingdom

Abstract

Short pulse, low emittance electron beams are necessary to drive bright FEL X-rays, for this reason it is important to preserve and limit emittance growth. The strong bunch compression required to achieve the short bunches, can lead to coherent synchrotron radiation (CSR)-induced emittance growth, and while there are some methods of CSR cancellation, these methods may be less effective when the CSR kicks are distorted. In an attempt to understand why CSR kicks become distorted, we compare the CSR kicks calculated using the whole beam parameters to the CSR kicks calculated using the longitudinally sliced beam parameters, when propagated to the end of the bunch compressor. We find that CSR kicks can become distorted when calculated with non-uniform slice beam parameters. While slice beam parameters that are uniform along the centre of the bunch, do not result in distorted CSR kicks.

INTRODUCTION

Free-electron lasers are a fourth generation light source which aim to provide bright, coherent light over a wide range of wavelengths [1]. The demand for research using FELs is driving demand for shorter pulse, brighter FEL X-rays. As such it is necessary for high quality electron bunches driving the FELs, which have small emittance and short bunch lengths.

Bunch compressors are used to compress the bunch longitudinally, however this can lead to unwanted collective effects such as coherent synchrotron radiation (CSR) [2–7] and microbunching instability (MBI) [8]. CSR causes kicks in the horizontal coordinates, which increases the projected emittance (as in Fig. 1). This projected emittance growth can be managed using CSR cancellation techniques, however these methods may be less effective if the CSR kicks become distorted [9]. In this paper we explore how CSR kicks could be distorted by considering how the slice Twiss parameters vary.

MAX-IV

MAX-IV facility located in Lund, Sweden, hosts 1.5 GeV and 3 GeV electron storage rings and the short pulse facility (SPF), all driven by the same linear accelerator. The laboratory provides a wide range of spectroscopy techniques for industry and research. In this study we focus on the existing

* sgadixon@liverpool.ac.uk

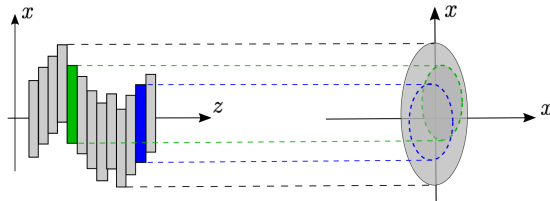


Figure 1: Horizontal slice offset leading to increased projected emittance [10].

short pulse facility (SPF) [11] and soft X-ray laser (SXL) [12], which is in the conceptual design phase [13]. The layout of the MAX-IV linac is shown in Fig. 2.

COHERENT SYNCHROTRON RADIATION

Synchrotron radiation is emitted by relativistic electrons when the bunch goes through a dipole. The electron bunch will radiate coherently when the bunch length is shorter than the radiation emitted and the following inequality is satisfied,

$$\lambda \geq 2\pi\sigma_z, \quad (1)$$

where σ_z is the bunch length and λ is the wavelength of synchrotron radiation.

Coherent synchrotron radiation leads to a redistribution of energy in the bunch due to some electrons reabsorbing emitted radiation. This effect can be approximated by the 1-D CSR wake as, excluding entrance and exit transient effects [14–17]. The 1-D CSR wake is defined as

$$\frac{dE}{cdt} = \frac{-2e^2}{4\pi\epsilon_0(3\rho^2)^{1/3}} \int_{\tilde{z}-s_L}^{\tilde{z}} \frac{df}{dz} \left(\frac{1}{\tilde{z}-z} \right)^{1/3} dz, \quad (2)$$

where ϵ_0 is the permittivity of free space, ρ is the bending radius of the dipole, $\frac{df}{dz}$ is differential of the linear charge density, \tilde{z} is the position within the bunch, and s_L is the slippage length.

CSR leads to projected emittance growth by causing longitudinal slices of the beam to become offset in the horizontal coordinates (see Fig. 1) [2–7]. The projected emittance growth can be mitigated by using CSR cancellation techniques, such as CSR kick matching [5, 18, 19] and optical balance [2, 3, 18–20].

Point-Kick Model

The point-kick model is an analytical method of evaluating the CSR kick from a dipole, by approximating the CSR

200 MV RECORD VOLTAGE OF vCM AND LCLS-II-HE CRYOMODULES PRODUCTION START AT FERMILAB*

T. Arkan†, J. Kaluzny, D. Bafia, D. Bice, J. Blowers, A. Cravatta, M. Checchin, B. Giaccone, C. Grimm, B. Hartsell, M. Martinello, T. Nicol, Y. Orlov, S. Posen, Fermilab, Batavia, USA

Abstract

The Linac Coherent Light Source (LCLS) is an X-ray science facility at SLAC National Accelerator Laboratory. The LCLS-II project (an upgrade to LCLS) is in the commissioning phase; the LCLS-II-HE (High Energy) project is another upgrade to the facility, enabling higher energy operation. An electron beam is accelerated using superconducting radio frequency (SRF) cavities built into cryomodules. It is planned to build 24 1.3 GHz standard cryomodules and one 1.3 GHz single-cavity Buncher Capture Cavity (BCC) cryomodule for the LCLS-II-HE project. Fourteen of these standard cryomodules and the BCC are planned to be assembled and tested at Fermilab. Procurements for standard cryomodule components are nearing completion. The first LCLS-II-HE cryomodule, referred to as the verification cryomodule (vCM) was assembled and tested at Fermilab. Fermilab has completed the assembly of the second cryomodule. This paper presents LCLS-II-HE cryomodule production status at Fermilab, emphasizing the changes done based on the successes, challenges, mitigations, and lessons learned from LCLS-II; validation of the changes with the excellent vCM results.

INTRODUCTION

LCLS-II-HE cryomodule (CM) production started at Fermilab with the assembly and testing of the verification cryomodule (vCM). Fermilab is responsible for the cryomodule design. The vCM design is the same as the LCLS-II CM; one major difference is that the superconducting radio frequency (SRF) cavities are treated with a new processing protocol for the required performance specifications.

With contributions from Fermilab, Jefferson Lab and SLAC, an R&D effort has been successfully completed to develop the new processing protocol and transfer the technology to industry. Ten fully dressed cavities were fabricated and processed with the newly developed treatment in industry, and successfully tested at Fermilab; performance exceeded the specification with average $Q_0=3.6e10$ and $E_{acc}=25.6$ MV/m (specifications are $Q_0=2.7e10$, $E_{acc}=21$ MV/m).

vCM was successfully tested at Fermilab with a 5-month test program and achieved an acceleration voltage of 200 MV in continuous wave mode, corresponding to an average accelerating gradient of 24.1 MV/m, significantly exceeding the specification of 173 MV. The average Q_0 (3.0×10^{10}) also exceeded its specification (2.7×10^{10}).

* Work supported by U.S. Department of Energy Offices of High Energy Physics and Basic Energy Sciences under Contracts No. DE-AC05-06OR23177 (Fermilab), No. DE-AC02-76F00515 (SLAC),
† email address: arkan@fnal.gov

After quench processing, no field emission was observed up to the maximum gradient of each cavity. At Fermilab, with this world record performance of vCM, we started the production of series cryomodules.

VCM ASSEMBLY AND TEST

vCM is assembled using eight of the best performing cavities fabricated with the new processing protocol. R&D to develop the new processing protocol, transfer the technology to industry, test and qualify the cavities processed with the new protocol is the first part of the equation to declare success. The second part is to assemble these cavities into the cryomodule and prove that the performance of the cavities can be preserved. vCM was assembled very soon after completing the last LCLS-II CM (keeping the momentum). Based on lessons learned from our successes and from unwanted outcomes of LCLS-II cryomodules production, some infrastructure upgrades were done and validated [1].

vCM cavity string was assembled (Fig. 1) in two months which is twice the duration of the LCLS-II production CM string assembly. We had to ensure that the new procedures, tooling, and infrastructure upgrades were fully understood and utilized by the team.



Figure 1: vCM cavity string assembly.

A few of the changes done to the cavity string assembly:

- Beamline slow vacuum pumping & nitrogen gas backfill / purge systems upgrades
- Leave beamline under active vacuum during CM assembly, pumping with NEG/ion pump
- Eliminate fundamental power cold coupler (FPC) assembly workstation in the cleanroom and combine the cavity interconnect bellows and cold end FPC assembly into one workstation. This is mainly

3 YEARS OF OPERATION OF THE SPIRAL2 SC LINAC - RF FEEDBACK

M. Di Giacomo[†], M. Aburas, P-E. Bernaudin, O. Delahaye, A. Ghribi, J-M. Lagniel, J-F. Leyge, G. Normand, A.K. Orduz, F. Pillon, L. Valentin, A. Dubosq, GANIL, Caen, France
 F. Bouly, LPSC, Université Grenoble-Alpes, CNRS/IN2P3, Grenoble, France
 S. Sube, CEA-DRF-IRFU, Saclay, France

Abstract

The superconducting LINAC of SPIRAL2 at the GANIL facility has been in operation since October 2019. The accelerator uses 12 low beta and 14 high beta superconducting quarter wave cavities, cooled at 4°K, working at 88 MHz. The cavities are operated at a nominal gradient of 6.5 MV/m and are independently powered by a LLRF and a solid-state amplifier, protected by a circulator. Proton and deuteron beam currents can reach 5 mA and beam loading perturbation is particularly strong on the first cavities, as they are operated at field levels much lower than the nominal one.

This paper presents a feedback after three years of operation, focuses on the RF issues, describing problems and required improvement on the low level, control and power systems.

RF SYSTEM DESCRIPTION

The SPIRAL2 accelerator [1] uses independently phased RF cavities, operated at 88.0525 MHz, to accelerate a multitude of ion beams within wide intensity and energy ranges (up to 5 mA and from 0.75 to 20 MeV/A).

Table 1: Main cavity parameters @ opt beta

| Parameter | $\beta = 7\%$ | $\beta = 12\%$ |
|-----------------------|------------------|------------------|
| Eacc (MV/m) | 6.5 | 6.5 |
| Field integral (MV) | 1.56 | 2.66 |
| 5mA beam loading (kW) | 7 | 12 |
| Qext | $5.5 \cdot 10^5$ | $1.1 \cdot 10^6$ |

The SC LINAC cavities [2] are quarter wave resonators (QWR), hosted in two families of cryomodules (CM). The 12 low beta ones host one QWR each, while the high beta CMs host a couple of QWR each. Table 1 gives the main parameters for both type of cavities.

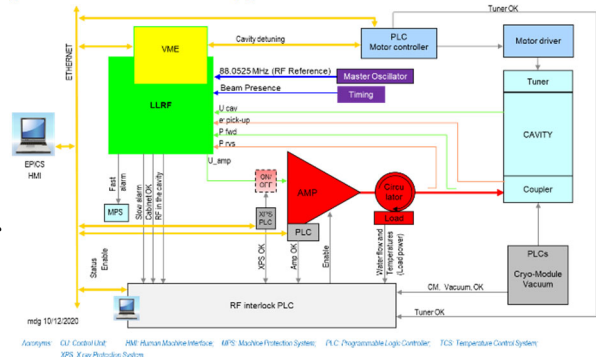


Figure 1: SC cavity RF system block diagram.

[†] digiacomo@ganil.fr

Each cavity has its own RF system equipped with digital LLRF, solid state amplifier (SSA) and circulator as shown in Fig. 1.

Reference and timing signals are provided by two sub-systems: the master oscillator (MO) with its distribution line and the timing electronics (ECSF in the picture). The circulators are installed out of the LINAC tunnel but as near as possible to the cavities, and each system has two sections of transmission lines: TL1 and TL2, the second being designed to withstand strong mismatched conditions (high VSWR).

Commissioning of the first beams took the first three years of operation, and showed several issues that had not arisen during the RF equipment commissioning or that had been insufficiently addressed during the design phase.

CALIBRATIONS

Calibration of the accelerating field amplitudes (Eacc) and of the external Q factors (Qext) was one of the first tasks to check whether it would have been possible to accelerate all ion species at nominal current and energy. That was particularly important for the first low beta cavities, which are used at much lower fields and are driven by 2.5 kW (cavity 1 to 6) and 5 kW (7 to 9) amplifiers (with respect to 10 kW for the last ones and to 19 kW for the high beta cavities).

Eacc

Cavity probes and LLRF acquisition channels had been characterised on the test benches while cables and attenuators had been measured in situ, after installation. Nevertheless, during the acceleration of the first beams showed that most of the cavity fields were over-estimated (see Fig. 2).

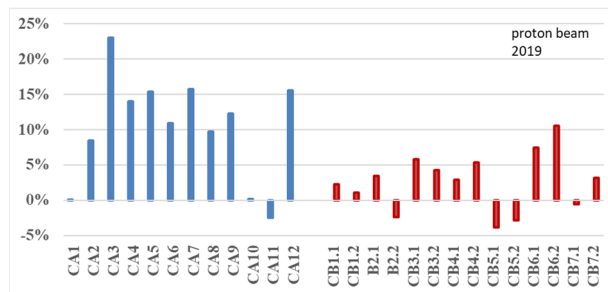


Figure 2: field error before calibration.

The accelerating fields were then calibrated looking at the effect of the first proton beam on each single cavity. Smaller corrections have followed, while accelerating various beam species and improving the measurement methods.

Content from this work may be used under the terms of the CC BY 4.0 licence (© 2021). Any distribution of this work must maintain attribution to the author(s), title of the work, publisher, and DOI

UNILAC HEAVY ION BEAM OPERATION AT FAIR INTENSITIES

W. Barth^{1,2,†}, M. Miski-Oglu¹, U. Scheeler, H. Vormann, M. Vossberg, S. Yarymyshev¹
 GSI Helmholtzzentrum für Schwerionenforschung, Darmstadt, Germany

¹ also at Helmholtz Institute Mainz, Germany

² also at Johannes Gutenberg-Universität Mainz, Mainz, Germany

Abstract

The GSI-UNILAC as well as the heavy ion synchrotron SIS18 will serve as a high current heavy ion injector for the FAIR synchrotron SIS100. In the context of an advanced machine investigation program acceleration and transport of space charge dominated argon beam inside entire UNILAC have been explored. The conducted high current argon beam measurements throughout the UNILAC-poststripper and transferline to SIS18 show a transversal emittance growth of only 35% for the design current of 7 emA (⁴⁰Ar¹⁰⁺). By horizontal collimation of the UNILAC beam emittance, the space charge limit could be reached at slightly lower pulse currents, but accordingly longer injection times. Further improvements in brilliance can be expected from the planned upgrade measures, in particular on the high-current injector linac.

INTRODUCTION

Besides two ion source terminals and a low energy beam transport system (LEBT) the High Current Injector (HSI) of the UNILAC (Fig. 1) comprises a 36 MHz IH-RFQ (2.2 keV/u up to 120 keV/u) and an IH-DTL with two separate tanks, accelerating the beam up to the final HSI-energy of 1.4 MeV/u. After stripping and charge state separation the Alvarez DTL provides for beam acceleration up to $\beta = 0.155$. In the transfer line (TK) to the synchrotron SIS18 a foil stripper and another charge state separator system can be used. In order to provide the highest heavy ion beam currents (15 emA, U²⁸⁺), as required for FAIR, the HSI must deliver up to $2.8 \cdot 10^{12}$ U⁴⁺ ions per pulse [1-12].

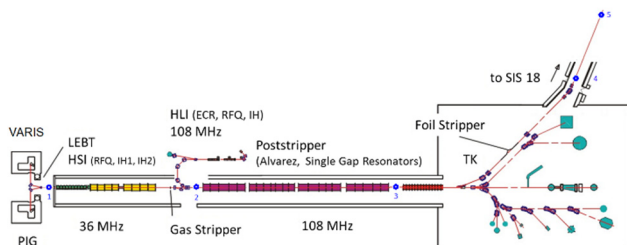


Figure 1: GSI-UNiversal Linear ACcelerator (UNILAC); the slit-grid-emittance measuring devices are shown in blue; 1: LEBT/UH1, 2: gas stripper section/US4, 3: poststripper/UA4, 4: transfer line/TK5, 5: transfer line/TK8.

The positions of the emittance meters (slit-grid devices) used for the measurements presented in this paper are also shown in Fig. 1. With the AC beam transformers installed behind each accelerator cavity and along all transport

† email address: w.barth@gsi.de

routes, the beam transmission in all sections can be permanently monitored and measured with high precision.

Highly charged heavy ion beams with high average intensities (but low pulse intensities), from an ECR ion source of CAPRICE-type are accelerated in the High Charge State Injector (HLI) to 1.4 MeV/u. The HLI as well as the HSI serve in a time sharing mode for the Alvarez DTL. The FAIR proton linac has to provide the high intensity primary proton beam for the production of antiprotons. It will deliver a 70 MeV beam to the SIS18 with a repetition rate of 4 Hz. The proton linac will be located north of the existing UNILAC complex.

HEAVY ION BEAMS AT THE SPACE CHARGE LIMIT

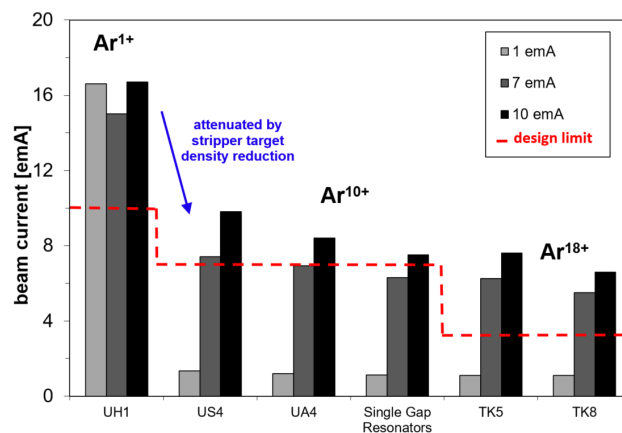


Figure 2: Argon beam variation beyond UNILAC design limitations.

For medium heavy ions beams (⁴⁰Ar¹⁰⁺) the HSI-intensity level behind gas stripper exceeds the space charge limit of 7 emA specified for SIS18. This enables to investigate acceleration and transport for space charge dominated beams inside entire UNILAC and transfer line to the SIS18. As depicted in Fig. 2, for further high intensity measurements the stripper gas density was chosen such that the desired Ar¹⁰⁺ current of 7 emA was achieved after optimization of the poststripper and TK. Also for highly charged ions (Ar¹⁸⁺), stripping with a suitable carbon foil (400 μg/cm²) allows to reach intensities that enable to fill the SIS18 up to the so-called space charge limit. The design current limit given in Fig. 2 (dashed line in red) is based on the FAIR requirements or the space charge limit achievable by multiturn injection of the high current beam from UNILAC into the SIS18.

Intensity variation at UNILAC is achieved by varying the gas stripper target density, which allows the particle

RF COMMISSIONING OF THE FIRST-OF-SERIES CAVITY SECTION OF THE ALVAREZ 2.0 AT GSI

M. Heilmann*, L. Groening, C. Herr, M. Hörr, S. Mickat, B. Schlitt, G. Schreiber
 GSI Helmholtz Centre for Heavy Ion Research, 64291 Darmstadt, Germany

Abstract

The existing post-stripper Drift Tube Linac (DTL) of the GSI UNILAC will be replaced with the new Alvarez 2.0 DTL to serve as the injector chain for the Facility for Antiproton and Ion Research (FAIR). The 108.4 MHz Alvarez 2.0 DTL with a total length of 55 meters has an input energy of 1.36 MeV/u and the output energy is 11.32 MeV/u. The presented First-of-Series (FoS) cavity section with 11 drift tubes and a total length of 1.9 m was planned as the first part of the first cavity of the Alvarez 2.0 DTL. After copper plating and assembly of the FoS-cavity the RF-conditioning started in July 2021. These contribution gives an overview on the results of the successful RF-conditioning to reach the necessary gap voltage for uranium operation including a comfortable safety margin.

INTRODUCTION

The UNiversal Linear ACcelerator UNILAC (Fig. 1) at GSI (Helmholtzzentrum für Schwerionenforschung, Darmstadt, Germany) will serve as main operation injector for the Facility for Antiproton and Ion Research FAIR (Fig. 2 and [1, 2]). The UNILAC is able to deliver ion beams (protons [3] up to uranium) for different experiments in parallel (pulse-to-pulse switch mode) with individual ion species and energies. For the upcoming FAIR project an update of the UNILAC in terms of high beam intensities, quality, and high availability is required. The construction of a completely new Alvarez-DTL 2.0 will fulfill these requirements with new beam dynamics [4]. Additionally, an increased shunt impedance per surface field on the drift tubes [5] is essential for the new RF-design (Table 1) [6]. The First-of-Series (FoS) Alvarez-Cavity was planned as the first section of the first tank of the new Alvarez 2.0 and was used for extensive prototyping. The RF-design study with CST-simulations [7] of the FoS-Cavity [8, 9] was verified with a scaled model [10–12] and the mechanical cavity design [13] ended with successful LLRF-measurements of the copper plated FoS-cavity [14].

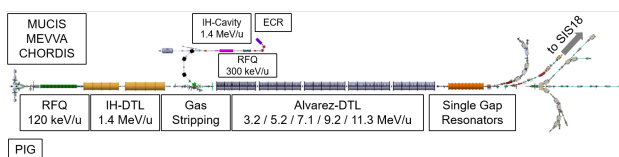


Figure 1: Schematic overview of the upgraded GSI UNILAC with five individual Alvarez-type post-stripper DTLs.

* m.heilmann@gsi.de

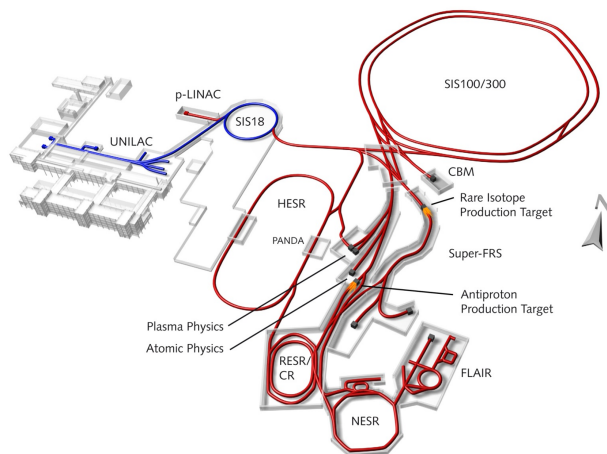


Figure 2: Schematic overview of the current GSI (blue) and the new FAIR complex in the complete expansion stage (red).

Table 1: Parameters for the Upgraded UNILAC

| Parameter | Unit | Value |
|------------------------------|---------------|-------------------|
| RF-frequency | MHz | 108.408 |
| A/q | | ≤ 8.5 |
| Max. Current | mA | $1.76 \times A/q$ |
| Synchronous phase | deg. | -30 / -25 |
| Input beam energy | MeV/u | 1.358 |
| Output energy | MeV/u | 3.0 – 11.3 |
| Hor. emittance (norm., tot.) | μm | ≤ 0.8 |
| Ver. emittance (norm., tot.) | μm | ≤ 2.5 |
| Beam pulse length | ms | ≤ 1.0 |
| Beam repetition rate | Hz | ≤ 10 |
| Alvarez-cavities | # | 5 |
| Drift tubes / cavity | # | 25 – 52 |
| Drift tube length | mm | 109.9 – 327.0 |
| Drift tube diameter | mm | 180 – 190.3 |
| Aperture diameter | mm | 30 / 35 |

FOS ALVAREZ CAVITY SECTION

The First-of-Series cavity (Table 2) [15] is the first tank section of the Alvarez 2.0-DTL (Fig. 3). The empty drift tubes were fabricated internally at the GSI workshop for a cost-effective high power RF-test campaign. After copper-plating of all components [14], time-consuming mounting, and challenging adjustment of the drift tubes including media supply had to be carried out in preparation for the RF-test.

HIGH INTENSITY HEAVY ION BEAM OPTIMIZATION AT GSI UNILAC

H. Vormann^{1,*}, W. Barth^{1,2,3}, M. Miski-Oglu^{1,2}, U. Scheeler¹, M. Vossberg¹, S. Yaramyshev¹

¹ GSI Helmholtz Centre for Heavy Ion Research, 64291 Darmstadt, Germany

² HIM Helmholtz Institute Mainz, 55099 Mainz, Germany

³ KPH Johannes Gutenberg University Mainz, 55128 Mainz, Germany

Abstract

In order to improve the UNILAC performance for the upcoming use as heavy ion injector for the FAIR accelerator chain, dedicated beam investigations have been carried out. In particular measurements with Bismuth and Uranium beam require the maximum accelerating voltage of rf cavities, power of rf transmitters and exciting current of magnet power converters. After four years without regular Uranium high current beam operation (2017-2020), recently the UNILAC has been operated again with full performance. Several upgrade measures will improve the UNILAC capability. In combination with the prototype pulsed hydrogen gas stripper, beam intensities close to the FAIR requirements are achievable.

INTRODUCTION

The UNILAC is designed as a universal linear accelerator for all ion types of different mass from protons to uranium. The UNILAC consists of different ion source terminals, the High Current Injector HSI with the adjacent stripping section, the poststripper, a chain of ten single gap resonators and the transfer channel to SIS18 (Fig. 1).

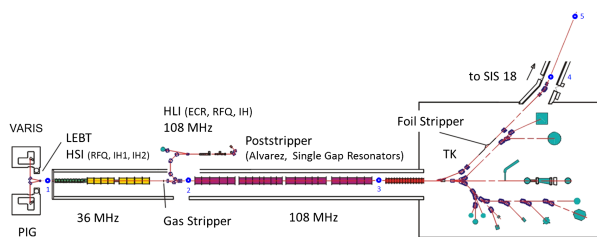


Figure 1: Overview of the GSI Universal Linear Accelerator (UNILAC) [1]; numbered blue dots mark positions of installed emittance measurement devices.

In the HSI ion beams are accelerated from 2.2 keV/u to 1.4 MeV/u with an RFQ and two IH-DTL-tanks. The poststripper contains five Alvarez tanks and ten single gap resonator cavities. Its nominal output beam energy is 11.4 MeV/u. Lower energy steps can be chosen by individually turning off Alvarez cavities, fine tuning is accomplished with the single gap resonator chain.

High current Uranium beam machine experiments were carried out in 2015 and 2016 for the last time before a four year break. At this time only three of the five Alvarez DTL post stripper tanks were available, due to upgrade and maintenance work at the RF-amplifier systems. For this the achiev-

* h.vormann@gsi.de

able high current beam brilliance at injection into the heavy ion synchrotron SIS18 could be estimated only on the base of front-to-end high-current measurements with proton beam performed in 2014 [1–14].

HEAVY ION BEAM INVESTIGATIONS

In 2021 and 2022 measurement campaigns have been conducted with high intensity heavy ion beams (Uranium, Bismuth, Tantalum, Xenon) and with medium and light ion beams (Argon, p⁺). Bismuth and Uranium beams have been utilised for an advanced optimization campaign along entire UNILAC (described in this report), while an Argon beam has been used to test space charge dominated beam operation [15].

HSI-RFQ- and the superlens-operation (SL) were suffering from performance restrictions, nevertheless since heavy ion beam operation is again possible the U²⁸⁺ beam performance at the end of the transfer channel could be significantly improved.

HSI RFQ and Superlens Optimization

After a beam line modification during shutdown 2017, the RF performance of the HSI-RFQ was strongly degraded (while RFQ kept under atmosphere conditions for almost one year). During recommissioning in 2018 only 70% of the nominal RF-voltage could be reached. As the the copper surfaces were degraded, new electrodes (rods) have been installed (2019). After recommissioning with light ions and U⁵⁺, the working point of the HSI-RFQ has been re-defined: With a medium heavy ion beam (Ar²⁺ and Ar¹⁺), the beam transmission through the HSI has been scanned in a wide range from voltages far below the working point to high voltages well above. The result was a surprisingly long plateau of almost full transmission and sufficient beam performance. The working point was sufficiently re-defined at an RF voltage closely above the kink point to the plateau. This was confirmed by measurements with Uranium (A/Z = 59.5), and also with ion beams of an even higher mass-over-charge ratio: ¹⁸¹Ta³⁺ (A/Z = 60.3) and ¹²⁴Xe²⁺ (A/Z = 62) [16].

The superlens suffered from short breakdowns during beam operation at high RF voltages, probably when the SL electrodes were hit by the ion beam. In order to avoid further breakdowns, the beam was partly collimated in the LEPT right before RFQ-injection. Additionally an RF high power coupler with an enlarged loop surface was mounted. However, this only slightly improved the HF performance, so that the SL rods will be exchanged in the next shutdown.

PREPARATION FOR COMMISSIONING WITH BEAM OF THE ADVANCED DEMONSTRATOR MODULE WITH HEAVY ION BEAM

M. Miski-Oglu^{1,2*}, W. Barth^{1,2,3}, M. Basten², C. Burandt^{1,2}, F. Dziuba^{1,2,3},
 V. Gettmann^{1,2}, T. Kuerzeder^{1,2}, J. List^{1,2,3}, S. Lauber^{1,2,3}, H. Podlech⁴, M. Schwarz⁴, S. Yaramyshev²
¹Helmholtz Institute Mainz, Mainz, Germany
²GSI Helmholtzzentrum für Schwerionenforschung
³KPH, Johannes Gutenberg-University, Mainz, Germany
⁴IAP Goethe-Universität Frankfurt, Frankfurt, Germany

Abstract

The integration of the accelerator components in to the cryogenic module prototype (Advanced Demonstrator) is a major milestone of the R&D for the superconducting heavy ion continuous wave linear accelerator **HELMholtz LI**near **AC**celerator (HELIAC) at GSI. The HELIAC is a joint project of Helmholtz Institute Mainz (HIM) and GSI developed in collaboration with IAP Goethe University Frankfurt. This module is equipped with three superconducting (sc) Cross bar **H**-mode (CH) acceleration cavities CH0-CH2 and a sc rebuncher cavity, as well as two sc solenoids. The commissioning of the cryogenic module with Argon beam at GSI is scheduled for August 2023. In preparation for the beam test activities, the beam line, which connects the High Charge State Injector (HLI) with the testing area, has been installed. The beamline comprises a pair of phase probes for **Time Of Flight** (TOF) measurement of the incoming beam energy, quadrupole lenses and a 4-gap RF-buncher cavity. The beam diagnostics bench behind the cryo module is equipped with phase probe pairs, a slit grid device, a **Bunch Shape Monitor** (BSM Feshenko monitor) for measurements of the longitudinal beam profile. The bench allows complete 6 d characterization of the ion beam.

INTRODUCTION

The design and construction of continuous wave (cw) high intensity Linacs is a crucial goal of worldwide accelerator technology development [1]. In the low- and medium-energy range, cw-Linacs can be used for several applications and user experiments, as Accelerator Driven subcritical nuclear reactor Systems (ADS) [2, 3], synthesis of Super Heavy Elements (SHE) [4] and material science. In particular the increased projectile intensity, preferably in cw mode, would remarkably improve the SHE yield. The need for compactness and energy efficiency of such cw facilities requires the use of superconducting (sc) technology in modern high intensity ion linacs [5–9]. For this purpose the heavy ion superconducting (sc) cw linear accelerator HELIAC is developed at GSI Helmholtzzentrum für Schwerionenforschung at Darmstadt and Helmholtz Institute Mainz (HIM)[10, 11] under key support of Institut für Angewandte Physik (IAP) of Goethe University Frankfurt (GUF) [12, 13].

* m.miskioглу@gsi.de

Table 1: General Characteristics of the HELIAC Accelerator

| Property | Value |
|----------------------------|--------------------------------------------|
| Frequency | 108.408 MHz (216.816 MHz ¹) |
| Mass-to-charge ratio | ≤ 6 |
| Repetition rate | Continuous wave |
| Beam current | ≤ 1 mA |
| Output energy | 3.5 MeV/u to 7.3 MeV/u |
| Injector energy | 1.4 MeV/u |
| Normal conducting cavities | 5 |
| Superconducting cavities | 12 |

¹ SC CH cavities operate at the second harmonic

Table 1 shows the key parameters of the HELIAC. Heavy ion beams with a mass-to-charge ratio up to $A/z = 6$ will be accelerated by twelve multi-gap CH cavities, operated at 216.816 MHz. The HELIAC should serve for physics experiments, smoothly varying the output particle energy from 3.5 to 7.3 MeV/u and simultaneously preserving high beam quality [14].

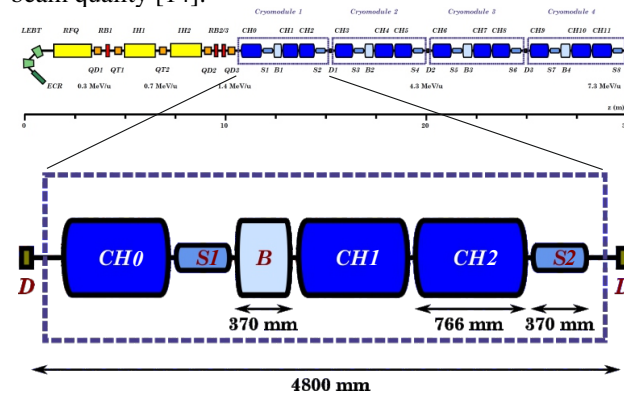


Figure 1: Layout of the HELIAC (top) and of the first cryogenic module i.e. "Advanced Demonstrator" (bottom).

Figure 1 shows the schematic layout of HELIAC, it comprising of ECR source, warm injector LINAC [15, 16] and four cryogenic modules [17].

Following the successful beam test of the first cavity cavity (CH0) within the Demonstrator [6, 10, 18] research project, the next step towards realization of HELIAC is the development, manufacturing and operation of the first cryogenic module (CM1) within the "Advanced Demonstrator" project [18]. As shown in Fig. 1 it contains the demonstrator cav-

Q DROP TENDENCY OF HALF-WAVE RESONATOR CAVITY*

Yoochul Jung[†], Heetae Kim, Hyunik Kim, Hyojae Jang, Juwan Kim

Institute for Basic Science, Daejeon, Republic of Korea

Sungmin Jeon¹, Kyungpook National University, Daegu, Republic of Korea

Abstract

Half-wave resonator superconducting cavities (HWRs) have been fabricated and tested. HWRs have been installed in the low energy section of the LINAC and being ready to be cooled down for the next step. All HWR cavities have been completely tested in two ways: vertical test and horizontal test. For the vertical test, HWRs were tested both at 4.2 K and 2.1 K cryogenic surroundings although the operating temperature is 2.1 K. Good cavity having higher quality factor than that of the target value showed the Q_0 drop tendency of 2.1 K was very similar to that of 4.2 K. However, in many cases, Q_0 drop tendency of 2.1 K was not similar with 4.2 K, rather Q_0 decreased more rapidly than 4.2 K which means the surface resistance of the cavity rapidly increased at 2 K surrounding. In this study, we will report that various Q_0 results of HWRs and discuss their Q_0 drop tendencies as a function of temperature, 2.1 K and 4.2 K along with field emission.

INTRODUCTION

One of factors determining the performance of the cavity is a quality factor, Q_0 . The quality factor decreases as electric field increases due to the increase of the surface resistance. The surface resistance consists of temperature dependent term (R_{BCS}) and temperature independent term (R_{res}). The residual resistance, R_{res} , originates from the material itself such as a lattice structure, impurities and grain boundaries. On the contrary, the BCS resistance, R_{BCS} , coming from how much the material depends on the temperature, increases with temperature [1].

In addition to temperature effect on the cavity, a field emission, detected as x-ray radiation, is also a critical factor for limiting the cavity performance. Field emission current causes x-ray radiation known as Bremsstrahlung radiation [2]. With the existence of a proper field emission tip, the field emission current starts to flow at or above a specific electric field. Consequently, x-ray radiation starts to turn on at or above this electric field. The intensity of field emission current and the turn-on electric field depends on the size and the curvature of the tip. And the x-ray radiation increases as electric field increases similar to the field emission current.

At cryogenic temperature, a cavity must be conditioned with a proper range of the electric field in order to achieve the target applied electric field (E_{acc}) in the cavity. Technically, the cavity conditioning consists of two different purposes.

One is "RF surface conditioning", which means cleans RF surface of the cavity to apply RF power effectively by removing the gases from the cavity surface such as H_2O and other gases. This process takes a few hours depending on the states of the cavity, and the low temperature baking is well known method to cut down conditioning time dramatically [3]. The other is "field emission conditioning", which means removes (lowers) field emission (x-ray radiation) with proper RF power. This conditioning process is to remove field emission tip itself or smoothen the tip. The RF power can be applied either as a pulse mode or a continuous mode depending on the intensity of x-ray radiation. This process must be carefully carried out at high gradient because a long time RF exposure to the cavity surface can degrade the cavity performance severely by damaging cavity surface such as creating craters, thus the RF mode and conditioning time must be carefully chosen in this case [2].

VERTICAL TEST

Similar to a quarter wave resonator cavity (QWR) in RISP, HWR cavity showed a very similar Q_0 drop tendency, which means Q_0 decreased linearly with E_{acc} as long as no x-ray radiation observed, while Q_0 decreased dramatically after the onset of x-ray radiation. Figs. 1–3 show the typical three types of test results. For the HWR vertical test, the field emission conditioning was carried out in 2K while the RF surface conditioning was performed at 4K because HWR cavity operates at 2K and the RF power is more effectively applied at 2K due to the less surface resistance of the cavity.

RF Surface Conditioning

When the cavity reaches 4K, the input RF power is set 1 Watt and check out the pickup signal monitored through both a power meter and a spectrum analyser. The input RF power is controlled in order to increase the pickup signal of the cavity very slowly. This process ends when E_{acc} in the cavity reaches target E_{acc} , 6.6 MV/m, or a moderate amount of x-ray radiation begins, for example, 50 ~ 100 μ Sv/h in RISP test facility.

Field Emission Conditioning

The HWR cavity is cooled down to 2K cryogenic temperature for measuring quality factor. Increase input RF power CW/pulse mode to remove (lower) x-ray radiation while checking out E_{acc} of x-ray turn-on and the vacuum pressure in the cavity. It is good evidence to observe the change of x-ray turn-on and vacuum pressure because not only turn-on E_{acc} increases but the sharp vacuum peak appears when the field emission tip is removed or smoothened. Depending on the size and geometry of the field emission tip. The effect of

* This work was supported by the Rare Isotope Science Project of Institute for Basic Science funded by Ministry of Science and ICT and NRF of Korea 2013M7A1A1075764.

[†] email address: sulsiin@ibs.re.kr

RF BEAM SWEEPER FOR PURIFYING IN-FLIGHT PRODUCED RARE ISOTOPE BEAMS AT ATLAS FACILITY*

A.C. Araujo Martinez, R. Agustsson, S.V. Kutsaev[†], J. Peña Gonzalez, A.Y. Smirnov
 RadiaBeam Technologies, LLC, Santa Monica, CA, USA
 B. Mustapha, Argonne National Laboratory, Lemont, IL, USA

Abstract

RadiaBeam is developing an RF beam sweeper for purifying in-flight produced rare isotope beams at the ATLAS facility of Argonne National Laboratory. The device will operate in two frequency regimes – 6 MHz and 12 MHz – each providing a 150 kV deflecting voltage, which doubles the capabilities of the existing ATLAS sweeper. In this paper, we present the design of a high-voltage RF sweeper and discuss the electromagnetic, beam dynamics, and solid-state power source for this device.

INTRODUCTION

The Argonne Tandem Linac Accelerator System (ATLAS) is the national user facility, providing stable and radioactive low-energy heavy ion beams. The latter have supported multiple astrophysics experiments for about two decades [1]. One way of producing Radioactive Ion Beams (RIB) at ATLAS is the in-flight method, providing access to more than 100 short-lived isotopes in the mass range up to $A \sim 60$ [2]. During this process, the primary beam traverses the production target. Its energy is degraded, and the beam acquires a long low-energy tail from the multiple-scattering processes in the target material. These tails can easily dominate the low-intensity RIB beams of interest.

To handle the large divergence and energy spread of the in-flight produced beam, an in-flight radioactive beam separator (AIRIS) was recently commissioned to enhance the radioactive beam capabilities of the ATLAS facility [3]. This system, shown in Fig. 1 (top), consists of a production target placed at the end of ATLAS followed by a two-step ion separator. The first step is a magnetic achromat while the second consists of an RF sweeper or chopper [4,5].

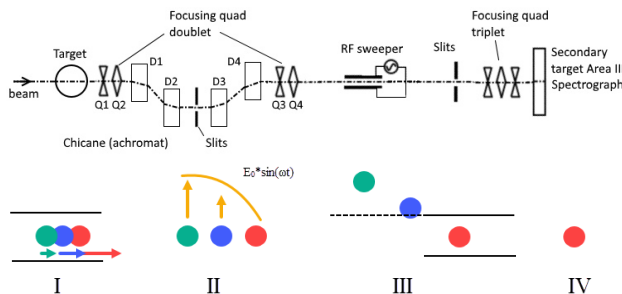


Figure 1: Layout of the ATLAS in-flight RIB facility (top) and the scheme of rare isotope RF separation (bottom).

The RF sweeper provides contaminant beam reduction through velocity differences: a time difference eventually develops between the two beam components due to the velocity difference and results in a varying deflection in the time-dependent electric deflecting field (see Fig. 1) [6]. For many cases of interest at ATLAS, the currently existing sweeper, operating at an ATLAS sub-harmonic of 6 MHz with a maximum voltage of 55 kV, was sufficient for a clean separation with 1-meter-long sweeper plates and a 10 cm gap. However, there are still many other beams that require at least twice as high voltage.

One class of experiments that could benefit from a higher-voltage separator would be those beams produced in fusion evaporation, such as the $(^3\text{He}, n)$ reaction used for production of ^{22}Mg from ^{20}Ne and ^{44}Ti from ^{42}Ca . These beams are also wanted at low energy (< 5 MeV/u). Another class of experiments could be the beams that are created with (d, p) for $A > 30$. Here, the issue is the primary beam charge states, so, it would be helpful to have a larger kick of these beams, which are typically requested at more like 10 MeV/u, as the fully stripped primary beam is close in energy to the beam of interest. For lower energy beams ~ 5 MeV/u, 6 MHz would be better because of the flight time. Hence a new RF sweeper design that includes 12 MHz high voltage for fast beams > 10 MeV/u, and 6 MHz with moderately high voltage for low energy beams ~ 5 MeV/u is needed.

In order to enable these experiments, RadiaBeam is developing the RF sweeper capable to operate at both 6 MHz and 12 MHz frequencies with about triple the voltage of the existing ATLAS sweeper. We have completely revised the electrical and engineering design of the original sweeper to allow operation at 150 kV.

In this paper, we present the electromagnetic design of the high voltage RF sweeper, beam dynamics, the conceptual engineering design, and the design of the solid-state RF power supply to feed the system.

ELECTROMAGNETIC DESIGN

We designed a structure capable to operate at both 6 MHz and 12 MHz frequency. The maximum operation voltage in both regimes is up to 150 kV. The design relies on the idea of establishing resonance between the capacitor (electrodes) and variable inductance (coil). We decided to use a sliding contact (switch) that electrically divides two coils in series. Figure 2 shows the circuit diagram of the device and its 3D model in CST Microwave Studio.

The operation principle of the sliding switch is the following: the switch is disconnected to enable the 6 MHz mode in which the two coils are in series, and when the

* This work was supported by the U.S. Department of Energy, Office of Nuclear Physics, under SBIR grant DE-SC0019719.

[†] kutsaev@radiabeam.com

HIGH-GRADIENT ACCELERATING STRUCTURE FOR HADRON THERAPY LINAC, OPERATING AT kHz REPETITION RATES*

A.C. Araujo Martinez, R. Agustsson, S.V. Kutsaev[†], A.Y. Smirnov, S.U. Thielk
RadiaBeam Technologies, LLC, Santa Monica, CA, USA
B. Mustapha, G. Ye, Argonne National Laboratory, Lemont, IL, USA
V.A. Dolgashev, SLAC National Accelerator Laboratory, Menlo Park, CA, USA

Abstract

Argonne National Laboratory and RadiaBeam have designed the Advanced Compact Carbon Ion Linac (ACCIL) for the acceleration of carbon and proton beams up to the energies of 450 MeV/u, required for image-guided hadron therapy. Recently, this project has been enhanced with the capability of fast tumour tracking and treatment through the 4D spot scanning technique. Such solution offers a promising approach to simultaneously reduce the cost and improve the quality of the treatment. In this paper, we report the design of an accelerating structure, capable of operating up to 1000 pulses per second. The linac utilizes an RF pulse compressor for use with commercially available klystrons, which will dramatically reduce the price of the system.

INTRODUCTION

Radiation therapy with X-ray, electron and hadron beams, is used to treat over 60% of cancer patients. Compared to X-ray therapy, which is currently the standard treatment method, hadron therapy offers significant advantages, such as a sharp Bragg peak and the capability to treat “radioresistant” tumours [1]. Unless the position of the tumour and treated organs are accurately known both before and during the treatment, and the therapy system can track the motion of the patient’s organs, the small beam spot benefit of ion therapy may not be realized. However, by combining ion beam therapy with real-time image guidance and fast transverse and longitudinal (i.e. beam energy variation) scanning is potential game changer in the future of cancer radiation therapy [2].

Argonne National Laboratory, in collaboration with RadiBeam Technologies has been working on the development of the Advanced Compact Carbon Ion Linac (ACCIL), an ultra-high gradient linear accelerator for cancer therapy capable of delivering the full energy range from ion source to 450 MeV/u for $^{12}\text{C}^{6+}$ and protons [3]. The latter can also be used for imaging. However, its design must be adjusted for the pulse repetition and the beam energy variation rates up to a thousand per second (~ 1000 Hz). Such flexibility in beam tuning will enable the fast and efficient beam scanning and 3D dose painting, as well as real-time image-guided range calculation and targeting of

moving targets, while reducing the treatment time to several minutes [4].

One of the key technical challenges of the ACCIL system is the need for a high gradient accelerating structure to limit the footprint to ~ 45 m and improve the overall efficiency of the linac [5]. In ACCIL the high-gradient section starts from the energy of 45 MeV/u ($\beta=0.3$), allowing to replace ~ 3 meters of low-frequency DTLs with a 30 cm long S-band structure, operating at 50 MV/m gradient. In order to achieve such high gradients at so low velocity, the beam is accelerated by the negative -1^{st} harmonic. Such negative harmonic accelerating structure (NHS), consisting of 15 magnetically coupled cells [6], was build and tested at ANL. The structure was conditioned up to 33-MW peak power, corresponding to 50 MV/m gradient with RF breakdown rate of 1 per 1000 pulses [7].

In this paper we will discuss the improvements made to this structure design to enable its operation at 1 kHz repetition rates. The second challenge to be addressed is the requirement for the RF power system. With the current prototype, up to 33 MW of RF power is required for each accelerating section. At 1 kHz repetition rate, this would require the development of a custom klystron and modulator system. Instead, we have designed the accelerating structure for operation with standard medical klystrons (~ 5 -MW, up to 1% duty cycle) that are available at reasonable costs. Such breakthrough improvement was enabled by relaxing the peak gradient from 50 MV/m to 40 MV/m reducing a peak power requirement to 20 MW. Thanks to short 300 ns beam pulses such peak power can be achieved by utilizing an RF pulse compressor (SLED) [8].

RF DESIGN

The goals of the upgraded negative harmonic structure (NHS) design are to reduce peak power requirements from 34 MW to 20 MW and reduced the filling time to 300 ns to be used with SLED. This was achieved by reducing the accelerating gradient to 40 MV/m, improving the shunt impedance (R_{sh}), and adjusting the group velocity of the structure.

In order to improve its shunt impedance, we modified the cell design of the previous NHS [9]. We reduced the gap between the noses, adjusted the nose shape, and increased the blending radius of the outer wall (Fig. 1). These modifications allowed to increase the shunt impedance from 32 $\text{M}\Omega/\text{m}$ up to 47 $\text{M}\Omega/\text{m}$ while maintaining the peak fields below 180 MV/m at 40 MV/m. The number of coupling holes was reduced from eight to five, and the

* This work was supported by the U.S. Department of Energy, Office of High Energy Physics, under STTR grant DE-SC0015717 and Accelerator Stewardship Grant, Proposal No. 0000219678.

[†] kutsaev@radiabeam.com

HIGH-BRIGHTNESS RFQ INJECTOR FOR LANSCE MULTI-BEAM OPERATION*

Y.K. Batygin[†], D.A. Dimitrov, I.N. Draganic, D.V. Gorelov, E. Henestroza, S.S. Kurennoy
 Los Alamos National Laboratory, Los Alamos, New Mexico, 87547, USA

Abstract

The LANSCE accelerator facility has been in operation for 50 years performing important scientific support for national security. The unique feature of the LANSCE accelerator facility is multi-beam operation, delivering beams to five experimental areas. The LANSCE front end is equipped with two independent injectors for H⁺ and H⁻ beams, merging at the entrance of a Drift Tube Linac (DTL). The existing Cockcroft-Walton (CW) – based injector provides high beam brightness before injection into DTL. To reduce long-term operational risks and support beam delivery with high reliability, we designed an RFQ-based front end as a modern injector replacement for the CW injectors. Proposed injector includes two independent low-energy transports merging beams at the entrance of a single RFQ, which accelerates simultaneously both protons and H⁻ ions with multiple flavors of the beams. The paper discusses details of beam physics design and presents injector parameters.

INTRODUCTION

LANSCE linear accelerator consists of 201.25 MHz Drift Tube Linac accelerating particles from 0.75 MeV to 100 MeV and 805 MHz Coupled-Coupled Linac (CCL), accelerating particles from 100 MeV to 800 MeV. Accelerator facility simultaneously delivers various beams to multiple targets. Proton 100-MeV beam is delivered to Isotope Production Facility (IPF), while 800-MeV H⁻ beams are distributed to four experimental areas: the Lujan Neutron Scattering Center, the Weapons Neutron Research facility (WNR), the Proton Radiography facility (pRad), and the Ultra-Cold Neutron facility (UCN). The existing front end of accelerator is based on 50-years old Cockcroft-Walton (CW) accelerating columns and Drift Tube Linac. Analysis of beam availability within the last decades shows that a significant fraction of beam downtime (around 30%) is due to failures of the existing injector and Drift Tube Linac. Continuation of operation of that obsolete equipment leads to the risk of complete failure of facility operation.

To reduce long-term operational risks and to realize future beam performance goals in support of the laboratory missions, we develop a novel Front End including a high-brightness Radio-Frequency Quadrupole (RFQ) based injector [1]. The layout of the proposed injector is illustrated in Fig. 1 and the parameters are presented in Table 1. The new Front-End must provide the existing capabilities with a possible upgrade in beam intensity.

* Work supported by US DOE under contract 89233218CNA000001

[†] batygin@lanl.gov

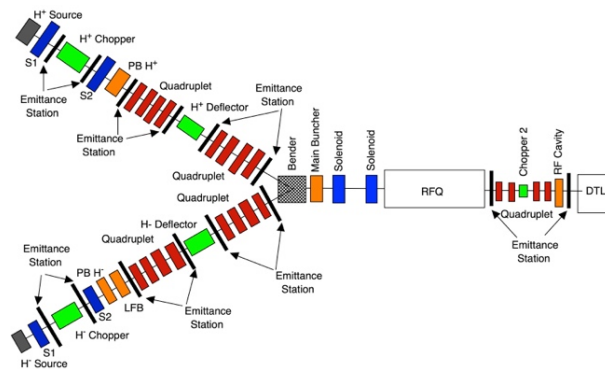


Figure 1: Layout of proposed RFQ-based 3-MeV injector.

Table 1: Parameters of the Proposed LANSCE Injector

| Ions | H ⁺ /H ⁻ |
|--------------------------------|--------------------------------|
| Ion sources extraction voltage | 100 keV |
| RF Frequency | 201.25 MHz |
| RFQ energy | 3 MeV |
| Repetition rate | 120 Hz |
| Max beam peak current | 32 mA |
| Average current | 1.25 mA |
| Beam pulse | 625-1000 μs |
| Number of RFQ cells | 187 |
| RFQ Length | 4.2 m |

DESIGN ISSUES FOR THE PROPOSED INJECTOR

The optimal operation of the accelerator facility critically depends on the emittance and brightness of the beam extracted from the ion sources and beam formation in the low-energy beam end. Normalized beam brightness is determined as

$$B = \frac{I}{8\pi^2 \epsilon_{x_rms} \epsilon_{y_rms}}$$

where I is the beam current, and ϵ_{x_rms} , ϵ_{y_rms} are normalized beam emittances in x - and y - directions. The H⁺ beam injector operates with a duoplasmatron proton source which delivers a high-brightness beam with a current $I = 10 - 30$ mA, normalized rms emittance in the range $\epsilon_{rms} = 0.003 - 0.004 \pi$ cm mrad, and beam brightness $B = 20 \text{ A}/(\pi \text{ cm mrad})^2$ [2]. The H⁻ beam injector is based on a cesiated, multicusp- field surface-production ion

LINAC DESIGN WITHIN HITRIplus FOR PARTICLE THERAPY

U. Ratzingerer[†], B. Koubek, H. Hoeltermann, H. Podlech, Bevatech GmbH, Frankfurt, Germany
M. Vretenar, CERN, Geneva, Switzerland

Abstract

Within the EU Horizon 2020 programme a linac was designed, which is starting from the concept as used at the 4 European cancer therapy centers applying light ions up to carbon. The new linac will in its simplest version allow ion beam injection into synchrotrons at 5 A MeV, with high beam transmission and allowing currents up to 5 mA α -particles. An advanced ECR – ion source will inject into an RFQ – IH-DTL combination. The DTL concept allows upgraded versions for A/q – values up to two and with beam energies of 7.1 A MeV from IH – tank2 and 10 A MeV from IH-tank3. The higher beam injection energies for light ions allow for relaxed synchrotron operation conditions at lowest magnetic field levels. A main argument for the DTL extensions however is an additional linac function as radioisotope facility driver. The 7.1 A MeV are especially defined for the clean production of ²¹¹At, which may play a future role in cancer therapy. The linac will allow for high duty-factors – up to 10%, to fulfil the needs for efficient radioisotope production. Solid state amplifiers with matched design RF power levels (up to 600 kW for IH3) will be used.

INTRODUCTION

With the development of the carbon therapy in Europe a 7 A MeV linac for C⁴⁺ was developed in a cooperation with GSI Darmstadt and IAP Frankfurt and was put into operation in 2008 at the therapy facility HIT Heidelberg [1]. The linac serves there as a synchrotron injector, as well as at 4 other facilities.

This linac is extremely compact. The acceleration from 8 A keV to 7 A MeV is accomplished within 5.5 m. The inter-tank section between RFQ and IH – DTL with a length of 0.25 m consists of a quadrupole doublet and beam diagnostics only. The system is easy to operate. Main key parameters can be seen from Table 1.

Table 1: Key Parameters of the HIT Injector

| | |
|----------------------------------------------|------------------------------------------|
| Design ion | ¹² C ⁴⁺ |
| Operating frequency | 216.816 MHz |
| Final beam energy | 7 MeV/u |
| Beam pulse length | ≤ 300 μs |
| Beam repetition rate | ≤ 5 Hz |
| Pulse current after stripping | 100 μA (¹² C ⁶⁺) |
| Transv. norm. emittances (95 %) ¹ | 0.8 π mm mrad |
| Exit energy spread ¹ | ±0.3 % |
| Total injector length ² | ≈ 13 m |

¹ straggling effects in the stripper foil not included

² including ECRIS, LEBT and foil stripper

For a new therapy facility one would like to get rid of the big tetrode driven RF amplifiers in the present design. The RF power losses within the present IH -DTL are 870 kW.

* Work supported by EU Horizon2020 – No. 101008548

† email address: u.ratzingerer@iap.uni-frankfurt.de

There is a chance for a drastic reduction, as the synchrotron not necessarily needs such a high injection energy. Moreover, the carbon stripper foil after the linac, which provides a C⁶⁺ - beam to the synchrotron was proven to be sufficiently effective at 5 A MeV beam energy. For α - and p - beams energies of 7.1 A MeV and 10 MeV are envisaged. These will allow higher injection energies for those lighter ions (stable synchrotron operation at lowest magnetic field levels) and furthermore, an efficient production of radioisotopes for medical purposes. Production of At²¹¹ is the reason for a 7.1 A MeV α - beam from the linac. In this operation-mode up to 10% linac duty-factor are requested. This is – besides RF power reduction – an additional reason for reduced acceleration fields: to overcome water-cooling limitations on the cavities. A new generation ECR – ion source AISHA is foreseen for this injector [2]. To allow combined function operation of this linac as synchrotron injector and as a radioisotope facility driver linac the design duty-factor is 10% for A/q – values up to 2.0, and below 1 % for A/q – values up to 3.0.

GENERAL LAYOUT

RFQ –Design

The detailed layout of the RFQ was not part of this study. However, the main parameters are fixed: The injection energy is 15 A keV, which is an upper limit for the ECR ion source as long as a high-voltage platform is avoided for simplicity. The end energy of 700 keV resulted from extensive beam dynamics studies on the DTL and its acceptance improvement by rising the exit energy from 400 keV (HIT Heidelberg design) to this new value. It is expected, that the new RFQ will have a total length of about 2.5 m. An improved 4 – Rod design is suggested, which safely can be operated at 10% duty factor.

DTL –Design

Figures 1 and 2 show the scheme of the HITRIplus Linac, consisting of one RFQ, 3 IH – cavities, one rebuncher and two debunchers for matching the beam longitudinally to the synchrotron at all injection energies. Table 2 shows the simulated beam parameters, Fig. 3 shows the exit cluster plots (with norm. eff. emittance values printed). It should be mentioned, that HITRIplus offers many linac options to a potential customer:

- The basic version with a 5 A MeV injector and one IH – cavity only
- The 5 / 7.1 A MeV version with two IH – cavities and the option of At²¹¹ – production
- The full version with three synchrotron injection energies and extended isotope production program at 5 mA He²⁺ nominal beam current after debunching.

STATUS OF THE TOP-IMPLART PROTON LINAC

P. Nenzi[†], A. Ampollini, M. D. Astorino, G. Bazzano, F. Fortini, L. Picardi, C. Ronsivalle, V. Surrenti, E. Trinca, ENEA Frascati Research Center, Frascati, Italy

Abstract

The TOP-IMPLART (Intensity Modulated Proton Linear Accelerator for Radio Therapy) proton linac, is a RF pulsed linac, designed for proton therapy, consisting of a low frequency (425 MHz) 7 MeV injector followed by a sequence of accelerating modules operating at 3 GHz under construction, assembly and test at the ENEA Frascati Research Center. The accelerator features also a vertical low energy (3-7 MeV) line for irradiation of samples in horizontal position. The segment currently completed includes 8 SCDTL modules up to 71 MeV grouped in two sections each one powered by a 10 MW klystron driven by a SCANDINOVA K100 modulator with a variable pulse length (1-5 us) at a repetition frequency of 25 Hz. The output current can be varied up to 30 μ A. The beam is mainly used for radiobiology experiments and dosimetry systems tests, but the flexibility in beam characteristics makes it suitable also for applications different from proton therapy, as the irradiation of electronics components to verify their behavior in the space environment. In this work, the current status of the accelerator and beam characteristics measurements are presented with an overview of the experiments carried on it.

INTRODUCTION

The TOP-IMPLART linac is a pulsed proton linear accelerator under construction and commissioning at the ENEA Frascati Research Center in a partnership with the Italian Institute of Health (ISS) and the oncological hospital Regina Elena-IFO in Rome. Accelerator development is funded by Regione Lazio with the aim of developing a technological demonstrator for a linear accelerator for proton therapy. The final particle energy expected for the TOP-IMPLART linac is 120 MeV, the maximum achievable energy compatible with the available space in the 27 meters long ENEA bunker.

Linac development and construction has been intermixed with experiments directed to optimize beam delivery strategies and design beam diagnostic systems adapted to the peculiar beam pulsed structure.

THE TOP-IMPLART LINAC

The TOP-IMPLART linac (see Fig. 1) is composed by a commercial injector, PL-7 model, developed by AccSys Technology Inc. (Pleasanton (CA), USA) and an high frequency booster composed of two SCDTL (Side Coupled DTL) sections designed by ENEA. PL7 is a 7 MeV linac consisting of a compact duoplasmatron H⁺ ion source working at a voltage of 30 kV.

The beam extracted from the source is focused by an einzel lens into a 3 MeV RFQ followed by a 7 MeV DTL, each powered by a 350 kW triode based amplifier. The nominal operation frequency of the injector is 425 MHz (with a tuning range of ± 100 kHz).

The high frequency booster consists of two sections of 4 SCDTL accelerating module each. The first section accelerates the beam to an energy of 35 MeV and the second one to an energy of 71 MeV. Each section is powered by a 10 MW peak power klystron amplifier operating at a frequency of 2997.92 MHz (S-band). The main beam parameters are listed in Table 1.

The output beam current can be varied by changing the voltage on the einzel lens in the injector or acting on the length or the temporal superposition of the two klystrons pulses. A magnetic scanning system is under realization and will be installed to test and demonstrate the implementation of 4D irradiations based on active control of energy and intensity and x-y spot scanning.



Figure 1: TOP-IMPLART linac.

Table 1: Main Beam Parameters

| Parameter | Value |
|-------------------------------|--------------|
| Max. Output Current (pulsed) | 30 μ A |
| Beam pulse width | 1 -5 μ s |
| Beam pulse repetition rate | 10 – 100 Hz |
| Beam size at the linac output | <3 mm |

The MEBT line features also a vertical extraction line for the injector 3-7 MeV beam consisting of a 90° bending magnet directing the beam toward the ceiling for irradiation of samples that must stay in horizontal position, like cell cultures in Petri dishes.

Work supported by Regione Lazio
[†] paolo.nenzi@enea.it

DESIGN OF A LINEAR ACCELERATOR FOR ISOTOPE PRODUCTION

A.Pisent, C.Baltador, L. Bellan, M. Comunian, J.Esposito, L.Ferrari, A.Galatà, F.Grespan
 INFN/LNL, Legnaro, Italy
 P. Mereu INFN/Torino, Italy
 L. Celona INFN/LNS, Catania, Italy

Abstract

The recent accelerator developments allow the design of very efficient linear accelerators for various applications. The possible use of concepts, components and developments well established or recently achieved in larger projects will be illustrated, with some examples related to isotope production for medical applications.

INTRODUCTION

The accelerator driven production of radioisotope for medical applications (for diagnostics, therapy and combined, so called theranostic) is one of the most important applications of nuclear techniques. The focus of INFN in the field has grown up in the last years, also in connection with the possible use of the new cyclotron at LNL able to deliver 0.5 mA of protons with variable energy range (35-70 MeV). Novel as well as already established radionuclides of medical interest may alternatively be produced using alpha particle beams [1-3], having energy ranging between few and 40 MeV. This new approach may allow to yield radionuclides hard to be obtained with more traditional nuclear reactors or by proton accelerators by exploiting new reaction routes. This approach may lead to better radionuclidic impurity profile, simplifying the radiochemical separation/purification process.

Interesting cases are, e.g., the alternative supply of ^{99m}Tc through the $^{96}\text{Zr}(\alpha,n)^{99}\text{Mo}$ reaction route, or the very important theranostic ^{67}Cu (under the spotlight at international level) by using the $^{64}\text{Ni}(\alpha,p)$ route. Other interesting products are based upon the reaction routes $^{209}\text{Bi}(\alpha,2n)^{211}\text{At}$, or $^{\text{nat}}\text{Mo}(\alpha,x)^{97}\text{Ru}$. The use of cyclotron for α particles has an intensity limitation (mainly related to the extraction system): the IBA cyclotron at Aronax is for example limited to about 35 μA .

THE ALPHA DTL LINAC DESIGN

With the project alpha-DTL, presently under evaluation by INFN as interdisciplinary accelerator research program (CSN5 call), we propose an alternative approach with a high duty cycle normal conducting linac (high frequency, i.e. 352 MHz), composed by an ECRIS (electron cyclotron resonance ion source), an RFQ (radio frequency quadrupole) and a DTL (drift tube linac), as sketched in Fig.1; an average of 0.5 mA of fully stripped He can be delivered to the target (one order of magnitude better than cyclotrons). Moreover, we intend to develop an original idea to allow in the DTL the energy regulation on a large range. This accelerator will represent a clear step forward in the field of accelerator driven isotope production.

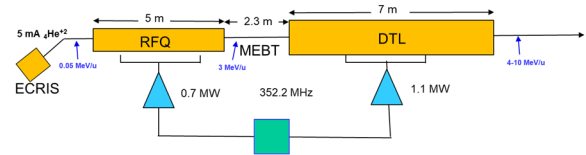


Figure 1: Block diagram of the alpha-DTL linac.

The design is based on the high power linac development by INFN in the last years. In particular, the RFQ uses the mechanics of TRASCO RFQ [4,5], 4 modules, and the tuning procedure developed for IFMIF-EVEDA [6]. The DTL uses the design developed for ESS [7, 8]. The RF system, two klystron and a single modulator, is the same of ESS normal conducting section.

The Background

Alpha-DTL project makes the best use of the unique competences and edge technologies developed by INFN, with application in a different field, new in terms of particle kind and applications. Moreover, the energy variation in a DTL is a substantial innovation in itself and opens to new applications; the DTL (well known for excellent efficiency in terms of beam dynamics and power consumption) can now be used as a flexible main linac to track energy dependent cross sections.

The implementation of the research program moves in four main directions, the beam dynamic design, the linac component development, the ion source and the solid target development. The first WP has the very important task to optimize the design (which for TRASCO RFQ and ESS DTL was though for high current protons) with $A/q=2$, with all the key performances, interfaces and limitations that characterize our system; moreover, the idea of energy variation is integrated in the design. A key ingredient of this optimization are the new algorithms developed for linac design based on genetic and AI techniques and heavy parallelization of the processes [9]. The second WP considers the design of the cavities and of the RF system, with a program of dedicated prototypes (actuated post-couplers for the DTL, new power couplers, new DT-tank interface...); also, 3D RF simulations allow unprecedented performances (for example a full DTL tank with all tuning and stabilizing devices). New milling machines allow substantial advantage with new geometry optimization. This WP has preeminent aspects in mechanics, rf design and control system. The third WP considers the ion source development, with a specific assessment of the reliable performances. The fourth task is dedicated to assessing the solid target design for this specific application (10 kW beam power).

Content from this work may be used under the terms of the CC BY 4.0 licence (© 2021). Any distribution of this work must maintain attribution to the author(s), title of the work, publisher, and DOI

CELL GEOMETRY OPTIMIZATION FOR DIPOLE KICK CORRECTION IN A HIGH FREQUENCY IH STRUCTURE*

R. López López^{†1}, J. Giner Navarro, D. Gavela Pérez, G. Moreno Fernández-Baíllo, P. Calvo Portela, C. Oliver Amorós, J.M. Pérez Morales, CIEMAT, Madrid, Spain

A. Lombardi, CERN, Geneva, Switzerland

J.M. Carmona, C. Battaglia, AVS, Elgoibar, Spain

¹also at Universidad Carlos III de Madrid, Madrid, Spain

Abstract

Given the asymmetry in the stem configuration of an IH-DTL structure, an electric dipole component is always present between drift tubes, and it is especially significant for reduced dimensions in high-frequency regimes. Here we study the effect of different modifications of the drift tubes geometry of a 750 MHz IH-DTL to eliminate the impact of the dipole component in the transverse beam dynamics. Tracking simulations through a single cell are also performed to assess the outcomes in particle's trajectory offset and angle.

INTRODUCTION

Interdigital H-mode structures are common components in linac injectors due to their high power efficiency performance in the acceleration of beams below 25% of the speed of light [1]. Following the recent progress at CERN on a "bent-linac" design for carbon ion beams [2] that comprises a highly compact RFQ [3] operating at 750 MHz, here we present a conceptual study of a high frequency IH-DTL structure for the injector, downstream the mentioned RFQ, accelerating in the energy range of 5 to 10 MeV/u. The baseline design tries to continue the work in [4] on the optimized cell geometry of a 750 MHz IH-type structure.

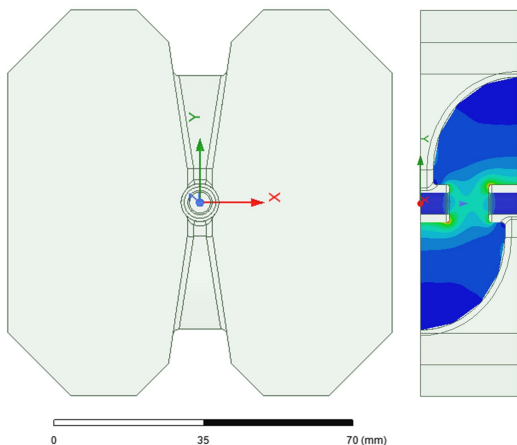


Figure 1: Front view (left) and lateral cross-section (right) of one standard IH cell. Electric field map is represented in the YZ plane.

Structures with very small apertures, and high frequency regimes, require special attention to the beam dynamics which is strongly affected by small errors in geometry dimensions. In addition, the asymmetry with opposing stems introduces a very significant transverse component of the electric field. Benedetti et al [4] proposed the mitigation of such dipole kick by adjusting the length of the first and last cells of the rf tank. In this study, we consider several proposals of geometrical modifications of the drift tubes that aims at either reducing or compensating the transverse electric fields. Simulations of the electromagnetic fields were performed in ANSYS HFSS [5], and calculations of different figures of merit were compared for each model.

Figure 1 shows the conformed geometry in vacuum of one regular cell of an IH structure, which respects the idea in [4] of using flat copper walls for the outer cavity profile, but has been revised with a round profile in seek of smaller power losses [6]. The model in Fig. 1 is used as baseline for this study. The cell length is 23.085 mm, corresponding to an ion speed of $\beta = 0.12$. The internal bore diameter of the drift tube is 5 mm, its thickness is 2 mm, and the gap length is 9.315 mm. The horizontal and vertical sizes of the outer profile of the cavity are 91.35×91.35 mm.

For such a model, the electric field along the ideal particle path is represented in Fig. 2 by the axial (z) and transverse (y) components. The transverse voltage, responsible of deflecting the beam, entails 8.4% of the total axial voltage in a single cell. The goal of this study is to reduce the deflecting effect by modifying the standard drift tube geometry close to the gap.

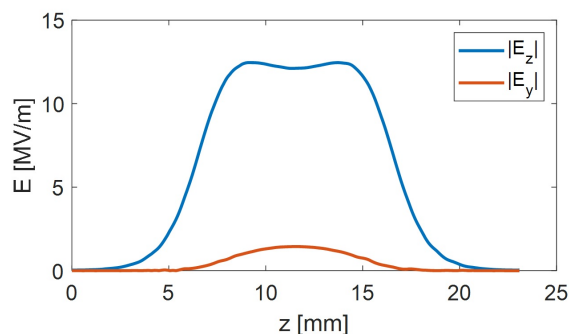


Figure 2: Axial (blue) and transverse (red) field profile along the centre of the rf cell. Fields are scaled to an axial effective voltage of 120 kV.

* Work supported by IKERTU-II grant, ZE-2021/00050

[†] ricardo.l.lopez.eng@gmail.com

EFFECT OF HIGH-MAGNETIC FIELD REGION GEOMETRY ON THE EFFICIENCY OF A 750 MHz IH STRUCTURE*

G. Moreno Fernández-Baillo[†], J. Giner Navarro, D. Gavela Pérez, R. López López[‡]
P. Calvo Portela, C. Oliver Amorós, J.M. Pérez Morales, CIEMAT, Madrid, Spain
A. Lombardi, CERN, Geneva, Switzerland
J.M. Carmona, C. Battaglia, AVS, Elgoibar, Spain

Abstract

High frequency structures generally translate to high efficiency performances thanks to reduced surfaces of the inner cavity. Two round-profiles geometry and some variations of two important parameters of a 750 MHz IH-DTL are proposed in this paper in order to improve shunt impedance performance regarding an existing solution with flat-walled cavity developed by CERN. The proposed designs are shaped such that they guarantee an easy connection of RF and vacuum auxiliaries. Electromagnetic simulations are checked with CST Microwave Studio.

INTRODUCTION

H-mode accelerator structures, which work in transverse electric (TE) modes, stand out mainly because of their high efficiency performance in low β regimes, compared to other accelerator structures such as Alvarez linac type cavities [1]. Among the different types of H-mode DTL structures, two are emphasised above all, the so-called crossbar H-mode (CH), which operates in TE₂₁₀ mode; or the interdigital H-mode (IH) structure, operating in TE₁₁₀ mode. It is for a specific particle's velocity range, below $\beta \sim 0.15$, where IH cavities show the most efficient performance [2], and become a necessary component in linac injectors for light and heavy ions. An example is the bent-linac injector for medical applications with carbon ion beams [3] proposed at CERN, which comprises a compact 750 MHz RFQ in the first RF acceleration stage (0.4-5 MeV/u) [4]. After such cavity, the use of an optimised 750 MHz IH structure capable of covering the first range up to 5-10 MeV/u range has been proposed [5].

There are some factors that can define the high value of the RF cavity efficiency, such as its external structure. Refining the shape in the auto-inductive dominated regions of the cavity allows for further optimisation of the power consumption. Concerning this idea, this work explores the shaping and geometry parametrisation of a 750 MHz IH cell aiming at improving its efficiency.

The shunt impedance (Z) parameter is a good variable to study the optimisation of the cavity. This variable is defined as the ratio between the square of the longitudinal voltage in the cavity and the consumed power. Thus, with a constant longitudinal voltage, the value of Z reaches its highest value when the power dissipated in the cavity walls is minimised.

One usually deals with the effective shunt impedance (Z_{TT}), which includes the transit time factor of the voltage noticed by the beam. Under this consideration, in order to achieve the objective of this study, some proposals for geometric modifications to the 750 MHz IH structure together their Z_{TT} values are presented here. These structures are capable of reducing the dissipated power while maintaining the dimensions of the drift tubes.

With a view to carry out this analysis, the CST Studio Suite 2021 software was used. This software allows for the simulation of the resonance frequencies of an RF cell, EM fields and some determining parameters such as the effective impedance Z_{TT} .

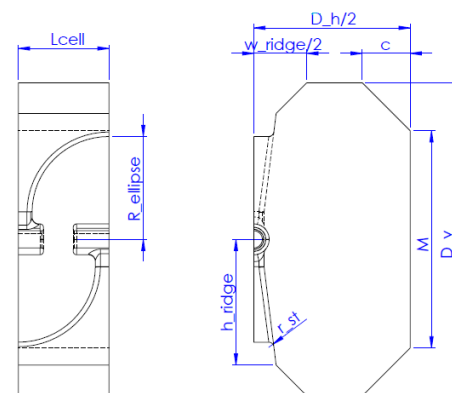


Figure 1: Front view (right) and lateral cross section (left) of half standard IH cell.

Figure 1 shows the baseline cavity in which the analysis was carried out, as well as the nomenclature of key parameters that have been studied in the optimisation. It is a regular cell that belongs to an IH cavity with a structure inspired by the S. Benedetti et al. study [5]. With a length of 25.16 mm and a gap equal to 8.99 mm, this cell has a series of flat copper walls for the outer profile, motivated by an easy machining and insertion of auxiliaries. These flat walls will be modified during this study.

EFFICIENCY AND CAVITY WALLS

Choosing the best acceleration structure for a given application is a complicated task. To narrow down the spectrum of possibilities, it is useful to set some constraints. In this work, the orifice size, the gap and the operating frequency were fixed. The decision on the orifice radius comes from

* Work supported by IKERTU-II grant, ZE-2021/00050

[†] Gabriela.moreno@ciemat.es

[‡] also at Universidad Carlos III de Madrid, Madrid, Spain

AUTOMATIC RF CONDITIONING OF S-BAND CAVITIES FOR COMMERCIAL PROTON THERAPY LINACS

S. Benedetti[#], M. Cerv, S. Magnoni, L. Navarro, D. Soriano, AVO-ADAM, Geneva, Switzerland

Abstract

The CERN spinoff company ADAM owned by Advanced Oncotherapy plc (AVO-ADAM) is completing the construction and testing of its first LIGHT (Linac for Image-Guided Hadron Therapy) system. Each LIGHT machine is composed by 20 accelerating modules: one 750 MHz RFQ, four 3 GHz Side-Coupled Drift Tube Linac (SCDTL) and 15 3 GHz Coupled-Cavity Linac (CCL). The company aims at delivering several similar LIGHT machines in the next years. A prerequisite to achieve such goal is the capability to complete the RF conditioning of the accelerating modules in a systematic and automatic way, with minimal inputs from RF engineers. In the past years ADAM developed an automatic conditioning system capable of increasing the main conditioning parameters – RF power, pulse width, repetition rate – while controlling the cavity breakdown rate and vacuum level. The system has been so far tested on about twenty accelerating structures with different brazing methodologies and RF accelerating voltages, proving its robustness. This paper discusses the ADAM automatic conditioning system design and its implementation.

INTRODUCTION

RF accelerating structures must undergo a process of conditioning before being accepted for operation in an accelerator facility. The conditioning is considered finished when the breakdown rate (BDR) meets the requirements and the RF parameters – pulse width and repetition rate – are nominal. The conditioning process consists of an iterative algorithm that smoothly increases the average power in the cavity until the working conditions are reached. During this process, the BDR and other parameters, such as the cavity vacuum pressure, are acquired to characterize the conditioning status. A fast RF inhibit is recommended to protect the cavity from clusters of breakdowns that could damage the inner surface of the cavity. A schematic of an RF system suitable for accelerating cavity conditioning is sketched in Fig. 1.

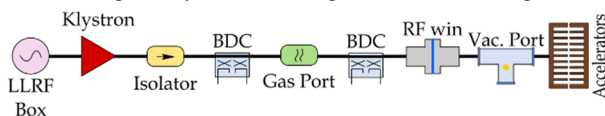


Figure 1: Overview of an RF network layout for cavities conditioning.

Such systems are typically composed of a low-level RF (LLRF) box or RF generator, a modulator and klystron system (MKS), an RF network (RFN), vacuum system and gauges, temperature sensors and thermos-switches, SF6

gauge and reading, a cooling system and a trigger system to synchronize the LLRF, the MKS and the acquisition system.

AVO-ADAM developed in the past years an automatic tool for conditioning its accelerating cavities, called Event Detection System (EDS), building on the initial work discussed in [1]. The EDS permitted to condition more than 19 accelerating cavities so far with a reproducible and standardized process.

SYSTEM COMPOSITION

The Event Detection System (EDS) is a system consisting of software and hardware. It monitors the RF signals in the RF network and in the accelerating cavity. If any of the signals exceeds predefined limits, the EDS marks it as an event. After a user-defined number of consecutive events, it can inhibit the trigger of the RF generator to protect the RF cavity from physical damage. In addition, the EDS accepts external digital inhibit signals from the cooling and vacuum systems.

EDS is fully controlled by a supervisory control system, where also sends the data for monitoring, archiving and further processing. Triggers arrive from the trigger generator and are conditionally forwarded to the RF generator.

When the EDS detects a trigger, it will perform data acquisition on 8 analogue inputs, process the acquired waveforms, detect whether some of those processed values are out of preconfigured limits and appropriately flag this data. Typically acquired signals are the MKS voltage and current, the MKS and accelerating cavity bi-directional coupler (BDC) forward and reflected power as well as the accelerating cavity pickups (PKPs). This system capability proved very useful during the data postprocessing to discern between recorded events originating from breakdowns in the accelerating cavities, rather than in the RFN or in the klystron.

If the number of consecutive events is higher than a user-defined limit, an internal inhibit signal is raised. EDS also detects externally produced inhibit signals, typically those coming from the cooling and the vacuum systems. If an inhibit signal is raised, the EDS will no longer forward the triggers from its input to its power output.

The EDS computes the rate of recognized events in a dynamic way, as 2 divided by the number of pulses since the second to last event to the present time. This number is the accelerating cavity BDR monitored by the system, though as explained above during the data postprocessing several recorded events can be discarded as breakdowns non-originating from the accelerating cavity.

[#] stefano.benedetti@avo-adam.com

HIGH POWER RF TRANSMISSION LINES OF THE LIGHT PROTON THERAPY LINAC

J.L. Navarro Quirante*, D. Aguilera Murciano, S. Benedetti, G. Castorina, C. Cochrane, G. De Michele, J. Douthwaite, A. Eager, S. Fanella, M. Giles, D. Kaye, V. F. Khan, J. Mannion, J. Morris, J. F. Orrett, N. Pattalwar, E. Rose, D. Soriano Guillén, AVO-ADAM, Meyrin, Switzerland

Abstract

The Linac for Image-Guided Hadron Therapy (LIGHT) machine [1] is designed to accelerate a proton beam up to 230 MeV to treat deep seated tumours. The machine consists of three different kinds of accelerators: Radio-Frequency Quadrupole (RFQ), Side Coupled Drift Tube Linac (SCDTL) and Coupled Cavity Linac (CCL). These accelerating structures are fed with Radio Frequency (RF) power at 750 MHz (RFQ) and 3 GHz (SCDTLs and CCLs). This power is delivered to the accelerating structures via the high power RF transmission network (RFN). In addition, the RFN needs to offer other functionalities, like protection of the high RF power feeding stations, power splitting, phase and amplitude control and monitoring. The maximum power handling of the RFN corresponds to a peak RF power of 8 MW and an average RF power of 9 kW. It functions either in Ultra-High Vacuum (UHV) conditions at an ultimate operating pressure of 10^{-7} mbar, or under pressurized gas. The above listed requirements involve different challenges. In this contribution we exhibit the main aspects to be considered based on Advanced Oncotherapy's (AVO) experience during the commissioning of the RFN units.

OVERVIEW OF LIGHT SYSTEM

The Linac for Image-Guided Hadron Therapy (LIGHT) machine [1] consists of several subsystems to produce, accelerate, transport and deliver protons to treat deep seated

tumours. It has the capability to deliver the required dose sending pulses with a duration of 5 μ s, 200 times per second and being able to change the proton energy electronically pulse by pulse. The main subsystems are:

- LIGHT Proton Injector (L-PIA) that produces continuous proton pulses of 5 μ s at 200 Hz and modulates their intensity.
- LIGHT Radiofrequency Quadrupole subsystem (L-RFQ) that comprises the necessary devices to produce, amplify, transport, monitor and control RF at 750 MHz to feed an RF quadrupole cavity that is capable of capturing the proton pulses produced by the source, bunching and accelerating them up to 5 MeV.
- LIGHT Side Coupled Drift Tube Linac subsystem (L-SCDTL) composed of two units with the necessary equipment to produce, amplify, transport, monitor and control the 3 GHz RF power to feed accelerating cavities boosting protons up to a fixed energy of 37.5 MeV.
- LIGHT Coupled Cavity Linac subsystem (L-CCL) composed of 10 units able to produce, amplify, transport, monitor and control the 3 GHz RF power to feed 15 CCL cavities able to dynamically modulate the energy of the protons from 70 to 230 MeV.
- After the main Linac other subsystems transport and deliver the beam to one or several treatment rooms, which are out of the scope of this contribution.

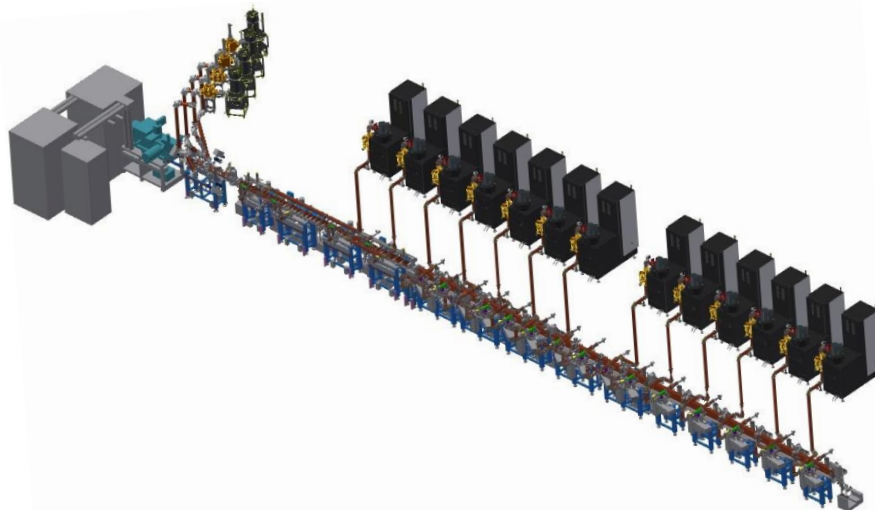


Figure 1: 3D model of the full LIGHT. The 3 GHz RF Network is visible connecting the high power stations to the accelerator.

* l.navarro@avo-adam.com

LOW LEVEL RF SYSTEM OF THE LIGHT PROTON THERAPY LINAC

D. Soriano Guillen[†], G. De Michele, S. Benedetti, Y. Ivanisenko, M. Cerv
AVO-ADAM, Meyrin, Switzerland

Abstract

The LIGHT (Linac for Image-Guided Hadron Therapy) project was initiated to develop a modular proton accelerator delivering beam with energies up to 230 MeV for cancer therapy. The machine consists of three different kinds of accelerating structures: RFQ (Radio-Frequency Quadrupole), SCDTL (Side Coupled Drift Tube Linac) and CCL (Coupled Cavity Linac). These accelerating structures operate at 750 MHz (RFQ) and 3 GHz (SCDTL, CCL). The accelerator RF signals are generated, distributed, and controlled by a Low-Level RF (LLRF) system. The LIGHT LLRF system is based on a commercially available solution from Instrumentation Technologies with project specific customization. This LLRF system features high amplitude and phase stability, monitoring of the RF signals from the RF network and the accelerating structures at 200 Hz, RF pulse shaping over real-time interface integrated, RF breakdown detection, and thermal resonance frequency correction feedback. The LLRF system control is integrated in a Front-End Controller (FEC) which connects it to the LIGHT control system. In this contribution we present the main features of the AVO LLRF system, its operation and performance.

INTRODUCTION

AVO-ADAM designed and is currently commissioning the LIGHT (Linac for Image Guided Hadron Therapy) proton cancer therapy LINAC [1], which is a modular normal conducting RF accelerator fed by 4 Inductive Output Tubes (IOTs) and 13 klystrons grouped in 14 power stations. At each power station the RF power can be modulated independently every pulse. The pulse repetition rate is 200 Hz allowing accurate dose delivery within tumour volume and longitudinal layer switching on a pulse-to-pulse basis, given the low emittance of the proton beam. These features of the LIGHT LINAC are key to have image-guided adaptive radiation therapy with protons [1]. The modular structure of the LIGHT system consists of:

- A proton source injecting 40 keV protons with currents up to 300 uA and pulses up to 20 us at 200 Hz repetition rate.
- An RFQ (Radio Frequency Quadrupole) with a resonant frequency of 749.48 MHz accelerating the protons up to 5 MeV. This is the fourth sub-harmonic of the 2997.92 MHz LINAC frequency. The RFQ is fed by an IOT powering system driven by the first LLRF unit. Several signals are monitored in the LLRF from the RFQ system: 4 probe signals from the RFQ cavity and 4 pairs of directional couplers (forward and reflected power) in the RF network.

- Four SCDTL (Side Coupled Drift Tube LINAC) structures powered by two klystrons at the main LIGHT frequency of 2997.92 MHz. Passing through the four SCDTL cavities, the beam will accelerate to 37.5 MeV. A SCDTL RF unit consists of a LLRF driving power to a Modulator Klystron System (MKS) that amplifies the 5 microseconds duration RF pulses to MW levels. From each SCDTL RF unit, the associated LLRF receives 4 probe signals (2 per cavity) and 3 pairs of directional couplers (forward and reflected) signals in the RF network. The power is split from main line and there is a coupler on each branch before the SCDTL cavities.
- Fifteen CCL (Coupled Cavity LINAC) structures powered by eleven klystrons at 2997.92 MHz, bringing the beam energy up to 230 MeV. Four CCL RF units split power between two CCL cavities and the other six are fed directly from the MKS. In the first case, the associated LLRF receives 4 probe signals (2 per cavity) and 3 pairs of directional couplers (forward and reflected) signals in the RF network (as in the SCDTL case); and in the latter case only 2 probe signals from the cavity and 2 pairs of directional couplers are received.

Figure 1 shows a schematic view of the LIGHT LINAC design. The three types of RF accelerating cavities are highlighted with the final energy at each section. The RF peak power required for the RFQ, SCDTL and CCL units is 400 kW, 8 MW and 45 MW respectively [2].

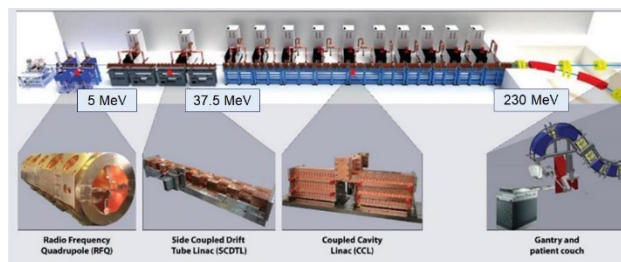


Figure 1: LIGHT system schematic with expected beam energy reached after each type of RF accelerating cavity section.

The LIGHT beam production system is currently being commissioned at AVO-ADAM Daresbury integration site (DIS) in UK.

LLRF SYSTEM DESCRIPTION

Each high-power RF unit is fed by a LLRF device, which makes a total of 14 LLRF units for the whole LIGHT LINAC. The LLRF system has been built and delivered by Instrumentation Technologies [2] and on top of the LLRF

[†] d.soriano@avo-adam.com

COMMISSIONING STATUS OF THE iBNCT ACCELERATOR

M. Sato[†], Z. Fang, M. Fukuda, Y. Fukui, K. Futatsukawa, K. Ikegami, H. Kobayashi, C. Kubota, T. Kurihara, T. Miura, T. Miyajima, F. Naito, K. Nanmo, T. Obina, T. Shibata, T. Sugimura, A. Takagi, High Energy Accelerator Research Organization (KEK), Ibaraki, Japan
H. Kumada, Y. Matsumoto, S. Tanaka, University of Tsukuba, Ibaraki, Japan
T. Ohba, N. Nagura, NAT, Ibaraki, Japan
T. Toyoshima, ATOX, Ibaraki, Japan
H. Oguri, Japan Atomic Energy Agency, Ibaraki, Japan

Abstract

An accelerator-based boron neutron capture therapy (BNCT) has been studied intensively in recent years as one of the new cancer therapies after many clinical research with nuclear reactors. In the iBNCT project, the accelerator configuration consists of an RFQ and a DTL which have proven achievements in J-PARC. Meanwhile, a high duty factor is required to have a sufficient thermal neutron flux needed by BNCT treatments. After a failure of the klystron power supply occurred in Feb. 2019, beam operation was resumed in May 2020. To date, an average current of about 2 mA with the beam repetition rate of 75 Hz has been achieved with stable operation. Irradiation tests with cells and mice are ongoing together with characteristic measurements of the neutron beam. In parallel with that, we have been gradually improving the accelerator cooling-water system for further stability. In this contribution, the present status and prospects of the iBNCT accelerator are reported.

INTRODUCTION

Boron Neutron Capture Therapy (BNCT) has been attracting attention recently as a new type of cancer therapy. It has been originally studied with thermal neutrons generated in a nuclear reactor, but recently many activities have started with accelerator-based neutron generation methods to get rid of many regulations against nuclear reactors. The iBNCT (Ibaraki BNCT) project, which started in 2010, is an industry-academia-government collaborative project organized by High Energy Accelerator Research Organization (KEK), Tsukuba University, and private companies together with support from Ibaraki prefecture in Japan [1].

In the iBNCT project, the linear accelerator consists of an RFQ and Alvarez-type DTL which is the same configuration as the J-PARC linac. The RFQ is the same type as J-PARC RFQ II, and the length of the DTL is reduced to 3 m to have optimized proton kinetic energy. Detailed parameters are found in Ref. [2]. Primary 50-keV protons extracted from a multi-cusp ECR ion source are accelerated by RFQ and DTL up to 3 MeV and 8 MeV, respectively. The proton beam is bombarded onto a three-layer neutron-generation beryllium target [3] to generate neutrons by the ${}^9\text{Be}(p, n)$ reaction. In this reaction, generated neutrons mainly have a kinetic energy of a few MeV, so a moderator is installed after the target to reduce neutron kinetic energy

to the epi-thermal region suit for BNCT treatment. In BNCT, a desired epi-thermal neutron flux is formulated by IAEA-TECDOC to be greater than 1×10^9 n/cm²/sec [4]. To achieve this value with the iBNCT accelerator configuration, averaged proton current must be more than 1 mA. Assuming the peak current of around 30 mA which is presently obtained in the iBNCT ion source, a high duty factor is required compared with J-PARC linac.

Presently, the iBNCT accelerator is operated with a beam width of 920 μs under the repetition of 75 Hz. The resulting averaged beam current is about 2 mA which is sufficient to enable the iBNCT project to proceed with non-clinical studies. In Nov. 2021, non-clinical studies have started and we aim to complete them in the fiscal year 2022. Presently, the iBNCT project is preparing to take safety reviews to start clinical studies in the fiscal year 2023.

FACILITY STATUS

Failure of Klystron High-Voltage Power Supply

In Feb. 2019, a failure of the high-voltage power supply of the klystron occurred during the cavity RF conditioning. High-voltage pulses were not delivered to the klystron due to a breakdown of the high-voltage switching device (HVS) in the power supply. In HVS, gate voltage to the IGBT was not generated due to a failure of the control board of HVS. Since HVS was manufactured by a Korean company, HVS together with its insulation-oil tank was shipped to Korea for repair. Unfortunately, there was no backup of HVS, the beam operation was completely suspended during the period. After repair, HVS was reinstalled at the end of Nov. 2019, however, at the beginning of resuming operation, we could not increase the high-voltage to the rated voltage due to the over-current protection of the power supply. As a result of investigations, we found that the insulation of a high-voltage supply cable between HVS and the klystron was broken. It may be valid that the cable and HVS failure occurred at the same time, though the relationship between them has not been understood yet. Another problem was a malfunction of the RF interlock triggered by the switching noise of HVS. After some measures to the noise, cavity RF conditioning resumed from Feb. 2020 with the repetition of 75 Hz.

Replacement of the Neutron-Generation Target

After a long shutdown for the repair of the klystron power supply, the neutron-generation beryllium target was

[†] masaharu.sato@kek.jp

A MEDICAL LINAC FOR AFFORDABLE PROTON THERAPY

S. M. Hunt, Joël Adélise, Elsa van Garderen, Wolf-Dieter Klotz, Rebecca Seviour¹

Alceli Limited, Aberdeen, Scotland

Dora Correia, PSI, Villigen, Switzerland

¹also at University of Huddersfield, Huddersfield, UK

Abstract

Proton Therapy (PT) was first proposed in the 1940s. Application of this knowledge was largely led over the next fifty years by accelerator laboratories, but now also by commercial companies. Availability of PT is increasing but is limited by three factors: facility size, prompt/induced radiation, and treatment cost. Compact cyclotrons/synchro-cyclotrons for single-room facilities have reduced space requirements. Linacs can avoid high radiation levels. Yet treatment costs have remained stubbornly high, driven largely by maintenance and staffing costs over the typical 20-30 year facility lifetime. Current technology cannot simultaneously reduce these three factors. By using a long Linac, the Alceli approach sacrifices size limitations, to gain massive improvements in treatment cost and radiation levels. Quadrupling the length of a Linac results in a sixteen-fold reduction in RF power per cavity. Along with other innovations in our design, this leads to a modular warm Linac with distributed solid-state RF amplification, easy and cheap to manufacture and maintain, requiring no water cooling, and a treatment cost of 1/10th of current facilities, making PT much more affordable.

WHAT IS PROTON THERAPY?

Traditional radiotherapy uses X-rays, a form of high energy electromagnetic radiation, to kill cancer cells. The X-rays pass through the body, depositing energy as they do so, and this energy kills both cancer and normal cells on the way. The beam is quite large, but by rotating the beam around the patient, and always pointing at the tumour, the tumour receives the maximum dose, and other tissue receives a lower, although non negligible, dose. Proton Therapy (PT) is an advanced form of radiotherapy that can treat tumours with minimal damage to the surrounding tissue. It uses protons instead of X-rays to destroy the cancer cells. The advantage of using protons is that instead of destroying cells all the way as they pass through the body most of the energy is deposited, and therefore damage occurs, at a specific depth known as the Bragg Peak. The depth of the Bragg Peak is dependent on the kinetic energy of the proton, and therefore can be controlled.

HISTORY OF PROTON THERAPY

The idea of using this effect for treating cancer was already proposed in the 1940's by Wilson [1], and first experiments treating patients were made in the 1950's at the Lawrence Berkeley Laboratory in California using their cyclotron [2] However, the high cost of the accelerators needed to accelerate protons to the necessary energy meant that for many years Proton Beam Therapy was restricted to

accelerator laboratories treating small numbers of patients. The first dedicated accelerator to treat patients was a synchrotron designed and built by Fermi lab National Laboratory in the USA and installed at the Loma Linda Hospital in California in the 1970s [3].

Commercial companies only became involved in Proton Beam Therapy in the 1990's. The first commercial accelerator for PT was ordered by the Massachusetts General Hospital in the USA [4]. They were already making use of the Harvard Cyclotron to deliver PT and wanted their own dedicated machine. The contract to supply the machine was won by IBA, a Belgian company that already produced small cyclotrons used for science and other medical purposes. This one order has led to PT now being IBA's main business, and they have become the world leader in producing PT systems. Soon after, the Paul Scherrer Institute (PSI) in Switzerland which already had a very successful PT program treating patients using protons from its large cyclotron used primarily for high energy physics, ordered a superconducting cyclotron from Accel AG [5], a German Accelerator company. Having a dedicated accelerator for PT meant patients could be treated all year around rather than relying on the availability of the physics machine. Accel gained enough knowledge of PT from this project to offer machines to other sites, and Accel was eventually sold to Varian and has become a major supplier of PT systems including two NHS facilities in UCLH London, and the Christie in Manchester. So, from these two commercial contracts the PT industry was born. It is interesting to note that the prevalence of cyclotrons (and the related synchro-cyclotrons) as accelerators for PT came as a result of these two contracts from centres already using cyclotrons for other purposes.

LIMITATIONS TO THE WIDE AVAILABILITY OF PT

Three factors have held back the wide adoption of PT world-wide.

Cost

The cost of treatment using PT is partly due to the high capital cost of building the facilities (circa £100M for the Christie in Manchester, significantly more for UCLH in London). But as that capital cost can be amortised over a long lifetime of the facility, even more important is the re-occurring cost of operation and maintenance of the facility (circa £20M per year for the Christie and UCLH).

UPDATE ON THE FIRST 3D PRINTED IH-TYPE LINAC STRUCTURE - PROOF-OF-CONCEPT FOR ADDITIVE MANUFACTURING OF LINAC RF CAVITIES*

H. Hähnel[†], A. Ateş, U. Ratzinger

Institute of Applied Physics, Goethe University, Frankfurt a. M., Germany

Abstract

Additive manufacturing ("AM" or "3D printing") has become a powerful tool for rapid prototyping and manufacturing of complex geometries. A 433 MHz IH-DTL cavity has been constructed to act as a proof of concept for additive manufacturing of linac components. In this case, the internal drift tube structure has been produced from 1.4404 stainless steel using AM. We present the concept of the cavity as well as first results of vacuum testing, materials testing and low level rf measurements. Vacuum levels sufficient for linac operation have been reached with the AM linac structure.

INTRODUCTION

Additive manufacturing (AM) of metal parts may provide an interesting new way to manufacture accelerator components. As technology is evolving, the quality and accuracy of parts manufactured this way is improving. Recently, a number of studies on the topic of AM for linear accelerator components have been published [1–5]. Based on these promising results, we aim to evaluate the suitability of AM parts for direct manufacturing of normal conducting linac structures. To that end, a reproduction of the beam pipe vacuum tests in [2, 3] was performed [6, 7]. Motivated by these successful preliminary experiments, a prototype cavity with a fully printed drift tube structure was constructed. The cavity is designed to be UHV capable and includes cooling channels reaching into the stems of the drift tube structure for power testing with a pulsed 30 kW rf amplifier.

Prototype Design and Concept

The prototype cavity was designed for a resonance frequency of 433.632 MHz, which is a harmonic of the GSI UNILAC operation frequency [8]. In combination with a targeted proton beam energy of 1.4 MeV this scenario allows for a compact accelerator at the limits of feasibility and is therefore a good benchmark for the new approach. The internal drift tube structure is fully 3D printed from stainless steel (1.4404), see Fig. 1a. Due to the lower complexity of the cavity frame and lids, they are manufactured by CNC milling of bulk stainless steel. Printing those parts would not be cost efficient.

The cavity is just 22 cm wide and 26 cm high (outer walls), with a length of 20 cm on the beamline (flange to flange). A center frame acts as the foundation for the cavity. This 7 cm high center frame provides the precision mount points for

the girder-drift tube structures and end-drift tubes. While the end-drift tubes are mounted in vacuum, the girders have a vacuum sealing surface at the bottom. Two half shells are mounted on the top and bottom of the center frame. The cavity is equipped with four CF40-Flanges for vacuum, rf-coupler and tuner, as well as metal sealed KF40 flanges for the beamline and smaller ports for diagnostics. Rf simulations show that the bulk of the rf losses during the operation of this cavity is concentrated on the drift tube structure and the cavity frame. Therefore, water channels are included in the girders up to the drift tubes and also in the center frame. A 3D CAD view of the full construction is shown in Fig. 1b.

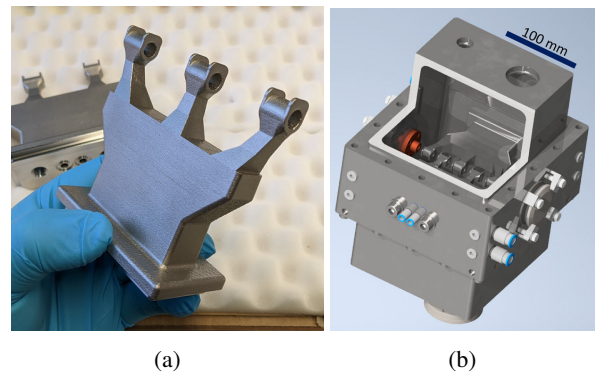


Figure 1: Overview of the cavity geometry and printed parts. (a) 3D printed girder drift tube structure. (b) Cross section of the assembled cavity model.

RF Simulations

The cavity design was optimized for a frequency of 433.632 MHz. To minimize the need for support structures during the manufacturing process, the shape of the girder-drift tube structure was optimized to reduce overhang. Simulations of electromagnetic fields in the cavity were performed with the CST Microwave Studio eigenmode solver. From the idealized design model, the simulated dissipated power for the effective acceleration voltage of $U_{eff} = 1$ MV is $P_{loss} = 24.82$ kW. With an inner wall length of 146 mm, this corresponds to an effective shunt impedance of $Z_{eff} = 287.13$ M Ω /m¹, showing the high efficiency of such an IH-type structure.

EXPERIMENTS

Since the first construction of the cavity in late 2020/early 2021, several experiments have been conducted to evaluate

¹ The stated value in [6] was much too low, due to a typo.

* Work supported by BMBF 05P21RFRB2

[†] haehnel@iap.uni-frankfurt.de

CAVITY R&D FOR HBS ACCELERATOR

N. F. Petry*, K. Kümpel, M. Schwarz, S. Lamprecht, O. Meusel, H. Podlech¹
 IAP, Goethe University Frankfurt, Frankfurt am Main, Germany

¹also at Helmholtz Research Academy Hesse for FAIR, Frankfurt am Main, Germany

Abstract

The demand for neutrons of various types for research is growing day by day worldwide. To meet the growing demand the Jülich High Brilliance Neutron Source (HBS) is in development. It is based on a high power linear proton accelerator with an end energy of 70 MeV and a proton beam current of 100 mA. The main part of the accelerator consists of about 45 CH-type cavities. As the current beam dynamic layout is still work in progress the number of cavities can change for the final design. For this beam dynamic layout the design of the CH-type cavities was optimized to handle the high accelerating gradient. The results of the performance of the CH-type cavities will be presented in this paper.

HBS

The High Brilliance Neutron Source (HBS) was first presented and published as a project in 2015/2016 [1,2]. Having a source at hand which relies on a proton linear accelerator with a high current to achieve the level of currently existing medium to high flux neutron sources in terms of neutron brilliance and flux is the goal. To reach that goal, the following specification, summarized in Table 1, need to be fulfilled by the linear accelerator.

Table 1: HBS Top-Level Requirements [3]

| Parameter | Specifications |
|--------------------|----------------------|
| Final energy | 70 MeV |
| Peak beam current | 100 mA |
| Particle type | Protons |
| Peak beam power | 7 MW |
| Average beam power | 952 kW |
| Beam duty factor | 13.6 % |
| RF duty factor | 15.3 % |
| Pulse length | 208/833/2000 μ s |
| Repetition rate | 96/24/48 Hz |

The initial approximated design consisted of 36 cavities. Due to the high proton current the first cavities need a lower acceleration gradient in order to keep the emittance of the beam as low as possible and the acceptance of the linear accelerator as high as possible. Furthermore additional CH-type cavities are needed as rebuncher cavities to assure a sufficient beam quality.

CH-TYPE CAVITIES

The 176.1 MHz linac should be as efficient as possible while being easy to maintain, as modular as possible and

* petry@iap.uni-frankfurt.de

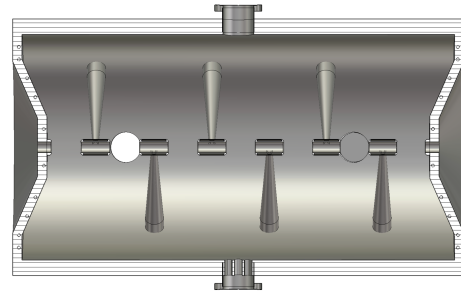


Figure 1: Side view of cross section of the used design for the HBS CH-type cavities.

have a low R&D effort. To meet those requirements with normal conducting accelerating cavities CH-type cavities will be used for the linac. The proposed design is shown in Fig. 1. The expected thermal load for the cavities will reach a maximum value of 25 kW/m. Therefore a cooling design was initially developed for the CH cavities and has been improved to handle the high acceleration gradient. The cooling design consists of one cooling channels for each stem, one for each tuning device, one for the power coupler, two for the lids and 24 for the tank. A view of the front of the cooling design is shown in Fig. 2. The highest thermal load and thus the most cooling effort will be on and around the stems, since those are the regions with the highest current inside the cavity. Hot spots are also in the middle section of the tank possible due to the mode used for acceleration, which is the TE₂₁₁-Mode. To account for the high acceleration gradient changes to the cooling design of the stems were made. The results of a thermal simulation and thus the operation of the enhanced cooling design is shown in Fig. 3. For a better comparison between the new design and the old design the enhanced design was applied only on the stem in the middle

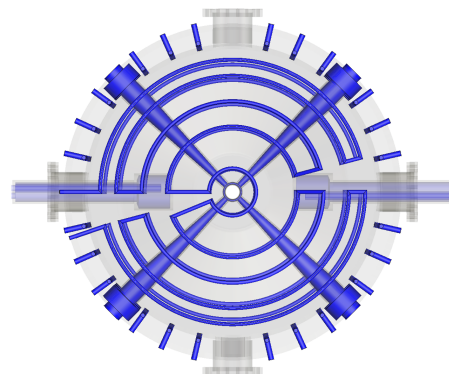


Figure 2: Front view of the enhanced cooling design from the CH-type cavities.

ACCELERATION EFFICIENCY OF TE-MODE STRUCTURES FOR PROTON LINACS

J. Tamura*, Y. Kondo, T. Morishita, JAEA/J-PARC, Ibaraki, Japan
 F. Naito, M. Otani, KEK/J-PARC, Ibaraki, Japan

Abstract

High-energy proton linacs generally consist of various types of cavity structures because the acceleration efficiency of a cavity depends on the velocity of the beam particle. Alvarez drift-tube linacs (DTLs) and transverse-electric (TE)-mode accelerating structures such as interdigital H-mode (IH) DTL and crossbar H-mode (CH) DTL are widely used in the low-energy section of the proton linacs. In this study, shunt impedances of these cavity structures, including higher-order TE₃₁ and TE₄₁ DTLs, are simulated by applying a very simple structural configuration. This study shows that TE_{*m*1} DTLs with smaller angular index *m* have higher shunt impedances whereas the axisymmetry of the electric field improves as *m* increases, and that the shunt impedances of TE₁₁ and TE₂₁ DTLs are higher than those of Alvarez DTLs especially in the low energy region immediately after a radiofrequency quadrupole (RFQ).

INTRODUCTION

Various types of cavity structures are generally used in high-energy proton linacs. This is, particularly in normal-conducting structures, because cavity's acceleration efficiency varies with the velocity of the beam particle. For low-energy proton beam acceleration, while Alvarez DTLs are the most prevalent, TE-mode structures, which could also be called H-mode structures, are also widely used. At present, the typical TE-mode accelerating structures are IH-DTL and CH-DTL [1–3], which are based on TE₁₁-mode and TE₂₁-mode pillbox cavities, respectively. Because the optimal cavity structure for proton linacs may be a subject of frequent argument [4], we investigated the acceleration efficiency of Alvarez DTLs and TE-mode accelerating structures including higher-order TE₃₁ and TE₄₁ DTLs. In this study, the shunt impedances of these cavity structures for proton energies of 2-100 MeV were simulated by using the CST Studio Suite.

SIMULATION MODEL

In this simulation study, 162 MHz TE-mode DTLs and 324 MHz Alvarez DTLs were examined by applying the following very simple structural configuration. Each cavity has four drift tubes (DTs) supported by stems and two end-cell half-DTs attached to the entry and exit lids, respectively. Therefore, Each cavity has five accelerating gaps. The stems were all rod-shaped with a fixed diameter of 20 mm for simplicity. The cell length, which is defined by the distance between adjacent gap centers, changes with the beam

velocity as $\beta\lambda/2$ for TE-mode DTLs and as $\beta\lambda$ for Alvarez DTLs, where β is the beam velocity relative to the speed of light and λ is the wavelength. For a given proton energy, the cell length of 162 MHz TE-mode DTLs is always the same as that of 324 MHz Alvarez DTLs.¹ Giving a priority to the structural simplicity, all cell lengths within a cavity were kept the same. Figure 1 shows the applied DT geometry. Whereas the ratio of gap length (*g*) to cell length was set to $g/(\beta\lambda/2) = 0.50$ for TE-mode DTLs, two ratios of $g/\beta\lambda = 0.50$ and 0.25 were applied for Alvarez DTLs. Figures 2-6 show examples of the simulation models for TE_{*m*1} DTLs (*m* = 1, 2, 3, 4) and Alvarez DTL ($g/\beta\lambda = 0.50$), which cell lengths and cavity diameters are adjusted for a 10 MeV proton beam. Each electric field distribution of the corresponding pillbox cavity is shown on the left side.

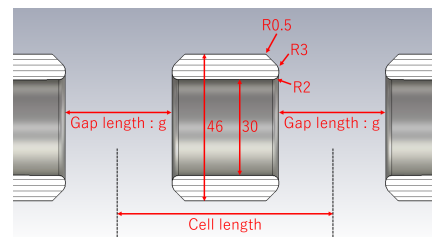


Figure 1: DT geometry applied to the simulation.

FIGURES OF MERIT

In each simulation model, only the cavity's transverse diameter was adjusted so that the resonant frequency becomes 162 MHz and 324 MHz for TE-mode DTLs and Alvarez DTLs, respectively. Obtained cavity diameters are shown in Fig. 7. The TE_{*m*1}-mode DTL has a smaller transverse diameter with smaller angular index *m*.

The longitudinal electric field distribution along the beam axis is essential for evaluating the cavity's acceleration efficiency. Figure 8 shows the obtained field distribution for the cavities accelerating a 10 MeV proton beam. In this figure, each field amplitude is normalized so that the stored energy is 1 Joule. Whereas the flat field distributions are produced in the Alvarez DTLs, the electric fields of the TE-mode DTLs decrease toward the end of the cavity because the TE field cannot exist parallel to the end walls of a conducting cavity. As shown in Fig. 8, the TE_{*m*1} DTL with smaller *m* provides higher gap voltage with respect to the unit stored energy, in other words, the so-called *r/Q* is larger in the lower-order

¹ For example, the cell lengths corresponding to the proton energies of 2, 10, 20, and 100 MeV are 60.3, 134.0, 188.1, and 396.2 mm with β 's of 0.065, 0.145, 0.203, and 0.428, respectively.

* jtamura@post.j-parc.jp

CURRENT STATUS OF THE SPOKE CAVITY PROTOTYPING FOR THE JAEA-ADS LINAC

J. Tamura*, Y. Kondo, B. Yee-Rendon, S. Meigo, F. Maekawa, JAEA/J-PARC, Ibaraki, Japan
 E. Kako, K. Umemori, H. Sakai, T. Dohmae, KEK/iCASA, Ibaraki, Japan

Abstract

The Japan Atomic Energy Agency (JAEA) has proposed an accelerator-driven system (ADS) to efficiently reduce high-level radioactive waste generated at nuclear power plants. As a first step toward the full-scale design of the CW proton linac for the JAEA-ADS, we are now prototyping a low- β (around 0.2) single spoke cavity. In 2021, we have started welding the cavity parts together. By preliminarily investigating the optimum welding conditions, each cavity part was joined with a smooth welding bead. Consequently, we have succeeded to fabricate the body section of the prototype spoke cavity.

INTRODUCTION

JAEA has proposed an ADS as a future project to efficiently reduce high-level radioactive waste generated at nuclear power plants. In the ADS, long-lived nuclides are transmuted to short-lived or stable ones. One of the challenging R&D aspects of the ADS is the reliability of the accelerator [1, 2]. In the JAEA-ADS, a high-power (30 MW) proton beam with a final beam energy of 1.5 GeV is required with high reliability. Because the accelerator needs to be operated in CW mode to be compatible with the reactor operation, a super-conducting (SC) linac would be a suitable solution. The latest design of the JAEA-ADS linac is reported in Refs. [3, 4]. As shown in Fig. 1, the proposed linac consists of a normal-conducting radio-frequency quadrupole (RFQ), half-wave resonator (HWR), low- β and high- β single-spoke resonators (SSR1 and SSR2, respectively), and low- β and high- β elliptical cavities (ELL1 and ELL2, respectively).



Figure 1: Accelerating structure proposed for the JAEA-ADS linac.

In preparation for the full-scale design of the JAEA-ADS linac, we have decided to prototype a low- β single-spoke cavity and conduct a high-field performance test of the prototyped cavity at liquid helium temperature. This prototyping will provide us with various insights on the development of SC cavities with $\lambda/2$ -mode resonance. Furthermore, through the high-field cavity testing, we will acquire valuable information such as how much accelerating gradient would be achievable with reasonable stability. Therefore, both prototyping and performance testing are essential to ensure the

feasibility of the JAEA-ADS linac. In this paper, the current status of the spoke cavity prototyping is presented.

DESIGNED CAVITY

The prototype spoke cavity with an operating frequency of 324 MHz was designed by electromagnetic simulation [5–7]. Figure 2 shows the cross-sectional views of the designed cavity. The cavity's design parameters are listed in Table 1. The multipactor analysis for the designed cavity without the coupler ports is presented in Ref. [6].

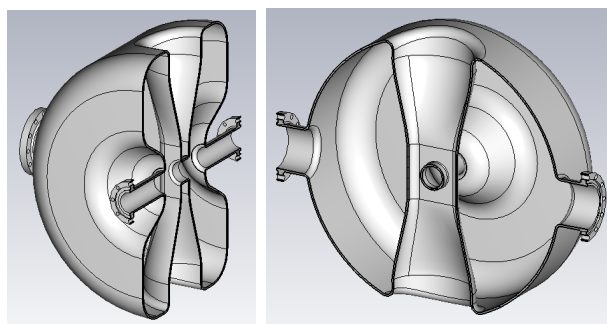


Figure 2: Cross-sectional views of the designed cavity.

Table 1: Design parameters of the prototype spoke cavity.

| Parameter | Value |
|--------------------------------|------------------|
| f_0 | 324 MHz |
| β_g | 0.188 |
| β_{opt} | 0.24 |
| Beam aperture | 40 mm |
| Cavity diameter | ≈ 500 mm |
| Cavity length | 300 mm |
| $L_{eff} = \beta_{opt}\lambda$ | 222 mm |
| $G = Q_0 R_s$ | 90 Ω |
| $T(\beta_{opt}) = V_{acc}/V_0$ | 0.81 |
| $r/Q = V_{acc}^2/\omega W$ | 240 Ω |
| E_{peak}/E_{acc} | 4.1 |
| B_{peak}/E_{acc} | 7.1 mT/(MV/m) |

CAVITY FABRICATION

The fabrication process for the prototype spoke cavity was reviewed in fiscal year 2019, and the actual cavity fabrication started in 2020. The prototype spoke cavity is made of pure niobium (Nb) except for the niobium-titanium alloy (Nb-Ti) flanges for the RF ports and beam ports. These materials were provided by Tokyo Denkai Co., Ltd. Most of the cavity

* jtamura@post.j-parc.jp

OPERATION OF THE H⁻ LINAC AT FNAL*

K. Seiya[†], T. Butler, D. Jones, V. Kapin, K. Hartman, S. Moua, J. -F. Ostiguy, R. Ridgway, R. Sharankova, B. Stanzil, C. Y. Tan, J. Walters, M. Wesley
Fermi National Accelerator Laboratory, Batavia 60510 IL, USA
M. Mwaniki
Illinois Institute of Technology, Chicago, IL 60616, USA

Abstract

The Fermi National Accelerator Laboratory (FNAL) Linac has been in operation for 52 years. In approximately four years, it will be replaced by a new 800 MeV superconducting machine, the PIP-II SRF Linac. In the current configuration, the Linac delivers H⁻ ions at 400 MeV and injects protons by charge exchange into the Booster synchrotron. Despite its age, the Linac is the most stable accelerator in the FNAL complex, reliably sending 22 mA in daily operations. We will discuss the status of the operation, beam studies, and plans.

INTRODUCTION

FNAL is leading the intensity frontier by providing high intensity proton beams to high energy experiments. The Linac delivers H⁻ ions at 400 MeV to inject protons by charge exchange into the Booster, a 15 Hz rapid cycling booster synchrotron.

H⁻ beam is supplied to the Linac by an RFQ injection line (RIL) which consists of a magnetron ion source, a low energy beam transport (LEBT), a radio frequency quadrupole (RFQ) with acceleration from 35 to 750 keV and a medium energy beam transport (MEBT) with a buncher cavity [1]. The Linac is divided into two sections: (1) a 201.25 MHz Drift Tube Linac (DTL) where the H⁻ beam is accelerated to 116 MeV [2] and (2) a 805 MHz Side Coupled Linac (SCL) which further accelerates the beam to 400 MeV [3].

The Linac has been in operation for 52 years and reliably sends 22 mA in daily operations. Our present goals are:

- Minimizing machine downtime and providing stable beam to users.
- Increasing the output current to more than 30 mA.
- Using Machine Learning (ML) to optimize RF parameters and automate machine tuning.

In this paper, we present the history and status of the beam operation and machine studies for the last 5 years.

STATUS OF OPERATION

The Proton Improvement Plan (PIP) aimed to run 4.3E12 protons per pulse in the Booster at 15 Hz and successfully accomplished its goal in 2017 [4]. As a part of PIP, modulators for the DTL RF system were upgraded for more reliable operations [5]. With 24/7 user support as our first

priority, the Linac has been providing 22 mA consistently with 96 % machine up-time for the last 5 years.

Beam Current and Efficiency

The beam current in the LEBT, upstream of the Linac, and end of the Linac at 400 MeV are shown in Fig. 1. The transmission efficiency in RIL has been 40 % and Linac 92 %. In 2017, a collimator with an aperture size of 9.9 mm × 14.5 mm was installed in front of the Linac in order to minimize beam loss in the Booster. The average RMS beam sizes are ±2.7 mm horizontal and ±3.5 mm vertical.

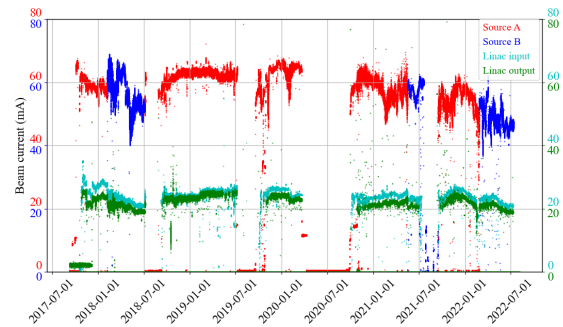


Figure 1: Linac beam current over last 5 years.

Two major machine failures occurred in the last 5 years (Fig. 2). A water leak damaged a quadrupole magnet in a drift tube (DT) in Tank 5 and caused an intermittent short on the wire around the quadrupole magnet. Replacing the exposed wires on the tank and isolating the quadrupole magnet from the ground took 72 hrs. An end plate on Tank 4 was missing one push screw, which was supposed to push the plate to the flange for a good RF contact, thus creating a gap which caused a spark in the cavity. A comparison between the three gradient detector signals at low, mid, and high energies in the tank indicated that the spark occurred at lower energy. Finding the source and completing the repair took 112 hrs.

Drift Tube Replacement and Alignment

Rebuilding DT The DTL has 207 DTs in Tank 1 - Tank 5. Each DT was built with oxygen free high conductivity copper and contains a quadrupole magnet that isolates it from a vacuum. The length varies from 48 mm to 409 mm throughout the Linac, and the bore size varies in different tanks. Twelve DT failures have been recorded since 1986 and four DTs were replaced in the last 4 years in Tank 2 –

* Work supported by Fermilab Research Alliance, LLC under Contract No. DE-AC02-07CH11359 with the United States Department of Energy

[†] kiyomi@fnal.gov

DEVELOPMENT OF HIGH-GRADIENT ACCELERATING STRUCTURES FOR PROTON RADIOGRAPHY BOOSTER AT LANSCE

S. S. Kurennoy, Y. K. Batygin, and E. R. Olivas, LANL, Los Alamos, NM 87545, USA

Abstract

Increasing energy of proton beam at LANSCE from 800 MeV to 3 GeV improves radiography resolution ~ 10 times. We propose accomplishing this energy boost with a compact cost-effective linac based on normal conducting high-gradient (HG) RF accelerating structures. Such an unusual proton linac is feasible for proton radiography (pRad), which operates with very short beam (and RF) pulses. For a compact pRad booster at LANSCE, we have developed a multi-stage design: a short L-band section to capture and compress the 800-MeV proton beam from the existing linac followed by the main HG linac based on S- and C-band cavities, and finally, by an L-band de-buncher. Here we present details of development, including EM and thermal-stress analysis, of proton HG structures with distributed RF coupling for the pRad booster. A short test structure is designed specifically for measurements at the LANL C-band RF Test Stand.

INTRODUCTION

Proton radiography employs high-energy proton beams to image material behavior under extreme conditions. It was invented and developed at LANL. The pRad program at the Los Alamos Neutron Science Center (LANSCE) has performed hundreds of successful experiments, both static and dynamic. While the LANSCE 800-MeV linac accelerates both protons and H^- ions, the pRad uses H^- beam, which is presently the only beam species that can be chopped in the front end and directed to the pRad facility. For dynamic experiments, pRad uses multiple pulses from the linac, which produce movies up to a few tens of frames. Each short pRad beam pulse consists of several successive bunches from the linac, which follow at the linac DTL repetition rate of 201.25 MHz, to multiply the pulse total intensity. This is because the H^- bunch current at 800 MeV is limited to ~ 10 mA, mainly by the ion source, but also by losses in the linac. On the other hand, the pRad pulses are restricted to 80 ns in length, i.e., contain no more than 16 linac bunches, to prevent image blur.

Increasing the beam energy for pRad at LANSCE from present 800 MeV to 3 GeV would provide significant improvements: for thin objects, the radiography resolution would increase about 10 times, and much thicker objects could be also imaged [1]. A superconducting (SC) option for a pRad booster to 3 GeV was considered in [1]. With a real-estate gradient of 15 MV/m, it leads to a rather long booster, more than 150 m only in accelerating structures. This option is also expensive because it requires a new cryogenic plant and significant tunnel modifications. We proposed a shorter and cheaper pRad booster based on normal-conducting RF accelerating structures with higher gradients operating at low duty factors [2].

HIGH-GRADIENT PRAD BOOSTER

Requirements for pRad Booster Cavities

HG structures with phase velocity $\beta = 1$ were developed for acceleration of electrons [3]. Accelerating gradients up to 150 MV/m have been demonstrated in X-band copper cavities at room temperature. When such cavities are operated at cryogenic temperatures (cryo-cooled), gradients up to 250 MV/m were achieved. HG C-band cavities at room temperature provide gradients 50-60 MV/m, but at liquid-nitrogen (LN_2) temperature one can expect gradients two times higher. 800-MeV protons at the exit of the LANSCE linac have velocity $\beta = v/c = 0.84$, and at 3 GeV $\beta = 0.97$. Therefore, HG cavities must be modified for protons to cover this velocity range.

Operating the HG pRad booster at liquid-nitrogen temperatures makes structures more efficient and reduces the required RF power by a factor of 2-3. Such operation of pRad booster seems practical: the pRad needs only 1-20 beam pulses per event spread by about 1 μ s; no more than a few events per day. Even if some nitrogen evaporates due to heating caused by RF losses in cavity walls during one event, it can be easily refilled before the next one.

There are additional requirements for HG structures for pRad booster. First, they must accept the large proton bunches out of the existing linac both longitudinally – this limits RF frequency from above – and transversely, which limits the cavity aperture from below. Second, high accelerating gradients lead to beam defocusing by RF fields, so a strong focusing is required. There are also important requirements to the output beam: energy stability pulse-to-pulse, pulse timing, and low energy spread. For better quality of radiographs, it is desirable to reduce the relative momentum spread, $dp/p = 10^{-3}$ at the exit of our 800-MeV linac, as $1/p$, i.e., to $3.3 \cdot 10^{-4}$ at 3 GeV.

Further considerations are related to the LANSCE layout and operations. The facility delivers five different beam types [4] to multiple users, and it is important to preserve this capability. The closest point where a new booster can start is about 38 m away from the 800-MeV linac exit, after the existing switchyard. The exiting beam spreads in this drift, so we need to lower RF frequency in the first cavities to capture it longitudinally. All the above requirements led to a multi-stage compact booster design [5].

pRad Booster Design

The booster starts with an L-band buncher operating at 1408.75 MHz, the 7th harmonic of the linac bunch frequency 201.25 MHz, to capture 800-MeV linac bunches. The booster includes S-band structures at 2817.5 MHz to the energy of 1.6 GeV and continues with C-band struc-

CST MODELING OF THE LANSCE COUPLED-CAVITY LINAC

S. S. Kurennoy and Y. K. Batygin, LANL, Los Alamos, NM 87545, USA

Abstract

The 800-MeV proton linac at LANSCE consists of a drift-tube linac, which brings the beam to 100 MeV, followed by 44 modules of a coupled-cavity linac (CCL). Each CCL module contains multiple tanks, and it is fed by a single 805-MHz klystron. CCL tanks are multi-cell blocks of identical re-entrant side-coupled cavities, which are followed by drifts with magnetic quadrupole doublets. Bridge couplers – special cavities displaced from the beam axis – electromagnetically couple CCL tanks over such drifts within a module. We have developed 3D CST models of CCL tanks. The models are used to calculate electromagnetic fields in the tanks. Beam dynamics is modeled in CST for bunch trains with realistic beam distributions using the calculated RF fields and quadrupole magnetic fields. Beam dynamics results are crosschecked with other multi-particle codes and applied to evaluate effects of CCL misalignments.

INTRODUCTION

Realistic 3D models of accelerator structures proved to be useful for studying various EM effects, mechanical tolerances, and beam dynamics. One example is CST models of LANSCE drift-tube linac (DTL) tanks [1]. On various occasions, they were used to calculate details of DTL element heating, tuning sensitivities, fine features of beam dynamics and particle losses. Another example is CST modeling of the FNAL 4-rod RFQ. We received a CAD model of this RFQ from its manufacturer, Kress GmbH, to help us evaluate a 4-rod RFQ option for LANL. The CAD model was imported into CST [2] and simplified for EM analysis. Our EM calculations revealed unexpected longitudinal fields in the end gaps, which are purely 3D effects and were not (and could not be) taken into account in the RFQ designed with standard codes. The beam dynamics study with CST Particle Studio showed that the end-gap field reduced the beam output energy. This incidental discovery helped our FNAL colleagues to understand the reason for the incorrect RFQ output energy, which puzzled them for over a year before that, and showed how to correct it [3]. Fortunately, the fix was easy: just removing an end-wall plug in the RFQ outer box.

Here we apply a similar approach to the LANSCE coupled cavity linac (CCL). As a first step, we build a simplified CST model of the first CCL tank (T1) in the module 5 (M5T1). The model is fully parametrized and applicable for all tanks in the CCL modules. More details and pictures can be found in the report [4]. All geometrical and design electromagnetic parameters of CCL cavities are summarized in the original 1968 document [5].

CST MODELING OF CCL

EM Model of Module 5 Tank 1 (M5T1)

The first module of CCL, module 5 (M5; the count includes four preceding DTL modules), starts at beam energy of 100 MeV and consists of four tanks. Each tank in M5 contains 36 identical re-entrant accelerating cavities (cells, AC), which are side coupled by 35 coupling cavities (CC). The coupling cavities are located off axis (side-coupled structure) and alternate their transverse positions on both sides of the beam path. Drifts after each tank contain a doublet of two EM quadrupole magnets. For M5T1, the AC length is 8.0274 cm and inner radius 12.827 cm. The tank total length is 289 cm, and the drift after T1 is 72.3 cm.

The CST model of the AC cavity starts with creating a parametrized profile curve for a quarter of the cavity vacuum volume, making a figure of rotation, and its mirroring. The CC vacuum volume is then added to the AC, and the edges of the coupling slot formed by the AC-CC intersection are rounded. After that, the cavity frequency is tuned to the operating mode frequency, 805 MHz, by adjusting the AC gap. In practice, some additional metal was left on the drift-tube noses of manufactured half-cavities, and it was scraped by a special tool to adjust the frequency before cavity brazing. We follow a similar procedure in our CST model by adjusting the AC gap width, using an optimizer in the CST eigensolver. To find all the tank modes, we need to consider bridge couplers. The end cells are tuned such that the field amplitudes there for operating mode are the same as in inner cells, so it is sufficient to calculate fields in one structure period, shown in Fig. 1.

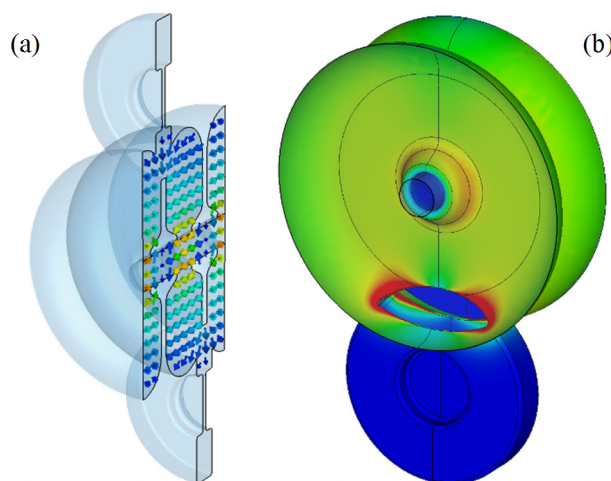


Figure 1: Electric field (a) and surface-current magnitude on the cavity inner surface (b) in one period of M5T1. Red color indicates higher values, blue – lower ones.

DESIGN OF IH-DTL TO ACCELERATE INTENSE LITHIUM-ION BEAM FOR COMPACT NEUTRON SOURCE

S. Ikeda, T. Kanetsue, and M. Okamura

Collider-Accelerator Department, Brookhaven National Laboratory, Upton, NY, USA

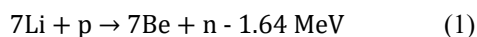
Abstract

We are studying feasibility of a compact neutron source with a lithium-ion beam driver. The neutron source comprises a laser ion source, an RFQ linac, and an IH-DTL. Recently, we demonstrated 35-mA ${}^7\text{Li}^{3+}$ ion beam acceleration by an RFQ linac with a laser ion source. Based on the result, we performed beam dynamic design of an IH-DTL to accelerate the lithium-ion beam to the energy required for the neutron production, 14 MeV. To obtain a realistic field distribution, we made a rough model of the IH-DTL cavity with Microwave studio. It was confirmed with GPT 3D beam simulation that 1.7-m and 200-kW IH-DTL with two triplets can accelerate 30-mA ${}^7\text{Li}^{3+}$ beam.

INTRODUCTION

Accelerator-driven compact neutron sources have attracted great attention because of the wide range of the applications, such as non-destructive inspection for defects of buildings and explosive material in cargo[1]. They are composed of an MeV-class accelerator and a neutron conversion target. The availability coming from the compactness and the relatively low cost is also desirable for industrial and educational users. Recently, even portable neutron source has been developed for the purpose of inspection of infrastructures. They are also interested as alternative for small neutron reactors.

For the moderate range of neutron flux, proton accelerators with lithium or beryllium targets are used. Especially for lithium target, the neutrons are generated by the nuclear reaction.



The proton energy is slightly higher than the threshold value, typically 2.4 MeV. Because this reaction is endothermic, the energy distribution of the neutrons is narrow. Meanwhile, the neutrons are produced in all direction due to the small velocity of the center of mass. Only the part in the forward direction is used for the applications. In contrast to the conventional neutron sources, we are proposing a lithium-ion beam driver with a laser ion source[2]. It is composed of a laser ion source, an RFQ linac, and an IH-DTL. The features of the use of the laser ion source are lithium projectile 1) and a pulsed beam with high peak current and short width 2). The type of ion is ${}^7\text{Li}^{3+}$. The peak current, the pulse width, the repetition rate will be 30 mA, 0.1 to 10 μs , and 1 to 1 kHz, respectively. With a lithium projectile, the velocity of the center of mass is larger than with a proton projectile. This leads to a narrow angular distribution of the neutrons. This effect is called kinematic focusing demonstrated with simulation and experiments[3]. The generated neutrons are in forward direction and can be

used at downstream. The enhancement factor compared with proton injection can be factor of ten[3]. Furthermore, the background neutrons are less and the shielding can be lighter, which leads to lower cost and better portability. Regarding the pulse and peak current, laser ion sources are known with the ability to produce intense pulsed beam. The beam current is several orders of magnitudes higher than conventional heavy ion sources. The pulse width can be adjusted to 1 μs or shorter. The beam with the high peak current and short width is advantageous for pulsed neutron beam applications since the short pulse neutron beam will enable users to separate the background neutrons from the probe beam, resulting in a good signal-to-noise ratio.

The advantage of the lithium projection is obvious, but it was not practical because the beam current of conventional heavy ion machines is low. Meanwhile, it was proved that a combination of a laser ion source and an RFQ linac can produce large beam current by using Direct Plasma Injection Scheme[4]. By applying this scheme, the intense lithium driver will be able to be used to neutron sources.

In previous study, we recently succeeded to accelerate 35 mA of ${}^7\text{Li}^{3+}$ ion beam by an RFQ linac[5]. As a next step, we designed an IH-DTL to accelerate the beam to the nuclear reaction threshold, 14 MeV[3]. We are considering IH-DTL as the second accelerator after the RFQ linac because of the high efficiency for the energy range. We checked the feasibility and the specification of the IH-DTL for the intense beam. The design was mainly about the beam dynamics. An RF simulation with a rough model was done with CST studio to obtain the electric field distribution for particle tracking. More practical cavity design will be next step.

IH-DTL DESIGN

The parameters of the input beams were from the beam parameters from the existing RFQ linac. The input energy is 1.43 Me, the transverse and longitudinal 90 % normalized emittances are 3 π mm mrad and 0.54 MeV-deg, respectively. The beam current was set to 40 mA to have some margin to accelerate the 35 mA from the RFQ linac. The longitudinal emittance was the calculated value by Parmteq in design. To estimate the transverse emittance, trace3D simulation was performed for the analyzing line in the previous study to compare with the experimental result. The simulation revealed that the maximum emittance to propagate the dipole is 3 π mm mrad containing 90 % of ions. In other word, with larger emittance than 3, the transmission was worse than the previous experiments. So, 3 π mm mrad was selected as the input parameter for the IH-DTL.

PRELIMINARY STUDY ON THE CRYOGENIC CONTROL SYSTEM WITHIN RF SUPERCONDUCTIVE LINAC PROJECTS

H. Sibileau, M. Beniken, T. Junquera, Accelerators and Cryogenic Systems, Orsay, France
D. Masson, Isii-Tech, Saint-Étienne-du-Rouvray, France

Abstract

Several RF Superconductive LINAC projects are underway in different laboratories around the world, with various objectives such as research in physics, irradiation tests, production of radioisotopes for medical purposes. Superconducting operation of the accelerating cavities requires them to be maintained at cryogenic temperatures (2K - 4K) by the use of cryogenic fluids. This requires a complete cryogenic control system, including sensors, actuators, local controllers and PLCs. We describe the process by which the preliminary design of the cryogenic control system for the accelerator's cryomodules and valve boxes may be built. It starts with the functional and performance requirements of the system, followed by the definition of use cases and the study of the necessary cryogenic instrumentation. This leads to a preliminary design of the architecture of the cryogenic control system using Siemens hardware, as well as cryogenic sequences describing standard phases of operation of the LINAC. We also discuss how to take advantage of the modularity of cryomodules for control system implementation and some recent developments in PLC simulation.

INTRODUCTION

In general, the cryogenic infrastructure installed on a SC Linac includes 3 major layers (Fig. 1):

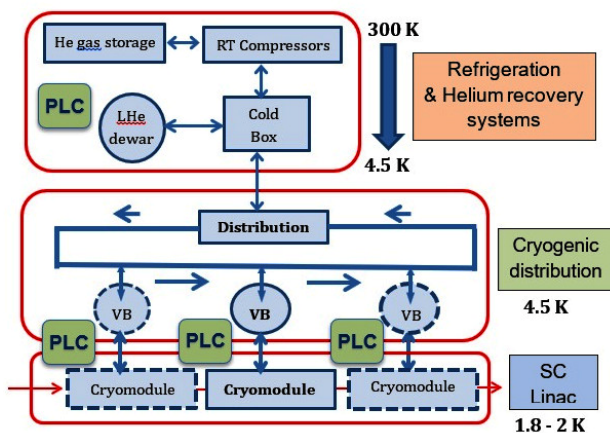


Figure 1: SC Linac, main cryogenic components.

- Refrigerator, helium recovering and storage systems
- Cryogenic distribution: multi lines connecting the refrigerator to the SC Linac.
- SC Linac components (Cryomodules, Valve Boxes)

All the 3 layers are controlled, for cryogenic operation, by industrial PLC systems. A standard solution adopted in many facilities is to install a PLC for the control of each pair {Cryomodule + Valve Box}. This is a major requirement in order to adapt to the different accelerating gradients and associated dynamic losses.

In this paper we focus on the control system (PLC) of the pair {Cryomodule + Valve Box}. For the prototyping phase, a close development is to control only a pair (CM+VB). In this case the CM + VB are installed in a test room, connected to different cryogenic supply systems (LHe dewars, He pumping systems, ...) but using most of the sensors and actuators that will be installed in the final SC Linac.

PHYSICAL EQUIPMENT, SENSORS, ACTUATORS, INTERFACES

Safe operation and stability of the SC Linac Cryogenic systems (Cryomodules and Valve Boxes) are two major requirements for all the operation phases. The associated control system based on PLC must assume this responsibility. Other important requirements are the connection of these "local" PLC to the overall Linac security systems (machine protection system MPS, personnel protection system PPS) and to the facility infrastructures (electrical distribution, cooling, HVAC, vacuum systems, etc.)

All the operation process are based on dedicated sensors and actuators installed within the SC Linac Cryogenic systems, connected through special interfaces to the PLC. On the other side, using supervisory tools and networks, the PLC must be interfaced to the high-level control process (databases, MPS, PPS, infrastructures etc.) using adapted IOC (Input/Output Controllers) operating under EPICS [1] software environment.

Sensors within the Cryomodules and the Valve Boxes, are difficult to be replaced in short delays, and need to be redundant. Other redundancy that may be considered are the process controllers (complete PLC or partial critical hardware as CPU and I/O systems), data networks and associated power supplies.

In parallel with the major control role and safety aspects, the Cryogenics Instrumentation will deliver interesting measurements for the SC Cavities and RF Couplers

A SUPERCONDUCTING 217 MHz SINGLE SPOKE CAVITY FOR THE HELMHOLTZ LINEAR ACCELERATOR AT GSI *

F. Dziuba^{1,2,4†}, K. Aulenbacher^{1,2,4}, W. Barth^{1,2,4}, M. Basten², C. Burandt², T. Conrad³,
 V. Gettmann^{1,2}, T. Kürzeder^{1,2}, S. Lauber², J. List^{1,2,4}, M. Miski-Oglu^{1,2}, H. Podlech³,
 M. Schwarz³, S. Yaramyshev²

¹HIM Helmholtz Institute Mainz, 55099 Mainz, Germany

²GSI Helmholtzzentrum für Schwerionenforschung GmbH, 64291 Darmstadt, Germany

³IAP Goethe University Frankfurt, 60438 Frankfurt am Main, Germany

⁴KPH Johannes Gutenberg University Mainz, 55128 Mainz, Germany

Abstract

A new superconducting (SC) continuous wave (CW) linac, providing high efficient heavy ion acceleration above the coulomb barrier, is going to be built at GSI to fulfill the upcoming demands in the research field of super heavy element (SHE) synthesis. The so-called HELIAC (HELMholtz LInear ACcelerator) delivers ion beams in the energy range of 3.5 MeV/u and 7.3 MeV/u with a mass to charge ratio (A/z) of up to 6. Superconducting multi-gap crossbar-H-mode (CH) cavities with a resonance frequency of 217 MHz are used for beam acceleration. In addition, SC single spoke buncher cavities should ensure longitudinal beam matching to the following CH sections. Therefore, the first 217 MHz single spoke cavity with $\beta = 0.07$ has been developed at HIM/GSI. In this paper the design of the cavity and first RF measurements during manufacturing are presented.

INTRODUCTION

After the reliable operability of SC CH cavities [1, 2] with beam at 4 K was successfully shown within the demonstrator project [3–7], the next step on the way realizing the proposed HELIAC [8–10] is the construction, commissioning and operation of the so called 'Advanced Demonstrator' CM1 cryomodule [11]. In future, the Advanced Demonstrator is foreseen to be used as the first of a series of up to four cryomodules (CM1–CM4) of the entire HELIAC accelerator. The new CM1 will be fully equipped with three SC CH cavities, a SC single spoke resonator (SSR) and two SC solenoids (see Fig. 1). In 2021, cryomodule CM1 has been successfully tested within SAT at HIM/GSI under 4 K conditions. Meanwhile, all mentioned components have been built and delivered to GSI. Currently, cold string assembly of CM1 is taking place in the ISO4 cleanroom at HIM [12].

BUNCHER CAVITY LAYOUT

The first layout of a SC 217 MHz SSR with a particle velocity of $\beta = 0.07$ for CM1 has been presented in [13, 14]. Based on this early design, the cavity has been optimized regarding compactness, electrical and magnetic peak fields, the appearance of multipacting and its pressure sensitivity.

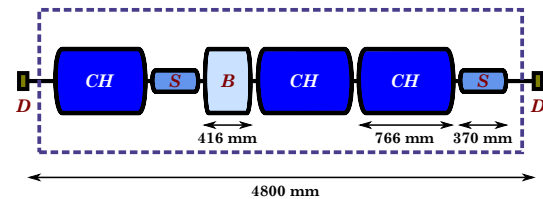


Figure 1: Layout of cryomodule CM1 containing three CH cavities, a single spoke buncher (B) and two solenoids (S).

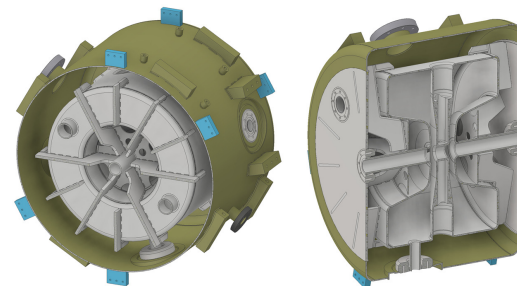


Figure 2: 3D-model of the SC 217 MHz SSR.

The optimized cavity (see Fig. 2) is 416 mm long and has an equidistant gap length of 13 mm. A dynamic bellow tuner inside the cavity allows slow and fast frequency adjustment during operation at 4 K. Furthermore, a helium jacket made from titanium provides a closed helium circulation around the cavity. Two additional flanges at each end cap of the cavity allow adequate surface processing. The main parameters of the cavity are summarized in Table 1. Due to its compact geometry within the mentioned velocity and frequency domain the resonance frequency of the cavity is extremely sensitive to external influences. This makes the design, the construction and operation of such a type of cavity to be extremely challenging tasks. Nevertheless, as described in [15] stable cavity beam operation is quite possible.

RF MEASUREMENTS

The manufacturing of the SSR started in 2020. Several RF measurements during the production process have been performed in order to achieve the target frequency. All important steps were carried out on the basis of detailed RF and structural-mechanical simulations. Initially, the resonance frequency was designed to be higher than the target fre-

* Work supported by BMBF Contr. No. 05P18UMRB2

† f.dziuba@gsi.de

CONSERVATION OF QUALITY FACTOR FOR SUPERCONDUCTING CAVITY AND HEARTBEAT UNDER RELATIVISTIC MOTION

Heetae Kim

Rare Isotope Science Project, Institute for Basic Science, Daejeon, Republic of Korea

Abstract

The conservation of quality factor under relativistic motion is applied to the superconducting cavity as well as the heartbeat of mammal. The quality factor of the superconducting cavity is conserved under relativistic motion. The frequency of the cavity decreases and the decay time increases as the velocity and acceleration are increased. The quality factor of the superconducting cavity is comparable with the total heartbeat of the mammal. The quality factor for the heartbeat of the mammal representing the total number of heartbeat is also conserved under relativistic motion. Therefore, the heart rate is inversely proportional to the life expectancy under relativistic motion.

INTRODUCTION

Superconducting niobium cavity was developed well and was shown to have very high quality factor. Thermionic emission, field emission, and generalized electron emission were studied [1-5]. The superconducting cavities of the quarter-wave resonator (QWR) and the half-wave resonator (HWR) for RAON accelerator were developed [6-9]. Generalized Doppler effect was investigated for arbitrary velocity and acceleration [10]. The heart rate and life expectancy of mammal were studied [11, 12]. In this research we show the quality factor conservation for the superconducting cavity and the heartbeat of the mammal. The frequency-energy relation, Doppler effect, and energy conservation are presented. The frequency and the decay time of the superconducting cavity in reference frame is shown as a function of velocity and acceleration. The heart rate and lifespan of the mammal in reference frame are also calculated as a function of velocity and acceleration.

FREQUENCY-ENERGY RELATION

We postulate the conservation of frequency-energy relation. The product of frequency and energy for a particle is always conserved as

$$E(i)f(i) = \text{constant}, \quad (1)$$

where E is the energy and f is the frequency. The frequency-energy relation can also be expressed as

$$E(x)f(x) = E(v)f(v) = E(a)f(a), \quad (2)$$

where x is the position, v is the velocity, and a is the acceleration.

DOPPLER EFFECT

Frequency shift for constant velocity and acceleration can be calculated from Doppler effect.

The frequency for constant velocity in reference frame is shifted to

$$f(v) = f_o \sqrt{1 - (v/c)^2}, \quad (3)$$

where c is the speed of light.

The frequency for constant acceleration in reference frame is shifted to

$$f(a) = f_o \sqrt{1 - (2ax/c^2)}. \quad (4)$$

The frequency decreases as the velocity and acceleration are increased.

ENERGY FOR MOTION

From the frequency-energy relation and Doppler effect, the energy of a body can be calculated. The frequency-energy relation for constant velocity is

$$E(v) = E(0) \frac{f(0)}{f(v)}. \quad (5)$$

The energy for constant velocity can be expressed as

$$E(v) = \frac{m_o c^2}{\sqrt{1 - (v/c)^2}}, \quad (6)$$

where m_o is the rest mass of the body.

The frequency-energy relation for constant acceleration becomes

$$E(a) = E(0) \frac{f(0)}{f(a)}. \quad (7)$$

The energy for constant acceleration can be expressed as

$$E(a) = \frac{m_o c^2}{\sqrt{1 - \frac{2ax}{c^2}}}. \quad (8)$$

The energy for constant velocity is the same as that of special relativity. The energy of the body increases as the velocity and acceleration are increased.

* This work was supported by the Rare Isotope Science Project of Institute for Basic Science funded by the Ministry of Science and the National Research Foundation (NRF) of the Republic of Korea under Contract 2013M7A1A1075764.

† kimht7@ibs.re.kr

UNDERSTANDING Q SLOPE OF SUPERCONDUCTING CAVITY WITH MAGNETIC DEFECT AND FIELD EMISSION

Heetae Kim^{1,*}, Sungmin Jeon², Yoochul Jung¹, Juwan Kim¹, Hyunik Kim¹
¹Rare Isotope Science Project, Institute for Basic Science, Daejeon, Republic of Korea
²Department of Physics, Kyungpook National University, Daegu, Republic of Korea

Abstract

RF test for quarter-wave resonator (QWR) and half-wave resonator (HWR) superconducting cavities is performed at low temperature. The quality factors of the superconducting cavities are measured as a function of accelerating field. The magnetic heating effect for the quarter-wave resonator (QWR) is studied. For the half-wave resonator (HWR), the Q slope degradation is investigated with x-ray radiation and field emission.

INTRODUCTION

Development of superconducting cavities is very important to construct a heavy ion accelerator. Vertical test facility to test the performance of the superconducting cavities was designed and constructed [1, 2]. Field emission and thermionic emission were studied in terms of dimensions [3-5] and the unified theory for the field emission and thermionic emission was also investigated [6, 7]. The field emission of a superconducting niobium cavity was investigated [8]. The quarter-wave resonator (QWR) and the half-wave resonator (HWR) cavity of RAON accelerator at Rare Isotope Science Project (RISP) were developed [9-12], and the cryomodule and cavity for the HWR were tested at 2 K [13, 14]. In this research we show the Q slopes for the quarter-wave resonators (QWRs) and the half-wave resonators (HWRs). The Q slope degradation for the QWR cavities is studied with magnetic defects while the Q slope degradation for the HWR cavities is investigated with x-ray radiation and the field emission.

MAGNETIC HEATING AND FIELD EMISSION

The quality factor of a superconducting cavity is degraded by magnetic heating, field emission, and x-ray radiation. The quality factor of the cavity is denoted as

$$Q_o = \frac{G}{R_{\text{Sur}}}, \quad (1)$$

where G is the geometric factor and R_{Sur} is the surface resistance. The surface resistance can be represented as

$$R_{\text{Sur}} = R_{\text{Res}} + R_{\text{BCS}}, \quad (2)$$

where R_{Res} is the residual resistance and R_{BCS} is the BCS resistance.

* This research was supported by the RISP of ibs funded by the Ministry of Science and the National Research Foundation (NRF) of the Republic of Korea under Contract 2013M7A1A1075764.

* kimht7@ibs.re.kr

Dissipated power on the cavity surface is

$$P_{\text{dis}} = \frac{1}{2} \int R_s |H(r)|^2 dS, \quad (3)$$

where H is the magnetic field strength.

The BCS resistance is expressed as

$$R_{\text{BCS}} = \frac{C_1 f^2}{T} \exp\left(-\frac{\Delta}{k_B T}\right), \quad (4)$$

where Δ is the band gap and C_1 is the constant.

The band gap is expressed as [15]

$$\Delta = \Delta_0 - MB_{\text{peak}}, \quad (5)$$

where M is the magnetic moment and B_{peak} is the peak magnetic field strength.

From Eq. (2), Eq. (4), and Eq. (5) the surface resistance can be denoted as

$$R_{\text{Sur}} = \frac{C_1 f^2}{T} \exp\left(-\frac{\Delta_0}{k_B T} + \frac{MB_{\text{peak}}}{k_B T}\right) + R_{\text{Res}}. \quad (6)$$

The current density of field emission is denoted as

$$J = \frac{e\sqrt{E_F} F^2}{2\pi h(\Phi_W + E_F)\sqrt{\Phi_W}} e^{-4k\Phi_W^{1.5}/3F}, \quad (7)$$

where F is the electric field, E_F is the Fermi energy, and Φ_W is the work function. The field emission current is generated by the particles and surface curvatures from the superconducting cavity.

The average current from the field emission for AC current is [14]

$$\langle I \rangle = \frac{C_2 e\sqrt{E_F} F^{2.5} \beta^{2.5}}{h\sqrt{k}(\Phi_W + E_F)\Phi_W^{0.75}} e^{-4k\Phi_W^{1.5}/3F\beta}, \quad (8)$$

where β is the field enhancement factor and C_2 is the proportional constant. The field emission site is heated with Joule heating and the electrons generated from the field emission are accelerated and generate x-ray. The x-ray generation increases with increasing pressure of gases such as hydrogen and oxygen. The counting rate of the x-ray radiation from the superconducting cavity is

$$I_{X\text{-ray}} = I_0 + \frac{C_3 \sqrt{E_F} F^{2.5} \beta_X^{2.5}}{(\Phi_W + E_F)\Phi_W^{0.75}} e^{-4k\Phi_W^{1.5}/3F\beta_X}, \quad (9)$$

where β_X is the field enhancement factor of the x-ray and C_3 is the proportional constant.

RF MEASUREMENT AND CHARACTERISATION OF EUROPEAN SPALLATION SOURCE CAVITIES AT UKRI-STFC DARESBUARY LABORATORY AND DESY

P.A. Smith*, A. Akintola, K. Dumbell, M. Ellis, S. Hitchen, P. Hornickel, C. Jenkins, G. Jones, M. Lowe, D. Mason, A. J. May, P. McIntosh, K. Middleman, G. Miller, A. Moss, J. Mutch, A. Oates, S. Pattalwar, M. Pendleton, O. Poynton, S. Wilde, J. Wilson, A.E. Wheelhouse
 UKRI-STFC Daresbury Laboratory, Keckwick Lane, Daresbury, UK
 L. Steder, M. Wienczek, and D. Reschke
 Deutsches Elektronen-Synchrotron DESY, Hamburg, Germany

Abstract

The Accelerator Science and Technology Centre (ASTeC) is responsible for delivering 88 High Beta (HB) cavities as part of the European Spallation Source (ESS) facility in Sweden. The bulk Niobium Superconducting Radio Frequency (SRF) cavities operate at 704 MHz. They have been fabricated in industry and are currently being tested at Daresbury Laboratory and Deutsches Elektronen-Synchrotron (DESY). They will then be delivered to Commissariat à l’Energie Atomique et aux Energies Alternatives (CEA) Saclay, France for integration into cryomodules. To date 50 cavities have been conditioned and evaluated and 36 cavities have been delivered to CEA. This paper discusses the experiences and testing of the cavities performed to date at both sites.

INTRODUCTION

As part of the UK In-Kind-Contribution (IKC) to the European Spallation Source (ESS) facility in Sweden, STFC are providing 88 704 MHz high-beta superconducting RF cavities. These cavities are to be delivered to CEA-Saclay, France for integration into 21 cryomodules which will then be delivered to ESS. The cavities are required to have a quality factor (Q_0) of 5×10^9 at an accelerating gradient of 19.9 MV/m.

The test system used at STFC is quite different to most others used around the world. Cavities were tested horizontally, and cooled only by filling the LHe tanks [1] whereas most other systems use complete bath immersion. The other significant difference was that the radiation detectors at each end of the cavity were much closer. At STFC the detectors at each end were typically 25 to 30 cm from the ends of the cavities. This results in detection of radiation onset much earlier in the STFC system. A schematic of the STFC setup is presented in Fig. 1. The detectors are at each end of each cavity, immediately outside the cryostat, but are not shown in the diagram.

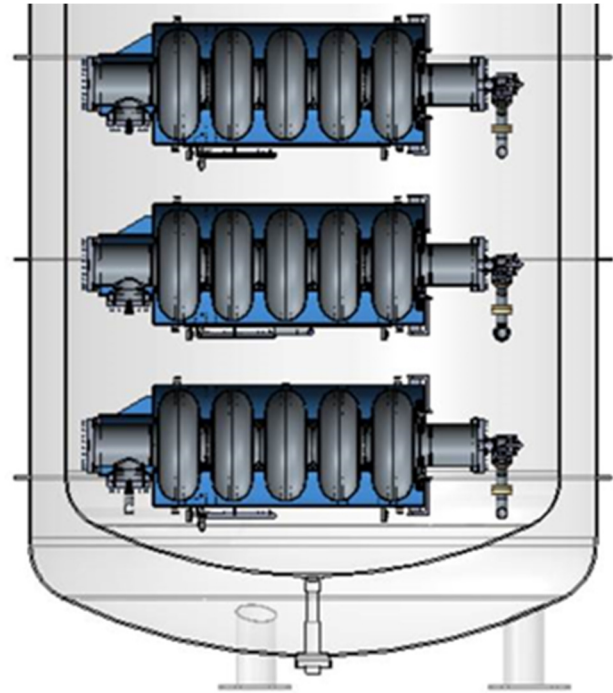


Figure 1: Schematic of STFC test system. Showing 3 cavities inside the cryostat.

Most other systems place the detectors 2 or 3m from the ends. A schematic of the test system at DESY [2] is shown in Fig. 2. Thus, the detectors at STFC are approximately 10 x closer. It was therefore expected, that the dose rate reading would be about 100x higher, from the simple $1/r^2$ effect. At STFC there is also significantly less shielding material between the ends of the cavity and the detectors. Overall these two effects resulted in a dose rate reading at STFC that was approximately 300x larger than that measured at DESY.

*paul.a.smith@stfc.ac.uk

A MULTI-CAMERA SYSTEM FOR TOMOGRAPHIC BEAM DIAGNOSTICS

A. Ateş*, G. Blank, H. Hähnel and U. Ratzinger
Institute of Applied Physics, Goethe University, Frankfurt, Germany

Abstract

A prototype of a beam-induced residual gas fluorescence monitor (BIF) has been developed and successfully tested at the Institute of Applied Physics (IAP) at the Goethe University Frankfurt. This BIF is based on ten single-board cameras inserted into the vacuum and directed onto the beam axis. The overall goal is to study the beam with tomography algorithms at a low energy beam transport section. Recently, we tested the detector with a 60 keV, 33 mA hydrogen beam at 20 Hz and 1 ms puls length. In this paper we present the ongoing investigations on image processing and application of the algebraic reconstruction technique (ART).

INTRODUCTION

Beam-induced fluorescence (BIF) monitors are standard detectors at accelerator facilities [1]. For ultrahigh vacuum beam diagnostics, scientific cameras are commonly used in combination with MCP photon amplifiers to determine the beam position and profile. New BIF monitors have been successfully tested at the low-energy beamline of the Frankfurt Neutron Source at the Stern Gerlach Center [2]. These developments lead to new ways to study the beam. One idea is to view the beam from multiple angles. This allows the use of tomography algorithms to reconstruct the intensity distribution of the transverse beam profile. Beam tomography has previously been studied using a camera and a rotating vacuum chamber to rotate the camera and obtain any number of views. Another approach is to view the beam through viewing windows.

Our goal is to maximize the number of viewing angles and develop a fast tomographic detector with minimal size to be as flexible as possible. Our approach is to use non-scientific single-board cameras with single-board computers and integrate the system into the vacuum. Figure 1 shows a photo of the cameras mounted on the holder. It is designed to fit into a vacuum chamber with a diameter of 200 mm and a length of 300 mm.

The detector is built for low energy beam transport sections in high vacuum regions of about 10^{-7} mbar. To amplify the emitted light, a buffer gas can be introduced during image acquisition. We introduced argon gas and tested the cameras at a residual gas pressure of up to 1×10^{-4} mbar. Figure 2 shows the position of the tomography detector. This position is of particular interest since the RFQ will be placed at this location.

There were several challenges to overcome in developing such a detector. One challenge was to have all the cameras work in parallel and transmit all the data from the vacuum. Another challenge was to align all cameras so that the center

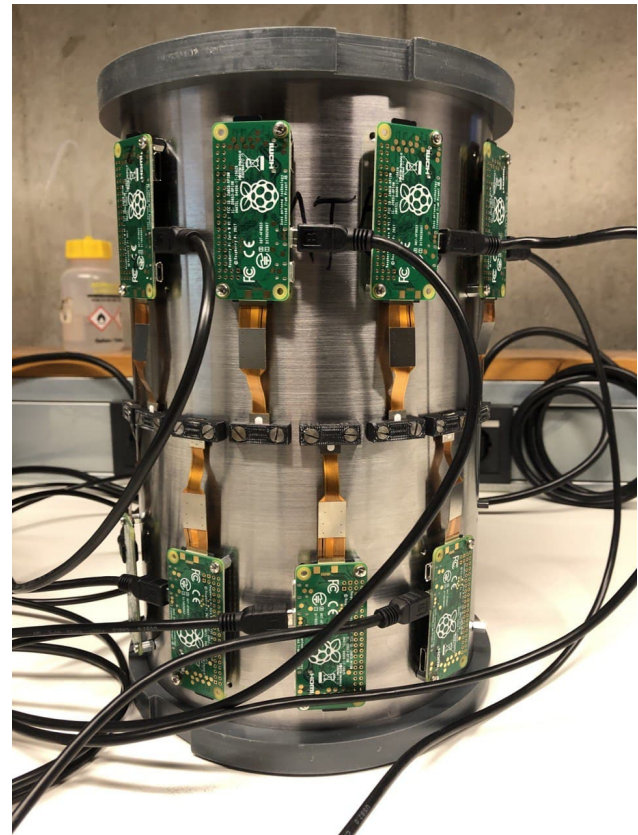


Figure 1: The picture shows a photo of the tomography detector with the Raspberry Pi Zero and its camera modules attached to a stainless steel pipe.

of their field of view matched. For more information about calibration and alignment, see [3].

HARDWARE SET UP

Raspberry Pi Zero and its Camera

The cameras you see in Fig. 1 are single-board cameras with so-called Raspberry Pi Zero single-board computers. The Raspberry Pi Zero is the one with the smallest dimensions among the Raspberry Pi computer models. The computer and especially its camera are gaining more and more attention not only in the Maker scene, but also in the scientific community [4]. Due to its compact dimensions and low power consumption of about 15 mW, they are predestined for projects like drones, robots or any mobile devices. The camera consists of a 5 MP high resolution Omnivision OV5647 CMOS image sensor. The sensor size is $3.76 \text{ mm} \times 2.74 \text{ mm}$ and has a pixel size of $1.4 \mu\text{m} \times 1.4 \mu\text{m}$. It has a focal length (3.6 mm) with a single aperture (F2.9). The sensor sensitivity can be varied between ISO values from 100 to 800, and it is possible to vary the analogue gain of the ADC for the blue and red color pixels, i.e. to change the white balance

* ates@iap.uni-frankfurt.de

IMPLEMENTATION OF AN ADVANCED MicroTCA.4-BASED DIGITIZER FOR MONITORING COMB-LIKE BEAM AT THE J-PARC LINAC

E. Cicek*, K. Futatsukawa, T. Miyao, S. Mizobata, KEK, Tsukuba, Ibaraki 305-0801, Japan
 N. Hayashi, A. Miura, K. Moriya, JAEA/J-PARC, Tokai, Ibaraki 319-1195, Japan

Abstract

The Japan Proton Accelerator Research Complex (J-PARC) linac beam pulse, generated by a beam chopper system placed at the MEBT, comprises a series of intermediate pulses with a comb-like structure synchronized with the radio frequency of the rapid cycling synchrotron (RCS). The sequentially measuring and monitoring the comb-like beam pulse ensures the beam stability with less beam loss at the current operation and higher beam intensity scenarios at the J-PARC. However, signal processing as a function of the pulse structure is challenging using a general-purpose digitizer, and monitoring the entire macro pulse during the beam operation is unavailable. To this end, an advanced beam monitor digitizer complying with the MicroTCA.4 (Micro Telecommunications Computing Architecture.4) standard, including digital signal processing functions, has been developed. This paper reports the implementation, performance evaluation, and the first results of this unique beam monitor digitizer.

INTRODUCTION

The Japan Proton Accelerator Research Complex (J-PARC) linac front-end comprises a negative hydrogen H^- ion source (IS), low-energy beam transport line (LEBT), 3 MeV radiofrequency quadrupole linac (RFQ), medium-energy beam transport line (MEBT1), housing two buncher cavities and RF choppers, 50 MeV drift-tube linac (DTL), 190.8 MeV separated type DTL (SDTL), and 400 MeV annular ring coupled structure ACS [1], see Fig. 2. A 50 mA H^- beam is injected into the rapid cycling synchrotron (RCS) through an L3BT (linac-to-3-GeV RCS beam transport) line. The linac also has an additional line, called medium-energy beam transport line 2 (MEBT2), which is equipped with two buncher cavities (B1 and B2).

Figure 1 shows the time structure of the beam from the linac. The IS generates macro-pulses of widths ranging from 50 to 500 μs (ω_{ma_p}). The beam pulse is formed by an RF chopper system [2] placed at MEBT1 and consists of a series of intermediate pulses with a comb-like structure, synchronized with RF frequency (f_{rf}) of the RCS ring. The beam is modulated by an RCS chop signal from the RCS low-level RF (LLRF) system [3]. It has different patterns in chopped-beam operations to achieve the comb-like structure. Thus, relying on this signal, the linac provides various pulse structures with different intermediate pulse widths (ω_{int_p}), thinning rates (TRs), and 1-bunch operation for the Material

and Life Science Experimental Facility (MLF) and main ring (MR) in J-PARC [4].

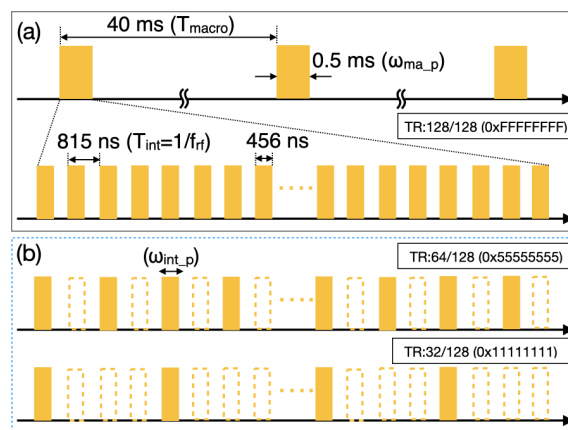


Figure 1: (a) Time structure of the linac beam; macro-pulses (upper), intermediate pulses (lower), (b) intermediate pulses with different thinning rates. 0xFFFFFFFF denotes the existence of all intermediate pulses in a macro-pulse, while dashed orange color blocks represent thinned-out pulses.

Numerous beam monitors are employed in J-PARC linac, such as the beam current monitor (slow current transformer, SCT), beam phase monitor (fast current transformer, FCT), and beam position monitor (BPM) [5, 6]. The extant WE7000 measurement station [7], has proven reliable over the past 15 years. However, obsolescence and the desire to monitor the entire macro-pulse necessitate the development of a new monitoring system. Monitoring the entire macro-pulse while performing signal processing in a field-programmable gate array (FPGA) during beam operation with a general-purpose digitizer is challenging. Consequently, we developed a new beam monitor digitizer (henceforth called "BMONDIG"), which complies with MicroTCA.4 (Micro Telecommunications Computing Architecture.4) standards and includes a digital signal processing (DSP) function. It sequentially measures the comb-like beam together with the duty cycle and averaging calculation processes, enabling the monitoring of the linac beam pulse structure. The aim is to achieve stable beam operation with lower beam loss for all intensities at J-PARC. This paper introduces the new monitor digitizer, its installation procedure, and the test results of beam pulse measurements.

HARDWARE

The BMONDIG architecture, as shown in Fig. 3, was implemented by the Mitsubishi Electric TOKKI Systems

* ecicek@post.kek.jp

DEVELOPMENT OF QUANTUM GAS JET BEAM PROFILE MONITOR FOR sub-mm BEAMS

N. Kumar*, O. Stringer, J. Wolfenden, H. D. Zhang, C. P. Welsch
University of Liverpool and Cockcroft Institute, Warrington, UK
I. Maltusch, FH Aachen, University of Applied Science, Jülich, Germany

Abstract

The development work of a high-resolution quantum gas jet beam profile monitor for highly energetic sub-mm particle beams is in progress at the Cockcroft Institute (CI), UK. This device is designed on the principle of detecting the secondary ions from the ionisation induced in the interaction between the quantum gas jet and charged particle beams. This monitor aims to generate an intense gas jet with a diameter of less than 100 μm , which can ultimately lead to superior position resolution and high signal intensity resulting from a strongly focused quantum gas jet. This is done by exploiting the quantum wave feature of the neutral gas atoms to generate an interference pattern with a single maximum acting as an ultra-thin gas jet using an 'atom sieve' which is similar to the light focusing with a Fresnel zone plate. This device will be minimally interceptive and will work analogously to a mechanical wire scanner. This contribution gives a general overview of the design, working principle of the monitor and experimental results obtained from the electron beam profile measurements carried out at the Cockcroft Institute.

INTRODUCTION

Beam diagnostics are essential for the operation, optimization and protection of accelerators and their subsystems. The requisite of non-invasive high resolution beam diagnostics has been increasing with the growing demand for high intensity and high power accelerators worldwide. Wire scanners are the currently existing invasive monitors for high power accelerators such as the Spallation Neutron Source (SNS) or Accelerator Driven System, having the limitation of handling the huge beam peak power and hence, will be used at low beam duty cycle [1, 2]. Non-invasive monitors such as residual gas ionization profile monitors (IPM) suffer from distortions due to the non-uniformity of the extraction field, space charge effects of the primary beam and the initial momentum spread of the ionization products [3]. These concerns have triggered a demand for the development of a new generation of non-invasive beam profile monitors with high resolution and the least distorted beam profiles. Development work for a quantum gas jet scanner based beam profile monitor is in progress at the Cockcroft Institute (CI), Daresbury. This monitor is based on the previous development work on the supersonic gas jet based IPM carried out by the QUASAR group at CI for high intensity beams such as the CLIC Drive beam and the European Spallation Source [4-6].

A focused gas jet with a diameter less than a few 10 μm named as Quantum gas jet will be used to generate the beam profile in this profile monitor instead of a gas jet curtain. In order to generate the complete beam profile of the primary beam, this quantum gas jet will be scanned over the beam, analogous to a wire scanner. The quantum gas jet can be used in several other applications i.e. for generating a confined plasma source [7], as a probe for microscopy [8], etc. Initial design calculations for this monitor were carried out using the fundamental physics principles and results obtained from the CST simulations [9, 10]. In this work, the general overview of the design and working principle of the quantum gas jet monitor are presented along with the beam profile measurement results obtained for a 3.7keV electron beam at CI.

OVERVIEW AND WORKING PRINCIPLE OF THE MONITOR

The schematic of the whole setup is shown in Fig. 1. In this setup, supersonic gas jet curtain is created using a nozzle-skimmers assembly with differential pumping stages. Details of the gas jet curtain generation can be found in our previous work [4].

In this development work, the pinhole shown in Fig. 1 will be replaced by an atom sieve designed on the principle of Fresnel zone plate (FZP) for x-rays to generate quantum jet. The design details of atom sieve can be found in previous work done by our group [9]. A FZP designed for x-rays is usually made up of concentric metallic rings embedded in an x-ray transparent substrate. However for an atom sieve, holes are required to provide passage for the gas molecules. Figure 2 shows the design of the atom sieve to be used for this work. The atom sieve is fabricated on a 2 μm thick silicon nitride membrane grown on a silicon wafer of diameter 150 mm. The circular holes in the pattern are within 60 μm diameter.

The interaction chamber is coupled with an electron gun that can generate a beam of energy up to 10 keV which propagates perpendicular to the direction of the flow of the quantum gas jet. The interaction between the electron beam and the supersonic gas leads to ionization of the gas molecules and these ions will be extracted using an external electrostatic field generated by a series of hollow metallic electrodes. The ion signal is amplified using a Micro-channel plate (MCP) which is converted into scintillating light using phosphor screen stacked after the MCP. This light is then viewed by a CMOS camera.

* Email: Narender.Kumar@cockcroft.ac.uk

A GAS JET BEAM HALO MONITOR FOR LINACS

O. Stringer^{†,1}, H. Zhang¹, N. Kumar¹, C. Welsch¹
 University of Liverpool, Liverpool, United Kingdom
¹also at the Cockcroft Institute, Warrington, United Kingdom

Abstract

The gas jet beam profile monitor is a non-invasive beam monitor that is currently being commissioned at the Cockcroft Institute. It utilises a supersonic gas curtain which traverses the beam perpendicular to its propagation and measures beam-induced ionisation interactions of the gas. A 2D transverse beam profile image is created by orientating the gas jet 45 degrees to obtain both X and Y distributions of the beam. This paper builds upon previously used single-slit skimmers and improves their ability to form the gas jet into a desired distribution for imaging beam halo. A skimmer device removes off-momentum gas particles and forms the jet into a dense thin curtain, suitable for transverse imaging of the beam. The use of a novel double-slit skimmer is shown to provide a mask-like void of gas over the beam core, increasing the relative intensity of the halo interactions for measurement. Such a non-invasive monitor would be beneficial to linacs by providing real time beam characteristic measurements without affecting the beam. More specifically, beam halo behaviour is a key characteristic associated with beam losses within linacs.

INTRODUCTION

Beam halo is typically regarded as a region of particles outside the beam core but the distinction of the boundary between beam profile and beam halo is highly dependent on the application. A geometric perspective could be chosen, describing it as density distributions beyond n sigma or from a formation perspective, as a function of the space charge or parametric resonance [1]. In linear accelerators,

beam halo forms due to factors such as dark current in the cathode, emittance mismatch or skewness. In this paper, beam halo shall be defined simply by a low-density region surrounding the higher density central beam core. Further clarification of this definition is not required due to the proof of concept demonstration in this contribution. A low energy, 5 keV electron beam is used to demonstrate the available imaging region intended on capturing the halo, however it is unable to produce a measurable halo itself.

Typical diagnostics methods for beam halo include wire scanners, scrapers and screens [1]. These are all inherently destructive in nature to the beam. As such, non-invasive techniques are preferred for halo monitoring, such as coronagraphing synchrotron radiation with optical masks [2, 3]. However, this method also has drawbacks due to the energy requirements of generating synchrotron radiation suitable for imaging. The Beam Gas Curtain (BGC) aims to provide an alternative method of non-invasive beam diagnostics that may be more suited to specific beamlines.

The BGC diagnostics tool utilises a thin, supersonic gas curtain, inclined at a 45-degree angle which produces ionisation and fluorescent interactions between the working gas and beam [4-6]. The setup used in this contribution was configured as an Ionisation Profile Monitor (IPM). The gas ions created are collected upon a Micro Plate Channel (MCP) and imaged on a phosphor screen above the interaction point. This provides a real-time recreated 2D image of the beam at the location of interaction.

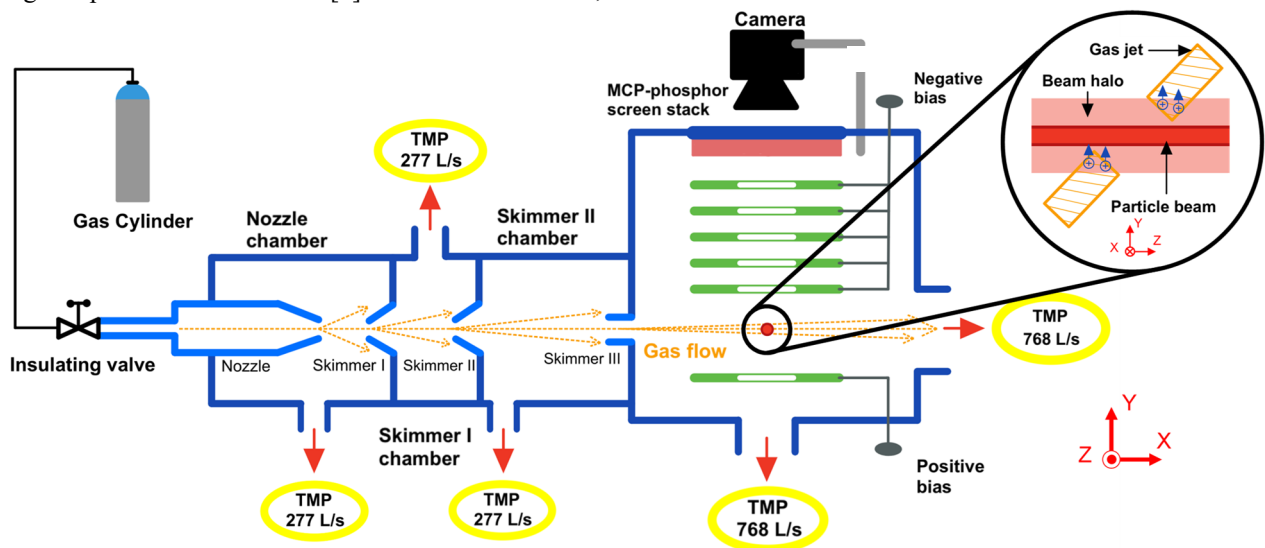


Figure 1: The layout of the Beam Gas Curtain setup configured as an Ionization Profile Monitor for halo monitoring.

[†] O.Stringer@liverpool.ac.uk

APPLICATION OF VIRTUAL DIAGNOSTICS IN THE FEBE CLARA USER AREA

J. Wolfenden^{*1}, C. Swain¹, C. P. Welsch¹, University of Liverpool, Liverpool, UK
T. H. Pacey¹, A. E. Pollard¹, J. Jones¹, D. Dunning¹, ASTeC/STFC, Daresbury, UK
¹also at Cockcroft Institute, Daresbury, UK

Abstract

Successful user experiments at particle beam facilities are dependent upon the awareness of beam characteristics at the interaction point. Often, properties are measured beforehand for fixed operation modes; users then rely on the long-term stability of the beam. Otherwise, diagnostics must be integrated into a user experiment, costing resources and limiting space in the user area. This contribution proposes the application of machine learning to develop a suite of virtual diagnostic systems. Virtual diagnostics take data at easy to access locations, and infer beam properties at locations where a measurement has not been taken, and often cannot be taken. Here the focus is the user area at the planned Full Energy Beam Exploitation (FEBE) upgrade to the CLARA facility (UK). Presented is a simulation-based proof-of-concept for a variety of virtual diagnostics. Transverse and longitudinal properties are measured upstream of the user area, coupled with the beam optics parameters leading to the user area, and input into a neural network, to predict the same parameters within the user area. Potential instrumentation for FEBE CLARA virtual diagnostics will also be discussed.

INTRODUCTION

The interaction point (IP) in a particle accelerator is the focal point at which the attention of users and operators converge. At this point users require certain beam parameters in order to achieve their desired output, whilst operators monitor this location and tune the machine settings accordingly. The balance of these two sets of goals is key to any successful exploitation plan. If the user blocks the operators diagnostic efforts then they cannot be certain of the beam parameters their instrumentation receives; likewise if operator diagnostics interfere with the users ability to receive the beam in a manner suited to their needs, their output is affected. A utilitarian approach is therefore required to proceed. Standard practise is therefore to operate in nominal "user modes". These are machine settings which provide a stable beam with known parameters. These parameters are measured in great invasive detail ahead of user operation, and the machine stability utilised to reliably reproduce these parameters once invasive high resolution diagnostics are removed. In general, this approach works well. Other lower resolution non-invasive measures can be used to monitor the beam away from the IP, and machine jitter can be quantified and converted into an uncertainty for users, which can then

be baked directly into their output. However, issues can arise when users require non-standard beam parameters or when the facility is using a novel acceleration scheme, such as plasma wakefield acceleration [1, 2]. The former requires operators to tune the machine settings on-the-fly, meaning either the beam is tuned with less resolution due to a lack of diagnostics, or the user loses beam time as the required diagnostics are inserted and then removed from the IP. The latter suffers, at this time, from a fundamental shot-to-shot instability, which means a much larger error is introduced when relying upon machine stability with certain machine parameters. An obvious solution one might suggest is the implementation of several novel non-invasive diagnostics that have been developed in recent years [3–6]. Unfortunately these methods would still fall foul of the user-operator balance described above as the instrumentation would need to be placed close to the IP, and hence user instrumentation. It is here that the concept of a virtual diagnostic (VD) can be deployed. A VD is a technique based upon machine learning which uses beam measurements from one location on a beamline to infer, with high accuracy, beam parameters at another location. This practise could therefore be used to move high resolution IP diagnostics away from the IP, freeing the space for users, whilst still providing shot-to-shot beam measurements, even in exotic operational modes.

Presented in this contribution is a case study into the application of such VDs in the framework of the full energy beam exploitation (FEBE) CLARA (STFC, UK) [7] user area IP. This simple example focuses solely on transverse beam size measurements from particle tracking simulations (Elegant [8]), but other beam parameters will be discussed. The goal is to maintain an alignment with experimental plans for the facility, providing actionable VD implementations. Two VD options will be discussed, along with the accompanying diagnostic instrumentation.

SIMULATION

As with any application of machine learning, a significant quantity of quality input and output data is required in order to facilitate model training. To produce this data, the particle tracking code Elegant was used. A lattice file for a nominal FEBE CLARA operational mode was chosen. This lattice had been tuned to maximise the beam current at the IP; however, the actual absolute values of the machine settings are unimportant at this stage. In order to produce a random sampling of the transverse beam parameters at the IP, the K1 values of several quadrupole magnets in the beamline were chosen, presented in Fig. 1, and randomly

* joseph.wolfenden@cockcroft.ac.uk

IMPROVEMENTS ON THE MODIFIED NOMARSKI INTERFEROMETER FOR MEASUREMENTS OF SUPERSONIC GAS JET DENSITY PROFILES

C. Swain*, J. Wolfenden, A. Salehilashkajani, H D. Zhang, O. Apsimon, C. P. Welsch
 Cockcroft Institute, Daresbury Laboratory, Warrington, UK
 University of Liverpool, Liverpool, UK

Abstract

For supersonic gas jet based beam profile monitors such as that developed for the High Luminosity Large Hadron Collider (HL-LHC) upgrade, density profile is a key characteristic. Due to this, non-invasive diagnostics to study the jet's behaviour have been designed. A Nomarski interferometer was constructed to image jets 30 μm to 1 mm in diameter and study changes in their density. A microscope lens has been integrated into the original interferometer system to capture phase changes on a much smaller scale than previous experiments have achieved. This contribution presents the optimisation and results gained from this interferometer.

INTRODUCTION

The use of supersonic gas jets is becoming more common within accelerator facilities, meaning it is important that suitable diagnostics are developed to properly characterise them. An example of this is the beam gas curtain (BGC) currently under development by the Cockcroft Institute (CI), CERN, and GSI. The BGC is a non-invasive beam profile monitor being developed for installation on the HL-LHC [1], and is designed for use on both the proton beam and hollow electron lens (HEL) [2, 3]. There are two working principles for the BGC, beam induced fluorescence (BIF) [4], and ionisation profile monitoring (IPM) [5]. In both operating modes, results are proportional to the density profile of the gas jet, making this an important property which must be properly understood to allow for accurate measurements. Whilst density distributions of the jet have been simulated [5], measured values for comparison and validation are still needed. Therefore, a diagnostic setup has been designed and tested at CI for this purpose. A modified Nomarski interferometer [6] was chosen to provide non-invasive imaging from which the density profile could be attained. Utilising a single optical path and compact design, this style of interferometry was chosen due to its benefits over other systems [7, 8]. An example of one such benefit is that the single path length allows for reductions in the alignment requirements and susceptibility to instability shown by split path interferometers, such as the Mach Zender system [9]. This paper presents updates to the system previously developed at CI [10], including the integrated microscope, new measurements, and possible improvements to be made.

* Catherine.Swain@liverpool.ac.uk

INTERFEROMETRY THEORY

Interferometry relies on the interference of coherent light sources creating fringes which can be imaged. From these images, or interferograms, properties of the media the light has propagated through can be found through studying changes in phase shift. In this interferometry system, a Wollaston prism was used to create the interferograms. The prism is made of birefringent material, in this case magnesium fluoride. Two triangular prisms are fit together with orthogonal optical axes, creating a polarising beam splitter with a fixed opening angle between the resulting rays [11]. A linearly polarised laser which is passed through the prism will diverge into an ordinary and extraordinary ray as it crosses the centre axes, as shown in Fig. 1.

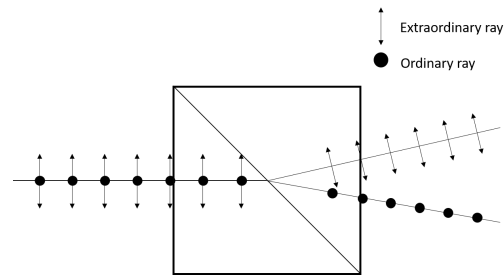


Figure 1: Diagram of Wollaston prism showing how light is split as it crosses the optical axis.

A focusing lens is used to focus the two rays into an interferogram, from which the phase shift they have undergone can be observed. These changes in phase shift can be directly linked to density gradients the laser has experienced via the Lorentz-Lorenz equation (Eq. 1). For gases with a density of less than 10^{19} cm^{-3} , it can be assumed that the refractive index (η) is close to 1. Therefore, Eq. (1) gives an approximation for the density [12]

$$\rho \approx (\eta - 1) \frac{2}{3} \frac{N_A}{A} \quad (1)$$

where density is given in m^{-3} , N_A is Avogadro's constant ($6.022 \times 10^{23} \text{ mol}^{-1}$), and A is the molar refractivity (for nitrogen, used in this study, $A = 4.46 \text{ m}^3 \text{ mol}^{-1}$ [13]). This equation can then be used to form a relationship between density and phase shift, as given in Eq. (2) [12]

$$\Delta\phi = l \frac{3\pi}{\lambda} \frac{A}{N_A} \rho \quad (2)$$

where l is the laser path length through the media and λ is the laser wavelength. In this study l was taken as being equal

BEAM MAPPING LINEARITY IMPROVEMENT IN MULTI-DIMENSIONAL BUNCH SHAPE MONITOR*

A.C. Araujo Martinez, R. Agustsson, S.V. Kutsaev[†], A. Moro, A.Y. Smirnov, K.V. Taletski
 RadiaBeam Technologies, LLC, Santa Monica, CA, USA
 A.V. Aleksandrov, A. Menshov, Oak Ridge National Laboratory, TN, USA

Abstract

RadiaBeam is developing a Bunch Shape Monitor (BSM) with improved performance that incorporates three major innovations. First, the collection efficiency is improved by adding a focusing field between the wire and the entrance slit. Second, a new design of an RF deflector improves beam linearity. Finally, the design is augmented with both a movable wire and a microwave deflecting cavity to add functionality and enable measuring the transverse profile as a wire scanner. In this paper, we present the design of the BSM and its sub-systems.

INTRODUCTION

Direct measurement of the full multi-dimensional phase space is crucial for the operation and development of linear accelerators. Obtaining an accurate initial distribution of the beam entering the linac system is required for realistic simulations of the beam dynamics [1]. The Bunch Shape Monitor (BSM) is a device used to measure the longitudinal bunch distribution in hadron linacs, originally developed by A. Feschenko at the Institute for Nuclear Research (INR) in Moscow [2].

The principle of operation of the BSM is shown in Fig. 1. The primary ion beam with a longitudinal structure passes through a tungsten wire biased at high voltage (-10 kV) and generates a low-energy secondary electron beam with an equivalent temporal profile. The electron beam is accelerated towards the input slit (anode) and is focused with an electrostatic lens (focusing system). Then, an RF deflector with a superimposed electric potential is used to focus, steer, and deflect the electrons. Hence, the temporal distribution is converted into a spatial distribution via an RF deflecting field. Finally, the electrons are measured by a multichannel plate detector (MCP) and a phosphor screen.

Modern hadron linacs require several BSMs to suite their beam diagnostics [3]. For example, the Spallation Neutron Source (SNS) at Oak Ridge National Laboratory (ORNL) has seven BSM systems originally delivered by INR [4]. Although these systems have been operational for several years, they have technical limitations such as poor electron collection efficiency, beam mapping non-linearity, and are limited to one-dimensional measurement of the phase coordinate [5]. An improved design of the BSM is needed to solve these issues and could potentially be used to perform more advanced beam dynamics experiments using the six-dimensional phase space scan technique developed at SNS [1].

* This work was supported by the U.S. Department of Energy, Office of Basic Energy Sciences, under contract DE-SC0020590.

[†] kutsaev@radiabeam.com

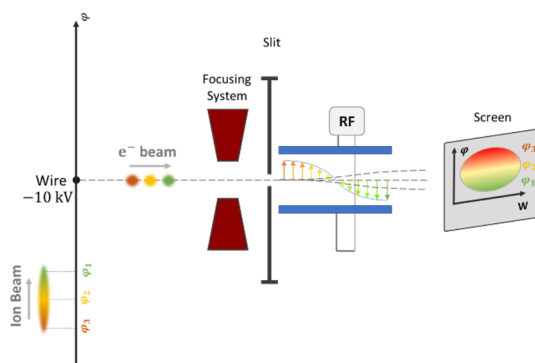


Figure 1: BSM operation principle.

RadiaBeam is developing an improved multi-dimensional BSM to be used at SNS. The specifications for this system are the following: 402.5 MHz operating frequency, 2.5 MeV ion energy, and phase resolutions smaller than 1° . The design includes three major innovations: focusing system to improve collection efficiency, new RF deflector to improve beam linearity, and a moving mechanism to enable measurement of the transverse profile [6]. Recently, we have developed and fabricated the focusing system to improve the electron collection efficiency and beam linearity for the current BSM at the SNS Beam Test Facility. This focusing system prototype was tested at SNS and demonstrated excellent vertical focusing properties, improved electron collection efficiency by a factor of 2.9, and improvement in the measured signal-to-noise ratio.

In this paper, we report further progress, which includes the following innovations: a new RF deflector cavity that allows improved vertical beam focusing and provides a linear horizontal beam mapping from wire to the screen, and a movable wire system that allows proton beam scan in the transverse dimension.

RF DEFLECTOR

One of the major improvements of the BSM design is the addition of a new RF deflector cavity. This deflector allows a symmetric geometry to reduce distortions in the vertical focusing, which was an issue with the original BSM. Its design also facilitates moving the wire and deflector together for transverse beam measurements.

The new RF deflector was designed by ORNL [7] and provided to RadiaBeam for RF testing. This deflector consists of an RF cavity with input and output slits, and two electrode plates that are attached to two pairs of support rods for a symmetric geometry as displayed in Fig. 2. The target operational frequency for the cavity is 402.5 MHz. However, ORNL manufactured the cavity with longer

LINEAR ACCELERATOR FOR DEMONSTRATION OF X-RAY RADIOTHERAPY WITH FLASH EFFECT*

S.V. Kutsaev†, R. Agustsson, S. Boucher, K. Kaneta, A.Yu. Smirnov, V. Yu
RadiaBeam Technologies, LLC, Santa Monica, CA, U.S.A.
A. Li, K. Sheng, Department of Radiation Oncology, University of California,
Los Angeles, CA, U.S.A.

Abstract

Emerging evidence indicates that the therapeutic window of radiotherapy can be significantly increased using ultra-high dose rate dose delivery (FLASH), by which the normal tissue injury is reduced without compromising tumor cell killing. The dose rate required for FLASH is 40 Gy/s or higher, 2-3 orders of magnitude greater than conventional radiotherapy. Among the major technical challenges in achieving the FLASH dose rate with X-rays is a linear accelerator that is capable of producing such a high dose rate. We will discuss the design of a high dose rate 18 MeV linac capable of delivering 100 Gy/s of collimated X-rays at 20 cm. This linac is being developed by a RadiaBeam/UCLA collaboration for a preclinical system as a demonstration of the FLASH effect in small animals.

INTRODUCTION

Ultra-fast radiation delivery, also known as FLASH radiotherapy, may become a breakthrough technology for oncology treatment. Compared to conventional radiotherapy with dose rate ~ 0.1 Gy/s, FLASH radiotherapy markedly reduced the normal tissue toxicity without compromising tumor response [1]. The FLASH effects have been consistently observed across different animal species, using different modalities including electrons, X-rays, and protons. Moreover, the FLASH effect was recently demonstrated in a human study for treating skin lesions [2].

It is believed that with a sufficiently high dose rate, depleted oxygen cannot be replenished via diffusion before the full radiation dose is given, reducing the cell damage and leading to the hypothesized FLASH effect [3]. Other mechanisms, including inflammatory response, were also indicated [4]. Regardless of the FLASH-therapy mechanism, the promising initial results warrant further investigation and human clinical trial studies.

One possibility for delivering FLASH would be an X-ray system [5]. However, there are significant technical challenges to achieving the $\sim 500\times$ greater dose rate for FLASH in human patients. Unfortunately, the physical process for generating X-rays is not very efficient, therefore a high-power accelerator is needed. Conventional 6 MV medical linacs produce a flattening filter free dose rate of around 0.2 Gy/s at one meter from the X-ray target – 3 orders of magnitude too low – however they are on the low end of the spectrum of linac powers [6]. A typical medical

linac has a beam power on the order of 1 kW, while industrial accelerators for sterilization of food and medical products can achieve beam powers of several hundred kW.

Another factor that allows for improvement in dose rate is increasing the beam energy. The conversion efficiency from electron beam power to X-ray power scales approximately with E^3 , so a small increase in energy can make a large difference in X-ray intensity. The increased X-ray energy also allows greater penetration.

RadiaBeam and UCLA are working on a clinical solution for X-ray FLASH therapy that takes advantage of a single linac based on already-demonstrated technology and an innovative, yet straightforward, method for intensity modulation [7, 8]. This linac will be capable of producing 18 MV X-ray radiation with 100 Gy/s collimated dose rate in the tumor, located at 80 cm from the source. Such dose will be achieved by accelerating a >300 mA beam with 2.5% duty factor. Since the complexity of this linac is extensive, the expected timeline for its completion is estimated to be several years. Therefore, in parallel to a clinical system, we are developing a scaled linac that can be used for demonstration of the FLASH effects in small animals. The linac will benefit from using the infrastructure of a 9 MeV NDT linac (FLEX) [9] available at RadiaBeam, and therefore can be developed and fabricated in a much shorter time scale by only replacing the accelerating structure.

LINAC CONCEPT

The goal of this project is to design and build an inexpensive linac for demonstration of gamma FLASH therapy. The following considerations are taken into account. The designed accelerator must be able to provide at least 100 Gy/s dose, collimated, at 20 cm from the target. This corresponds to 16.5 cGy/s uncollimated dose at 1 m from the target. Second, the accelerator must be able to utilize the existing FLEX linac RF power system, available at RadiaBeam, based on 5 MW peak power klystron, operating at 2.856 GHz frequency with 0.4% duty factor.

The other consideration is to maximize the X-ray dose conversion from the accelerated electron beam. In order to do this, we pursued two approaches. First, the dose yield scaled linearly with the beam current I and cubically with the energy W as:

$$D = k \cdot I \cdot W^{2.7-3.0}$$

Where k is a yield factor that depends on the particular X-ray conversion target design. For example, we know that for 6 MeV linacs produced at RadiaBeam, $k=10.6$ cGy/min/ μ A [10] and $k\sim 30$ cGy/min/ μ A for a Varian 9 MeV Linatron.

* This project is funded by National Institutes of Health (NIH), award number NIH R01CA255432

† kutsaev@radiabeam.com

FIRST STUDIES OF 5D PHASE-SPACE TOMOGRAPHY OF ELECTRON BEAMS AT ARES

S. Jaster-Merz^{*1}, R. W. Assmann², R. Brinkmann, F. Burkart, T. Vinatier
Deutsches Elektronen-Synchrotron DESY, Germany

¹also at Department of Physics Universität Hamburg, Germany

²also at Laboratori Nazionali di Frascati, Italy

Abstract

A new beam diagnostics method to reconstruct the full 5-dimensional phase space (x, x', y, y', t) of bunches has recently been proposed. This method combines a quadrupole-based transverse phase-space tomography with the variable streaking angle of a polarizable X-band transverse deflecting structure (PolariX TDS). Two of these novel structures have recently been installed at the ARES beamline at DESY, which is a linear accelerator dedicated to accelerator research and development, including advanced diagnostics methods and novel accelerating techniques. In this paper, realistic simulation studies in preparation for planned experimental measurements are presented using the beamline setup at ARES. The reconstruction quality of the method for three beam distributions is studied and discussed, and it is shown how this method will allow the visualization of detailed features in the phase-space distribution.

INTRODUCTION

The ARES linear accelerator [1–4] at DESY is designed to deliver stable and well-characterized electron bunches at a repetition rate up to 50 Hz with energies up to 155 MeV and charges from 0.05 pC to 200 pC. Its research program focuses on performing advanced accelerator research and development. This includes the production and measurement of bunches with down to sub-fs durations [5–9] for the study of novel dielectric-based acceleration techniques [10–13] and medical applications; the application of machine learning to accelerator operation [14, 15]; and the development of diagnostic devices and methods [16–21]. As part of these activities, a tomographic method is being developed that would allow for the reconstruction of the 5-dimensional (5D) phase space of electron bunches. The method takes advantage of the polarizable X-band transverse deflecting structure (PolariX TDS) that has recently been developed in a collaboration between CERN, DESY, and PSI [22–24]. Two of these structures are installed at ARES and will be operational in 2023. The variable streaking angle has already enabled the reconstruction of the 3D charge density (x, y, t) at other beamlines [8, 9, 23, 25]. In the technique presented here, it is used to perform a slice-wise 4D transverse phase-space tomography [26–29], effectively reconstructing the 5D (x, x', y, y', t) phase space of the bunches. This information is useful to optimize and improve the beam quality, detect correlations and other features in the distribution, or

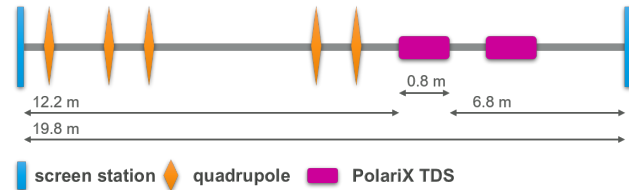


Figure 1: Sketch of the ARES beamline layout used for the 5D phase-space tomography simulation studies.

perform detailed simulation studies. The method and its working principle were first presented in [21]. Here, simulation studies in preparation for experimental measurements using the beamline setup at ARES are presented. These studies investigate the accuracy of the method for three different beam distributions.

WORKING PRINCIPLE

The method is based on performing a longitudinally sliced transverse phase-space tomography. In order to perform a transverse tomography, the transverse phase space needs to be rotated. This rotation is performed in normalized phase space, where the phase advance $\mu_{x,y}$ is equivalent to the rotation angles $\theta_{x,y}$ [30]. The conversions from real phase-space coordinates x, y and x', y' to normalized phase-space coordinates x_N, y_N and x'_N, y'_N are given by $x_N, y_N = x, y / \sqrt{\beta_{x,y}}$ and $x'_N, y'_N = x, y (\alpha_{x,y} / \sqrt{\beta_{x,y}}) + x', y' \sqrt{\beta_{x,y}}$, where $\beta_{x,y}$ and $\alpha_{x,y}$ are the Courant-Snyder parameters [31]. The longitudinal information of the bunch is obtained by streaking the bunch with the PolariX TDS at various transverse angles. By using a tomographic reconstruction algorithm such as the SART (Simultaneous Algebraic Reconstruction Technique) [32], this allows the reconstruction of the 3D charge density (x, y, t) [8, 9, 23, 25] for each (θ_x, θ_y) combination. Then, with the same algorithm, the 4D distribution (x, x', y, t) is reconstructed by using all the 3D reconstructions for a fixed θ_y . Finally, by combining the 4D reconstructions of all scanned θ_y , the 5D distribution (x, x', y, y', t) is obtained.

ACCURACY OF 5D PHASE-SPACE TOMOGRAPHY

The accuracy of the tomographic reconstructions is affected by several factors. Firstly, a larger number of transverse rotations and streaking angles is in general beneficial, especially when the distribution has detailed features. Secondly, chromatic effects due to a finite energy spread result

* sonja.jaster-merz@desy.de

SEISMIC ANALYSIS FOR SAFETY REQUIREMENTS OF SPIRAL2 ACCELERATOR

C. Barthe-Dejean, F. Lutton, M. Michel, GANIL-SPIRAL2, Caen, France
 M. Dubuisson, ADDL, Paris, France

Abstract

The SPIRAL2 Accelerator at GANIL is a superconducting ions continuous wave LINAC with two associated experimental areas. Mechanical engineers have been highly involved in the design of SPIRAL2 equipment since the beginning of the project in 2004. During the development phase, Computer Aided Design and calculation codes have been used throughout the complete process: from the ion sources, the LINAC, the beam transport lines and the experimental halls equipped with detectors. SPIRAL2 has to meet different safety requirements, among which seismic hazard. This involves justifying that the integrity of the radiologic containment barrier is always maintained in case of earthquake. This paper reports the improvement in design and calculation methods performed by GANIL engineers to meet the seismic safety requirements, specifically the non-missility feature of the equipment. The modal-spectral simulations, used to demonstrate the mechanical strength of equipment in case of earthquakes, was an important part of this design activity in the past 10 years. New methods have been used to calculate welds, fasteners and the ground anchor of the structural supports of the heaviest equipment.

INTRODUCTION

The non-missility criteria consists in preventing equipment weighing more than 500 kg at height 1.5 m to be projected on ground floor or walls of the building, which is used as containment barrier. The mechanical supports and frames have to withstand dynamic load corresponding to earthquake S.M.S (Security Maximum Seism) [1]. Also, fasteners and anchors to ground have to be analysed to prove that they withstand such loads. For example, LINAC supporting frame had to be reinforced for seismic load after first installation (Fig. 1).

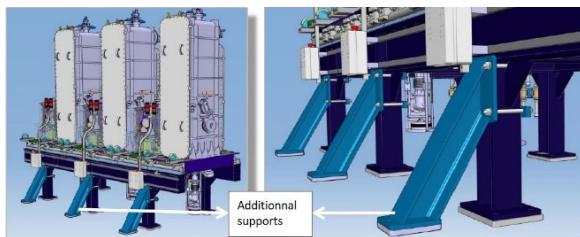


Figure 1: Additional supporting features LINAC A.

All calculation have been performed with the Finite Element Analysis Code ANSYS 2020 R1. The spectral load in three directions X, Y and Z is provided by Civil Engineering (Fig. 2) and implemented in the Finite Element Model and combined to gravity. First, a modal analysis is performed to identify the Eigen modes of the structure.

Then two load cases will be compared to identify the most severe: gravity + seism or gravity - seism. The X, Y and Z direction loads are also combined to each others: either by quadratic combination, or by Newmark combination.

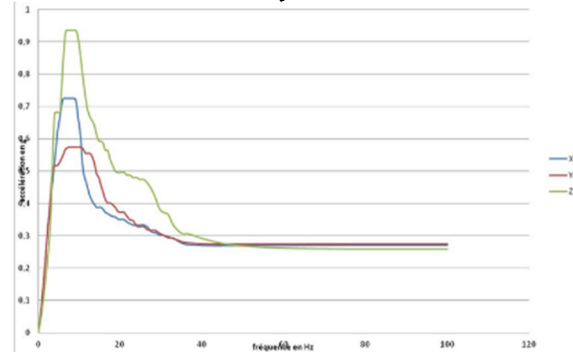


Figure 2: Spectral load based on S.M.S.in S3.

EXAMPLE 1 : NFS DETECTOR

NFS (Neutron for Science) is the first experimental area linked to SPIRAL2 accelerator. NFS is composed of a time-of-flight baseline and irradiation stations. A new detection system named FALSTAFF has been installed in the Time-of-flight NFS area as shown. This detector fully equipped weighs 592 kg, and hence is subject to non-missility requirements, has been clamped to ground as shown in Fig. 3.

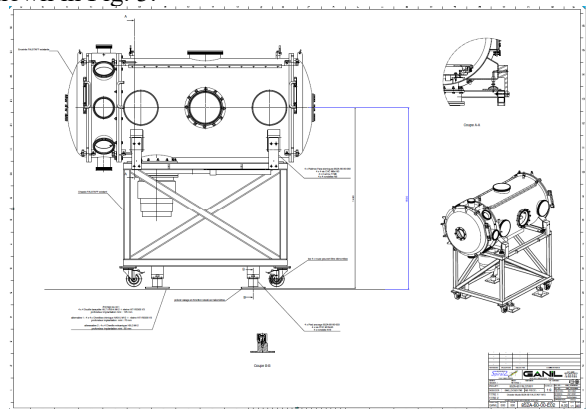


Figure 3: FALSTAFF detection assembly drawing.

In this example, only the structural frame and the feet of the vacuum chamber has to be calculated in order to prove that the FALSTAFF detector will not be projected under seismic load. We will focus on the fasteners and anchorage analysis even if welds and stresses are also post-treated.

Figure 3 shows how the equipment is clamped to the frame with metal plates and to the ground. The bonded anchors that have been calculated and selected according to the method described in [2].

DEVELOPMENT OF COMMERCIAL RFQ TOWARD CW APPLICATIONS

M. Masuoka†, H. Yamauchi, TIME Co., Mihara, Hiroshima, Japan

Abstract

TIME Co. developed a new 4-vane RFQ structure that can be used for a very high-duty factor operation. We eliminated the tuners to flatten the field distribution. The tuners increase RF contacts which may trigger unexpected local heat spots and subsequent discharges. In addition, we hollowed out the entire vane to achieve large cooling water channels. A high-power test showed that the commissioning was completed within one day. We could input a nominal RF power without experiencing almost any discharge. The applied duty factor was 5 % at the 200 MHz resonant frequency, and the measured frequency shift was not detected.

INTRODUCTION

In recent years, linear accelerators have been becoming superconducting, especially in the high energy range [1]. Also, applications that require high beam power, such as neutron generation [2] including BNCT [3] and alpha emitter production, have been increasing. These trends have led to strong worldwide demand for high-duty RFQ accelerators. However, the strategy for producing high-duty RFQs is not well established.

Time co. has been supplying three-layered structure RFQs [4] and IH-type linear accelerators, mainly for the Japanese domestic market for more than 10 years. Based on our accumulated technologies and experiences, we have decided to develop a new 4-vane RFQ that can be operated at a high duty factor. Although it is relatively not difficult to achieve a high duty factor by employing a long and large accelerating cavity with a low Kilpatrick limit and a low frequency, this approach [5] is not suitable for industrial use. We developed an RFQ that has a resonant frequency of 200 MHz, a total length of 3.0 m, and an output beam energy of 2.5 MeV. By eliminating stub tuners for voltage distribution and frequency adjustment and significantly strengthening the water channels for cooling passage, the accelerator was able to operate very stably. The first production unit of the RFQ has now been delivered to the Hungarian Academy of Sciences (MTA) is waiting for beam commissioning. The design parameters of the RFQ are summarized in Table 1.

Table 1: Design Parameters of RFQ

| | |
|------------------------|-------------------|
| Frequency | 200.3 MHz |
| Q Value | 14600 (Simulated) |
| | 13400 (Measured) |
| Design species | Proton |
| Beam Current | 20 mA |
| Injection beam energy | 35 keV |
| Extraction beam energy | 2.5 MeV |
| Length of Cavity | 3060 mm |
| Weight of Cavity | 2.3 ton |

† masuoka@time-merit.co.jp

THREE-LAYER STRUCTURE

The three-layer structure has been employed by some IH-Linacs in the past. This structure enables us to easily access the inside of the cavity. This means that precisely controlled machining can be applied directly to any interior segment of the cavity. We employed this structure to a 4-vane RFQ and provided several cavities to the market in Japan. The structure is illustrated in Fig. 1.

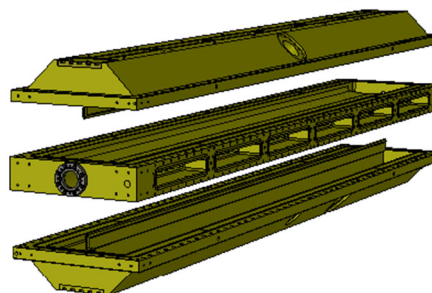


Figure 1: Three-layer structure of TIME RFQs.

As seen in the figure, the 4-vane acceleration cavity is composed of three parts, which are called the upper minor vane, major vane, and lower minor vane, respectively.

The upper minor vane has the vertical vane facing downwards, which is machined as a part of the upper vacuum vessel. The structure of the lower minor vane is the same as that of the upper minor vane but is arranged facing upward. The major vane, the centerpiece, consists of a rectangular frame with two horizontal vanes facing each other. Each of these three pieces is machined from a single forged oxygen-free copper block.



Figure 2: In process of assembling three-layer structure RFQ.

The major vane has grooves in its flange part and an O-ring and RF contact is installed. Although not visible in the Fig. 2, the back side of the major vane has the same structure and vacuum tight and good RF contact conditions are achieved. This structure allows the cavity to be disassembled and reassembled with a high degree of reproducibility. Furthermore, the inside of the vane can be hollowed out directly from the outside of the cavity. Thus, additional

ON THE UNILAC PULSED GAS STRIPPER AT GSI

P. Gerhard*, M. Maier

GSI Helmholtzzentrum für Schwerionenforschung GmbH, Darmstadt, Germany

Abstract

The UNILAC (UNIversal Linear ACcelerator) will serve as injector linac for heavy ion beams for the future FAIR (Facility for Antiproton and Ion Research), with the commissioning being anticipated in 2025. One of the crucial steps in the course of acceleration along the UNILAC is the stripping of the ions by a gas stripper in front of the main linac. Its efficiency is decisive in reaching the intensities required and may be increased by more than 50% by introducing hydrogen as stripping target, instead of the nitrogen used so far. This requires the stripper to be operated in a pulsed mode, since otherwise the pumping speed is not sufficient to maintain suitable vacuum conditions. The proof of principle was demonstrated in 2016. A dedicated project aims for a setup suitable for routine operation. Main issues are safety, reliability and automated operation. This project started in 2016, the realisation coming within the next few years. Recently, systematic measurements on the properties of the valves and their impact on the properties of the stripping target were carried out in order to specify proper operating parameters.

INTRODUCTION

The GSI UNILAC (UNIversal Linear ACcelerator) together with the heavy ion synchrotron SIS18 will serve as a high current, heavy ion injector for the future FAIR (Facility for Antiproton and Ion Research). The ions will be provided by the high current injector HSI. A stripper, situated at the end of the HSI, is necessary to increase the (very) low charge states of the heavy ions produced by the high current sources in order to enable further acceleration in the poststripper DTL (Drift Tube Linac) of Alvarez type. The present stripper employs a continuous nitrogen gas jet as stripping target. Out of the charge state spectrum resulting from the stripping process, one charge state has to be separated for further acceleration. For heavy ions like uranium, this results in the loss of up to 85% of the beam.

In order to increase the yield into the particular charge state desired, the introduction of hydrogen as stripping target was investigated from 2012–16. With H₂, in comparison to N₂, the width of the charge state distribution is reduced for heavy ions, thereby increasing the stripping efficiency e. g. for ²³⁸U by approximately 50%. Additionally, for all ions an increase of the mean charge state can be achieved. This was demonstrated successfully in 2016 [1–3].

Introducing H₂ into regular operation poses several challenges. Main concern is safety, since hydrogen is highly combustible. Apart from that, it is much more difficult to

extract from the vacuum system. Finally, a fully automated setup suitable for regular operation has to be developed.

A modified gas stripper setup had been developed in the course of the original investigations [1]. It exploits the low duty factor of the UNILAC in order to reduce the gas load by delivering only short pulses of high gas density synchronised with the beam pulse. This was realised by using a fast injection valve. The gas is injected into a stripping cell, which confines the highly volatile hydrogen. After the proof of principle, a dedicated project was initiated to devise the regular operation of this pulsed gas stripper. An extensive risk assessment had to be conducted and several risk mitigation measures developed. A test stand was set up to investigate the properties of the valves under worst case conditions. The liquid fuel injection valve initially chosen proved unsuitable for prolonged operation with gases [4]. Consequently, the type of the valves had to be changed and the setup adapted accordingly. The current pulsed gas stripper setup is shown in Fig. 1.

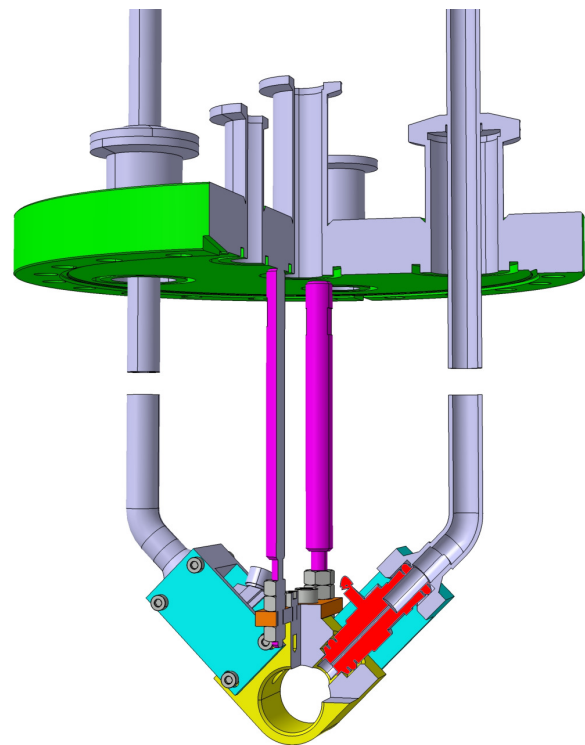


Figure 1: Sketch of the latest stripper setup accommodating two fast valves for gaseous media. One valve is indicated as cross section in red. Gas supply is from top via the tubes (grey). After injection into the accelerator vacuum, the gas is confined within the interaction zone in the yellow tube at the bottom, which surrounds the beam axis.

* p.gerhard@gsi.de

UPDATE OF ADJUSTABLE PMQ LENS

Y. Iwashita, KURNS, Kyoto University, Kumatori, Osaka, Japan
 T. Hosokai, D. O. Espinos, ISIR, Osaka University, Ibaraki, Osaka, Japan
 Y. Fuwa, JAEA/J-PARC, Tokai, Ibaraki, Japan

Abstract

Gluckstern's adjustable permanent magnet quadrupole (PMQ) lens based on five rings is revisited to achieve a compact focusing system for laser-accelerated beams. The first prototype was fabricated for bore diameter of 50 mm. The integrated gradient was up to 6.8 T. A new PMQ with a bore diameter of 25 mm is under fabrication based on the same geometry. While the first prototype unit was developed for the final focus magnet of the ILC, the second unit is the first doublet element for laser-accelerated electron beam focusing to be combined with this first unit. The current status of the development is reported.

INTRODUCTION

Adjustable Permanent Magnet Quadrupole lens based on Gluckstern's five-ring configuration has been studied [1]. While changing the intensity of the PMQs is not easy, Gluckstern proposed a method to adjust the strength without skew rotating the five PMQs alternately in opposite directions around the beam axis. The rotation angle ϕ at even positions of the PMQ ring is opposite in sign to the rotation angle ϕ at odd positions (see Fig.1).

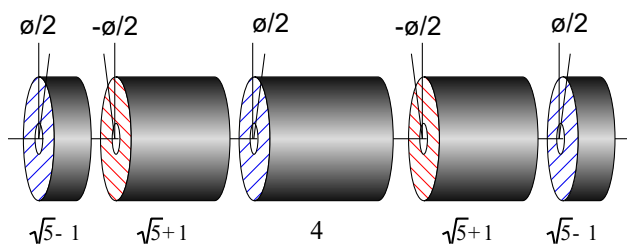


Figure 1: Gluckstern's five ring singlet.

The transfer matrix of such a system is represented by a 4 x 4 matrix M_n to account for the x-y coupling and the matrix of n-th PMQ is written as:

$$M_n = \begin{pmatrix} M_{n,xx} & \mathbf{0} \\ \mathbf{0} & M_{n,yy} \end{pmatrix}, \quad (n=1,2,3,4,5). \quad (1)$$

Since $M_5 = M_1$ and $M_4 = M_2$, the total transfer matrix M is calculated as:

$$M = R \cdot M_1 \cdot R^{-1} \cdot M_2 \cdot R \cdot M_3 \cdot R^{-1} \cdot M_2 \cdot R \cdot M_1, \quad (2)$$

where R represents the rotation of a magnet. By rewriting with 2 x 2 sub matrices, equ. (2) 4 x 4 matrix M can be written as

$$M = \begin{pmatrix} M_{xx} & M_{xy} \\ M_{yx} & M_{yy} \end{pmatrix}. \quad (3)$$

The off-diagonal sub matrices M_{xy} and M_{yx} , can be negligible when the lengths of the rings satisfy a relation. It should be noted that the distances d between rings are zero ($d=0$) in above case. A similar problem was solved for a case with $d=1\text{cm}$ case where summed PMQ length $2L_1+2L_2+L_3+4d$ is 26cm, keeping $2L_1-2L_2+L_3=0$. The rotation matrix R should be substituted by $R \cdot D$, where the transfer matrix D denotes a 1cm drift space. The off-diagonal sub matrices are expanded in series up to 5th order for a solution. The ratios are solved as $L_1:L_2:L_3 = 1.81046:5:6.37909$. Actual lengths are rounded to 20 mm, 55 mm, and 70 mm, respectively. The first prototype developed for the ILC was built with a 50mm bore diameter to get practical experience at ATF2 [2-7]. External dimensions are designed to fit into the beam tube of the detector at the interaction point (see Fig. 2). The exit hole is located 56 mm from the incoming axis to allow the outgoing beam to escape at a crossing angle of 14 milli-radians at 4 m from the interaction point.

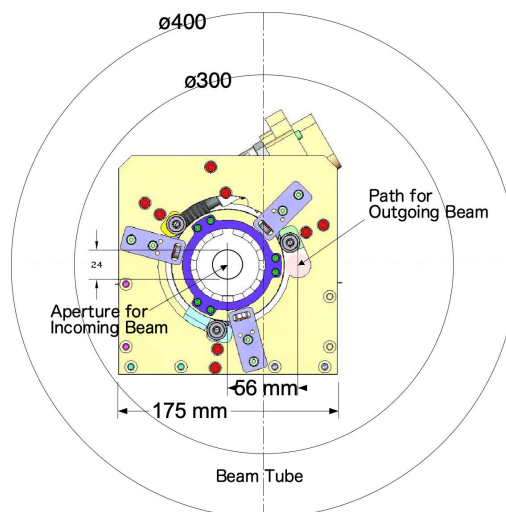


Figure 2: Adjustable PMQ in a beam tube.

REVIEW OF THE FIRST UNIT

Figure 3 shows the fabricated magnet. The five rings are rotated around an axis with three rollers holding the circumference of each ring, assuming that the circumference of each ring is a regular circle. The positions of the three rollers must be adjusted so that the axis of each ring is aligned. Therefore, care must be taken to ensure roundness. The odd-numbered rings were connected by a bridge and rotated by a single motor, while the even-numbered rings were rotated by individual motors. Thus, three motors were used in all. Because the rings strongly repel and attract each other, a large force is required to rotate them against each other, and a worm gear is used to rotate the

THE ESS FAST BEAM INTERLOCK SYSTEM: FIRST EXPERIENCE OF OPERATING WITH PROTON BEAM

S.Gabourin*, S. Pavinato, M. Carroll, S. Kövecses, A. Nordt, K. Rosquist
European Spallation Source, Lund, Sweden

Abstract

The European Spallation Source (ESS), Sweden, currently in its early operation phase, aims to be the most powerful neutron source in the world. Proton beam pulses are accelerated and sent to a rotating tungsten target, where neutrons are generated via the spallation effect. The damage potential of the ESS proton beam is high and melting of copper or steel can happen within less than 5 microseconds. Therefore, highly reliable and fast machine protection (MP) systems have been designed and deployed. The core system of ESS Machine Protection is the Fast Beam Interlock System (FBIS), based on FPGA technology. FBIS collects data from all relevant accelerator and target systems through 300 direct inputs and decides whether beam operation can start or must stop. The architecture is based on two main building blocks: Decision Logic Node (DLN), executing the protection logic and realizing interfaces to Higher-Level Safety, Timing System and EPICS Control System. The second block, the Signal Condition Unit (SCU), implements the interface between FBIS inputs/outputs and DLNs. This paper gives an overview on FBIS and a summary on its performance during beam commissioning phases since 2021.

INTRODUCTION

At ESS [1] the MP system has been designed in order to have an optimum balance between appropriate protection of equipment from damage and high beam availability [2]. Since the proton beam power of 125 MW per pulse (5 MW average) will be unprecedented and its uncontrolled release can cause serious damage of equipment within a few microseconds an FBIS is required to provide a minimum latency. The FBIS is responsible of collecting several types of information from different kind of so-called Sensor Systems. As for example slow systems (Vacuum, magnets and position of insertable devices) or fast systems (Radio Frequency Control Systems and Beam Instrumentation). These are inputs for signal processing units that make the decision on maintaining or not the beam production.

ARCHITECTURE OF FBIS

The FBIS architecture is fully redundant to ensure it can reach the Protection Integrity Level requested by the Protection Functions. Hundreds of Sensor Systems connection are foreseen along the 600m Linac, leading to a specific architecture with two component types: the “Signal Conversion Unit” (SCU) and the “Decision Logic Node” (DLN).

Signal Conversion Unit (SCU)

The SCU, Fig. 1, is a concentrator for Sensor Systems connections. It is based on a cPCI standard chassis with custom electronic cards. An SCU hosts up to 12 Mezzanine Cards (MC) on which Sensor Systems connect. Two more cards, called Serializers, host a MPSoC Zynq Ultrascale+ to manage the connection to the MC by the backplane, and the communication with the DLN through serial links, redundant optical connections using the Xilinx Aurora 64b/66b core IP.

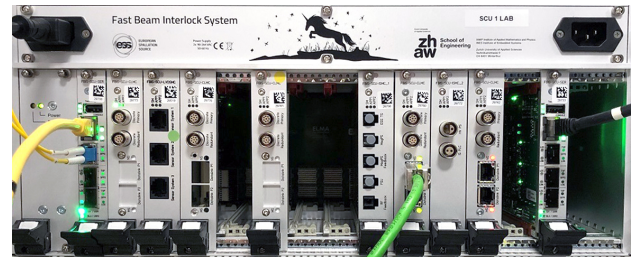


Figure 1: Signal Conversion Unit - SCU.

Several kind of MC were designed to interface with various types of Sensor Systems. One of them manages PLC-based Sensor Systems [3], and two others fast electronic Sensor Systems, mainly FPGA-based. Twenty five SCUs are foreseen along the Linac and in the Target building. The two first SCUs, installed close to the Ion Source, host also specific MC to interface with five hardware Actuators, acting to stop the Beam Production upon DLNs request.

Decision Logic Node (DLN)

The DLN, Fig. 2, performs the protection logic implemented by the FBIS. It also realizes the interfaces to the Higher-Level Safety, Control System and the ESS Timing System. It is based on mTCA, using the 3U chassis to host the redundant DLN carrier boards, heart of the FBIS functionality. It also contains the Timing System Event Receiver EVR, and a Concurrent CPU to host the FBIS EPICS Control System IOCs.



Figure 2: Decision Logic Node - DLN.

* stephane.gabourin@ess.eu

OVERVIEW OF STFC DARESBUURY LABORATORY VACUUM OPERATIONS FOR THE TESTING OF ESS HIGH BETA CAVITIES*

S. Wilde^{1,2}, K. Middleman^{1,2}, O. Poynton^{1,2}, M. Pendleton³, D. Mason³, J. Mutch³, G. Miller³

¹ASTeC, STFC Daresbury Laboratory, Warrington, UK

²Cockcroft Institute, STFC Daresbury Laboratory, Warrington, UK

³Technical Department, STFC Daresbury Laboratory, Warrington, UK

Abstract

This paper describes the vacuum systems and operations that are used at the STFC Daresbury Laboratory superconducting radio frequency (SuRF) lab during cold RF testing of European Spallation Source (ESS) high beta superconducting radiofrequency (SRF) accelerating cavities. Dedicated slow pump slow vent (SPSV) systems are used to perform vacuum acceptance testing of each cavity before, during and after cold RF testing. Details of the vacuum systems, acceptance criteria and test results will be discussed in detail.

INTRODUCTION

The ESS will be the most powerful linear proton accelerator that has ever been built. The accelerated protons will impact a helium cooled tungsten target wheel and produce neutrons that can be used to analyse the nanostructure of materials at the atomic level. STFC will supply 84 high beta SRF accelerating cavities to ESS as part of the UK's in-kind contribution to the facility. The SuRF lab was purpose built to conduct acceptance testing of the ESS high beta cavities once they have been built by industry partners. A range of acceptance testing is performed, including mechanical, cleanroom, vacuum, and RF. However, this paper will concentrate on the vacuum acceptance testing.

VACUUM ACCEPTANCE CRITERIA

Vacuum acceptance criteria have been developed so that each SRF accelerating cavity can be expected to work at optimal performance when installed into the ESS beamline. The acceptable helium leak rate is $<1\text{E-}9$ mbar l/s within the cavity beamline vacuum space and $<2\text{E-}10$ mbar l/s within the helium jacket vacuum space. The helium jacket vacuum space was given a more stringent helium leak rate acceptance criterion so that there is reduced risk of a cold superfluid helium leak once the cavity is installed within cryomodules. All helium leak rates are measured using a Leybold Phoenix Vario leak detector.

Cavities must be delivered to STFC with a total pressure of <1 mbar within the cavity beamline vacuum space. Cavities are at risk of particulate contamination if they are delivered with total pressure of >1 mbar as this puts the vacuum characteristics within the molecular flow regime [1].

The cavity beamline vacuum space must be measured using a residual gas analyser (RGA) and meet the specifications described in table 1. RGA measurements are performed using an MKS Microvision 2 and ensure that the cavity beamline vacuum space is within ultra-high vacuum

(UHV) specification [2]. Each vacuum acceptance testing step is performed at pre-defined junctures within the overall process of testing the ESS SRF cavities for SRF performance. An overview of the testing procedure, including the vacuum acceptance testing schedule is described in Fig. 1. A full and detailed description of the SRF testing and setup is given in [3].

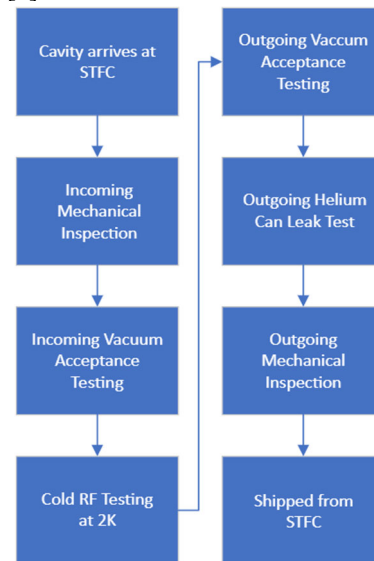


Figure 1: Simplification of the cavity testing process at STFC.

VACUUM TESTING SYSTEMS

Purpose built slow pump slow vent (SPSV) vacuum systems have been designed and built to perform vacuum acceptance testing. Two SPSV systems, comprising three separate pumping lines, are used during cold RF testing of cavities. A schematic of the SPSV systems is shown in Fig. 2. Each of these two systems is housed on a test insert that can hold up to three cavities. The cavities are loaded onto the test insert, located at a parking stand, and incoming vacuum acceptance testing is performed. The incoming acceptance testing begins by making vacuum connections to the right-angle valve (RAV) of the cavity within an ISO 4 glovebox and recording particulate counts. The SPSV system is then slow pumped at a rate of 10 mbar / min and a helium leak test of the cavity connection and RGA analysis of the SPSV system is performed. If the SPSV is accepted, then the cavity RAV is opened and leak testing and RGA analysis of the cavity is performed. Valve V7, as described in Fig. 2, is closed when opening the cavity RAV, and protects the SPSV system from overpressure. So long

FABRICATION, FIELD MEASUREMENT, AND TESTING OF A COMPACT RF DEFLECTING CAVITY FOR ELBE

Gowrishankar Thalagavadi Hallilingaiah^{*, 1}, André Arnold², Sebastian Köppen², Peter Michel^{1, 2}, Ursula van Rienen^{1, 3}

¹ University of Rostock, Rostock, Germany

² HZDR, Dresden, Germany

³ Department Life, Light & Matter, University of Rostock, Rostock, Germany

Abstract

A transverse deflecting cavity is being developed for the electron linac ELBE (Electron Linac for beams with high Brilliance and low Emittance) to separate the bunches into two or more beamlines so that multiple user experiments can be carried out simultaneously. A normal conducting double quarter-wave cavity has been designed to deliver a transverse kick of 300 kV when driven by an 800 W solid-state amplifier at 273 MHz. The main challenges in fabrication were machining the complex cavity parts with high precision, pre-tuning the cavity frequency, and the final vacuum brazing within the tolerances, which are described in this paper. The reason for a low intrinsic quality factor measured during the low power test was investigated, and suitable steps were taken to improve the quality factor. The cavity field profiles obtained from the bead-pull measurement matched the simulation results. Further, the cavity was driven up to 1 kW using a modified pick-up cup, and eventually, vacuum conditioning of the cavity was accomplished. The cavity fulfills the design requirements and is ready to be installed in the beamline.

INTRODUCTION

The linear electron accelerator, ELBE (Electron Linac for beams with high Brilliance and low Emittance) at Helmholtz-Zentrum Dresden-Rossendorf (HZDR), Germany, is a versatile machine that drives six distinct secondary particle and radiation sources used in a wide range of experiments related to health, matter, transmutation, and accelerator development [1]. In the current beamline setup, the accelerated high energy beam can only be transported to a single experimental station at any given time. This limits the utilization of the accelerator to one user at a time. To overcome this limitation, a new radio-frequency (RF) deflecting cavity was proposed in [2], which can distribute the bunches from the existing single beam into two or more beamlines. This cavity would enable the simultaneous operation of the multiple downstream secondary sources, thus significantly enhancing the accelerator's capabilities. Furthermore, this deflecting cavity is being actively considered as a beam separator for the proposed future accelerator facility at HZDR [3]. The complete geometry of the deflecting cavity is shown in Fig. 1, and its parameters are listed in Table 1. The design of the cavity is discussed in [2], and this paper focuses on its fabri-

Table 1: Important Parameters of the Deflecting Cavity

| Parameter | Value | Unit |
|---------------------------------|---------------|------------------------|
| Cavity: width x height x length | 275x181x500 | mm |
| Cavity aperture | V_{ap} | 30 mm |
| Resonance frequency | f_0 | 273 MHz |
| Frequency tuning range | Δf_0 | -1.67 to 1.86 MHz |
| Shunt impedance | R_{\perp}/Q | 9.96 M Ω |
| Intrinsic Q-factor | Q_0 | 11188 |
| Geometry factor | G | 57.03 Ω |
| Deflecting voltage | V_{\perp} | 300 kV |
| RF power loss | P_0 | 810 W |
| Peak electric field | E_{pk} | 2.49 MV/m |
| Peak magnetic field | S_{pk} | 1.21 W/cm ² |

cation. Additionally, we discuss the results of the frequency pre-tuning, on-axis field measurement and RF conditioning of the cavity.

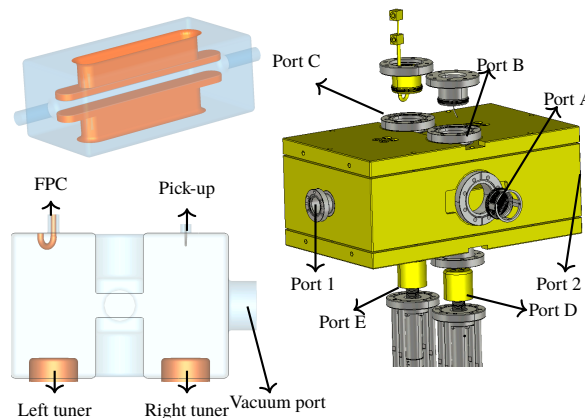


Figure 1: The cavity geometry showing all the cavity ports and the cavity components associated with the ports.

FABRICATION

Manufacturing a cavity out of a single solid copper block is not viable, either technically or financially. The cavity must therefore be divided into smaller parts so that these parts can be machined with greater accuracy. However, the tolerances achieved during machining may be impacted by brazing since the number of brazing joints increases with the number of cavity parts. Therefore, the cavity should be divided into fewer parts to reduce the number of brazing joints while maintaining the required tolerances. The cavity

* gowrishankar.hallilingaiah@uni-rostock.de

HIGH-POWER TEST OF AN APF IH-DTL PROTOTYPE FOR THE MUON LINAC

Y. Nakazawa*, H. Iinuma, Ibaraki University, Mito, Ibaraki, Japan
Y. Iwata, National Institute of Radiological Sciences, Chiba, Japan
E. Cicek, H. Ego, K. Futatsukawa, N. Kawamura, T. Mibe, S. Mizobara, M. Otani, N. Saito,
T. Yamazaki, M. Yoshida, KEK, Tsukuba, Ibaraki, Japan
Y. Kondo, R. Kitamura, T. Morishita, JAEA, Tokai, Naka, Ibaraki, Japan
Y. Sue, K. Sumi, M. Yotsuzuka, Nagoya University, Nagoya, Japan
Y. Takeuchi, Kyushu University, Fukuoka, Japan
N. Hayashizaki, Tokyo Institute of Technology, Tokyo, Japan
H. Yasuda, University of Tokyo, Hongo, Tokyo, Japan

Abstract

We conducted a high-power test of a prototype cavity of a 324-MHz inter-digital H-mode drift tube linac (IH-DTL) for the muon g -2/EDM experiment at J-PARC. This prototype cavity (short-IH) was developed to verify the fabrication methodology for the full-length IH cavity with a monolithic DT structure. After 40 h of conditioning, the short-IH has been stably operated with an RF power of 88 kW, which corresponds to 10% higher accelerating field than the design field (E_0) of 3.0 MV/m. In addition, the thermal characteristics and frequency response were measured, verifying that the experimental data was consistent with the three-dimensional model. In this paper, the high-power tests of this IH-DTL for muon acceleration are described.

INTRODUCTION

At the Japan Proton Accelerator Research Complex (J-PARC), an experiment is planned to measure the anomalous magnetic moments of muons [1] and search for electric dipole moments using accelerated muons by a muon linear accelerator (linac) [2]. The muon linac consists of a radio-frequency quadrupole linac (RFQ), an inter-digital H-mode drift-tube linac (IH-DTL), disk and washer coupled cavity linacs (DAW-CCL), and disk-loaded accelerating structures (DLS) [3, 4]. Muons are accelerated from an energy of 25 MeV to 212 MeV ($\beta = 0.95$), avoiding significant emittance growth to satisfy the experimental requirement of a transverse divergence angle of less than 10^{-5} .

The muons bunched and accelerated by the RFQ are accelerated from 0.34 MeV to 4.3 MeV ($\beta = 0.08 - 0.28$). The Alvarez DTL is widely used for this β region. However, reducing construction costs is critical for the realization of our experiment. Therefore, we employed the alternating phase focusing (APF) [5] method. The APF method utilizes the transverse focusing force derived from the RF electric field by appropriately selecting each gap's positive and negative synchronization phases. With this scheme, the structure can be drastically simplified by omitting the complicated focusing-element-containing drift tubes (DT). The APF is

usually used for heavy ion linacs having relatively low beam currents [6–8]. For our muon linac, the beam current is very low, so we considered it applicable. However, more careful treatment of the RF transverse force was necessary in the beam dynamics design [9] because of the much lighter mass of the muon.

Moreover, for the APF IH-DTL cavity, a three-piece structure [10], which is also effective for cost reduction, can be applied. A center plate and two semi-cylindrical side shells made of oxygen-free copper (OFC) are bolted together to form the cavity structure. On the center plate, all DTs are monolithically machined. With this method, the time-consuming DT alignment procedure is not required.

However, because this is the first case that the monolithic DT structure is being applied to a 324 MHz IH-DTL cavity for muon acceleration, we developed a short-length IH-DTL (henceforth called “short-IH”) as a prototype. We already confirmed that the field accuracy of less than $\pm 2\%$, which is required by the beam dynamics design [11], was achieved only by machining [12]. In this paper, the results of the high power test of short-IH are described.

SHORT-IH

Figure 1 shows the short-IH structure, which corresponds to the upstream one-third of the full-length IH-DTL (full-IH). The short-IH has the same synchronous phase as the first

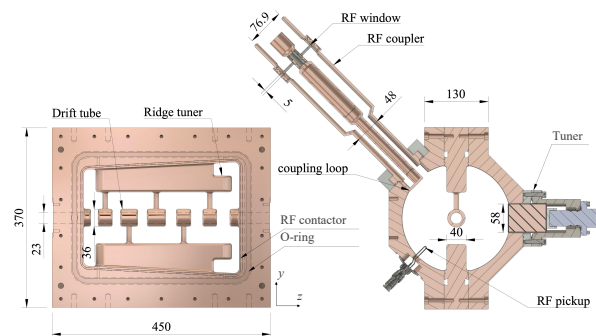


Figure 1: Mechanical structure of the short-IH. (A) Center plate. (B) Cross-sectional view.

* 20nd103s@vc.ibaraki.ac.jp

HIGH-POWER TESTING RESULTS OF X-BAND RF WINDOW AND 45 DEGREES SPIRAL LOAD

M. Boronat[†], N. Catalan-Lasheras, G. McMonagle, H. Bursali, A. Grudiev, I. Syrathev
CERN, Geneva, Switzerland

Abstract

The X-Band test facilities at CERN have been running for some years now qualifying CLIC structure prototypes, but also developing and testing high power general-purpose X-Band components, used in a wide range of applications. Driven by operational needs, several components have been redesigned and tested aiming to optimize the reliability and the compactness of the full system and therefore enhancing the accessibility of this technology inside and outside CERN. To this extent, a new high-power RF-window has been designed and tested aiming to avoid unnecessary venting of high-power sections already conditioned, easing the interventions, and protecting the klystrons. A new spiral load prototype has also been designed, built, and tested, optimizing the compactness, and improving the fabrication process. In these pages, the design and manufacturing for each component will be shortly described, along with the last results on the high-power testing.

INTRODUCTION

High-power RF (HP-RF) windows are crucial components used to isolate different sections of a vacuum line. When designing a RF window, the electric field on the surface of the ceramic window must be minimized, because high electric fields on this region could result in an electrical breakdown (BD) and eventually in the destruction of the ceramic itself. To be able to sustain high-power RF pulses, mixed-mode RF windows are normally used [1,2]. Based on this principle and in order to meet the requirement of the high-power X-Band test stands at CERN, a new design was proposed, optimized to sustain high peak power and high repetition rate.

High-power RF loads are components needed in many accelerator facilities, especially when using traveling wave structures, absorbing the remaining power after de acceleration. In X-band, due to the small size of the structures and the limited available space, new designs have been focused in making them more compact. A new concept of a spiral load has been developed at CERN, fabricated by additive manufacturing techniques out of titanium (3D metal printing) [3]. First prototypes were successfully tested on the high-power X-band test facilities (Xboxes) [4].

Recent designs are moving towards a more efficient fabrication procedure to overcome intrinsic limitations coming from the additive manufacturing process. Previous prototypes of spiral loads were printed at 45 degrees (Fig. 2

left) to avoid the horizontal segments and the associated waste of printed titanium volumes and supports. To improve the procedure of manufacturing, a new spiral load design was proposed [5] with an optimized cross-section and a twisted input waveguide, which allows horizontal 3D printing, with less support posts required and the possibility of stacking them vertically.

In these pages we will present the results obtained during the high-power tests of both components. The high-power tests were carried out at CERN, on the X-Band high-power test stand 3 (Xbox3) which consist of a combination of two 5.5 MW klystrons, feeding two test benches, providing up to 40 MW after pulse compression (50 ns pulse length), with a maximum repetition rate up to 200 Hz per line [6].

X-BAND RF WINDOW

The X-Band HP-RF window was designed to sustain up to 75 MW peak power. The design includes a mode converter from TE₁₀ (rectangular) to TE₀₁ (circular), which allows higher flexibility in terms of integration, taking advantage of the rotational symmetry of the circular mode. The electric field on the ceramic window was designed to be below 3.4 MV/m. To reduce the peak field, a ceramic disc of 65 mm of diameter was chosen. The thickness of the ceramic was defined as 2,43 mm and the transition, from the circular waveguide diameter to the window diameter was done in two-stages to preserve the required TE₀₁ mode purity.

High Power Test

The historic of peak power and average power put into the window is shown in Fig. 1. The component was tested at different pulse length and repetition rate combinations, reaching up to 40 MW peak power at 150 Hz and 1.9 kW average power (35 MW peak at 200 Hz). Table 1 shows a summary of the main parameters measured during the processing. The RF window was tested up to the performance limits of the facility, and no breakdowns were detected.

Table 1: Measured Parameters on the Flat Regions

| | R ₁ | R ₂ | R ₃ | R ₄ |
|----------------------|----------------|----------------|----------------|----------------|
| Power [MW] | 35 | 35 | 35 | 40 |
| Average [kW] | 1.47 | 1.9 | 1.6 | 1.64 |
| Transmission [dB] | -0.19 | 0.18 | -0.16 | -0.15 |
| Pulse Length [ns] | 50 | 50 | 100 | 50 |
| Repetition Rate [Hz] | 150 | 200 | 150 | 150 |

[†] boronat.arevalo@cern.ch

MONTE CARLO MODEL OF HIGH-VOLTAGE CONDITIONING AND OPERATION

W. L. Millar*, W. Wuensch, CERN, 1211 Geneva 23, Switzerland
G. Burt, Cockcroft Institute, Lancaster University, Lancaster LA1 4YW, UK

Abstract

To synthesise the experimental results and theory pertaining to high-field phenomena, a model has been developed to simulate the conditioning and operation of high-field systems. By using a mesh-based method, the high-field conditioning of any arbitrary geometry and surface electric field distribution may be simulated for both RF and DC devices. Several phenomena observed in previous high-field tests such as the probabilistic behaviour of vacuum arcs and the inhomogeneous distribution of arc locations are described by this approach.

INTRODUCTION

High-voltage conditioning is the progressive increase in an electrode's resistance to arcing which is developed during high-field operation. The process is a relevant topic for any technology where breakdown limits performance and numerous RF and DC test facilities have been established in this context [1–7]. To better understand the results from these facilities and offer insight into how current conditioning procedures could be improved, a new discretised model has been developed.

THE MODEL

The model is based on the progressive modification of the electrode surface and relies on several assumptions. Given the often inhomogeneous field distribution in high-field devices, the electrode geometry divided into individually treated mesh elements. Each element is assigned a scaling factor, k_i , to allow calculation of the local electric field relative to the maximum, E_O , for a given operating voltage. To facilitate inhomogeneous meshing, the number of elements and the area of each, a_i , is also user-definable. Devices may then be simulated with any arbitrary spatial resolution.

Generally, in existing conditioning procedures the field is increased gradually, as the rate at which devices condition quickly decreases when operating at fixed voltages [8–11]. If a constant breakdown rate is maintained during this ramping, the increase in operating field is asymptotic, and this is regularly observed in high-gradient RF cavity tests [8–10]. In one instance, a cavity tested at CERN showed no reduction in the breakdown rate when operated under fixed conditions in the later stages of testing [10]. Results from these, and similar RF cavity tests elsewhere, have also shown that the conditioning of similar devices is most comparable when plotted against the cumulative number of pulses, as opposed to cumulative number of breakdowns [8].

Based on these characteristics, the model assumes a maximum attainable electric field, E_L , for a given reference breakdown rate i.e. probability of arcing, P_{Ref} . The level of conditioning of each element is denoted $E_{S,i}$. In a device with a homogeneous field distribution, E_S then refers to the surface electric field which can be established at the reference breakdown rate. To provide the conditioning effect the model assumes that, in the absence of breakdowns, $E_{S,i}$ is increased with each pulse as:

$$\Delta E_{S,i} = \gamma \cdot \frac{E_O \cdot k_i}{E_{S,i}} \cdot \left[1 - \frac{E_{S,i}}{E_L} \right] \quad (1)$$

where γ is a constant to allow fitting to existing data and has units of V/m. The latter term in Eq. (1) then remains unitless and is scalable for different materials, a characteristic which aligns with existing test results in which different materials were recorded as having conditioned at different rates and to different field levels [12]. In RF cavities, the breakdown rate has been shown to scale with the electric field as [13]:

$$BDR \propto E^{30} \quad (2)$$

However, as conditioning progresses the breakdown rate for a given field level decreases. As such, it is assumed that the probability of breakdown for a given mesh element on each pulse, $P_{BD,i}$, scales with the ratio of the applied electric field to its conditioned state as:

$$P_{BD,i} \propto \left[\frac{E_O \cdot k_i}{E_{S,i}} \right]^{30} \quad (3)$$

Experiments have also shown that it is common for several breakdowns to occur in quick succession, followed by a quiescent period. This has led to the proposal that breakdowns may be classified as primary events, which occur stochastically, and secondary events, which are a consequence of the primary event [8, 9]. It is postulated then, that breakdowns are capable of effectively diminishing the conditioned state the surface. However, as devices are capable of reliably establishing high fields after several breakdowns, improvement is also possible. This could correspond physically, for instance, to the removal of field emission sites capable of nucleating future breakdowns. To capture this effect, a unitless enhancement factor, ψ , is added to Eq. (3) as:

$$P_{BD,i} \propto \left[\frac{E_O \cdot k_i}{E_{S,i} \cdot \psi_i} \right]^{30} \quad (4)$$

* lee.millar@cern.ch

LIMITS ON STANDING WAVE CAVITY PERFORMANCE DUE TO THERMAL EFFECTS*

S. Smith[†], G. Burt, Lancaster University, Lancaster, UK
Cockcroft Institute, Daresbury Lab, UK

Abstract

After an RF cavity has been designed, a thermal analysis is typically performed to assess the effects of RF heating on the operating frequency and field flatness. A multi-physics approach (coupled electromagnetic, thermal, and mechanical) is normally employed, sometimes combined with computational fluid dynamics (CFD) simulations to incorporate flowing water, which is used for cooling in normal conducting structures. Performing a CFD analysis can add significant time to the design process because of the long and complex simulations and instead, approximations of the heat transfer coefficients and inlet/outlet water temperature rises are made and used directly in the multi-physics analysis. In this work, we explore these approximations, through the use of coupled electromagnetic-thermal-structural simulations and a preliminary CFD analysis.

INTRODUCTION

Normal conducting RF cavities are typically cooled by passing water through copper pipes around the structure, with the temperature being changed to compensate for frequency shifts. These shifts are caused by the thermal expansion of the cavity which is in-turn caused by RF power dissipation in the cavity walls. An analysis of these heating effects is generally left until the end of a design, and approximations are normally made about the heat transfer coefficient between the water and the copper walls and the temperature rise of the water as it passes through the pipes [1]. A self consistent approach that takes all the physics of the heating problem into account can be used to identify when these approximations are valid and eventually can be used to investigate the ultimate power limits on normal conducting cavities.

ELECTROMAGNETIC DESIGN

The first step in the thermal analysis requires the RF losses to be calculate on the cavity walls. The cavity used for this study is a C-band (5.712 GHz) bi-periodic standing wave structure that has been designed for industrial use. The nominal average input power is 850 W and it produces a 2 MeV electron beam. The electromagnetic analysis was performed in Ansys HFSS with the RF surface losses being shown in Fig. 1 [2]. Once these losses have been calculated they are scaled to the average input power of the linac and exported for use in thermal simulations.

* Supported by Research Grant: ST/P002056/1

[†] s.smith26@lancaster.ac.uk

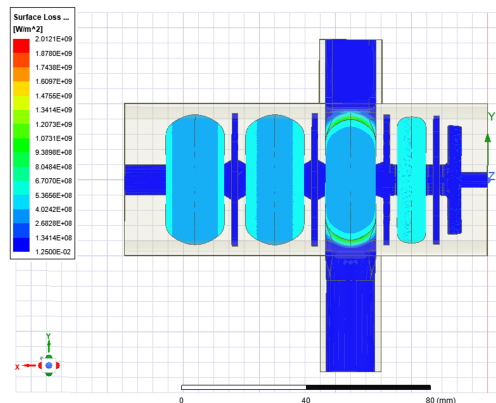


Figure 1: C-band linac showing RF surface losses.

BACKGROUND THEORY

The average temperature rise in the water used for cooling the structure can be estimated using [3]:

$$\Delta T = \frac{\dot{Q}}{c_p \cdot \dot{m}}, \quad (1)$$

where \dot{Q} is the heat added to the system, c_p is the specific heat of the fluid and \dot{m} is the mass flow rate of the fluid:

$$\dot{m} = \rho v A, \quad (2)$$

where v is the fluid velocity and A is the pipe cross sectional area. For an average input power of 850 W, and a mass flow rate of 0.08 kg/s a water temperature rise of 2.53 °C is obtained. The temperature difference between the water and the walls of the copper pipes is given by:

$$\Delta T = \frac{\dot{Q}}{hL\pi D}, \quad (3)$$

where L is the length of the pipe system, D is the hydraulic diameter and h is the heat transfer coefficient:

$$h = \frac{Nu \cdot \kappa}{D}, \quad (4)$$

where k is the thermal conductivity of the fluid and Nu is the Nusselt number given by:

$$Nu = \frac{(\frac{f}{8})(Re - 1000)Pr}{1 + 12.7(\frac{f}{8})^{1/2}(Pr^{2/3})}. \quad (5)$$

Re is the Reynold's number which provides information about whether the flow is turbulent or not. It is given by:

$$Re = \frac{\rho v D}{\eta} = \frac{994.1 \cdot 2.85 \cdot 0.06}{7.2 \times 10^{-4}} = 23608 \quad (6)$$

COMPACT TURN-KEY SRF ACCELERATORS*

N.A. Stilin[†], A. Holic, M. Liepe, T. O’Connell, J. Sears, V.D. Shemelin and J. Turco
 Cornell Laboratory for Accelerator-Based ScienceS and Education (CLASSE), Ithaca, USA

Abstract

The development of simpler, compact Superconducting RF (SRF) systems represents a new subject of research in accelerator science. These compact accelerators rely on advancements made to both Nb₃Sn SRF cavities and commercial cryocoolers, which together allow for the removal of liquid cryogenics from the system. This approach to SRF cavity operation, based on novel conduction cooling schemes, has the potential to drastically extend the range of application of SRF technology. By offering robust, non-expert, turn-key operation, such systems enable the use of SRF accelerators for industrial, medical, and small-scale science applications. This paper provides an overview of the significant progress being made at Cornell, Jefferson Lab, and Fermilab (FNAL), including stable cavity operation at 10 MV/m. It also introduces the primary challenges of this new field and their potential solutions, along with an overview of the various applications which could benefit the most from this technology.

INTRODUCTION

Various workshops and investigations have shown that numerous applications exist for particle accelerators which could further benefit from the use of SRF technology [1, 2]. These applications cover several fields of interest, including: energy and environment, such as wastewater or flue gas treatment; medicine, such as device sterilization and isotope production; security and defense, such as cargo inspection; industry, such as biofuel production. Many of these applications fall within a similar range of beam parameters, requiring only moderate energies but high current and average power; see Table 1 [1, 2].

Table 1: Typical Beam Parameters

| Property | Value | Units |
|----------|---------|-------|
| Energy | 1 – 10 | MeV |
| Current | 0.1 – 1 | A |
| Power | 1 – 10 | MW |

These applications can benefit from the use of SRF technology, which offers significantly more efficient operation compared to normal conducting cavities. However, the use of SRF cavities has not been possible until the recent improvements made to both Nb₃Sn cavities and cryocoolers. Together, these improvements allow compact accelerators to operate at the energies required while not being reliant

on liquid helium for cooling. This shift to conduction-based cooling greatly simplifies the system while also being much cheaper than the extensive infrastructure required for operating with helium. Combined, these developments have brought SRF technology within reach of important small-scale applications such as the ones discussed above.

KEY COMPONENTS

This section will briefly describe the improvements made to both Nb₃Sn cavities and commercial cryocoolers which are essential to the design of new compact accelerators.

Nb₃Sn Cavities

Nb₃Sn is an alternative material for SRF cavities which has seen significant interest and growth over the last couple decades. The main advantage offered by Nb₃Sn is that its critical temperature is 18 K, almost twice that of pure Niobium [3]. This affects the BCS component of the surface resistance, which means Nb₃Sn cavities can operate with lower losses and/or at a higher temperature compared to Niobium cavities.

Since 2013, Nb₃Sn cavities have been improved to the point of operating at 4.2 K at 15 MV/m or higher while still maintaining a high Q₀ of 1 – 2 E10 [?, 3–7, 9]. These high Q₀ values correspond to a very small cavity heat load of less than one watt for a single-cell 1.3 GHz cavity; see Fig. 1. This means that we can now achieve highly efficient cavity operation at field levels which are relevant to small-scale operations. Since these achievements have been demonstrated at 4.2 K, these cavities are also capable of using a new cooling scheme which does not require liquid helium.

Cryocoolers

The cryocooler concept was first introduced in the 1960’s, but only in the last few years have they reached the cooling capacity required for use with Nb₃Sn cavities. For example, initial models of Cryomech’s 4.2 K pulse-tube type cryocoolers, which were released around 2000, could only remove less than 1 W of heat from a system at 4.2 K [10]. By comparison, the most recent models are able to remove more than 2 W [10], which means they are capable of being used as the primary cooling source of current Nb₃Sn cavities operating at medium fields. Figure 1 shows this improvement of cryocooler performance.

CONDUCTION COOLED CAVITIES

With the current state of Nb₃Sn cavities and commercial cryocoolers, it is possible to design a system which uses an entirely new cooling scheme compared to standard LHe cooling; see Fig. 2. The first possibility is to use direct conduction cooling, in which the cryocooler cold head and

* Cornell’s work was supported by U.S. DOE award DE-SC0021038 “Next Steps in the Development of Turn-Key SRF Technology,” which supports the full development of a conduction cooling based cryomodule.

[†] nas97@cornell.edu

R&D TOWARDS HIGH GRADIENT CW CAVITIES

D. Bafia*, P. Berrutti, B. Giaccone, A. Grassellino,
D. Neuffer, S. Posen, A. Romanenko
Fermi National Accelerator Laboratory, 60510 Batavia, IL, USA

Abstract

We discuss Fermilab's recent progress in the surface engineering of superconducting radio-frequency (SRF) cavities geared toward producing simultaneously high quality factors and high accelerating gradients in cryomodules. We investigate possible microscopic mechanisms that drive improved performance by carrying out sequential RF tests on cavities subjected to low temperature baking. We compare performance evolution to observations made with material science techniques and find correlations with material parameters. We also discuss other key advancements that enable high gradient operation in cryomodules.

INTRODUCTION

Bulk Nb superconducting radio-frequency (SRF) cavities remain as the primary accelerating technology for current and future accelerators. While these resonant structures are capable of sustaining high Q_0 at high accelerating electric fields E_{acc} in continuous wave (CW) operation, the realization of the next generation of accelerators relies on the further advancement of these metrics as this translates into potentially dramatic reductions in associated cryogenic and construction costs. To further improve these metrics, fundamental R&D aimed at understanding the microscopic mechanisms that drive RF losses in these structures is required. Moreover, other key technologies which improve or preserve the gradient reach of cavities, such as the *in situ* mitigation of field emission in a cryomodule, must be explored.

In this contribution, we present recent efforts at Fermilab that focus on extending the performance of bulk Nb SRF cavities. First, we discuss new insights on the role of impurities in the performance of SRF cavities by studying the evolution of cavity $Q_0(E_{acc})$ as we gradually increase the concentration of thermally diffused oxygen impurities within the RF layer *via* sequential vacuum baking treatments. By correlating cavity performance with observations made in time-of-flight secondary ion mass spectrometry, we confirm the positive role that diffused oxygen from the native niobium oxide has on cavity performance. We show evidence that diffused oxygen captures hydrogen and prevents the precipitation of poorly superconducting niobium nano-hydrides. In turn, this results in i) the elimination of high field Q-slope up to quench after *in situ* vacuum baking and ii) the ability to tune cavity quench field by simple thermal diffusion. Next, we discuss two new technologies which enable a dramatic improvement in cavity performance. First, as part of the ILC cost reduction program, we demonstrate the new 2-step bak-

ing + cold electropolishing (EP) surface treatment, which has been shown to consistently yield single-cell cavities of ultra-high gradients (>49 MV/m) and nine-cell cavities which routinely quench at high gradients. The second key technology is plasma processing, which has been recently fully validated for 1.3 GHz cryomodules, and has the potential to mitigate hydro-carbon related field emission and multipacting *in situ*. Lastly, we briefly discuss the application of these recent advancements in SRF technology to a new proposed accelerator, namely, in a linac to replace the current booster at Fermilab which will enable 2.4 MW of power on target for LBNF/DUNE.

EXTENDING MICROSCOPIC UNDERSTANDING OF THE ROLE OF IMPURITIES IN CAVITIES

One major performance determining factor of bulk Nb SRF cavities is the impurity structure within the first 100 nm from the inner RF surface. By combining various chemical and baking treatments, it is possible to tailor this impurity structure to redirect supercurrent flow and/or minimize deleterious inclusions that ultimately limit RF performance. Fig. 1 depicts four different cavities subjected to four such surface treatments: N-doping [1], N-Infusion [2], 120 C LTB [3], and electropolishing [3].

Cavities subjected to EP are clean from extrinsic impurities except for hydrogen. As shown in Fig. 1, cavities subjected to this surface treatment yield a dramatic decrease in Q_0 above 25 MV/m, dubbed the high field Q-slope (HFQS). It is now well known that this phenomenon is driven by the breakdown of proximity coupled niobium nano-hydrides which precipitate at cryogenic temperatures [4].

Nitrogen has been a key impurity in mitigating HFQS and enabling excellent RF performance in SRF cavities. It has been shown by Grassellino *et al.* that dilute and uniform concentrations of nitrogen interstitial are capable of yielding ultra-high Q_0 at moderately high gradients in cavities [1]. On the other hand, nitrogen infusion shows that surfaces which contain a sharp concentration gradient of N within the RF layer produce very high gradients with moderately high Q_0 's [2].

Another key surface treatment is the 120 C *in situ* vacuum bake, which has been shown to mitigate HFQS and yield cavities with high gradients at moderate Q_0 , the so-called 120 C bake effect. This surface treatment requires that a cavity be fully assembled for testing and be evacuated prior to undergoing an *in situ* vacuum bake at 120 C in a low temperature oven. It has only been recently found by Romanenko *et al.* that oxygen diffused from the native niobium oxide is respon-

* dbafia@fnal.gov

SWELL AND OTHER SRF SPLIT CAVITY DEVELOPMENT

F. Peauger*, O. Brunner, M. Garlasche, S. Gorgi Zadeh, T. Koettig, G. Rosaz, I. Syratchev,
 M. Timmins, M. Therasse, W. Venturini Delsolaro, CERN, Geneva, Switzerland
 G. Burt, Lancaster University, Lancaster, UK

Abstract

An innovative superconducting cavity topology has been recently proposed at CERN. It integrates longitudinal waveguide slots crossing perpendicularly the RF surface to damp transverse higher order modes. The RF current lines of the fundamental mode run along the slots, inducing no perturbation of the accelerating mode. Thanks to this approach, the cavity can be built by sectors, which is well appropriate to precise manufacturing techniques. This configuration allows direct access to the RF surface, thus facilitating the surface preparation and thin film deposition process in the case of cavities based on Nb/Cu technology. This paper covers the latest development of a 600 MHz slotted elliptical cavity called SWELL, which has been proposed as an alternative option for the FCC-ee RF system as well as the prototyping of a simplified SWELL version of a single cell 1.3 GHz elliptical cavity. The development of a new type of 6 GHz split resonator is also on-going at Lancaster University. This cavity is made of two halves and is dedicated to superconducting thin film characterization. An overview of this new development will be given.

INTRODUCTION

Elliptical radio frequency (RF) cavities operating on the TM_{010} accelerating mode have RF current lines running longitudinally along the cavity surface. It is possible to divide the cavity geometry into sectors with an arbitrary angle without perturbing the field pattern of the accelerating mode. Each cavity sector becomes an open structure, which opens new opportunities to fabricate highly performant superconducting RF (SRF) cavities. In such an approach, longitudinal slots can even be added provided that the slot width is small compared to the cavity outer diameter. The slots can act as high frequency waveguides to extract and propagate transverse Higher Order Modes (HOM) outside the resonator in order to efficiently damp them.

In the CLIC Test Facility CTF3 at CERN, the 3.5 A drive beam electron accelerator was equipped with 3 GHz Slotted Irises Constant Aperture (SICA) copper structures which adopted this strategy [1]. The CLIC 12 GHz Power Extraction and Transfert Structure (PETS) was designed to decelerate a more intense electron beam of 100 A and was built of 8 copper sectors (octants) to allow extremely strong HOM damping [2].

The slotted cavity concept was also explored in the superconducting domain for high current Energy Recovery Linac (ERL) applications [3]. A 3-cell 1.3 GHz cavity was built

in bulk niobium and was preliminary tested in a vertical cryostat [4].

In this paper, we present a novel scheme of a slotted SRF cavity where the sectors are made of copper and are precisely machined, as experienced in the CLIC RF structures, and are coated with a niobium (Nb) thin film to provide an inner superconducting surface. We describe the RF design and development plan of a new Slotted Waveguide ELLiptical (SWELL) cavity proposed as an alternative solution for the FCC-ee RF system [5]. We finally give an overview of the development of 6 GHz split cavities dedicated to the exploration and RF characterization of new superconducting thin films.

SWELL SUPERCONDUCTING CAVITY DEVELOPMENT FOR FCC

The original idea of the SWELL cavity concept applied to the FCC-ee machine came up in December 2020 [6]. The wish was to improve the cavity performances, to optimize the installation scenario of the RF system and to reduce its overall cost. Since the SWELL cavity is made to operate at high beam current and high accelerating gradient at the same time, it is a good candidate to have a single cavity type for the Z, W and H working energies of FCC-ee which are listed in Table 1.

Table 1: FCC-ee Operating Modes.

| Mode | RF Voltage (GV) | Beam Current (mA) |
|-------|-----------------|-------------------|
| Z | 0.120 | 1280 |
| W | 1 | 135 |
| H | 2.08 | 26.7 |
| ttbar | 11.3 | 5 |

600 MHz SWELL RF Design

The operating RF frequency of 600 MHz has been chosen as an intermediate frequency between the two FCC-ee baseline frequencies (400 MHz and 800 MHz). It is a good compromise between different factors. For example, low cavity impedance is crucial especially for the Z operating point, which runs at a beam current of 1.28 A with long trains of bunches. It prevents risks of beam instabilities and of high power RF losses due to HOMs. This is favored at low RF frequencies as the longitudinal and transverse loss factors scale with the RF frequency to the power of two and three, respectively. On the other hand, the size of the cavity and its superconducting RF surface is smaller at high RF frequency, thus reducing the risk of having surface defects, which may induce parasitic losses or may trigger quenches.

* franck.peauger@cern.ch

NEXT-GENERATION Nb₃Sn SUPERCONDUCTING RF CAVITIES*

N. Verboncoeur[†], R. Porter[‡], G. Gaitan, M. Liepe, L. Shpani, N. Stilin, Z. Sun
Cornell University, Ithaca, NY, USA

Abstract

Nb₃Sn currently is the most promising alternative material for next-generation, higher-performance SRF cavities. Significant recent progress has been made in further increasing efficiency, maximum field, and demonstrating readiness for first applications in actual accelerators. This paper will present an overview of worldwide recent progress in making this material a viable option for future accelerators.

INTRODUCTION

The use of superconducting RF (SRF) cavities was once considered outlandish. Today, modern facilities use niobium (Nb) SRF cavities, however the future of both scientific research and industrial accelerators would greatly benefit or would be possible only if a superconducting material that supports higher performance exceeding the material limitations of Nb for use in SRF cavities can be found.

Why Nb₃Sn?

Niobium has served us well for years, so why is Nb₃Sn a better choice? First we must understand several figures of merit by which we judge an SRF cavity.

First and foremost is the accelerating gradient, E_{acc} . This determines the amount of energy that a cavity can deliver to a beam per length, typically reported in MV/m. The ultimate limit on the accelerating gradient is directly proportional to the superheating field, H_{SH} , of the superconducting material used.

The BCS surface resistance is another important factor in cavity performance defined by

$$R_{BCS} = f^2 e^{-const \cdot T_c/T}.$$

The total surface resistance that determines the cavity's quality factor, Q_0 , is made up of the BCS resistance and the residual resistance. By increasing the critical temperature, the BCS resistance decreases allowing us to achieve a higher Q_0 .

The quality factor, $Q_0 = \frac{G}{R}$, is a figure which describes the cavity's efficiency, where G is the cavity's geometry factor. The quality factor plays a roll in determining the cooling power needed, and is also related to the cavity's resonant frequency. The dissipated power, P_{diss} , depends on Q_0 and is defined by

$$P_{diss} = \frac{V^2}{\frac{R}{Q_0} Q_0},$$

where V is the accelerating voltage and $\frac{R}{Q_0}$ is a factor describing how effectively power can be delivered to a beam.

Finally, the cooling power, $P_{AC, Cooling}$, depends on the AC wall power needed to do one watt's worth of cooling in your system and Q_0 . The cooling power is defined by

$$P_{AC, Cooling} = COP^{-1} \cdot P_{diss},$$

where P_{diss} is as defined above and COP is the coefficient of performance for the system in W/W , as seen in Fig. 1.

Nb₃Sn is predicted to outperform Nb in a number of significant ways. First, the quality factors at 4.2 K of Nb₃Sn are predicted to be even higher than that of pure Nb at 2 K as seen in Fig. 2 where the Q_0 is visibly much higher for Nb₃Sn than for Nb at SRF operating temperatures [1]. This means that we could, in principle, operate Nb₃Sn cavities at 4 K

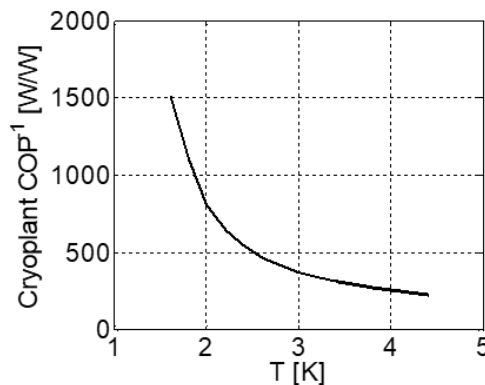


Figure 1: The cooling power, which is in watts of AC wall power needed to remove one watt of power from the cryogenic system, is much higher for low temperatures [2, 3].

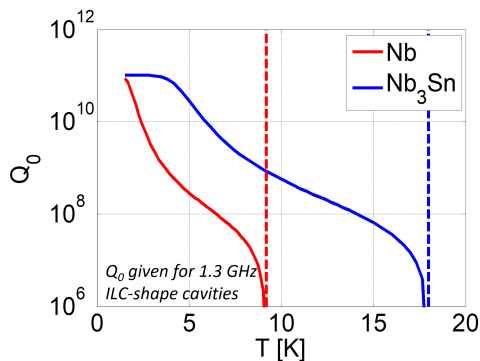


Figure 2: Q_0 versus temperature. At 4.2 K, Nb₃Sn significantly outperforms pure Nb. This figure shows that a 1.3 GHz Nb₃Sn cavity could efficiently operate at 4.2 K rather than 2 K, which is the typical operation temperature for Nb cavities

* This work is supported in part by NSF grant No. PHY-1549132 and DOE grant No. DE-SC0008431

[†] nmv39@cornell.edu

[‡] Now at SLAC

OVERVIEW OF ADS PROJECTS IN THE WORLD

B. Yee-Rendon*

Japan Atomic Energy Agency (JAEA), Tokai, Japan

Abstract

Accelerator-driven subcritical systems (ADS) offer an advantageous option for the transmutation of nuclear waste. ADS employs high-intensity proton linear accelerators (linacs) to produce spallation neutrons for a subcritical reactor. Besides the challenges of any megawatt (MW) proton machine, ADS accelerator must operate with stringent reliability to avoid thermal stress in the reactor structures. Thus, ADS linacs have adopted a reliability-oriented design to satisfy the operation requirements. This work provides a review and the present status of the ADS linacs in the world.

INTRODUCTION

With the increase in the necessity for a safe, sustainable, and zero-emission energy source, nuclear energy represents a suitable option [1]. However, society has concerns about nuclear safety and the long-time residual waste it produces. The partitioning and transmutation strategy offers an effective way to reduce the burden of geological storage, as shown in Fig. 1. Partitioning comprises the selective separation of radioactive isotopes of the spent fuel, where some of them are reused as a fuel, and the other part, the so-called nuclear waste, is transmuted to reduce the radiotoxicity level. Accelerator-driven subcritical system (ADS) is an advanced nuclear system that could be used for the transmutation of minor actinides, therefore reducing the burden of geological disposal. Additionally, it can produce electricity, as the energy amplifier proposed by Rubbia [3], and fissile material, known as Accelerator- Breeding [4].

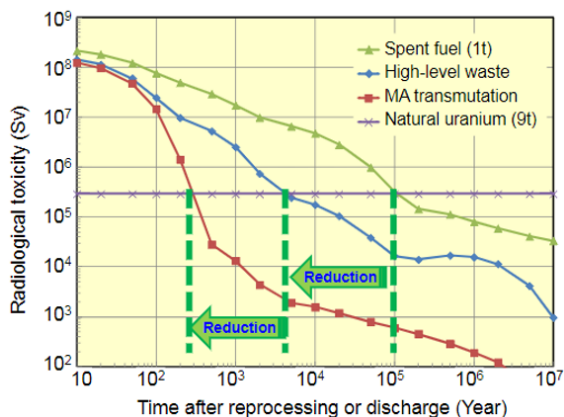


Figure 1: Reduction of radiotoxicity by applying partitioning and transmutation strategy [2].

ADS is composed of a high-power accelerator, a spallation target, and a subcritical reactor [1]. Figure 2 shows the

* byee@post.j-parc.jp

design of the JAEA-ADS. The accelerator drives the beam, usually protons, to a spallation target to produce neutrons for the subcritical reactor. Because the reactor is subcritical, it requires an external source of neutron to sustain the nuclear fission. Thus, if the accelerator is stopped, the fission process is also stopped. This feature enhanced the safety of these nuclear reactors. In addition, the ADS provides greater flexibility concerning the fuel composition.

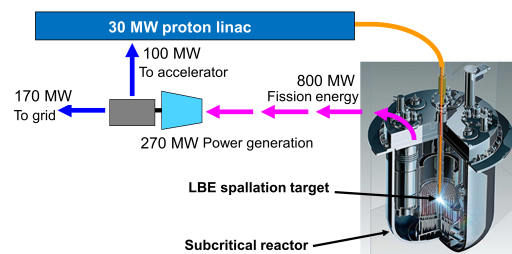


Figure 2: JAEA-ADS design.

With the advancement of high-power accelerators, especially superconducting radio frequency (SRF) technology, ADS accelerators have benefited from those developments. However, the ADS accelerator is expanding the intensity frontier to operate with high reliability and stability in the MW beam power regime. This work provides a review of the key features of the ADS accelerators and presents a summary of ADS activities around the world.

ADS ACCELERATOR FEATURES

The ADS accelerator must meet specific requirements to make the ADS technology suitable:

- Stable and efficient continuous wave (cw) operation of a beam power of few to tens of MW, which is defined by the thermal power and subcritical of the reactor [5, 6].
- Final beam energy is about 1 to 2 GeV for efficient neutron production through a spallation process.
- Beam current of few to tens of mA.
- Operating with beam loss less than 1 W/m to facilitate maintenance.
- High reliability to avoid thermal stress in the reactor structures. The number of allowing beam trips is more strict than other high-power accelerators, as shown in Fig. 3.
- High beam stability is necessary to ensure the integrity of the beam window.

To this end, a reliability-oriented design based on a robust lattice design, fault tolerance, and easy repairability is pursued [10].

SPIRAL2 FINAL COMMISSIONING RESULTS

A.K. Orduz*, P-E. Bernaudin, M. Di Giacomo, R. Ferdinand, B. Jacquot,
 O. Kamalou, J-M. Lagniel, G. Normand and A. Savalle
 Grand Accélérateur National d'Ions Lourds (GANIL), Caen, France
 D. Uriot, IRFU, CEA, Université Paris-Saclay, F-91191 Gif-sur-Yvette, France

Abstract

The commissioning of SPIRAL2 was carried out in different steps and slots from 2014 to end 2021. In a first phase, the proton-deuteron and heavy ion sources, LEBT lines and RFQ were commissioned and validated with $A/Q=1$ up to 3 particles. The validation of the MEBT (between the RFQ and the linac, including the Single Bunch Selector), linac and HEBT lines (up to the beam dump and to the NFS experimental room) started on July 2019, when GANIL received the authorization to operate SPIRAL2. The linac tuning is now validated with H^+ , $^4He^{2+}$ and D^+ and nominal H^+ and D^+ beams were sent to NFS for physics experiments. The main results obtained during the commissioning stages and the strategy used by the commissioning team are presented.

INTRODUCTION

GANIL (Grand Accélérateur National d'Ions Lourds) is principally carrying studies in fundamental nuclear physics, but also in other fields such as atomic physics, radiobiology, condensed matter physics and medical and industrial applications [1]. The laboratory has a first radioactive ions beams facility operating since 1983, now equipped with 3 sources and 5 cyclotrons with an energy range up to 95 MeV for stable beams, 50 MeV for fragmented beams and 25 MeV for post-accelerated radioactive beams [2]. A second facility started operating in 2019, SPIRAL2 (Système de production d'ions radioactifs accélérés en ligne de 2e génération), is now based on a SC (Super Conducting) linac producing H^+ beams up to 33 MeV, D^+ and $A/Q=2$ up to 20 MeV/A and heavy ions ($A/Q<3$) up to 14.5 MeV/A. The SPIRAL2 beam characteristics are listed in Table 1.

Table 1: Beam specifications including the NewGain project.

| Parameter | H^+ | D^+ | $A/Q < 3$ | Newgain |
|-----------------|-------|-------|-----------|---------|
| A/Q | 1 | 2 | 3 | 7 |
| Max I (mA) | 5 | 5 | 1 | 1 |
| Max E (MeV/A) | 33 | 20 | 14.5 | 7 |
| Beam power (kW) | 165 | 200 | 45 | 49 |

SPIRAL2 comprises a heavy ion source $A/Q<3$ and a H^+/D^+ source [3], two LEBT (Low Energy Beam Transport) [4] to transport and match the beams to the RFQ (Radio Frequency Quadrupole) [5], a MEBT (Medium Energy Beam Transport) [6], the SC linac with 26 cavities in two cryostat families. The first cryostat family each containing one low beta cavity ($\beta=0.07$) was designed by CEA [7]

* angie.orduz@ganil.fr

and the second one, each containing two high beta cavities ($\beta=0.12$), designed by CNRS [8]. Three HEBT (High Energy Beam Transport) lines drives the beam to the beam dump and two to experimental rooms: NFS (Neutrons For Science) [9] and S3 (Super Separator Spectrometer) [10, 11].

A Single Bunch Selector (SBS) is located in the MEBT line to select one bunch over N , N ranging between 100 and 10000, for Time-of-Flight experiments and power reduction with same particle density [12]. The beam diagnostics along the linac are positioned in the warm sections (in-between cryomodules) as shown in Fig. 1.

The sources, LEBT, RFQ and beam diagnostics were commissioned in different steps between 2014 and 2018 [13]. The commissioning of SPIRAL2 linac took place from July to December in 2019, 2020 and 2021. During these periods, the MEBT, linac, HEBT and the NFS experimental room were successfully commissioned with the reference particles H^+ , $^4He^{2+}$ and D^+ . This paper describes the main results obtained during the commissioning, the transition between commissioning and operation, and the first results obtained by the NFS experiments. The future projects at SPIRAL2 are finally presented.

COMMISSIONING PHASES AND RESULTS

The SPIRAL2 commissioning was managed in four phases. The first phase was the beam qualification of the ion sources and LEBT in the laboratories in charge of the development. The project decided to preinstall the ECR (Electron Cyclotron Resonance) ion sources and the LEBT in the two French laboratories where they were designed (CEA-Saclay and LPSC-Grenoble), in order to commission them with beam before the SPIRAL2 building availability. These successful tests were achieved by late 2012 [3].

The second phase comprised the qualification of the injector (sources and RFQ) on a diagnostic plate (D-Plate). This was a relevant step with the achievement of various goals:

- (i) Reproduce the results from the ion source pre-commissioning, i.e. validate the source performances on SPIRAL2 site,
- (ii) Validate the RFQ performances for the various main reference particles (Table 1): transmission, beam energy, output emittances in the three planes, and bunch extension,
- (iii) Provide a development platform for various beam diagnostics required either to validate the RFQ beams or later to tune and validate the linac beams, and

COMMISSIONING OF IFMIF PROTOTYPE ACCELERATOR TOWARDS CW OPERATION*

K. Masuda^{†1}, T. Akagi¹, A. De Franco¹, T. Ebisawa, K. Hasegawa, K. Hirosawa¹, J. Hyun, T. Itagaki, A. Kasugai, K. Kondo, K. Kumagai¹, S. Kwon¹, A. Mizuno², Y. Shimosaki³, M. Sugimoto¹,
 QST-Rokkasho, Aomori, Japan

P. Cara, Y. Carin¹, F. Cismondi¹, D. Duglué, H. Dzitko, D. Gex¹, A. Jokinen, I. Moya¹, G. Phillips,
 F. Scantamburlo¹, Fusion for Energy, Garching, Germany

N. Bazin, B. Bolzon, T. Chaminade, N. Chauvin, S. Chel, J. Marroncle, CEA Paris-Saclay, Gif sur
 Yvette, France

F. Arranz, B. Brañas, J. Castellanos, C. de la Morena, D. Gavela, D. Jimenez-Rey, Á. Marchena,
 P. Méndez, J. Molla, O. Nomen, C. Oliver, I. Podadera, D. Regidor, A. Ros, V. Villamayor, M. We-
 ber, CIEMAT, Madrid, Spain

L. Antoniazzi, L. Bellan, M. Comunian, A. Facco, E. Fagotti, F. Grespan, A. Palmieri, A. Pisent,
 INFN-LNL, Legnaro, Italy

¹also at IFMIF/EVEDA Project Team, Aomori, Japan

²also at JASRI/Spring-8, Hyogo, Japan

³also at KEK, Ibaraki, Japan

Abstract

A beam commissioning phase has started since July 2021 to pursue the world highest D⁺ beam current of 125 mA in CW at 5 MeV. Pilot beam operation as the first step with reduced beam currents of 10 mA H⁺ and 20 mA D⁺ identified needs of improvements in some newly installed components. The pilot beams were characterized, and comparisons were made with simulations for verification. CW commissioning of subsystems, namely injector, RFQ and RF power system, are being conducted in preparation to the nominal 125 mA D⁺ operation targeting CW.

INTRODUCTION

Construction of Linear IFMIF Prototype Accelerator (LIPAc) have been and are being conducted in Rokkasho, Aomori, Japan, within the EU-JA collaborative framework of the IFMIF/EVEDA project under the Broader Approach agreement [1]. The IFMIF, an accelerator-based D-Li neutron source, aims to provide highly intense neutron fluxes with appropriate energy spectrum in order to characterize materials for future fusion reactors. Because the IFMIF requires an accelerator with unprecedented performances to provide 40 MeV, 125 mA D⁺ beams in CW, the feasibility is being tested with a 1:1-scale prototype until the first cryomodule of the superconducting linac up to 9 MeV, namely the LIPAc. In this context, the LIPAc is to consist, in its final configuration in what is called the Phase C (see Fig. 1), of a 100 keV D⁺ beam Injector [2-4] incorporating an ECR ion source, the world longest RFQ [5-8] driven by eight 200 kW tetrode-based chains of RF power system (RFPS) at 175 MHz [9-10] to accelerate the beam up to 5

MeV, followed by a Medium Energy Beam Transport line (MEBT) [11] with highly space charged and beam loaded Buncher cavities [11,12], a superconducting RF (SRF) Linac, and a High Energy Beam Transport (HEBT) line [13] with a state-of-the-art Diagnostic Plate (D-Plate) [14,15], ending in a Beam Dump (BD) [16] designed to stop the world highest D⁺ current of 125 mA CW at 9 MeV.

A stepwise strategy as shown in Fig. 1 has been and will be applied to the installation and beam commissioning of the LIPAc [1]. The beam commissioning in the Phase B by temporary use of a Low Power Beam Dump (LPBD) has led to a successful acceleration of 125 mA D⁺ beam up to 5 MeV at the exit of RFQ in pulsed mode [17,18], without significant trace of unexpected beam loss [19]. Confirmation of the designed beam dynamics has been conducted successfully in terms of the beam transmission through the RFQ [20]. Following these milestones achieved in the

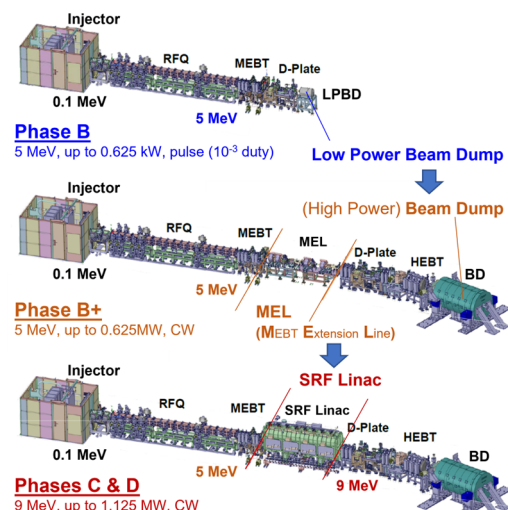


Figure 1: Three different layouts for the stepwise installation and commissioning of the LIPAc.

* This work was undertaken under the Broader Approach Agreement between the European Atomic Energy Community and the Government of Japan. The views and opinions expressed herein do not necessarily state or reflect those of the Parties to this Agreement.

[†] masuda.kai@qst.go.jp

A DISCUSSION OF KEY CONCEPTS FOR THE NEXT GENERATION OF HIGH BRIGHTNESS INJECTORS

T. G. Lucas, P. Craievich, S. Reiche, Paul Scherrer Institut, 5232 Villigen PSI, Switzerland

Abstract

The production of high brightness electron beams has been key to the success of the X-ray free-electron laser (XFEL) as the new frontier in high brilliance X-ray sources. The past two decades have seen the commissioning of numerous XFEL facilities, which quickly surpassed synchrotron light sources to become the most brilliant X-ray sources. Such facilities have, so far, heavily relied on S-band RF photoguns to produce the high brightness electron bunches required for lasing, however, such photoguns are beginning to reach their performance limit. This paper aims to discuss some key ideas which are important for the development of the next generation of high brightness photoguns. A particular emphasis will be placed on the newly developing topic of intrabeam scattering which recent measurements have found to be responsible for performance limitations in a handful of injector.

INTRODUCTION

For the viability of future X-ray Free Electron Laser (XFEL) projects, it is vital for a significant improvement in the beam brightness. Current XFELs predominantly use S-band injectors which are beginning to reach the performance limit with only minor improvements possible, on paper, without a shift in technologies [1]. This limitation comes as the result of physical limits set by the intrinsic emittance in the cathode determined in part by the achievable gradient for a room temperature S-band Standing Wave (SW) Photogun. In order to make the leap to a higher brightness future, some key concepts are the focus of investigations at various labs around the world. In this paper, we aim to describe the possible benefits of moving towards two new technologies: high gradient photoguns and cold cathode technology. Each technology offers the ability to achieve a significant increase in 5D brightness. However, with these benefits there's a caveat in the form of an enhanced sliced energy spread due to intrabeam scattering (IBS). This enhanced sliced energy spread will limit the performance, particularly so in compact FELs where the beam energy is lower. These effects of IBS on the sliced energy spread require us to rethink the development of injectors for future compact FELs.

FEL PERFORMANCE AND BRIGHTNESS

Crucial to the performance of an FEL is the power generated in the lasing process. This power grows exponentially, until the amplification saturates (P_{sat}), dictated by the equation:

$$P_{\gamma}(s) = P_0 e^{s/L_g} < P_{sat}, \quad (1)$$

where $L_g = \frac{\lambda_u}{4\sqrt{3}\pi\rho}$ is the ideal 1D gain length. We find that this gain length is dependent on the parameter ρ , known as the 'FEL parameter' or 'Pierce parameter'. This unitless parameter is fundamental to defining several conditions of the FEL process. It can be shown, using the common definition for 5D brightness $B_{5D} \equiv 2I/\epsilon_n^2$ and ρ , that ρ has a proportionality [1]:

$$\rho \propto B_{5D}^{\frac{1}{3}}. \quad (2)$$

This is a commonly quoted proportionality in injector design and has proven to be a good figure of merit for the first generation of photoinjectors, still motivating the most recent generation of high brightness injector projects. To understand what ideas must be investigated in order to develop the next generation of high brightness photoguns, it is important to understand what limits current photoguns.

THE S-BAND ROOM-TEMPERATURE PHOTOINJECTOR

A common design of an XFEL injector consists of an S-band room temperature RF Photogun feeding a pair of S-band accelerating structures [2–4]. Table 1 details the performance of a handful of such S-band injectors. We find that each of these facilities uses very similar operational parameters particularly with a gradient between 100 and 120 MV/m. These ultimately achieve a 5D brightness in the range 200–1800 TA/m². Moving beyond this performance is limited by achievable gradients and the thermal emittance of the beam generated by the cathode. The following two sections will describe efforts to move beyond this 5D brightness regime through the use of high gradient photoguns and cryogenic photoguns.

HIGH GRADIENTS PHOTOGUNS

Arguably the most important development in the next generation of compact FELs is the development of high gradient technology. Along with the benefits of reducing the overall length of the linac, important for allowing the development of XFEL facilities in places with reduced space or financial means, an increase in gradient is highly beneficial to the machine brightness. In [5], it was demonstrated that the 5D brightness is proportional to:

$$B_{5D} \propto E_0^n \quad (3)$$

where E_0 is the electric field at extraction and n is between 1.5 and 2 depending on the initial bunch shape. This gives a strong motivation for moving to greater cathode gradients. Achieving a greater gradient without a significant increase in

COMMISSIONING PLAN OF THE IFMIF-DONES ACCELERATOR*

I. Podadera^{†,1}, A. Ibarra¹, M. Weber¹, Consorcio IFMIF-DONES España, Spain
B. Bolzon, N. Chauvin, S. Chel, A. Madur, Université Paris-Saclay, CEA, France

T. Dézsi, CER, Hungary

F. Arranz, C. de la Morena, M. García, D. Jimenez-Rey, J. Molla, C. Oliver, D. Regidor
CIEMAT, Spain

D. Bernardi, G. Micciché, F. S. Nitti, ENEA Brasimone, Italy

C. Prieto, Empresarios Agrupados, Spain

P. Cara, Daniel Duglue, Fusion for Energy, Germany

W. Królas, U. Wiacek, IFJ-PAN, Poland

L. Bellan, A. Palmieri, A. Pisent, INFN/LNL, Italy

Ll. Macià, M. Sanmarti, B. K. Singh, IREC, Spain

V. Hauer, Y. Qiu, T. Lehmann, KIT, Germany

M. J. Ferreira, C. Martins, Lund University, Sweden

J. Aguilar, S. Becerril-Jarque, M. Luque, J. Maestre, D. Sánchez-Herranz, C. Torregrosa
Universidad de Granada, Spain

J. Castellanos, Universidad de Castilla-La Mancha, Spain

¹ also at CIEMAT, Madrid

Abstract

IFMIF-DONES (International Fusion Materials Irradiation Facility- DEMO-Oriented Neutron Early Source) - a powerful neutron irradiation facility for studies and certification of materials to be used in fusion reactors - is planned as part of the European roadmap to fusion electricity. Its main goal will be to characterize and to qualify materials under irradiation in a neutron field similar to the one faced in a fusion reactor. The intense neutron source is produced by impinging deuterons, from high-power linear deuteron accelerator, on a liquid lithium curtain. The facility has accomplished the preliminary design phase and is currently in its detailed design phase. At the present stage, it is important to have a clear understanding of how the commissioning of the facility will be performed, especially the commissioning of a 5 MW CW deuteron beam, together with the lithium curtain and the beam optimization for the neutron irradiation. In this contribution, the present plans for the hardware and beam commissioning of the accelerator will be given, focusing on the most critical aspects of the tiered approach and on the integration of the procedure with the lithium and test systems.

IFMIF-DONES ACCELERATOR

The IFMIF-DONES facility [1,2] is a fusion-like neutron source, generating a neutron flux of 5×10^{14} neutrons/cm²/s

* This work has been carried out within the framework of the EUROfusion Consortium, funded by the European Union via the Euratom Research and Training Programme (Grant Agreement No 101052200 — EUROfusion). Views and opinions expressed are however those of the author(s) only and do not necessarily reflect those of the European Union or the European Commission. Neither the European Union nor the European Commission can be held responsible for them.

[†] ivan.podadera@ifmif-dones.es

for the assessment of materials damage in DEMO and future fusion reactors. Neutrons are generated by the interaction between the lithium curtain and the deuteron beam from a Radio Frequency LINear ACcelerator (RF LINAC) at 40 MeV and nominal Continuous Wave (CW) current of 125 mA. The facility is divided in three major group of systems: 1) the ~100 m long Accelerator Systems (AS), grouping those systems involved in the beam production, acceleration and shaping, 2) the lithium systems (LS) which generate and control the liquid lithium target, and where the Li(d,xn) stripping reaction (with a neutron spectrum up to 50 MeV) between the deuterons and the lithium occurs, and 3) the experimental material test areas or test systems (TS), where the main component is the High Flux Test Module containing 100 cm³ of material under test with up to 20 dpa y⁻¹ to 50 dpa y⁻¹. The Accelerator Systems [3] will be formed by Fig. 1: 1) an Injector [4], composed of an ion source and a Low Energy Beam Transport (LEBT) section at 100 keV to guide the low energy ions up to the Radio Frequency Quadrupole (RFQ) and match its injection acceptance, 2) the RFQ [5] to accelerate the ions from 100 keV up to 5 MeV, 3) a Medium energy Beam Transport Line (MEBT) [6] to match the RFQ extracted beam to the injection of the Superconducting RF LINAC (SRF LINAC), 4) an SRF LINAC [7] with five cryomodules to bring the energy of the deuterons up to 40 MeV, 6) a High Energy Beam Transport (HEBT) [8] line to transport and shape the beam from SRF Linac towards the lithium target or the Beam Dump Transport Line (BDTL), in pulsed mode, 7) an RF Power System (RFPS) [9] based on solid-state technology to supply and control the RF injection into the cavities for beam acceleration and bunching, and 8) the AS Ancillaries (ASA) providing the services to the accelerator, including the vacuum generation and exhaust, the

MULTI-HARMONIC BUNCHER (MHB) STUDIES FOR PROTONS AND IONS IN ESS-BILBAO*

J. L. Muñoz[†], I. Bustinduy, L. C. Medina, P. González
 ESS-Bilbao, Zamudio, Spain

Abstract

Multi-harmonic buncher cavities (MHB) are used in ion linacs to increase the bunch separation, so the beam can be injected in rings or used in applications like time-of-flight experiments. ESS-Bilbao will develop a MHB intended to be tested in the CERN-ISOLDE facility. The design and prototyping include the buncher device itself as well as the solid-state power amplifier (SSPA) to power it. The buncher design (finite elements and beam dynamics) will be carried out to optimize it for ISOLDE beams and frequencies of 1/10th of their RF frequency. The testing of the cavity at ESS-Bilbao proton beam injector has also been studied.

INTRODUCTION

The RF frequency of radioactive ion beams accelerators is usually around 100 MHz [1]. In the case of HIE-ISOLDE [2], the frequency is $f_0=101.28$ MHz. The bunching of the beam carried out in the RFQ results then in a bunch separation of 9.87 ns. An increased bunch spacing to approximately 100 ns is requested by several research groups targeting experimental physics at this facility. The increased bunch spacing can be obtained by bunching the beam before the RFQ to a frequency of 1/10th of the RF frequency, $f=10.128$ MHz, that will result in a bunch separation of 98.7 ns. This task can be done by a MHB device, located external to the RFQ. For low intensity beams where space charge effects are not relevant, a MHB can also be used to pre-bunch the beam and to reduce the length and the longitudinal emittance of the RFQ [3]. In this paper, the preliminary design of a MHB device is presented. The design is done with the HIE-ISOLDE application as objective, but the performance of the MHB installed in the ESS-Bilbao injector [4, 5] is also studied, with the aim of the future testing of the cavity in this facility prior to tests in HIE-ISOLDE(*).

MULTIHARMONIC BUNCHING

The optimum electric field time profile to bunch a continuous beam with bunch separation of $1/f$ is that of a saw-tooth wave profile of frequency f [3], with a linear ramp of field centered at the middle of the bunch at time $t = t_0$. The saw-tooth profile can be synthesized by summing up the first harmonics of its Fourier expansion. Usually, four harmonic terms are enough to generate an adequate approximation of the wave shape. In the MHB, the electric field is applied

between two electrodes that are powered up with the combined multiharmonic RF wave. In the ideal case, the actual electric field profile will be a uniform value between the electrodes, modulated by the MHB wave. In a real device the electric field between the electrodes depends on the electrode geometry and the aperture needed for the beam, so the actual performance of the MHB will be lower than the ideal one. The shape of the electrodes is usually designed by assuming a constant voltage and computed as an electrostatics problem to obtain the electric field shape. Then this field is modulated to obtain the adequate field spatial and temporal distribution and beam dynamics simulations are run to evaluate the bunching [3, 6–8]. For low frequencies the differences in the electric field shape between an electrostatics and a RF calculations are very low.

FEM-BEAM DYNAMICS SIMULATIONS

For this work, different electrode geometries are explored. The electrode geometry and the FEM calculations are done using an integrated simulation platform that makes use of GMSH [9] and FEniCS [10] open source libraries. Beam dynamics tracking simulations are done with GPT [11]. The integrated platform is driven by Python scripts that allow for quick parametric exploration or optimization.

RESULTS

For HIE-ISOLDE a preliminary MHB electrode design has been selected after parametric exploration. The beam characteristics are shown in Table 1. The MHB electrodes have an aperture of 20 mm in diameter, and the MHB vessel has a total length of 250 mm, to keep the values already defined in [6].

Table 1: Beam Characteristics for Simulations

| | ISOLDE beam | ESS-Bilbao beam |
|--------------------------|--------------|--------------------|
| A/q | 4.5 | 1 |
| β | 0.003 28 | 0.0098 |
| ϵ_x, ϵ_y | 0.62 mm mrad | 0.25π mm mrad |
| Intensity | 1 mA | 45 mA |

Different geometries have been explored and the beam dynamics results compared to the basic results shown in [6]. Geometries with a tail shape (as in [7]) or conical (as in [8]) have been explored. It is worth mentioning that the main aim of this work is not to find an optimum geometry of the buncher, but to explore the possibility of testing a MHB optimized for HIE-ISOLDE radioactive beams in ESS-Bilbao

* This work is presented in the framework of the "Agreement for the Spanish Contribution to the Upgrade of the ATLAS, CMS, and LHCb Experiments and the new Projects for ISOLDE and n_TOF"

[†] jlmunoz@essbilbao.org

OPTIMIZED BEAM OPTICS DESIGN OF THE MINERVA/MYRRHA SUPERCONDUCTING PROTON LINAC

U. Dorda †, L. de Keukeleere, SCK CEN, Mol, Belgium
 E. Bouquerel, E. Traykov, IPHC, CNRS/IN2P3 Strasbourg, France
 F. Bouly, E. Froidefond, LPSC Université Grenoble-Alpes, CNRS/IN2P3 Grenoble, France
 L. Perrot, S. Chance, IJCLab, CNRS/IN2P3 Orsay, France

Abstract

The MYRRHA design for an accelerator driven system (ADS) is based on a 600 MeV superconducting proton linac. The first stage towards its realization is called MINERVA and was approved in 2018 to be constructed by SCK CEN in Belgium. This 100 MeV linac, will serve as a technology demonstrator for the high MYRRHA reliability requirements as well as a driver for two independent target stations, one for radio-isotope research and production of radio-isotopes for medical purposes, the other one for fusion materials research. This contribution gives an overview of the latest accelerator machine physics design with a focus on the optimized medium (17 MeV) and high energy (100 MeV) beam transfer lines

INTRODUCTION

The MINERVA project at SCK CEN, Belgium, is the fully funded first implementation stage of the MYRRHA project, which aims to demonstrate transmutation of nuclear waste in a subcritical nuclear reactor driven by a high power accelerator (ADS). This use case also dictates the high reliability requirements to the accelerator of maximal 10 beam trips longer than 3 sections within a 90 day work period.

While the accelerator has been studied in the context of several design studies [1], with the decision by the Belgium government to implement MINERVA, the accelerator design was critically reviewed in terms of a) beam physics robustness b) reliability c) practical feasibility and d) cost and schedule-effectiveness. The final overall layout which is currently being implemented with the aim of operating a first beam at 100 MeV by the end of 2027, is shown in Fig 1.

The main linac beam parameters are given in Table 1.

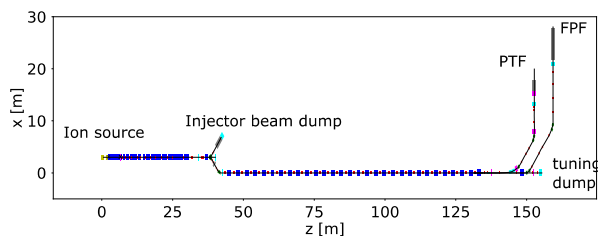


Figure 1: Layout of the 100 MeV MINERVA linac including the transfer lines to the two user facilities (PTF, FPF). The blue boxes indicate RF cavities.

Table 1: MINERVA Linac Specifications

| Parameter | Value |
|---------------|-------------------------------------------|
| Particle | Protons |
| Energy | 100 MeV |
| Beam current | 4 mA |
| Duty factor | CW (or pulsed with 4ms cycles) |
| Inj. RF | Normal conducting 176 MHz CH-cavities |
| Main linac RF | Superconducting 352.2 MHz single spoke |

INJECTOR

The injector starts with an ECR ion source (providing a 30 keV beam) coupled to a LEBT containing two solenoids, a fast beam chopper and various beam diagnostic devices e.g. an Allison emittance meter. The subsequent 4 vane 176.1 MHz RFQ [2-3] bunches and accelerates the beam to 1.5 MeV. The following two normal conducting quarter wave cavities re-bunch the beam. SCK CEN currently operates these elements in a dedicated injector test stand [Fig 2.] which is about to be extended with an emittance meter and a longitudinal bunch shape measurement device [4-6].



Figure 2: The Injector test stand featuring an ECR ion source, a LEBT, the RFQ and 2 quarter wave rebunching cavities

The following series of 15 normal conducting CH-type cavities accelerates the beam to 17 MeV. The beam optics remained mainly unchanged in this design iteration except for an elaboration of the beam diagnostics and orbit correction scheme.

In order to achieve the required reliability objectives, the final design foresees the installation of two parallel injectors which can be alternatively delivering beam to the SC-

R&D FOR THE REALIZATION OF A VERY HIGH FREQUENCY CROSSBAR H-MODE DRIFT TUBE LINAC

M. Heilmann^{*1}, C. Zhang¹, and H. Podlech^{2,3}

¹GSI Helmholtz Centre for Heavy Ion Research, Darmstadt, Germany

²IAP, Goethe University, Frankfurt, Germany

³Helmholtz Research Academy Hesse for FAIR (HFHF), Frankfurt, Germany

Abstract

A 704.4 MHz Crossbar H-mode (CH) drift tube LINAC has been proposed for performing a radio frequency jump at $\beta \approx 0.2$. Up to now, the highest frequency of the constructed CH cavities is 360 MHz. In principle the operation frequency for an H₂₁₀-mode cavity can be up to 800 MHz. At 704.4 MHz, the cavity dimensions become small, which bring challenges for many practical problems e.g. construction, vacuum pumping and RF coupling. This paper presents the performed R&D studies for the realization of such a very high frequency cavity.

INTRODUCTION

The crossbar H-mode (CH) drift tube LINAC (DTL) has been developed as a kind of efficient RF-structure for accelerating low- and medium- β beams [1, 2]. In principle, the operation frequency for a CH-structure can be up to 800 MHz [1], but up to now, the highest frequency of all realized CH-cavities is 360 MHz [2]. In a recent study [3], a kind of novel 704.4 MHz CH-DTL has been proposed to enable a radio frequency jump from 176.1 MHz to 704.4 MHz at $\beta \approx 0.2$ for a large-scale LINAC (Fig. 1). This fourfold increase in radio frequency can shorten the entire LINAC [4,5] as well as can reduce the related construction and operation costs considerably. 704.4 MHz is almost twice the highest frequency of already constructed CH-cavities. The preliminary RF-structure design results have shown that such a very compact cavity can work in CW-mode both at room temperatures and at liquid helium temperatures [3]. As a further step towards the realization of a 704.4 MHz CH-DTL cavity (firstly normal conducting), more practical aspects e.g. mechanical design, vacuum pumping and RF coupling are being investigated carefully.

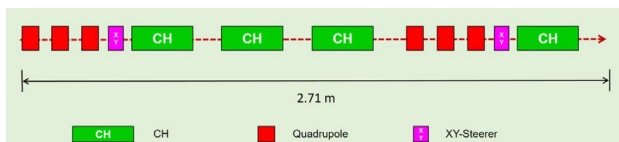


Figure 1: Schematic overview of the frequency jump section based on four 704.4 MHz CH-DTLs (taken from [3]).

VERY HIGH FREQUENCY CH-DTL

The normal conducting CH-DTL for 704.4 MHz will have an octagonal tank cross-section to mount for the first time

* m.heilmann@gsi.de

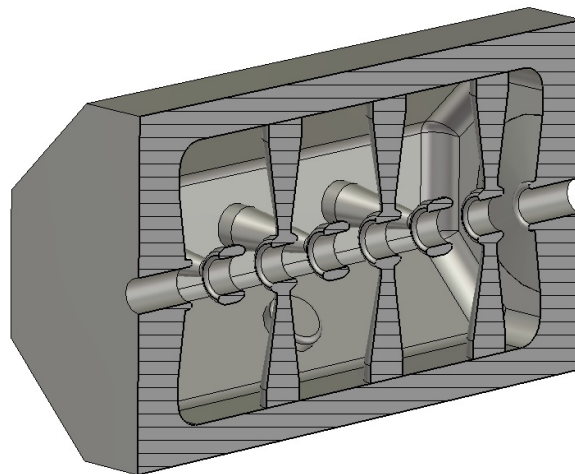


Figure 2: CST-MWS [6] model of the recent design of the 704.4 MHz CH-DTL (side view).

Table 1: Design Parameters of the NC CW CH-DTL

| Parameter | Unit | Value |
|------------------------|---------------|-------|
| RF-frequency | MHz | 704.4 |
| β | | 0.186 |
| Gaps | # | 7 |
| Gap length | mm | 19.8 |
| Drift tubes | # | 6 |
| Drift tube length | mm | 19.8 |
| Drift tube aperture | mm | 20.0 |
| Tank diameter (inner) | mm | 160.0 |
| Tank length | mm | 337.0 |
| Total RF-power | kW | 1.5 |
| Acceleration gradient | MV/m | 0.5 |
| Shunt impedance (sim.) | M Ω /m | 53.46 |
| Kilpatrick Factor | | 0.24 |

CH-drift tubes with its stems into a tank (Fig. 2, Table 1). For superconducting [7–9] and room temperature CH-DTLs [10, 11], the standard way is to weld the drift tubes into the tank. The drift tubes are not welded into this very high frequency CH-structure to reduce the risks and challenges at copper plating of the cavity (Fig. 3). The copper plating of a normal conducting CH-structure becomes more critical for a smaller diameter in combination with an increased cavity length, so another option for this small cavity can be to manufacture the tank from copper.

WELDING AND COPPER PLATING INVESTIGATIONS ON THE FAIR PROTON LINAC

A. Seibel, T. Dettinger, C. Kleffner, K. Knie, C. Will, GSI, Darmstadt, Germany
 M. Breidt, H. Hähnel, U. Ratzinger, IAP, University of Frankfurt, Germany
 J. Egly, PINK GmbH Vakuumtechnik, Wertheim, Germany

Abstract

A FAIR injector linac for the future FAIR facility is under construction. In order to meet the requirements for copper plating of the CH-cavities, a variety of tests with dummy cavities has been performed and compared to simulation. Further dummy cavities have been produced in order to improve the welding techniques. In addition, the results on 3d-printed stems with drift tubes will be presented.

OVERVIEW

The present GSI injector UNILAC (universal linear accelerator) [1] will serve as one injector for the future Facility for Antiproton and Ion Research (FAIR) [2]. However, a large part of the FAIR experiments will be conducted with secondary antiprotons which will be produced by bombarding a target with an intense proton beam. Because the UNILAC is optimized for heavy ions, i.e., particles with an $A/q \gg 1$, a dedicated proton injector is presently under construction. It consists of a ladder RFQ [3] followed by six CH structures (Crossbar H-mode).

Figure 1 shows the structure of the proton linac [4]. The main acceleration from 3 MeV up to 33 MeV will be realized with three coupled CH-cavities (CCH) connected by a coupling tank housing a focusing magnetic quadrupole triplet lens, followed by a diagnostic section at 33 MeV and finalized up to 68 MeV by three single CH-modules. The cavity design of all six CH-type cavities has been developed by IAP University of Frankfurt [5]. They operate at a resonance frequency of 325.224 MHz. It is designed to provide a proton beam with an energy of 68 MeV and a current up to 70 mA at a rf pulse repetition rate of 2.7 Hz.

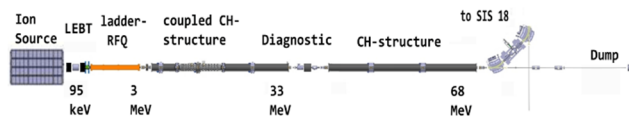


Figure 1: Layout of the proton linac.

Figure 2 shows the first coupled CH-DTL cavity. The low energy part consists of ten gaps, followed by the coupling cell and by the eleven-gap high energy part. The whole cavity has an inner length of about 1.4 m and the cylindrical tanks have an inner diameter of about 307 mm (first section) and 316 mm (second section). The coupling cell has a length of about $2\beta\lambda$. Twelve fixed (five in tank one and seven in tank two) and three movable tuners (located at each cavity and at the coupling cell) are foreseen.

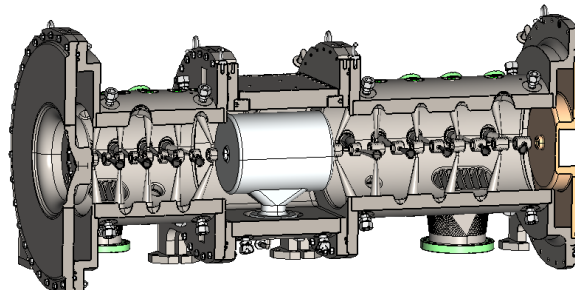


Figure 2: 3d-model of the first coupled CH-cavity.

WELDING AND COPPER PLATING STUDIES

Due to these complex monolithic structures with tiny distances of the stems and aperture of the tank design, there is no possibility of conventional welding from the inside. Other welding techniques (outside welding) are not well established at GSI. In addition, copper plating for these novel structures is particularly challenging. Therefore, four types of test dummies are planned for CCH1, which can be considered as the most complex structure. Table 1 shows our learning process for the new welding technique from the outside, as well as the copper plating process.

Table 1: Learning Process Outside Welding and Copper Plating Per Dummy In Percent

| Learning Process | Copper Plating | Welding |
|------------------|----------------|---------|
| Dummy 1 | 50 % | 0% |
| Dummy 2 & 2.1 | 90% | 10% |
| Dummy 3 | 95% | 70% |
| Dummy 4 | 98% | 100% |

DUMMY 1

Dummy 1 (see Fig. 3) is a simple rolled steel sheet with straight stems tacked inside. This dummy has already been copper plated at GSI.



Figure 3: Dummy 1 consists of a simple rolled steel sheet with straight stems tacked inside.

DESIGN AND TEST OF BEAM DIAGNOSTICS EQUIPMENT FOR THE FAIR PROTON LINAC

T. Sieber[†], P. Forck, C. Kleffner, S. Udrea, GSI, Darmstadt, Germany
J. Herranz, PROACTIVE R&D, Sabadell, Spain
I. Bustinduy, A. Rodriguez Paramo, ESS Bilbao, Zamudio, Spain
A. Navarro Fernandez, CERN, Geneva, Switzerland

Abstract

A dedicated proton injector Linac (pLinac) for the Facility of Antiproton and Ion Research (FAIR) at GSI, Darmstadt, is currently under construction. It will provide a 68 MeV, up to 70 mA proton beam at a duty cycle of max. $35\mu\text{s} / 2.7\text{ Hz}$ for the SIS18/SIS100 synchrotrons, using the existing UNILAC transfer beamline. After further acceleration in SIS100, the protons are mainly used for antiproton production at the Pbar ANnihilations at DArmstadt (PANDA) experiment. The Linac will operate at 325 MHz and consists of a novel so called ‘Ladder’ RFQ type, followed by a chain of CH-cavities, partially coupled by rf-coupling cells. In this paper we present the beam diagnostics system for the pLinac with special emphasis on the Secondary Electron Emission (SEM) Grids and the Beam Position Monitor (BPM) system. We also describe design and status of our diagnostics testbench for stepwise Linac commissioning, which includes an energy spectrometer with associated optical system. The BPMs and SEM grids have been tested with proton and argon beam during several beamtimes in 2022. The results of these experiments are presented and discussed.

INTRODUCTION

The FAIR [1] facility at GSI will provide antiproton and ion beams of worldwide unique intensity and quality for fundamental physics research.

The accelerator facility of FAIR, shown in Fig. 1, will include three linear accelerators, the existing UNILAC (for which a refurbishing program is currently on the way), a

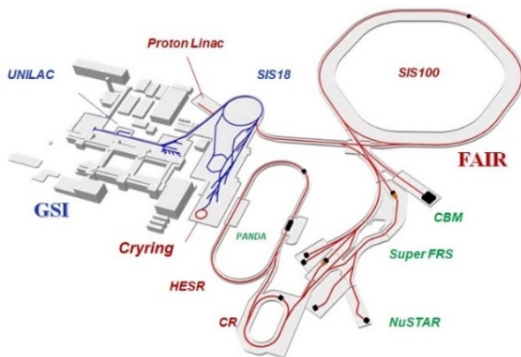


Figure 1: Layout of the FAIR facility.

superconducting cw-Linac, designed mainly for intermediate energy experiments [2], and the new proton Linac [3] (pLinac). The UNILAC and pLinac will be the main injectors of SIS18, which will in turn be an injector for SIS100, the central accelerator component of FAIR.

[†]T.Sieber@gsi.de

The pLinac consists of a novel so called ‘Ladder’ RFQ [4] followed by two $\sim 10\text{ m}$ sections of Cross Bar H-drift-tube accelerator (CH) structures [5]. The first section includes six CH modules, which are pairwise rf-coupled (Coupled CH or CCH). The second section consists of three separate modules, each connected to its own klystron. The pLinac will deliver a current up to 70 mA with a macropulse length of $35\mu\text{s}$ (at max. 4 Hz) and a typical bunch length of 100 ps. The design energy is 68 MeV. Figure 2 shows a schematic of the pLinac and its beam instrumentation.

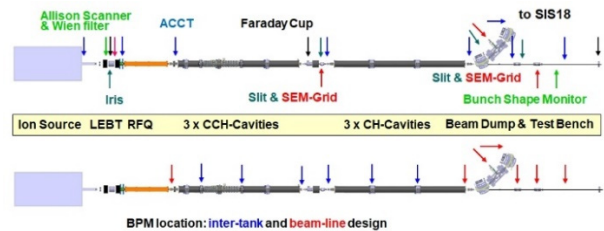


Figure 2: Schematic of the FAIR pLinac, side view, showing the location of diagnostics (upper) and BPMs, divided in cavity (inter-tank) and beamline BPMs (lower).

The overall diagnostics concept and layout of pLinac has been described in various reports, e.g. [6]. Because of the compact structure of the two CH sections, diagnostics (except BPMs) will be concentrated in the LEBT, in the MEBT behind the RFQ and in a diagnostics/rebuncher (so called SD) section between the CCH and CH parts of the pLinac. Additional beam diagnostics elements are placed in the transfer line to SIS18 as well as in a straight line to the beam dump.

Concerning the SEM Grid design (Fig. 3), we expect a 1σ beam radius of 1.5 mm at best possible beam quality in pLinac, therefore the wire pitch cannot be larger than 0.5 mm to obtain reasonable profiles. To compensate for thermal expansion of the wires, a stretching mechanism is required - even if the grids are operated in a ‘grid protection mode’ at reduced duty cycle. Gold plating on the tungsten wires has to be considered carefully because of possible melting and agglutination during irradiation.

The BPM system of pLinac [7] comprises button BPMs, as shown in Fig. 4, in combination with a custom made preamplifier including narrowband amplification (single button signals) for the frequency domain LIBERA (Single Pass H, LSPH) electronics and wideband amplification (sum signal) for oscilloscope based time of flight (TOF) measurements.

UPGRADE AND COMMISSIONING OF THE 60 KEV LOW ENERGY BEAM TRANSPORT LINE FOR THE FRANKFURT NEUTRON SOURCE FRANZ

H. Hähnel^{1*}, A. Ateş¹, D. Bänsch¹, G. Blank¹, M. Breidt¹, R. Gössling¹, R. Hollinger³, T. Metz¹,
H. Podlech^{1,2}, U. Ratzinger^{1,2}, A. Ruffer¹, K. Volk¹, C. Wagner¹, C. Zhang³

¹Institute of Applied Physics, Goethe University, Frankfurt a. M., Germany

²Helmholtz Forschungsakademie Hessen für FAIR (HFHF), Frankfurt a. M., Germany

³GSI Helmholtzzentrum für Schwerionenforschung, Darmstadt, Germany

Abstract

The Low Energy Beam Transport line (LEBT) for the Frankfurt Neutron Source (FRANZ) has been redesigned to accommodate a 60 keV proton beam. Driven by a CHORDIS ion source, operating at 35 kV, a newly designed electrostatic postaccelerator has been installed to reach the desired beam energy of 60 keV. Additional upgrades to the beamline include two steerer pairs, several optical diagnostics sections and an additional faraday cup. We present the results of beam commissioning up to the point of RFQ injection. Emittance measurements were performed to prepare matching to the RFQ and improve the beam dynamics model of the low energy beamline. Due to the successful operation of the beamline at 60 keV, retrofitting of the RFQ for the new energy has been initiated.

INTRODUCTION

The Frankfurt Neutron Source (FRANZ) is a compact accelerator driven facility originally initiated in the early 2000s [1–6]. It is designed to provide a 2 MeV proton beam for neutron production via the ${}^7\text{Li}(p,n){}^7\text{Be}$ reaction [7]. The produced neutrons with a thermal spectrum around 30 keV can be used for a number of experiments in the fields of applied physics and experimental astrophysics [8].



Figure 1: Photograph of the current FRANZ LEBT beamline (Aug. 2022).

Significant progress on the driver linac was made recently. The commissioning of the new CHORDIS ion source [9, 10] in late 2020 was a first milestone. Since the CHORDIS ion source only provides a 35 keV proton beam, an electrostatic post-accelerator was developed and commissioned at IAP to reach the desired beam energy of 60 keV. After stable operation was confirmed, the Low Energy Beam Transport line (LEBT), see Fig. 1, was commissioned and the beam was transported up to the point of injection into the RFQ-Accelerator. This presents an important milestone for the

* haehnel@iap.uni-frankfurt.de

initial beam commissioning of the FRANZ facility. Meanwhile, emittance measurements to further improve an efficient injection into the RFQ are well under way. We will present the recent progress since ca. 2019 and show a path to operation for first experiments with neutrons within the next two years.

RECENT DEVELOPMENTS

In recent years, the FRANZ project faced some delays in commissioning. Failure to reach the designated RFQ injection energy of 120 keV with protons posed a significant hurdle for the project. As a consequence, the RFQ injection energy was reduced to 60 keV, necessitating a redesign of the RFQ electrodes, as well as the desire to acquire a reliable ion source for operation. A turning point was reached, when the decision landed on the well known CHORDIS ion source which was provided to IAP by GSI Darmstadt. Since then, several adjustments and upgrades to the high voltage terminal and LEBT have been made.

CHORDIS Ion Source

The CHORDIS ion source is a filament driven volume type ion source [9, 10] (see Fig. 2). Plasma confinement is realized with a permanent magnet multi-cusp field. When operated with hydrogen gas at an extraction voltage of 35 kV, the CHORDIS produces up to 60 mA of total beam current with a proton fraction of typically 45 %, the rest being H_2^+ and H_3^+ .

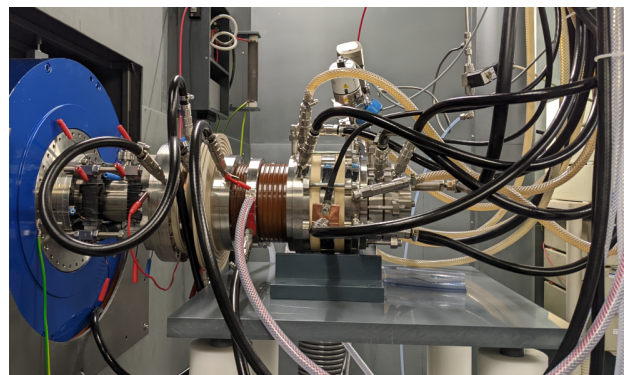


Figure 2: CHORDIS ion source mounted at the FRANZ high voltage terminal complete with electrostatic post-accelerator and steerer pair. The first solenoid of the LEBT can be seen on the left side (blue casing).

HIGH POWER RF CONDITIONING OF THE ESS DTL1

F. Grespan[†], ESS, Lund; INFN/LNL, Legnaro (PD)

B. Jones, D. Nicosia, L. Page, A.G. Sosa, E. Trachanas, R. Zeng, C. Plostinar, ESS, Lund
L. Antoniazzi, C. Baltador, L. Bellan, D. Bortolato, M. Comunian, E. Fagotti, M. Giacchini,
M. Montis, A. Palmieri, A. Pisent, INFN/LNL, Legnaro (PD)

Abstract

The first tank of Drift Tube Linac (DTL) for the European Spallation Source ERIC (ESS), delivered by INFN, has been installed in the ESS tunnel in Summer 2021. The DTL-1 is designed to accelerate a 62.5 mA proton beam from 3.62 MeV up to 21 MeV. It consists of 61 accelerating gaps, alternate with 60 drift tubes (DT) equipped with Permanent Magnet Quadrupole (PMQ) in a FODO lattice. The remaining drift tubes are equipped with dipole correctors (steerers), beam position monitors (BPMs) or empty. The total length of the cavity is 7.6 m and it is stabilized by post couplers. Two waveguide couplers feed the DTL with the 2.2 MW of RF power required for beam operation, equally divided by RF power losses and beam power. This paper first presents the main systems required for the DTL conditioning. Then it summarizes the main steps and results of this high-power RF conditioning done at ESS to prepare the DTL for the consequent beam commissioning.

INTRODUCTION

The high-power RF conditioning process wants to make the cavity ready to sustain beam operation, in terms of RF parameters (field, pulse length, repetition rate) and vacuum level. For ESS DTLs the two main goals of the conditioning process are [1]:

- To maintain 14 Hz, 3.2 ms, nominal field level (3 MV/m for DTL1) for 12 hours with low interlock rate (> 95% RF ON over 12 hours).
- To keep the vacuum level $5.0e-07$ mbar at nominal RF level.

After a description of the main systems necessary for the conditioning and the integrated tests performed, the paper will go through the main steps of the conditioning process and finally will comment the main results.

RF CONDITIONING SYSTEMS

The block diagram of Fig. 1 shows the main systems involved in the DTL1 high power RF conditioning, their physical and functional links, in particular the signals to interlock the RF power and protect the cavity.

DTL1 Cavity

After the tuning and stabilization [2], the entire cavity DTL1 has been transported and installed in the ESS accelerator tunnel in August 2021 (Fig. 2). Once on the supports, the 2 power couplers and RF windows have been installed, then DTL1 has been aligned, connected to the cooling system, leak tested. The RF parameters measured at the end of

the tuning process [2] have been confirmed with measurement in the tunnel. DTL1 has a flat acc. field $E_0 = 3$ MV/m, corresponding to a cavity power $P_{cav} = 1150$ kW, without beam. DTL1 has 9 RF pick-ups to monitor E_0 flatness, and 3 movable tuners to maintain the cavity at 352.21 MHz.

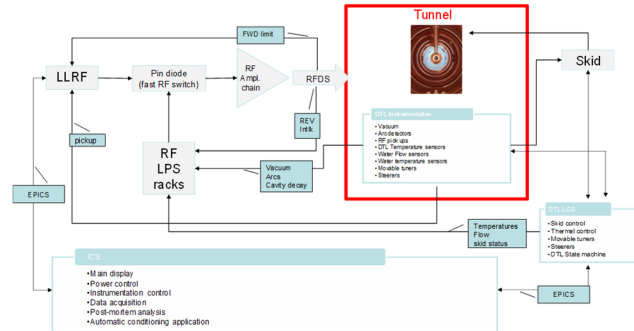


Figure 1: Block diagram of DTL1 systems and protections.



Figure 2: DTL1 in the ESS beam line.

RF System

A 2.8 MW klystron serves the DTL1 as RF source, sharing the modulator with RFQ. The klystron is followed and protected by a circulator. Then a Magic-Tee splits the power in 2 wave guide lines, which arrive to feed the cavity by 2 power couplers. FWD and REV power are monitored at many points all along the RF line. Two circular alumina RF windows separate the DTL cavity vacuum from the in-air wave guide system. Each RF window is protected by 2 arc detectors (air and vacuum side), with two additional view ports for light test. The RF windows were previously conditioned at CEA-Saclay, up to 1.4 MW.

RF system includes the RF Local Protection System (LPS), the key protection system during conditioning.

Cooling System

A water skid provides cooling and thermal stability to the 5 DTL tanks. Each tank has its own cooling circuit with a

[†] francesco.grespan@lnl.infn.it

HARDWARE COMMISSIONING WITH BEAM AT THE EUROPEAN SPALLATION SOURCE: ION SOURCE TO DTL1

B. Jones[†], R. Baron, C. Derrez, C. Plostinar, A. Garcia Sosa, S. Grishin, F. Grespan[‡], Y. Levinsen, N. Milas, R. Miyamoto, D. Nicosia, D. Noll, E. Trachanas, R. Zeng, ESS, Lund, Sweden
C. Baltador, L. Bellan, M. Comunian, A. Palmieri, INFN, Legnaro, Italy
L. Neri, INFN, LNS, Italy
I. Bustinduy, N. Garmendia, G. Harper, S. Varnasseri, A.R. Páramo, ESS Bilbao, Spain

Abstract

The European Spallation Source (ESS) aims to build and commission a 2 MW proton linac ready for neutron production in 2025. The normal conducting section of the ESS linac is designed to accelerate a 62.5 mA, 2.86 ms proton beam to 90 MeV at 14 Hz. The section consists of a microwave-discharge ion source, Radio Frequency Quadrupole (RFQ) and 5-tank Drift Tube Linac (DTL). All sections are provided to ESS by in-kind partners from across Europe.

This paper reports the recent progress on the assembly, installation, testing and commissioning of the ESS normal conducting linac.

INTRODUCTION

The project to build and commission the ESS accelerator is progressing well. In particular, the Normal Conducting Linac (NCL) has been installed, RF conditioned and commissioned with full peak current beam up to the first DTL tank. A description of the ESS LINAC can be found in [1] and a previous status update here [2].

ION SOURCE AND LEBT

The ion source and Low Energy Beam Transport (LEBT) section, an in-kind contribution from INFN-LNS, Catania, was first operated at ESS in 2019 and now meets all specifications as far as can be measured at this stage. A maximum beam current of $>74\text{mA}$ can be produced with a 3ms flat-top stable to $\pm 2\%$. Emittance has not yet been accurately measured but downstream transmission and beam size is consistent with expectation.

The source was disassembled for inspection in January 2022 and a fault with the repeller cable was discovered. Beam measurements after correction of this fault confirmed that the repeller had been unbiased during all previous commissioning at ESS and this was the cause of an over-estimation of the extracted current and its dependence on solenoid 1 current as shown in Fig. 1. Further details are given in [3].

Another fault was found on the LEBT collimator thermocouple. The thermocouple feedthrough is upstream of the LEBT BCM whereas the collimator is downstream. The thermocouple was providing a conductive path through the BCM so it has temporarily been disconnected.

A test-stand for ion source and LEBT testing and development is under construction at ESS. A complete spare ion source was provided by INFN and this will form the first phase of the test stand. The second phase will include the LEBT and duplicate solenoids, beam instrumentation and vacuum vessels are being procured for this. A hydrogen generator has also been purchased for the test stand and is under test in the vacuum lab. If successful, this generator will remove the hazards associated with the pressurised hydrogen bottle currently used on the ESS ion source. Further optimisation of source parameters will also be performed at the test stand, building upon recent studies of high-stability operation [4].

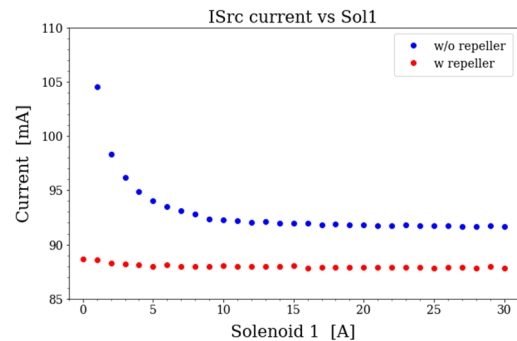


Figure 1: Effect of LEBT solenoid 1 on the measured ion source current with/without repeller bias.

The LEBT chopper is critical to the safe operation of the ESS LINAC since the beam extracted from the ion source is several milliseconds and the MEBT and DTL Faraday cups can only withstand 10-100 μs of beam. It is therefore important to note that the chopper has met all requirements and performed faultlessly during normal beam operations and beam abort scenarios.

The LEBT iris is equally important at this commissioning stage when low current diagnostic beams are required. The iris is a six-blade collimator used to control the beam diameter and thereby peak current. It has been tested extensively at ESS for normal operating modes and full aperture scans and has worked perfectly. However, a small water to vacuum leak has been detected and a new unit is to be manufactured with a revised design for cooling channel routes and connections.

[†]bryan.jones@ess.eu

[‡]also at INFN, Legnaro, Italy

DESIGN OF BEAM FOCUSING SYSTEM WITH PERMANENT MAGNET FOR J-PARC LINAC MEBT1*

Y. Fuwa[†], K. Moriya, and T. Takayanagi,
 J-PARC Center, Japan Atomic Energy Agency, Ibaraki, JAPAN

Abstract

MEBT1 (Medium Energy Beam Transport 1) of the J-PARC LINAC is a 3 MeV beam transport system located between the RFQ (Radio Frequency Quadrupole) and DTL (Drift Tube Linac). In the MEBT1, the beam-optical matching for injection into DTL and chopping for injection into acceleration phase of 3 GeV synchrotron, located downstream to the LINAC, are performed. The characteristics of MEBT1 are an important factor in determining the beam quality in the J-PARC accelerator facility. To achieve beam power of 1 MW and beyond, improving the stability and reliability of MEBT1 is an important development issue. The application of permanent magnets to the beam focusing system to the MEBT1 is under consideration to achieve improved stability and reliability. In this presentation, we report the design of focusing magnets using permanent magnet material and the results of the lattice study of MEBT1 with permanent magnets.

INTRODUCTION

J-PARC (Japan Proton Accelerator Research Complex) is an experimental facility with a nominal proton beam output power of 1 MW [1,2]. The J-PARC accelerator has been gradually increasing its beam power since it started operation in 2006. As of 2022, steady operation is being conducted with a beam output power of 850 kW, and continuous operation with 1 MW is planned in a few years.

J-PARC LINAC is a 400 MeV negative hydrogen beam injector of the J-PARC accelerator facility [3]. For the J-PARC LINAC to achieve output power of 1 MW, the one of the important issues is to reduce the degradation of beam quality due to the space charge effect. Since the beam degradations such as emittance growth and formation of beam fragmentation cause beam loss and radioactivation of accelerator components. In the future, it is also planned to enhance the accelerated beam current of the LINAC from current nominal value of 50 mA to 60 mA. For the stable long-term operation with higher beam power, it is necessary to understand emittance growth mechanism and to reduce beam loss.

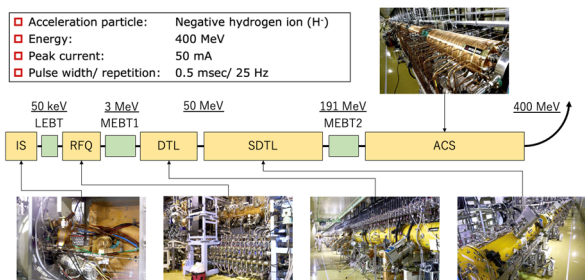


Figure 1: Configuration of J-PARC LINAC.

J-PARC LINAC MEBT1

The space charge effect is especially severe in the low energy part of the LINAC. MEBT1 (Medium Energy Beam Transport 1) is a beam transport section, where 3-MeV negative hydrogen beam is transported between RFQ (Radio Frequency Quadrupole) and DTL (Drift Tube Linac) (see Fig. 1). The MEBT1 consists of eight focusing magnets used for transverse matching of the beam for injection into the DTL, and two buncher cavities and two chopper cavities used for longitudinal matching for injection acceptance of the DTL and acceleration RF phase of the RCS (Rapid Cycling Synchrotron) at a later stage of the LINAC. The configurations of the devices are shown in Fig. 2.

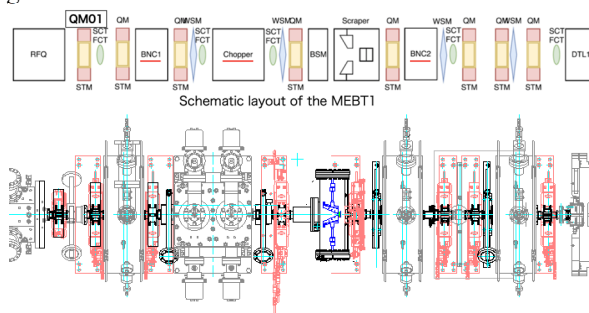


Figure 2: Layout of MEBT1.

Emittance Growth Mitigation with Octupole Focusing Field

In the current MEBT1, the formation of the beam fragmentation and beam emittance growth occurs due to the space charge effect [4]. From theoretical consideration, it is estimated that the emittance of MEBT1 is increased because the phase advance is lowered due to the space charge effect at the point where the transverse width of the beam is large [5].

To mitigate the emittance growth in MEBT1, a compensation technique which apply higher order focusing field is proposed [5]. Since the repulsive force due to the space charge effect has a higher-order nonlinear component, the emittance growth can be reduced by externally applying a focusing force to cancel the component. From the symmetry of the beam distribution, the divergence force due to space charge has an odd-order component, and the most influential component of the nonlinear term is the lowest third-order term. The octupole magnetic field component has a third-order focusing force. Therefore, externally applied octupole magnetic field can cancel the space charge effect. To verify the effectiveness of this method, we are investigating combined function magnet to apply external high-order magnetic field.

DEVELOPMENT OF EMITTANCE METER INSTRUMENT FOR MYRRHA

A. R. Páramo[†], I. Bustinduy, S. Masa, R. Miracoli, V. Toyos, S. Varnasseri
 Consorcio ESS-Bilbao, Spain

F. Doucet, L. de Keukeleere, A. Ponton, A. Tanquintic, SCK-CEN, Belgium
 J. Herranz, ProActive R&D, Spain

Abstract

For the commissioning of the MYRRHA proton Linac an Emittance Meter Instrument (EMI) has been foreseen. The EMI will be installed in a dedicated test bench for linac commissioning. The test bench will be initially placed after the RFQ with energies of 1.5 MeV, and in later stages moved to other sections of the Normal Conducting Linac for operation at 6 and 17 MeV.

The MYRRHA EMI is composed of two slit and grid subsystems for measurement of the phase space in the horizontal and vertical directions. For collimating the beam, graphite slits are used, and the beam aperture is measured in the SEM grids placed downstream. The control system performs signal amplification, data acquisition, and motion control, with the different systems integrated in an EPICs IOC.

The system, manufactured by ESS-Bilbao and Proactive R&D, has been tested on the ESS-Bilbao 45 keV and soon will be integrated in MYRRHA facilities. We present the EMI design, with irradiation analysis and emittance reconstruction, and the integration tests results.

INTRODUCTION

The MYRRHA project aims for the development of accelerator driven subcritical fission reactor. The current phase of the project, named MINERVA, will realise a 100 MeV, 4 mA superconducting linac. A prototyping of the normal conducting MINERVA injector is ongoing at SCK CEN in Belgium [1]. Currently commissioning of RFQ and Normal-Conducting Linac is in progress. For characterization of beam emittance and phase-space the Emittance Meter (EMI) has been developed. The EMI will be installed in a test bench used for Linac commissioning at different energies, 1.5, 6 and 17 MeV (see Table 1).

Table 1: Main Design Parameters for MYRRHA EMI

| Parameter | Value |
|------------------------|------------------|
| Current | 4 mA |
| Pulse duration | 100 μ s |
| Freq. | 10 Hz |
| Duty Cycle | 0.1 % |
| Minimum Beam Size, rms | 1 mm |
| Max. Beam Extension | ± 20 mm |
| Max. Beam Divergence | ± 20 mrad |
| Beam Energy | 1.5 / 6 / 17 MeV |
| Beam Power | 6 / 24 / 68 kW |
| Average Power | 6 / 24 / 68 W |

[†] arparamo@essbilbao.org

The MYRRHA EMI is developed with a similar design as the ESS MEBT Emittance Meter [2]. The EMI is based on a slit/grid system (see Figure 1). For measuring the phase-space the beam is sliced in the slit, getting the beam position. Then downstream the beam opens and with the signal measured in the grid the beam divergence is estimated. By performing the operation for different slit and grid positions the emittance can be reconstructed.

We have performed validation that the emittance meter can be operated under the irradiation conditions expected in MYRRHA. For the slit graphite blades have been chosen to withstand beam irradiation with a slit aperture of 100 μ m. After the slit a grid is placed. The grid is composed of 16 tungsten wires of $\phi 35$ μ m and separated 500 μ m. The grid is enclosed between two bias plates allowing for effective suppression of secondary electrons. When positive bias voltages are applied the secondary electrons emitted in the tungsten wires are attracted by the bias plates and leave the grid.

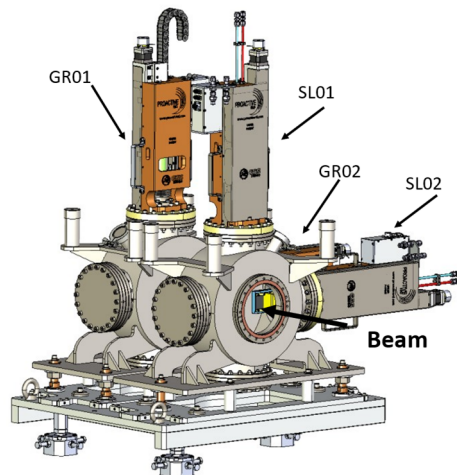


Figure 1: MYRRHA EMI assembly with slit & grids in the x/y planes.

EMI DESIGN

To characterize the performance of the EMI, we have studied the expected emittance, from the Tracewin source term we perform slit/grid simulations using linear particle tracing with python scripts, comparing the reconstructed emittance to the source values.

In Figure 2 we show a simulation at 1.5 MeV, for an emittance scan of 29 slit positions from -7 mm to +7mm of the beam centre, and a grid with an aperture of ± 3.75 mm or ± 10 mrad (16 wires separated 0.5 mm for a slit grid distance of 350 mm). The analysis of emittance reconstruction

WIRE SCANNER SYSTEMS AT THE EUROPEAN SPALLATION SOURCE (ESS): TESTS AND FIRST BEAM COMMISSIONING RESULTS

C. Derrez*, V. Grishin, T. Shea, E. Donegani, R. Tarkeshian, C. Thomas, H. Kocevar, N. Milas, R. Miyamoto, P. Van Velze, J. Martins, ESS, Lund, Sweden
 I. Bustinduy, I. Mazkaran, A.R. Páramo, ESS Bilbao, Bilbao, Spain
 M. Ferianis, S. Grulja, R. De Monte, S. Cleva, Elettra Sincrotrone Trieste, Trieste, Italy

Abstract

The ESS beam instrumentation includes 3 different type of Wire Scanners (WS). Double wires systems are deployed in the Medium Energy Beam Transfer (MEBT) part of the Normal Conducting Linac (NCL), and single wires and flying wire instruments are being tested and installed in the higher energy sections of the ESS linac. First beam tests results from the MEBT systems will be presented. The superconducting linac (SCL) WS shower detection systems are based on scintillator detectors coupled to long haul optical fibers, which carry the signals to custom front end electronics sitting in controls racks at the surface. The acquisition chain have been characterized at IHEP (Protvino, Russia), Elettra (Trieste, Italy), CERN PSB, COSY (IKP, Germany) and SNS (USA) before installation in the ESS tunnel. The test results of this system design, differing from the standard approach where photomultipliers are coupled to the scintillator will be presented.

INTRODUCTION

The ESS is since 2018 in a phase of commissioning with beam of the NCL [1, 2], while installation in the high energy sections progresses. When running at full installation completion, a 62.5 mA proton beam at a repetition rate of 14 Hz and pulse length of 2.86 ms will be accelerated up to 2 GeV, resulting in an average beam power of 5 MW. Wire scanners are part of the ESS beam diagnostics design to measure the beam profile and transverse halo at a number of locations along the Linac (Fig. 1).

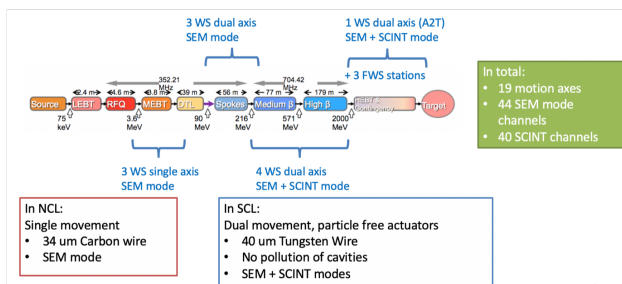


Figure 1: ESS LINAC WS installation layout.

The overall system architecture and installation status is first presented, before introducing beam commissioning results in the MEBT. Last but not least, the first tests results

* clement.derrez@ess.eu

with beam of the WS scintillator detectors and their complete data acquisition chain are presented.

WS SYSTEM STATUS

The WS system measurement principle consists of moving a wire across the beam in step by step mode or at constant speed while monitoring a signal proportional to the number of particles interacting with the wire. Key specifications of the system include a time resolution of $1 \mu\text{s}$, an accuracy of $\pm 0.1 \text{ mm}$ and a dynamic range of 10^3 .

At low energy, the mode of detection is based on Secondary Emission (SE), while at energies above 200 MeV, the primary mode of detection will be the measurement of the hadronic shower created in the wire. These high-energy secondaries are detected with scintillator detectors installed around the beam pipe.

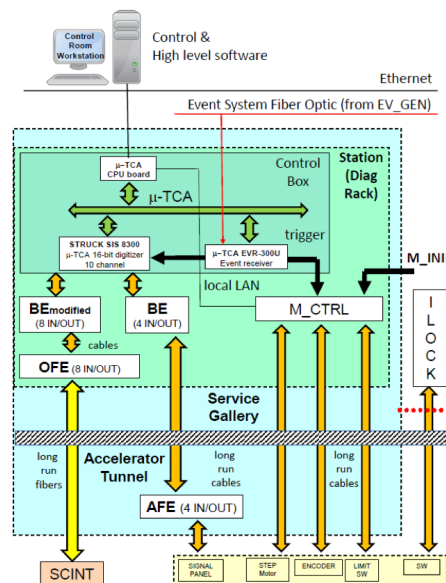


Figure 2: WS signal acquisition chain.

The beam power at ESS is a challenge for this type of interceptive diagnostics. The ESS WS are therefore only used in beam modes where the beam power is reduced, in order to preserve the device integrity by limiting thermal load. Carbon wires are used on double-wire actuators in the MEBT, while the high energy stations on Linac Warm Units (LWU) are equipped with single tungsten wire forks to measure each transverse plane. These actuators are assembled and tested in ISO class 8 clean rooms to allow final installation on the

STATUS OF TESTING AND COMMISSIONING OF THE MEDIUM ENERGY BEAM TRANSPORT LINE OF THE ESS NORMAL CONDUCTING LINAC

A. Garcia Sosa[†], R. Baron, H. Danared, C. Derrez, E. Donegani, M. Eshraqi, V. Grishin, A. Jansson, M. Jensen, B. Jones, E. Laface, B. Lagoguez, Y. Levinsen, J. Martins, N. Milas, R. Miyamoto, D. Nicosia, D. Noll, C. Plostinar, T. Shea, R. Tarkeshian, C. Thomas, E. Trachanas, P. van Velze, R. Zeng, ESS, Lund, Sweden
I. Bustinduy, A. Conde, D. Fernandez-Cañoto, N. Garmendia, P.J. Gonzalez, G. Harper, A. Kaftoosian, J. Martin, I. Mazkarian, J.L. Muñoz, A.R. Páramo, S. Varnasseri, A. Zugaza, ESS-Bilbao, Bilbao, Spain

Abstract

The latest beam commissioning phase of the Normal Conducting LINAC at ESS delivered a proton beam through the Medium Energy Beam Transport (MEBT) into the first Drift Tube LINAC (DTL) tank. The probe beam in MEBT consisted of 3.6 MeV protons of <6 mA, <5 μ s pulse length and 1 Hz repetition rate. Following the delivery of the components at ESS in Lund in June 2019, the commissioning phase with the MEBT was completed in July 2022. In March 2022, the maximum beam current of 62.5 mA was transported up to the MEBT Faraday cup. This proceeding focuses on the status of MEBT including magnets, buncher cavities, scrapers and beam diagnostics designed and tested in collaboration with ESS Bilbao.

NORMAL CONDUCTING LINAC

The ESS LINAC starts with a Microwave Discharge Ion Source (MDIS). This source is capable of producing a 75 keV, 74 mA proton beam with a pulse length of 6 ns and 14 Hz repetition rate. An extraction system with a repeller electrode is employed to limit the back-streaming electrons [1]. The LEBT at ESS is roughly 2.5 m long and consists of two focusing solenoids with a pair of corrector magnets embedded in each of them, an iris with a changeable aperture is used to limit the beam current, a diagnostics tank with a pair of Allison emittance probes, a Faraday cup, and an electrostatic chopper. Two sets of Non-invasive Profile Monitors (NPMs) measure beam size and position and a Doppler monitor that measures the proton fraction. A collimator cone sits at the end of the LEBT as an interface with the RFQ. The IS and the LEBT are in-kind contributions from INFN Catania in Italy [2,3].

The beam dynamics design of the Radio Frequency Quadrupole (RFQ) is optimized for minimal losses and high beam quality in terms of transverse and longitudinal emittance [4]. The RFQ is an in-kind contribution from CEA [5].

The MEBT is described in the next section, and after that begins the DTL section, another successful in-kind

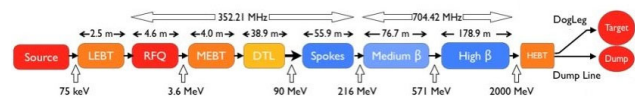


Figure 1: ESS LINAC.

contribution from INFN Legnaro [6]. The 39 m long DTL section is designed to accelerate the proton beam from 3.6 MeV to 90 MeV at a frequency of 352.21 MHz (see Fig. 1).

MEBT

The MEBT section, located between the RFQ and the DTL tanks, focuses the beam transversally and longitudinally, and chops the beam pulse as it is transported down the LINAC. A schematic of the ESS MEBT is shown in Fig. 2.

The Medium Energy Beam Transport (MEBT) has several functions. It matches the RFQ output beam characteristics to the DTL input both transversally and longitudinally. The transverse focusing and matching is achieved with quadrupole magnets whereas the longitudinal matching is achieved with buncher cavities. Moreover, the beam trajectory correction is done by steering magnets. A stripline chopper removes longitudinal edges of the beam pulse, and subsequently the chopped beam is intercepted by a beam dump.

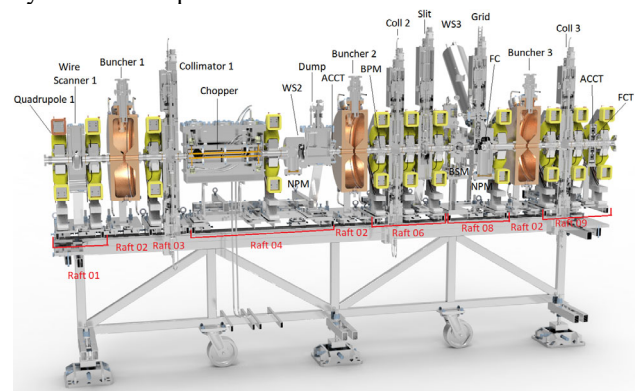


Figure 2: Schematic of the ESS MEBT.

Diagnostic instruments are used to measure a wide range of beam parameters, such as the beam matching and

[†]Alejandro.sosa@es.eu

COMMISSIONING OF UKRI-STFC SRF VERTICAL TEST AND HPR REPROCESSING FACILITY

M. D. Pendleton*, A. Akintola, R. Buckley, G. Collier, K. Dumbell, M. Ellis, S. Hitchen, P. Hornickel, G. Hughes, C. Jenkins, G. Jones, M. Lowe, D. Mason, A. J. May, P. A. McIntosh, K. Middleman, G. Miller, C. Mills, A. Moss, J. Mutch, A. Oates, S. Pattalwar, O. Poynton, P. A. Smith, A. E. Wheelhouse, S. Wilde, J. Wilson,
 UKRI-STFC Daresbury Laboratory, Keckwick Lane, Daresbury, WA4 4AD, UK

Abstract

The UK's first and only vertical test facility and associated cleanroom reprocessing suite has been developed, commissioned, and entered steady-state operations at the UKRI-STFC Daresbury Laboratory. The facility is capable of 2 K testing of 3 jacketed SRF cavities in a horizontal configuration per 2-week test cycle. We report on the associated cryogenic, RF, UHV, mechanical, cleanroom, and HPR infrastructure. SRF cavity workflows have been developed to meet the requirements of the ESS high- β cavity project within a newly developed quality management system, SuraBee, in accordance with ISO9001:2015. To support standardisation of measurements across the collaboration, reference cavities have been measured for cross-reference between CEA, DESY, and UKRI-STFC. We further report on commissioning objectives, observations, and continuous improvement activities.

INTRODUCTION

A new Superconducting Radio Frequency Lab (SuRF Lab) which includes a Vertical Test Facility (VTF) and Reprocessing Facility (Cleanroom and High Pressure Rinse (HPR)) has been commissioned at the UKRI STFC Daresbury Laboratory. The facility is currently undertaking a 2-year program to qualify high- β cavities for the European Spallation Source (ESS).

The VTF supports 2 K characterisation of three jacketed SRF cavities in a single cool-down run. Measurements of HOMs and passband modes are made at low power. Q vs E field measurements are made at high power levels (up to 200 W). A novel cryogenic architecture is used to significantly reduce the liquid helium (LHe) consumption compared with conventional facilities.

The HPR system has been developed to reprocess cavities that do not meet specification following their first vertical test; this system is currently in its commissioning phase.

VTF CRYOSTAT DESIGN

The conventional method for VTF SRF cavity testing is to fully immerse the cavities in a large LHe bath, and then cool to 2 K using a cold compressor/vacuum pump to reduce the vapour pressure over the bath. RF testing is then carried out with the cavities at 2 K. This approach has been used successfully for many programs, including XFEL cavity

testing at DESY [1]. Whilst well-proven, this technique requires both a large cryoplant and, for this activity, would require ~8500 L of LHe per test cycle.

Given the diminishing global supply of He, and associated rise in cost, an alternative cryostat architecture has been developed for vertical testing of jacketed SRF cavities which requires significantly less LHe and a much smaller cryoplant throughput [2]. The cryostat is based on a cavity support insert (CSI) where three cavities are mounted horizontally inside LHe jackets below a header tank, each fed by a common fill/pumping line; this may be seen in Fig. 1 which shows a photograph of an assembled insert. By using this design approach, far less LHe is required per testing run (~1500 L, all of which is recovered) compared with the conventional designs.



Figure 1: Photograph of CSI on stand with three jacketed cavities installed (top and middle cavities dressed in MLI jackets)

The insert is mounted into a cryostat vessel which comprises the outer vacuum chamber, magnetic shielding (see

* mark.pendleton@stfc.ac.uk

HIGH EFFICIENCY, HIGH POWER, RESONANT CAVITY AMPLIFIER FOR PIP-II

Rebecca Simpson, David Cope, Marcel. P.J. Gaudreau, Erik Johnson, Michael Kempkes, Nigel Stuart, Diversified Technologies, Inc., Bedford, MA, USA

Abstract

An advanced high-power, high power density, solid state power amplifier (SSPA) was developed to replace legacy Vacuum Electron Devices (VEDs). Diversified Technologies, Inc. (DTI) developed and integrated a resonant-cavity combiner with solid state amplifiers for the Proton Improvement Plan-II (PIP-II) at Fermilab. The architecture combines the power of N-many (up to 100+) RF power transistors into a single resonant cavity that are surface-mounted and -cooled. The system is designed so that failure of individual transistors has negligible performance impact. Due to the electrical and mechanical simplicity, maintenance and logistics are simplified leading to reduced capital and operating costs.

DTI demonstrated the basic feasibility of a 50-100 kW class amplifier resonant cavity combiner system at 650 MHz. A single-cavity system reached 15 kW at 66% power-added efficiency with ten of 12 slots filled, on only one of two cavity faces. The system further demonstrated the expected graceful degradation - an intermittent fault occurred on one of the ten modules and the only observable effect was a reduction in output power to 13.3 kW with a slight reduction in efficiency. Combining of multiple cavities was also demonstrated at low power.

INTRODUCTION

Achieving high power from solid state amplifiers is only possible by combining the outputs of multiple transistors. Each UHF transistor is limited to relatively modest power levels (less than 1000 watts CW), so hundreds to thousands of devices must be combined to compete with large conventional Vacuum Electron Devices, such as klystrons. In contrast to phased array radars, where space combining enables the contribution of thousands of individual, low power amplifiers to create a high power beam, the RF power for accelerators must be available at a single coupler to drive the accelerator cavity. Efficiently combining multiple transistors, while delivering high reliability at an affordable cost, are the main challenges for high power solid-state amplifiers (SSAs).

Binary combining (2N) is common at lower power, but high total insertion losses rule it out for most accelerator applications. DTI's cavity combiner is a unique form of the so-called N:1 combiner. The amplifier module combines the power of more than 96 transistors in one step. While there are other types of N:1 combiners, they typically require high power RF connectors and water cooling lines for each individual amplifier stage, leading to a level of complexity which scales with output power and total number of transistors. DTI's approach avoids most of this complexity, while the demonstrated graceful degradation

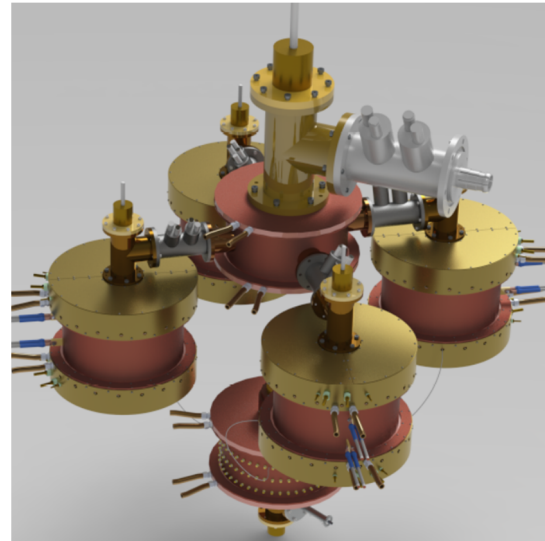


Figure 1: Conceptual layout of a high power solid-state transmitter based on four DTI cavity amplifier modules combined in a passive 4:1 cavity combiner. Power level of this concept scales to at least 500 kW

feature ensures high reliability.

In this approach, the cavity serves as both a power combiner and also as an integral part of the transistor output matching network. The low output impedance transistors are not matched to an arbitrary 50 ohm impedance level; rather the coupling loop and associated transmission line (when operated in the cavity) operates at a lower impedance level, presenting the optimum load impedance at the drain of the devices. This configuration is simple, has low losses and is responsible for the graceful degradation property.

DTI's design is a radical simplification of high-power, narrow band transistor-based amplifiers, and allows for straightforward scaling to increased power levels (hundreds of kilowatts) via combining multiple amplifier modules into a passive combiner (Fig. 1).

In Phase II of this Small Business Innovation Research (SBIR) grant, DTI built and tested a single-cavity system which reached 15 kW at 66% power-added efficiency with ten of 12 slots filled, on only one of two cavity faces. Combining of multiple cavities was also demonstrated at low power.

In a related effort, DTI has extended this design from 650 MHz to 1.3 GHz with similar results and hardware performance.

CAVITY QUALIFICATION AND PRODUCTION UPDATE FOR SNS-PPU CRYOMODULES AT JEFFERSON LAB*

P. Dhakal^{1,†}, N. Huque¹, J. Fisher,¹ E. F. Daly¹, M. Howell², and J. D. Mammosser²

¹Thomas Jefferson National Accelerator Facility, Newport News, VA, USA

²Spallation Neutron Source, Oak Ridge National Lab, Oak Ridge, TN, USA

Abstract

The Proton Power Upgrade (PPU) project at Oak Ridge National Lab's Spallation Neutron Source (SNS) currently being constructed will double the proton beam power capability from 1.4 to 2.8 MW by adding seven cryomodules, each containing four six-cell high-beta ($\beta=0.81$) superconducting radio frequency cavities. Research Instruments, located in Germany, built and processed the cavities at the vendor site, including electropolishing as the final active chemistry step. Twenty-eight cavities for seven cryomodules and an additional four cavities for a spare cryomodule were delivered to Jefferson Lab and the first qualification tests were completed on all cavities as received from the vendor. The performance largely exceeded the requirements on quality factor and accelerating gradient. Six cryomodules have been assembled into strings with three cryomodules shipped and high power rf tested successfully at SNS to date.

INTRODUCTION

The Spallation Neutron Source (SNS) at Oak Ridge National Laboratory is the world's first megawatt-class pulsed neutron source with the proton energy of 1 GeV. The Proton Power Upgrade (PPU) project will double the proton beam power from 1.4 to 2.8 MW by adding 7 additional cryomodules each contains four six-cell high beta (HB) $\beta=0.81$ superconducting radio frequency cavities. Modifications were made to both cavities and helium vessels based on operating experience of earlier SNS cryomodules and one of the prototypes currently installed in the linac [1]. The end groups of the cavities were made from high purity niobium whereas the original SNS cavities were fabricated from reactor-grade niobium. Cooling blocks were added to the end groups to increase the thermal contact between the end group and the helium bath. Higher order mode couplers were also removed from the upgrade design, making the cavities easier to chemically polish and clean. Furthermore, some modifications were made to the fundamental power couplers and cryomodule end cans based on the operational experience of the original SNS project. Table 1 shows the cavity parameters for original and upgrade high beta SRF cavities. Here, we present the status of initial cavity qualification tests, rework of unqualified cavities, and final cavity qualification with helium vessel prior to installation in cryomodules. In addition, an update on cryomodule production and high power rf test at SNS will be presented.

* This manuscript has been authored by Jefferson Science Associates, LLC under U.S. DOE Contract No. DE-AC05-06OR23177.

† dhakal@jlab.org

Table 1: Cavity Parameters for Original and Upgrade High Beta SRF Cavities

| Parameters | Original Cavities | PPU Cavities |
|------------------|-----------------------------|-----------------------------|
| E_{acc} (MV/m) | 15.8 | 16 |
| Q_0 | $>5 \times 10^9$ | $>8 \times 10^9$ |
| FPC Power (kW) | 550 | 700 |
| Q_{FPC} | $7 \times 10^5 (\pm 20 \%)$ | $8 \times 10^5 (\pm 20 \%)$ |
| HOM | 2 | None |

Table 2: PPU Acceptance Criteria for Vertical Test

| Test Conducted | Acceptance Value |
|-----------------------|------------------------------|
| E_{acc} (MV/m) | ≥ 18.0 |
| Q_0 | $>8 \times 10^9$ at 16 MV/m |
| Field Emission | ≤ 20 mrem/hr at 16 MV/m |
| Q_{FP} | $(0.7 - 2.0) \times 10^{12}$ |
| Fundamental frequency | 805.6 ± 0.25 MHz |

CAVITY QUALIFICATIONS

Design modifications to PPU cavities were based on operational experience of original SNS HB cryomodules as well as the results of prototype cryomodules installed in the SNS tunnel. A quality assurance plan was put in place to ensure optimal performance of PPU cavities from production steps at the vendor sites to the cavity qualification at Jefferson Lab [2]. The incoming cavities are checked for RF and mechanical acceptance followed by a wipe-down to ensure no particulates are transferred into the clean room. While in the clean room each cavity was attached to a vertical test stand using clean assembly procedures, followed by a leak check. Once on the test stand the cavity is transferred to a bake box, where all cavities were baked at 120 °C for 24 hours. Analog scans employing a residual gas analyzer before and after baking were recorded. Also, the partial pressure of various gas species were recorded during low-temperature baking. The cavity was cooled down to 2.1 K in a vertical Dewar with a residual magnetic field < 20 mG [3]. The performance acceptance criteria are summarized in Table 2.

Bare Cavities rf Performances

All 32 cavities were rf tested as received from the vendor with only 16 cavities meeting the PPU specification for accelerating gradient (>18.0 MV/m) and quality factor ($>8 \times 10^9$). Typical failures during rf qualification test were due to gradient limitation either by early field emission onset or final field emission reaching an administrative limit

PROGRESS ON THE PROTON POWER UPGRADE PROJECT AT THE SPALLATION NEUTRON SOURCE*

M. Champion[†], C. Barbier, M. Connell, N.J. Evans, J. Galambos, M. Howell, G. Johns, S. Kim, J. Moss, B. Riemer, K. White, Oak Ridge National Laboratory, Oak Ridge, USA
 E. Daly, Thomas Jefferson National Accelerator Facility, Newport News, USA
 D. Harding, Fermi National Accelerator Laboratory, Batavia, USA

Abstract

The Proton Power Upgrade Project at the Spallation Neutron Source at Oak Ridge National Laboratory will increase the proton beam power capability from 1.4 to 2.8 MW. Upon completion of the project, 2 MW of beam power will be available for neutron production at the existing first target station with the remaining beam power available for the future second target station. The project will install seven superconducting radiofrequency (RF) cryomodules and supporting RF power systems and ancillaries to increase the beam energy to 1.3 GeV. The injection and extraction region of the accumulator ring will be upgraded, and a new 2 MW mercury target has been developed along with supporting equipment for high-flow gas injection to mitigate cavitation and fatigue stress. Equipment is being received from vendors and partner laboratories, and installation is underway with three major installation outages planned in 2022-2024. The project is planned to be completed in 2025.

INTRODUCTION

The SNS accelerator routinely delivers a 1.4 MW proton beam to a liquid mercury spallation target to provide neutrons to 19 instruments [1]. The existing Linac produces a 1 ms pulse train of H- ions at a repetition rate of 60 Hz. The H- ions are stripped of their electrons as they enter the accumulator ring, which compresses the proton beam to a sub-microsecond pulse that is extracted and sent to the target 60 times per second. The Linac presently provides a beam energy of 1.0 GeV that will be increased to 1.3 GeV through the addition of 28 superconducting cavities contained in 7 cryomodules. The Linac H- current will be increased from 26 to 38 mA, which will increase beam loading throughout the Linac. Three Drift Tube Linac (DTL) radiofrequency (RF) stations will be upgraded to provide needed additional power by means of new higher-rated klystrons. Otherwise, the existing Linac can accelerate the increased H- current.

The mercury target and supporting utilities in the existing First Target Station (FTS) are being upgraded to accept 2 MW of proton beam power, and the remaining beam power will drive the future Second Target Station (STS) that is being constructed as a separate project. The 2 MW beam delivered to the FTS will improve performance

across the entire existing and future instrument suite, and the future STS will provide a wholly new capability in the form of a transformative new source optimized to produce the world's highest peak brightness of cold neutrons.

SUPERCONDUCTING LINAC

Eight cryomodules are being produced by Thomas Jefferson National Accelerator Facility (TJNAF). Three cryomodules have been delivered to SNS and exceeded performance requirements during RF testing at 2 K. Delivery of the 4th cryomodule is planned in Sep. 2022, and the final cryomodule is due for delivery in Aug. 2023. The first two cryomodules (Fig. 1) will be installed in Aug.-Sep. 2022.



Figure 1: The first two cryomodules staged for installation in the front-end building.

The superconducting cavities were received from industry ready for vertical testing. Roughly 50% of the cavities required additional high pressure rinsing to eliminate field emission [2]. The helium vessels were attached at TJNAF [3], and then the cavities were again vertically tested to qualify for cryomodule cavity string assembly. It has been challenging to qualify the tanked cavities, and numerous cleaning cycles have been needed in many cases. A few cavities have required light buffered chemical polishing (BCP) to meet performance requirements.

Fundamental power couplers were RF tested at SNS and delivered to TJNAF ready for installation. U-tubes for connecting the cryomodules to existing cryogenic distribution lines are being fabricated by industry.

RADIO FREQUENCY SYSTEMS

Twenty-eight new 700 kW, 805 MHz klystrons are being installed to power the 28 superconducting RF cavities. The RF systems are largely the same as the existing RF systems with some improvements based on operations experience since the SNS construction was completed in 2006. Three new alternate-topology high voltage converter modulators will power 9, 9, and 10 klystrons. The modulators have been received, and the first unit has been installed in the

*ORNL is managed by UT-Battelle, LLC, under contract DE-AC05-00OR22725 for the U.S. Department of Energy. This research was supported by the DOE Office of Science, Basic Energy Science, Scientific User Facilities.

[†]championms@ornl.gov

PROGRESS OF THE ESS PROTON BEAM IMAGING SYSTEMS*

Erik Adli[†], Håvard Gjersdal, Kyrre N. Sjøbæk, Grey Christoforo, Eric D. Fackelman, Ole M. Røhne, Jonas S. Ringnes, Simen R. Solbak, Maren C. Lithun (University of Oslo, Oslo, Norway)
Cyrille Thomas, Yngve Levinsen, Kaj Rosengren, Thomas Shea (ESS ERIC, Lund, Sweden)
Gerard Bell (STFC), Mark Ibison (University of Liverpool and Cockcroft Institute, Daresbury, UK)
Shrikant Joshi, Stefan Björklund (University West, Trollhattan, Sweden)

Abstract

The ESS Target Proton Beam Imaging Systems has the objective to image the 5 MW ESS proton beam as it enters the spallation target. The imaging systems has to operate in a harsh radiation environment, leading to a number of challenges : development of radiation hard photon sources, long and aperture-restricted optical paths and fast electronics required to provide rapid information in case of beam anomalies. This paper outlines how main challenges of the imaging systems have been addressed, and the status of deployment as ESS gets closer to beam.

INTRODUCTION

The European Spallation Source (ESS) [1], currently under construction, has as objective to deliver neutron beams with a 95% overall availability (average beam power of 5 MW) for ~5000 h per year. In order to achieve these goals it is critical to monitor all aspects of the spallation process and the proton beam characteristics. The beam will be rastered (painted) onto the rotating target by specially designed rastering magnets [2], in order reduce the current density at the target. The Oslo in-kind contribution [3] consists of delivering the ESS target and tuning dump imaging systems. We report here on the recent progress on the two systems, including electronics development and related beam dynamics studies.

TUNING DUMP SYSTEMS: Two imaging systems are provided for the tuning beam dump, and are vital to characterise the beam on dump parameters. These will have insertable screens made of large, custom cut Chromox ceramic plates [4, 5], special camera inserts deep into the concrete walls to protect them from radiation, and an optical system design to give an optimal field of view. The tuning dump imaging system design is described in [6].

TARGET SYSTEMS: The two target imaging systems are key diagnostics for monitoring the proton beam in the target region, including verifying that the rastering is functioning correctly. A thin layer of luminescent coating is thermal sprayed on the target surface and on the proton beam window surface. Optical systems will image the photons emitted when the proton beam passed through the coated surfaces. The two surfaces, and the beginning of the optical path, are depicted in Fig. 1a). The target imaging system is further described in [3].

* This work is part of the Norwegian in-kind contribution to ESS.

[†] Erik.Adli@fys.uio.no

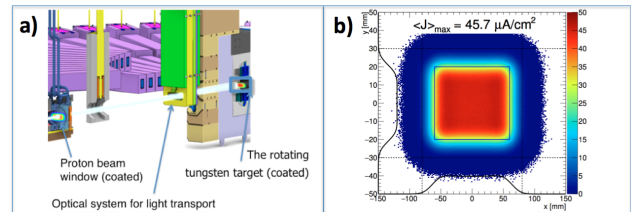


Figure 1: a) The target imaging systems, imaging the proton beam window and the target wheel, will operate in an intense neutron flux and must withstand the 5 MW proton beam. b) Beam density map of the rastered proton pulse at the target wheel. From [2].

TUNING DUMP SYSTEMS

Two tuning dump systems have been completed and were delivered to ESS in June 2022. One of systems is shown in Fig. 2, integrated in the vacuum vessel provided by STFC.

The vacuum vessel is fitted with an actuator that moves a frame that can hold two Chromox scintillating screens. When a screen is placed in the beam path, the beam footprint can be imaged from the emitted photons by a camera that is installed in the wall next to the chamber. Two mirrors are installed on the wall to transport the light from the Chromox screen to the camera. The images produced by the system will be used by the operators to tune the beam during commissioning.

Camera Insert

To minimise the radiation damage and increase the expected lifetime of the cameras, holes have been core drilled into the concrete wall next to the vacuum vessels. Pipes with rails will be installed and fixed in the holes. For each system, a camera with a lens, two neutral density (ND) filters, and a microcontroller are mounted on a custom camera insert.

The Allied Vision Manta G-419b PoE Gig-E camera is attached to an adapter at a tilted angle with respect to the optical axis as calculated from the Scheimpflug principle [7]. The Chromox screens are tilted 45 degrees to the optical axis, the camera tilt is there to make it possible to have the whole screen in focus. An off-the-shelf lens, Canon EF 135 F/2L, is also connected to the adapter. A microcontroller makes it possible to remote control the lens focus and aperture. Two ND filters (OD 2.0, 3.0) are installed on actuators in the adapter, so they can be moved in or out of the light-path.

The adapter is connected to a wagon and to rectangular pipes. The pipes are used as cable guides, as well as a handle

THE PRE-INJECTOR UPGRADE FOR THE ISIS H⁻ LINAC

S. R. Lawrie*, R. Abel, C. Cahill, D. C. Faircloth, A. P. Letchford,
 J. H. Macgregor, T. Sarmiento, J. Speed, O. A. Tarvainen, M. O. Whitehead, T. Wood
 UKRI Science and Technology Facilities Council, Rutherford Appleton Laboratory,
 Harwell Campus, Oxfordshire, OX11 0QX, UK

Abstract

A new maintenance-free, high current, high duty-factor H⁻ linac pre-injector is being commissioned for the ISIS pulsed spallation neutron and muon facility. As well as delivering a low emittance-growth, loss-free beam, the pre-injector incorporates a chopper to facilitate arbitrary bunch time-structures. A 50 Hz, 0.9 ms (4.5% duty factor) RF-driven H⁻ ion source operates extremely reliably and with a large available parameter space via a novel microwave ignition gun and a wideband solid-state RF amplifier. A 202.5 MHz medium energy beam transport (MEBT) incorporates eight quadrupole magnets with integrated xy steerers, four quarter-wave re-bunching cavities, four extremely compact beam position monitors and an electrostatic chopper in just two metres of footprint. Beam has been extracted from the ion source and MEBT commissioning is due Spring 2023. Thereafter, the entire pre-injector will be soak-tested offline for a year before installing on the user facility.

ISIS LINEAR ACCELERATOR HISTORY

An H⁻ linac is used at ISIS for charge-exchange injection into a rapid-cycling proton synchrotron. This delivers protons to two targets, which produce neutrons and muons for materials science studies. A pre-injector based around a solenoid low energy beam transport (LEBT) and 202.5 MHz radio-frequency quadrupole (RFQ) is used to form a high quality low energy bunched beam for subsequent acceleration by a drift-tube linac (DTL). In order to revert to the retired Cockcroft-Walton multiplier stack in the event of a problem, old equipment was left installed in the area. The consequent lack of space meant that no matching components could fit between the RFQ and DTL. It was known that this would result in significant beam loss at two major locations in the linac. Therefore, having proven itself as extremely reliable over 15 years, space has been cleared such that the pre-injector may be moved back away from the DTL and a medium energy beam transport (MEBT) installed. The improvement in beam delivered by the MEBT is highlighted in Table 1. Because far less beam-loss is expected, the ion source no longer needs to generate as much beam current. This opens the door to modern long-life, high efficiency H⁻ technology. This paper describes the pre-injector installation status and the initial commissioning results of the ion source.

Table 1: Improved beam transport afforded by the pre-injector upgrade.

| Location | Existing | Upgrade |
|------------|----------|-----------------|
| Ion source | 55 mA | 38 mA |
| LEBT | 36 mA | 36 mA |
| RFQ | 35 mA | 35 mA |
| DTL | 25 mA | 35 mA (chopped) |

MEDIUM ENERGY BEAM TRANSPORT

The design of the MEBT has been described previously in detail [1]. It consists of eight quadrupole magnets, four re-bunching cavities, four beam position monitors and an electrostatic chopper.

Re-bunching Cavities

Four two-gap quarter-wave resonator (QWR) cavities operating at 202.5 MHz and -90° phase maintain the longitudinal structure of the beam bunched by the RFQ. Each QWR shown in Fig. 1 consists of a copper drift tube suspended inside a copper-plated stainless steel cylindrical cavity. Each QWR also incorporates four RF pickups, water cooling channels, fixed and dynamic slug tuners and a vacuum-pumping port. Features on the beam ports are used to align the drift tube bore to within 20 μm. Difficulties meeting the required welding and plating tolerances have necessitated prototypes being manufactured by several vendors. The QWRs are on the critical path for the project, but it is hoped that a satisfactory solution will be found to meet the MEBT beam delivery schedule of Summer 2023.



Figure 1: Quarter-wave resonator cavity prototype.

* scott.lawrie@stfc.ac.uk

PROGRESS OF PIP-II ACTIVITIES AT IJCLab

P. Duchesne†, N. Gandolfo, D. Le Dréan, D. Longuevergne, R. Martret, T. Pépin-Donat, F. Rabehasy, S. Roset, L. M. Vogt, Université Paris-Saclay, CNRS/IN2P3, IJCLab, Paris, France
P. Berrutti, M. Parise, D. Passarelli, Fermilab, Batavia, USA

Abstract

Since 2018, IJCLab is involved in PIP-II project on the design and development of accelerator components for the SSR2 (Single Spoke Resonator type 2) section of the superconducting linac. First pre-production components have been fabricated, surface processing and cavity qualification in vertical cryostat are on-going. IJCLab has upgraded its facilities by developing a new set-up to perform rotational BCP. The progress of all processing and testing activities for PIP-II project will be reported and, in particular, a dedicated study to qualify removal uniformity compared to static BCP will be presented.

INTRODUCTION

The Proton Improvement Plan-II (PIP-II) encompasses a set of upgrades and improvements to the Fermilab accelerator complex aimed at supporting a world-leading neutrino program over the next several decades and more specifically at providing an intense neutrino beam to the future DUNE project (Deep Underground Neutrino Experiment). PIP-II benefits from a strong commitment as in-kind contributions of international partners among which France is involved through CEA and CNRS/IN2P3 agencies. Since 2018, IJCLab, unique actor for CNRS/IN2P3 contribution, is strongly involved in the pre-production and production phases of PIP-II project and more specifically on the design and development of accelerator components for a section of the superconducting linac named SSR2 [1]. CNRS/IN2P3 contribution consists of:

- Supporting design of SRF components as tuners, power couplers and cavities.
- Procuring several pre-production components as tuners and power couplers.
- Supporting fabrication, validating in vertical cryostat and re-processing cavity surfaces if required of pre-production SSR2 cavities.
- Supporting fabrication, validating in vertical cryostat of 33 production cavities and re-processing a maximum of 25% of cavities if required.

The manufacturing and the surface processing of the first prototype cavities procured by Fermilab* are ongoing [2]. The first step of surface preparation consists in a bulk BCP (Buffered chemical polishing) performed on the bare cavity, followed by a light BCP and heat treatment after the helium tank integration. The required average material removal will be in the range of 150-200µm to eliminate the damaged layer created during the manufacturing.

In this context, IJCLab has upgraded its facilities by developing a new setup to perform rotational BCP (Figure 1) starting from the existing one used to perform static BCP of Spoke resonators equipped with their helium vessel [3]. The heat generated during the chemical reaction is dissipated through both the chilled acid bath and the cooling water flowing through the helium vessel. In the case of static BCP setup, as the cavity remained fixed during the process, it has to be emptied, rinsed, disassembled, flipped and re-assembled after half the time to etch as homogeneously as possible the overall surface. The implementation of rotational BCP will now avoid this intermediate disassembly and thus reduces drastically the operators' intervention and risk occurrence.

Moreover, previous studies proved that the implementation of a rotation during chemical etching improves significantly the homogeneity [4,5] and surface quality by avoiding patterns as grooves, stripes or bubble marks.



Figure 1: Rotational BCP setup at IJCLab

The new setup developed at IJCLab was experimented on a SSR2 prototype bare cavity equipped with a removable dummy tank. Static and rotational treatments were performed in order to measure wall thicknesses and induced frequency shift. Surface quality and homogeneity of the niobium removal have thus been addressed.

This paper aims at summarizing all preliminary results obtained on the first SSR2 prototype.

EXPERIMENTAL SETUP

The new rotational BCP setup was developed by taking into account our experience matured on ESS and MYRRHA projects. To efficiently keep the cavity walls cold during the treatment, a chilled water flow is maintained around the cavity. To achieve this, a removable dummy tank was designed for the SSR2 bare cavity. Its geometry is very similar to the helium vessel to have identical interfaces.

Dummy Tank

The dummy tank is composed of two half shells in stainless steel and closing parts in PVC (Figure 2). EPDM seals

*Work supported, in part, by U.S. Department of Energy, Office of Science, Office of High Energy Physics, under U.S. DOE Contract No. DE-AC02-07CH11359

†patricia.duchesne@ijclab.in2p3.fr

ACCELERATED LIFETIME TEST OF SPOKE CAVITY COLD TUNING SYSTEMS FOR MYRRHA

N. Gandolfo¹, S. Blivet¹, F. Chatelet¹, V. Delpech¹, D. Le Dréan¹, G. Mavilla¹, M. Pierens¹,
 H. Sagnac¹, IJCLab, CNRS/IN2P3 Orsay, France
¹also at Université Paris-Saclay, Orsay, France

Abstract

Within the framework of MINERVA, the first Phase of MYRRHA (Multi-purpose hYbrid Research Reactor for High-tech Applications) project, IN2P3 labs are in charge of the developments of several accelerator elements. Among those, a fully equipped Spoke cryomodule prototype was constructed, it integrates two superconducting single spoke cavities operating at 2K, the RF power couplers and the associated cold tuning systems. The extreme reliability specified for this project motivated to conduct accelerated lifetime tests (ALT) on two cold tuning systems in a cryomodule-like environment. By gathering experimental data, many critical aspects can be enhanced like maintenance plan consolidation, determination of aging indicators and design optimization of the whole system and its sub components. This paper describes the complete ALT process from the studying elements and the test environment design, to the experimental findings.

INTRODUCTION

MYRRHA [1] is the combination of a subcritical nuclear reactor driven by a proton accelerator. One of its goals is to provide answers to the feasibility of nuclear waste transmutation at a massive level. Because the accelerator is coupled to the reactor, its reliability requirement is significantly higher than for any other operational high power proton beam accelerator. This key parameter encouraged to build the accelerator components conservatively but also to design and operate dedicated tools to assess the reliability of systems that are considered the most critical for the beam acceleration, either because of the low accessibility or the high risk to provoke a loss of beam scenario.

The early stage of the superconducting linac will bring the beam energy up from 16.6 MeV to 100 MeV [2] thanks to 30 cryomodules [3], which contains each two single-spoke cavities ($\beta = 0.37$, 352 MHz). Each cavity is equipped with a cold tuning system [4], which allows a fine control of the resonant frequency required to operate at the nominal accelerator field. Four tuners were built, two for the prototype cryomodule development purpose, and two dedicated for the ALT campaign.

TUNER DESCRIPTION

The MINERVA cavity cold tuning systems is a double-lever class tuner (see Fig. 1) based on the design of ESS double-spoke cavity tuner [5]. The tuner is actuated using a low temperature stepper motor (VSS57.200) with a 6.25:1 planetary gearhead from Phytron [6] and two piezo actuators (NAC2022-H72) from Noliac [7] for coarse and

fine tuning respectively. The motor is mechanically coupled to a full stainless steel satellite roller screw coated with MoS2 dry lubricant built by Elitec [8]. The lever arms are guided by a set of four stainless steel hybrid ball bearings built by JESA [9]. All of those components are considered critical in terms of reliability due to the combination of small motions, high forces, and material fatigue in vacuum environment at cryogenic temperatures.



Figure 1: Prototype tuner assembled on a single-spoke cavity during cryomodule integration.

TEST ENVIRONMENT

In order to mimic the cryomodule environment, a dedicated tuner test cryostat has been designed and built

STATUS AND RF DEVELOPMENTS OF ESS BILBAO RFQ*

N. Garmendia[†], J. L. Muñoz, I. Bustinduy, P. González, A. Kaftoosian, J. Martin, A. Conde, A. Rodríguez, S. Masa, ESS Bilbao Consortium, Zamudio, Spain

Abstract

Within the framework of the plans for study of a light-ion linear accelerator, ESS Bilbao is manufacturing a radio frequency quadrupole (RFQ) aimed at accelerating up to 3 MeV the protons generated in the ion source. The progress made and the difficulties encountered with the RFQ are discussed in this paper. A power coupler prototype for the RFQ has been developed while several mechanical constraints were also studied in the final coupler. This prototype operates at a lower power, then it can work using PEEK window for the vacuum interface and it does not require neither brazing nor cooling system. Also, a complete RF test stand is being implemented to perform the high-power conditioning in traveling and standing wave mode, to verify the power handling capability of the coupler and its thermal behaviour. The RF test stand, based on EPICS environment, can provide up to 2 MW peak power at 352.2 MHz in a pulse operation of 14 Hz and a duty cycle of 4.9%.

INTRODUCTION

ESS Bilbao oversees the Spanish in-kind contributions to the contributions to the European at the same time we are involve in developing local project such as the study of a multi-purpose light ion linear accelerator of 30 MeV proton beam [1].

The first part, an Electron Cyclotron Resonance (ECR) proton ion source and Low Energy Beam Transport (LEBT), which already are under operation at the ESS Bilbao premises, can provide a proton beam of up to 40 mA at an energy of 45 kV.

The next linac part is the Radio Frequency Quadrupole (RFQ), which is under manufacturing [2].

Table 1: ARGITU-RFQ Main Specifications

| Parameter | Value |
|-------------------|----------------------|
| Specimen | H+ |
| Beam current | 32 mA |
| Beam energy | 45 keV → 3 MeV |
| RF Frequency | 352.2 MHz |
| Pulse Operation | 30 Hz; 1.5 ms; 4.5 % |
| Intervane Voltage | 85 kV |
| Kilpatrick | 1.85 |
| Input emittance | 0.25 π mm rad |

The next steps of the RFQ project have been launched, such as the coupler and the RF system for the conditioning. The main details of each phase are presented in the next sections.

* This work is part of FEDER -TRACKS project, co-funded by the European Regional Development Fund (ERDF)

[†]ngarmendia@essbilbao.org

RFQ STATUS

The ESS Bilbao RFQ has a total length of about 3.12 m (3,66 λ) and 273 cells, composed of 4 segments of 800 mm in length. Each segment is itself an assembly of four components using O-ring system, with polymeric vacuum gaskets, therefore avoiding the brazing.

The RFQ first segment is already manufactured and experimentally validated [3], so the next segment manufacturing has started. The metrology of the one vane has let validate one of the key parameters of the RFQ design, the 2-term modulation curve. The design and experimental data of the modulation curve of the vane have been compared and it can be checked the good agreement with a 5 μ m of tolerance (Fig. 1).

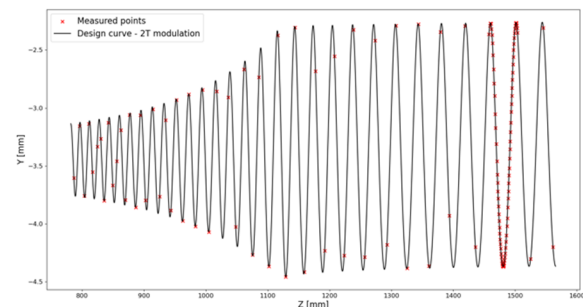


Figure 1: Modulation curve of the major vane of the second RFQ segment. Metrology results of vane seems to agree within 5 μ m tolerance

POWER COUPLER DESIGN

The injection of the RF power as well of the vacuum interface in the RFQ is achieve by means of adequate RF power couplers. The designed coupler is based in magnetic loop coupling with a mechanical interface of standard Con-Flat 2 3/4". Two couplers are required to provide the required power.

Due to the reduced size of the mechanical interface, several difficulties have appeared to fulfil all the coupler requirements in terms of maximum electric field and thermal behaviour. With the aim to overcome these issues

FIRST BEAM MATCHING AND TRANSMISSION STUDIES ON THE ESS RFQ

D. Noll*, R.A. Baron, C.S. Derrez, E.M. Donegani, M. Eshraqi, F. Grespan, H. Hassanzadegan, B. Jones, Y. Levinsen, N. Milas, R. Miyamoto, C. Plostinar, A. Garcia Sosa, R. Zeng (ESS, Lund), A.-C. Chauveau, O. Piquet (CEA-IRFU, Gif-sur-Yvette)

Abstract

The European Spallation Source will be driven by a 5 MW, 2 GeV linear accelerator, producing 2.86 ms long proton beam pulses with a peak current of 62.5 mA at 14 Hz. Following the source commissioning in 2018 and 2019, the RFQ was successfully conditioned and subsequently commissioned with beam in 2021. In this paper, we will present results of studies on beam matching to the RFQ, both for low and high current beam modes, and will compare these results to model predictions.

INTRODUCTION

The normal-conducting part of the ESS accelerator (NCL) consists of an ion source, a low-energy beam transport section, an RFQ, a medium-energy beam transport line and five DTL tanks. The commissioning of the NCL is ongoing [1]. The RFQ has been conditioned in the summer of 2021 and first protons were accelerated to 3.62 MeV on the 26th November of 2021. After a period of tests and studies at low beam current, with a so-called probe beam with 5 μ s long pulses at 6 mA and a repetition rate of 1 Hz, the beam current was increased to the design value of 62.5 mA on 12th of March 2022 using 5 μ s and later 20 μ s long pulses at 1 Hz.

Two solenoids in the 2.5 m-long low-energy beam transport line match the beam from the proton source to the RFQ. The solenoids are outfitted with internal steerers for trajectory correction. After the first solenoid, an iris – a set of three movable blades which form a hexagonal aperture – is installed in the LEBT [2]. Closing the iris allows an operator to change the beam current without adjusting the plasma conditions of the source. Compared to relying on adjustments of both the plasma parameters and the extraction to match the changes in space charge forces and the extracted beam distribution, this makes it easier to produce low-current beams with lower emittance compared to the full current beam. A repeller is present in front of the RFQ to prevent electrons from being injected into the RFQ.

The 4.6 m-long four-vane RFQ, designed by CEA/Saclay, accelerates the beam from an energy of 75 keV to 3.62 MeV. Its RF performance is presented in [3]. The inter-vane voltage is ramped from 80 kV at the entrance to 120 kV, requiring a forward RF power of approximately 800 kW.

The injected and accelerated beam current can be measured by three beam current monitors (BCM): one directly in front of the RFQ, one directly after the RFQ and one further downstream in the MEBT. During all studies presented

here, the beam was stopped at a Faraday Cup at the center of the MEBT. Details on the MEBT can be found in [4].

A number of studies were performed to help understand the performance of the RFQ and associated components.

VOLTAGE SCANS

The behavior of beam transmission as function of the inter-vane voltage is a good quantity to compare to model predictions to verify the expected performance of the beam dynamics of the RFQ. In simulation, for small changes in the voltage (< 10 %), output beam energy and transmission will remain relatively constant while for larger decreases, the energy spread will be large as transmission drops.

The power injected into the RFQ was scanned over the entire available range. Figure 1 shows the behavior of the transmission through the RFQ, for different matching conditions, as measured by the BCs at the start and the end of the RFQ in comparison to the model prediction. Figure 2 shows the input distributions as predicted by a model.

The beam current for this study was approximately 6 mA. Multiple, quite different settings of the solenoid magnets were found that give beam transmission of close to 100 %. The measurements fit the expected behavior with voltage: independent of solenoid settings, the transmission remains

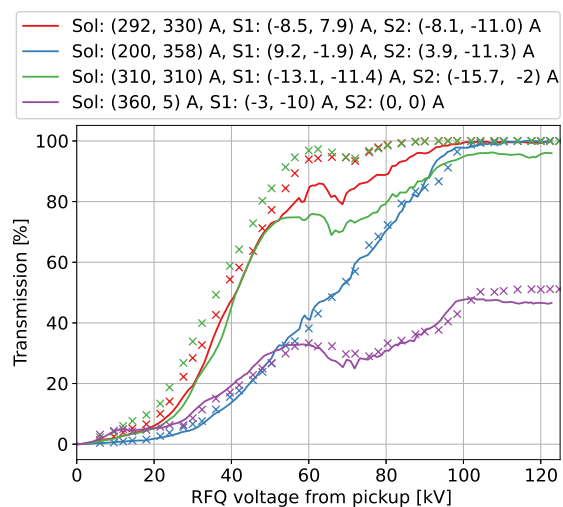


Figure 1: Beam transmission through the RFQ for different inter-vane voltages and four different LEBT configurations. The data shown as lines are measurements, the data shown as crosses are predictions by a model built upon ion source commissioning data.

* daniel.noll@ess.eu

RFQ PERFORMANCE DURING RF CONDITIONING AND BEAM COMMISSIONING AT ESS

R. Zeng[†], B. Jones, D. Noll, R. Miyamoto, A. Svensson, G. Fedel, E. Trachanas, D. Nicosia,
 A. Garcia Sosa, European Spallation Source ERIC (ESS), Lund, Sweden
 O. Piquet, M. Desmons, M. Baudrier, A-C. Chauveau, P. Hamel
 CEA-IRFU, University Paris-Saclay, Gif-sur-Yvette, France
 F. Grespan, INFN, Italy

Abstract

The RFQ at ESS has been successfully gone through RF conditioning, RF re-conditioning and low duty cycle beam commissioning. The RFQ fulfils all required functions and overall performance is satisfactory. RF conditioning, three RF re-conditionings after LEBT interventions and beam commissioning will be reported and RFQ performance during these periods will be described. RFQ performance in a large extent is reflected by dynamics and interactions between RF, cavity and beam. Thanks to advanced hardware capabilities and flexible software intelligence, observation of those dynamics and interactions are done at a detailed level. Analysis of those dynamics and interaction will be introduced. Some techniques to deal with challenges resulting from those dynamics and interactions will also be discussed.

INTRODUCTION AND RFQ OVERALL PERFORMANCE

RFQ has been installed and tuned in the ESS tunnel following its delivery to ESS in 2019. The overall parameters are listed in Table 1. RFQ high power conditioning started in June 2020 and after 7 weeks RFQ was conditioned up to full duty cycle (14 Hz and 3.2 ms) at 800 kW (corresponding to 776 kW net power in cavity). After high power conditioning, the RFQ reached stable operation condition and RF breakdown rates reduced to 1~2 times per hour at full duty cycle, compared to 200 times per hour in the peak of conditioning. After a trip when RF power is shut down completely, it takes around 3 minutes for RFQ to thermally stabilise with nominal power nominal power and full duty cycle [1].

In late 2021 and early 2022 when there were three interventions in the LEBT to fix and exchange components, the RFQ end flange had to be disconnected. During these periods, nitrogen gas was purged through RFQ to avoid exposure to air. RF re-conditioning was performed immediately after each intervention to enable RFQ to recover to its full capacity. It was noticed that the longer intervention time it took, the longer re-conditioning time it required for RFQ to recover. During the beam commissioning phase (beam destinations to Faraday cup in MEBT and Faraday cup after DTL1), beam pulse length is limited to be less than 50 μ s, and RFQ was set to run in low duty cycle (1 Hz and 100 μ s) to avoid damage of Faraday cups in case of chopper failure in LEBT. RFQ performance has been very stable and robust throughout this low duty cycle beam commissioning phase, and very few RF breakdown occurred.

Table 1: RFQ Overall Parameters

| RFQ | Design | Measured |
|-------------------------------------------------|--------------------------|-----------------------------|
| Frequency (MHz) | 352.21 | |
| Beam Duty Cycle | 4% (14 Hz, 3.2 ms) | |
| P _{cu} (kW) | 713-1375 | 713 |
| P _{beam} (kW) | 241 (67.5 mA) | 200 (58 mA) |
| Vane Voltage (kV) | 80~120 | 118 (max.) |
| Max. E field (Kilpatrick) | 1.9 | |
| Power Coupler | 2 | |
| Coupling factor (beta) | 1.337-1.175 | 1.321 |
| Phisync (deg) | -43.4 | -43 |
| Q ₀ | 4055-7821 | 7436 |
| W _{in} (MeV) | 0.075 | |
| W _{out} (MeV) | 3.62 | 3.60 |
| 3 dB bandwidth (kHz) | \pm 52.4 | \pm 55.0 |
| Cooling skid stability at full duty cycle | \pm 0.1 @30° (Vane) | \pm 0.04@28.81° (Vane) |
| (deg.) | \pm 0.1 @30° (Body) | \pm 0.06@28.80° (Body) |

RF AND CAVITY INTERACTION

Transient Thermal Effect

The RFQ experiences a transient thermal effect that induces significant frequency shift when RF power is on or off. The RF power does not heat up directly the whole RFQ body and vane, instead it affects first only 3.5 μ m thick skin of RFQ body and vane. The transient temperature rise, especially over vane surface, can be very high when RF is on. In the case of RF off due to interlock trips, it leads to significant frequency due strong RFQ frequency sensitivity to temperature. A frequency jump up to 50 kHz over seconds was observed during conditioning when RF is suddenly triggered off from full power at full duty cycle. This value is also consistent with thermal simulation of RFQ and its cooling system [2]. To deal with the issue of frequency jump, a dedicated RF ramp up procedure using RF frequency tracking method has been developed, which adjusts RF frequency to track cavity resonance, instead of adjusting cavity resonance to track RF frequency. In this way,

MICROSCOPY INVESTIGATION ON DIFFERENT MATERIALS AFTER PULSED HIGH FIELD CONDITIONING AND LOW ENERGY H⁻ IRRADIATION

C. Serafim^{†1,2}, S. Calatroni¹, F. Djurabekova², A. T. Perez Fontenla¹, R. Peacock¹, W. Wuensch¹,
S. Sgobba¹, A. Grudiev¹, A. Lombardi¹, E. Sargsyan¹, S. Ramberger¹, G. Bellodi¹

¹CERN Organisation Européenne pour la Recherche Nucléaire, Geneva, Switzerland

²University of Helsinki, Helsinki, Finland

Abstract

During operation the RFQ (Radio-Frequency-Quadrupole) of the LINAC4 at CERN is exposed to high electric fields which can lead to vacuum breakdown. It is also subject to beam loss that can cause surface modification, including blistering, which can result in reduced electric field handling and an increased breakdown rate. An experimental study has been made to identify materials with high electric field capability and robustness to low-energy irradiation. In this paper we briefly discuss the selection criteria, and we analyse these materials investigating their metallurgical properties using advanced microscopic techniques such as Scanning Electron Microscope, Electron Back Scattered Diffraction, Energy-dispersive X-ray Spectroscopy and conventional optical microscopy. These allow to observe and characterize the different materials on a micro and a nanoscale and to compare results before and after irradiation and breakdown testing.

INTRODUCTION

Surface modifications of materials due to the blistering phenomenon caused by the hydrogen retention it is a known problem [1]. Blistering is dependent on many factors, such as the radiation dose (minimum dose required for appearance of blisters), the ion energy, the temperature of the target and angle of incidence [2], as well as the metallurgical properties of the material. In the case of the RFQ the energy of the incident H⁻ beam at its entrance, where most beam losses are localised, is 45 keV. This corresponds to a range of approximately 250 nm in copper, with the H possibly accumulating under the surface and leading to blistering.

Two pairs of anode-cathode electrodes (see below) of different materials were manufactured for the purpose of the studies. For the study of the blistering phenomena, and the material properties at its origin, a test stand that replicates the low energy beam transport in the LINAC4 tunnel at CERN was used. In this test stand, specific hardware was developed to use a cathode as the target for irradiation and allows for a rapid turn-over for various irradiation runs. For the study of the breakdown phenomena, we have used the Large Electrode system (LES) in which we tested the electrodes that were manufactured to be compatible with the

chamber geometry. Detailed information about this system can be found in [3].

For a better understanding if any blistering phenomena caused by the beam irradiation could have a consequent effect in triggering breakdowns, we have irradiated first the materials on the LINAC 4 test stand and then tested them on the LES. For comparison, a pair of non-irradiated electrodes was also tested in the system. All electrodes underwent systematic metallurgical analyses, as detailed in this paper.

METODOLOGY

A list of candidate materials was carefully selected for manufacturing of a future RFQ with better performance. In this paper we will focus on the results for three different materials, Oxygen Free Electronic Grade Copper (Cu OFE, UNS C10100), Niobium (Nb) purity of 99.9%, RRR300, and a Titanium grade 5 alloy (TiAl6V4), premium grade forged in α - β range with a final α -microstructure.

The materials were selected based on their usability for meter-long high gradient RF cavities and their potential resistance to blistering and breakdown phenomena. Nb and Ti grade 5 were chosen for their high hydrogen diffusivity, which should prevent accumulation of hydrogen and thus blistering. Ti grade 5 should also provide comparatively easier machinability. The machining of the electrodes was performed with high precision tooling. After machining electrodes have been submitted to metrology testing to assure that all the requirements are within the stipulated ranges. After this, electrodes have been submitted to a cleaning process and a brazing cycle, for the case of Cu, of 100 °/h up to 795 °C for 6 hours and 100 °/h up to 835 °C for 45 minutes.

Irradiation was performed at CERN for different materials using a low energy H⁻ beam at 45 keV. Each irradiation had a duration of approximately 40 hours, with a pulse duration of 600 μ s, a repetition rate of 0.83 Hz and a peak current of 20 mA, which resulted in a deposition of 1.2×10^{19} H^p/cm² on the target, corresponding to about ten days of beam losses during RFQ operation.

The LES testing was performed in electrodes after being exposed to irradiation and in electrodes that were not exposed to irradiation. This allows us to compare if the irradiation had a significant impact on the performance of each material in reaching a maximum and stable field. Detailed information for the results of the high electric field testing, on the studied electrodes, can be found in [4].

[†] catarina.serafim@cern.ch

RF MEASUREMENTS AND TUNING OF THE CERN 750 MHz ELISA-RFQ FOR PUBLIC EXHIBITION

M. Marchi,^{*,1} H. W. Pommerenke,[†] A. Grudiev, S. Mathot, CERN, Geneva, Switzerland
¹also at La Sapienza University of Rome, Italy

Abstract

Over the last few years, CERN has successfully designed, built, and commissioned the smallest RFQ to date, the one meter long PIXE-RFQ operating at 750 MHz. Its compactness offers a unique opportunity for education and public presentation of the accelerator community: A duplicate machine called ELISA-RFQ (Experimental Linac for Surface Analysis) will be exhibited in the Science Gateway, CERN's upcoming scientific education and outreach center. It will allow the public to approach within a few centimeters a live proton beam injected into air, which is visible to the naked eye. The construction of the ELISA-RFQ has been completed in 2022. In this paper, we present the results of low-power RF measurements as well as field and frequency tuning.

INTRODUCTION

The 750 MHz ELISA-RFQ, constructed at CERN, is a compact 1-meter long four-vane RFQ, an identical copy of the previous project PIXE-RFQ [1–4]. The small stand-alone RFQ will accelerate protons to 2 MeV and will be exhibited in the CERN's scientific education and outreach center, Science Gateway. There the audience will observe a live proton beam in air, visible to the naked eye. The RFQ key parameters are listed in Table 1.

The RFQ is subject to manufacturing imperfections and misalignments which lead to variations of the capacitance and inductance distribution. Therefore, the ideal quadrupole field of the TE₂₁₀ operating mode is perturbed [5], and tuning of field and frequency is required. For ELISA-RFQ, the tuning algorithm developed for the HF-RFQ [6] based on Ref. [5] and improved for PIXE-RFQ [4] has been used.

SINGLE MODULE MEASUREMENTS

The ELISA-RFQ consists of two mechanical modules, brazed individually and then clamped together to form the full assembly. For each construction step, the vane positions were measured with respect to the ideal beam axis. The displacements after the final brazing step were within $\pm 10 \mu\text{m}$ for the first module and $\pm 17 \mu\text{m}$ for the second module.

Bead-pull measurements were performed on both the single modules to assess manufacturing quality. Very close agreement was observed by comparing measured resonance frequency and field profile to the simulation (eigenmode solver of CST Microwave Studio® 2020 [7]), thus no special measures were needed. Figs. 1a and 1b report the spectra

Table 1: Key Parameters of the ELISA-RFQ

| Species | Proton | (H ⁺) |
|-------------------------------------------|----------|-------------------|
| Input energy | 20 | keV |
| Output energy | 2 | MeV |
| RF frequency | 749.480 | MHz |
| Inter-vane voltage | 35 | kV |
| RFQ length | 1072.938 | mm |
| Vane tip transverse radius | 1.439 | mm |
| Mid-cell aperture | 1.439 | mm |
| Minimum aperture | 0.706 | mm |
| Final synchronous phase | -15 | deg |
| Output beam diameter | 0.5 | mm |
| Beam transmission | 30 | % |
| Unloaded quality factor (Q ₀) | 6000 | |
| Peak RF power loss | 65 | kW |

of the two modules. Each was measured by placing two aluminum extension tubes at the upstream and downstream ends to have boundary conditions that can be reproduced in a 3D eigenmode simulation. For the quadrupole mode the observed deviations between the measured and simulated frequencies amount to 700 kHz for module 1 and less than 100 kHz for module 2. Fig. 2 shows the field components profiles of the single modules, where the dipole components show small deviations from the ideal zero simulation value ($\pm 3\%$), whereas the quadrupole component has a deviation of less than $\pm 1\%$ for both modules.

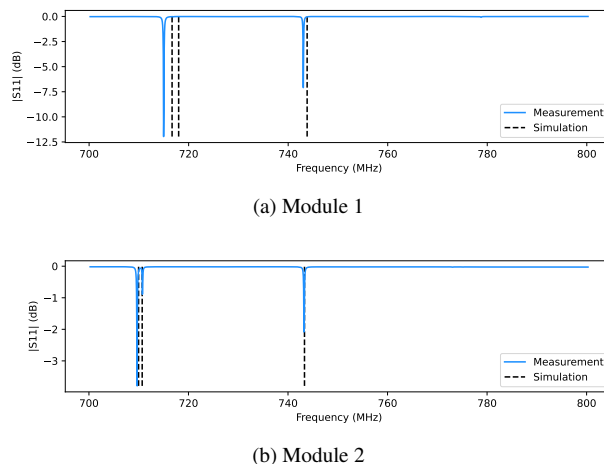


Figure 1: Measured reflection coefficient vs frequency for the single modules.

* mariangela.marchi@cern.ch

† hermann.winrich.pommerenke@cern.ch

BEAM DYNAMICS AND RF DESIGN STUDIES FOR A PROPOSED NEW RFQ FOR CERN LINAC4

H. W. Pommerenke*, G. Bellodi, A. Grudiev, S. Kumar, A. Lombardi, CERN, Geneva, Switzerland

Abstract

The 352 MHz Linac4-RFQ is the first rf accelerating structure of the CERN accelerator complex, accelerating an H-beam to 3 MeV. After successful commissioning in 2013, superficial vane damage has been observed in 2020. In view that the RFQ is a single point of failure, in parallel to the production of a near identical spare (RFQ2), design studies on a longer-term upgrade have been launched: Linac4-RFQ3. Main goals are to achieve a design with higher beam acceptance, reduced beam losses, and reduced rf breakdown rate. Several versions of RFQ are under study: conventional RFQs built by brazing copper, as well as an RFQ with titanium vane tips (brazed on copper). High-gradient experiments suggest that titanium vane tips support higher surface fields compared to copper, up to 40 MV/m, and are more resistant against beam irradiation. In this paper, we present beam dynamics and rf design of various RFQ3 designs.

INTRODUCTION

Linac4-RFQ1, currently installed in the tunnel, was designed when the source development was not yet completed and an emittance of 0.25π mm mrad (rms normalized) was used as input design parameter. A safety factor was built into the design fixing the RFQ acceptance to about 0.35π mm mrad for a current of 70 mA. Whereas such value was eventually achieved for source beam peak currents up to 40 mA, any larger current was extracted with an emittance that exceeded the RFQ acceptance: For a peak current of 70 mA an emittance of 0.5π mm mrad, has been measured at the Linac4 source test stand (Fig. 1).

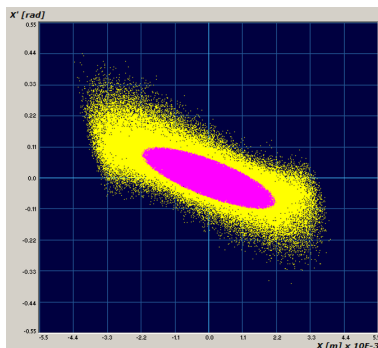


Figure 1: Measured beam out of Linac4 source (yellow) vs. RFQ1 acceptance (pink). The expected transmission (TOUTATIS [1]) is only 75 %.

To overcome this bottleneck, a study was launched to design an RFQ better targeted to the source performance and yet maintaining several of the successful design choices of

* hermann.winrich.pommerenke@cern.ch

the original RFQ: full compatibility with Linac4 in terms of input and output energy and final longitudinal emittance, a two-term potential vane profile, a constant average aperture radius and a constant transverse radius of curvature for easier tuning (constant capacitance) and the possibility of machining with a 2D cutter.

DESIGN GUIDELINES

The main redesign effort has been to balance the phase ramp with the increased input transverse emittance and optimize the trade-off between the transverse acceptance and the final longitudinal emittance. The result of this optimization has been either a longer RFQ or a higher surface electric field on the vane tips. The main RFQ parameters for three different solutions are reported in Table 1. All solutions present a transmission higher than 90 % for a beam current of 70 mA in an emittance of 0.5π mm mrad. Figure 2 compares the beam transmissions of RFQ1 with the proposed designs as function of input beam emittance. It is noted that the acceptance for a 60 mA beam from the source is doubled with respect to RFQ1: A current of 60 mA needs to fit in an emittance of 0.4π mm mrad for RFQ1, but in just 0.8π mm mrad for RFQ3 to give 48 mA out of the RFQ.

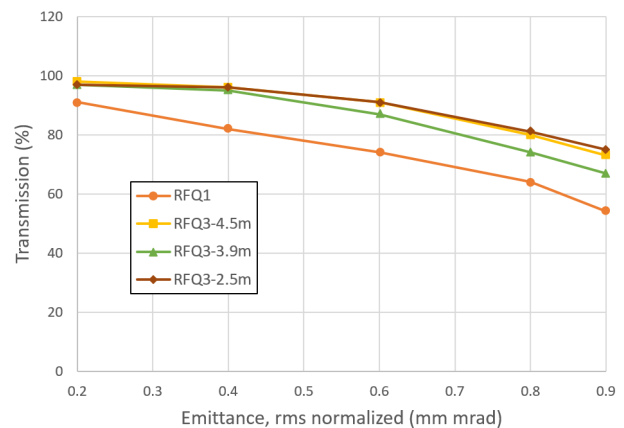


Figure 2: Performance comparison: Transmission vs. emittance for fixed beam current of 60 mA for RFQ1 and considered RFQ3 designs.

Like most RFQs, Linac4-RFQ1 has been designed with the Kilpatrick criterion [2] as ultimate surface electric field limit. In 1961, Maitland [3] pointed out the "gap scaling" relation

$$E_{\text{norm}} = \frac{V}{V_{\text{DC}}} \left(\frac{d_{\text{DC}}}{d} \right)^\alpha, \quad (1)$$

for dc electrodes separated by distance d subject to pulsed dc voltage V . This has been recently confirmed through dc sparking tests at CERN, where empirically $V_{\text{DC}} = 7.75$ kV,

Content from this work may be used under the terms of the CC BY 4.0 licence (© 2021). Any distribution of this work must maintain attribution to the author(s), title of the work, publisher, and DOI

COMPACT PROTON ACCELERATOR IN UHF BAND AT KAHVELab*

S. Esen[†], A. Adiguzel, O. Kocer, Istanbul University, Turkey

A. Caglar, Yildiz Tech. University, Turkey

E. Celebi, S. Oz, V. E. Ozcan, Bogazici University, Turkey

A. Karatay, F. Yaman, O. H. Yilmaz, Izmir Institute of Technology, Turkey

U. Kaya, Istinye University, Turkey

A. Kilicgedik, Marmara University, Turkey

G. Turemen, Turkish Energy, Nuclear and Mineral Research Agency, Turkey

N. G. Unel, UCI, Irvine, California, USA

Abstract

Proton Test Beam at KAHVELab (Kandilli Detector, Accelerator and Instrumentation Laboratory) project aims to design and produce a radio frequency quadrupole (RFQ) operating at 800 MHz in Istanbul, Turkey using the local resources. The beamline consists of a proton source, a low energy beam transport (LEBT) line including the beam diagnostic section and the RFQ cavity itself. This RFQ is 4-vane, 1-meter-long cavity to accelerate the 20 keV beam extracted from plasma ion source to 2 MeV. Its engineering prototype is already produced and subjected to mechanical, low power RF and vacuum tests. In this study, the results of the first test production, especially the bead-pull test setup will be discussed.

GENERAL DESIGN

PTAK (Proton Testbeam At KAHVELab) RFQ design process aimed to achieve a state of the art accelerator with the local production capability. Design goals as chosen to achieve a 30% acceleration of a 1 mA proton beam to roughly 2 MeV using less than 60 kW pulsed RF power at 800 MHz. In process we iterated our initial cavity design and decided on a new intervane voltage value all to achieve a better power usage. With the intervane voltage set to 33 kV and the cavity geometry designed, we were left with a challenge of designing the vane-tip geometry out of the standard process. We decided to replace shaper and gentle buncher sections with a much shorter design. Then we set the acceleration section modulation and the synchronous phase. Also we kept both intervane voltage and the R_0 constant throughout the accelerator. In the end only two values for the replacement section needed to be determined along its length; modulation and the synchronous phase. We wrote a script that randomly tests different values of modulation and phase with PARMTEQM. Batches of these simulation results were tabulated and bounds of values adjusted. The minimum longitudinal radius of curvature for the vane tip value also important machinability of the parts and promising designs were evaluated accordingly. After few iterations of limits we found the design and manually tweaked the

values a bit more to achieve the final design which is shown in Figure 1 [1, 2]. The parameters are shown in Table 1.

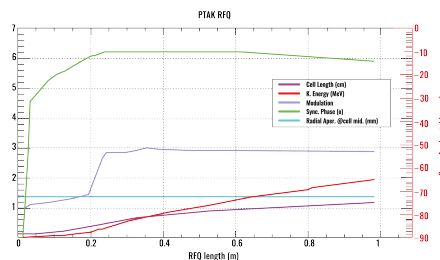


Figure 1: General design parameters of PTAK.

Table 1: Design Parameters

| Parameters | PTAK-RFQ |
|--------------------------|-------------------|
| RF Frequency | 800 MHz |
| Length | 980 mm |
| Input Energy | 20 keV |
| Output Energy | 2 MeV |
| Vane Voltage | 33 kV |
| Minimum Aperture | 0.64 mm |
| Maximum Aperture | 3.0 mm |
| Vane Tip Radius ρ | 1.4 mm |
| Transmission | 30 % |
| Acceptance (Total Norm.) | 0.16 π mmmrad |
| RF Peak Power | 48.5 kW |

PROTOTYPE PRODUCTION

The production of the trial RFQ module, whose vanes were designed using Parmteq programs, was manufactured in DORA MAKİNA company in Ankara, Turkey. Manufacturing error of the prototype is below 20 micron. Parameters of prototype in Table 2 and the picture of it can be seen in Figure 2 [3].

Table 2: The Prototype Measurement Results

| Parameters | Prototype RFQ |
|---------------------|---------------|
| Frequency | 799.6 MHz |
| Max. Assembly Error | ± 18 um |

* Work supported by TUBITAK Project No: 118E838

[†] yavuzzseyma@gmail.com

RF MEASUREMENTS AND TUNING OF THE TEST MODULE OF 800 MHz RADIO-FREQUENCY QUADRUPOLE

A. Kilicgedik†, Marmara University, Istanbul, Turkey

A. Adiguzel, S. Esen, Istanbul University, Istanbul, Turkey

B. Baran, Ankara University, Ankara, Turkey

A. Caglar, Yildiz Technical University (YTU), Istanbul, Turkey

E. Celebi, V. E. Ozcan, Bogazici University, Istanbul, Turkey

U. Kaya, Istinye University, Istanbul, Turkey

G. Turemen, Turkish Energy, Nuclear and Mineral Research Agency (TENMAK-NUKEN), Ankara, Turkey

N. G. Unel, University of California Irvine (UCI), California, USA

F. Yaman, Izmir Institute of Technology (IZTECH), Izmir, Turkey

Abstract

The 800 MHz RFQ (radio-frequency quadrupole), developed and built at KAHVELab (Kandilli Detector, Accelerator and Instrumentation Laboratory) at Bogazici University in Istanbul, Turkey, has been designed to provide protons that have an energy of 2 MeV within only 1 m length. The RFQ consists of two modules and the test module of RFQ was constructed. The algorithm developed by CERN, based on the measurements generated by the tuner settings estimated through the response matrix [1, 2, 3], has been optimized for a single module and 16 tuners. The desired field consistent with the simulation was obtained by bead-pull measurements. In this study, we present low-power rf measurements and field tuning of the test module.

INTRODUCTION

At KAHVELab, there is an ongoing effort to make the proton beamline operational. It will attain 2 MeV exit energy using the world's smallest Radio Frequency Quadrupole (RFQ, see Table 1 for a quick comparison), which is an important accelerator structure [4, 5, 6, 7, 8] (Fig. 1).

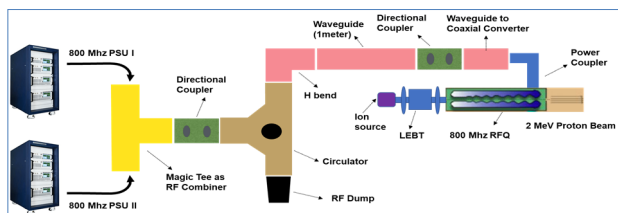


Figure 1: Layout of 800 MHz rf system and proton accelerator at KAHVELab.

The RFQ consists of four vanes, which are connected to each other without any soldering. It is designed to be reassembled with screws, a 3-D O-ring and RF guards. Thanks to the portable and easy installation nature of the RFQ, it will be easy to do material analysis using PIXE technique

on the objects of historical value that are difficult to transport from museums.

Table 1: Comparison of PTAK at KAHVELab with similar RFQs

| Parameter | Symbol | HF | PIXE | PTAK |
|--------------------|-----------|------|------|------|
| Input E (keV) | W_{in} | 40 | 20 | 20 |
| Output E (MeV) | W_{out} | 5 | 2 | 2 |
| RF (MHz) | f_0 | 750 | 800 | 800 |
| Number of Modules | - | 4 | 2 | 2 |
| RFQ length (mm) | - | 1964 | 1073 | 980 |
| Quality Factor | Q_0 | 6440 | 5995 | 7036 |
| RF Power Loss (kW) | P_0 | 350 | 64.5 | 48.5 |

THE TEST MODULE OF RFQ

General Layout

The test module of 800 MHz RFQ was manufactured from ordinary copper to reduce production costs. Naturally, the final 2 MeV RFQ will be built from OFE-Cu (Oxygen-free electric copper) material.

The bead-pull measurements [2, 6, 8] were performed to ensure of the manufacturing quality and to tune the EM field in the cavity. The construction errors are compensated with a total of 16 tuners with micrometer precision, four in each quadrant of the test module (Fig. 2).

The tuners are numbered as T_1 - T_{16} starting at quadrant-1 and moving in a helical orbit. Two extra tuners on the vertical plane where the pick-up antennas are located are on the module to be used if needed. The two ports with the aforementioned extra tuners are included in the design as vacuum ports.

* Work supported by The Scientific and Technological Research Council of Turkey (TUBITAK)

† atacanfz@gmail.com

PULSED DC HIGH FIELD MEASUREMENTS OF IRRADIATED AND NON-IRRADIATED ELECTRODES OF DIFFERENT MATERIALS

R. Peacock^{†1,2}, W. Wuensch¹, G. Burt², S. Calatroni¹, A T. Perez Fontenla¹, C. Palma Serafim¹,
 A. Grudiev¹, S. Ramberger¹, A. Lombardi¹, S. Sgobba¹, G. Bellodi¹, E. Sargsyan¹

¹CERN, Organisation Européenne pour la Recherche Nucléaire, Geneva, Switzerland

²Lancaster University, Lancaster, United Kingdom

Abstract

Beam loss occurs in Radio Frequency Quadrupoles (RFQ), and has been observed in the H⁻ linear accelerator Linac4 (L4) at CERN. To determine if beam loss can induce breakdowns, and to compare the robustness of different materials, tests have been done using pulsed high-voltage DC systems. Electrical breakdown phenomena and conditioning processes have been studied using these systems. Cathodes of different materials were irradiated with 1.2×10^{19} H⁻ p/cm², the estimated beam loss of the L4 RFQ over 10 days. The irradiated electrodes were installed in a system to observe if the irradiated area coincided with the breakdown locations, with pulsing parameters similar to the RFQ. Tests of irradiated and non-irradiated electrodes of the same material were done for comparison. The main difference observed was an increase in the number of breakdowns during the initial conditioning that returned to non-irradiated sample values with further running. Visual observations after irradiation show the beam centre and a halo the same diameter of the beam pipe. Breakdown clusters occur in the centre and halo regions, suggesting irradiation is not the only factor determining the breakdown probability.

BACKGROUND

The first stage of acceleration for the Large Hadron Collider (LHC) is L4 [1]. H⁻ ions are generated by the RF ciated source and pass through the Low-Energy Beam Transport (LEBT) to the Radio Frequency Quadrupole (RFQ) [2]. An endoscopy of the L4 RFQ showed signs of vane surface damage and breakdowns [2]. It was postulated that the damage was due to H⁻ losses irradiating the Copper OFE (Cu-OFE), creating blisters causing RF breakdowns.

To gain more knowledge of the effects of irradiation on field holding, tests were carried out using a pre-existing DC setup. For this, electrodes were irradiated at the H⁻ source test stand, as seen in Fig. 1 [3], with the same dose as the RFQ, estimated to be 1.2×10^{19} H⁻ p/cm² [4].

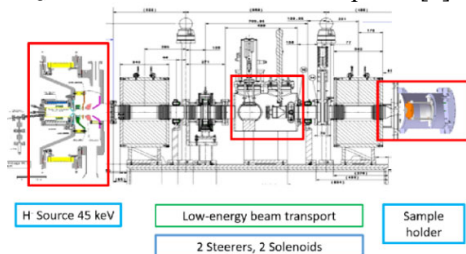


Figure 1: Irradiation setup for DC system electrodes [3].

[†] ruth.peacock@cern.ch

LARGE ELECTRODE SYSTEM

The pulsed DC Large Electrode System (LES) seen in Fig. 2, consists of 2 high precision machined electrodes placed in parallel between 20 μm and 100 μm apart in vacuum to which pulses of voltage up to 10 kV, pulse lengths between 1 μs and 1 ms, and repetition rates up to 6 kHz can be applied [5]. This system is used for the study of conditioning and vacuum breakdown phenomena. The instrumentation has the ability to detect breakdowns using voltage, current, pressure, and light and give the location of each breakdown during operation [6].

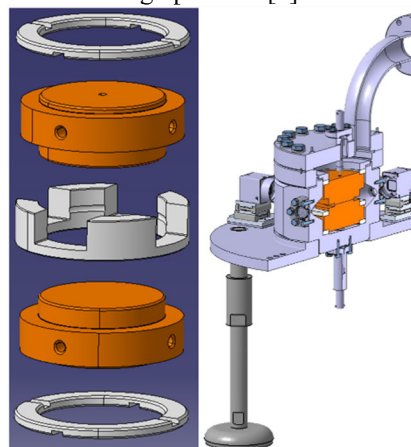


Figure 2: Exploded view of the electrode sandwich and cross section of the system.

Tests were made of different materials including Cu-OFE and CuCr1Zr, due to being the materials of the L4 and the now decommissioned L2 RFQs respectively [7]. TiAl6V4, Ta, and Nb were chosen due to their increased resistance to blistering as this was believed to be the main cause of breakdowns in the RFQ. Due to limited space, all materials except CuCr1Zr are described in this report and all results are included in the summary plots.

Two pairs of each material were tested of which one pair included an irradiated cathode. Irradiation produced visually distinct areas including the beam central area, a halo shaped by the beam pipe outlet (40 mm, 30 mm or half circle 30 mm diameter) and areas with no change, a detailed example of the areas is given in reference [8]. For these tests a small anode (40 mm or 30 mm diameter) to large cathode (60 mm or 40 mm diameter) configuration was used to avoid field enhancements on the cathode, leaving a 40 mm or 30 mm radius high-field area, depending on the electrode design used.

To replicate conditions occurring in the RFQ as closely as possible whilst keeping testing time to a minimum, a

MULTIPACTOR STUDIES: SIMULATIONS AND MEASUREMENTS ON THE RF COAXIAL RESONATOR TEST BENCH*

Y. Gómez Martínez[†], J. Angot, M. Baylac, T. Cabanel, M. Meyer

Univ. Grenoble Alpes, CNRS, Grenoble INP, LPSC-IN2P3, Grenoble, France

D. Longuevergne, G. Sattonnay, Université Paris-Saclay, CNRS/IN2P3, IJCLab, Paris, France

Abstract

Multipactor is an undesired phenomenon triggered by electromagnetic fields in accelerator components and more specifically in RF structures, such as accelerating cavities and power couplers, and may lead to Electron Cloud build up in beam tubes.

The accelerator group at LPSC has developed an experimental setup dedicated to multipactor studies. It consists in a coaxial resonator, tunable and operational between 100 MHz and 1 GHz. It allows to characterize under real conditions the efficiency of surface treatment mitigation processes (coatings, cleaning procedures) at room temperature.

This paper presents the experimental measurements performed with this setup confronted to simulations.

INTRODUCTION

Multipacting (MP) occurs under vacuum when an electron is accelerated by the electromagnetic field and hits the device's wall. Depending on the secondary electron yield of the surface, more than one electron can be emitted and, if accelerated by the electromagnetic field, a self-sustained electron avalanche can be created.

We define:

- The 1-point multipactor: The impacts sites are localised very close on the same surface. The time between two impacts is an integer number of a RF period (T_0). This integer number is called order of the 1-point multipactor.
- The 2-point multipactor: The impacts sites are localised on two distinct surfaces. The time between two impacts ($T_{2\text{-point}}$) is an odd number of a half RF period. The order of the 2-point multipacting (n) is given by the Eq. (1):

$$T_{2\text{-point}} = \frac{2n-1}{2} T_0 \quad (1)$$

The LPSC's experimental setup, based on a coaxial (1"5/8 EIA) copper resonator, can be used in a travelling wave configuration when the measurement vessel is loaded with 50 Ω . It can also be used as a cavity in a standing wave mode (Fig. 1). This configuration benefits from a voltage amplification (represented by a K factor) allowing measurements of multipacting barriers at higher field amplitude than injected. This allows the measurement of multipacting barriers at higher frequencies using the same RF amplifiers of 500 W.

* Work supported by IN2P3 (CNRS).

[†] gomez@lpsc.in2p3.fr.

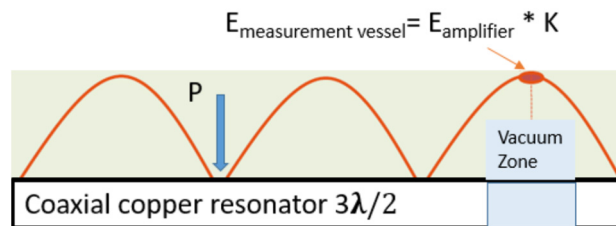


Figure 1: Schematic view of the electric fields in the measurement vessel as a cavity.

This paper presents the results of the multipacting simulations with the SPARK3D software, including MP barriers as well as the type of MP, and compares them to measurements on the experimental setup.

SPARK3D SIMULATIONS

SPARK3D (@Dassault Systemes) [1] is part of a commercial electromagnetics (EM) package. The main output of SPARK3D is the curve of the electron number (called in SPARK3D electron evolution) analysed in time for each RF power. For a given field level, if the electron number increases, multipacting occurs. For the same duration, the higher the electron number, the stronger the multipactor. At a given frequency, the simulation was stopped when the electron number reaches 10^{15} .

We define the electron growth rate (EGR) as the slope of the electron number curve (Eq. (2)). Two points (e_1/t_1 and e_2/t_2) have been chosen once the electron number curve become a straight line, (e_2/t_2) corresponds when the simulation stops.

$$\text{Electron growth rate} = \frac{e_2 - e_1}{t_2 - t_1} \quad (2)$$

The electron re-emission is given by the Secondary Emission Yield (SEY) as a function of the impact energy.

The SEY data used in the simulations in the Vaughan model is shown in Table 1. It corresponds to a clean surface where SEY_{max} , SEY_0 , E_1 and E_{max} is defined as shown in Fig. 2.

Table 1: SEY of the Copper, Al_2O_3 and TiN Coating

| Parameter | Copper | Al_2O_3 | TiN |
|-----------------------|--------|-----------|------|
| SEY_{max} | 2,3 | 5,78 | 1,75 |
| SEY_0 | 0,5 | 1 | 0,5 |
| E_1 (eV) | 35 | 24 | 35 |
| E_{max} (eV) | 165 | 950 | 250 |

COMPLETE STUDY OF THE MULTIPACTOR PHENOMENON FOR THE MYRRHA 80 kW CW RF COUPLERS*

Y. Gómez Martínez[†], P.O. Dumont, M. Meyer

Univ. Grenoble Alpes, CNRS, Grenoble INP, LPSC-IN2P3, 38000 Grenoble, France

P. Duchesne, C. Joly, W. Kaabi, Université Paris-Saclay, CNRS/IN2P3, IJCLab, Paris, France

Abstract

MYRRHA (Multi Purpose Hybrid Reactor for High Tech Applications) is an Accelerator Driven System (ADS) project. Its superconducting linac will provide a 600 MeV - 4 mA proton beam. The first project phase based on a 100 MeV linac is launched. The Radio-Frequency (RF) couplers have been designed to handle 80 kW CW (Continuous Wave) at 352.2 MHz. This paper describes the multipacting studies on couplers.

INTRODUCTION

Multipacting is an undesired phenomenon of resonant electron build up encountered in electromagnetic field regions under vacuum. It appears when an electron is accelerated by the electric field and hits the enclosure's wall. Depending on the secondary electron yield of the wall, more than one electron can be emitted and accelerated by the electric field, creating a self-sustained electron avalanche. The coupler aims to transfer energy from the RF source to the accelerating cavities of the linac. It also provides a vacuum and a thermal barrier between air and the superconducting cavity while preserving its cleanliness.

As part of an ADS ('Accelerator Driven System'), the MYRRHA (Multi Purpose Hybrid Reactor for High Tech Applications) [1] coupler is laid out for the highest achievable reliability. To improve the reliability, the coupler is studied and tested up to 80 kW CW, well above its nominal power (8 kW CW), to allow the fault-tolerance schema [2]. The study includes a complete calculation of the multipactor phenomenon. MUSICC3D [3] and SPARK 3D codes have been chosen for the simulations.

COUPLER DESIGN OVERVIEW

The power coupler [4] is made (Fig. 1) of an inner conductor (antenna) and an outer conductor (cuff) brazed on a high purity alumina ceramic window. The antenna has a radius 13.1 mm (R_{ant}) and the outer conductor, fixed by the cavity, is 28 mm. The coupler allows some mechanical flexibility to compensate differential thermal expansions and mechanical misalignments thanks to bellows. The antenna having a water cooling, a double input tee has been designed. This tee has a flange on one side to transport the RF power, and on the other side, a special short stub, to support cooling pipes all the way up through the antenna. The length of this short stub (L_{ss}) was studied to eliminate the mismatch created by the bellows, which was a length of 270 mm.

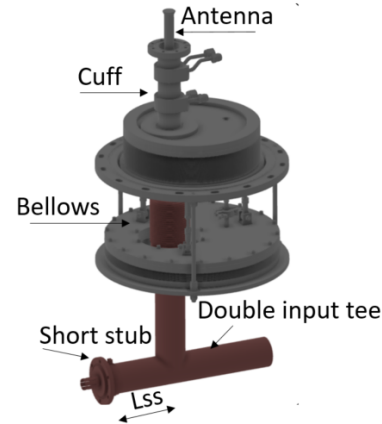


Figure 1: Main elements of the power coupler.

MUSICC3D CALCULATIONS

MUSICC3D (@IJCLab/ IN2P3/France) uses a model of one virtual particle, where the output 'charge number' represents the product of SEYs (Secondary Electrons Yields) occurring at each interaction with the wall. It is considered that there is a multipacting barrier at a given field level, if the charge number increases at this field gradient.

The particle emission is based in the secondary emission Yield in function of the impact energy (SEY curves)

First simulations were made with MUSICC3D around the window because it is the most fragile and important region to prevent of multipactor. If window breaks the accelerator is no longer under vacuum.

The worst case was simulated, with no TiN anti-multipactor coating on the Al₂O₃. The Secondary Electron Yield (SEY) curves used are shown in Fig. 2.

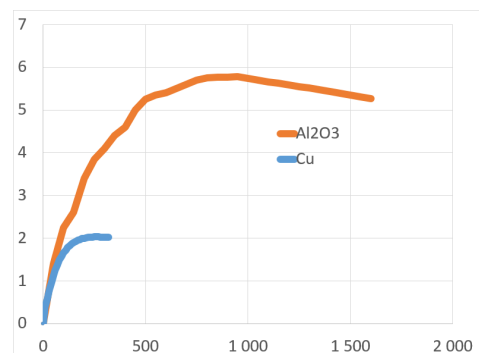


Figure 2: Al₂O₃ SEY curve (in red) and cu SEY curve (in blue).

* Work supported by SCK•CEN and IN2P3 (CNRS)

[†] gomez@lpsc.in2p3.fr.

SOLVING THE USB COMMUNICATION PROBLEM OF THE HIGH-VOLTAGE MODULATOR CONTROL SYSTEM IN THE EUROPEAN XFEL

M. Bousonville*, S. Choroba, S. Göller, T. Grevsmühl, A. Hauberg, T. Weinhausen
Deutsches Elektronen-Synchrotron, Hamburg, Germany

Abstract

Since the commissioning of the modulators in the European XFEL in 2016, it happened from time to time that the modulator control system hung up. The reason for the problem was unknown at that time. Initially, the MTBF (Mean Time Between Failure) was 104 days, which was so rare that other problems with the RF system clearly dominated and were addressed first. Over the next 2 years, the error became more frequent and occurred on average every 18 days. After the winter shutdown of the XFEL in 2020, the problem became absolutely dominant, with an MTBF of 2 days. Therefore, the fault was investigated with top priority and was finally identified. Two units of the control electronics communicate via USB 2.0 with the main server. Using special measurement technology, it was possible to prove that weak signal levels in the USB signal led to bit errors and thus to the crash of the control electronics. This article describes the troubleshooting process, how to measure the signal quality of USB signals and how the problem was solved in the end.

INTRODUCTION

The European XFEL is equipped with 26 RF stations [1]. One RF station can generate up to 10 MW of RF power with a pulse width of 1.7 ms and a repetition rate of 10 Hz.

The stations are operated with 0.7 to 6.5 MW. The failure of an RF station leads to a reduction in the electron beam energy of 600 to 700 MeV, which stops the generation of the X-ray pulses in the undulator sections. The failure of one station therefore interrupts operation of the free-electron laser as a whole.

Each RF station consists of a multibeam klystron, high-voltage pulse modulator and pulse transformer, RF waveguide power distribution and several other subsystems. While a number of childhood diseases were eliminated after the commissioning of the European XFEL in 2016 [2], a fault that occurred from time to time in the high-voltage modulators played only a minor role. The modulators generate the high-voltage pulses for the klystrons with an amplitude of 6.3 to 9.2 kV, which are transformed upwards by a factor of 12 by a pulse transformer. So, 75 to 110 kV are available for the klystron operation. The initially unknown error led to the failure of a modulator, which could be fixed by a manual power cycle of the control system. When the error occurred, the GUI of the control system displayed a red spider, which is why this error was internally called the red spider. This error message is always displayed when the communication between the two electronic boards and the server controlling the modulator is disturbed (Fig. 1).



Figure 1: High voltage modulator, GUI and control system.

* michael.bousonville@desy.de

TEST AND COMMISSIONING OF THE HELIAC POWER COUPLER

J. List^{1,2,4*}, K. Aulenbacher^{1,2,4}, W. Barth^{1,2,4}, M. Basten²,
 C. Burandt², T. Conrad³, F. Dziuba^{1,2,4}, V. Gettmann^{1,2}, T. Kürzeder^{1,2}, S. Lauber^{1,2,4},
 M. Miski-Oglu^{1,2}, M. Schwarz³, H. Podlech³, S. Yaramyshev²

¹ Helmholtzinstitut Mainz (HIM), Mainz, Germany

² GSI Helmholtzzentrum (GSI), Darmstadt, Germany

³ Goethe-Universität-Frankfurt (GUF), Frankfurt am Main, Germany

⁴ Johannes Gutenberg-Universität Mainz, Mainz, Germany

Abstract

The superconducting continuous wave (cw) heavy ion HELMholtz LInear ACcelerator (HELIAC) is intended to be built at GSI in Darmstadt. With its high average beam current and repetition rate the HELIAC is designed to fulfill the requirements of the super heavy element (SHE) research user program and the material sciences community at GSI. The accelerating cavities are of the superconducting Crossbar H-mode (CH) type, developed by GUF. Within the Advanced Demonstrator project, the first cryomodule, consisting of four cavities is scheduled for commissioning with beam in 2023. The former RF power couplers introduced a high heat input into the cryostat. Therefore, the coupler is re-designed at HIM in order to not only reduce the heat input but to provide an overall improved power coupler for the HELIAC. It is designed for a maximum power of 5 kW cw at the frequency of 216.816 MHz. A prototype has been tested and commissioned recently. This includes several RF-tests at room temperature and in cryogenic environments. The results of these tests will be presented in this paper.

INTRODUCTION

The superconducting HELIAC (Fig. 1) is foreseen to serve as the main accelerator for SHE research [1] and material sciences at GSI while the UNIVersal LinAC (UNILAC) is upgraded as injector for the Facility for Antiproton and Ion Research (FAIR) [2]. HELIAC consists of a normal conducting injector [3, 4] and a superconducting linac [5] comprising twelve CH-cavities [6, 7]. After completion of the Demonstrator project, and first successful operation of a CH cavity [8] with heavy ion beam [9], the linac is currently in an advanced R&D-phase, called the Advanced Demonstrator project [10]. For this purpose, the first complete cryomodule consisting of three CH cavities, a CH-buncher [11, 12] and two superconducting solenoids is going to be prepared for a beam test.

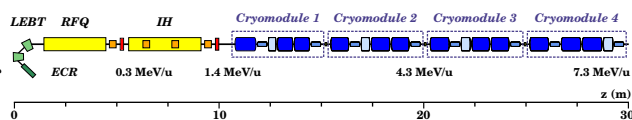


Figure 1: Layout of the HELIAC with its normal conducting 1.4 MeV/u injector and the superconducting part, comprising four cryomodules with three CH-cavities (beam energies up to 7.3 MeV/u).

* j.list@gsi.de

HELIAC POWER COUPLER

In order to overcome serious operational problems, the original design approach of the power-couplers [13] has been further improved and thus a new advanced design could be developed [14]. The revised coupler can be disassembled modularly into individual components, to allow easy cleaning and assembly; potentially the replacement of individual components is possible in case of malfunction. As the previous coupler, the current design (see Fig. 2) is based on a coaxial, capacitive 3 1/8"-RF-line (2, 4) and comprises two ceramic windows (1). The diameter of the line is tapered (3)

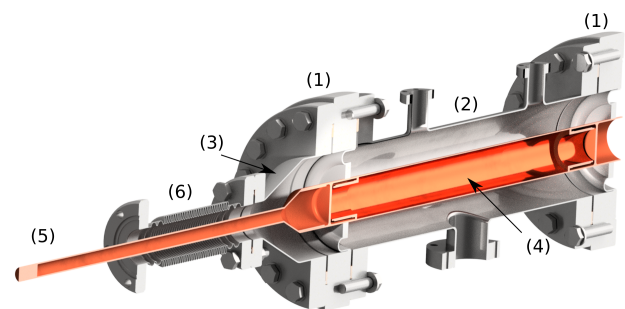


Figure 2: Cross section of the recent power coupler design for the HELIAC.

to fit the cut-off tube of the resonators in the cold section. In order to allow variable coupling, the coupler is equipped with a bellow (6) which has a total stroke of 30 mm. With 28 corrugations and a wall thickness of only 0.15 mm the bellow also ensures a minimal static heat load into the cavity.

Figure 3 depicts the RF window flange (1), where an U-shaped spring connects a CF100-flange with an Al₂O₃-disk-window. This spring is made of Invar42, a nickel-iron alloy

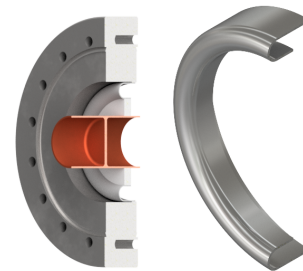


Figure 3: Cross-section of coupler window flange (left) and U-shaped spring (right).

with the same coefficient of thermal expansion as Al₂O₃ and thus minimizes the probability of damage caused by thermal

DESIGN OF AN X-BAND BUNCHING AND ACCELERATING SYSTEM FOR THE AWAKE RUN 2

J. M. Arnesano[†], S. Doebert, CERN, Geneva, Switzerland

Abstract

In Run2 AWAKE aims to demonstrate beam quality and increase the accelerating gradient in the plasma even further and in order to be able to serve high-energy physics experiments. In this framework, a new electron injector, consisting of an S-band RF-gun and a subsequent X-band bunching and accelerating sections, able to produce very short bunches with a small emittance, has been designed. In this paper, two different configurations of the X-band section and their corresponding high power distribution systems are presented. The first one consists of three identical travelling wave cavities to bunch and accelerate the beam while the second one uses a separate short structure for velocity bunching followed by three long pure accelerating structures. A discussion of the strengths and weaknesses of each configuration is carried out; the X-band power distribution systems are described with particular attention to the choice of the high-power klystron, the pulse compression system and the waveguide distribution.

INTRODUCTION

In 2018, RUN 1 of the AWAKE experiment at CERN achieved all its milestones, demonstrating for the first time, the acceleration of electrons to GeV energies using proton-driven plasma wakefields [1]. In 2021 the AWAKE Run 2 started, aiming to demonstrate acceleration of high-quality electron beams appropriate for future high-energy physics experiments. Preservation of beam quality, emittance and low energy spread, is the main goal of the Run 2. Therefore, it is necessary to use two plasma cells, one for seeding the microbunching and one for pure acceleration and a new electron injector to inject high quality electron bunches into the second plasma cell.

The new injector has to produce an energy of about 150 MeV, a small emittance and very short bunches to be able to reach the “blow out regime” during acceleration. The bunch length has to be a fraction of the plasma wavelength to keep the energy spread low. In addition, the injector has to be very compact due to the severe space constraints in the existing tunnel.

In this framework, a novel injection scheme has been proposed, consisting of an S-band Rf-gun followed by X-band structures used for velocity bunching and acceleration to ~200 fs and 150 MeV, respectively.

This paper is focused on the new AWAKE injector’s baseline and its RF power distribution system for Run 2c. More details about the experimental program and its phases are described at this conference [2]. The main parameters of the new electron source are listed in table 1. Its installation is scheduled in 2027 in the AWAKE experimental area while a reduced prototype of the injector, called ARTI

[†]jordan.arnesano@cern.ch

(AWAKE Run 2 test injector), is being developed in collaboration with CLEAR. In the following sections, the injection baseline is explained in detail, an analysis of the X-Band power compression system is performed and an estimation of the power required for each system is compared.

Table 1: Injector parameters

| Parameter | Value |
|--------------------------|---------|
| Energy [MeV] | 150 |
| Charge [pC] | 100 |
| Spread [%] | 0.2 |
| Bunch length [fs] | 200-300 |
| Nor. Emittance [mm mrad] | 2 |

INJECTOR BASELINE

Initially, two different configurations for the X-band injection system have been considered and are shown in Fig. 1. The first configuration consists of three identical cavities of ~0.9 m; the first one is used for bunching and the other two for pure acceleration. The second configuration includes a small cavity of 30 cm for bunching and three cavities of ~0.9 m for pure acceleration. In both cases, a S-band 1.5 cell photoinjector is used as electron source. To prevent emittance growth, the buncher has been placed in the so-called “Ferrario’s working point” and a solenoid is placed right after the GUN and around the first two cavities [3].

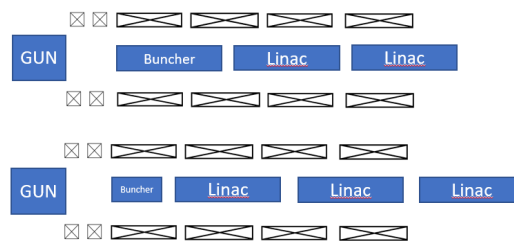


Figure 1: On top the first configuration with 3 identical cavities, on the bottom the second with the small buncher.

When considering the RF power system, which layouts are shown in Fig. 2, each configuration presents strengths and weaknesses. The main advantage of the first layout over the second, is the use of a single klystron. In the second layout an additional “small” klystron is required to feed the buncher. The first choice leads to economic savings and increased simplicity however presents a major disadvantage, i.e., there is a risk of a high breakdown rate due to the energy requirement of 150 MeV which forces the two acceleration cavities to work with a high gradient of 80 MV/m in a magnetic solenoid field. In the second case the gradient of each cavity is only 53 MV/m, significantly reducing the risk of RF breakdowns [4]. For this reason and the lower peak power requirements, the second setup has been

DESIGN, MANUFACTURING, ASSEMBLY, TESTING, AND LESSONS LEARNED OF THE PROTOTYPE 650 MHz COUPLERS *

J. Helsper[†], S. Chandrasekaran, N. Solyak, S. Kazakov, K. Premo, G. Wu, F. Furuta, J. Ozelis, B. Hanna, FNAL, Batavia, IL 60510, USA

Abstract

Six 650 MHz high-power couplers will be integrated into the prototype High Beta 650 MHz (HB650) cryomodule for the PIP-II project at Fermilab. The design of the coupler is described, including design optimizations from the previous generation. This paper then describes the coupler life-cycle, including manufacturing, assembly, testing, conditioning, and the lessons learned at each stage.

INTRODUCTION

The prototype High Beta 650 MHz (pHB650) couplers will provide radio frequency (RF) input to the superconducting accelerating cavities housed within the pHB650 cryomodule (CM) [1], which is part of the PIP-II Project [2]. Six pHB650 couplers are used in the pHB650 CM string. Eight pHB650 couplers with three additional vacuum sides were procured. These pHB650 couplers are predated by ‘proof of concept’ 650 couplers, which validated the overall design and testing regime [3].

DESIGN

The critical design components of the pHB650 coupler design are shown in Fig.1.

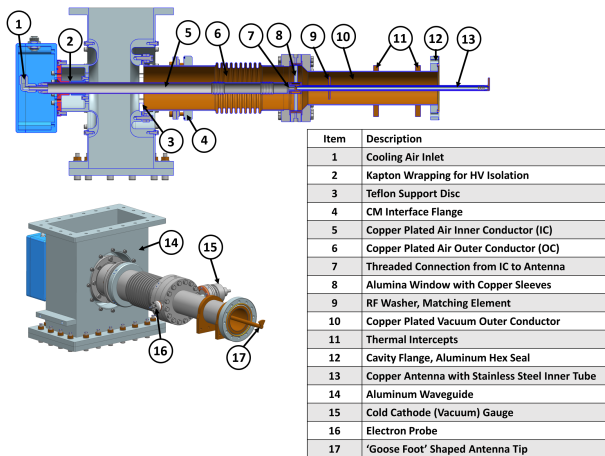


Figure 1: The full pHB650 coupler assembly.

Brazed copper sleeves connect the window (Item 8) to its surrounding components, allowing for thermal expansion without undue stress. The stainless steel (SS) tube within the antenna provides an air cooling path and the stiffness

necessary for transportation and handling. Ti-N coating was not applied to the Alumina window as a high voltage (HV) bias of 5 kV suppresses multipacting. The antenna tip (Item 17) has a non-symmetric ‘goose foot’ shape which allows for modulation of cavity Qext. The antenna assembly (Item 8+13), cold outer conductor (OC) (Item 10), air inner conductor (IC) (Item 5), and air OC (Item 6) were all designed to be vacuum furnace brazed.

Changes from Previous Design

The two proof of concept coupler designs [3, 4] are shown in Fig.2. Design A used solid copper electromagnetic shielding, while design B used copper plating over the SS outer conductor.

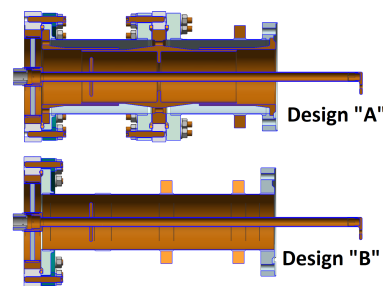


Figure 2: Section view, proof of concept couplers.

Design B was chosen as the basis for the pHB60 couplers as it was less complex, easier to assemble, and better for UHV cleaning. Several features of Design B were changed for the pHB650 coupler, which included a larger waveguide, a different electron probe location, inclusion of a vacuum gauge, increased OC wall thickness, a fully brazed SS tube within the antenna (previously removable design left the antenna easily deformed), and thru hole mounting on thermal straps instead of threaded inserts.

Analysis

The RF and Thermal analyses performed for the pHB650 coupler [5] are similar in methods and results to those for the proof of concept couplers [4, 6], which show the couplers meet all necessary requirements. Previous structural analysis verified the thermal stress of the ceramic window sleeves [5], and recent analysis verified the coupler will have acceptable resonant frequencies and stress levels during shipment of the CM [7].

MANUFACTURING

The manufacturing life cycle shown above in Fig. 3 was driven by Fermilab’s technical and procurement specifica-

* Work supported, in part, by the U.S. Department of Energy, Office of Science, Office of High Energy Physics, under U.S. DOE Contract No. DE-AC02-07CH11359.

[†] jhelsper@fnal.gov

CONCEPTUAL ANALYSIS OF A COMPACT HIGH EFFICIENCY KLYSTRON

J. P. Edelen, S. D. Webb, RadiaSoft LLC, CO, USA
K. Nichols, LANL, Los Alamos, NM, USA

Abstract

Traditional klystron efficiencies are limited by the output electron beam harmonic current and energy spread. Increasing the amount of harmonic current produced in the klystron requires increasing the velocity bunching in the input cavity. Additional cavities may be used to improve the bunching, however they do so at additional cost and space requirements for the klystron. Moreover, at higher currents space charge counteracts this velocity bunching reducing the amount of harmonic current that can be produced. Our concept resolves these challenges by employing a new type of high-efficiency, multi-beam klystron. Our design consists of a single two-frequency input cavity, a wiggler, and an output cavity. The two-frequency input cavity approximates a linear function in time thereby increasing the harmonic content of the beam, while the wiggler provides strong longitudinal focusing to mitigate the effects of space charge. In this paper we provide the theoretical foundation for our design and present initial numerical calculations showing improved bunching from the harmonic mode and the wiggler.

INTRODUCTION

In a klystron the efficiency is determined by how much DC current can be converted into current at the fundamental frequency of the output cavity (harmonic current). The effectiveness of this bunching is usually limited by nonlinear velocity bunching and space-charge forces [1, 2]. Two common methods for improving klystron efficiency are the core oscillation method (COM) and the Bunch-Align-Compress (BAC) methods [3–5]. The COM method uses gain cavities spaced at the bunch oscillation length in order to allow the anti-bunching particles to smoothly merge into the central bunch. This has been shown in simulation to achieve efficiencies of up to 90%. There is a significant space cost however in that these klystrons tend to be between 50% and 100% larger than their more traditional counterparts. The BAC method has recently been a popular alternative to the COM method due to its more compact design, [6, 7]. Here cavities are strung together in triplets in order to more efficiently focus the beam longitudinally. These designs have shown an improvement in efficiency on the same scale as the COM designs however only a 10% to 20% increase in size compared to traditional klystrons. In both of these cases however the klystron design requires a number of bunching cavities and they tend to be large compared to other sources such as magnetrons.

Our paper explores a novel klystron circuit that enables a compact, high efficiency, source to be produced at low cost. We utilize two-frequency bunching combined with

wiggler focusing to increase the harmonic current output while simultaneously decreasing the overall footprint.

THEORETICAL PRINCIPLES

High-efficiency RF amplifiers, such as klystrons, require harmonic current amplitudes I_1 about equal to the average input current I_0 . The efficiency of a klystron is roughly proportional to $I_1/2$, therefore a tube with 100% harmonic current is approximately 50% efficient. To reach 80% efficiency, a harmonic current of about 160% is required. Starting with small-signal modulation of the electron beam from an input cavity, a klystron uses a series of gain cavities and large-signal cavities to increase the beam's harmonic current. These cavities are all powered parasitically by the beam. An output cavity at the location of peak harmonic current is phased to decelerate the bunch and, produces the klystron's output power. Ballistic bunching in a two cavity klystron can be described analytically by propagating a velocity modulated beam over some finite distance.

The velocity of a particle that exits the two frequency input cavity as a function of time can be described in the zero current limit by Eq. (1),

$$v_{\text{exit}} = v_0 (1 + X \sin(\omega t_0) + Y \sin(2\omega t_0)). \quad (1)$$

Here $X = TV_{\text{gap}}^f e / (mc^2 \gamma^3 \beta^2)$ and $Y = TV_{\text{gap}}^h e / (mc^2 \gamma^3 \beta^2)$. The time of flight from the cavity to some position z can be approximated by $t - t_0 = z/v_0(1 - X \sin(\omega t_0) - Y \sin(2\omega t_0))$. Note that here we have both the fundamental, ω , and the second harmonic, 2ω , affecting the beam velocity modulation. We can then calculate the harmonic current at z by decomposing the beam into Fourier harmonics,

$$I(t) = I_0 + \sum_{n=1}^{\infty} a_n \cos(n(\omega t - \theta)) + b_n \sin(n(\omega t - \theta)). \quad (2)$$

Here a_n and b_n are the Fourier coefficients and θ represents a phase shift characterized by the bulk propagation time of the beam $\omega z/v_0$. The magnitude of the a_1 term gives a first approximation of how efficient the klystron will be. When solving for the Fourier coefficients it is useful to define the instantaneous current as $I(t) = I_0 dt_0/dt$, which transforms the integrals of a_n and b_n to be over t_0 . Then using a change of variables, we can compute the a_n terms by solving Eq. (3),

$$a_n = \frac{I_0}{\pi} \int_{-\pi}^{\pi} \cos(n(\phi - X \sin(\phi) - Y \sin(2\phi))) d\phi. \quad (3)$$

DESIGN ENHANCEMENTS FOR THE SNS RFQ COAXIAL COUPLER*

G. Toby[†], C. Barbier, S. Lee, A. Narayan, J. Moss, Y. Kang
Oak Ridge National Laboratory, Oak Ridge, USA

Abstract

The H⁻ ion linear accelerator at the Spallation Neutron Source (SNS) at Oak Ridge National Laboratory operates with reliability that routinely surpasses 90% during scheduled beam operation. With the ambitious goal of eventually achieving at least 95% availability, several upgrade and improvement projects are ongoing. One such project is the modification of the coaxial couplers that transfer radio frequency (RF) power to the accelerator's Radio Frequency Quadrupole (RFQ). The proposed modification utilizes stub sections and capacitive coupling to construct a physically separable assembly with DC isolation. With a separated coupler assembly, the section that includes the magnetic coupling loop can be permanently mounted to the RFQ which would eliminate the need to re-adjust the couplers after maintenance activities, upgrades, and repairs. Additionally, the modified design would provide increased multipaction suppression with DC biasing and potentially lower thermal gradients across the device. This paper presents the design and simulation results of the project.

INTRODUCTION

Beam acceleration at the SNS starts with the front-end systems where an ion source, an RFQ and two beam transport sections are utilized. The 65 keV beam from the ion source is focused, bunched, and accelerated to 2.5 MeV in the RFQ [1]. The 402.5 MHz RFQ is powered by two coaxial couplers that deposit up to 700 kW peak power in 60 Hz, 1 msec pulses. Each coupler is conditioned up to 400 kW, but nominally run at 300 kW during baseline operation [2, 3].

While not a source of significant downtime, the goal of achieving 95% availability during scheduled beam operation necessitated a coupler improvement project. The design of the current RFQ couplers requires each unit to be manually adjusted after repairs and maintenance activities to achieve the proper RF coupling for beam loading. Given the non-autonomous nature of this task, significant time, energy, and several iterations are often needed. Figure 1 shows the current coupler design with a permanent connection that forms a loop antenna between the inner and outer conductors.

RF Systems and Mechanical Engineering personnel at SNS explored several modification ideas with the goal to improve the electrical and mechanical performance of the couplers while reducing accelerator downtime. Of several potential solutions determined, three were selected as candidates for the next phase.

* ORNL is managed by UT-Battelle, LLC, under contract DE-AC05-00OR22725 for the U.S. Department of Energy. This research was supported by the DOE Office of Science, Basic Energy Science, Scientific User Facilities

[†] tobygd@ornl.gov

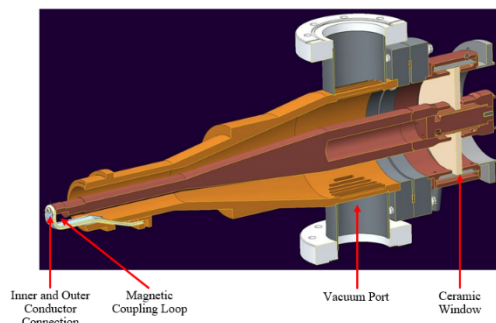


Figure 1: Cross sectional view of the current coupler.

RF DESIGN

The first target of the improvement project was a design capable of maintaining fixed coupling with the RFQ. The coaxial coupler needed to be separated into two subsections, one containing the ceramic, vacuum window and the other incorporating the coupling loop. This change would make maintenance activities and some repairs, including vacuum window replacements, possible without the need to remove the entire coupler assembly. This separation, however, would require rigid support for the inner conductor with no RF disruption. The need intuitively derived utilizing transmission line short-circuited stub sections and capacitive coupling to achieve that goal. Quarter-wave transmission line sections optimized to transform RF short circuits to open circuits at the center conductor were employed. This approach was selected based on impedance matching, mechanical rigidity and heat sinking. Three types of short-circuited, quarter-wave transmission line sections capable of meeting the requirements were considered. Of the three types shown in Fig. 2, option 1 was selected for simplicity and proof of concept.

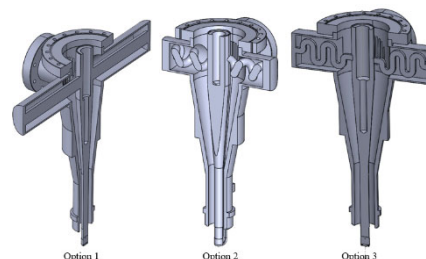


Figure 2: Quarter-wave short-circuited stub design concepts.

DEVELOPMENT AND TESTING OF HIGH POWER CW 1497 MHz MAGNETRON

M. Popovic¹, T. Blassick², M.A. Cummings¹, A. Dudas¹, R. P. Johnson¹, K. Jordan³, R. Lentz¹,
M. Neubauer¹, R. Rimmer³, H. Wang³, J. Wessel², T. Wynn¹

¹Muons, Inc., Batavia, IL, USA

²Richardson Electronics Ltd., LaFox, IL, USA

³Thomas Jefferson National Accelerator Facility, Newport News, VA, USA

Abstract

We have designed, built, and tested a new magnetron tube that generates RF power at 1497 MHz. In the tests so far, the tube has produced CW 9 kW RF power, where the measured power is limited by the test equipment. The final goal is to use it to power superconducting (SC) cavities.

INTRODUCTION

This tube was designed under DOE NP STTR that Mike Neubauer directed as the PI. The design itself was primarily the work of Alan Dudas working with our advisors from California Tube Laboratory (CTL), Tony Wynn and Ron Lentz. The tube, shown in Fig. 1, was constructed by companies in California, but final repairs, reassembly, and testing were done at Richardson Electronics (RELL) in Illinois.



Figure 1: Tube at RELL ready to be baked.

DESIGN

This tube is like a 75 kW CW 915 MHz tube designed and built by CTL. The water-cooled tube has 10 strapped cavities. Power is extracted using a three-legged antenna that is enclosed in a ceramic dome. The cathode stalk has a

* Work supported by DOE NP STTR DE-SC0013203 and Muons Inc. and Jefferson Lab CRADA JSA 2016S004

† email: popovic@muonsinc.com

2 liter/s ion pump and connectors for high voltage and filament power input. These elements are shown in Figs. 2a and 2b.



Figure 2a: Picture showing 10 cavities, straps, and antenna posts attached to the vanes of the anode body.



Figure 2b: Antenna attached to anode body.

The design process involved special consideration regarding heat distribution and removal. The biggest concern with heat dissipation was related to the cathode stalk. After assembling the filament, the temperature of the helical filament was measured in a Bell jar for several different currents. The conclusion was that 75 amps and around 8 volts will create conditions for large electron emission.

COMMISSIONING OF THE VECC CRYOMODULE

Z. Yao[†], R. Bjarnason, J. Cheung, K. Fong, J. Keir, D. Kishi, S. Kiy, P. Kolb, D. Lang, R.E. Laxdal, B. Matheson, R.S. Sekhon, B.S. Waraich, Q. Zheng, V. Zvyagintsev, TRIUMF, Vancouver, Canada

Abstract

A quarter-wave resonator (QWR) cryomodule was designed and assembled at TRIUMF for the energy upgrade of the VECC ISOL-RIB facility to boost radioactive isotopes from 1 MeV/u to 2 MeV/u. The top loading cryomodule was chosen based on the ISAC-II low energy section design, consisting of four superconducting QWRs and one superconducting solenoid. The major change from the ISAC-II concept is separating the RF space vacuum from the isolation vacuum. The cryogenic commissioning was recently completed. The cold mass alignments and the cryogenic heat loads were measured. The cavity performance was qualified in both test regime and operating regime. The cavity degradations caused by magnetic pollution from solenoid and the recovery procedure were verified. This paper will report the detailed results of the commissioning.

INTRODUCTION

The radioactive ion beam (RIB) facility at the Variable Energy Cyclotron Centre (VECC) at Kolkata in India uses the isotope separation on-line (ISOL) technique to produce rare isotopes. The post-accelerators consist of a radio frequency quadrupole (RFQ) that accelerates heavy ions with a mass-to-charge ratio of $A/q \leq 14$ to 100 keV/u, and five IH-type linear accelerator (linac) tanks for further acceleration to 1 MeV/u [1]. The energy upgrade of the VECC RIB facility will add two superconducting (SC) heavy ion quarter-wave resonator (QWR) cryomodules (CM) downstream of the IH tank 5 to boost the isotopes with $A/q \leq 7$ to 2 MeV/u. TRIUMF has been in collaboration with VECC to develop the QWR CM.

DESIGN

The VECC CM is a top loading CM based on the ISAC-II low energy section design. The major change from the ISAC-II concept is separating the RF space vacuum from the isolation space. The CM consists of four SC QWRs and one 7 T SC solenoid. The cavity frequency is specified at 113.61 MHz and the cavity geometry β is selected at 5.5% for maximizing the transit time factor (TTF) in the energy range from 1 MeV/u to 2 MeV/u. The general cavity geometry is the same as ISAC-II low β cavity, including a coaxial structure with a diameter ratio of 1/3 and a flat short plate that has been demonstrated to eliminate high level multipacting (MP) barriers (~ 1 MV/m) in ISAC-II [2]. The beam aperture region has been redesigned to accommodate the specified geometry β and to minimize the peak surface field ratio. The iris shape is the axisymmetric nose cone to simplify the manufacture. The vertical steering effect in QWR is to be corrected by aligning the cavity aperture axis

below the beam axis by 0.76 mm at 4 K. The resonant frequency is tuned by adjusting the cavity length on the coaxial axis. The distance from the tip of the inner conductor to the tuner plate on the bottom is optimized to achieve the frequency tuning sensitivity at 2.5 kHz/mm. The optimized RF parameters include $E_{\text{peak}}/E_{\text{acc}} = 4.7$, $B_{\text{peak}}/E_{\text{acc}} = 8.7$ mT/(MV/m), $R/Q = 490 \Omega$ and the geometry factor at 21Ω . The cavity is specified to operate at 6.6 MV/m and to provide 1 MV effective voltage with < 10 W RF loss. The cavity is made with RRR > 250 niobium, while the helium jacket is made with reactor grade niobium to avoid differential thermal contraction and to act as a Meissner shield at 4 K against the fringe magnetic field from the solenoid. The cavity is mounted on the strong-back and connected to the helium space via the thick stainless-steel top flange that also supports the mechanical damper in the inner conductor to mitigate the microphonics.

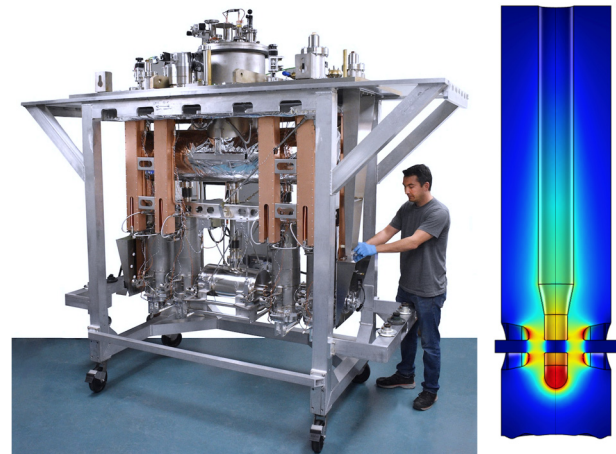


Figure 1: VECC QWR CM in the dirty assembly area (left), and the QWR geometry with the electric field distribution (right).

A few design changes have been developed to accommodate the separated vacuum. Niobium-titanium alloy (NbTi) flanges are added to the beam pipes and the RF ports and are sealed with diamond shaped aluminium gaskets. A set of hermetic variable loop RF coupler and RF pickup has been developed. The cavity bottom assembly is also redesigned. A 1 mm niobium tuning plate is attached the cavity bottom flange as ISAC-II QWR to close the RF volume. A thick stainless-steel flange is sealed with indium to the cavity bottom flange separately to provide the hermetic seal. The tuning plate connects to the tuner lever via the bellow assembly in a small space. The cavity beam port and the tank wall are connected with a warm-cold transition (WCT) with the double-layer bellows and an 80 K intercept with the liquid nitrogen (LN2) shield. The multi-layer insulation (MLI) is wrapped on the liquid helium (LHe) reservoir above the strong back, and on both interior

[†] zyyao@triumf.ca

THREE YEARS OF OPERATION OF THE SPIRAL2 LINAC: CRYOGENICS AND SUPERCONDUCTING RF FEEDBACK

P.-E. Bernaudin[†], M. Aburas, M. Di Giacomo, A. Ghribi, P. Robillard, L. Valentin,
GANIL, Caen, France

Abstract

The superconducting LINAC of SPIRAL2 at the GANIL facility is in operation since October 2019. Its 26 superconducting quarter wave resonating cavities (88 MHz) are operated at a nominal gradient of 6.5 MV/m, but most of the cavities can be operated up to 8 MV/m. They are integrated into 19 cryomodules and cooled down at 4 K by a dedicated refrigeration cryogenic system.

In this paper, we will present a feedback after five years of operation of the cryogenic system, focusing on the main problems that have been faced, and on the diverse evolutions performed in order to improve the cryogenic system and to increase its reliability. We will also provide a feedback of the superconducting cavities performances status after three years of operation.

THE CRYOGENIC SYSTEM

Cryogenic System Overview

The SPIRAL2 cryogenic system is based on a HELIAL LT Air Liquide cold box. Fed by two Kaeser screw compressors, this cold box supplies 4 K liquid helium (1.3 kW) and 60 to 70 K helium gas to cool down cavities and thermal screens respectively.

The cryogenic distribution is composed of a 9 m long vertical line, linking the ground floor located cryoplant to the LINAC tunnel, and by 19 cryogenic valves boxes, connected one to the next to form the horizontal cryolines. Five valves per valves box supplies the cryogenic fluids to each cryomodule (2 valves for the thermal screen circuit, 2 valves for the liquid helium one, and 1 valve for the cryomodule cool down). Various non insulated, auxiliary lines are available for conditioning, warm gas collection, etc. For more details about the SPIRAL2 cryogenics system please refer to Ref. [1].

LINAC Cool Down

From 2017 up to today, the LINAC has been cooled down and warmed up once a year. Each cool down lasts three full weeks, plus a fourth week dedicated to thermalization of cryomodules and various controls and tuning operation. Hence the accelerator's cryogenics is in nominal configuration four weeks after the beginning of cool down.

As the niobium cavities have not been baked against the 100 K effect, the LINAC cool down is performed in a way that minimizes the time spent by each cavity in the 50-150 K temperature window. The temperatures of all the cavities are slowly decreased to 150 K, to allow homogeneous cool down of the cold mass, and once the 150 K

threshold is reached, the process is accelerated as fast as possible. The acceleration is applied to only one cryomodule at a time, due to the volumetric flow rate capacity of the compression station and takes one full day per cryomodule. The volumetric flow rate capacity of the compression station limits the number of simultaneous fast cool down to one cryomodule at a time, so these phases shall be properly programmed to avoid any overlap.

Thermo-acoustic Oscillations (TAO)

The cryogenic operation has been hampered by two TAO (Taconis) issues since 2017 [2].

The cryoplant's main dewar (5 000 L) suffered from TAO once connected to the LINAC. This problem was detected early and easily solved using a dedicated buffer volume of a few litres.

More critical was the TAO that appeared on the cryogenic valves boxes. Positioned on the 5 K helium return line, it was detected only thanks to the cavity RF instabilities. A solution was hastily developed: the helium vessels inside the cryomodules were linked to the faulty connection point on the valves boxes using a warm line and a needle valve. This solution allowed RF operation, but it has some drawbacks; thus an alternative, more suitable solution based on a pre-tuned hydraulic RLC circuit, was developed in parallel with operation. After preliminary tests in 2021, it was installed early this year and successfully tested in July 2022.

Other Cryogenic Issues

The main cause of downtime over the last five years of cryogenic operation were linked to utilities. Several air utility failures were suffered, stopping completely the cryoplant. These failures were overcome thanks to upgrades performed on the GANIL air utility system in 2020; the cryogenic team is also working on a backup air supply system, to provide 2-hours autonomy to the cryoplant.

Main electrical power failures cause one cryogenic emergency stop per year. In particular, the cycle compressors are sensitive to voltage drops. Water refrigeration stops also caused several compression station trips.

In such cases, 3-5 hours are necessary to recover the LINAC's operational status from a cryogenic point of view.

During the five years of cryogenic operation, only two failures were caused by the cryogenic system, both in 2021. During the cool down, the cryoplant stopped. This stop was caused by mishandling of cryomodules cool down sequence by the cryogenics operators. During cold box restart, another operator mistake caused one turbine break. Thanks to the availability of spare turbines, the installation was quickly restarted with no impact on beam schedule.

[†] bernaudin@ganil.fr

ADVANCED CRYOGENIC PROCESS CONTROL AND MONITORING FOR THE SPIRAL2 SUPERCONDUCTING LINAC

A. Ghribi^{*1,2}, M. Aburas^{1,3}, P-E. Bernaudin^{1,3}, P. Bonnay^{3,4}, F. Bonne^{3,4},
 A. Corbel^{1,2}, M. Di-Giacomo^{1,3}, F. Millet^{3,4}, A. Ngueguim Tsafak^{3,4}, A. Trudel^{1,3}, Q. Tura^{1,2}

¹Grand Accélérateur National d'Ions Lourds (GANIL), Caen, France

²Centre National de la Recherche Scientifique (CNRS - IN2P3), Caen, France

³Commissariat à l'Énergie Atomique (CEA), Caen, France

⁴Univ. Grenoble Alpes, CEA, IRIG-DSBT, Grenoble, France

Abstract

SPIRAL2 is a superconducting accelerator for protons, deuterons and heavy ions delivering a maximum beam power of 200 kW at 40 MeV (for deuteron beams). 26 superconducting quarter wave cavities are operated at 4.4 K, plunged in a liquid helium bath with a drastic phase separator pressure control. Previous years have seen the development of advanced process control for cryogenics allowing to cope with high heat load dynamics thanks to an automatic heat dissipation compensation and a model based control. The latter is based on models, using the Simcryogenics library, optimized and linearised in the Programmable Logic Controllers. The SPIRAL2 operation has demonstrated that such control allows to keep the specified conditions for RF and beam operation even at levels of heat load dissipation approaching the physical limits of the cryogenic system. These developments allowed to synthesise a virtual observer of the dynamic heat load dissipated by the cavities. The present paper summarises the development of such observer based on the physical thermodynamic model and on machine learning techniques.

INTRODUCTION

SPIRAL2 [1] at GANIL (Grand Accélérateur National d'Ions Lourds) is a state of the art accelerator that aims at delivering some of the highest intensities of rare isotope beams. Its driver should accelerate protons, deuterons and heavy ions at intensities up to 5 mA and a maximum beam power of 200 kW (see Table 1) [2]. The driver is composed of ECR (Electron Cyclotron Resonance) sources, a RFQ (Radio-Frequency Quadrupole) and a superconducting LINAC (LINEar Accelerator). The latter is made of 26 QWR (Quarter Wave Resonating) independently phased superconducting cavities. SPIRAL2 cavities are of two families: low beta ($\beta_0 = 0.07$) and high beta ($\beta_0 = 0.12$) [3]; where β_0 is the relative velocity of the accelerated particles. The low beta cavities are the first 12 cavities of the LINAC. They are made of bulk Niobium for their upper part and copper for the bottom part. Each low beta cavity is housed in a different cryostat and separated by room temperature quadrupole magnets. The cryostats, that we call cryomodules, integrate passive RF, vacuum and other components needed for the operation of the cavities. The last part of the LINAC comprises

Table 1: SPIRAL2 Beam Specifications

| Particles | H ⁺ | ³ He ²⁺ | D ⁺ | ions | [Units] |
|--------------------|----------------|-------------------------------|----------------|------|---------|
| Q/A | 1 | 3/2 | 1/2 | 1/3 | |
| Maximum current | 5 | 5 | 5 | 1 | [mA] |
| Maximum beam power | 165 | 180 | 200 | 45 | [kW] |

7 cryomodules, housing 2 high beta cavities each. These cavities are made of bulk niobium. All cavities are operated at 88.0525 MHz. To be operated, the superconducting cavities are plunged in liquid helium baths with a stringent pressure control to avoid detuning. Every cryomodule has a dedicated satellite valves-box that insures liquid helium distribution and pressure/level regulations. These satellite cryostats form the cryodistribution. The latter can be decomposed in two branches: A left branch made of 12 valves boxes (for all low beta cryomodules) and a right branch made of 7 valves boxes (for all high beta cryomodules). More details on the cryoplant and the cryodistribution can be found in Ref. [4].

The last years have seen the commissioning of the different parts of the accelerators leading to the beam commissioning and the current ramp up to achieve the target requirements [1]. Cryogenics proved more challenging than initially expected [5]. This pushed the developments of advanced model based control bringing immunity to high dynamic heat loads and uneven heat load distributions effects. One of the consequences was the ability to introduce model based virtual observers which opened the way to machine learning based diagnostics. This paper depicts these developments. The first part details the specific challenges of the cryogenics of the SPIRAL2 LINAC and the strategies to overcome them. The second focuses on virtual heat load observers.

CRYOGENIC CONTROL: CONSTRAINTS AND STRATEGIES

The first purpose of the cryogenic system is to cool down the superconducting cavities under their transition temperature and keep them in optimal operating conditions. Apart from the cool down, which poses its own set of challenges due to Q-disease (see Ref. [5]), maintaining optimal operating conditions can be difficult. Superconducting cavities operate around a center frequency f_0 with an admissible bandwidth Δf_0 . Micrometric shape deformations due to sur-

* adnan.ghribi@cnrs.fr

AN APPROACH FOR COMPONENT-LEVEL ANALYSIS OF CRYOGENIC PROCESS IN SUPERCONDUCTING LINAC CRYOMODULES*

C. Lhomme^{†,2}, H. Saugnac, P. Duthil, F. Chatelet, IJClab, Orsay, France
F. Dieudegard, T. Junquera, ACS, Orsay, France
M. D. Grosso Xavier, D. Berkowitz Zamora, SCK•CEN, Mol, Belgium
²also at ACS, Orsay, France

Abstract

Powerful superconducting linear accelerators feature accelerating sections consisting in a series of cryomodules (CM), each hosting superconducting radiofrequency (SRF) cavities cooled by a cryogenic process. Despite the extensive instrumentation used for the tests and validation of the prototype cryomodules, it is usually very complex to link the measured global thermodynamic efficiency to the individual component performance. Previous works showed methods for assessing the global efficiency and even for allocating performances to sets of components, but few went down to a component level. For that purpose, we developed a set of techniques based on customized instrumentation, on dedicated test protocols, and on model-based analysis tools. In practice, we exposed the components to various operating conditions and we compared the measured data to the results from a detailed dynamic component model at the same conditions. This method was applied to the cryogenic debugging phase of the tests of the MINERVA prototype cryomodule, which, despite the liquid helium shortage, led to an extensively detailed characterisation, for its validation towards the serial construction.

INTRODUCTION

One advantage of superconducting cavities over normal conducting ones is the power savings, which are directly linked to the amount of heat captured by the cryogenic process. Thus, precise estimate and break-down of the heat loads of a CM during the prototyping phases are crucial to further optimize its efficiency for the series operation.

Along its path, a cryogenic loop collects heat from different components. In the cryomodule field, heat load measuring method based on the knowledge of the mass flowrate and of the specific enthalpy difference can be as accurate as +/- 5%, with properly calibrated sensors and perfect steady-state conditions. One problem is that the conditions are never steady, as cryogenic operation may feature long transients, spanning over several days. Another problem is that those methods only provide the total heat load received by a given heat sink. Without careful measurements and expensive instrumentation, it is hard to break them down.

What we propose, instead, is to rely on a model-based diagnostic tool associated to a specific comparison method. In the following, we first describe the cryomodule

cryogenic process, then we present our diagnostic tool, and finally we give two use cases of our method.

CRYOMODULE CRYOGENIC PROCESS

In the superconducting accelerating section of most modern linear accelerators, like GANIL or FRIB, a modular architecture based on a series of up to tens of cryomodules, is chosen [1-2].

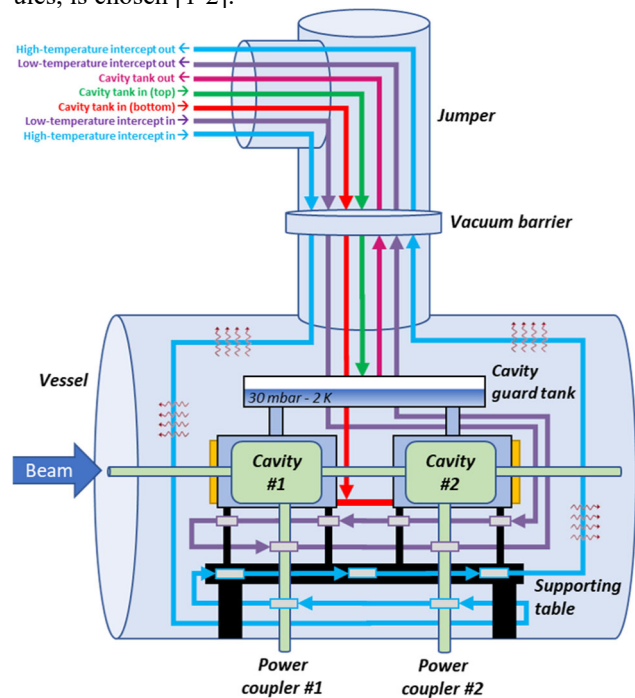


Figure 1: The simplified flow schematics of the MINERVA prototype SPOKE cryomodule.

Over this paper, we consider the MINERVA prototype cryomodule [3-4] – currently being tested at IJClab in Orsay, France – to illustrate our approach.

This cryomodule contains a pair of SRF cavities which are maintained at 2 K by a pool of saturated helium at about 30 mbar. To optimize the global thermal efficiency, two cryogenic lines intercept the incoming heat from the parts in contact with the 2 K tanks:

- A high-temperature line circulating saturated nitrogen at about 80 K (in prototype test mode).
- A low-temperature line circulating saturated helium between 5 and 10 K (in prototype test mode).

All the lines are supplied by a test valve box; the flow schemes and the cryomodule main components are displayed in Fig. 1.

* Work supported by MYRRHA programme at SCK CEN (Belgium)
[†] cedric.lhomme@ijclab.in2p3.fr cedric.lhomme@acsfrance.com

PERFORMANCE TEST OF MASS-PRODUCTION HWR CRYOMODULES FOR SCL32*

Youngkwon Kim[†], Danhye Gil, Hyojae Jang, Hyunik Kim, Yong Woo Jo, Jaehee Shin, Jong Wan Choi, Moo Sang Kim, Min Ki Lee, Jongdae Joo, Hoechun Jung, Myeun Kwon, IBS, Daejeon, Korea
 Younguk Sohn, PAL, Pohang, Korea

Abstract

Mass production of the HWR (half wave resonator) cryomodules for SCL32 of RAON had been conducted since 2018 and all cryomodules were installed in the SCL3 tunnel in 2021. Total number of the HWR cavities and the HWR cryomodules are 106 and 34, respectively. Cryomodule performance test was started in September 2020 and finished in October 2021, except for one bunching cryomodule that will be installed in front of the high energy linac. The detailed procedure and the results of performance test is reported in detail.

INTRODUCTION

The Rare isotope Accelerator Complex for ON-line Experiments (RAON) has been built for providing beam of exotic rare isotope of various energies at the Institute for Basic Science (IBS) [1-2]. The layout of RAON is shown in Figure 1. The low energy superconducting linac (SCL3) of RAON is composed of 22 quarter wave resonator (QWR) cryomodules and 35 half wave resonator (HWR) cryomodules including two bunching HWR cryomodules in a post-accelerator to driver linac (P2DT). The high-energy superconducting linac (SCL2) use two types of single spoke resonator (SSR1 and SSR2). 23 SSR1 cryomodule and 23 SSR2 cryomodule are required for SCL2. Total number of the QWR cavity is 22 and that of the HWR cavity is 106 since 15 HWR cryomodules are holds two cavities in them (HWR CMA) while 19 HWR cryomodules have four cavities in them (HWR CMB). The RF parameters of QWR

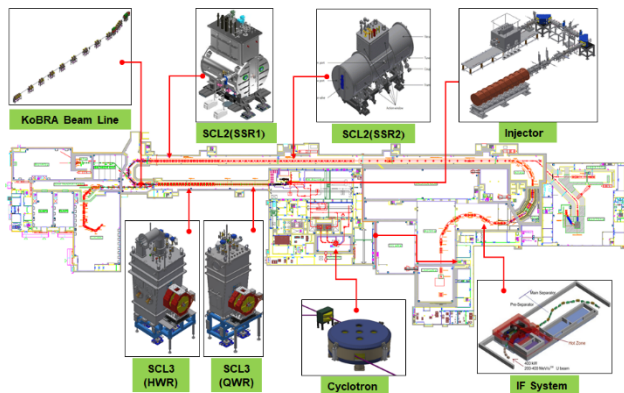


Figure 1: Layout of RAON

Table 1: RF Parameters of QWR and HWR Cavity

| | QWR | HWR |
|-----------------------------------------|-------|-------|
| β_{opt} | 0.047 | 0.12 |
| f [MHz] | 81.25 | 162.5 |
| L_{eff} | 173.5 | 221.5 |
| R/Q [Ω] | 469 | 295 |
| E_p/E_{acc} | 5.7 | 5.2 |
| B_p/E_{acc} [mT/(MV/m) ²] | 10.4 | 9 |
| E_{acc} [MV/m] | 6.1 | 6.6 |
| V_{acc} [MV] | 1.06 | 1.46 |
| QR_s | 18.1 | 36.8 |

and HWR cavities are listed in Table 1. Total number of SSR1 and SSR2 cavities are 69 and 138, respectively. The mass-production of QWR and HWR cryomodules were already finished and the prototyping of the cryomodules for SCL2 section are still on-going.

The mass-production of HWR cryomodules was started in May, 2018. Fabrication of the sub-components such as cavity, coupler, tuner and cryomodule was done by the domestic vendor and the surface treatment of the cavity and the assembly of cryomodule were done in both vendor site and own facility of IBS. The vertical test (VT) and the horizontal test (HT) had been done in two SRF test facilities of IBS. One is off-site test facility that has 2 VT pits, 2 HT bunkers, and 70 L/h helium liquefier and another is on-site test facility that has 3 VT pits, 3 HT bunkers, and 140 L/h helium liquefier. The cavities that had passed the vertical test were assembled in the cryomodules. Performance test of HWR cryomodules was started in September 2020 and finished in November 2021 except for one cryomodule that will be installed at the end of P2DT section. The low energy linac of RAON was installed in the tunnel on December 2021. SCL3 will be cooled down in September 2022 and the first beam injection to SCL3 is planned to be in October 2022[3].

TEST SETUPS AND PROCEDURE

Performance test of cryomodules were conducted in the HT bunkers at both test facilities. Figure 2 shows the test setups in the bunker. Cryogenic fluid such as liquid nitrogen and liquid helium were supplied from the helium liquefier and LN2 tanks, respectively through the flexible insulated transfer lines. Two RF transmission lines were installed in the bunkers and connected with power couplers.

* This work was supported by the Rare Isotope Science Project of Institute for Basic Science funded by Ministry of Science and ICT and NRF of Korea (2013M7A1A1075764)

[†] ykkim78@ibs.re.kr

MAGNETIC FIELD MEASUREMENTS AND SHIELDING AT THE UKRI-STFC DARESBUURY LABORATORY SRF VERTICAL TEST FACILITY

A. E. T. Akintola[†], A. Bainbridge, S. Hitchen, M. Lowe, A. J. May, D. Mason, S. Pattalwar, A. Shabalina, P. A. Smith
UKRI-STFC Daresbury Laboratory, Warrington, United Kingdom

Abstract

A novel vertical test facility has been developed, commissioned, and entered steady-state operations at the UKRI-STFC Daresbury Laboratory. The cryostat is designed to test 3 jacketed superconducting RF cavities in a horizontal configuration in a single cool-down run at 2 K. A 2-year program is currently underway to test ESS high-beta cavities. Upon completion of this program, the facility will undertake a testing program for PIP-II HB650 cavities. In the current configuration, a solution combining passive and active magnetic shielding has been validated for the ESS requirement of field attenuation to the level of $<1 \mu\text{T}$, although continuous field measurements are not provided. This paper reports the implementation of passive and active shielding, along with simulation and experimental measurements thereof.

INTRODUCTION

UKRI-STFC Daresbury Laboratory (DL) houses a Vertical Test Facility (VTF) located in the Superconducting Radio Frequency (SuRF) Laboratory. This facility is used for testing and qualifying the performance of jacketed SRF niobium cavities at 2 K for users before their final installation into cryomodules and subsequent integration into particle accelerators.

For cavity testing, the SuRF lab is equipped with two cavity support inserts (CSIs) which can mount 3 jacketed SuRF cavities each, allowing Daresbury to test three cavities per run. The dressed cavities are loaded into the top, middle and bottom cradle positions as shown in Fig. 1b). The facility is enabled by a closed cycle warm compression Air Liquide Helial ML¹ cryoplant that provides cold helium gas at 50 K for cooling the cryostat's thermal shield and liquid helium at 4 K for cooling the cavities and CSI. The liquid produced is stored in a 3000 L liquid helium dewar. The spent (boil-off) helium is recovered at 300 K, dried, purified, and then stored in a clean gas buffer tank or reliquefied/cooled depending on the state of the cryoplant. Once liquid transfer into the cryostat is complete, a set of 2 K pumps pump the vapour pressure above the helium liquid down to 30 mbar which provides the operating temperature of 2 K where RF testing and qualification of the SRF cavities take place. The dressed cavities are also actively pumped throughout except when being transferred from the CSI stand to the VTF bunker. Further detail is given in Ref. [1].

[†]ayo.akintola@stfc.ac.uk

¹advancedtech.airliquide.com

²magneticshields.co.uk

³3ds.com/products-services/simulia/products/opera/

Currently, the SuRF lab is undertaking cavity testing for the European Spallation Source (ESS) to be built in Lund, Sweden. The ESS cavity testing specification requires that the ambient magnetic field present in the test environment does not exceed $1 \mu\text{T}$. The main sources of field within the lab are the Earth's ambient field, steel rebar in concrete used to provide radiation shielding and, stray field from pumps and other miscellaneous equipment located in the vicinity. In order to meet the magnetic hygiene requirements of the ESS project, the VTF employs both passive magnetic shielding (Mu-Metal²) and active magnetic shielding (tuneable coils). The current system was validated in 2017 to meet the ESS requirement of $<1 \mu\text{T}$ during the VTF's commissioning although it does not have the capability for magnetic field measurements during cavity testing.

EXISTING SHIELDING

The magnetic shielding of the VTF comprises both passive magnetic shielding and active magnetic shielding, in order to meet the magnetic hygiene requirements of $<1 \mu\text{T}$ for the ESS project.

Passive Shielding (Mu-metal Shield)

The VTF's passive shield is a Mu-metal cylinder with an open lid at the top and 3 side ports as shown in Fig. 1a). The open lid allows the CSI to be lowered and removed from the cryostat with ease at the start and end of each test cycle. The cryostat is housed in the Mu-metal shield with the largest access for residual magnetic field being located at the top of the Mu-metal shield where the lid is open.

Active Shielding (Top and Bottom Coils)

The VTF's active magnetic shielding consists of 2 coils, one located just above the lid of the cryostat and the other located on the floor of the cryostat bunker as shown in Fig. 1b). The two coils are made of tri-rated cable with 2.5 mm^2 cross sections. However, the number of turns in the coils are not identical with the top coil being made up of 10 turns and the bottom coil comprised of 20 turns.

MAGNETIC FIELD SIMULATIONS

Simulations of a simplified version of the proposed magnetic shield were performed in OPERA³ using a background field strength and direction set according to a Hall probe survey conducted at the site before installation. The shield was modelled as an open-topped can of height 3.5 m and outer diameter 2.2 m, using the material BH curve for Mu-metal supplied with OPERA (a potential source of er-

DESIGN OF A TRANSPORT SYSTEM FOR THE PIP-II HB650 CRYOMODULE

M. Kane, T. Jones, E. Jordan, Science and Technology Facilities Council, Daresbury, UK
 J.P. Holzbauer, Fermi National Accelerator Laboratory, Batavia, IL, USA

Abstract

The PIP-II Project at FNAL requires the assembly of 3 high-beta 650MHz cryomodules at STFC Daresbury (DL) in the UK. These modules must be safely transported from DL to FNAL in the USA. Previous experience with cryomodule transport was leveraged at both labs to design a transport system to protect the cryomodules during transit. Requirements for the system included mitigation of shocks, drops, and vibrations, and acting as a lifting fixture. It is comprised of a tessellated steel frame which encompasses the module with a wire rope isolator arrangement which the module mounts to. The frame was designed to withstand the weight of the 12.5 tonne cryomodule in various load cases. Details of shock and vibration profiles were obtained from MIL-STD-810H and were used to guide the sizing of passive isolators. The frame and the isolation system were analysed via FEA using the shock and vibration profiles as an input. The transport system was found to be suitable for the given isolation, frame stiffness, and lifting code requirements. The frame has been fabricated and successfully load tested at FNAL. It will now be road tested with a dummy cryomodule before undergoing a trial run to DL.

INTRODUCTION

For the Proton Improvement Plan II project, 3 high-beta 650 MHz (HB650) cryomodules will be assembled at STFC Daresbury Laboratory (DL) in the UK. The completed modules will be transported to the Fermi National Accelerator Laboratory (FNAL) in the USA. A transportation system was designed to protect the cryomodules from forces experienced during transit and facilitate handling operations.

REQUIREMENTS

The principle design conditions were defined as follows:

1. Transport the 12.5t, 10m long HB650 cryomodule in its transport configuration from DL to FNAL.
2. Suitable for road and air transport, therefore must fit within their respective cargo envelopes.
3. Mitigate logistical drops and mishandling events.
4. Isolate cryomodule from external shocks such that shocks experienced are less than 2.5g peak vertically, 3.5g longitudinal, and 1.5g transverse.
5. Isolate vibrations above 10 Hz by at least 80% relative to input vibrations.
6. Enable the cryomodule to be lifted via frame lifting points.
7. Resist sustained transportation loads, e.g., braking, cornering, accelerating.

DESIGN

The transport frame was influenced by lessons learnt from the LCLS-II and ELI-NP projects. These utilised wire rope isolators mounted between a base frame and inner frame to isolate the modules from transport forces (Fig. 1). The stiffness of the inner frame and the positioning of the isolators was found to be critical [1]. The current design for the HB650 cryomodule is displayed in Fig. 2. The following features can be identified:

- A tessellated steel outer frame encompassing the module to provide protection and restrict access.
- A removable top section for loading.
- 4 lifting points suitable for a 30° direct lift.
- Isolator mounts welded directly to the cryomodule.
- 7 isolators on each side, one positioned under each strongback support.
- 7 cradles to link pairs of isolators and ease assembly.
- Frame envelope minimised for transport compatibility.

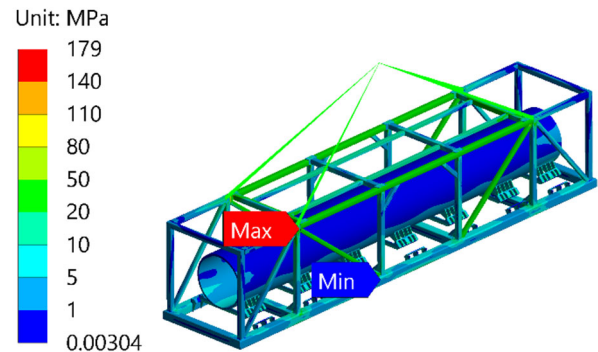


Figure 1: Von-Mises stress in the transport frame during a 200% lift.

Static Loading

BS EN 13155:2003 [2] was referenced to ensure that the outer frame met the requirements of a lifting fixture. Compliance required the frame to be designed to withstand 200% of the weight of the load, without exceeding the specified yield stress limits of the welds and main structure. Figure 1 shows the output of the FEA study for the design, which was used to iterate the design to achieve a 30° lift within the stress limits required.

Static loads associated with transport forces were also analysed against the lifting yield limits, though no case was as severe as the 200% lift.

STEADY-STATE CRYOGENIC OPERATIONS FOR THE UKRI-STFC DARESBURY SRF VERTICAL TEST FACILITY

A. J. May*, A. Akintola, R. Buckley, G. Collier, K Dumbell, S. Hitchen, G. Hughes, P. Hornickel,
C. Jenkins, S. Pattalwar, M. Pendleton, P. A. Smith
UKRI-STFC Daresbury Laboratory, Keckwick Lane, Daresbury, WA4 4AD, UK

Abstract

A novel vertical test facility has been developed, commissioned, and entered steady-state operations at the UKRI-STFC Daresbury Laboratory. The cryostat is designed to test 3 jacketed superconducting RF cavities in a horizontal configuration in a single cool-down run at 2 K. The cavities are cooled with superfluid helium filled into their individual helium jackets. This reduces the liquid helium consumption by more than 70% in comparison with the conventional facilities operational elsewhere. The facility is currently undertaking a 2-year program to qualify 84 high-beta SRF cavities for the ESS (European Spallation Source) as part of the UK's in-kind contribution. This paper reports on the steady-state operations, along with a detailed discussion of the cryogenic performance of the facility, including that of the cryoplant.

INTRODUCTION

The UKRI STFC Daresbury Laboratory Vertical test Facility (VTF) [1] has now been operating regularly for over a year. The VTF supports 2 K characterisation of three jacketed SRF cavities in a single cool-down run, with the 2-year ESS high-beta cavity testing program well underway. Measurements of HOMs and passband modes are made at low power. Q vs E field measurements are made at higher accelerating gradients (up to 200 W input power). A novel cryogenic architecture is used to significantly reduce the liquid helium (LHe) consumption compared with conventional facilities.

VTF CRYOSTAT DESIGN

The standard architecture for vertical SRF cavity testing is to fully submerge cavities in a large LHe bath, and then cool to ≤ 2 K using a vacuum pump/cold compressor to reduce the partial pressure over the bath. RF characterisation is then carried out. This method has been used successfully for many programs, including testing XFEL cavities at DESY [2]. Whilst well-proven, this technique requires both a large cryoplant and, for the activities at UKRI STFC, would require ~ 8500 L of LHe per test cycle.

Given the ever-diminishing global supply of He, and associated rise in cost, an alternative cryostat architecture has been developed for vertical testing of jacketed SRF cavities which requires significantly less LHe and a much smaller cryoplant throughput [1, 3]. The cryostat is based on a cavity

support insert (CSI) where three cavities are mounted horizontally inside LHe jackets below a header tank, each fed by a common fill/pumping line; this may be seen in Fig. 1 which shows a photograph of an assembled insert. By using this design approach, far less LHe is required per testing run (~ 1500 L, all of which is recovered) compared with the conventional designs.



Figure 1: Photograph of CSI on stand with three jacketed cavities (top and middle cavities dressed in MLI jackets).

The insert is mounted into a cryostat vessel which comprises the outer vacuum chamber, magnetic shielding, and thermal radiation shields. The cryostat was manufactured by Criotec¹.

SAFETY

In the operation of any cryogenic facility, safety is paramount. Accordingly, significant efforts have been devoted to understanding potential failure modes for the facility as described above, and introducing mitigation strategies in consideration of the relevant regulations. For a detailed report on the safety of this system, the interested reader is directed to Ref. [3].

CRYOGENIC INFRASTRUCTURE

An ALAT Hélium ML cryoplant, commissioned in 2018, supplies 50 K gaseous helium (GHe, produced by the first

* andrew.may@stfc.ac.uk

¹ criotec.com

A FINAL ACCEPTANCE TEST KIT FOR SUPERCONDUCTING RF CRYOMODULES

A. J. May*, A. Akintola, S. Pattalwar, A. A. J. White,
 UKRI-STFC Daresbury Laboratory, UK

Abstract

UKRI-STFC Daresbury Laboratory is currently undertaking several projects involving assembly of superconducting RF cryomodules, including HL-LHC crab cavities and PIP-II HB650 cavities. As part of the final acceptance tests before shipping of the modules, extensive leak testing, pressure testing, and thermal cycling with gaseous and liquid cryogenics must be performed. A Final Acceptance Test kit (FAT-kit) has been developed to support these tests. The FAT-kit, designed as a single portable unit, sits as an interface module between the cryomodule under test and the required utilities (liquid cryogen supply and return, gaseous cryogen supply and return, warm gas supply and return, vacuum pumps, leak detectors, etc.). The kit features a valve manifold to make or break connections to, from, and between circuits in the cryomodule, safety groupings to provide protection for the circuits as required, and various instrumentation. We report here on the design and commissioning of the kit.

INTRODUCTION

Several projects to assemble and test superconducting radio frequency (SRF) cryomodules for forthcoming accelerators are underway at UKRI-STFC Daresbury.

In 2018, operation of the prototype DQW crab cavity cryomodule was successfully demonstrated in CERN's Super Proton Synchrotron (SPS) as part of the HL-LHC project [1]. Following on from this, STFC Daresbury are working closely with CERN to assemble first the preseries RFD cryomodule and subsequently four series DQW cryomodules [2].

STFC-Daresbury are also responsible as part of the PIP-II project for the assembly of HB650 cryomodules [3].

FINAL ACCEPTANCE TESTING

After completion of assembly of the aforementioned cryomodules, final acceptance testing is required before shipping from STFC-Daresbury to their onward destinations. These tests vary by project [4, 5], but generally include the following cryogenic and vacuum tests:

- Leak testing of the insulating vacuum and various cryogenic circuits
- Pressure testing of the various cryogenic circuits
- Thermal cycling of the cryogenic circuits

Leak and pressure tests are generally to be repeated after thermal cycling back to room temperature to confirm

* andrew.may@stfc.ac.uk

mechanical integrity after thermal stresses have been experienced. As nearly all thermal contraction occurs above 80 K, this thermal cycling may be done using liquid nitrogen (LN₂).

FAT-KIT DESIGN

In order to support final acceptance testing of cryomodules at Daresbury, an interface module (FAT-kit) has been developed to sit between the assembled cryomodule and the required utilities for the tests. Originally, this design was developed for the HL-LHC crab cavity cryomodule, but can be modified as required for HB650 tests. The main goal of the kit is to improve consistency between, as well as safety and quality of FAT tests compared with connecting the various utilities in an ad hoc manner. The module is required to be portable between different experimental areas. The utilities required to interface to are as follows:

- High-pressure/low-pressure room-temperature He gas
- High-pressure/low-pressure room-temperature N₂ gas
- 80 K N₂ gas
- LN₂
- Vacuum pumping station
- Leak detector
- Vent lines

Figure 1 shows the top-level piping and instrumentation diagram (P&ID) with the FAT-kit between the utilities as described and the cryomodule.

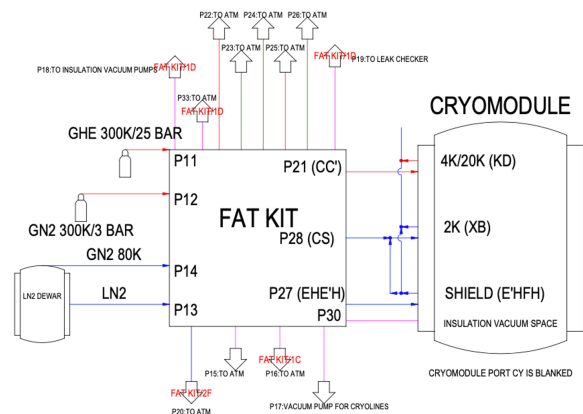


Figure 1: Top-level P&ID showing the FAT-kit sitting between utilities and cryomodule

APPLICATION OF THE ASME BOILER AND PRESSURE VESSEL CODE IN THE DESIGN OF SSR CRYOMODULE BEAMLINES FOR PIP-II PROJECT AT FERMILAB*

J. Bernardini[†], M. Parise, M. Chen, D. Passarelli
 FNAL, Batavia, IL 60510, USA

Abstract

This contribution reports the design of the main components used to interconnect SRF cavities and superconducting focusing lenses in the SSR Cryomodule beamlines, developed in the framework of the PIP-II project at Fermilab. The focus of the present contribution is on the design and testing of the edge-welded bellows according to ASME Boiler and Pressure Vessel Code. The activities performed to qualify the bellows to be assembled in cleanroom, for operation in high vacuum, cryogenic environments, and their characterization from magnetic standpoint, will also be presented.

INTRODUCTION

The PIP-II linac [1] will include a total of nine Single Spoke Resonator Cryomodules (SSR CMs), two SSR1 CM [2, 3] and seven SSR2 CM [4]. The SSR section of the linac will accelerate H⁻ ions from 10 MeV to 185 MeV. The PIP-II beam optics design requires that each SSR1 CM contains four focusing lenses (solenoids) and eight SSR1 cavities, and each SSR2 CM contains three focusing lenses and five SSR2 cavities. Each cavity is equipped with one high-power RF coupler, and one tuner, and each solenoid is followed by one Beam Position Monitor (BPM). Cavities, solenoids, and BPMs, together with their interconnecting elements, define the string assembly. The string assembly operates in a high vacuum cryogenic environment and in operation cavities and solenoids need to be aligned within the PIP-II permissible alignment error, reported in Table 1. Therefore, flexible interconnecting elements are needed in the string assembly to compensate for fabrication errors during the mechanical alignment, and to allow for the thermal contraction and expansion of the string's components during cool-down and warm-up cycles.

Edge welded bellows are the element of choice to make such interconnections. They are designed according to ASME Boiler and Pressure Vessel code satisfying all loading scenarios during assembly, cool-down, operation, and warm-up. The bellows are also designed to be cleanroom compatible, being the SSR strings assembled in an ISO 10 cleanroom [5]. The focus of the present contribution is on the design and testing of the bellows weldments used in the SSR2 string.

Table 1: PIP-II Alignment Requirements

| Cavities | Value |
|--------------------------------------------|-------|
| Transverse cavity alignment error, mm RMS | <1 |
| Angular cavity alignment error, mrad RMS | ≤10 |
| Solenoids | Value |
| Transverse cavity alignment error, mm RMS | <0.5 |
| Angular solenoid alignment error, mrad RMS | ≤1 |

BELLOWS DESIGN

Edge welded bellows have a higher stroke and can be moved laterally more than hydro-formed or expansion-formed bellows of equal length. These features make them a suitable choice for SSR CMs strings [6], where the space is limited and cavities and solenoids are supported from the bottom by the strongback, which stays at room temperature during operations. Lateral movement and stroke are determined by the bellows diameter and number of convolutions. Two different bellows geometries, type 1 - long and type 2 - short, are used among four different weldments in the SSR2 string. Figure 1 shows the four weldments, Table 2 summarizes the characteristics of short and long bellows.

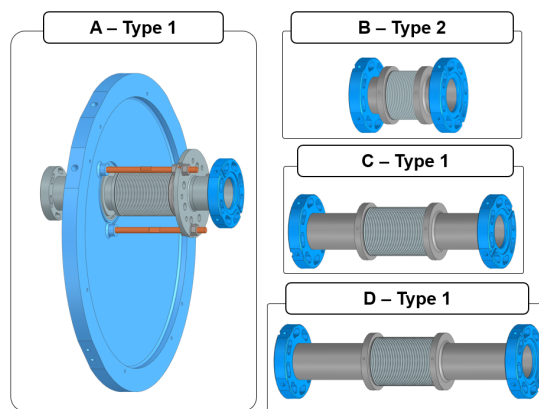


Figure 1: SSR2 edge welded bellows sub-assemblies. A, beamline end flange kit - B, cavity to cavity bellows weldment - C, cavity to BPM bellows weldment - D, cavity to solenoid bellows weldment.

The requirements on the axial stroke and lateral movement are driven by the thermal contraction of the string's components during cool-down / warm-up cycles (up to 1 mm), cavity tuning (up to 2 mm), fabrication errors (up to 4 mm), and installation misalignment. The internal diameter is cho-

* Work supported by Fermi Research Alliance, LLC under Contract No. DEAC02-07CH11359 with the United States Department of Energy, Office of Science, Office of High Energy Physics.

[†] jbernard@fnal.gov

FINAL DESIGN OF THE PRE-PRODUCTION SSR2 CRYOMODULE FOR PIP-II PROJECT AT FERMILAB*

J. Bernardini[†], D. Passarelli, V. Roger, M. Parise, J. Helsper, G. V. Romanov, M. Chen, C. Boffo, M. Kramp, F. L. Lewis, T. Nicol, B. Squires, M. Turenne
 FNAL, Batavia, IL 60510, USA

Abstract

The present contribution reports the design of the pre-production Single Spoke Resonator Type 2 Cryomodule (ppSSR2 CM), developed in the framework of the PIP-II project at Fermilab. The innovative design is based on a structure, the strongback, which supports the coldmass from the bottom, stays at room temperature during operations, and can slide longitudinally with respect to the vacuum vessel. The Fermilab style cryomodule developed for the prototype Single Spoke Resonator Type 1 (pSSR1) and the prototype High Beta 650 MHz (pHB650) cryomodules is the baseline of the current design, which paves the way for production SSR1 and SSR2 cryomodules for the PIP-II linac. The focus of this contribution is on the results of calculations and finite element analysis performed to optimize the critical components of the cryomodule: vacuum vessel, strongback, thermal shield, and magnetic shield.

INTRODUCTION

A total of seven production SSR2 CMs will be used in the PIP-II linac [1] to accelerate H⁻ ions from 35 MeV to 185 MeV. One ppSSR2 CM will be built during the prototyping and validation stages.

The design of the ppSSR2 CM is based on a novel concept developed at Fermilab [2, 3], the Fermilab style cryomodule, which was validated by cold testing the pSSR1 CM for PIP-II [4]. It also takes into account the standardization strategy set for the PIP-II CMs [5]. To minimize the movement of the beamline components and ancillaries during cooldown and to facilitate the assembly, the coldmass and the beamline components are based on a full-length strongback that is designed to be maintained at room temperature during operations. A High Temperature Thermal Shield (HTTS) and Low Temperature Thermal Source (LTTS), along with connections for intercepts are made available between the inner surface of the vacuum vessel and the 2 K helium to reduce radiation and conduction heat transfers. The current PIP-II beam optics design requires that each SSR2 cryomodule contains three focusing lenses and five identical SSR2 cavities, where each cavity is equipped with one high-power RF coupler, and one tuner.

Cavities and focusing lenses are supported by individual support posts, which are mounted on the strongback, located between the vacuum vessel and the HTTS. A two-phase

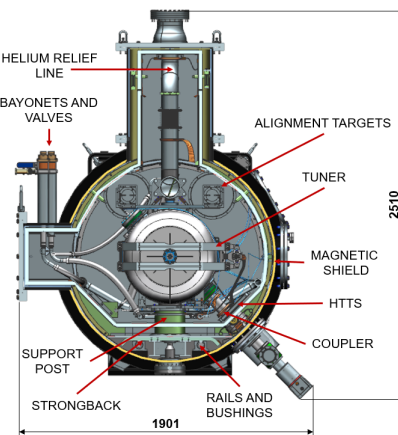


Figure 1: ppSSR2 CM transverse cross section showing the main components and subsystems (dimensions in mm).

helium pipe, running the length of the cryomodule, is connected to cavities by means of Ti-SS transition joints, and to the focusing lenses by means of thermal straps. The two-phase pipe is connected to the relief line through the top hat, and to the pumping line through the bayonets on the lateral extension of the vessel. The heat exchanger and the interfaces with 2 K relief line and pressure transducers are located on the top hat of the vacuum vessel. The interior of the vessel features an inner frame, which supports a global magnetic shield.

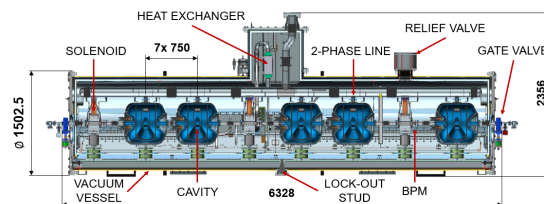


Figure 2: ppSSR2 CM longitudinal cross section showing main components and subsystems (dimensions in mm).

MAIN CRYOMODULE COMPONENTS

Vacuum Vessel

The vacuum vessel consists of a cylindrical shell in carbon steel (ASTM A-516) anchored to the floor with bottom supports and equipped with lugs for lifting purposes. The vessel shell is closed at the upstream and downstream side with endcaps, and it has ports for input RF power couplers,

* Work supported by Fermi Research Alliance, LLC under Contract No. DEAC02-07CH11359 with the United States Department of Energy, Office of Science, Office of High Energy Physics.

[†] jbernard@fnal.gov

NIObIUM TO TITANIUM ELECTRON BEAM WELDING FOR SRF CAVITIES*

M. Parise[†], D. Passarelli, J. Bernardini, Fermi National Accelerator Laboratory, Batavia, IL, USA

Abstract

Titanium and niobium are the main materials used for the fabrication of Superconducting Radio Frequency (SRF) cavities. These two metals are usually joined, using various welding techniques, using a third material in between. This contribution focuses on the development of an innovative electron beam welding technique capable of producing a strong bond between these two different materials. Several samples are produced and tested to assess the mechanical strength at room and cryogenic temperature as well as the composition of the resulting welded joint. Also, the first units of the Single Spoke Resonator type 2 (SSR2) cavities for the Proton Improvement Plan-II (PIP-II [1]) have been fabricated joining directly various grades of titanium to niobium and results gathered through the fabrication will be reported.

INTRODUCTION

SRF cavities used in particle accelerators are, for the most part, manufactured by forming, machining and Electron Beam (EB) or Tungsten Inert Gas (TIG) welding materials such as Niobium, Titanium and Stainless Steel. Niobium, and in particular high purity niobium, is the metal used for the fabrication of the superconducting resonators because of its high transition temperature, high critical magnetic field and its availability in the forms of sheets and rods/tubes. Given the low operating temperatures of the superconducting structures (around 2 - 4 K) and, in case of the need for proper heat dissipation, liquid helium is required. An external vessel (also called helium jacket), joined to the niobium resonator, is therefore needed. The search for vessel's materials that preserve appropriate strength and ductility at cryogenic temperatures and, among other characteristics, are also paramagnetic, commercially available and machinable/weldable sees the titanium as the one mostly used. One of the challenges of the cavity design is the development of the transition from the niobium resonator to the helium tank. Niobium resonators with titanium helium jackets, are historically joined using a third material that is an alloy of the 2: Nb55Ti. This approach increases the number of welded joints, and thus, the cost of the overall project with respect to joining the 2 materials directly together. While designing the new pre-production SSR2 (ppSSR2) cavity [2-4] for PIP-II it was decided to develop an EB welded joint between high purity niobium and 2 different types of titanium to prove that such joints can be suitably used for the fabrication. Such joints are mechanically characterized at Room

Temperature (RT) and at Liquid Nitrogen (LN) temperature. Energy Dispersive X-ray Spectroscopy (EDS) is also used to check if the titanium can diffuse into the niobium as part of the welding process and following heat treatment.

MATERIALS AND JOINT TYPES

The materials used for the weld development are:

- High purity niobium (Nb) (Residual Resistivity Ratio >300)
- Titanium Grade 2 (Ti Gr.2) (UNS R50400)
- Titanium Grade 5 (Ti Gr.5) (UNS R56400)

The Ti Gr.2 is a material that can be used for the construction of pressure vessel according to the ASME Boiler and Pressure Vessel Code [5]. Its characteristics are well suited for the fabrication of SRF cavities and it was chosen as helium jacket material for the ppSSR2 cavities. The Ti Gr.5 one of the most used titanium alloys and it has superior mechanical strength however is not a code [5] compliant material. The flanges outside the pressure boundary of the ppSSR2 cavities are fabricated using this titanium alloy so that the sealing surfaces of the Ultra High Vacuum connection have improved resistance to wear and require minimal or no maintenance throughout their lifecycle. Welded samples are prepared joining Nb to Ti Gr.2 and Nb to Ti Gr.5. The joint types for both material combinations are 2: butt welded joint 4.0 mm thick obtained welding in a straight line from one side only and a butt welded joint of a 1" Nb rod to a Ti flange (for both titanium grades). These 2 joint types serve to develop the EB welding parameters on the simplest joint configuration possible (straight line on flat sheets) and to be able to cut specimens for tensile testing and analysis at the Scanning Electron Microscope (SEM). The tensile testing is needed to assess the structural performance of the welded joint. The SEM analysis allows to obtain macrographs of the grain structure, and using the EDS technique we are able to establish the chemical composition of the joint and its Heat Affected Zone (HAZ). Also, flanges are used to verify the leak tightness and to reproduce the geometry of the real joint as present on the ppSSR2 cavity flanges. A total of 14 sheets 4" x 2.5" (8 made of Ti Gr.2 and 6 of Ti Gr.5) are EB welded to 14 Nb sheets with exact same dimensions. A total of 4 titanium flanges (2 made of Ti Gr.2 and 2 of Ti Gr.5) are EB welded to 4 Nb rods.

SETUP AND WELDED SAMPLES

All the EB welds are performed using a Sciaky 60kV EB welding machine capable to deliver 30 kW. The vacuum level in the welding chamber at the beginning of each weld is better than 10^{-4} Torr. Fig. 1 shows the test setup as described for the 2 joint types. Before welding each niobium part is lightly etched using an acid mixture to remove the

* This manuscript has been authored by Fermi Research Alliance, LLC under Contract No. DE-AC02-07CH11359 with the U.S. Department of Energy, Office of Science, Office of High Energy Physics.

[†] mparise@fnal.gov

BEAMLINE VOLUME RELIEF ANALYSIS FOR THE PIP-II SSR2 CRYOMODULE AT FERMILAB *

M. Parise[†], D. Passarelli, J. Bernardini, Fermi National Accelerator Laboratory, Batavia, IL, USA

Abstract

The beam volume of the Pre-Production Single Spoke Resonator type 2 (ppSSR2) cryomodule for the Proton Improvement Plan-II (PIP-II) project will be protected against over-pressurization using a burst disk. This contribution focuses on the analysis of the relief of such trapped volume during a catastrophic scenario with multiple systems failures. An analytical model, able to predict the pressure in the beam volume depending of the various boundary conditions, has been developed and will be presented along with the results.

INTRODUCTION

Superconducting Radio Frequency (SRF) cavities are the core of linear particle accelerators like PIP-II [1]. The new pre-production SSR2 (ppSSR2) cavities [2–5] as well as Single Spoke Resonator Type 1 (SSR1) [6], Low Beta (LB) [7] and High Beta (HB) [8] 650 MHz cavities and cryomodules [9] for PIP-II use liquid helium to cool the SRF cavities down to 2 K in order to harness the superconducting advantages. Figure 1 shows a generic section, transversal to the beam axis, of a PIP-II cryomodule. In operation the *insulating volume* and *beamline volume* are under vacuum (high vacuum and ultra-high vacuum respectively). The support post is made of insulating material and interface room temperature with the beamline components at 2 K. The liquid helium is contained in a circuit that encompasses the beamline components and at the operating temperature of 2 K is in a two-phase state. The circuit is connected with relief devices installed outside the *vacuum vessel* that are set to relieve the pressure above 4.1 bar-g when in operation. A *thermal shield*, maintained at a temperature around 50K screen the beamline components from the radiation coming from the vacuum vessel. A leak between the liquid helium circuit and the *beamline volume* may occur during the life of the PIP-II project. If this leak goes undetected, liquid helium may accumulate in the *beamline volume*. Once the insulating vacuum is spoiled the liquid helium trapped in the *beamline volume* may vaporize rapidly increasing the pressure in this space. To protect the cavities and beamline components from over-pressure, a burst disk is installed on the beamline outside of the cryomodule.

INPUTS AND ASSUMPTIONS

To purpose of this work is to analytically evaluate the pressure inside the *beamline volume* as a function of the time given the applied boundary conditions under certain

* This manuscript has been authored by Fermi Research Alliance, LLC under Contract No. DE-AC02-07CH11359 with the U.S. Department of Energy, Office of Science, Office of High Energy Physics.

[†] mparise@fnal.gov

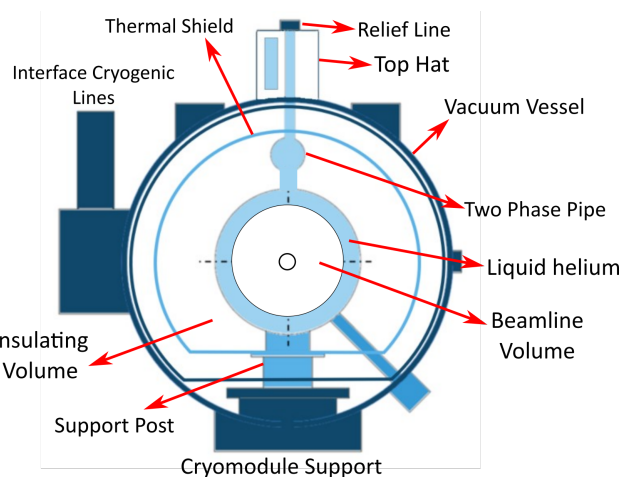


Figure 1: Schematic Section of a Generic PIP-II Cryomodule.

assumptions. Figure 2 schematically shows the main elements that are recalled in this section. The inputs used for the calculation are therefore:

- **Geometry:** the ppSSR2 cryomodule is chosen as geometry for the analysis. It includes 5 cavities and 3 solenoids connected by bellows and tubes. The solenoid *beamline volume* has the same shape and Internal Diameter (ID) of the interconnecting elements therefore it will be considered as straight pipe and the cavities are modeled as cylinders for the purpose of this analysis. The *beamline volume* is considered to be closed by 2 gate valves at each ends. The *beamline volume* is interfacing the *insulating volume* (the helium circuit is not included. This is a conservative assumption). The complex geometry that goes from the beamline to the burst disk is decomposed in several elemental shapes for which the resistance coefficient can be easily calculated.
- **Defect:** a defect with a determined leak rate connects the helium circuit with the textit{beamline volume}. Liquid helium fills the volume for a certain amount of time.
- **Heat load to helium:** the insulating vacuum is lost in 1 minute of time. As a consequence, a convective heat load is establish between the air in that volume and the helium. The presence of a *thermal shield* is also neglected and the helium therefore sees a radiative heat load from 300 K. The conductive heat load from the *support posts* is included as well. All these heat loads are absorbed 100% by the helium.

All the described assumptions and the one used as part of the calculation to establish diameter changes, simplify the geometry, etc. are conservative and contribute to increase

PROTOTYPE HB650 TRANSPORTATION VALIDATION FOR THE PIP-II PROJECT*

J.P. Holzbauer[†], S. Cheban, C. Grimm, J. Helsper, R. Thiede, A. Wixson,
Fermi National Accelerator Laboratory, Batavia, IL, USA

R. Cubizolles¹, CEA-IRFU, Gif-sur-Yvette, France

M. Kane², STFC-UKRI, Warrington, UK

Abstract

The PIP-II Project at Fermilab (FNAL) is centered around a superconducting 800 MeV proton linac to upgrade and modernize the Fermilab accelerator complex, allowing increased beam current to intensity frontier experiments such as LBNF-DUNE. PIP-II includes strong international collaborations, including the delivery of 13 cryomodules from European labs to FNAL (3 from STFC-UKRI in the UK and 10 from CEA in France). The transatlantic shipment of these completed modules is identified as a serious risk for the project. To mitigate this risk, a rigorous and systematic process has been developed to design and validate a transport system, including specification, procedures, logistics, and realistic testing. This paper will detail the engineering process used to manage this effort across the collaboration and the results of the first major validation testing of the integrated shipping system prior to use with a cryomodule.

INTRODUCTION

The PIP-II SRF linac is composed of five types of cryomodules at 3 sub-harmonics of 1.3 GHz (162.5, 325, and 650 MHz) [1]. The 650 MHz section of the linac is composed of two cryomodule types, Low-Beta (LB) and High-Beta (HB). The PIP-II Project has significant international contributions in almost every part of the machine, and the 650 section is no exception. The LB modules are being designed and produced by CEA in France while the HB modules are produced by STFC-UKRI in the UK as in-kind contributions to the project. The PIP-II project has adopted the design philosophy of convergent design, aligning the techniques and technologies between different modules as much as possible. This philosophy extends to transportation of the LB and HB modules from the partner labs in Europe to FNAL. Transportation experts at all three labs have worked closely to ensure that a consistent and systematic approach is used for assessing and mitigating the risks of these critical cryomodule transports.

TRANSPORT SYSTEM VALIDATION STRATEGY

A conservative approach to transportation and transport validation has been adopted by PIP-II driven by past experience with cryomodule shipping for LCLS-II [2]. This

includes the choice to forego sea and rail, relying on air transport for the transatlantic segments. The following major stages are chosen to systematically validate the integrated transport system design (cryomodule plus shipping frame) while minimizing risk to critical equipment.

- Design, fabrication, and integration of HB650 transport frame with cryomodule analog (Dummy Load)
- Local road testing with Dummy Load to validate isolation and handling performance
- Realistic transport of Dummy Load from FNAL to STFC-UKRI to validate air transport and handling
- Local road testing with a cold-tested and validated prototype HB650 (pHB650) to reverify isolation performance as well as any module-internal resonances
- Realistic transport of the pHB650 module from FNAL to STFC-UKRI and back, concluding with second cold-test to assess impacts of transatlantic shipment on cavity performance.

The transportation scope of each partner is distributed based on many factors which are outside the scope of this document. The diversity of activities and design details of both transport systems and cryomodules means that it is critical that the transportation approaches are aligned and designs and lessons learned are shared strongly as early as possible within the project to minimize duplicated effort or increased risk.

VALIDATION RESULTS

PIP-II uses a formal systems engineering approach, including strong documentation and review philosophies. Detailed risk assessments are matched to systematic risk mitigation and detailed validation efforts. All work is documented formally and reviewed, both internally and, periodically, by external transportation experts. This process and associated documentation is described below.

Risk Assessment and Planning

The foundational documents for the transport process are the Failure Mode and Effect Analysis (FMEA) and Prevention through Design (PtD) tables. The FMEA gathers all technical risks including human factors during all procedures (e.g., incorrect installation of shipping supports), design failure modes (e.g., resonant excitation and fatigue

* Work supported by Fermi Research Alliance, LLC under Contract No. DeAC02-07CH11359 with the United States Department of Energy.

[†] jeremiah@fnal.gov

STANDARDIZATION AND FIRST LESSONS LEARNED OF THE PROTOTYPE HB650 CRYOMODULE FOR PIP-II AT FERMILAB*

V. Roger[†], J. Bernardini, S. Chandrasekaran, C. Grimm, O. Napoly, J. Ozelis, M. Parise, D. Passarelli, Fermilab, Batavia, USA
N. Bazin, R. Cubizolles, CEA, Gif-sur-Yvette, FRANCE

Abstract

The prototype High Beta 650 MHz cryomodule (pHB650 CM) has been designed by an integrated design team, consisting of Fermilab (USA), CEA (France), STFC UKRI (UK), and RRCAT (India). The manufacturing and assembly of this prototype cryomodule is being done at Fermilab, whereas the production cryomodules will be manufactured and assembled by STFC-UKRI. As the first PIP-II cryomodule for which standardization was applied, the design, manufacturing and assembly of this cryomodule led to significant lessons being learnt and experiences gathered. These were incorporated into the design of the pre-production Single Spoke Resonator Type 2 cryomodule (ppSSR2 CM) and the pre-production Low Beta 650 MHz cryomodule (ppLB650 CM). This paper presents the pHB650 CM lessons learned and experiences gathered from the design to the lower coldmass assembly and how this cryomodule has a positive impact on all the next Proton Improvement Plan-II (PIP-II) cryomodules due to the standardization set up among SSR and 650 cryomodules.

INTRODUCTION

After the completion of the PIP-II prototype [1] Single Spoke Resonator 1 (SSR1) cryomodule [2, 3], a design strategy was set up among the 650 and SSR cryomodules to reduce the cost, to increase the quality and performances, and to mitigate risks [4]. This design strategy led to the standardization of several components, tooling, assembly processes, and procurements.

STANDARDIZATION

The PIP-II SSR and 650 cryomodules are designed adopting the Fermilab style cryomodule that uses a room temperature strongback as foundation. Due to the design of the cavities and requirements being different for SSR and 650 cryomodules, the strongback design has been optimized for each cryomodule type. With the 650 cryomodules being transported overseas, rigid connections in between the vacuum vessel and the strongback as presented in Fig. 1 were required to meet the specifications. Thus, it was necessary to insert the strongback into the vacuum vessel, then to adjust it up to its nominal position before locking it down using 14 studs, set of screws and pins [5, 6]. The SSR cryomodules being assembled at Fermilab, thus not requiring overseas transportation, it was allowed to ease the interface strongback/vacuum vessel. Calculations

have shown that bushing screwed to the vacuum vessel with rails connected to the strongback as presented in Fig. 2 met the requirements. The longitudinal position of the strongback is fixed using a central pin, and no lifting is needed [7].

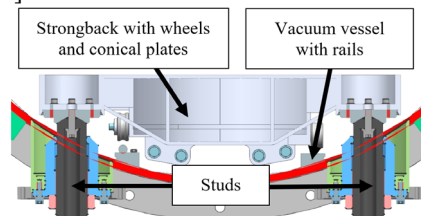


Figure 1: 650 vacuum vessel - strongback interface.

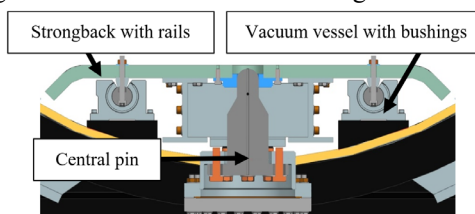


Figure 2: SSR vacuum vessel - strongback interface.

The 650 cavities are aligned using C-shape brackets [5, 8] at the interface with the cavity lugs, whereas SSR cavities use an alignment plate positioned at the bottom of the cavities. This concept was validated during the alignment of the prototype SSR1 string assembly [9].

All SSR and 650 cryomodules share the same cryogenic layout and the size of the cryogenic lines are identical for all cryomodules (Fig. 3). With the 650 production cryomodules manufactured in Europe and the SSR cryomodule assembled in the USA, it was decided to use ISO pipes which also match imperial pipe size to allow the procurement from the international market maintaining equivalence.

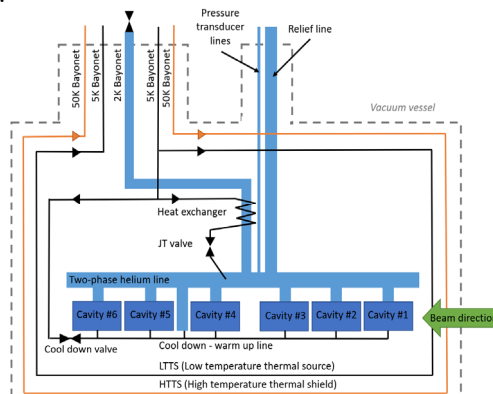


Figure 3: Schematic of the cryogenic lines.

* This manuscript has been authored by Fermi Research Alliance, LLC under Contract No. DE-AC02-07CH11359 with the U.S. Department of Energy, Office of Science, Office of High Energy Physics.

[†] vroger@fnal.gov

FABRICATION EXPERIENCE OF THE PRE-PRODUCTION PIP-II SSR2 CAVITIES AT FERMILAB*

M. Parise[†], D. Passarelli, P. Berrutti, V. Roger, FNAL, IL, USA
 D. Longuevergne, P. Duchesne, CNRS, IJCLab, France

Abstract

The Proton Improvement Plan-II (PIP-II) linac will include 35 Single Spoke Resonators type 2 (SSR2). A total of eight pre-production SSR2 jacketed cavities will be procured and five installed in the first pre-production cryomodule. The mechanical design of the jacketed cavity has been finalized and it will be presented in this paper along with fabrication and processing experience. The importance of interfaces, quality controls and procurement aspects in the design phase will be remarked as well as lessons learned during the fabrication process. Furthermore, development studies will be presented together with other design validation tests.

of spoke resonators are also considered carefully as of this process [4, 5]. Figure 1 shows the finalized design of the cavity and a section defining the helium space and beam volume.

Table 1: Parameters of the SSR2 Cavity.

| Parameter | Value |
|---------------------------------------------------------|------------|
| Nominal Frequency, MHz | 325 |
| df/dp , $\frac{\text{Hz}}{\text{mbar}}$ | <25 |
| Target Frequency Allowable Error, kHz | +/-50 |
| Maximum Allowable Working Pressure (MAWP) RT / 2 K, bar | 2.05 / 4.1 |

INTRODUCTION

The Radio-Frequency (RF) volume final design and the advanced (but not final) mechanical design of the pre-production Single Spoke Resonators type 2 (SSR2) cavities, for the Proton Improvement Plan-II (PIP-II, [1]), was presented 3 years ago at the 19th International Conference of RF Superconductivity (SRF'19) [2, 3]. An internal project Final Design Review was held in November 2019 and the procurement of niobium initiated shortly thereafter. The procurement of the jacketed cavities, to be manufactured in industry, initiated at the beginning of 2021 with the first bare cavity completed at the end of the same year. After bulk Buffered Chemical Polishing (BCP), High Pressure Rinse (HPR) of the RF volume and High Temperature Heat Treatment (HTHT) the jacketing and room temperature tests of the first unit were completed in July 2022. The next units are expected to be completed soon.

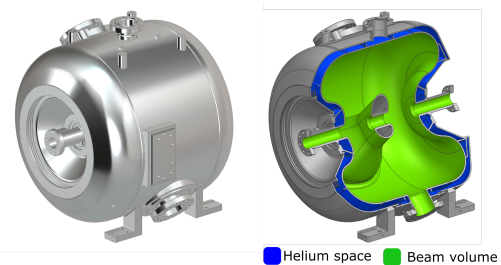


Figure 1: Cavity final design.

DESIGN OVERVIEW

Some of the main parameters used for the design of the SSR2 cavities are reported in Table 1. The RF volume is optimized to enable the best Electro Magnetic (EM) performance and to mitigate multipacting. The result is the starting point for the mechanical design: a multi-objective optimization problem revolving around not only the structural soundness but also involving RF parameters such as frequency sensitivity and Lorentz Force Detuning (LFD). The design of the SSR2 bare cavity and the helium jacket is carried out simultaneously as a integrated system opposed to trying to optimize the bare cavity first and only secondly the helium jacket which may have led to unnecessary design iterations. Lessons learned from the previous generation

Design Choices with an Impact on the Fabrication

As a result of the multipacting mitigation, the endwalls of the cavity present an elliptical profile with an inflection point and overall high depth to radius ratio making the part difficult to form. Moreover, the structural soundness, in compliance with Fermilab internal guidelines and the ASME Boiler and Pressure Vessel Code [6], whenever possible, required to procure niobium sheets with a minimum thickness close to 5 mm. This value is the maximum used among all superconducting cavities of PIP-II and above the usual thickness that cavity fabricators are used to. Thick material implies a more difficult forming and Electron-Beam (EB) welding operations. To simplify the procurement and reduce the number of joint types, the SSR2 cavities are manufactured only from 2 materials: high purity niobium and titanium. Not using nb-ti alloys means directly joining niobium and titanium through EB and Tungsten Inert Gas (TIG) joints, a practice that has never been used not only for PIP-II but at Fermilab in general.

BARE CAVITY FABRICATION

Figure 2 shows the first pre-production SSR2 cavity as fabricated. The cavity mostly consists of niobium sheets

* This manuscript has been authored by Fermi Research Alliance, LLC under Contract No. DE-AC02-07CH11359 with the U.S. Department of Energy, Office of Science, Office of High Energy Physics.

[†] mparise@fnal.gov

OPERATIONS OF COPPER CAVITIES AT CRYOGENIC TEMPERATURES*

H. Wang[†], U. Ratzinger, M. Schuett, IAP, Frankfurt University, Germany

Abstract

This work is focused on the anomalous skin effect in copper and how it affects the efficiency of copper-cavities in the temperature range 40-50 K. The quality factor Q of three coaxial cavities was measured over the temperature range from 10 K to room temperature in the experiment. The three coaxial cavities have the same structure, but different lengths, which correspond to resonant frequencies: around 100 MHz, 220 MHz and 340 MHz. Furthermore, the effects of copper-plating and additional baking in the vacuum oven on the quality factor Q are studied in the experiment. The motivation is to check the feasibility of an efficient, pulsed, ion linac, operated at cryogenic temperatures.

INTRODUCTION

The RF loss in copper is given by

$$P = \frac{1}{2} \int R_s \cdot H_0^2 \cdot dA \quad (1)$$

where H_0 is the magnetic field amplitude and R_s the surface resistance, which is given by

$$R_s = \sqrt{\pi f \mu_0 \mu_r \rho} \quad (2)$$

where ρ is the specific electrical resistivity.

From Eq. (2) we can see that R_s is proportional to $\sqrt{\rho}$. ρ decreases as the temperature decreases, see Fig. 1 [1].

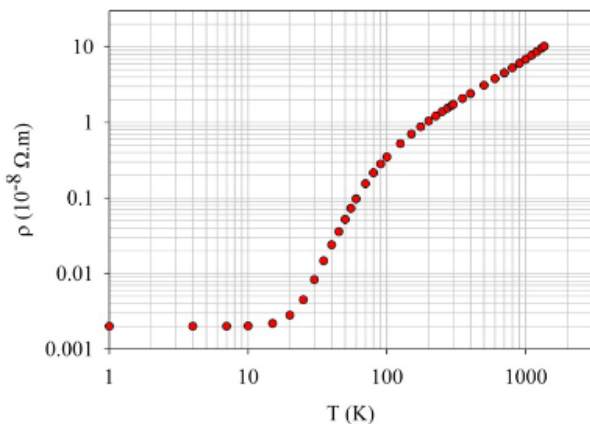


Figure 1: The electrical resistivity dependence on the temperature of very pure copper (RRR \approx 550).

Figure 1 shows how the electrical resistivity changes with temperature in the case of direct current (DC) with a high RRR value. This curve is still applicable for the RF case when the temperature drops to a certain value for a specific frequency. Below this temperature the mean free path of

electrons becomes comparable to or even greater than the skin depth $\delta = \sqrt{2\rho/\omega\mu_0\mu_r}$, the anomalous skin effect starts to play an increasing role and will reduce the advantage of rising conductivity. Below this temperature the RF resistivity will not change like the DC resistivity shown in Fig. 1. It still decreases with the temperature but more slowly.

The definition of the quality factor Q_0 of a cavity is

$$Q_0 = \frac{\omega W}{P} \quad (3)$$

where W is the stored energy. According to Eqs. (1), (2) and (3), $Q_0 \propto 1/P \propto 1/R_s \propto 1/\sqrt{\rho}$, which means, Q_0 increases with decreasing temperature. However, it increases slower in the cryogenic temperature region due to the anomalous skin effect. Even so, there might be still a potential for the cryogenic cavities at modest rf frequencies and at low duty factor such like in case of heavy ion synchrotron injectors. The goal of this work is to find out in which this approach might be attractive.

TEST CAVITY GEOMETRY

For this work three simple $\lambda/4$ coaxial cavities have been designed and were fabricated at the workshop in IAP. They have the same structure, see in Fig. 2, but different lengths, which correspond to the resonant frequencies: around 100 MHz, 220 MHz and 340 MHz. The designed parameters for the cavities are listed in Table 1.



Figure 2: Structure of the shortest $\lambda/4$ coaxial cavity and the cover.

Table 1: Design Parameters of the Cavities

| f (Design) (MHz) | Length (mm) | Gap (mm) |
|--------------------|-------------|----------|
| 100 | 735 | 54 |
| 220 | 324 | 54 |
| 340 | 201 | 54 |

The main parts of the cavities were made of copper and the top cover was made of stainless steel. The inner side of

* Work supported by HFHF.

[†] wang@iap.uni-frankfurt.de

STATUS OF THE NEW INTENSE HEAVY ION DTL PROJECT ALVAREZ 2.0 AT GSI

L. Groening*, S. Mickat, T. Dettinger, X. Du, M. Heilmann, M.S. Kaiser, E. Merz, A. Rubin, C. Xiao
 GSI Helmholtzzentrum für Schwerionenforschung GmbH, Darmstadt, Germany

Abstract

The Alvarez-type post-stripper DTL at GSI accelerates intense ion beams with $A/q \leq 8.5$ from 1.4 to 11.4 MeV/u. After more than 45 years of operation it suffers from aging and its design does not meet the requirements of the upcoming FAIR project. The design of a new 108 MHz Alvarez-type DTL has been completed and series components for the 55 m long DTL are under production. In preparation, a first cavity section as First-of-Series has been operated at nominal RF-parameters. Additionally, a prototype drift tube with internal pulsed quadrupole has been built and operated at nominal parameters successfully. High quality of copper-plating of large components and add-on parts has been achieved within the ambitious specifications. This contribution summarizes the current project status of Alvarez 2.0 at GSI and sketches the path to completion.

INTRODUCTION

The existing post-stripper DTL at GSI is in operation since more than 45 years. Accordingly, it suffers from increased failure rates especially of the e.m. quadrupoles inside the drift tubes. Its design has some conceptual shortcomings with respect to the high intensity demands of the upcoming FAIR facility [1]. These issues are addressed by the construction of a completely new DTL section. Subsequently, the DTL's design features are briefly summarized followed by description of extensive prototyping of critical components and procedures. Finally, the status of series production is reported, followed by an outlook on the future project planning.

GENERAL DESIGN

Like the current DTL, the new section will accelerate ions up to the injection energy of the subsequent synchrotron SIS18. All species up to the mass-to-charge ratio of $A/q=8.5$ are accelerated, corresponding to FAIR's reference ion of $^{238}\text{U}^{28+}$. Five cavities with lengths of about 11 m each are operated at 108.4 MHz with peak powers of up to 1.35 MW including beam loading. Figure 1 plots the new DTL together with some RF-design details of the first cavity. The normal conducting DTL covers a beam repetition rate of up to 10 Hz with flat top RF-pulse length of up to 1.0 ms corresponding to the beam pulse length. Within the cavities, transverse FDDF focusing is provided with a zero current phase advance of 65° . The large intensities cause transverse tune depressions of up to 40% along the first cavity [2]. Longitudinal focusing is from RF-phases of

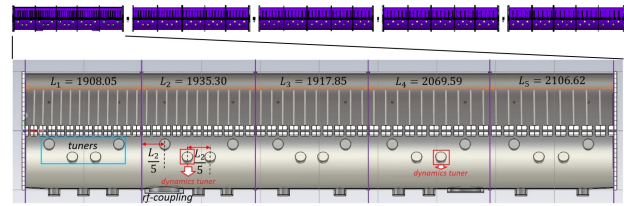


Figure 1: New post-stripper DTL Alvarez 2.0 being under construction at GSI.

-30° along the first three cavities and -25° along the last two ones. Cavities are separated by four identical inter-tank sections which serve for 3d beam envelope matching by three quadrupoles and one re-buncher. The inter-tank sections provide also for a beam current and phase probe, a sector valve, and a transverse beam profile measurement set-up.

Although the machine is mainly designed as an injector for the synchrotron SIS18, several low-energy experiments shall be served as well. The DTL design allows for switching off the RF-power of the last cavities while the transversely focusing quadrupoles inside the drift tubes remain switched on. Accordingly, the DTL output energies correspond to the individual cavity exit energies of 3.212, 5.173, 7.142, 9.237, and 11.318 MeV/u. The quadrupoles are pulsed, such that the focusing can be adapted individually to each ion species and design energy; the latter can be changed between the individual DTL pulses, i.e., within less than 100 ms. The DTL design is described in detail within the dedicated Technical Design Report [3] and the main design parameters are listed in Table 1.

Table 1: Main Design Parameters of GSI's New Post-stripper DTL Alvarez 2.0

| Parameter | Value |
|--------------------------|---------------------------------------|
| Ion A/q | ≤ 8.5 ($^{238}\text{U}^{28+}$) |
| Input beam energy | 1.358 MeV/u |
| Output beam energy | 3.212 – 11.318 MeV/u |
| Electrical beam current | 1.76 e mA · A/q |
| Transv. tune depression | $\leq 40\%$ |
| Beam pulse duration | 0.2 – 1.0 ms |
| Beam repetition rate | ≤ 10 Hz |
| Number of cavities | 5 |
| RF-frequency | 108.408 MHz |
| max. RF-power per cavity | 1.35 MW |
| RF-sources per cavity | 1 |
| Transv. focusing scheme | FDDF |
| Total length | 55 m |

* la.groening@gsi.de

OBSERVATION OF CURRENT-DRIVEN FEATURES OF 2.5 MeV ION BUNCH WITH COMPLETE AND EFFICIENT 5D MEASUREMENTS AT THE SNS BEAM TEST FACILITY*

K. Ruisard[†], A. Aleksandrov, S. Cousineau, A. Hoover, A. Zhukov
 Oak Ridge National Laboratory, Oak Ridge, TN 37830, USA

Abstract

The SNS Beam Test Facility (BTF) research program is focused on detailed studies of beam distributions for medium-energy ion beams, with the goal of reconstructing realistic 6D bunch distributions to enable halo prediction. For complete characterization of the initial distribution, scan time scales exponentially with scan dimension. Currently, a full 6D measurement with about 10 points across most dimensions requires 24 hours. However, measurement of the 5D distribution $f(x, x', y, y', w)$ can be done very rapidly using a hybrid slit/screen method. This approach requires approximately 4 hours to obtain at least 32 points/dimension, with very high resolution (0.5 keV) in the energy distribution. This presentation reports on the approach and results for 5D characterization of the initial RFQ-formed bunch. This includes higher-resolution views of previously reported transverse-longitudinal dependence and additional interplane dependencies that were not previously reported.

INTRODUCTION

Precise, predictive modeling of high current hadron beams is difficult, due to the complexity of accelerator systems. This complexity is a result of beamline elements, as well as the beam distribution itself. This complexity limits model accuracy. Model/measurement discrepancies are often attributed to incomplete knowledge of the initial beam distribution (e.g., [1]). Work at the Spallation Neutron Source (SNS) Beam Test Facility (BTF) is focused on directly mapping the 6D distribution of the bunched beam after the RFQ. The goal of this work is to enable predictive modeling of downstream beam distributions with halo.

Full and direct 6D measurement allows reconstruction of a realistic, fully-correlated phase space without imposing assumptions on the shape of the distribution. The feasibility of 6D measurement was demonstrated in Ref. [2]. More recently, high resolution measurements in a 5D phase space allow more detailed views of the space-charge driven correlations in the BTF H^- bunch.

MEASUREMENT APPROACH

A detailed description of the BTF is available in Ref. [3]. The system consists of an RF-driven H^- ion source, 65 keV LEBT and 402.5 MHz radiofrequency quadrupole (RFQ),

* Notice: This manuscript has been authored by UT-Battelle, LLC, under contract DE-AC05-00OR22725 with the US Department of Energy (DOE).

[†] ruisardkj@ornl.gov

all identical to the components in the SNS front-end. This is followed by a 2.5 MeV MEBT (medium energy transport). This MEBT is much longer than the SNS design, contains no re-bunching cavities, and includes a 4 meter, 9.5-cell FODO line consisting of permanent magnet quadrupoles.

The BTF is equipped for full-and-direct measurement of the 6D phase space distribution $f(x, x', y, y', \phi, w)$. The 6D apparatus is described in Ref. [2]. To summarize here, the measurement apparatus consists of 3 vertical slits, a 90-degree dipole, 1 horizontal slit and a bunch shape monitor with a horizontal wire for secondary electron emission. In order to fully map the 6D space, the 4 slits and 1 wire are scanned in a 5D grid pattern. For each coordinate in 5D space, the phase distribution $f(\phi)$ is measured instantaneously using a camera and viewscreen in the bunch shape monitor.

This is an inherently lengthy measurement, as a rectilinear scan with n points per dimension will record roughly n^5 data points. (Only roughly, because one slit is "flying" and the number of points recorded during a pass varies). A recent 6D measurement on a $10 \times 10 \times 32 \times 10 \times 258 \times 12$ grid in (x, x', y, y', ϕ, w) coordinates required 24 hours of measurement time for beam at 5 Hz. Due to the high dimensionality, if the data rate were doubled the resolution would only improve by 15%.

Reducing scan dimension is a much more effective method to increase resolution. The geometry for a 5D phase space measurement is shown in Fig. 1. Here, 3 slits and a viewscreen are used to map the distribution $f_{5D} = \int d\phi f(x, x', y, y', \phi, w)$. Because this measurement takes advantage of both viewscreen axes, a 3D scan can make a complete mapping of the 5D space with n^3 data points. Holding duration fixed and increasing scan resolution, a 5D scan should have $n^{\frac{2}{3}}$ times more points per dimension. The

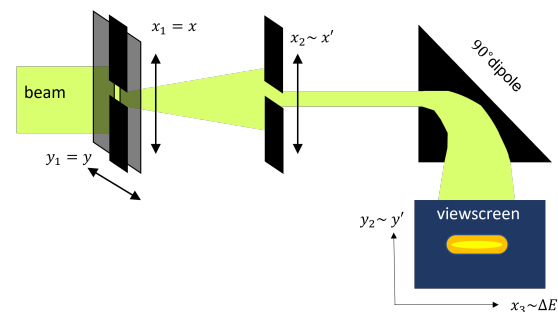


Figure 1: Geometry of 5D measurement apparatus, reproduced from Ref. [4].

NEW INJECTION BEAMLINE FOR TRIUMF CYCLOTRON*

Marco Marchetto[†], R. A. Baartman, Y. Bylinskii, P. E. Dirksen, M. Ilagan, O. Law, R. E. Laxdal, S. Saminathan, V. A. Verzilov, V. Zvyagintsev, TRIUMF, Vancouver, Canada
B. Dos Remedios¹, UBC, Vancouver, Canada ¹also at TRIUMF, Vancouver, Canada
P. M. Jung², UVic, Victoria, Canada ²also at TRIUMF, Vancouver, Canada

Abstract

The TRIUMF ion source and injection system beamline is used to transport the 300 keV H⁻ beam from the ion source to the injection into the 500 MeV cyclotron. The vertical section of the beamline, upgraded in 2011, is very robust and reliable, while the horizontal section, now 50 years old, is very demanding in maintenance, and it presents a high risk of downtime due to ageing. The horizontal beamline is being re-designed with well-proven optical concepts, and modern UHV technologies already used in the vertical section, and in the ARIEL RIB transport system; this will produce a more efficient system that is easier to maintain and tune. The beamline will use electrostatic optical modules like matching, periodic, and 90-degree achromatic bend sections; updated elements include bunchers, a high-energy pulser, a 5:1 selector, and a new set of diagnostics. A crucial aspect of the new beamline is a magnetic shield, to compensate the cyclotron's stray field, comprised of a μ -metal in-vacuum liner allowing HV feedthroughs and diagnostics insertion without breaking the shield's continuity. The new injection beamline will be controlled via EPICS. This paper presents the status of the project.

INTRODUCTION

The ion source and injection system is an electrostatic beamline that transports a 300 keV H⁻ beam from the ion source terminal to the injection point, the inflector, of TRIUMF 500 MeV cyclotron [1]. At the moment a single ion source terminal, I1, is in operation since 1974, while a second terminal, I2, is being developed. One of the project requirements is having the capability of feeding the H⁻ beam into the new transport section from two redundant terminals.

The beamline, from the ion source terminal to the inflector, is divided into a horizontal and a vertical section for practical purposes. The vertical section of the beamline was upgraded and commissioned in 2011 [2, 3], and, since then, it operates very reliably. The horizontal beamline, which still is the original installation, needs to be updated as well since it requires significant routine maintenance, and it presents a high risk of downtime due to ageing equipment (optics, diagnostics, vacuum, etc.). The overall layout of the new horizontal installation is represented in Fig. 1.

The re-design is taking advantage of the recent experience with the ARIEL RIB transport system [4], which is also a complex of electrostatic beamlines. New technologies are

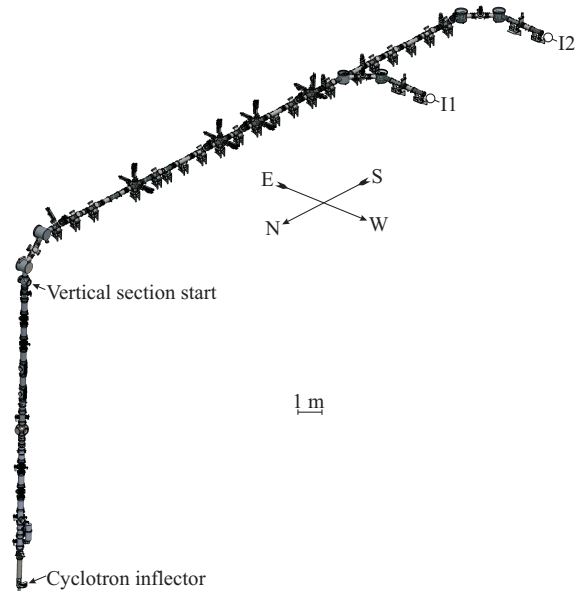


Figure 1: New injection beamline 3D model (including existing vertical section).

to be adopted including metal seals (ConFlat[®] flanges), and ultra-high vacuum (UHV) materials and assembly procedures in order to reach a lower pressure (10^{-8} Torr) with respect to the present installation, and hence reduce beam losses due to residual gas interaction.

The new injection beamline is planned to be controlled via EPICS like all the ISAC/ARIEL accelerator systems. The vacuum system of the present installation has already been migrated to EPICS. It is foreseen though that some cross talking with the original Central Control System (CCS) will still be necessary to exchange information and/or interlock signals from the cyclotron.

BEAM OPTICS

Basic beam transport requirements for the horizontal injection beamline are specified in table 1.

The injection beamline consists of electrostatic optics modules such as periodic sections, 90-degree achromatic bend sections and matching sections. The electrostatic optical elements (quadrupole, bender and steerer) have been modelled in OPERA[®] to calculate the realistic electric fields to be used in the beam dynamics simulations.

The ion beam transport calculations have been performed for the given beamline layout (see figure1) at the I1 and I2 injection terminals. The position of the ion source at I1

* Funded under a contribution agreement with NRC (National Research Council Canada)

[†] marco@triumf.ca

MODEL COUPLED ACCELERATOR TUNING WITH AN ENVELOPE CODE*

O. Shelbaya[†], R. Baartman, O. Kester, S. Kiy, S.D. Rädle, TRIUMF, V6T 2A3 Vancouver, Canada

Abstract

Frequent linac re-tuning is needed at TRIUMF-ISAC for the delivery of rare isotope beams at a variety of mass-to-charge ratios and beam energies. This operation is of appreciable complexity due to the nature of the accelerator, consisting of a separated function, variable output energy DTL paired with an RFQ. Reference tunes, computed from a variety of beam and accelerator simulation codes, are scaled according to the beam properties, though changing beam parameters at the sources requires manual tuning of matching section quadrupoles. Using an end-to-end envelope model of the machine in the code TRANSOPTR, these tunes can now be rapidly computed, and using beam diagnostic inputs to reconstruct the beam matrix, the model can be used to dynamically re-optimize the machine tune on-line.

INTRODUCTION

Unlike multiparticle (ray-tracing) simulations, which treat beam envelopes as emergent quantities, the infinitesimal transfer matrix approach is better suited for optimization of the ion-optics settings needed to configure the machine for optimum beam quality. At TRIUMF-ISAC, the heavy-ion post-accelerator which drives nuclear science investigations, consists of an RFQ-DTL pair, which can be configured at a variable output energy, for a range of $2 \leq A/q \leq 6$, shown in Fig. 1. By its design, this machine is constantly being re-tuned to produce the various requested beam properties by the network of experiment stations it services. To date, the operational tuning methodology has called for the manual establishment of reference machine configurations, whose optics settings are in turn scaled for mass and charge. Though this is informed by beam simulations, it is a decidedly empirical tuning approach. As the demands upon the apparatus have increased, thanks to a competitive and highly subscribed experiment schedule, the overhead time associated with empirical machine tuning have become difficult to sustain.

This has motivated the development of a full model of the ISAC linac in the envelope code TRANSOPTR[1], which is now capable of performing start to end envelope simulations and constrained optimizations. The lightweight nature of the computation means that full machine optimizations can be done in roughly one minute, using a conventional pc. In turn this enables the writing of software which performs start-to-end optics optimizations, by locally isolating groups of 4 to 6 parameters such as quadrupoles, or any element representable by an analytic Hamiltonian. Recent beam devel-

opment investigations have aimed to use a parallel envelope simulation, fed with real-time machine setpoints and using information on the beam distribution obtained from diagnostic readings. The envelope code is then used to compute optimized tunes, subject to user defined constraints upon the beam or transfer matrices, with setpoints then loaded back into the accelerator on-line. This interplay between apparatus and simulation is the premise for model coupled accelerator tuning, now under development at TRIUMF.

ENVELOPE MODEL

TRANSOPTR tracks a reference particle in a sliding Frenet-Serret frame, with trajectory s . Particles in this frame are located as $\mathbf{X} = (x, P_x, y, P_y, z, P_z)$. The beam distribution is represented through its covariance matrix σ ; The evolution of the rms size of the beam depends on the linear components of the forces[2]. Over a small displacement ds , σ transforms through the infinitesimal transfer matrix $\mathbf{M} = \mathbf{I} - \mathbf{F}ds$, and \mathbf{I} is the identity. This connects to the Hamiltonian via $\mathbf{M}' = \mathbf{F}\mathbf{M}$. The matrix $\mathbf{F}(s) = \mathbf{J}\mathbf{H}(s)$, where \mathbf{J} is the elementary symplectic matrix and $\mathbf{H}(s)$ is the Hessian matrix of the s -independent Hamiltonian. The continuous evolution of σ along the trajectory is given by the envelope equation:

$$\frac{d\sigma}{ds} = \mathbf{F}(s)\sigma + \sigma\mathbf{F}(s)^T. \quad (1)$$

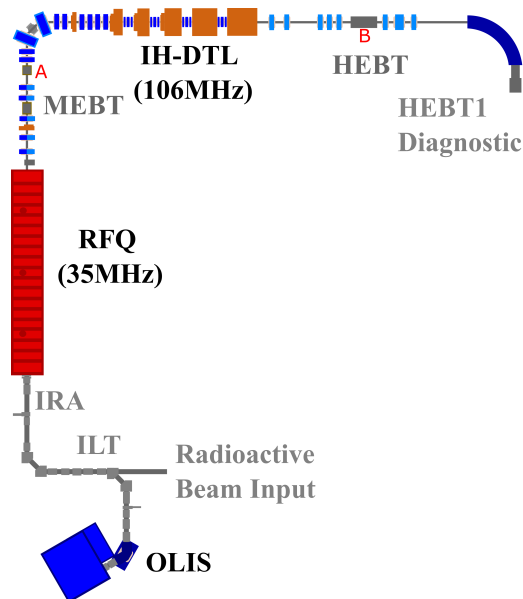


Figure 1: Overview of the ISAC-I component of the rare isotope beam (RIB) postaccelerator at the TRIUMF-ISAC facility. Stable pilot beams are provided by the OffLine Ion Source (OLIS). Movable stripping foils located at A & B.

* Funded under a contribution agreement with NRC (National Research Council Canada).

[†] oshelb@triumf.ca

CAVITY FAILURE COMPENSATION STRATEGIES IN SUPERCONDUCTING LINACS

A. Plaçais*, F. Bouly†

Univ. Grenoble Alpes, CNRS, Grenoble INP‡, LPSC-IN2P3, Grenoble, France

Abstract

RF cavities in linear accelerators are subject to failure, preventing the beam from reaching its nominal energy. This is particularly problematic for Accelerator Driven Systems (ADS), where the thermal fluctuations of the spallation target must be avoided and every fault shall be rapidly compensated for. In this study we present LightWin. This tool under development aims to create a database of the possible cavity failures and their associated compensation settings for a given accelerator. We apply it on the MYRRHA ADS, with a scenario including various faults distributed along the accelerator, and compare the settings found by LightWin to those found by the code TraceWin. We show that both tools find different compensation settings. We also outline the limitations of LightWin and explain the upcoming improvements.

INTRODUCTION

The efficiency, availability and reliability of particle accelerators is an important issue for high power linacs. In particular, accelerator-driven systems (ADS) have very stringent beam availability requirements. Their principal application is the transmutation of long-lived radioactive waste into shorter-lived fission products. To this end, they provide a continuous high-energy proton beam that subsequently produces a neutron flux thanks to a spallation target [1]. Repeated beam interruptions affect the ADS availability and sustainability: thermal stress, long restart procedures among others [2]. As an illustration, the Multi-purpose Hybrid Research reactor for High-tech Applications (MYRRHA) shall not exceed ten beam interruptions longer than three seconds per three-month operating cycle [3].

Consequently, such ADS machines require a robust linac design, to operate with margins and provide a large longitudinal acceptance. Mitigation strategies have been implemented to anticipate failure of RF cavities and their associated systems [4]. In such situations, the other cavities may be re-tuned to compensate for the malfunctioning ones [5]. The new tunings must achieve the same beam energy and must limit the increase in emittance. Plus, they must be set in a very short amount of time.

In the first Section, we introduce LightWin, a tool under development to rapidly find compensation settings. In the second Section, we present the results obtained by using LightWin to calculate multiple failure scenarios in the MYRRHA linac. The last Section is dedicated to the review

of LightWin as well as to the compensation strategies and optimisation algorithm that should be implemented in the future.

PRESENTATION OF LIGHTWIN

Several beam dynamics codes enabling to find compensation settings already exist, such as TraceWin [6]. They have been used and validated by the accelerators community for several years. However, they are multi-purpose and thus are not particularly optimised for compensation. In addition, there is only a limited choice for numerical solvers and methods. Thus, we have been developing a tool called LightWin, dedicated to finding cavity failure compensation tunings and revising the work presented in [7]. It aims at providing precise retuning settings as fast as possible and is focused on the longitudinal beam dynamics description (envelope mode). It uses 1D RF field map and space charge effects are neglected as for now. LightWin uses the same linac description file format as TraceWin, and was designed to be used in combination with TraceWin for the 3D studies. LightWin is implemented in Python, and the most time-consuming routines are implemented in Cython.¹

Computation of the beam and linac properties

The compensation process starts by the calculation of the energy and phase of the synchronous particle as well as of the longitudinal transfer matrix components, in absence of any fault (*nominal* linac).

Compensation zone

The second step is the set up of the compensation zone around every fault; it encompasses all the cavities to be retuned, all other cavities remaining untouched. It is the *local* compensation process – in the *global* compensation process, all the cavities after the faults are rephased. The global method should be less demanding in terms of RF power margins. However, it requires that a high number of cavities are rapidly rephased.

When two compensation zones overlap, the corresponding faults are fixed together. It corresponds in particular to the situation where a full cryomodule fails. When the scenario involves several faults, they are fixed in sequential manner starting from the linac entry. The choice of the number of compensating cavities per fault is up to the user. If a lattice period includes a least one compensating cavity, all other cavities of the lattice period will be compensating too. Fig. 1 represents the compensation zone strategy we adopted in this study.

¹ <https://cython.org>

* placais@lpsc.in2p3.fr

† bouly@lpsc.in2p3.fr

‡ Institute of Engineering Univ. Grenoble Alpes

BEAM DYNAMIC SIMULATIONS FOR THE DTL SECTION OF THE HIGH BRILLIANCE NEUTRON SOURCE

S. Lamprecht*, M. Droba, K. Kümpel, O. Meusel, N. Petry, H. Podlech¹, M. Schwarz, C. Zhang²
IAP, Goethe University Frankfurt, Frankfurt am Main, Germany

¹also at Helmholtz Research Academy Hesse for FAIR (HFHF), Frankfurt, Germany

²GSI Helmholtzzentrum für Schwerionenforschung GmbH, Darmstadt, Germany

Abstract

As various experimental reactors in Europe are already or will be decommissioned over the next years, new neutron sources will be necessary to meet the demand for neutrons in research and development. The High Brilliance Neutron Source is an accelerator driven neutron source planned at the Forschungszentrum Jülich. The accelerator will accelerate a proton beam of 100 mA up to an end energy of 70 MeV, using normal conducting CH-type cavities. Due to the high beam current, the beam dynamics concept requires special care. In this paper, the current status of the beam dynamics for the drift tube linac is presented.

OVERVIEW HBS, REQUIREMENTS AND BOUNDARY CONDITIONS

The HBS drift tube linac [1] will accelerate the 100 mA proton beam coming out of the MEBT2 section with an energy of 2.5 MeV up to an end energy of 70 MeV using CH-type normal conducting cavities [2]. The top level requirements and most important parameters of the HBS linac can be found in Table 1.

Table 1: General Parameters and Top Level Requirements for the HBS Linac

| Design Parameters | Value |
|----------------------|-----------------|
| Input energy | 2.5 MeV |
| End energy | 70 MeV |
| Beam current | 100 mA |
| Particles | Protons |
| Resonance frequency | 176.1 MHz |
| Number of cavities | 45 |
| Peak beam power | 7 MW |
| Average beam power | 336 kW |
| Duty cycle (beam/RF) | 4.8 / 10 % |
| Beam pulse length | 167/667 μ s |

The beam dynamics concept is carefully chosen to keep the emittance growth along the beam line as low as possible, which is the most challenging aspect concerning the beam dynamics calculations, due to the high beam current and the resulting space charge forces involved. Furthermore the linac is designed to accelerate the beam as efficient as possible, minimizing the number of cavities, required equipment and infrastructure.

* lamprecht@iap.uni-frankfurt.de

Three rebunching cavities will provide longitudinal focussing, while the transversal focussing lattice consists of quadrupole triplets installed between the cavities.

It can be observed that at low energies, the longitudinal phase spread of the beam will increase in the drift after an accelerating cavity to an extent so that the longitudinal acceptance of the next cavity would have to be much to high for efficient acceleration. Therefore, the three rebunchers are necessary to guarantee efficiency and stability. Another conclusion from this observation is that the distance between cavities should be kept as short as possible. Therefore, the lengths and transversal geometry of the quadrupole triplets are chosen to be identical and as short as technically feasible.

However, there are further boundary conditions concerning the feasibility of the parts. The length of the cavities should not exceed 1.5 m and the maximum magnetic field strength of the quadrupole lenses should be 1.2 T. All beam dynamics calculations have been performed with LORASR [3], a beam dynamics code developed at the IAP, Frankfurt, Germany.

AUTOMATION OF CALCULATION USING PARTICLE SWARM OPTIMIZATION

The high number of cavities naturally leads to a high number of free parameters for the beam dynamics concept. Therefore the beam dynamics calculations for the HBS DTL section have been largely automated using python programmes. For optimization of the beam dynamics layout, particle swarm optimization (PSO) has been chosen. This optimization algorithm has several advantages: It does not use gradients. This is necessary when optimizing beam dynamics, because one can not assume that a chosen cost function is differentiable. Furthermore, it is possible to parallelize the calculation of the candidate solutions in one iteration, which saves an considerable amount of time.

A particle swarm optimization algorithm which supports multithreading has been coded in python. The parameters to be optimized are the cavity phases and the magnetic field strengths of the lenses. The candidate solutions are fed to several instances of LORASR run in batch mode and calculated on different cores of the processor at the same time. The results are read out and the cost function is calculated. The python code runs over a fixed number of cavities at once, after which it moves automatically on to the next cavities. This way, creating the beam dynamics concept for the HBS

HARMONIC BUNCH FORMATION AND OPTIONAL RFQ INJECTION

E. Sunar *, U. Ratzinger, M. Syha and R. Tiede
Institute of Applied Physics, Goethe University, Frankfurt, Germany

Abstract

With the aim of reduced beam emittances, a pre-bunching concept into an RFQ or a DTL has been developed. The structure has been designed by using a two harmonics double drift buncher which consists of two bunchers: the first one is driven by a fundamental frequency whereas the other is excited with the second harmonic including a drift in between. This well-known "Harmonic Double-Drift-Buncher" is reinvestigated under space charge conditions for RFQ, cyclotron, and for direct DTL-injection. There are significant benefits for this design such as to catch as many particles as possible from a dc beam into the longitudinal linac acceptance, or to reduce/optimize by up to an order of magnitude the longitudinal emittance for low and medium beam currents. In accordance to these advantages, a new multi-particle tracking beam dynamics code has been developed which is called "Bunch Creation from a DC beam - BCDC". In this paper we present this new code and some stimulating examples.

INTRODUCTION

A source generates continuous particle beams, which need to be bunched before injection into the main part of an rf accelerator. This task can be performed either by a stand alone buncher cavity or by an RFQ. Both alternatives must fulfill certain design requirements like high transmission rates combined with low beam emittance. RFQs are common bunch forming systems. However, harmonic bunchers especially for low and medium current proton and ion beams at linac injection have also some potentials at special requirements like providing really small longitudinal emittance or a shorter length than the RFQ. Besides of this, the RF power need of a buncher cavity is in general much smaller than for an RFQ, which leads to an attractive, cost efficient alternative. Multi harmonic buncher systems have already been used at Argonne ANL-ATLAS [1] and by many others like FRIB at MSU in East Lansing [2, 3]. Based on the existing experience, we developed a two-harmonics double drift buncher (DDHB) scheme including a compact transverse focusing concept. In this paper, the DDHB concept as well as a new code for multi-particle tracking, BCDC, are explained briefly and an optimized example obtained by this new tool is presented in detail. The motivation of the development for the new beam dynamics code is the detailed study of the space charge action during bunch formation.

CONCEPT OF DOUBLE DRIFT HARMONIC BUNCHING SYSTEM

The ideal energy modulation is achieved by a saw-tooth waveform. A saw-tooth signal of amplitude V_{st} leads to

* sunar@iap.uni-frankfurt.de

the following energy spread when starting with a mono-energetic and continuous beam:

$$\Delta W_i = q \cdot V_{st} \cdot \frac{\Delta \phi_i}{\pi} \quad (1)$$

As seen in the formula, there is a linear dependence between the particles' energy ΔW_i and its relative phase, $\Delta \phi_i$. However, generating a direct saw-tooth waveform is not possible due to incapability of power electronics with current technologies. An approximate saw-tooth voltage can be obtained with a combination of a sine-wave and its superposition of higher harmonics. One option is to overlap the fundamental and the higher harmonics in one buncher cavity at one location, which mathematically corresponds to the Fourier analysis of the sawtooth [4]. However, the technical realization of such multi-harmonic bunchers (e.g. by combination of two or three $\lambda/4$ resonators [1]) is quite ambitious. Instead of that, the DDHB concept [5] adopted in our proposal is to use two bunching cavities each operated at one harmonic frequency (f or $2f$) and separated by a drift space L_1 , as schematically shown in Fig. 1. The length L_2 serves as an additional parameter for a longitudinal beam focus at the position $z = L_1 + L_2$.

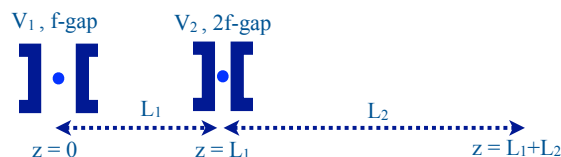


Figure 1: Schematic of the DDHB with four specific parameters.

In the simplified model as shown in Fig. 1, the first buncher cavity operated at the fundamental frequency f and the synchronous phase -90 deg is located at position $z = 0$ and has the gap voltage V_1 . This pure sinusoidal signal leads to the following energy variation for an initially mono-energetic and continuous beam [6]:

$$\Delta W_i(\Delta \phi_i(0)) = q \cdot V_1 \cdot \sin(\Delta \phi_i(0)) \quad (2)$$

Along the drift L_1 between the buncher cavities only the relative particle phases $\Delta \phi_i$ are transformed due to the energy modulation of the beam, described by the following formula (with beam current effects neglected):

$$\Delta \phi_i(L_1) = \Delta \phi_i(0) - \frac{\omega L_1}{\beta_s^3 \gamma_s^2 c} \cdot \frac{\Delta W_i(\Delta \phi_i(0))}{W_s} \quad (3)$$

The effect of the second accelerating gap at double harmonic $2f$ with a synchronous phase of $+90$ deg is given as:

$$\Delta W_i(\Delta \phi_i(L_1)) = \Delta W_i(\Delta \phi_i(0)) - q \cdot V_2 \cdot \sin(2\Delta \phi_i(L_1)) \quad (4)$$

END-TO-END SIMULATIONS AND ERROR STUDIES OF THE J-PARC MUON LINAC

Y. Takeuchi*, J. Tojo, T. Yamanaka, Kyushu University, Fukuoka, Japan
Y. Nakazawa, H. Iinuma, Ibaraki University, Ibaraki, Japan
Y. Kondo, R. Kitamura, T. Morishita, JAEA, Ibaraki, Japan
E. Cicek, H. Ego, K. Futatsukawa, N. Kawamura, M. Otani,
T. Yamazaki, M. Yoshida, T. Mibe, N. Saito, KEK, Ibaraki, Japan
Y. Iwashita, Kyoto University, Osaka
Y. Sue, K. Sumi, M. Yotsuzuka, Nagoya University, Nagoya, Japan
Y. Sato, Niigata University, Niigata, Japan
H. Yasuda, University of Tokyo, Tokyo, Japan

Abstract

A muon linac is under development for future muon g-2/EDM experiments at J-PARC. The linac provides a 212 MeV muon beam to an MRI-type compact storage ring. After the initial acceleration using the electrostatic field created by mesh and cylindrical electrodes, the muons are accelerated using four types of radio-frequency accelerators. To validate the linac design as a whole, end-to-end simulations were performed using General Particle Tracer. In addition, error studies is ongoing to investigate the effects on beam and spin dynamics of various errors in the accelerator components and input beam distribution. This paper describes the preliminary results of the end-to-end simulations and error studies.

INTRODUCTION

Muon g-2 is arguably one of the most important observables in modern particle physics. The long-standing existence of anomalies of more than three standard deviations between experimental values of muon g-2 measured by Brookhaven National Laboratory (BNL) [1] and the Standard Model (SM) predictions [2] has attracted many physicists, who believe that they suggest the existence of new physics beyond the SM. Recently, Fermilab's experimental group improved BNL's experimental equipment and new experiment now running in a similar method. The first result of the group was consistent with the previous experiment, and the discrepancy between the average of the two experiments and the SM prediction was updated to 4.2σ [3]. As a result, there is even more hope for the discovery of new physics. However, since the two experiments were performed using the same experimental method, it is very important to confirm the discrepancy by measuring with another new technique. Therefore, to verify the discrepancy, an experiment using a completely different method from the two previous experiments is being planned at the Japan Proton Accelerator Research Complex (J-PARC).

The J-PARC experiment aims to measure the muon g-2 with a precision of 0.1 ppm [4]. To reduce the muon beam-

derived systematic uncertainties that have dominated previous experiments, in this experiment, a beam obtained by accelerating low-emittance muons produced by laser ionization of muonium is required. In addition, to reduce decay loss, the muons must be accelerated in a time sufficiently shorter than the muon lifetime of $2.2 \mu\text{s}$. The linear accelerator was our choice because it is efficient in this respect. For highly efficient acceleration, muons are accelerated from thermal energy to relativistic energy using four RF structures, depending on the beam velocity. Figure 1 shows the configuration of the muon linac. The muon linac starts with an ultra-slow muon source which generates a muons by the laser ionization of thermal muonium with an extremely small momentum of 3 keV/c (kinetic energy $W=25$ meV). The generated muons are accelerated to 5.6 keV by electrostatic field and injected to a radio frequency quadrupole (RFQ). The acceleration is performed up to 0.34 MeV by a 324 MHz RFQ. Then, the energy of the muon beam is boosted to 4.5 MeV with a 324 MHz interdigital H-type drift tube linac (IH-DTL). Following the IH-DTL, a 1296 MHz disk-and-washer coupled cell linac (DAW CCL) structures are used to accelerate to 40 MeV. Finally, the muons are accelerated from 40 MeV to 212 MeV by using a 2592 MHz disk-loaded traveling wave structure (DLS). Details of the linac design are described in this separate paper [5].

Considering the injection of accelerated muon beams into the storage ring, beam parameters such as emittance and momentum spread at the exit of linac are important factors, since they directly affect the efficiency of injection into the storage ring. The exact muon beam parameters required for the experiment are currently being investigated in detail, but the results of the latest injection simulation studies suggest that a beam quality at the end of linac with a transverse rms emittance of $\sim 0.3 \pi$ mm mrad and a rms momentum spread of $\sim 0.04\%$ are desirable. Hereafter, in this study, these values will be used as reference values to evaluate beam parameters. The muon spin properties are also very important because they can be a source of systematic errors in this experiment. Therefore, it is necessary to fully understand how properties such as spin polarization and spin-momentum correlation, which is the correlation be-

* takeuchi@epp.phys.kyushu-u.ac.jp

BEAM DYNAMICS FOR THE MAX IV TRANSVERSE DEFLECTING CAVITY BEAMLINE

N. Blaskovic Kraljevic*, L. Isaksson, E. Mansten, S. Thorin, MAX IV Laboratory, Lund, Sweden

Abstract

The MAX IV 3 GeV linac delivers electron beams to two synchrotron rings and to a dedicated undulator system for X-ray beam delivery in the Short Pulse Facility (SPF). In addition, there are plans to use the linac as an injector for a future Soft X-ray Laser (SXL). For both SPF and SXL operations, longitudinal beam characterisation with a high temporal resolution is essential. For this purpose, a transverse deflecting cavity (TDC) system has been developed and is being installed in a dedicated electron beamline branch located downstream of the 3 GeV linac. This beamline consists of two consecutive 3 m long transverse S-band RF structures, followed by a variable vertical deflector dipole magnet used as an energy spectrometer. This conference contribution presents the beam dynamics calculations for the beam transport along the TDC beamline, and in particular the optics configurations for slice emittance and slice energy spread measurements. The operation of an analysis algorithm for use in the control room is discussed. The aim is to provide 1 fs temporal measurement resolution to access the bunch duration of highly compressed bunches and slice parameters for sub-10-fs bunches.

INTRODUCTION

The MAX IV light source in Lund, Sweden, consists of a 3 GeV electron linac, a 1.5 GeV storage ring and a 3 GeV storage ring [1]. The linac is used both as an injector for the two storage rings and as a source of short electron pulses for the Short Pulse Facility (SPF). The linac has also been designed as an injector to a future Soft X-ray Laser (SXL) [2].

For both SPF and SXL operations, longitudinal beam characterisation with a high temporal resolution is critical. For this purpose, a transverse deflecting cavity (TDC) system has been installed in a new, dedicated electron beamline branch located downstream of the 3 GeV linac. This TDC beamline (Fig. 1), which will be commissioned with beam in the coming months, contains two consecutive TDCs (TDC1 and TDC2), each of which is a 3 m long transverse RF structure operated at the zero crossing of the 2.9985 GHz linac RF. The TDC structures have been manufactured by Research Instruments (Fig. 2); further details of the RF design can be found in [3]. Initially, the deflecting TM_{110} mode will streak the beam horizontally, but, in the future, adjustment of the RF signal phases fed to the TDC structures will allow both horizontal and vertical beam streaking [4].

The TDC structures are followed by a variable vertical deflector dipole magnet, to be used as an energy spectrometer, deflecting the beam vertically down by 0° , 2.8° or 5.6° into three distinct beamline branches as shown in Fig. 1.

* neven.blaskovic_kraljevic@maxiv.lu.se

The beamline also contains five quadrupoles (QH) for optics control, five stripline beam position monitors (BPL), five horizontal and five vertical corrector magnets (COBXX and COBYY, respectively) for trajectory correction and ten insertable YAG screens (SCRN) as shown in Fig. 1.

BEAMLINE OPTICS

The optics through the TDC beamline has been optimised, using the beam tracking code elegant [6], for the end-of-line screens (SCRN9 and SCRNI0 in Fig. 1).

Beta Function

The horizontal beta function is maximised at the mid-point of the TDC structures (Fig. 3) in order to maximise the imparted horizontal kick [2], whilst the beta function is minimised both horizontally and vertically at the end-of-line screens to have a beam that is fully contained on the screen. For aperture considerations, the maximum beta function is limited to 1000 m throughout the TDC beamline.

Phase Advance

In order to maximise the horizontal deflection imparted by the TDC structures [2], as viewed on SCRNI9, the horizontal phase advance from the mid-point of the TDC structures to SCRNI9 has been optimised at $\frac{\pi}{2}$ (Fig. 4).

The TDC beamline will be used to perform beam emittance measurements by scanning the strength of quadrupole QH2 and measuring the vertical beam size at SCRNI9. In order to maximise the change in vertical beam size at SCRNI9 over the QH2 strength scan, the optimum vertical phase advance from QH2 to SCRNI9 is set to $\frac{\pi}{2}$.

As the beam will be streaked horizontally by the TDC structures, the optimum horizontal phase advance from QH2 to SCRNI9 is π in order to minimise the effect of the change in QH2 strength on the horizontal beam properties at SCRNI9.

SCREEN IMAGES

A beam consisting of 200 000 particles has been tracked along the full MAX IV linac and the TDC beamline using the code elegant [6]. Figure 5 shows the beam intensity on SCRNI9, with the TDC and spectrometer magnet both off.

Figure 6 shows the result of turning the TDC on. The colour-coding shows the particle arrival time, and the relationship between the horizontal beam coordinate and time is clear as expected.

Turning the TDC off, but turning the spectrometer magnet on, displays the energy structure of the beam, where the vertical position on the screen is correlated to the energy offset (Fig. 7).

BEAM LOADING SIMULATION FOR RELATIVISTIC AND ULTRARELATIVISTIC BEAMS IN THE TRACKING CODE RF-TRACK

J. Olivares^{*1,2}, A. Latina¹, N. Fuster², B. Gimeno², D. Esperante²
¹ CERN, Geneva, Switzerland

² Instituto de Física Corpuscular (IFIC), CSIC-University of Valencia, Paterna (Valencia), Spain

Abstract

Medical and industrial electron linacs can benefit from the X-band accelerating technology developed for the Compact Linear Collider (CLIC) at CERN. However, when high-intensity beams are injected in such high-gradient structures (>35 MV/m), the beam loading effect must be considered by design since this beam-cavity interaction can result in a considerable gradient reduction with respect to the unloaded case. Studying energy conservation, a partial differential equation (PDE) has been derived for injected beams in both the relativistic and ultrarelativistic limits. Making use of this, a specific simulation package within RF-Track has been developed, allowing realistic tracking of charged particle bunches under this effect regardless of their initial velocity. The performance of this tool has been assessed by reproducing previously obtained beam-loaded fields in CLIC main linac and CLIC Drive-Beam linac structures. In this paper, we present the analytic PDE derivation and the results of the tests.

INTRODUCTION

Accelerating cavities exhibit an ohmic response when electromagnetic waves travel through the structure, leading to energy losses. Furthermore, when a beam of charged particles enters the accelerating structure, it excites the cavity, and such excitation diminishes the stored energy and thus the accelerating gradient. This is called beam loading effect [1].

Previous attempts to model the beam loading effect rely on simplifications of the structure and beam properties. The most general analytic study is reference [2], which describes the beam-loading effect in arbitrary structures and shows that this interaction beam-cavity follows a transient model. However, [2] is limited to the ultrarelativistic case and focuses on the structure gradient rather than its implementation in a tracking routine.

So far, the way of performing tracking under this effect was using a beam-loaded precomputed field obtained from finite-difference solvers such as HFSS. This approach presents the inconvenience of being both computationally demanding and static, i.e. no transient behaviour can be retrieved.

To design a quick, flexible and non-ultrarelativistic tool to study the beam loading effect, the starting point is deriving a PDE describing the energy conservation in such a general scenario. Its numerical solution will be implemented in RF-Track, allowing tracking under the beam loading effect.

* javier.olivares.herrador@cern.ch

PDE THEORETICAL DERIVATION

Energy Conservation in Accelerating Structures

Instantaneous energy conservation can be studied starting from the differential version of Poynting's theorem [3]:

$$-\frac{\partial u(\mathbf{r}, t)}{\partial t} = \nabla \cdot \mathbf{S}(\mathbf{r}, t) + \mathbf{E}(\mathbf{r}, t) \cdot \mathbf{J}(\mathbf{r}, t), \quad (1)$$

where:

- u is the volumetric electromagnetic energy density stored in the accelerating cavity, defined in terms of the electric (\mathbf{E}) and magnetic (\mathbf{H}) fields as:

$$u(\mathbf{r}, t) = \frac{1}{2} \epsilon_0 \|\mathbf{E}(\mathbf{r}, t)\|_{\mathbb{R}^3}^2 + \frac{1}{2} \mu_0 \|\mathbf{H}(\mathbf{r}, t)\|_{\mathbb{R}^3}^2 \quad [\text{J/m}^3], \quad (2)$$

with ϵ_0 the electric permittivity and μ_0 the magnetic permeability in vacuum (empty cavity).

- \mathbf{S} is the Poynting vector defined as $\mathbf{S} = \mathbf{E} \times \mathbf{H}$. Its flux takes into account power flow (P_{flow}) and dissipation (P_{diss}) along the structure as it has been reported in [3]. In an arbitrary volume bounded by a surface \mathcal{S} , its flux can be described as:

$$P_{\text{total}}(z, t) = \oint_{\mathcal{S}} \mathbf{S}(z, t) \cdot d\mathbf{S} = P_{\text{diss}}(z, t) + P_{\text{flow}}(z, t). \quad (3)$$

- \mathbf{J} is the current density flowing along the structure, defined in terms of the volumetric charge density λ_q and the particle's velocity \mathbf{v} as:

$$\mathbf{J}(\mathbf{r}, t) = \lambda_q(\mathbf{r}, t) \mathbf{v}(\mathbf{r}, t) \quad [\text{A/m}^2]. \quad (4)$$

Accelerating Gradient

The main quantity whose evolution is aimed to be studied is the effective accelerating gradient, defined as the average electric field that affects a particle. In a given cell of length L located at position z , it can be described as:

$$G_{\text{eff}} = \frac{1}{L} \text{Re} \left[\int_z^{z+L} \tilde{E}_z(\zeta, t) e^{j\omega t_q(\zeta, t_0, \beta(\zeta, t, t_0, \beta_0))} d\zeta \right] \quad [\text{V/m}], \quad (5)$$

with ω the RF angular frequency, $j = \sqrt{-1}$ the imaginary unit, and t_q the time of flight of a particle with charge q entering the structure at a time t_0 , calculated as [4]:

$$t_q(z, t_0, \beta(z, t, t_0, \beta_0)) = t_0 + \int_0^z \frac{d\zeta}{\beta(\zeta, t, t_0, \beta_0)c} \quad [\text{s}]. \quad (6)$$

Here, c refers to the speed of light and β to the ratio of v to c , which evolves with the particle's energy gain.

A START-TO-END OPTIMISATION STRATEGY FOR THE CompactLight ACCELERATOR BEAMLINE

Y. Zhao*, A. Latina, CERN, Geneva, Switzerland

A. Aksoy¹, Ankara University, Ankara, Turkey

H. M. Castaneda Cortes, D. Dunning, N. Thompson

ASTeC and Cockcroft Institute, STFC Daresbury Laboratory, Warrington, United Kingdom

¹also at CERN, Geneva, Switzerland

Abstract

The CompactLight collaboration designed a compact and cost-effective hard X-ray FEL facility, complemented by a soft X-ray option, based on X-band acceleration, capable of operating at 1 kHz pulse repetition rate. In this paper, we present a new simple start-to-end optimisation strategy that is developed for the CompactLight accelerator beamline, focusing on the hard X-ray mode. The optimisation is divided into two steps. The first step improves the electron beam quality that finally leads to a better FEL performance by optimising the major parameters of the beamline. The second step provides matched twiss parameters for the FEL undulator by tuning the matching quadrupoles at the end of the accelerator beamline. A single objective optimisation method, with different objective functions, is used to optimise the performance. The sensitivity of the results to jitters is also minimised by including their effects in the final objective function.

INTRODUCTION

As the fourth and latest generation of synchrotron light source, free-electron-laser (FEL), can produce extremely high brightness radiation, based on linear electron accelerators and undulators. The CompactLight collaboration designed an X-ray FEL facility that is innovative, compact and cost effective, and recently published the Conceptual Design Report (CDR) [1]. In order to significantly reduce the cost and increase the efficiency of the facility, the design aims to bring together recent advances in many of the important technical systems that make up an X-ray FEL.

To meet the requirements from the user community that spreads across a multitude of scientific and engineering disciplines, the facility is supposed to be operated with a large flexibility, with different combinations of soft X-ray (SXR) and hard X-ray (HXR) operating modes, at high and low repetition rates. Two separate FEL beamlines are developed for this purpose:

1. A SXR FEL light source with wavelengths ranging from 5.0 nm to 0.6 nm (0.25 keV to 2 keV) with up to 1 kHz repetition rate.
2. A HXR FEL light source with wavelengths ranging from 0.6 nm to 0.08 nm (2 keV to 16 keV) with maximum 100 Hz repetition rate.

* yongke.zhao@cern.ch

The configuration and operation of the CompactLight FEL are proposed in three stages, including a baseline option and two upgrade options. The baseline configuration satisfies the majority of the user requirements, being able to generate two synchronised photon pulses in Self-Amplified Spontaneous Emission (SASE) mode [2], with either 250 Hz SXR or 100 Hz HXR. Upgrade-1 increases the SXR repetition rate to 1 kHz by using additional klystron power supplies for the accelerating structures while the average RF power is kept constant. Upgrade-2 allows the simultaneous generation of SXR and HXR FEL pulses at 100 Hz.

The required main parameters of the CompactLight FEL are summarised in Table 1. To achieve a good FEL performance and simplify the FEL design, some extra requirements are also considered in the optimisation, such as small transverse shears or offsets (in x, y, x', y') so that the beam centroid is steered on longitudinal axis.

Table 1: Main Parameters of the CompactLight FEL

| Parameter | Unit | SXR | HXR |
|--------------------------|---------|------------|----------|
| Electrons | | | |
| Beam energy | GeV | 0.97–1.95 | 2.75–5.5 |
| Peak current (minimum) | kA | 0.35–0.925 | 1.5–5 |
| RMS sliced energy spread | % | 0.02 | 0.01 |
| RMS sliced emittance | mm-mrad | 0.2 | |
| Bunch charge | pC | 75 | |
| Photons | | | |
| Photon energy | keV | 0.25–2 | 2–16 |
| Wavelength | nm | 5–0.6 | 0.6–0.08 |
| Repetition rate | Hz | 250–1000 | 100 |

This report presents an optimisation of the accelerator beamline for the HXR mode at the highest beam energy of 5.5 GeV. The beamline to be optimised is displayed in Fig. 1.

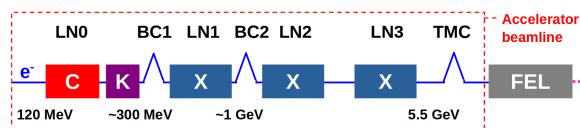


Figure 1: Schematic layout of the beamline to be optimised.

LN0 is Linac-0, consisting of 6 C-band structures, located downstream of a laser heater (LH) and upstream of a K-band lineariser. BC1 and BC2 are magnetic bunch compressors. LN1–3 are Linac-1 to Linac-3, all composed of X-band structures. The designed input beam energy for the optimised

THE PSI POSITRON PRODUCTION PROJECT

N. Vallis^{1,*}, B. Auchmann², P. Craievich, M. Duda, H. Garcia-Rodrigues, J. Kosse, M. Schaer, R. Zennaro, Paul Scherrer Institut, 5232 Villigen PSI, Switzerland

¹also at EPFL, Lausanne, Switzerland

²also at CERN, Geneva, Switzerland

Abstract

The PSI Positron Production project (P³ or P-cubed) is a demonstrator for a novel positron source for FCC-ee. The high current requirements of future colliders can be compromised by the extremely high positron emittance at the production target and consequent poor capture and transport to the damping ring. However, recent advances in high-temperature superconductors allow for a highly efficient matching of such an emittance through the use a solenoid around the target delivering a field over 10 T on-axis. Moreover, the emittance of the matched positron beam can be contained through large aperture RF cavities surrounded by a multi-Tesla field generated by conventional superconducting solenoids, where simulations estimate a yield higher by one order of magnitude with respect to the state-of-the-art. The goal of P³ is to demonstrate this basic principle by implementing the aforementioned solenoids into a prototype positron source based on a 6 GeV electron beam from the SwissFEL linac, two RF capture cavities and a beam diagnostics section.

INTRODUCTION

The Future Circular Collider (FCC) study group published in 2019 a Conceptual Design Report for an electron-positron collider (FCC-ee) with a centre-of-mass energy from 90 to 365 GeV and a beam current up to 1.4 A [1]. This high current requirement depends largely upon an injector complex (see Fig. 1) consisting of two separate sources and linacs for electrons and positrons up to 1.54 GeV, a damping ring (DR) to cool the positron emittance and a common linac up to 6 GeV [2].

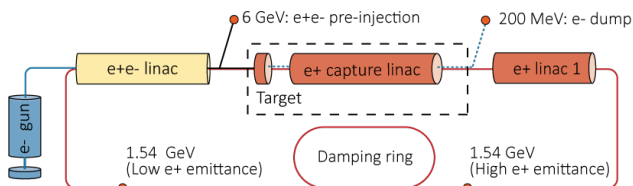


Figure 1: Latest proposal for the FCC-ee Injector Complex.

The principle method for positron production at FCC-ee is based on a 6 GeV electron beam impinging a 17.5 mm-thick (or 5X₀) amorphous W target, which generates a positron yield around 13 N_{e+}/N_{e-} at the target exit [3]. However, the extremely high emittance and energy spread of the secondary distribution can lead to poor capture rates, compromising the yield of positrons accepted at the DR. The state-of-the art for

* nicolas.vallis@psi.ch

a similar positron source is that of the SuperKEKB factory, allowing for 0.5 N_{e+}/N_{e-}, based on a 3.2 GeV electron drive beam with a bunch charge of 10 nC [4]. By contrast, the FCC-ee injection requires yield of 1 N_{e+}/N_{e-} at the DR, plus a safety factor of 2 in the design [5].

The PSI Positron Production project (P³ or P-cubed) was proposed as a demonstrator for a novel solution for the FCC-ee positron source and capture linac. The baseline design of P³ (see Fig. 2) consists of an adiabatic matching device (AMD) based on high-temperature superconducting (HTS) solenoids surrounding the target with a max. field on-axis of 12.7 T and two standing-wave (SW) capture RF cavities in S-band with a large iris aperture of 20 mm radius surrounded by conventional superconducting solenoids with a max. 1.5 T field on-axis. A beam diagnostics section will provide the first experimental estimations of the positron yield, which according to simulations is expected to improve the SuperKEKB record by one order of magnitude.

P³ will use a 6 GeV drive electron beam generated at the SwissFEL linac. On the one hand, SwissFEL can provide the desired beam energy and transverse size with extreme precision. On the other hand, due to the radioprotection limitations at SwissFEL, the drive beams of P³ and FCC-ee show substantial differences regarding bunch charge and time structure (see Table 1). This results in a significantly lower radiation load in the P³ target, excluding any thermo-mechanical studies from the scope of the experiment.

Table 1: Main Drive Linac Parameters

| | FCC-ee | P ³ (SwissFEL) |
|-----------------------|--------------------------|---------------------------|
| Energy [GeV] | | 6 |
| $\sigma_{x,RMS}$ [mm] | | 0.5 - 1.0 |
| Q_{bunch} [nC] | 0.88 - 1.17 ¹ | 0.20 |
| Repetition rate [Hz] | 200 | 1 |
| Bunches per pulse | 2 | 1 |

¹Based on 5.0 - 5.5 nC requirements at booster ring and preliminary yield estimations of 4.7 - 5.7 N_{e+}/N_{e-}.

KEY TECHNOLOGY

HTS Adiabatic Matching Device

HTS solenoids will be used to deliver a peak on-axis field of 12.7 T around the target in order to match the extremely high positron emittance. This technology can lead to significantly higher yields with respect a conventional, normal-conducting flux concentrator (FC) [6]. The solenoids will be implemented with non-insulated ReBCO tape, which does

EMITTANCE MEASUREMENT FROM THE PROTON TESTBEAM AT KAHVELab

D. Halis*, T. B. Ilhan, Yildiz Technical University, Istanbul, Türkiye
 A. Adiguzel, S. Esen, S. Oz, Istanbul University Istanbul, Türkiye
 S. Aciksoz, V. E. Ozcan, Bogazici University Istanbul, Türkiye
 H. Cetinkaya, Dumlupınar University Kutahya, Türkiye
 A. Kilicgedik, Marmara University Istanbul, Türkiye
 S. Ogur, Université Paris-Saclay, CNRS/IN2P3, IJCLab, Orsay, France
 N. G. Unel, University of California (UCI), California, USA

Abstract

A test beam using a Radio Frequency Quadrupole (RFQ) operating at 800 MHz, to accelerate a 1.5mA proton beam to 2 MeV energy has been designed, manufactured and is currently being commissioned at KAHVELab, Istanbul. The beam from the microwave discharge ion source (IS) must be matched to the RFQ via an optimized Low Energy Beam Transport (LEBT) line. The LEBT line consists of two solenoid magnets, two steerer magnets and a beam diagnostics station named MBOX. All the beamline components are locally designed, simulated manufactured and tested with local resources. The MBOX should be able to measure the beam current and profile, as well as the beam emittance, to ensure an accurate match between IS and RFQ. It includes a number of diagnostic tools: a Faraday Cup, a scintillator screen, and a pepper pot plate (PP). An analysis software is developed and tested for the PP photo analysis. This contribution will present the proton beam-line components and will focus on the MBOX measurements, especially on the PP emittance analysis.

This study is supported by Istanbul University Scientific Research Commission Project ID 33250 and TUBITAK Project no: 119M774.

INTRODUCTION

The proton beamline at KAHVELab consists of an ion source, a low energy beam transport (LEBT) section and a radio frequency quadrupole (RFQ). A simplified schema of the proton beamline can be seen in Fig. 1 [1].

The ion source consists of 3 sections: a transmission line to transfer 2.45 GHz microwaves from magnetron to the plasma chamber, a plasma chamber where ions are produced and an extraction system which transfers ions from plasma chamber to the beam line for a current of about 1.5 mA.

In this 140 cm LEBT line, there are two water-cooled solenoid magnets with the same physical dimensions and designs, different number of turns, two identical steerer magnets and a measurement box (MBOX). The sensors in the MBOX are moved into and out of the beam line by means of pneumatic motors. The solenoids are used to focus the beam to fit into the RFQ acceptance, and steerers are used

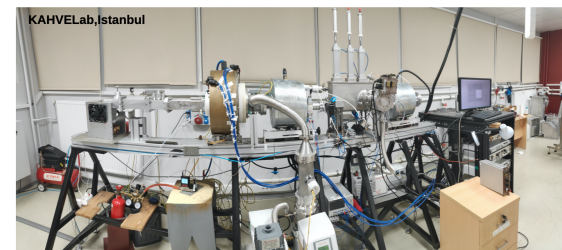
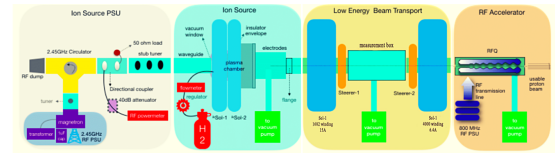


Figure 1: The schematic (Top) and the picture (Bottom) for the Proton test beam line at KAHVELab.

to direct the beam into the reference line of the RFQ. Simulation studies were carried out with DemirciPRO [2] and in-house software in Python3 [3] to optimize the solenoid positions and fields.

The MBOX vacuum chamber is designed and manufactured to keep the vacuum volume as small as possible, with a wall thickness of 5 mm and a polygonal geometry of $369 \times 130 \times 215$ mm from stainless steel alloy material. The MBOX upper cover houses the pneumatic controls. One can see the design of the system in Fig. 2. MBOX is used to measure the beam profile, beam spread, and the beam current. The Pepper Pot method is used for emittance measurement as it allows measuring beam emittance, both the X and Y components at once, simultaneously [4].

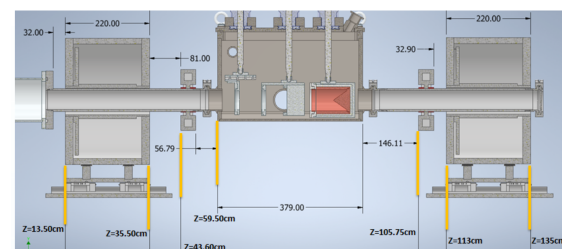


Figure 2: LEBT line components and their positions.

The simulated data taken at the exit location of the ion source was generated via IBSIMU program. Simulated with

* duygu17.dh@gmail.com

THE DESIGN OF THE FULL ENERGY BEAM EXPLOITATION (FEBE) BEAMLINE ON CLARA

D. Angal-Kalinin, A. R. Bainbridge, J. K. Jones, T. H. Pacey, Y. M. Saveliev, E. W. Snedden
ASTeC, STFC Daresbury Laboratory, UK

Abstract

The CLARA facility at Daresbury Laboratory was originally designed for the study of novel FEL physics utilising high-quality electron bunches at up to 250 MeV/c. To maximise the exploitation of the accelerator complex, a dedicated full energy beam exploitation (FEBE) beamline has been designed and is currently being installed in a separate vault on the CLARA accelerator. FEBE will allow the use of high charge (up to 250 pC), moderate energy (up to 250 MeV), electron bunches for a wide variety of accelerator applications critical to ongoing accelerator development in the UK and international communities. The facility consists of a shielded enclosure, accessible during beam running in CLARA, with two very large experimental chambers compatible with a wide range of experimental proposals. High-power laser beams (up to 100 TW) will be available for electron-beam interactions in the first chamber, and there are concrete plans for a wide variety of advanced diagnostics (including a high-field permanent magnet spectrometer and dielectric longitudinal streaker), essential for multiple experimental paradigms, in the second chamber. FEBE will be commissioned in 2024.

INTRODUCTION

The Compact Linear Accelerator for Research and Applications (CLARA) is an ultra-bright electron beam test facility being developed at STFC Daresbury Laboratory. CLARA has been designed to test advanced Free Electron Laser (FEL) schemes that could be later implemented on existing and future short wavelength FELs, such as a UK XFEL.

CLARA is being constructed in stages: Phase 1 was completed in 2018 and consisted of the CLARA Front End: electron bunch production at 50 MeV, 100 pC at 10 Hz. Bunch charge up to 250 pC was achieved from the upgraded gun at 10 Hz with a hybrid Cu-photocathode. Design and commissioning of the CLARA Front End is detailed in Reference [1]. Phase 2 is currently under construction, and elevates the beam to 250 MeV/c, 250 pC at 100 Hz. A novel 100 Hz photo-injector gun [2] is currently being commissioned on the Versatile Electron Linear Accelerator (VELA)[3], situated adjacent to CLARA, and will be swapped over to the CLARA line when fully characterised. Phase 3 will allow installation of an FEL, seeding laser and modulators along with associated photon diagnostics. Phase 3 of CLARA is not yet funded.

During the construction of CLARA, in Phases 1 and 2, access to electron beams at ~ 35 MeV/c was made available to users from academia and industry. This enabled the testing of novel concepts and ideas in a wide range of disciplines, including development of advanced accelerator

technology, beam diagnostics, medical applications and novel particle beam acceleration and deflection concepts [4]. Based on increasing user demand for access to the CLARA high brightness electron beam, a decision was made to design and build a dedicated beamline for user applications at the full CLARA beam momentum of 250 MeV/c.

The FEBE beamline is being built to transport 250 MeV/c beam to a dedicated hutch area, containing two experimental chambers, for user access. As a key component of the design, the hutch will be accessible without switching off the accelerator, allowing users to set up and access their experiments as required. The total beam power within the hutch is limited to ~ 6 W, which offers sufficient flexibility with available bunch charge (maximum 250 pC), bunch repetition rate (maximum 100 Hz) and beam momentum (up to 250 MeV/c).

The interaction of high-quality electron bunches with high instantaneous power laser light (>100 TW) is foreseen as a key component of the FEBE beamline exploitation, and will enable research in novel acceleration areas including LWFA, PWFA and dielectric laser acceleration (DLA). Beams accelerated inside the hutch can be accommodated up to 2 GeV/c.

FEBE DESIGN

The top-level overview of the CLARA and FEBE beamlines is shown in Fig. 1. The FEBE experiment hutch is a large ($10 \times 5.4 \times 3 \text{ m}^3$), shielded, and versatile area for performing electron beam exploitation experiments. Within the hutch, the beam transport is designed to deliver a strong focusing interaction point (IP) at two locations. Each IP is located within a large-volume ($\sim 2 \text{ m}^3$) vacuum experiment chamber.

A double-IP design is used to enable flexibility in experimental design and implementation, with most experiments having experimental apparatus situated in the first FEBE experimental chamber (FEC1) and diagnostics and other monitoring equipment situated in the second chamber (FEC2). A high power laser co-propagates with the electron beam to a common focus (IP1) in FEC1, with this capability included through a dedicated laser mirror box chamber (FMBOX1) upstream of the first experiment chamber, and a second mirror box (FMBOX2) between chambers to extract the laser following interaction.

The experimental hutch is connected to the main CLARA accelerator using a series of FODO arc cell structures optimised for minimal CSR emittance growth. The FEBE transverse offset is achieved using four 14° dipoles, which enables both sufficient space for an FEL seeding chicane, and fits within the existing CLARA shielding.

BEAM DYNAMICS FRAMEWORK INCORPORATING ACCELERATION USED TO DEFINE THE MINIMUM APERTURE OF RF CAVITY FOR FODO-LIKE FOCUSING SCHEME FOR PROTON RADIOTHERAPY LINAC

M. Southerby^{1,2*}, R. Simson^{1,2}

¹Lancaster University, Bailrigg, Lancaster, LA1 4YR, UK

²Cockcroft Institute, Daresbury Laboratory, Warrington, WA4 4AD, UK

Abstract

In this paper, we present a generalised analytical framework for beam dynamics studies and lattice designs, while incorporating longitudinal acceleration of bunches of charged particles. We study a ‘FODO-like’ scheme, whereby we have an alternating array of focusing and defocusing quadrupoles and study how this differs from a standard FODO lattice due to acceleration. We present optimisation techniques to provide quadrupole parameters, cavity lengths, and required drift lengths under different constraints.

particle Lorentz factor, γ_r , increases linearly in an RF cavity from $z = 0$ to $z = L_{cav}$ a transverse phase space map for an RF cavity can be shown to take the form of Eq. (1)

$$\begin{pmatrix} x_1 \\ x'_1 \end{pmatrix} = \begin{pmatrix} 1 & l_{cav} \frac{\gamma_{r0}\beta_{r0}}{\gamma_{r1}-\gamma_{r0}} \ln \left(\frac{\gamma_{r1}\beta_{r1}+\gamma_{r0}}{\gamma_{r0}\beta_{r0}+\gamma_{r1}} \right) \\ 0 & \frac{\gamma_{r0}\beta_{r0}}{\gamma_{r1}\beta_{r1}} \end{pmatrix} \begin{pmatrix} x_0 \\ x'_0 \end{pmatrix} \quad (1)$$

where β_{r0}/β_{r1} is the normalised longitudinal velocity of a particle before/after the cavity. The determinant of this map is non-unit and therefore it is non symplectic. A bunch of particles in phase space occupying an area, A , will not be a constant of motion along a cavity [3].

INTRODUCTION

In the recent decades improvements in particle accelerator technology and understanding have allowed a surge in applications to medicine. Two areas to have benefited from such improvements are cancer Radiotherapy and Medical imaging [1, 2]. An important figure of merit of a single RF cell is the shunt impedance, which wants to be maximised. A common method to increase shunt impedance for a given frequency is to reduce the beam aperture. The beam aperture can not be reduced indefinitely as peak surface fields, coupling requirements and most importantly, beam losses, limit the aperture radius. The premise of this paper is to calculate the minimum beam aperture that can be realised with respect to beam losses in a FODO-like scheme factoring in longitudinal acceleration. An accelerating RF cavity map is produced to allow for longitudinal acceleration of protons. Space-charge effects and electromagnetic field effects are ignored. The Twiss parameter mapping matrix is redefined to account for the increase in energy as a proton beam passes through a cavity. The mapping matrix as a function of the betatron phase advance, μ is also redefined to be consistent with increasing momentum. The method implemented minimises the beta function, β , at the cavity entrance and exit in order to maximise beam acceptance transversely.

The Twiss matrix defines the evolution of the Twiss parameters [4] β, α, γ from some point in a system. The matrix elements are strictly a function of the transfer map between the two points. Considering a system of maps where the only non-symplectic map is a cavity map, the Twiss matrix takes the form of Eq. (2).

The phase advance of a beam element represents the increase in the action angle variable of a particle. Normalising the transverse phase space ellipse using the normalising matrix will produce a phase space circle with the same area. The phase advance can be described as the rotation angle around the phase space circle. A transfer map of an element can, in general, be written as a function of the phase advance. When a cavity map is part of a beam line the total transfer map accumulates an additional term due to acceleration and takes the form shown in Eq. (3).

HALF-FODO CELL

The aim of this paper is to provide the quadrupole magnet strength and length such that the beam size is minimised at the cavity entrance for a FODO-like scheme.

The starting point of this scheme assumes that we at a point where α_x is 0 in the x transverse direction and β_x is at an extremal. We are free to define $\beta_x = \text{maximum}$. It is convenient to fix the transverse y beam dynamics to be minimum at this exact point: $\alpha_y = 0, \beta_y = \text{minimum}$. Our starting point is therefore some point in a focusing quadrupole of length l_{q1} and k-strength k_1 . We can produce the Twiss parameters at any point in a half-FODO cell, such as the cavity entrance, as well as the Twiss parameters at the end of the half-FODO at which point $\alpha_x = \alpha_y = 0$. A schematic of a half-FODO cell is shown in Fig. 1.

TRANSVERSE BEAM DYNAMIC RESULTS WITH ACCELERATION

RF Cavity Map

Consider a particle traveling along the z axis and that $p_x \ll p_z$. If the particle is given a longitudinal kick, p_x is unchanged ad p_z increases by δp_z . If it is assumed the

* m.southerby@lancaster.ac.uk

THE IMPACT OF BEAM LOADING TRANSIENTS ON THE RF SYSTEM AND BEAM BREAKUP INSTABILITIES IN ENERGY RECOVERY LINACS

S. Setiniyaz^{1,2*}, R. Apsimon^{1,2}, M. Southerby^{1,2}, and P. H. Williams²

¹Engineering Department, Lancaster University, Lancaster, UK

²Cockcroft Institute, Daresbury Laboratory, Warrington, UK

Abstract

In multi-turn Energy Recovery Linacs (ERLs), the filling pattern describes the order that which bunches are injected into the ERL ring. The filling patterns and recombination schemes together can create various beam loading patterns/transients, which can have a big impact on the RF system, namely the cavity fundamental mode voltage, required RF power, and beam breakup instability. In this work, we demonstrate one can lower the cavity voltage fluctuation and rf power consumption by carefully choosing the right transient by using an analytical model and simulation.

INTRODUCTION

Recirculating Energy Recovery Linac (ERL) is a promising technology as it combines the high brightness of conventional linacs with the high average powers of the storage rings. Unlike conventional linacs, the used bunches are not deposited directly, but rather decelerated in accelerator cavities [1], and their kinetic energy (KE) is recovered as the RF field energy of the cavities. As a result much less RF power is required to operate the ERLs compared to conventional linacs.

The accelerating and decelerating bunches in the multi-turn ERL can be grouped differently [2] to form various beam loading transients (or patterns) as shown in the examples in Fig. 1. The red/blue circles are accelerated/decelerated bunches and the number indicates their turn number. The sub-figure (a) shows a beam loading pattern where 3 accelerated bunches are followed by 3 decelerated bunches, while (b) shows accelerating and decelerating bunches come alternatively. In a 6-turn (3 accelerating and 3 decelerating) ERL, 6 bunches form a bunch packet, and many of these packets fill up the ring.

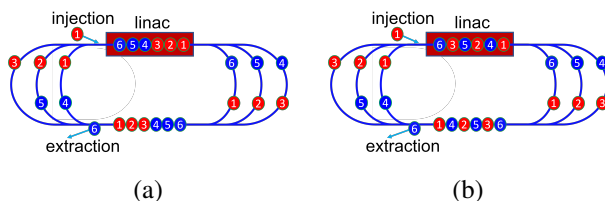


Figure 1: Beam loading patterns: (a) {123456} and (b) {142536}.

We will show one can minimize cavity voltage fluctuations and required RF power by carefully selecting the right beam loading patterns [3]. Lower cavity voltage fluctuations

* s.setiniyazi@lancaster.ac.uk

would improve beam stability and lower required RF power would reduce the energy consumption of the ERL. This has significant implications on beamline design as the beam loading patterns are determined primarily by the beamline topology and bunch recombination schemes.

BEAM LOADING PATTERNS

Beam loading patterns can be of two types depending on whether the bunches change their RF buckets. Generally, bunches are injected in every x RF cycle, and we refer to this x RF cycle as one RF bucket (or one intra-packet block). If the bunches don't change their RF buckets, the turn order in the bunch packet changes turn by turn, and we refer to this as the First In First Out (FIFO) scheme. In this scheme, bunches are injected into different RF buckets in every turn, which would require a complicated bunch injector with variable injection intervals. Currently, ERLs use various recombinations to maneuver the bunches between different RF buckets to maintain the bunch orders so we will refer to this as Sequence Preserving (SP) scheme. Recombination is achieved through path-length-differences to delay bunches differently, as can be seen in Fig. 1.

For FIFO schemes, the beam loading pattern changes turn by turn, so it is convenient to describe FIFO schemes by their filling pattern, which describes their filling order. We will use square brackets to indicate filling patterns. For example, filling pattern [123456] would describe the 1st bunch is injected to the 1st RF bucket, 2nd bunch is injected to the 2nd bucket, and so on so forth. Filling pattern [142536] would describe the 1st bunch is injected to the 1st RF bucket, 2nd bunch is injected to the 3rd bucket, and so on so forth. The number in the bracket is the bunch number, which describes the injection order. The index in the bracket is the RF bucket number.

In SP patterns, however, it is convenient to use beam loading patterns to describe them as the beam loading pattern does not change. We will use curly brackets to indicate beam loading patterns. For example, beam loading pattern {142536} would describe the 1st bunch passing through the cavity is at the 1st turn, the 2nd bunch is at 4th turn, and so on so forth. The number in the bracket is a bunch turn number, which describes the injection order. The index in the bracket is the RF bucket number.

If we call 1st bunch's RF bucket as the 1st RF bucket, for a N -turn ($N/2$ up and $N/2$ down turns) ERL, there are $(N - 1)!$ permutations of patterns. Therefore, there are 120 FIFO filling patterns and SP beam loading patterns for a 6-turn ERL. The pattern number i is used to indicate 120

INVESTIGATION OF THE BEAM PROPAGATION THROUGH THE FNAL LEBT*

Daniel C. Jones[†], Daniel Bollinger, Valery Kapin, Kiyomi Seiya
 Fermi National Accelerator Laboratory, 60510 Batavia, USA

Abstract

The Fermi National Accelerator Laboratory (FNAL) Pre-accelerator send 25 mA H⁺ beam with a 30 μs pulse length at 15Hz. The machine's uptime was increased in 2012 by the replacement of the Cockcroft Walton Accelerator with a Radio Frequency Quadrupole (RFQ) system to take the 35 keV beam from the ion source to 750 keV. The initial beam transmission efficiency from the ion source to the entrance of the Drift Tube LINAC (DTL) was 47%; however, the transmission efficiency has decreased over the last 10 years to 40% with no clear explanation. To better understand the cause of this reduction in transmission efficiency a vertically movable beam scraper was installed between the first two solenoids allowing the beam size to be investigated in the middle of the Low Energy Beam Line (LEBT). Utilizing this new diagnostic system in addition to the Ion Source R&D Laboratory's emittance probes the approximate emittance and beam size were able to be inferred. This experimental data was able to further inform our simulations and a more complete picture of the beams propagation through the LEBT has come into focus. The new simulations show the beam's spot size and emittance is to large for the RFQ's acceptance.

INTRODUCTION

The H⁺ injector for the FNAL LINAC was upgraded and has been in operation since 2012 as part of the Proton Improvement Plan that aimed to increase the proton flux in booster to 2.3 x 10¹⁷ protons per hour. The new design consisted of an ion source, a Low Energy Beam Transport (LEBT) that matches the beam to a 4-rod Radio Frequency Quadrupole (RFQ), and a Medium Energy Beam Transport (MEBT) that injects into the drift tube LINAC [1]. The transmission efficiency from the ion source to the start of the LINAC is approximately 40% which is significantly lower than expected. Previous studies looking at the transmission efficiency focused on the MEBT and other beam line qualities [2]. Recent data exploring the possibilities that the LEBT is the main cause of the inefficiency are presented in this paper.

EXPERIMENTAL SETUPS

FNAL LINAC Injector

Figure 1 displays the FNAL 750 keV injector line. Prior to the 2021 shutdown the only beam diagnostic elements

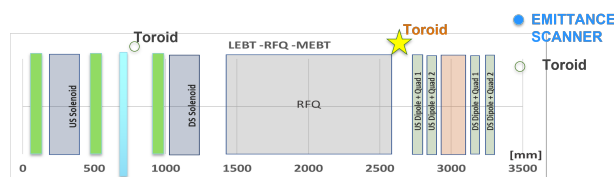


Figure 1: FNAL 750 keV injector line. The light blue line between the solenoids is the vertical beam scraper. The yellow star is where the MEBT toroid was placed during the 2021 shutdown period.

within the injector were a toroid in the LEBT and the toroid and emittance probes at injection into Tank 1 of the LINAC. In order to obtain more information about the beam two more diagnostic elements were used for this research. The MEBT toroid, the yellow star, was installed during the 2021 shutdown for a brief study period but had to be removed for the 2021-2022 run for the laser notcher re-installation. The vertical beam scraper, light blue line, was installed for the 2021-2022 run for continued diagnostics throughout the entire run.

Ion Source R&D Laboratory

The Ion Source R&D Laboratory houses a test bench which is identical to the operational LEBT through the first solenoid. After the first solenoid a set of emittance probes, located analogous to the beam scraper, were used to measure the beams transverse emittance in the middle of the LEBT.

FNAL LINAC INJECTION BEAM PROFILES

Utilizing the beam scraper in the LEBT and the emittance probes at Tank 1 beam profiles were obtained for both operational ion sources during the 2021-2022 run. Figure 2 displays several days of beam profiles within the 2021-2022 run period. The red dashed line corresponds to ion source A and the solid black line corresponds to ion source B. Ion source A displays a clear peak intensity approximately 1.5 cm above the center of the pipe. This is in stark contrast to the beam profiles of ion source B which display a much more uniform beam around the center of the pipe. This difference in beam profile was unexpected and is not easily explained.

The effect of this difference in beam profiles, between the two ion sources, appears to be minimized by the RFQ when observing the beam at the entrance to the FNAL LINAC in Fig. 3. The horizontal beam profiles delivered by ion source A, the solid black lines, tend to have a peak position closer to the center of the pipe than the beam profiles delivered by ion source B, the dashed red lines though the delivered

* Work supported by Fermilab Research Alliance, LLC under Contract No. DE-AC02-07CH11359 with the United States Department of Energy

[†] dcjones@fnal.gov

BEAM DYNAMICS STUDIES AT THE PIP-II INJECTOR TEST FACILITY *

J.-P. Carneiro[†], B. Hanna, E. Podzeyev, L. Prost, A. Saini, A. Shemyakin

Abstract

A series of beam dynamic studies were performed in 2020-2021 at the PIP-II Injector Test Facility (PIP2IT) that has been built to validate the concept of the front-end of the PIP-II linac being constructed at Fermilab. PIP2IT is comprised of a 30-keV H⁻ ion source, a 2 m-long Low Energy Beam Transport (LEBT), a 2.1-MeV CW RFQ, followed by a 10-m Medium Energy Beam Transport (MEBT), 2 cryomodules accelerating the beam to 16 MeV and a High-Energy Beam Transport (HEBT) bringing the beam to a dump. This paper presents beam dynamics - related measurements performed at PIP2IT such as the Twiss parameters with Allison scanners, beam envelopes along the injector, and transverse and longitudinal rms emittance reconstruction. These measurements are compared with predictions from the beam dynamics code Tracewin.

INTRODUCTION

The PIP-II linac is an 800 MeV, 2 mA H⁻ CW-capable superconducting (SC) linac for injection into the Booster [1]. A model of the front-end of the PIP-II linac, the PIP-II Injector Test Facility (PIP2IT), has been built at Fermilab and commissioned from Summer 2020 to Spring 2021 [2]. After a description of the PIP2IT injector, this paper presents beam dynamics measurements performed during the commissioning.

PIP2IT OVERVIEW

Figure 1 shows an overview of the PIP2IT injector. The injector is made of an ion source, a Low Energy Beam Transport (LEBT) that matches the beam into a 162.5 MHz Radiofrequency Quadrupole (RFQ), a Medium Energy Beam Transport (MEBT) that prepares the beam for injection into two SC cryomodules and a High Energy Beam Transport (HEBT) that brings the beam to a dump. The overall length of the facility is around 35 m.

The PIP2IT ion source operates at 30 kV with long pulses (typically few ms) and at 20 Hz. The beam is focused into the RFQ with 3 solenoids and, as indicated in Figure 1, a dipole is located between the first and second solenoid to deviate the beam by a 30° angle. A beam chopper is located in the LEBT between the second and third solenoid and cuts pulses of up to 0.55 ms. As indicated in [3], the LEBT operates in an original scheme. It is kept neutralized up to the middle of the second solenoid and un-neutralized downstream of the second solenoid in the portion that contains the chopper. The RFQ accelerates the beam to an energy of 2.1 MeV. The MEBT has two main purposes: first, it performs a bunch-by-

bunch selection using two kickers (that deviates the kicked beam into an absorber, as shown in Fig. 1) and, second, it matches the beam into the first cryomodule using 2 doublets, 5 triplets and 3 bunchers operating at 162.5 MHz. The first cryomodule contains 8 SC Half-Wave Resonators (HWR) cavities operating at 162.5 MHz, and the second cryomodule contains 8 Single-Spoke Resonators (SSR1) cavities operating at 325 MHz. The transverse focusing in the cryomodules is performed with 8 SC solenoids (HWR) and 4 SC solenoids (SSR1). The HEBT has 2 quads to transport the beam from the exit of the SSR1 cryomodule to the dump. Two correctors (horizontal and vertical) are associated with each solenoid, doublet and triplet. The PIP2IT injector has been designed to deliver a beam energy of 25 MeV at the dump and an average current of 2 mA (decreased from 5 mA by the MEBT kickers) at a maximum pulse length of 0.55 ms and 20 Hz.

Diagnostics

Five current monitors are installed along the PIP2IT injector: two in the LEBT (at the ion source exit and RFQ entrance), two in the MEBT (at the RFQ exit and at the HWR entrance) and one at the exit of the SSR1 cryomodule. The beam dump allows also for the monitoring of the current at the end of the injector. Each doublet and triplet of the MEBT and each solenoid in the cryomodules has an associated Beam Position Monitor (BPM). The HEBT contains also 3 BPMs. Two Allison scanners allow for vertical phase space measurements at the ion source exit and downstream the second MEBT doublet. In order to protect the injector from unexpected beam deviations, 4 sets of 4 scrapers (Vertical Top/Bottom, Horizontal Right/Left) are installed in the MEBT. The MEBT scrapers are also used to perform beam size measurements. Two Wire Scanners are installed in the HEBT which allow to perform beam size measurements in both horizontal and vertical planes. A movable BPM (Time-of-Flight, TOF) installed in the HEBT is used for energy measurement. A Fast Faraday Cup (FFC) located at the end of the HEBT is used for bunch length measurements.

Injector Settings

The first 3 HWR cavities were not operational during the commissioning of the injector because of a frequency offset for the first 2 cavities and a coupler issue with the third one. Furthermore, due to multipacting, the last 2 HWR cavities had to be operated at lower accelerating gradient than anticipated (respectively 8.5 MV/m and 8 MV/m vs. 9.7 MV/m). In order to compensate for that, the beam was longitudinally matched from the MEBT into the fourth HWR cavity by reaching a longitudinal waist at its entrance with a proper adjustment of the MEBT Bunchers.

* This work was supported by the U.S. Department of Energy under contract No. DE-AC02-07CH11359

[†] carneiro@fnal.gov

FINDING BEAM LOSS LOCATIONS AT PIP2IT ACCELERATOR WITH OSCILLATING DIPOLE CORRECTORS*

A. Shemyakin[†], Fermilab, Batavia, IL 60510, USA

Abstract

The PIP2IT accelerator was assembled in multiple stages in 2014 – 2021 to test concepts and components of the future PIP-II linac that is being constructed at Fermilab. In its final configuration, PIP2IT accelerated a 0.55 ms x 20 Hz x 2 mA H- beam to 16 MeV. To determine location of the beam loss in the accelerator's low-energy part, where radiation monitors are ineffective, a method using oscillating trajectories was implemented. If the beam is scraped at an aperture limitation, moving its centroid with two dipole correctors located upstream and oscillating in sync, produces a line at the corresponding frequency in spectra of BPM sum signals downstream of the loss point. Comparison of these responses along the beam line allows to find the loss location. The paper describes the method and results of its implementation at PIP2IT.

INTRODUCTION

The PIP-II Injector Test (PIP2IT) [1, 2] was an H⁻ ion linac modelling the front end of the PIP-II accelerator currently under construction at Fermilab [3]. In its final configuration, the PIP2IT consisted of a 30 kV, 15 mA H⁻ DC ion source, a 2 m long Low Energy Beam Transport (LEBT), a 2.1 MeV CW 162.5 MHz RFQ, a 10 m Medium Energy Beam Transport (MEBT), two cryomodules (HWR and SSR1) accelerating the beam up to 16 MeV, a High Energy Beam Transport (HEBT), and a beam dump (Fig. 1).

Beam loss inside the cryomodules was measured by comparison of the beam current read by beam current monitors (ACCT) placed at the exits of the MEBT and SSR1. This comparison indicated the beam loss in the long-pulse mode ~2%. However, such measurement could not point out to a specific location where the loss occurred. In the last days of PIP2IT run, a different method was implemented, where the Beam Position Monitor (BPM) signals were used to identify the loss location.

METHOD

The method is a development of the idea originally proposed by V. Lebedev and used in CEBAF [4]. It relies on the usually sharp dependence of the current loss on the beam position at the location of the loss. In such case, oscillating a dipole corrector current upstream of the loss location produces a signal at that frequency in BPM sum signals (intensities) downstream. Such measurement does not provide an absolute value of the loss but rather the difference in the loss over the range of the beam oscillation. While this loss variation can be low, the detection at a fix

frequency greatly improves the overall sensitivity. For sufficiently long measurement time, even oscillations with amplitude small enough to do not affect the beam emittance can result in a detectable signal.

Ref. [5] proposed to oscillate simultaneously two correctors (in one plane) to check in one measurement all locations in a beam line or linac. The initial test of the procedure is described in Ref. [6]. The proposal is to oscillate currents in two dipole correctors separated by the betatron phase advance of $\varphi_x \neq \pi n$ with a specific choice of amplitudes of resulting deflections θ_1 and θ_2 and the time phase difference φ_t (similar to Ref. [7]):

$$\theta_2 \sqrt{\beta_{x2}} = \theta_1 \sqrt{\beta_{x1}}, \quad \varphi_t = \pi + \varphi_x, \quad (1)$$

where β_{x1} and β_{x2} are betatron functions in the location of corresponding corrector. At these conditions, the deviation of the trajectory downstream is simplified to

$$x_0(z, t) = \theta_1 \sqrt{\beta_x(z) \beta_{x1}} \sin \varphi_x \sin(\omega t + \varphi_1(z)), \quad (2)$$

where $\beta_x(z)$ is the beta-function along the line. The Fourier component of BPM readings at the oscillation frequency $\omega/2\pi$ is determined by the beta-function in the BPM location, and its phase relates to the betatron phase advance $\varphi(z)$ as $\varphi_1(z) = \varphi(z) + \varphi_x$. Oscillation described by Eq. (2) move the beam around a circle in canonical phase coordinates, shifting the beam by the same portion of its rms size $\sigma_b = \sqrt{\beta_x(z) \varepsilon_0}$ everywhere along the beam line (ε_0 is the rms beam emittance).

Let's assume that the 1D current density distribution is scaled in various locations as the beam rms size:

$$j(x) = \frac{I_0}{\sigma_b} J\left(\frac{x}{\sigma_b}\right), \quad (3)$$

where I_0 is the total beam current, and $J\left(\frac{x}{\sigma_b}\right)$ is a dimensionless function, the same for all locations. If a flat scraper is inserted into the beam to the distance d from the beam center, the intercepted current I_s is modulated at the oscillation frequency:

$$\begin{aligned} I_s &= \int_d^\infty j(x - x_0) dx = \int_d^\infty j(x) dx + j(d)x_0 - \frac{dj}{dx}(d) \cdot \frac{x_0^2}{2} + \dots \approx \int_d^\infty j(x) dx + j(d)A_s \sin(\omega t + \varphi_1(z_s)) + \\ & j'(d) \cdot \frac{1}{2} (A_s \sin(\omega t + \varphi_1(z)))^2 \equiv I_{s0} + I_{s1} \sin(\omega t + \varphi_1(z_s)) + I_{s2} (1 - \cos(2 \cdot (\omega t + \varphi_1(z_s))))). \end{aligned} \quad (4)$$

where $A_s \equiv \theta_1 \sqrt{\beta_x(z_s) \beta_{x1}}$ is the trajectory oscillation amplitude at the scraper location z_s . The amplitude of the first harmonic depends only on the relative penetration of the scraper:

* This manuscript has been authored by Fermi Research Alliance, LLC under Contract No. DE-AC02-07CH11359 with the U.S. Department of Energy, Office of Science, Office of High Energy Physics
[†]shemyakin@fnal.gov

LONGITUDINAL BEAM DYNAMICS IN ARRAY OF EQUIDISTANT MULTICELL CAVITIES*

Y.K. Batygin[†], Los Alamos National Laboratory, Los Alamos, NM 87545, USA

Abstract

Linear accelerators containing the sequence of independently phase cavities with constant geometrical velocity along each cavity are widely used in practice. The chain of cavities with identical cell length is utilized within a certain beam velocity range, with subsequent transformation to the next chain with higher cavity velocity. Design and analysis of beam dynamics in this type of accelerator are usually performed using numerical simulations. In the present paper, we provide an analytical treatment of beam dynamics in such linacs. Expressions connecting beam energy gain and phase slippage along the cavity are implemented. The dynamics of the beam around the reference trajectory and matched beam conditions are discussed.

DYNAMICS IN ACCELERATING SECTION WITH EQUIDISTANT CELLS

Consider longitudinal beam dynamics in a structure with identical cells (see Figs. 1 and 2). Most of such structures in ion accelerators are π -structures with cell length $\beta_g \lambda / 2$, where β_g is the geometrical velocity and $\lambda = 2\pi c / \omega$ is the RF wavelength. Acceleration of particles in such field can be considered as dynamics in an equivalent traveling wave propagating along with the structure with constant phase velocity β_g and with amplitude $E = E_o T(\beta)$, where E_o is the average field per accelerating gap, $T(\beta)$ is the transit time factor and φ is the phase of a particle in traveling wave [1]:

$$\varphi = \omega t - \int_0^z k_z dz, \quad (1)$$

where $k_z = 2\pi / (\beta_g \lambda)$ is the wave number. The phase φ is also a phase of a particle in the standing wave at the moment of time when the particle crosses the center of the accelerating gap. Differentiation of Eq. (1) along the longitudinal coordinate z together with the equation for particle energy gain provides a set of equations for on-axis particle dynamics in traveling wave [2]:

$$\frac{d\varphi}{dz} = \frac{2\pi}{\lambda} \left(\frac{1}{\beta} - \frac{1}{\beta_g} \right), \quad \frac{d\gamma}{dz} = \frac{qE}{mc^2} \cos \varphi, \quad (2)$$

where m and q are mass and charge of particle, and $\gamma = (1 - \beta^2)^{-1/2}$ is the normalized particle energy. Equations (2) can be derived from Hamiltonian

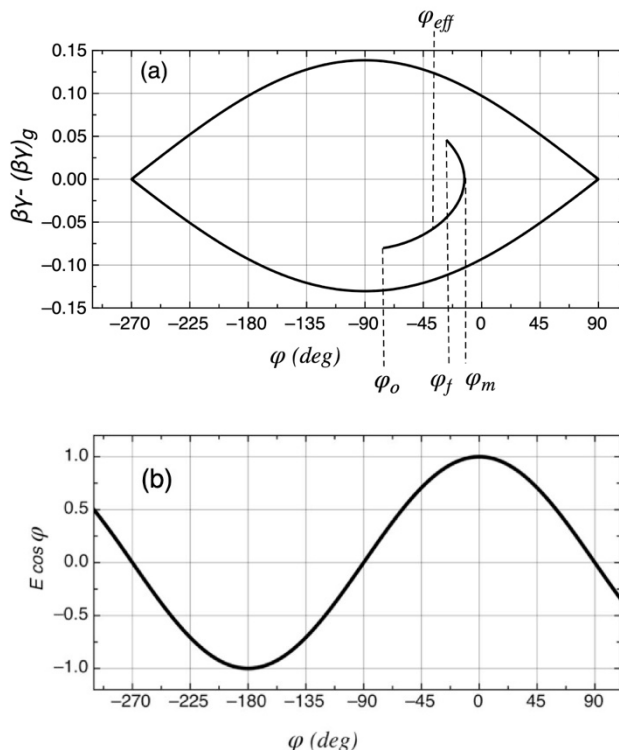


Figure 1: (a) Phase space trajectory of a particle in an RF structure with equidistant cells, (b) equivalent traveling wave with amplitude E .

$$H = \frac{2\pi}{\lambda} (\sqrt{\gamma^2 - 1} - \frac{\gamma}{\beta_g}) - \frac{qE}{mc^2} \sin \varphi, \quad (3)$$

where Hamiltonian equations are $d\gamma/dz = -\partial H / \partial \varphi$ and $d\varphi/dz = \partial H / \partial \gamma$. In the standing wave structure with identical cells, the average field per cell is constant, $E_o = const$, and variation of particle velocity along the cavity is typically small, $\Delta\beta / \beta \ll 1$, therefore, the amplitude of accelerating field can be approximated to be constant $E = E_o T(\beta) \approx const$. Because the geometrical velocity is also a constant, $\beta_g = const$, the Hamiltonian, Eq. (3), is a constant of motion. From Hamiltonian, Eq. (3), the integral of particle motion in such field, $C = H\lambda / (2\pi)$, is

$$\sqrt{\gamma^2 - 1} - \frac{\gamma}{\beta_g} - \frac{qE\lambda}{2\pi mc^2} \sin \varphi = C. \quad (4)$$

* Work supported by US DOE under contract 89233218CNA000001

[†] batygin@lanl.gov

PRELIMINARY STUDY ON THE IMPLEMENTATION OF THE ORBIT CORRECTION TO THE 100 MeV PROTON LINAC AT KOMAC

S. Lee*, H.-J. Kwon, H.-S. Kim, J.-J. Dang, D.-H. Kim, S.-P. Yun
KOMAC, Korea Atomic Energy Research Institute, Gyeongju, Korea

Abstract

At KOMAC (Korea Multipurpose Accelerator Complex), we have been operating a 100 MeV linac consisting of 11 DTLs (Drift Tube Linacs) with several BPMs (Beam Position Monitors), WSs (Wire Scanners) and SMs (Steerer Magnets) installed for the orbit correction of the proton beam. The orbit correction can be performed through the response matrix between the position measurements from the BPMs/WSs and the field strength of the steering magnets. In this work, we will show the calculated response matrix from the simulation results, and describe the detailed plans for the implementation of the orbit correction in the real linac system at KOMAC.

INTRODUCTION

The performance of the high current linac greatly depends on the alignment of the linac and the performance of the orbit correction. At KOMAC, we have a 100 MeV proton linac consisting of 11 DTLs. Using information on beam center at various BPM and WS locations in the linac, we can guide the proton beams to avoid beam loss. For this, SVD (Singular Value Decomposition) technique [1–3] is performed to calculate the steering angles to apply by building a response matrix relating between the beam centers at BPM/WS and the steering angles applied by SMs from the beam dynamics simulations. Here, we show some of the preliminary results of the orbit correction and future plans for the implementation of the orbit correction in the real system at KOMAC.

METHOD

In this section, we will describe how the orbit correction is implemented based on the beam dynamics simulation.

Layout for Beam Position Monitor, Wire Scanner and Steerer Magnet

For the orbit correction, there are 10 BPMs, 2 WSs and 8 SMs (including 3 additional SMs to be installed in future) in the linac and the dump beamline as shown in Fig. 1a. Depending upon the size of the free space, 2 types of steerer magnets, a and b are installed and also shown in Fig. 1a. The steering angle $\Delta\theta$ applied by the steerer magnet of size L and magnetic field B is given as

$$\Delta\theta = \frac{qBLc}{mc^2\beta\gamma} \quad (1)$$

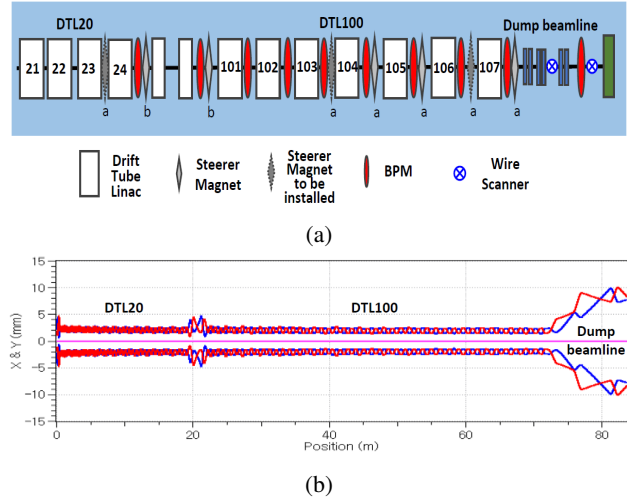


Figure 1: (a) Layout for Beam Position Monitor, Wire Scanner and Steerer Magnet. (b) Beam envelope graph shows x and y envelopes in blue and red respectively. Beam x, y centers are shown in magenta.

In Fig. 1a, we label DTL21~24 and DTL101~107 as DTL20 and DTL100 sections. Beam envelope for our 100 MeV proton linac is calculated and shown in Fig. 1b.

Scheme for Orbit Correction

The orbit correction is carried out utilizing a SVD which inverts a response matrix. We construct a response matrix, R_{ij} relating M BPMs and WSs, and N SMs used for the orbit correction of the 100 MeV proton linac,

$$R_{ij} = \frac{\Delta x_i}{\Delta \theta_j} \quad (2)$$

where x_i is beam center at i^{th} BPM and $\Delta\theta_j$ is a steering angle applied by j^{th} SM. This means that the change in the beam center by the steering angle is

$$\Delta x = R \cdot \Delta \theta \quad (3)$$

Response matrix, R can be written as a product of three matrices, U , Σ and V as

$$R = U \cdot \Sigma \cdot V^T \quad (4)$$

where U and V are $M \times M$ and $N \times N$ unitary matrix respectively. Σ is an $M \times N$ diagonal matrix with diagonal elements s . This decomposition is unique only to a certain extent, not in every case. To calculate the steering angle to apply the orbit correction,

$$\Delta\theta = R^{-1} \cdot \Delta x \quad (5)$$

* shl@kaeri.re.kr

INJECTOR SYSTEM DEVELOPMENT FOR 1 MeV/n RFQ AT KOMAC*

Han-Sung Kim[†], Jeong-Jeung Dang, Dong-Hwan Kim, Sang-Pil Yun, Seung-Hyun Lee,
Hyeok-Jung Kwon

Korea Multi-purpose Accelerator Complex/Korea Atomic Energy Research Institute,
Gyeongju, Korea

Abstract

A Radiofrequency quadrupole (RFQ) system with 200 MHz frequency and 1 MeV/n output energy is under development at KOMAC (Korea Multi-purpose Accelerator Complex) for multiple purposes such as a test-stand for an ion source and low energy beam transport study, ion beam implantation for semiconductors and polymers and neutron generation for material study. We developed an injector system for the RFQ, which is mainly composed of a 2.45 GHz microwave ion source, low energy beam transport with two solenoids and a vacuum system with diagnostic chamber. The RFQ was designed to be able to accelerate beam with 2.5 mass-to-charge ratios (A/q) but we used a proton beam for initial test to characterize the injector system. Detailed description of the constructed injector system along with test results will be given in this paper.

INTRODUCTION

An RFQ (radio-frequency quadrupole) with the output beam energy of 1 MeV/n is under development at KOMAC, mainly for a test-stand to perform an ion injector and low energy beam acceleration study. We expect several research items to be carried out such as an advanced ion source operation based on the AI (artificial intelligence) technology, low energy beam diagnostics including multi-dimensional phase space reconstruction and testing of an advanced RF control technologies (adaptive feed-forward, non-IQ sampling).

In addition, the developed system can be used for the acceleration of helium beam with applications including semiconductor irradiation and membrane fabrication. The designed output energy of helium beam is 4 MeV, which is enough to penetrate the silicon wafer up to 18 μm . To reduce the irradiation time and to increase throughput of ion beam treatment, higher beam current is preferred. With consideration of the ion source performance for He^{2+} , the beam current of the RFQ was determined to be 10 mA [1].

Through the acceleration of deuteron beam up to 2 MeV, a small-scale accelerator based neutron source for the neutron science and the nuclear material study is another important application in consideration.

The layout of the ion beam irradiation system based on RFQ is shown in Fig. 1. The system includes the ion injector, low energy beam transport (LEBT), RFQ, beam lines and the irradiation target. For the ion source, we use a microwave ion source with 2.45 GHz magnetron. The same

type of the ion source is routinely used for the 100-MeV proton linac at KOMAC. For the LEBT system, we use two solenoids to match the beam parameters suitable for injection into RFQ. The magnetic LEBT system includes a vacuum system with a diagnostic chamber which is equipped with an emittance scanner and a beam profile monitor.

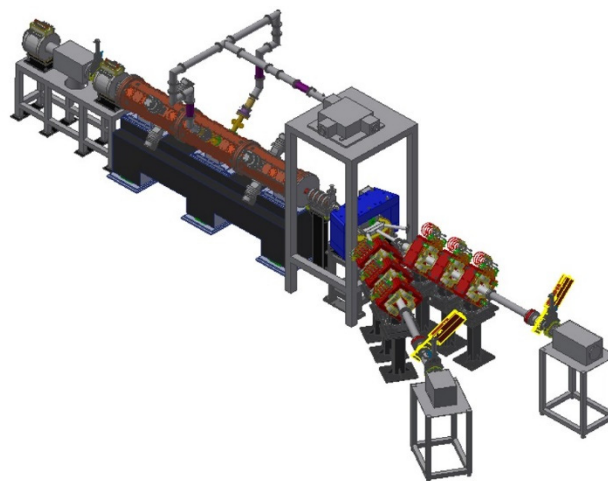


Figure 1. Layout of the ion beam system based on 200 MHz, 1 MeV/n RFQ and two beam lines.

The operation frequency of the RFQ is 200 MHz and with this choice of the RF frequency, we designed the RFQ with a four-vane type. Generally, a four-vane type RFQ is known to show better performance than the four-rod type in high duty operation point of view, while keeping the overall size of the RFQ within reasonably compact size [2].

We used PARMTEQ code for beam dynamics optimization for the RFQ. The optimization design parameters include the shaper energy, gentle buncher energy, vane voltage, and the aperture radius. During the optimization, we restricted the RF power and total length no more than 130 kW and 3.2 m, respectively. Design parameters are summarized in Table 1.

RFQ cavity consists of 3 sections and each section is about 1 m long. Under cut region at both ends of the structure is designed such that it results in flat field distribution better than 1 %. Each quadrant of single section contains four ports and total number of ports are 48. Eight of them are used for vacuum pumping with turbo-molecular pumps, two of them are for the coaxial type RF power couplers and another two of them are used for RF pickup ports. Rest of them are dedicated for slug tuner ports as shown in Fig. 2. Water-cooled slug tuner diameter is 70 mm and the frequency shift of 1 MHz is estimated with 9.7 mm insertion.

* This work was supported through KOMAC operation fund of KAERI by the National Research Foundation of Korea (NRF) grant funded by the Korea government (MSIT)(KAERI-524320-22).

[†] kimhs@kaeri.re.kr

SPACE CHARGE AND ELECTRON CONFINEMENT IN HIGH CURRENT LOW ENERGY TRANSPORT LINES: EXPERIENCE AND SIMULATIONS FROM IFMIF/EVEDA AND ESS COMMISSIONING

L. Bellan[†], M. Comunian, F. Grespan¹, A. Pisent, INFN-LNL, Legnaro, Italy

E. M. Donegani, M. Eshraqi, A. Garcia Sosa, B. Jones, E. Laface, N. Milas, R. Miyamoto, D. Noll, C. Plostinar, Y. Levinsen, ESS, Lund, Sweden

L. Neri, INFN-LNS, Catania, Italy

¹also at ESS, Lund, Sweden

Abstract

The mechanism of space charge compensation given as a result of the residual gas ionization is a key factor for the emittance containment in the low energy beam transport (LEBT) lines of high intensity hadron injectors. A typical front end including an ion source, a LEBT and Radio Frequency Quadrupole (RFQ), is equipped with two repellers at each interface to prevent electrons from flowing back, to the source, or forward, to the RFQ. In this paper we will emphasize the importance of the ion source and LEBT repellers on giving the appropriate boundary conditions for the space-charge compensation build-up mechanism. The theory and simulations are supported by experiments performed in the high intensities facility such as ESS and IFMIF/EVEDA.

INTRODUCTION

The Linear IFMIF Prototype Accelerator (LIPAc) [1, 2] is a high intensity D^+ linear accelerator; demonstrator of the International Fusion Material Irradiation Facility (IFMIF). The final linac [3] will send 40 MeV of 125 mA deuteron beam onto a liquid lithium target, in order to reproduce the future fusion reactor neutron spectra. In summer 2019 the IFMIF/EVEDA Radio Frequency Quadrupole (RFQ) accelerated its nominal 125 mA deuteron (D^+) beam current to 5 MeV, with >90% transmission for pulses of 1 ms at 1 Hz, reaching its nominal beam dynamics goal [4, 5].

The European Spallation Source (ESS) [6], currently under construction in Lund, Sweden will send a 62.5 mA proton beam at 14 Hz and 2.86 ms pulse length will be accelerated to 2 GeV. The resulting average beam power of 5 MW will be used to drive the production of spallation neutrons, enabling ESS to become a flagship research facility and to carry out world class science. The normal conducting part is the first section of the machine to transition from installation to integrated testing and commissioning with beam. In spring 2022 the first DTL tank [7] was commissioned at full peak current reaching its nominal beam dynamics goal [8, 9].

Both of these high power high intensity facilities implement a similar low energy stage composed of:

- high intensity ion source of ECR (Electron Cyclotron Resonance) type
- magnetostatic LEBT (Low Energy Beam Transfer) line.

THE INJECTORS

In this paper we will focus on the extraction and LEBT optics of these two facilities (Fig. 1). The ESS ion source plasma phenomena are described in [10] and the beam modulation techniques in [11].

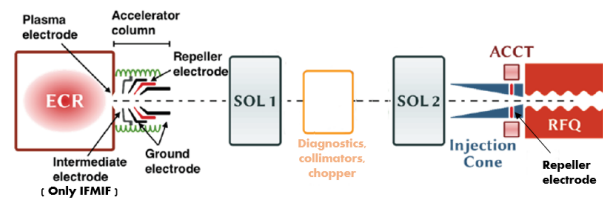


Figure 1: Common layout of the LEBTs of ESS and IFMIF/EVEDA.

The ion sources produce light ions beams: deuteron/protons for IFMIF, protons for ESS. The LEBT are based on a magnetostatic transfer line that uses two solenoids for transport and matching the beam into the RFQs. Two repellers are supplied, one in the extraction region, the other one at the RFQ entrance. As far as the diagnostics are concerned, both injectors are equipped with non intercepting current monitors that allows to read extracted beam current from the PE (Plasma Electrode) and to the RFQ injection point. Additionally, the ESS LEBT [12] is equipped with a Faraday Cup. In the following sections we will explain the differences between the injectors.

IFMIF Injector

The injector, an ECR source, in-kind contribution of CEA Saclay [13] consists of a 2.45 GHz RF power source with a two coil magnetic structure. The nominal CW beam extracted consists of 140 mA D^+ at 100 kV. For commissioning purposes, the source can also extract tens of mA of H^+ at 50 kV and can operate in pulsed mode. From the beam dynamics point of view, these beams are characterized by a high perveance beam transport: the general perveance (un-compensated) ranges from 5×10^{-4} for the probe up to 5×10^{-3} for the nominal beam. The extraction, differently to the ESS case, is characterized by a five-electrode system: the addition of an intermediate electrode can

[†] luca.bellan@lnl.infn.it

APPLICATION OF PERMANENT MAGNETS IN SOLENOID AND QUADRUPOLE FOCUSING

J. D. Kaiser*¹, A. Ateş, H. Haehnel, U. Ratzinger, IAP, Goethe University, Frankfurt, Germany
¹Helmholtz Research Academy Hesse for FAIR (HFHF), Frankfurt, Germany

Abstract

Permanent magnets can be used to design compact high gradient focusing elements for particle accelerators. Based on cheap industrial standard Neodym permanent magnets, design studies for Solenoids and Quadrupoles are presented.

The Solenoid design consists of three segments, where the outer segments possess a radial magnetization and the inner segments an axial magnetization. This increases the mean field strength in comparison to a singlet hollow cylinder solenoid.

The quadrupole design consists of 16 block magnets and is designed to be rather simplistic. The casing consists of two half shells, which can be easily mounted around a beam pipe. For a quadrupole triplet configuration the influence of different geometric parameters on beam transport regarding focusing strength and emittance growth is investigated.

Furthermore, a variation of the quadrupole design was mounted in vacuum in a triplet configuration. Using custom 3D-printed mounts for small raspberry pi cameras the beam could be observed inside the quadrupoles. A first prototype was constructed.

PERMANENT MANGETIC SOLENOIDS

In its simplest form, a permanent magnetic solenoid (PM-Solenoid) can be realized by a single axially magnetized hollow cylinder. A maximization of the coupling of the magnetic field across the aperture volume is crucial for the mean flux density along the beam axis. This is particularly weakened when the cylinder is lengthened. To counteract this, the solenoid is extended by two outer cylinder segments with a radial magnetization (Fig. 1).

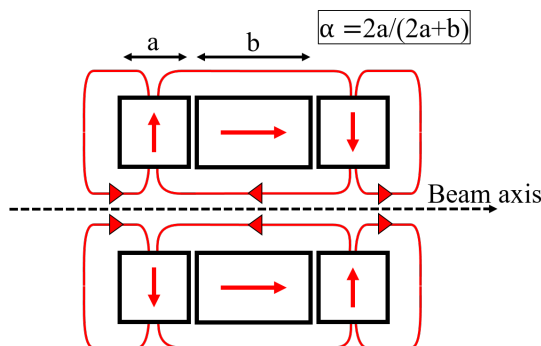


Figure 1: Cross-section of a PM solenoid consisting of three segments.

The ratio of the segment lengths α can be adjusted according to the geometrical parameters to a maximization

* kaiser@iap.uni-frankfurt.de

of the mean flux density. For suitable parameter combinations, this can be increased by a factor of 2. Compared to a single hollow cylinder, the magnetic fields are concentrated in a smaller area as this changes direction between segments (Fig. 2). For an aperture radius of 20mm, the average magnetic flux density increases by 20% radially for both designs. This results in overfocusing only for the combined cylinders due to the concentrated field. This problem can be circumvented by reducing the illumination or designing the solenoid with smaller aperture radii.

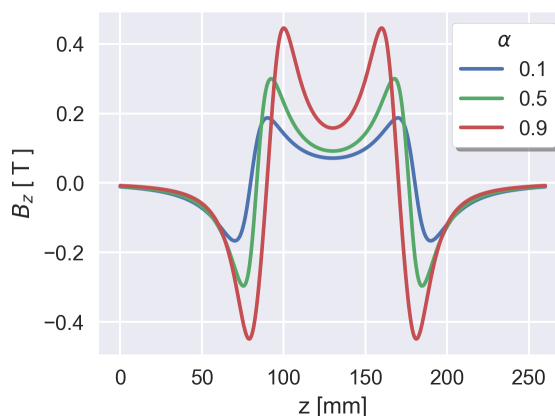


Figure 2: Field progression along the solenoid axis for three segment aspect ratios α .

For a cheap realization an arrangement of cuboid magnets can be derived, whose geometry is industrial standard and thus available at a low price compared to individually manufactured magnets (Fig. 3). The pole faces of the magnets, which correspond to the largest surface of the individual cuboids, are oriented according to Fig. 1. In this configuration, an average flux density of 0.5T can be achieved for an 80mm long solenoid and an aperture radius of 12mm with an outer radius of 32mm.

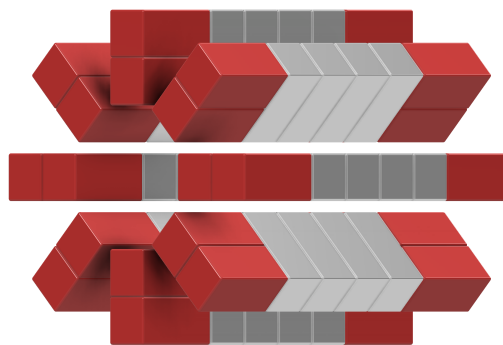


Figure 3: Arrangement of cuboid magnets to mimic the segmented PM solenoid.

Content from this work may be used under the terms of the CC BY 4.0 licence (© 2021). Any distribution of this work must maintain attribution to the author(s), title of the work, publisher, and DOI

RUN 2 OF THE ADVANCED PLASMA WAKEFIELD EXPERIMENT (AWAKE) AT CERN

G. Zevi Della Porta[†] (CERN, Geneva, Switzerland)
for the AWAKE Collaboration

Abstract

After successful completion of Run 1 of the Advanced Plasma Wakefield Experiment (AWAKE) at CERN, the experiment started Run 2 in 2021. The goals of AWAKE Run 2 are to accelerate electrons in proton-beam-driven plasma wakefields to high energies with gradients of up to 1 GV/m while preserving the electron beam normalized emittance at the 10 μm level, and to demonstrate the acceleration of electrons in scalable plasma sources to 50-100 GeV. The first milestone towards these final goals is to demonstrate electron seeding of the self-modulation of the entire proton bunch. This was achieved in the 2021 run and some highlight results are shown. In the next phases of AWAKE Run 2, a new X-band electron source will provide a 150 MeV, 200 fs, 100 pC electron beam, to be accelerated in the plasma wakefields.

INTRODUCTION

The Advanced Plasma Wakefield Experiment (AWAKE) at CERN [1] has been developed as a proof-of-principle R&D experiment to study proton-driven plasma wakefield acceleration of electrons. AWAKE relies on 400 GeV proton bunches of the SPS accelerator at CERN, which could potentially accelerate electrons to energies as high as 200 GeV in a 400 m long plasma [2]. Approved in 2013, AWAKE observed Self-Modulation (SM) of a proton bunch travelling in a 10 m plasma in 2016-2017 [3-5], and plasma wakefield acceleration of electrons from 19 MeV to 2 GeV in 2018 [6], completing its Run 1 programme.

After the successful demonstrations obtained in Run 1, the AWAKE Run 2 programme [7-9] aims to demonstrate the possibility to use proton-driven wakefield acceleration for high-energy physics applications, starting with experiments where a high-energy bunch collides with a target. Such fixed-target experiments do not require colliding bunches and their physics performance is determined by the energy and number of electrons on target. Demonstrating the ability to deliver beams for such an experiment is the goal of Run 2 and is a prerequisite for designing more complex facilities such as laser-electron and electron-proton colliders.

Experimental Layout

In its current layout, the AWAKE experiment includes a 10 m long rubidium vapor source supporting vapor densities in the range 10^{14} - 10^{15} cm^{-3} and a 120 fs laser, with central wavelength of 780 μm and energy of 120 mJ, used to singly ionize the rubidium vapor, creating plasma. The 18 MeV electron beam, with charge ranging from 100 to 800 pC, is provided by an S-band RF photo-injector with a

UV-illuminated Cs₂Te cathode, followed by a 1 m long booster structure. Both the injector and the booster are powered at 3 GHz by a 30 MW klystron, with a repetition rate of 10 Hz. The beam is then delivered to the entrance of the plasma by a 15 m long beamline of dipole and quadrupole magnets, instrumented with beam screens and beam position monitors. The beamline downstream of the vapor source includes a magnetic spectrometer to measure accelerated electrons and several Optical Transition Radiation (OTR) screens whose light, when crossed by the proton bunch, is sent to transverse and longitudinal diagnostics, producing both time-integrated and time-resolved distributions of the proton bunch charge density.

Seeded Self-Modulation

The proton bunches of the SPS are longer (6-8 cm r.m.s.) than the wavelength of the plasma used by AWAKE (1 mm), and they are subjected to the Self-Modulation Instability (SMI) as soon as they enter a dense plasma. During SMI, the wakefields generated by a long proton bunch act back on the bunch itself, creating focusing and defocusing regions that modulate the long bunch into a train of micro-bunches at the scale of the plasma wavelength [10]. SMI can develop from noise or from controlled initial wakefields. When the SMI is 'seeded' by an initial modulation, its timing and amplitude become reproducible, creating the Seeded Self-Modulation (SSM) process which is necessary to achieve reproducible electron acceleration.

AWAKE has experimented with two types of SSM. In Run 1, it was observed that by timing the ionizing laser pulse to overlap the proton bunch, the subsequent sharp onset of the beam-plasma interaction could drive well-defined seed wakefields and produce SSM in the second half of the proton bunch [3]. In Run 2a, an electron bunch preceding the proton bunch provided the seed, modulating the entire proton bunch [11].

AWAKE RUN 2 PROGRAMME

The goal of the Run 2 programme is to demonstrate stable acceleration of electron bunches with high gradient (0.5-1 GV/m) over significant distances (10 m), while maintaining small electron bunch emittance (10 μm) and relative energy spread (few %), as well as to demonstrate a scalable plasma source technology to support O(100) m of plasma [9]. In order to achieve these goals, several challenges must be met, resulting in the research programme described below.

AWAKE Run 2a (2021-2022)

The first phase of the Run 2 programme relies on the Run 1 infrastructure and focuses on the SSM process. Run 2a aims to demonstrate that an electron bunch can

[†] gzevi@cern.ch

FACET-II*

C. Clarke[†], J. Allen, L. Alsberg, C. Emma, A. Edelen, H. Ekerfelt, E. Gerstmayr,
S. Gessner, C. Hast, M.J. Hogan, R. Loney, S. Meuren, S. Miskovich,
B. O'Shea, M. Parker, D.A. Reis, D. Storey, R. Watt, G. Yocky
SLAC National Accelerator Laboratory, Menlo Park, CA, United States
R. Ariniello, C. Doss, C. Hansel, V. Lee, M. Litos, University of Colorado, Boulder, CO, USA
S. Corde, A. Knetsch, P. San Miguel, Laboratoire d'Optique Appliquée, France
C. Joshi, K. Marsh, Z. Nie, C. Zhang, UCLA, Los Angeles, CA, USA
G.J. Cao, University of Oslo, Norway
J. Wang, University Nebraska-Lincoln, NE, USA

Abstract

FACET-II is a National User Facility at SLAC National Accelerator Laboratory providing 10 GeV electron beams with μm -rad normalised emittance and peak currents exceeding 100 kA. FACET-II operates as a National User Facility while engaging a broad User community to develop and execute experimental proposals that advance the development of plasma wakefield accelerators. FACET-II is currently commissioned and has started with first experiments. The special features of FACET-II will be shown and first results from the experiments.

INTRODUCTION

Though conventional technology can satisfy near-term needs, the practical limits to the size and cost restrict the energy reach of linear colliders. A revolution in acceleration technology is needed to realise a multi-TeV linear collider. Such a new technology needs to meet criteria: it needs to be high gradient, efficient and result in high luminosity at the collision point.

Plasma Wakefield Acceleration (PWFA) is a scheme initially proposed four decades ago [1, 2] for high (GV/m) gradient acceleration, 1,000 times the acceleration in a given distance compared to conventional RF technologies. Extremely large electric fields can be sustained in a plasma wave caused by an intense, charged particle bunch and used to accelerate a second (trailing) bunch of electrons to high energies.

Experimental beam test facilities are essential in the development of the scheme. There are few facilities with the high beam intensities required to study PWFA in the regime for future collider applications. SLAC National Accelerator Laboratory has supported three generations of facility for the study of PWFA [3]: Final Focus Test Beams (FFTB), FACET and the upgraded facility FACET-II.

Experiments at FACET (2011-2016) demonstrated 9 GeV acceleration in one metre with 30% efficiency and low energy spread [4]. The studies at FACET were limited by the relatively high emittance of the incoming electron beam

which used a thermionic gun and damping ring to produce the electron bunches. The years between 2016 and 2020 were used to upgrade the facility, renamed FACET-II, with a new low emittance photo-cathode injector and new bunch compression scheme and final focus. The new facility allows these studies to continue with a focus on aspects of emittance preservation with a single 10 GeV acceleration stage.

FACET-II began commissioning in 2020. The first experiment run was in 2022. The goal of the initially invited experiments was to demonstrate the capabilities of the FACET-II facility and commission the experimental hardware. First science results from this initial run will inform the direction of more in-depth studies in the next FACET-II runs.

FACET-II National User Facility

The FACET-II accelerator provides uniquely high intensity beams. Science meetings were held over several years to develop a programme that could use these beams [5]. The programme encompasses not only GeV-level PWFA studies but also the development of ultra-high brightness electron beams from plasma-based injectors and high-intensity x-ray and gamma-ray sources plus the study of high-energy high-intensity electron beams and their interaction with lasers, plasmas and solids. Novel diagnostics to characterize the extreme beams are being developed combining beam-physics, machine learning (ML) and artificial intelligence (AI).

FACET-II operates as a Department of Energy National User Facility for High Energy Physics. Proposals are welcome from scientists all around the world and evaluated through a peer review process for beamtime at FACET-II [6]. Operating a broad science program draws expertise and the opportunity to collaborate with scientists in different fields, which benefits each of the individual science thrusts.

BEAM DELIVERY STATUS

Commissioning of the new FACET-II facility (Fig. 1) began in 2020. The single electron bunch configuration has been commissioned (Table 1) and will be further optimised. Future configurations include a two bunch configuration for PWFA demonstrations.

* This work performed under DOE Contract DE-AC02-76SF00515 and also supported under FES Award DE-SC0020076.

[†] cclarke@slac.stanford.edu

THE MUON LINAC PROJECT AT J-PARC

Y. Kondo*, R. Kitamura, Y. Fuwa, T. Morishita, K. Moriya, T. Takayanagi,
JAEA, Tokai, Naka, Ibaraki, Japan
M. Otani, E. Cicek, H. Ego, Y. Fukao, K. Futatsukawa, N. Kawamura, T. Mibe, Y. Miyake,
S. Mizobata, N. Saito, K. Shimomura, T. Yamazaki, M. Yoshida,
KEK, Oho, Tsukuba, Ibaraki, Japan
Y. Nakazawa, H. Inuma, Ibaraki University, Mito, Ibaraki, Japan
Y. Takeuchi, J. Tojo, Kyushu University, Fukuoka, Japan
K. Sumi, M. Yotsuzuka, T. Iijima, K. Inami, Y. Sue, K. Suzuki,
Nagoya University, Nagoya, Aich, Japan
K. Ishida, RIKEN, Wako, Saitama, Japan
N. Hayashizaki, Tokyo Institute of Technology, Tokyo, Japan
Y. Iwashita, Kyoto University, Kyoto, Japan
K. Hasegawa, Y. Iwata, QST, Chiba, Japan
H. Yasuda, University of Tokyo, Hongo, Tokyo, Japan
S. Bae, H. Choi, S. Choi, B. Kim, H. S. Ko,
Seoul National University, Seoul, Republic of Korea
E. Won, Korea University, Seoul, Republic of Korea
G. P. Razuvaev, BINP, Novosibirsk State University, Novosibirsk and
Pulkovo Observatory, St. Petersburg, Russia

Abstract

The muon linac project for the precise measurement of the muon anomalous magnetic and electric dipole moments, which is currently one of the hottest issues of the elementary particle physics, is in progress at J-PARC. The muons from the J-PARC muon facility are once cooled to room temperature, then accelerated up to 212 MeV with a normalized emittance of $1.5 \pi \text{ mm mrad}$ and a momentum spread of 0.1%. Four types of accelerating structures are adopted to obtain the efficient acceleration with a wide beta range from 0.01 to 0.94. The project is moving into the construction phase. We already demonstrated the re-acceleration scheme of the decelerated muons using a 324-MHz RFQ in 2017. The high-power test of the 324-MHz Interdigital H-mode (IH) DTL using a prototype cavity has been performed in 2021. The fabrication of the first module of 14 modules of the 1296-MHz Disk and Washer (DAW) CCL will be done to confirm the production process. Moreover, the design work of the traveling wave accelerating structure for the high beta region has been almost finished and prototyping is started. In this paper, the recent progress toward the realization of the world first muon linac will be presented.

INTRODUCTION

The muon anomalous magnetic moment $(g-2)_\mu$ is one of the most promising probe to explore the elementary particle physics beyond the standard model (SM). The most recent experiment FNAL E989 measured the $(g-2)_\mu$ with a precision of 0.46 ppm, and the measured value indicates 4.2 standard

deviations from the SM prediction [1]. The J-PARC E34 experiment aims to measure the $(g-2)_\mu$ with a precision of 0.1 ppm. In addition, the electric dipole moment (EDM) also can be measured with a precision of $1 \times 10^{-21} e\text{-cm}$ [2]. Figure 1 shows the experimental setup of J-PARC E34.

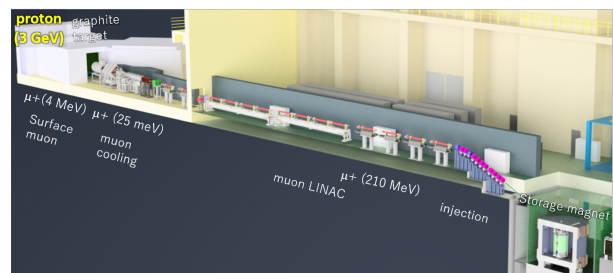


Figure 1: Experimental setup of the J-PARC E34 experiment.

The experimental method of E34 is completely different from that of the previous experiments. The previous experiments directory used decay muons from the secondary pions generated on the production target. The emittance of such muon beam is very large (typically, $1000\pi \text{ mm mrad}$); this is a major source of uncertainty of the measurement. On the other hand, E34 will use a low emittance muon beam to improve the precision. The required beam divergence $\Delta p_t/p$ is less than 10^{-5} , and assumed transverse emittance is $1.5\pi \text{ mm mrad}$. To satisfy this requirement, we are planning to use ultra-slow muons (USMs) generated by laser-dissociation of thermal muoniums ($\text{Mu: } \mu^+e^-$) from a silica-aerogel target [3]. The room temperature USMs (25 meV) should be accelerated to 212 MeV to obtain the required

* yasuhiko.kondo@j-parc.jp

THE CompactLight DESIGN STUDY

A. Latina, CERN, Geneva, Switzerland
G. D’Auria, R. Rochow, Elettra ST, Trieste, Italy
on behalf of the CompactLight Collaboration

Abstract

CompactLight (XLS) is an H2020 Design Study funded by the European Union under grant agreement No. 777431 and carried out by an international collaboration of 23 international laboratories and academic institutions, three private companies, and five third parties. The project, which started in January 2018 with a duration of 48 months, aimed to design an innovative, compact, and cost-effective hard X-ray FEL facility complemented by a soft X-ray source. In December 2021, the Conceptual Design Report was completed. The result is an accelerator that can be operated at up to 1 kHz pulse repetition rate, beyond today’s state of the art, using the latest concepts for high brightness electron photoinjectors, very high gradient accelerating structures in X-band, and novel short-period undulators. This paper gives an overview of the current status, focusing particularly on the technological challenges addressed and their future applications to compact accelerator-based facilities.

INTRODUCTION

Synchrotron Radiation is a fundamental and indispensable research tool in a broad spectrum of scientific and technological fields and their applications, including materials science, condensed-matter physics, atomic and molecular physics, life science and medicine, chemistry, and environmental sciences. For this reason, the use of synchrotron radiation has increased tremendously in the last decades, as testified by the number of synchrotron light sources built to serve increasingly large users communities across many scientific and engineering disciplines.

The CompactLight project aimed to design an innovative, compact, cost-effective Hard X-Ray (HXR) FEL facility complemented by a Soft X-Ray (SXR) source. The FEL specifications that drove the design were based on the demands of potential users, considering the photon characteristics required by their current and future experiments. XLS used the latest concepts for high brightness electron photoinjectors, very high gradient X-band accelerating structures based on CLIC technology developed at CERN [1], and novel short-period super-conducting undulators. The result is a normal-conducting accelerator that can be operated at up to a 1 kHz repetition rate, well beyond today’s state of the art.

The design presented in the Conceptual Design Report (CDR) [2] includes a facility baseline layout and two main upgrades, with the most advanced option allowing the simultaneous operation of both FEL beamlines, in SXR/HXR pump-probe configuration, at 100 Hz repetition rate. Fig-

ure 1 shows a schematic layout of the CompactLight facility Upgrade II.

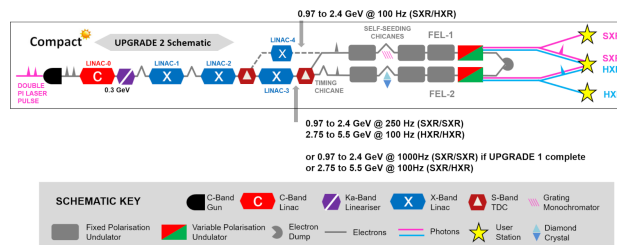


Figure 1: Schematic layout of the CompactLight facility including Upgrade II.

Compared to existing facilities with the same operating wavelengths, the technical solutions adopted by CompactLight allow the proposed facility to operate with a lower electron beam energy on a significantly smaller footprint. These enhancements make the facility more attractive and more affordable to build and operate. Figure 2 shows a 3D view of the different subsystems and their estimated lengths. The total length of the facility is just below 485 m, which is more than 250 m less than the total length of SwissFEL, for example.

The CompactLight CDR also includes preliminary evaluations of a soft X-ray FEL and an extremely compact and relatively inexpensive photon source based on Inverse Compton Scattering (ICS) using CompactLight technology. Compared with the entire CompactLight facility, this soft X-ray FEL can be considered quite an affordable solution in terms of cost and complexity, in case of limited funding capabilities. In addition, the ICS source, with its wide range of applications, is very attractive and could be easily installed and operated on university campuses, small laboratories, and hospitals.

FEL PERFORMANCE

The main features of CompactLight have been based on the users’ requests and include: High FEL stability in pulse energy and pulse duration; FEL synchronization better than 10 fs; photon pulse duration less than 50 fs; a repetition rate from 1 Hz up to 1 kHz; FEL pump-probe capabilities with a large photon energy difference; small focused spot size; variable polarization, linear and elliptical; tunability up to higher photon energies; two-bunch operation and two-colour pulse generation.

Based on these requirements, CompactLight has been designed as a hard X-ray facility covering the wavelength range from 0.08 nm to 5 nm with two separate FEL beamlines:

ELECTRON BEAM BASED LEATHER TANNING

R. Apsimon^{1,2,*}, D. Turner^{1,2}, K. Dewhurst^{1,2,†}, S. Setiniyaz^{1,2,‡}, R. Seviour³, and W. Wise⁴

¹Engineering Department, Lancaster University, Lancaster, LA1 4YW, UK

²Cockcroft Institute, Daresbury Laboratory, Warrington, WA4 4AD, UK

³Ion Beam Centre, University of Huddersfield, Huddersfield, HD1 3DH, UK

⁴Institute for Creative Leather Technologies, University of Northampton, Northampton, NN1 5PH, UK

Abstract

Tanning of leather for clothing, shoes, and handbags uses potentially harmful chemicals that often run off into local water supplies or require a large carbon footprint to safely recover these pollutants. In regions of the world with significant leather production, this can lead to a significant environmental impact. However recent studies have suggested that leather can instead be tanned using a combination of electron beams in a process inspired by the industrial crosslinking of polymers, to drastically reduce the quantity of wastewater produced in the process; thereby resulting in a reduced environmental impact as well as potential cost savings on wastewater treatment. In this talk, initial studies of leather tanning will be presented as well as accelerator designs for use in leather irradiation.

INTRODUCTION

Particle accelerators have been used for many industrial applications like radiotherapy treatment, cargo scanning, material modification, medical sterilization, food processing, and polymer crosslinking [1, 2]. Particle accelerators have great potential for developing disruptive technologies in a world with an increasing demand for green technology and sustainability. One of those potential applications is using an electron beam from accelerators for leather manufacturing, which we call e-beam tanning for brevity. The e-beam tanning process is similar to the crosslinking of polymers. The collagen in the animal hide is equivalent to polymers; similarly, tannin is the cross-linking agent. The whole e-beam tanning process is shown in the diagram in Fig. 1. The hide is soaked in the tanning agent bath before the treatment so the tannin is permeated throughout the hide. The mixture of tannin and hide is then irradiated by the electron beam, which will initiate the cross-linking process. The leftover tanning bath is replenished and reused. The hides are placed on a conveyor belt and irradiated by the electron from the top. The electron beam is scanned in the perpendicular direction to the hide movement.

In the conventional tanning process, the hides are tanned inside a tanning drum with a tanning bath. When tanning is finished, the leftover tanning bath is discharged as wastewater, which will require treatment as it contains tannins and other chemicals. The wastewater treatment process is an energy-intensive and costly process. In the e-beam tanning

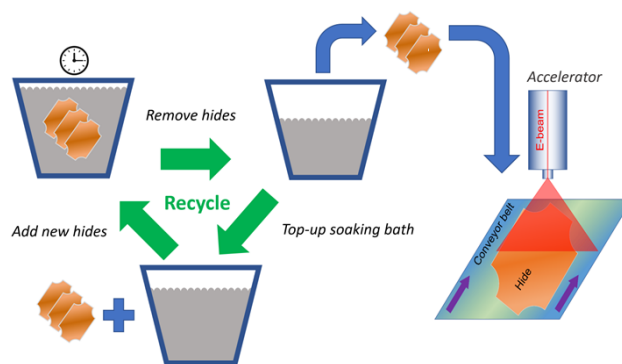


Figure 1: E-beam tanning process diagram.

process, however, the hide is only soaked inside the bath, hence it can be replenished and reused and no substantial amount of wastewater is generated. The tannin uptake efficiency can be close to 100%. Another advantage of e-beam tanning is it is able to occur over a wider range of temperatures and pH, while also allowing for the use of novel tanning agents that would typically be too unstable in water or air to bind to the collagen.

One of the key challenges of e-beam tanning is the uniformity of the tanning reaction throughout the cross-section of a hide, which is crucial for the end product to achieve tight specification parameters set by the original equipment manufacturers (OEMs) as well as meeting legislative restrictions. Uniform tanning would require uniform energy deposition by the electron beam. In this study, we use Monte Carlo simulations to design and optimize the electron beam-based leather treatment system to achieve uniform dose deposition, while keeping the system design simple, scalable for industrial production, and energy efficient.

ELECTRON BEAM TREATMENT SYSTEM DESIGN

Electron Beam Energy

The first key parameter we need to find out for the irradiation system is the beam energy, as it will dictate the accelerator size, operating power, and related costs. The beam energy determines the penetration depths in the hide. When it is too low, the energy is only deposited on the surface, which will result in poor uniformity. On the other hand, when it is too high, most electrons will penetrate through without depositing enough energy, which results in low effi-

* r.apsimon@lancaster.ac.uk

† Now at CERN, Geneva, Switzerland

‡ s.saitiniyazi@lancaster.ac.uk

DATA ANALYSIS AND CONTROL OF AN MeV ULTRAFAST ELECTRON DIFFRACTION SYSTEM USING MACHINE LEARNING *

T. B. Bolin[†], M. A. Fazio, S. Sosa Guitron, M. Martínez-Ramón, S. G. Biedron^{1,2}

Department of Electrical and Computer Engineering, University of New Mexico, NM 87131, USA

M. Babzien, M. Fedurin, J. Li, M. Palmer

Brookhaven National Laboratory, Upton, NY 11973, USA

¹also at Department of Mechanical Engineering, University of New Mexico, NM 87131, USA

²also at Element Aero, Chicago, IL 60643, USA

Abstract

An MeV ultrafast electron diffraction (MUED) instrument system is a unique characterization technique used to study ultrafast processes in a variety of materials systems by a pump-probe method. This relatively young technology can be advanced further into a turnkey instrument by using data science and artificial intelligence (AI) mechanisms in conjunction with high-performance computing. This can facilitate automated operation, data acquisition, and real-time or near-real-time processing. The AI-based system controls can provide real-time feedback on the electron beam, or provide virtual diagnostics of the beam. Deep learning can be applied to the MUED diffraction patterns to recover valuable information on subtle lattice variations that can lead to a greater understanding of a wide range of material systems. A data-science-enabled MUED facility will also facilitate the application of this technique, expand its user base, and provide a fully automated state-of-the-art instrument. Updates on research and development efforts for the MUED instrument in the Accelerator Test Facility of Brookhaven National Laboratory are presented.

INTRODUCTION

MeV ultrafast electron diffraction (MUED) system is a pump-probe characterization technique for studying ultrafast processes in materials. The use of relativistic electron beams leads to decreased space-charge effects compared to typical ultrafast electron diffraction experiments employing energies in the keV range [1-3]. MUED has a higher scattering cross section with material samples as compared to other probes such as X-ray free electron lasers, and as such allows access to higher-order reflections in the diffraction patterns due to the short electron wavelengths.

However, this is a relatively young technology, and several factors contribute to making it challenging to utilize, such as beam instabilities that can lower the effective spatial and temporal resolution. In recent years, machine learning (ML) approaches to materials and characterization techniques have provided a new path towards unlocking new physics by improving existing probes and increasing the user's ability to interpret data. Ideally, anomalous contribution detection and removal should not require *a priori* knowledge of what those contributions would be or how they would present themselves in the data. Particularly, with proper preprocessing, ML methods can be employed

[†] email address: tbolin@unm.edu

to control characterization probes in near-real time, acting as virtual diagnostics, or ML can be deployed to extract features and effectively denoise data. With respect to denoising, convolutional neural network architectures, such as auto encoder models, are an attractive and more powerful alternative to conventional denoising techniques. The autoencoder models provide a method of unsupervised learning of latent space representation of data that can help reduce the noise in the data. It should be noted that noise and anomalies aren't necessarily the same thing, as systematic stochastic noise issues may be present. In principle, AI/ML can facilitate distinguishing both.

By supplying a paired training dataset of "noisy" and "clean" data, these ML models can denoise measurements quite effectively [4, 5]. This method relies on the existence of an ideal dataset with no noise, which can be obtained by simulation or by averaging existing noisy datasets. However, in some cases these are not accessible or practical to use. Generative adversarial networks (GANs) are a more suitable option when no "clean" data are available and have been proven to perform well for blind image denoising [6]. They can be trained to estimate and generate the noise distribution, thus producing paired training datasets that can be fed to an autoencoder model. These approaches can lead to increased resolution if employed to denoise, for example, diffraction patterns. In addition, deep convolutional neural network architectures can be used for data analysis. Laanait *et al.* measured diffraction patterns of different oxide perovskites using scanning transmission electron microscopy and, by applying a custom ML algorithm, were able to invert the materials structure and recover 3-dimensional atomic distortions [7]. ML has yet to be applied to the MUED technique, where it can certainly enable advances that can further understanding of ultrafast material processes in a variety of systems.

EXPERIMENTAL

The MUED instrument is located at the Accelerator Test Facility at Brookhaven National Laboratory. A schematic of the experimental setup is presented in Fig. 1. The details of data collection are very briefly described here. The femtosecond electron beam is generated using a frequency-tripled Ti:Sapphire laser that illuminates a copper photocathode, generating a high brightness beam. The electrons are bunched in a 1.6-cell rf cavity and accelerated to 5 MeV. Current parameters of the electron beam source optimized for stability are presented in Table 1. The sample

DEVELOPMENTS TOWARDS FRIB UPGRADE TO 400 MeV/u FOR THE HEAVIEST URANIUM IONS

K. McGee, K. Elliott, A. Ganshyn, W. Hartung, S. Kim, P. Ostroumov, J. Popielarski,
 L. Popielarski, A. Taylor, T. Xu, FRIB/MSU, East Lansing, MI, USA
 G. V. Ereemeev, F. Furuta, M. Martinello, O. Melnychuk, A. Netepenko
 Fermilab, Batavia, IL, USA
 B. Guilfoyle, M. P. Kelly, T. Reid, ANL, Argonne, IL, USA

Abstract

High- Q_0 medium-velocity ($\beta_{\text{opt}} \approx 0.6$) 5-cell elliptical cavities for superconducting linacs are critical technology for current and future hadron linac projects such as Fermilab's Proton Improvement Plan II (PIP-II) and the proposed energy upgrade of Michigan State University's Facility For Rare Isotope Beams (FRIB400). Previous work established the validity of the novel geometry of the FRIB400 prototype 644 MHz 5-cell elliptical $\beta = 0.65$ superconducting rf cavities for future high- Q_0 development. In collaboration with Fermilab, two leading-edge high- Q_0 recipes, N-doping and furnace/medium-temperature baking (FMTB), were tested in the 5-cell cavity. N-doping ("2/0") + cold electropolishing was successful at achieving the FRIB400 and PIP-II requirements for Q_0 , achieving an unprecedented 3.8×10^{10} at 17.5 MV/m, which is 1.75 times higher than the FRIB400 requirement for Q_0 . With FMTB, Q_0 was 1.4 times higher than the FRIB400 requirement. Additionally, systematic studies of bulk Nb material parameters suggest a relationship between the flux pinning force measured in a sample and the flux expulsion properties of a cavity fabricated from the same material.

INTRODUCTION

The Facility for Rare Isotope Beams (FRIB) at Michigan State University (MSU), a first-in-class nuclear research facility, was fully commissioned in January 2022, and has successfully provided beam to three user experiments, with 34 more having been approved [1]. The FRIB accelerator consists of 3 linac segments and 2 folding segments, with a total of 324 superconducting radio-frequency (SRF) cavities (divided among quarter-wave and half-wave resonators) in 46 cryomodules. The FRIB400 project proposes to double the energy of the current superconducting FRIB linac for the heaviest uranium ions from 200 MeV per nucleon (MeV/u) to 400 MeV/u [2]. The increased rare isotope production from higher-energy drive beams would bring many important foci of nuclear physics research within reach of FRIB, including the ability to probe parameters of the nuclear matter equation of state to new levels of precision, which would provide critical information for the study of neutron star mergers. Further, the facility's reach along the neutron drip line would be significantly increased. [2].

In support of the FRIB400 proposal, a design study identified the novel $\beta_{\text{opt}} = 0.65$ 5-cell elliptical 644 MHz SRF cavity with an accelerating gradient (E_{acc}) of

17.5 MV/m as the best candidate for the upgrade accelerator [3]. Of the three frequencies studied for elliptical cavities, the 644 MHz 5-cell $\beta_{\text{opt}} = 0.65$ case was the only one capable of delivering the necessary accelerating voltage within the 80 m of space available in the FRIB linac tunnel without increasing the current standards for the peak surface electric field, around 40 MV/m [3]. This design also has the lowest cryogenic heat load and the largest longitudinal acceptance [3]. The principal cavity design parameters and operating goals can be found in Table 1, and Figure 1 shows the cavity design.

Table 1: FRIB400 Cavity Parameters

| | |
|-----------------------------------------------|--------------------|
| Frequency | 644 MHz |
| Geometric β | 0.61 |
| Optimal β | 0.65 |
| Aperture diameter | 83 mm |
| Effective length L_{eff} | 71.0 cm |
| Number of cells | 5 |
| Geometric shunt impedance R/Q | 368 Ω |
| Geometry factor G | 188 Ω |
| $E_{\text{peak}}/E_{\text{acc}}$ | 2.28 |
| $B_{\text{peak}}/E_{\text{acc}}$ | 4.42 mT/(MV/m) |
| 2 K operating goals | |
| Accelerating gradient E_{acc} | 17.5 MV/m |
| Peak surface electric field E_{peak} | 40 MV/m |
| Peak surface magnetic field B_{peak} | 77.5 mT |
| Intrinsic quality factor Q_0 | 2×10^{10} |

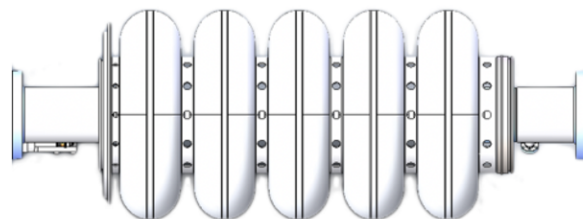


Figure 1: Drawing of the FRIB400 5-cell cavity.

The proposed 5-cell cavity operating at medium gradient bridges a hitherto unfilled gap from low- β TEM-type cavities to $\beta = 1$ elliptical-type cavities for continuous wave (CW) operation. Requiring a minimum Q_0 of 2×10^{10} , these large, sub-GHz cavities pose novel rf surface processing challenges. The European Spallation Source (ESS) and the Spallation Neutron Source (SNS), both of which operate in pulsed mode, employed buffered

ACCELERATOR DEVELOPMENT FOR GLOBAL SECURITY

S. G. Biedron

Element Aero, Chicago, IL 60643, USA

Abstract

Many particle accelerator facilities and projects can help with global security concerns, but not all accelerators used for security applications are designed specifically for these security applications. From direct interrogation to microelectronics radiation testing, there are myriad security applications of particle accelerators. This paper reviews several accelerator applications of security as well as design and technology activities to specifically better enable global security. Finally, this paper also points to many references discussing accelerators in global security.

INTRODUCTION

Global security means different things to different people. Global security includes military and diplomatic measures that nations and international organizations such as the United Nations [1] and the North Atlantic Treaty Organization (NATO) [2] take to ensure mutual safety and security. An individual may only focus on their own security.

The United Nations has its own definition of global security [3, 4]: “*With the advocacy of the United Nations Office for the Coordination of Humanitarian Affairs (OCHA) human security elements have acquired a wider dimension, for they go beyond military protection and engage threats to human dignity. Accordingly, it has become necessary for states to make conscious efforts towards building links with other states and to consciously engage in global security initiatives. OCHA’s expanded definition of security calls for a wide range of security areas:*

- *Economic: creation of employment and measures against poverty.*
- *Food: measures against hunger and famine.*
- *Health: measures against disease, unsafe food, malnutrition and lack of access to basic health care.*
- *Environmental: measures against environmental degradation, resource depletion, natural disasters and pollution.*
- *Personal: measures against physical violence, crime, terrorism, domestic violence and child labour.*
- *Community: measures against inter-ethnic, religious and other identity tensions.*
- *Political: measures against political repression and human rights abuses.”*

Looking through this broad definition of security that considers the collection of individual security concerns throughout the globe, we immediately recognize that particle accelerators and their peripherals can be of great assistance as a tool for global security applications (including defense).

Here are a few areas that might have come to mind as to why (in general terms) accelerators (and lasers and accelerator peripherals) are interesting for global security and defense [5, 6]:

- The identification and detection of materials, including chemical, biological, radiological, nuclear, and explosive (CBRNE);
- Preserving the water – energy – food nexus;
- Directed energy (applications: materials “modification” at a distance, propulsion, power transfer);
- Laser-sensing, communications, etc.;
- Materials research;
- Stockpile stewardship;
- Electronics testing for space and other applications;
- Medical applications (x-ray technologies, imaging, cancer treatments) to treat individuals located in environments that do not have access to state-of-the-art hospitals to preserve global health;
- Active radiation-belt remediation to improve the lifetime of satellites transiting the radiation belts;
- Sterilization capability for foods and surfaces to prevent contamination and infection.

Although this paper can cover a few ideas, it cannot cover all ideas and applications of accelerators and peripherals for global security. For this reason, many references are provided. Many of these publications have been based on comprehensive community studies and their subsequent publications to address accelerators, peripherals, and lasers, including:

- Accelerators for America’s Future, Department of Energy Report, March 2010 [7];
- Workshop on Energy and Environmental Applications of Accelerators, Department of Energy Report, 2015 [8];
- Workshop on Laser Technology for Accelerators, Department of Energy Report, 2013 [9];
- Workshop on Ion Beam Therapy, Department of Energy Report, 2013 [10];
- Task Force Report on Accelerator R&D commissioned by Jim Siegrist, Associate Director High Energy Physics, Office of Science [11];
- National Research Council, Scientific Assessment of High-Power Free-Electron Laser Technology, Washington, DC: The National Academies Press, 2009 [12];
- Summary Report – International FEL Expert Meeting: “Use of free-electron lasers and beyond: Scientific, technological, and legal aspects of dual use in international scientific cooperation” [13];
- The need for compact accelerators has been outlined in numerous documents, including the Basic Research Needs Workshop Report for Compact Accelerators for Security and Medicine: Tools for the 21st Century,

*sgbiedron@elementaero.com

SPATIOTEMPORAL STRUCTURE IN INTENSE THz PULSED BEAMS

G. A. Hine*, Oak Ridge National Laboratory, Oak Ridge, TN, USA

Abstract

Optically generated terahertz radiation, with gigavolt per meter (GV/m) electric fields accessible in tabletop experiments, provides a promising source of accelerating gradients for future particle accelerator applications. Manipulation and characterization of radiation is essential for efficiently producing high fields and effectively delivering them to an accelerating structure or interaction region. A method of generating and characterizing high quality and structured terahertz pulsed laser beams for compact particle acceleration is presented.

INTRODUCTION

Electromagnetic radiation with linear frequency in the 0.3-300 terahertz (1THz = 10^{12} Hz) band is referred to as Terahertz, THz, or T-Wave radiation. It comprises millimeter and sub-millimeter spatial scales and few picosecond to subpicosecond time scales. The production of coherent THz radiation has been demonstrated by a wide range of mechanisms from vacuum electronics to nonlinear optics using intense lasers. Although achieving high radiative power in this band has been historically difficult, this is an active field of research in which significant improvements are rapidly being demonstrated [1–3].

Because of its short length- and time-scales compared to microwaves, tightly focused THz pulses with high temporal (sub-picosecond) compression are possible, yielding extremely high electric fields even with modest pulse energy [4]. This has enabled a breadth of research from advanced particle acceleration and manipulation schemes [5–7] to fundamental physics and materials science [8–10]. At Spallation Neutron source, we are investigating using high THz fields to emulate the conditions inside a

superconducting cavity to improve cavity processing and mitigate deleterious effects like field emission [11] and as a possible source of accelerating gradients for novel ion acceleration schemes.

One method of THz generation (Fig. 1), optical rectification in nonlinear ($\chi^{(2)}$) materials has been shown to produce pulses with high fields (> 10 V/m) in free-space (no resonant structure) at comparatively high conversion efficiencies (2%) [4]. In these materials, a local quasi-static polarization develops in proportion to the time-averaged intensity of the pump laser pulse. As each unit cell in the crystal polarizes and depolarizes, it radiates a pulse with a single electromagnetic cycle. The radiation from each cell superposes like a phased antenna array, producing a directed pulse of THz radiation with a transverse profile determined by the pump transverse properties. With a conventional nonlinear optics treatment (one temporal dimension + one longitudinal

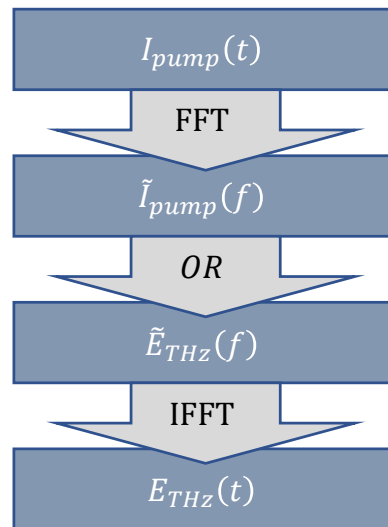


Figure 1: Calculation of THz pulses by optical rectification. The 1350 nm pump temporal profile is estimated from measurements of the 800 nm pulse input into the OPA. The power spectrum of the pump is calculated by FFT of the estimated pump profile. The THz amplitude spectrum generated in a $\chi^{(2)}$ medium like OH1 is proportional to the pump spectrum with a frequency-dependent prefactor Eq. (1). The THz temporal profile is Then calculated by IFFT of the generated THz amplituded spectrum.

dimension) as in [12], the generated THz pulse can be described by Eq. (1). Since the crystal itself is uniform, a pump which overfills a circular aperture should produce a THz pulse with a flat-top profile with a uniform spectrum throughout,

$$\begin{aligned} \tilde{A}_0 &= B(f)L(f, z)\tilde{I}_{pump}(f) \\ B(f) &= \frac{2d_{THz}f^2}{n_0\epsilon_0c^3\left(\frac{2\pi f}{c}(n_{THz}(f) + n_g) + i\left(\frac{\alpha_{THz}(f)}{2} + \alpha_0\right)\right)} \\ L(f, z) &= \frac{e^{i\left(\frac{2\pi f}{c}n_{THz} + i\alpha_{THz}/2\right)z} - e^{i\left(\frac{2\pi f}{c}n_g + i\alpha_0\right)z}}{\left(\frac{2\pi f}{c}(n_{THz}(f) - n_g) + i\left(\frac{\alpha_{THz}(f)}{2} - \alpha_0\right)\right)} \end{aligned} \quad (1)$$

The variables in Eq. (1) are described and their values defined in Table 1. Since the refractive index and absorption coefficient varies significantly over the generated THz range of interest, the refractive index $n_{THz}(f)$ and absorption coefficient $\alpha_{THz}(f)$ are expressed as functions of frequency according to the a lorentz multiple oscillator model described in [13].

The resulting THz spectrum is extremely broadband in the sense that its frequency spread is on the order of the peak or center frequency. While effects like “chirping” due to material dispersion are important for pulses with a few percent

* hinega@ornl.gov

R&D OF LIQUID LITHIUM STRIPPER AT FRIB*

T. Kanemura[†], N. Bultman, M. LaVere, R. Madendorp, F. Marti, T. Maruta, Y. Momozaki¹,
J. A. Nolen¹, P. N. Ostroumov, A. S. Plastun, J. Wei, and Q. Zhao, FRIB, Michigan State University,
East Lansing, MI, USA

¹also at Argonne National Laboratory, Lemont, IL, USA

D. B. Chojnowski, C. B. Reed, J. R. Specht, Argonne National Laboratory, Lemont, IL, USA

Abstract

Charge stripping is one of the most important processes for the acceleration of intense heavy ion beams, and the charge stripper greatly affects the performance of the accelerator facility such as the final beam power. In this paper, the design method and the achieved performance of the liquid lithium stripper recently developed for FRIB will be reported.

INTRODUCTION

The Facility for Rare Isotope Beams (FRIB) at Michigan State University is a 400 kW continuous wave (CW) high intensity heavy ion linear accelerator (linac) facility for the study of rare isotopes that don't exist on the earth [1]. A charge stripper is used in the FRIB driver linac as a critical device that allows increasing the energy gain of ion beams by a factor of 2. Charge stripping occurs at energies of 17-20 MeV/u, where the beam power will be 40 kW during full power operations. No solid materials that are available today can serve as a long-life stripper under these severe thermal and radiation conditions. Therefore, FRIB has developed a state-of-the-art self-replenishing liquid lithium charge stripper (LLCS) to overcome the technological bottlenecks [2].

In this paper we describe how we designed the FRIB LLCS system and report achieved performance. It would be worth noting that the process described in this paper could generally apply to other liquid lithium systems or even other fluid systems in which performance testing under operating conditions with the actual fluid is costly (both time and money) and simulation experiments are highly desired to test critical performance before the actual system is built.

DESIGN PROCESS

Conceptual Design

The LLCS concept was proposed by Nolen [3]. There were critical but unknown performance of the LLCS concept in the beginning; how could a stable and uniform thin (0.5-1 mg/cm²) liquid lithium film in a high vacuum environment be formed?; could the film withstand the foreseen extreme thermal load (56 MW/cm³) imposed by the full power uranium beam?; and could charge stripping charac-

teristics of the lithium film be acceptable for further acceleration of stripped beams? The first one: formation of a stable and uniform thin liquid lithium film was considered to be the most critical. To validate such a liquid lithium film, a series of R&Ds began at Argonne National Laboratory (ANL).

There are various methods to form a liquid film. One method is that when a round liquid jet impinges on the edge of a solid surface, a thin film is formed in the downstream (e.g. tap water from a faucet impinging on a spoon). This method was pursued at ANL.

It is not common to build a liquid lithium system until critical system performance is validated and there remain only validations that can be performed with liquid lithium. This is because liquid lithium systems are normally complicated thus expensive. The systems need heaters to melt solid lithium (the melting point of lithium is 180.5°C) and keep it liquid, heater controllers and temperature sensors to keep the temperature within a desired operating range. Tanks or vacuum chambers in liquid lithium systems are usually filled with argon or maintained under high vacuum to provide an inert environment. Otherwise the liquid lithium will be contaminated. For example, tanks / vacuum chambers must not be filled with air or nitrogen because lithium reacts with them, which could cause a lithium fire. Thus, dedicated sub-systems that provide an inert environment in the tanks / vacuum chambers are also required. To mitigate and prevent abnormal events, safety controls are required too.

To efficiently test concepts, usually water is used as a simulant of liquid lithium. The law of similarity guarantees that two different types of flow become similar when these flows are properly scaled and dimensionless numbers that are relevant to these flows (e.g. the Reynolds number) are the same. The dimensionless numbers that are relevant in this case are the Reynolds number and Weber number. The Reynolds number is defined as

$$Re = \frac{LU}{\nu}, \quad (1)$$

where L is the characteristic length, U is the characteristic speed, and ν is the kinematic viscosity.

The Weber number is defined as

$$We = \frac{\rho LU^2}{\sigma}, \quad (2)$$

where ρ is the density of the liquid, σ is the surface tension between the liquid and the gas.

* Work supported by the U.S. Department of Energy Office of Science under Cooperative Agreement DE-SC0000661

[†] kanemura@frib.msu.edu

LOW LEVEL RF CONTROL ALGORITHMS FOR THE CERN PROTON LINAC4

P. Baudrenghien[†], B. Bielawski, R. Borner, CERN, Geneva, Switzerland

Abstract

The CERN Linac4 Low Level RF (LLRF) uses a Linear Quadratic Gaussian regulator and an Adaptive Feed Forward to stabilize the accelerating field in the cavities in the presence of strong beam loading. A Klystron Polar Loop is also implemented to compensate the RF perturbations caused by the ripples and droop in the klystron High Voltage supply. The paper presents the important parts of the regulation, shows results as the system has evolved from first prototype (2013) to operational beams (2020), and mentions some important issues encountered during the commissioning and the first years of operation, with their mitigations.

LINAC4

The Linac4 machine accelerates H⁻ ions to 160 MeV Kinetic Energy and injects these into the PSB synchrotron, through a stripping foil. The RF operates at 352.2 MHz. It includes a chopper at 3 MeV removing the bunches that would fall outside the 1 MHz PSB bucket ($h=1$). The chopper also creates empty 2 μ s long beam gaps to cope with the switching time of the distributing magnet that routes the Linac beam to the four superposed PSB rings. As a consequence, the cavities see strong transient beam loading as the beam intensity changes from zero to maximum beam current (presently 25 mA DC) in just 3 ns. The machine operates at a 1.2 s repetition time. At each pulse it can accelerate up to 600 μ s of beam consisting of four batches (one per PSB ring) spaced by 2 μ s [1,2]. Linac4 has been producing protons for the CERN complex (PSB, PS, SPS, LHC) since Dec. 2020 [3]. Its first years of RF operation are presented in a companion paper [4]. The LLRF consists of a tuning system keeping the cavity at the tune that minimizes the required power [5], and a field regulation that modifies the generator drive to keep the cavity field at the desired value.

THE NEED FOR FIELD REGULATION

End-to-end beam dynamics simulations had been carried out, early in the machine design, to define (among other tolerances) the maximum level of RF phase and amplitude jitter that the system can tolerate before beam quality at injection in the PSB is compromised [6]. This study resulted in a one RF degree, one percent amplitude pk-pk budget during the beam pulse, for the (then) nominal 40 mA DC intensity. Although the source cannot presently give the target intensity, the RF performances presented here are scaled for the 40 mA.

[†] Philippe.Baudrenghien@cern.ch.

The causes for field fluctuations are numerous:

- Environmental causes (temperature and humidity) will affect the tunnel floor changing the cavity spacing, and the cable length, thereby introducing phase shifts.
- The cavities are subject to vibrations and microphonics that may be too fast to be corrected by the mechanical tuners.
- The power amplifiers suffer from RF gain/phase ripples caused by the noise in their High Voltage (HV) DC supply. This is very severe with klystrons: The changes in the HV modulate the velocity of the klystron electron beam, resulting in a change in the delay between input and output cavities. The LEP tubes (reused in Linac4) show 0.1 dB and 8 RF degree per percent HV drift. The slow drift during the pulse is called klystron *droop*. It will lead to a reduction of the field along the batch. The higher frequency (10 kHz) was traced to the switching frequency of the HV power converters. It is important to note that this affects the RF system as a *multiplicative* noise.
- Another source of perturbation is the beam current. An RF cavity is a resonant circuit excited by two currents, the RF amplifier output and the beam [7]. This is by far the largest perturbation in the Linac4 cavities. The 25 mA DC beam current induces almost 1 MV in the CCDTL1 cavity for example, to be compared to the 8 MV accelerating voltage. For nominal 40 mA, the beam induced voltage will be 1.6 MV, that is 20% amplitude variation. To respect the specifications, our LLRF must (and does) reduce the beam loading peak by twenty linear minimum. The beam loading is an *additive* perturbation in the RF system.

LLRF HARDWARE

This paper is focused on the algorithms. Yet a short presentation of the hardware will help the understanding.



Figure 1: VME crate housing the LLRF modules for one power amplifier and its cavity.

RF SYSTEM PERFORMANCE IN SwissFEL

C. D. Beard*, J. Alex, H.-H. Braun, P. Craievich, Z. Geng, N. Hiller, R. Kalt, C. Kittel,
 T. Lippuner, T. G. Lucas, R. Menzel, M. Pedrozzi, E. Prat, S. Reiche, T. Scheitinger,
 W. Tron, D. Voulot, R. Zennaro
 Paul Scherrer Institut, 5232 Villigen PSI, Switzerland

Abstract

The Hard X-ray FEL machine SwissFEL at the Paul Scherrer Institut in Switzerland is commissioned and transiting to user operation smoothly. FEL operation requires stringent requirements for the beam stability at the linac output, such as the electron bunch arrival time, peak current and beam energy. Among other things, a highly stable RF system is required to guarantee the beam stability. RF performance often dominates the overall performance and availability of FELs, and for this reason the SwissFEL RF system has been designed based on the state-of-the-art technologies that have enabled excellent RF stability, resulting in an arrival time jitter of 10 fs rms and relative beam energy stability of 10⁻⁴ rms. This paper aims to provide an understanding of the peak performance of the RF systems and to highlight possible limitations currently faced, focusing on the S-, C- and X-Band systems.

INTRODUCTION

SwissFEL [1] has been operational for regular users since early 2019, and over these past 3 years the linac operation in terms of both reliability and stability has been vastly improved. Through a better understanding of the instabilities, individual RF system performance and a gradual improvement of the infrastructure has been routinely carried out, with a long-term plan to increase the operational performance and reliability of the injector. RF stability is one of the most influential aspects of linear accelerator driven FELs, and often determine the achievable performance of the lasing capabilities. Operationally it is crucial to find a compromise between reliability and performance, however PSI have developed an RF system, which is capable of delivering low amplitude and phase jitter, whilst maintaining a highly reliable linac. The accelerator operates almost exclusively at 100 Hz, and consists of a 2.6 cell S-band photo-injector (electron source), four S-band accelerating modules (6 RF structures) and a single X-band station to linearise the energy-time curvature produced in the S-band injector stations and the non-linearities of the magnetic bunch compressors. Immediately following the injector and the first magnetic bunch compressor is the main C-band linac. SwissFEL is unique such that it operates in dual electron bunch mode that can provide a maximum beam energy up to 6.2 GeV to the Aramis undulator line, and 3.2 GeV to the Athos undulator line simultaneously. A schematic of the SwissFEL layout can be seen in Fig. 1.

* Carl.Beard@psi.ch

RF SYSTEM OVERVIEW

All RF stations (S-, C- and X-band) have the same overall RF system architecture with an individual LLRF feedback system controlling a solid state amplifier, which drives a 45 MW short-pulsed power klystron, which itself is powered by a high-voltage (HV) solid state modulator. A reference clock is distributed to components in the accelerator, with the trigger signal coming directly from the LLRF to the modulator and pre-amplifier.

Injector

The injector operates five accelerating stations (during user operation) and an X-band lineariser. At present due to limitations of the available RF power, configuration and mode of operation, each accelerating station operates at a different setpoint, whilst the specific energy gain of SINSB03/04 are regulated by the energy feedback system. Typical operating parameters for the Injector are displayed in Table 1. In the injector, each accelerating station (besides the gun) drives 1 or 2, 4-m long travelling wave (TW) accelerating structures. Due to excessive arcing in the SINSB04 klystron, the energy gain in SINSB04 has been compensated with SINSB03, to reduce the overall stress in the klystron and minimise downtime.

Table 1: Typical Injector Operating Parameters

| Station | Energy Gain (MeV) | RF Phase | HV Stab. (ppm) |
|-------------------|-------------------|----------|----------------|
| RF Gun (2.6 cell) | 7.1 | 90° | 19 |
| SINSB01 (1x4m) | 70.5 | 90° | 15 |
| SINSB02 (1x4m) | 62.4 | 90° | 45 |
| SINSB03 (2x4m) | 100 | 70° | 19 |
| SINSB04 (2x4m) | 79.5 | 70° | 60 |
| SINXB01 (1x0.9m) | -19.6 | 270° | 27 |

Linac

The main C-band linac is composed of three linacs as shown in Fig. 1. Between linac 1 and linac 2 is the second magnetic bunch compressor (BC2) while between linac 2 and linac 3 is the switchyard where the second bunch is extracted for the Athos beamline. The linac has a total of twenty six RF modules each feeding four accelerating structures, ~40 MW is required to achieve the specified 240 MeV energy gain per station. In the Athos beamline, there is an additional RF station to adjust the beam energy for the undulator chain by ±240 MeV. Each C-band station utilises an

PRODUCTION, TEST AND INSTALLATION OF ESS SPOKE, MEDIUM AND HIGH BETA CRYOMODULES

C. G. Maiano*, for the ESS SRF Collaboration,
ESS Lund, IFJ PAN Kraków,
IJCLAB Orsay, Uppsala University,
INFN-LASA Milano, STFC Daresbury, CEA Saclay

Abstract

We present here an overview of the ESS cryomodule production, test and preparation to tunnel installation, covering both families of modules: spoke and elliptical. Cryomodules and cavities for the ESS linac are in-kind contribution by several of the project partners.

PRODUCTION AND DELIVERY STATUS

Spoke cryomodules (CM) are in-kind contributions [1, 2] by IJCLAB and they undergo their site acceptance test (SAT) at the FREIA Laboratory, in Uppsala.

ESS will have a total of 14 spoke cryomodules (13 in the linac and one spare): presently 8 modules have passed SAT at FREIA and are in Lund. Incoming inspection for all the 8 received modules have been completed for all the several disciplines (mechanical, vacuum, electrical and SRF) and modules are currently stored, ready for transport and tunnel installation as soon as the CDS (Cryo Distribution System) will end its commissioning and qualification at the beginning of 2023. The current forecast is to complete the spoke testing at FREIA by the beginning of 2023. All reports are stored in the ESS Enterprise Asset Management (EAM) system for long term stewardship of the facility.

Elliptical cryomodules, 9 medium-beta (MB) and 21 high beta (HB) cryomodules, are in-kind contributions [1, 2] of CEA Saclay: MB and HB cavities are provided by INFN and STFC. CEA is responsible for assembly and delivery, and for the high RF power test for the first three CM of each family (and prototypes). The industrial assembly is performed by the B&S International company using the CEA infrastructure, under CEA supervision. Presently 12 modules have been fully assembled: 7 medium beta and 2 high-beta are currently at ESS. At the arrival in Lund incoming inspection reports are produced and released in EAM. Currently 5 medium beta have been successfully tested at Lund Test Stand (TS2) and are ready for installation. By the end of 2022 the seven available medium beta CM will be tested and high beta testing will start. CM installation in the tunnel will start in 2023. ESS has the responsibility of CM transport to site [3].

The staged facility commissioning will perform beam operation on the permanent beam dump at 570 MeV after the installation of the 7 MB and 2 HB CM already available, before the finalization of the target system, which will be ready in 2025. After the initial commissioning on the beam dump the remaining HB CM for the 800 MeV goal of 2 MW operation on target.

SPOKE CM TEST STATUS

After SAT at FREIA the spoke CMs are shipped to ESS, inspected and stored before tunnel installation.

FREIA team developed competences in SRF projects from 2015 to 2019, testing the prototype components several times. The 6-week test procedure was optimized, in order to achieve a yearly throughput of 8/9 CM tests. Series modules testing started in Oct 2020 and proceeded without interruptions during the Covid-19 pandemic. A total of 14 cold tests were performed, 8 modules were accepted and other 6 tests are currently planned to reach a total of 14 modules. The spoke CM series testing completion is forecast by March 2023.

The test plan performed at FREIA can be factorized in four main sections:

- Reception test (2 weeks): incoming frequency measurements and mechanical preparation for bunker.
- Warm test (1 week): cable calibration and then warm coupler conditioning.
- Cold test (2 weeks): measurement of frequency shift vs temperature/pressure; tuner steps to resonance and tuner frequency sensitivity; assessment of accelerating field, Lorentz force detuning and heat loads.
- Warm up and departure to ESS (1 week)

Spoke Cryomodules Tests Statistics

The statistics collected for all modules tested to now at FREIA is presented in Figure 1, which shows that most of the module reached the administrative test limit of 12 MV/m and all of them fulfilled the 9 MV/m specification. Eight out the eleven modules tested have fulfilled SAT and some modules required actions to resolve non conformities and retesting. The present nonconformities under resolution regard cold tuner motor failures (CM10 and CM11 have been repaired and re-tested at Uppsala) and vacuum leaks (CM09), requiring a string reassembly at IJCLab. The statistics account for all tested modules.

The assessment of the accelerating field during tests, E_{acc} , is performed in two different ways and comparison with VT (Vertical Test) results is systematically performed. The field k_t calibration factor is either computed using the forward power over-coupled relation or from the stored energy method. Calibration uncertain in power measurements was estimated in 0.5 dB (12%). For spokes the difference between VT and cryomodule, CM, calibration is not systematic (see Figure 2), while for elliptical medium the VT estimation leads to higher fields than the CM test.

*cecilia.maiano@ess.eu

THE ARES LINAC AT DESY

F. Burkart*, R.W. Assmann¹, H. Dinter, S. Jaster-Merz,
W. Kuropka, F. Mayet, B. Stacey, T. Vinatier
Deutsches Elektronen-Synchrotron DESY, Germany
¹also at Laboratori Nazionali di Frascati, Italy

Abstract

The generation and acceleration of ultra-short, high quality electron beams has attracted more and more interest in accelerator science. Electron bunches with these properties are necessary to operate and test novel diagnostics and advanced high gradient accelerating schemes. Furthermore, several medical and industrial applications require high-brightness electron beams. The dedicated R&D linac ARES at DESY (Deutsches Elektronen-Synchrotron) is now fully operational and able to produce these electron beams at the nominal energy of 155 MeV and deliver them to users. This paper gives an overview of the ARES linac and summarizes the beam parameter measurements. The possibilities for user operation will be described in detail.

THE SINBAD FACILITY

SINBAD (Short INnovative Bunches and Accelerators at DESY) is an accelerator R&D platform in the former DORIS accelerator tunnel at DESY, Hamburg. Its goals are to demonstrate the generation and acceleration of ultra-short electron bunches and to test advanced acceleration techniques such as laser driven plasma wake-field acceleration (LWFA), dielectric laser acceleration (DLA) and THz-driven acceleration, in multiple independent experiments [1–3]. ARES (Accelerator Research Experiment at SINBAD) at SINBAD represents one of these experiments. The construction of the linear RF accelerator with a target energy of 100–155 MeV was finished in 2021 followed by an extensive commissioning phase. The facility provides ultra-short, high brightness electron bunches with an excellent stability and reproducibility.

THE ARES LINAC

The ARES linac starts with a normal conducting RF photoinjector generating single electron bunches with a repetition rate of up to 50 Hz [4]. The bunch is afterwards accelerated by an S-band linac section, consisting of two travelling wave structures (TWS) accelerating the beam to its nominal momentum of 155 MeV/c. A first in-vacuum experimental area is installed downstream of the linac section. A movable magnetic bunch compressor (as part of the German Helmholtz-ATHENA project, [5]) will allow the generation of ultra-short bunches in the fs to the sub-fs regime based on the combined techniques of velocity bunching and magnetic bunch compression [6]. The high brightness beam will then serve as a test bench for novel diagnostic devices such as

the PolariX TDS, an advanced modular X-band transverse deflecting structure (TDS) system. It has the new feature of providing variable polarization of the deflecting force [7–10]. Further downstream and connected to the spectrometer section, two additional experimental stations were installed, allowing experimentalists to perform tests also in an in-air setup. A picture of the ARES linac is shown in Fig. 1.

Beam Parameters

The actual commissioning and design beam parameters are listed in Tab. 1. With additional high sensitive beam diagnostics it was possible to characterize the bunches down to 2.5 fC. The nominal bunch length of a few fs down to the sub-fs can only be measured with the PolariX TDS being fully operational, which is foreseen for mid 2023. Still without magnetic compression a bunch duration of 30 fs rms was reconstructed at the entrance of the second TWS using tomographic methods. This corresponds to the resolution limit of these methods on ARES. [11]. ARES has already demonstrated an outstanding stability with a relative momentum stability of 6E-5 over 16 hours at 155 MeV and a mean FWHM energy spread of 0.06 MeV.

Table 1: ARES design beam parameters and actual commissioning parameters.

| Parameter | Actual | Design |
|------------------|----------------|----------------|
| Momentum | 45 - 155 MeV/c | 45 - 155 MeV/c |
| Charge per pulse | 0.003 - 200 pC | 1 - 100 pC |
| Rep. rate | 1 - 50 Hz | 1 - 50 Hz |
| Bunch length | 30 fs | sub-fs |

Experimental Areas

ARES offers three experimental stations for DESY-internal and external user experiments and R&D purposes. The first experimental area is in the machine vacuum system and therefore only compatible with UHV, particle free setups. The experimental chamber is equipped with a hexapod. A screen and a nano-wirescanner are located on the hexapod. A quadrupole triplet as well as corrector magnets allow for an excellent beam control. A side view inside the chamber is depicted in Fig. 2 [12].

The second experimental area is located in the dispersive arm of the spectrometer section at the end of the linac. It consists of a vacuum chamber, separated from the machine vacuum by a 50 μm thick titanium foil. This experimental area is dedicated to detector tests with detectors in low-pressure or nitrogen atmosphere. A picture of the chamber is shown in

* florian.burkart@desy.de

COMMISSIONING OF A MOVABLE BUNCH COMPRESSOR FOR SUB-fs ELECTRON BUNCHES *

W. Kuroпка †, R. W. Assmann¹, F. Burkart, H. Dinter,
S. Jaster-Merz, F. Lemery, F. Mayet, B. Stacey, T. Vinatier,
Deutsches Elektronen-Synchrotron DESY, Notkestr. 85, 22607 Hamburg, Germany
¹also at Istituto Nazionale di Fisica Nucleare,
Laboratori Nazionali di Frascati, 00044 Frascati (Roma), Italy

Abstract

We present the first commissioning results of the movable bunch compressor (BC) designed for the ARES linac at DESY. The development and simulated performance has been reported earlier and predicts sub-fs electron bunches with high charge densities. Commissioning results of the injector part of the ARES linac delivered promising beam quality results to achieve these numbers. The bunch compressor system is foreseen to be used to bench mark numerical models for coherent synchrotron radiation (CSR) and space charge (SC) for ultra-short electron bunches. Here we will present first measurements of the dispersion as well as calculations for the longitudinal dispersion. In the future the PolariX transverse deflecting structure (TDS) will be commissioned to fully characterize the ARES electron beam.

ARES OVERVIEW

The ARES linac [1] is an S-band normal conducting linear electron accelerator for research and development of accelerator technology. The main focus lies on the production and characterization of high quality sub-fs electron bunches. Also the injection into laser driven electron acceleration schemes is pursued [2]. ARES is composed of a 1.6 cell gun and two 4 m long traveling wave structures (TWS). A vacuum chamber for exchangeable samples is located downstream of the radio frequency (RF) structures. A matching section comprises six quadrupole magnets and correctors connects to the BC section. The diagnostic line comprises the TDS [3] and dipole spectrometer. At the end of the diagnostic section the beam can be coupled out into air via a 50 μm titanium window. An overview of the installation can be found in another contribution [4].

Two modes of operation for short bunches are possible with the current setup: velocity bunching and magnetic compression. Hybrid Working points taking advantage of both concepts were studied also [5]. For the hybrid and magnetic compression working points the characteristics of the BC are essential. The beam is transported to the BC via the matching section and the longitudinal dispersion of the bunch compressor is adjusted to minimize the bunch length. Non-linearity of the longitudinal momentum correlation, uncorrelated energy spread, SC and CSR [6, 7] can be lim-

iting factors in bunch compression. The development and performance prediction have been published [8].

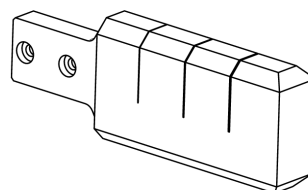


Figure 1: Drawing of the shape collimator blade. At the moment the attached blade has three slit apertures of 0.2 mm, 0.4 mm and 0.6 mm.

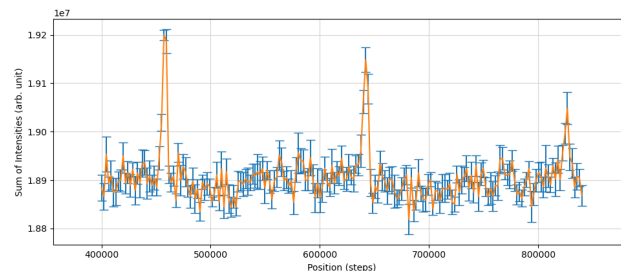


Figure 2: Beam intensity after the bunch compressor vs. position of the collimator mover. The three peaks correspond to the different apertures.

BUNCH COMPRESSOR

The magnetic chicane consists of four dipole magnets of which the two center ones can be moved up to 20 cm out from the center line to achieve large variability in the longitudinal dispersion. An overview of the BC is illustrated in Fig. 3. In between the two center magnets, where transverse dispersion is largest, an aperture collimator is installed to cut the real space of the bunch. A drawing of the collimator blade is shown in Fig. 1. Its function was checked by measuring the intensity on a down stream scintillating screen against the position of its transverse mover. Results are shown in Fig. 2. The collimator can be used to mitigate bunch lengthening from the non-linearity in longitudinal phase space due to RF curvature at the TWSs. A scintillating screen station is installed allowing the measurement of the transverse dispersion between the two center magnets. The first three dipole

* Work supported by Helmholtz Association HGF

† willi.kuroпка@desy.de

RF PERFORMANCE OF A NEXT-GENERATION L-BAND RF GUN AT PITZ

M. Krasilnikov*, Z. Aboulbanine, G. Adhikari, N. Aftab, P. Boonpornprasert,
M.-E. Castro-Carballo, G. Georgiev, J. Good, M. Gross, A. Hoffmann, L. Jachmann, W. Koehler,
C. Koschitzki, X.-K. Li, A. Lueangaramwong, D. Melkumyan, R. Niemczyk, A. Oppelt, S. Philipp,
M. Pohl, B. Petrosyan, H. Qian, C. Richard, J. Schultze, G. Shu, F. Stephan,
G. Vashchenko, T. Weillbach, DESY, Zeuthen, Germany
M. Bousonville, F. Brinker, L. Knebel, D. Kostin, S. Lederer, L. Lilje, S. Pfeiffer, M. Hoffmann,
R. Ritter, S. Schreiber, H. Weise, M. Wenskat, J. Ziegler, DESY, Hamburg, Germany

Abstract

A new generation of high-gradient normal conducting 1.3 GHz RF gun with 1% duty factor was developed to provide a high-quality electron source for superconducting linac driven free-electron lasers like FLASH and European XFEL. Compared to the Gun4 series, Gun5 aims for a ~50% longer RF pulse length (RF pulse duration of up to 1 ms at 10 Hz repetition rate) combined with high gradients (up to ~60 MV/m at the cathode). In addition to the improved cell geometry and cooling concept, the new cavity is equipped with an RF probe to measure and control the amplitude and phase of the RF field inside the gun. The first characterization of Gun5.1 included measurements of RF amplitude and phase stability (pulse-to-pulse and along 1 ms RF pulse). The dark current was measured at various peak power levels. The results of this characterization will be reported.

INTRODUCTION

The Photo Injector Test Facility at DESY in Zeuthen (PITZ) since more than 20 years develops, tests and characterizes high brightness electron sources for FLASH and European XFEL. Since these user facilities operate superconducting accelerators in pulsed mode, also the corresponding normal-conducting L-band RF gun has to operate with long RF pulses at 10 Hz repetition rate. To obtain high electron beam quality from a photocathode RF gun, a high acceleration gradient at the cathode is required. The peak RF electric field of 60 MV/m at the cathode is the goal parameter for the high brightness L-band photogun. Therefore, the RF gun has to provide stable and reliable operation at high average RF power. The previous gun cavity generation (Gun4) had a maximum RF pulse length of 0.650 ms, which implies a maximum of 27000 electron bunches per second. Growing interest from the FEL user community for even longer pulse trains motivated developments of the next generation of normal conducting L-band gun cavity (Gun5), which aims for 1 ms RF pulses. Combined with 6.5 MW of peak RF power, this results in a very high average power of ~65 kW. In addition to the improved resonator shape and cooling, Gun5 has a built-in RF probe to directly control the phase and amplitude of the RF field in the cavity. RF conditioning faces issues of

stability and reliability. Aspects of pulsed heating and dark current should also be considered.

GUN5.1 CAVITY

The RF gun cavity is a $1\frac{1}{2}$ -cell normal conducting copper cavity operating in the π -mode standing wave at 1.3 GHz. The Gun5 design includes several major improvements over the Gun4-generation aiming to enhance the gun performance. The elliptical shape of the internal geometry was applied in order to optimize the distribution of the peak electric field over the cavity surface [1]. Detailed studies to reduce the dark current resulted in an elliptical shape of the cathode hole at the back wall of the cavity. [2]. In order to control the RF field in the cavity directly an RF probe has been integrated in the front wall of the full cell. An optimized cavity cooling system and improved rigidity [1] should mitigate the challenges associated with the 1% duty cycle.

The cavity of the Gun5.1 prototype was tuned to the operation frequency and reasonable field balance of the π -mode electric field. The results of the bead-pull measurements after the last tuning step are shown in Fig. 1 together with eigenmode simulations for 0- and π -modes. Due to some technical issue a part of the π -mode measurement close to the cathode hole was corrupted, but simultaneous simulations of both modes are in a good agreement with both measurements. According to these results, the axial field distribution of the π -mode has a field balance $|E_{cath}/E_{fullcell}| \approx 1.097$.

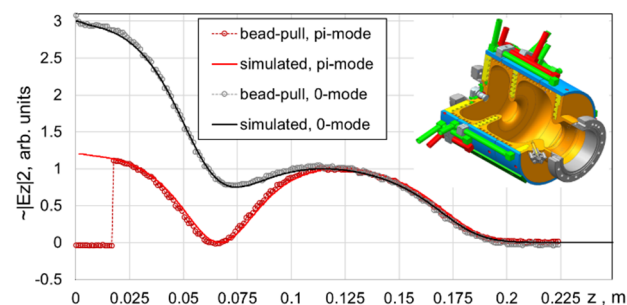


Figure 1: Results of the bead-pull measurements for 0- and π -modes after the last tuning step. The corresponding Superfish simulations are shown with solid curves. Inlet: 3D model of the Gun5.1.

* mikhail.krasilnikov@desy.de

STATUS AND RELIABILITY ENHANCEMENTS OF THE ALBA LINAC

D. Lanaia, R. Muñoz Horta, F. Pérez, ALBA Synchrotron, Cerdanyola del Vallès, Spain

Abstract

The pre-injector of the ALBA Synchrotron is a Linac that delivers 110 MeV electrons during regular operation. It consists in two Pre-bunchers, a Buncher and two Accelerating Sections fed by two pulsed 37 MW klystrons. Along the years, efforts to enhance the ALBA Linac performance and reliability have been devoted, resulting in an improvement of the Linac to Booster beam transmission efficiency, and of its Mean Time Between Failures (MTBF). The performance enhancement has been based on the use of optimization and control routines of the beam parameters (such as beam position and energy), but also by the application of regular preventive hardware maintenance procedures. Besides, the Linac reliability has been improved also by the implementation of alternative working modes in case of hardware failures, like operating at 67 MeV, with only one klystron and one Accelerating Section. In this respect, a new upgrade of the RF waveguide system is being implemented, with the aim to produce 80 MeV electron beam using only one klystron that will feed both Accelerating Sections. At this energy the injection to the Booster is expected to be more stable than with the existing 67 MeV mode. Furthermore, the possibility to install a thermionic RF-gun to inject directly into the first Accelerating Section is under study. This new gun will be installed in addition to the existing system, and will allow handling in short time any failure either from the DC-gun, the Pre-bunchers or the Buncher, ensuring the Linac's reliability even in case of a major event. Details of the Linac performance during the past years and a description of the new hardware upgrades are presented in this work.

INJECTOR WORKING MODES

Linac Operation Versatility

Two TH2100 klystrons (KA1 and KA2) power the ALBA Linac. In its nominal operation mode, KA1 feeds the Buncher cavities and the first Accelerating Section (AS1) whereas KA2 feeds exclusively AS2 [1].

Along the years other operation modes have been developed with the aim to enhance the reliability, not only of the ALBA Linac, but also of the ALBA injector.

In 2014, after a Linac waveguide upgrade, the ALBA injector was provided with the Single Klystron Injection Mode. This mode allows injecting a 67 MeV electron beam into the Booster using only one klystron (either KA1 or KA2), which feeds the Buncher and AS1 [2]. In fact, this mode has been also commissioned at 60 MeV to overcome arcs in the waveguide, although being less stable than the 67 MeV beam.

* With KA1 at nominal power, a 92 MeV beam should be achieved. However, arcs in the waveguide constrain the power delivered by KA2.

After an RF-window incident at AS1, such low energy beam was also injected into the Booster by operating with two klystrons while keeping AS1 disconnected: KA1 fed the Buncher and KA2 fed AS2. A summary of the ALBA injector different working modes is shown in Table 1.

Table 1: ALBA injector modes. The modes in grey are being implemented, but not tested.

| Energy [MeV] | KA1 | KA2 | Cavities fed |
|----------------|-----|-----|----------------|
| 110 | On | On | BU + AS1 + AS2 |
| 67 (60) | On | Off | BU + AS1 |
| 67 (60) | On | Off | BU + AS1 |
| 67 (60) | On | On | BU + AS2 |
| 80 | On | Off | BU + AS1 + AS2 |
| 80 | Off | On | BU + AS1 + AS2 |

Injecting into the Booster at 60 or 67 MeV is not straightforward [3]. The injection to the Booster at lower beam energies is affected by strong Booster magnetic field distortions produced by eddy currents induced at the bending magnet vacuum chambers. Because of its complexity this mode is tested every 6 months, to have it operationally when needed. Since its implementation, this mode has been required and used during the operation of ALBA for users at least in two occasions.

At present, another waveguide upgrade is being implemented at the ALBA Linac to feed all Linac cavities with only one klystron with the aim to inject a 80 MeV* beam into the Booster. The new waveguide configuration is shown in Fig. 1. The RF power sent by Klystron 1 to AS1 is now split in two equal branches: 50% to feed AS1 and 50% to feed AS2. As a consequence, for the same klystron power more cavities are fed. The total voltage applied to the electron beam increases by a factor $\frac{2}{\sqrt{2}}$.

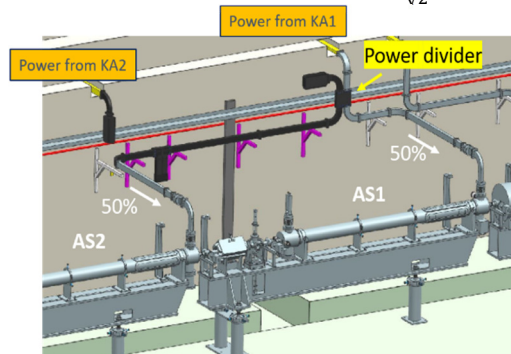


Figure 1: Waveguide modification for Single Klystron Injection Mode at 80 MeV.

RF DESIGN OF TRAVELING-WAVE ACCELERATING STRUCTURES FOR THE FCC-ee PRE-INJECTOR COMPLEX

H. W. Pommerenke*, A. Grudiev, A. Latina, CERN, Geneva, Switzerland
S. Bettoni, P. Craievich, J.-Y. Raguin, M. Schär, Paul Scherrer Institut, Villigen, Switzerland

Abstract

The linacs of the FCC-ee (Future Circular Electron-Positron Collider) injector complex will provide the drive beam for positron production and accelerate nominal electron and positron beams up to 6 GeV. Several linacs comprise different traveling-wave (TW) accelerating structures fulfilling the beam dynamics and rf constraints. Notably, high-phase advance large-aperture structures accelerate the positron beam at low energies. All TW structures are rotationally symmetric for easier production. Long-range wakes are damped by HOM detuning. Operating mode and HOM parameters were calculated based on lookup tables and analytic formulas, allowing for rapid scanning of large parameter spaces. In this paper, we present both methodology and realization of the rf design of the TW structures including their pulse compressors.

INTRODUCTION

The FCC-ee Conceptual Design Report (CDR) [1] considers a 6 GeV linac with 2 bunches per rf pulse at a repetition rate up to 200 Hz as baseline option for the FCC-ee injector complex. The bunches will have a charge of 5 nC each with an rms length of 1 mm or more and a spacing between 15 ns and 100 ns. The latest layout is shown in Fig. 1. Two separate linacs for electrons and positrons are foreseen up to 1.54 GeV. Both beams are then accelerated by the common linac to 6 GeV. To match the proposed filling scheme, the two low-energy linacs have to work at a repetition rate of 200 Hz and the common linac at 400 Hz, 200 Hz each for positrons and electrons [1, 2].

Over the last year, baseline parameters for the traveling-wave (TW) rf structures foreseen for each of the linacs have been determined. In the following, the methodology of the rf design and specific structures for positron, electron, and common linac are presented.

RF DESIGN METHODOLOGY

Large parameter spaces have to be considered when optimizing traveling-wave (TW) structures. In our case, one cell is characterized by its aperture radius (iris radius) a , iris thickness d , and synchronous rf phase advance ψ , where $L_c = \lambda\psi/(2\pi)$ is the cell length with the frequency $f = c/\lambda$. Structures are linearly tapered in aperture and iris thickness, such that 7 parameters describe one structure. To calculate millions of structures, cell parameter lookup tables and analytic formulas are used as far as possible.

* hermann.winrich.pommerenke@cern.ch

Cell Lookup Table

The general cell geometry (Fig. 2) is based on the Swiss-FEL C-band structure [3] and as such the lookup table database has been computed at its frequency of 5.712 GHz. However, this choice is arbitrary and it can be scaled to any frequency using appropriate proportionalities.

The lookup table contains over 200 reference geometries with different geometries ($0.08\lambda \leq a \leq 0.36\lambda$, $0.02\lambda \leq d \leq 0.19\lambda$, $2\pi/3 \leq \psi \leq 9\pi/10$). For each cell, iris ellipticity has been optimized for a maximum modified Poynting vector S_c [4] as small as possible. Rf parameters of the lowest higher-order modes (HOMs) have been numerically computed at the synchronous frequencies. The table contains frequencies, quality factors, shunt impedances, group velocities, and passband limits of the 20 lowest monopoles and dipoles each as well as high-gradient limits of the fundamental mode.

Analytic Formulas

The TW structures accelerate two bunches per rf pulse and thus profit from the widely-used SLED-type (SLAC energy doubler) rf pulse compressor [5]: A storage cavity with unloaded Q factor Q_c and coupling β is charged by the klystron. When the klystron phase is reversed, the storage cavity is discharged, adding to the klystron pulse. For a klystron pulse with arbitrary amplitude $A_k(t)$ (in units of \sqrt{W}), the amplitude into the TW structure is found to be

$$A_\ell(t) = A_k(t) - \alpha\mu e^{-\mu t} \int_0^t e^{\mu t'} A_k(t') dt', \quad (1)$$

where $\mu = \omega(1 + \beta)/2Q_c$ is the reciprocal storage cavity filling time and $\alpha = 2\beta/(1 + \beta)$. Assume now a rectangular klystron pulse of length T_k , amplitude $A_{k,0}$ and phase reversal at $t = T_k - T_f$, where T_f is the TW structure filling time. We obtain for $T_k - T_f \leq t \leq T_k$:

$$\frac{A_\ell(t)}{A_{k,0}} = 1 - \alpha \left(1 + \left[1 - 2e^{\mu(T_k - T_f)} \right] e^{-\mu[t - \tau(z)]} \right). \quad (2)$$

Following Ref. [6], the transient gradient during structure filling can be derived as

$$G(z, t) = A_\ell [t - \tau(z)] \sqrt{\omega \frac{\varrho(0)}{v_g(0)}} g(z), \quad (3)$$

where

$$g(z) = \sqrt{\frac{v_g(0)\varrho(z)}{v_g(z)\varrho(0)}} \exp \left[-\frac{\omega}{2} \int_0^z \frac{dz'}{v_g(z')Q(z')} \right] \quad (4)$$

STATUS OF CLARA AT DARESBURY LABORATORY

D. Angal-Kalinin^{*1}, A. Bainbridge¹, A. Brynes¹, R. K. Buckley¹, S. R. Buckley¹, R. J. Cash,
H. M. Castaneda Cortes¹, J. A. Clarke¹, R. F. Clarke, M. Colling, L. S. Cowie¹, G. Cox,
K. Dumbell¹, D. J. Dunning¹, B. D. Fell, A.J. Gilfellow¹, A. R. Goulden¹, S. A. Griffiths,
M. D. Hancock, T. Hartnett, J. Henderson¹, S. Hitchen¹, J. P. Hindley, C. Hodgkinson, F. Jackson¹,
C. Jenkins¹, J. K. Jones¹, M. Johnson¹, N. Y. Joshi¹, M. King¹, G. Marshall, S. L. Mathisen¹,
R. Mclean¹, J. W. McKenzie¹, K. J. Middleman¹, B. L. Militsyn¹, K. Morrow¹, A. J. Moss¹,
B. D. Muratori¹, T. C. Q. Noakes¹, A. Oates, W. Okell¹, H. L. Owen¹, T. H. Pacey¹, A. Pollard¹,
M. D. Roper¹, Y. M. Saveliev¹, D. J. Scott¹, B. J. A. Shepherd¹, R. J. Smith¹, E. W. Snedden¹,
N. Thompson¹, C. Tollervey¹, R. Valizadeh¹, A. Vick¹, D. A. Walsh¹, A. E. Wheelhouse¹,
P. H. Williams¹, J. T. G. Wilson

UKRI STFC, Sci-Tech Daresbury, Warrington, UK

¹also at Cockcroft Institute, Sci-Tech Daresbury, Warrington, UK

Abstract

CLARA (Compact Linear Accelerator for Research and Applications) is a test facility for Free Electron Laser (FEL) research and other applications at STFC's Daresbury Laboratory. The Front End of CLARA has been used for user exploitation programme from 2018. The second exploitation period in 2021-22 provided a range of beam parameters to 8 user experiments. We report on the status, further machine development, and future plans for CLARA including Full Energy Beam Exploitation (FEBE) beam-line which will provide 250 MeV/c high brightness beam for novel experiments.

INTRODUCTION

The first successful period of CLARA exploitation on CLARA Front End (FE) was reported at previous IPACs [1, 2]. The details of beam line and beam delivery of higher momentum (35 MeV/c) to users on CLARA FE and in Versatile Electron Linear Accelerator (VELA) Beam Area 1 (BA1) in 2018-2019 run is summarised in Ref. [3]. A shutdown for preparation for CLARA Phase 2 (acceleration to 250 MeV/c) begun in April'19 and completed in September'19. During this shutdown, a load lock system was installed on the 10 Hz gun and several improvements to other technical systems were undertaken. The shielded wall between the accelerator and user area was removed to prepare for Phase 2 shielding. A temporary wall at the end of BA1 allowed operation of CLARA FE/VELA line whilst Phase 2 preparation continued outside this shield wall.

After completion of the shutdown, beam commissioning programme was resumed. The upgraded 10 Hz gun with load lock system was successfully commissioned with a number of improvements made in the photoinjector laser. The planned start of second exploitation period was suspended due to COVID lockdown and technical issues with the gun waveguide. Additional diagnostics were added: a Bunch Compression Monitor on VELA line; and Electro-Optic in the experimental chamber in BA1 to provide information of longitudinal bunch profile.

*deepa.angal-kalinin@stfc.ac.uk

Offline build and testing of CLARA Phase 2 accelerator modules have progressed well in past two years. Accelerator modules have been installed in the accelerator hall, beyond the temporary wall, to allow commissioning and operation of CLARA FE for exploitation. The rest of the completed modules will be installed in the accelerator hall during planned shutdown in 2023. FEBE hutch modules are also being procured and assembled offline. Details of FEBE design are presented at this conference [4]. CLARA Phase 2 RF systems are currently being tested at low power and the build of rack rooms is ongoing.

Beam was delivered successfully to users at two locations; straight-on and transporting it through the CLARA-to-VELA S-bend to a dedicated user experimental chamber in BA1 during October'21 – April'22. We summarise here the beam commissioning, beam delivery to users as well as our near future plans.

PHOTOINJECTOR

The 10 Hz repetition rate photoinjector was upgraded for operation with interchangeable photocathode with a final goal to improve beam quality, increase duty factor, reduce the dark current and eventually allow for operation with different types of photocathode materials.

Hybrid photocathodes (Cu tip integrated with a Mo plug) were used during the user run. The Cu surface was cleaned by Ar plasma followed by a 250°C bake. Such activated photocathodes have QE at a level of high 10^{-5} and allow for generation of bunches with a charge of 100 pC and higher with a laser pulse energy on the photocathode of 10's μ J. More detailed description of gun upgrade and operation are presented at this conference [5, 6].

MACHINE STABILITY AND JITTER

Stability of RF system is paramount as it explicitly affects beam stability. Dependence of beam energy (E_b) on RF power (P) and phase (ϕ) can be simply described as,

$$E_b = \sqrt{PZ} \cos(\phi - \phi_0), \quad (1)$$

where, Z and ϕ_0 are equivalent cavity impedance and crest phase respectively. Impact of RF amplitude and phase jitter

RF DESIGN AND CHARACTERISATION OF THE CLARA 10HZ GUN WITH PHOTOCATHODE LOAD/LOCK UPGRADE

A. J. Gilfellow*, L. S. Cowie †, B. L. Militsyn ‡, T. J. Jones, R. Valizadeh, STFC, Daresbury Laboratory, UK.

Abstract

The 2.5 cell, S-band, 10Hz repetition rate electron gun (**Gun-10**) for the CLARA (**C**ompact **L**inear **A**ccelerator for **R**esearch and **A**pplications) accelerator underwent an upgrade during the scheduled shutdown period in the summer of 2019. The existing single photocathode/back plate component was replaced by a back plate with an integrated load/lock system capable of rapid exchanges of photocathode plugs. Here we outline the motivation and RF design of the back plate and also detail the RF testing and characterisation of the upgraded gun in terms of the unloaded quality factor, Q_0 , the RF power coupling match, β , the percent field flatness and the operating frequency of the cavity, calculated from the frequency measured in the laboratory. Finally, via simulations, a square root of the forward power, $\sqrt{P_F}$, vs. beam momentum plot was produced that we predict the gun will deliver once it goes back online.

INTRODUCTION

The need to change photocathodes arises from the degradation of the cathode's Quantum Efficiency over time, damage from the photoinjector laser and RF breakdown. CLARA photocathode exchanges have occurred approximately every 6 - 12 months. In the previous configuration, where the removable backplate of the gun also functioned as the photocathode, any exchange was invasive and time consuming (~ 3 weeks). The main motivations for the 10 Hz gun back plate upgrade, therefore, were:

- Exchanges can be carried out much more rapidly in-situ, ~30 minutes.
- Exchanges can take place under vacuum conditions.
- Eliminate the risk of an oxide layer forming on the cathode surface.
- Remove the need for lengthy RF reconditioning.
- Achieve more stable and repeatable RF characteristics during a cathode load and between load events.

In the following sections we highlight some of the RF concerns that went into the design of the upgrade, the post-upgrade characterisation of Gun-10 in terms of Q_0 , β , percent field flatness and the operating frequency. Finally we determine by how much the working surface of the photocathode is intruding on the internal space of the gun, cathode

penetration, which is the first step in constructing the $\sqrt{P_F}$, vs. beam momentum plot that we predict Gun-10 will deliver.

RF DESIGN

The introduction of a load/lock photocathode system into Gun-10 was not as simple as replacing the original cathode with a flat plate and a plug.

If the upgraded backplate was simply fitted in the same position as the original design, key RF parameters would change considerably, see table 1 for a comparison of simulated results between the original and a simple backplate replacement design.

In order to preserve the RF character of the cavity the majority of the cathode surface was recessed 300 μm further back than the pre-upgrade Gun-10 cathode. Contact between the upgraded backplate and the cavity wall includes a 300 μm step, which is 40 mm from the cavity centre. The step is rounded with a radius of 150 μm on both 90° angles. The centre of the step is at 40 mm radius, and the step extends from 39.85 mm to 40.15 mm. See Fig. 1 for the general design.

Table 1: A comparison of simulated results for the pre-upgrade design and the simple load/lock replacement design that shows how the RF characteristics would change and highlights the need for a more nuanced design approach.

| Mode | Stat. | Original Cathode | Upgraded Cathode |
|----------|-------------|------------------|------------------|
| π | freq. (GHz) | 2.99863 | 2.99908 |
| | β | 1.03 | 0.61 |
| | Q_0 | 12302 | 11270 |
| $3\pi/5$ | freq. (GHz) | 2.99550 | 2.99617 |
| | β | 0.81 | 1.5 |
| | Q_0 | 11093 | 11282 |
| $\pi/5$ | freq. (GHz) | 2.99048 | 2.99103 |
| | β | 1.228 | 0.272 |
| | Q_0 | 11108 | 11846 |

RF CHARACTERISATION

General Procedure

Once the backplate was fixed in its optimal position and the specially made dummy beadpull photocathode plug with an on-axis hole for the thread to pass through was installed, the beadpull experiments could begin. The perturbation

* anthony.gilfellow@stfc.ac.uk

† louise.cowie@stfc.ac.uk

‡ boris.militsyn@stfc.ac.uk

WAKEFIELD MONITOR SYSTEM FOR X-BAND LINEARISER LINAC ON CLARA *

N. Y. Joshi[†], A. C. Aiken, C. Jenkins, A. Moss
 ASTeC, STFC Daresbury laboratory, Warrington, UK.

Abstract

CLARA linear accelerator in phase-2 will utilise an X-band fourth harmonic linac to linearise bunch phase space. Beam induced transverse higher order modes (HOMs) between 15.3 to 16.2 GHz will be coupled out through HOM ports, which can be used to correct both position offset and angle misalignment to minimise beam degradation due to HOMs. In this paper we present design of a wakefield monitor system under development, with capability to use either baseband broadband signal for basic alignment, and also carry a detailed narrow-band spectrum analysis on all four (X and Y transverse modes from two couplers) signals. Initial laboratory testing of its subsystem is also presented.

INTRODUCTION

The CLARA linear accelerator is being developed in phases to serve as a test platform for new concepts and technologies for future large scale XFEL facilities, such as proposed UK-XFEL. It is undergoing a planned upgrade to phase-II which will accelerate electron bunches up to its nominal energy of 250 MeV [1,2], using normal conducting linac RF systems operating at ~3 GHz. It will also utilise a fourth harmonic X-band linac to linearise the bunch phase space. The X-band linac will be installed on a five axis precision mover. The linac was designed by PSI in collaboration with CERN. The relevant parameters of the X-band linac are summarised in Table 1 [3,4].

Table 1: Relevant specifications of the X-band linac cavity.

| Parameter | Value | Unit |
|-----------------------|-------------|-------------------------|
| Fundamental frequency | 11.994 | GHz |
| Length | 96.5 | cm |
| Number of cells | 73 | |
| HOM coupling cells | 2 | |
| HOM frequency range | 15.3 - 16.2 | GHz |
| HOM impedance | ~ 100 | $k\Omega/(mm \times m)$ |

An electron bunch passing through the linac induces electromagnetic (EM) field, known as wakefield, which can be expressed as sum of the field induced in fundamental and various higher order modes (HOMs). The induced HOM field interacts back with the bunch and degrades beam quality, hence it is desirable to minimise HOM excitation in the linac. The amplitude of the induced dipole HOMs depends on the bunch charge and transverse bunch offset from the

cylindrical axis of the linac [4]. The phase of the HOM field flips by 180° depending on the direction of offset from the centre. By coupling out and analysing the HOM field signals, bunch trajectory offset and angle can be determined and used to minimise HOM excitation. The linac cell iris and radius are varied along the linac length to achieve the desired gradient profile of the fundamental accelerating field, which also results in variation of the dipole HOM frequencies of the cells. As the HOM frequency varies along the cavity length, cell misalignment within the cavity can be studied in detail by analysing narrow band sections of the HOM spectrum.

The X band linac has two HOM couplers, the first is located in the mid section of the linac and couples to the HOMs from upstream cells. The second is at the end of the linac and couples to the HOMs from the downstream cells situated after the first HOM coupler. The HOMs are coupled out through the side coupled waveguides with cutoff frequency above the fundamental accelerating frequency to prevent the large accelerating field at 12 GHz. Each HOM cell has four ports, two each for X and Y bunch offset measurements, which can be combined to increase measurement sensitivity. The cavity misalignment can be minimised by measuring only the amplitude of the wideband HOM signals, but the ability to study the spectrum in detail and extracting the phase allows us to utilise it as a beam position monitor (BPM) system by knowing the direction of the offset. Hence the minimum requirement from the wakefield monitor system is to have four channels that can measure the amplitude of the wideband HOM signals, but additional functionality of spectrum analysis and phase measurement is highly desirable.

WAKEFIELD MONITOR SYSTEM

A wakefield monitor system is under development to facilitate HOM measurement and alignment of the cavity with 10 μm resolution for 200 pC bunch charge. A simplified block diagram of the system is shown in Fig. 1. It is designed as a modular system with signal processing in two stages. To minimise the cable losses at the higher HOM signal frequencies, the front-end box will be placed in the accelerator tunnel next to the linac and can either measure the baseband amplitude, or down convert the signal to less than 1.5 GHz and send it to the back-end box in an RF room through the long coaxial cables. The back-end box in the RF room can further process the amplitude, or scan the HOM spectrum for detailed narrowband analysis.

* STFC-UKRI

[†] Nirav.Joshi@stfc.ac.uk

LCLS-II-HE CRYOMODULE TESTING AT FERMILAB*

A. Cravatta[†], S. Posen, T. Arkan, D. Bafia, B. Chase, C. Contreras-Martinez, B. Giaccone, B. Hansen, E. Harms, B. Hartsell, J. Kaluzny, D. Lambert, J. Makara, H. Maniar, Y. Pischalnikov, J. Reid, N. Solyak, D. Sun, A. Syed, R. Wang, M. White, G. Wu
 Fermi National Accelerator Laboratory, Batavia, IL, USA
 S. Aderhold, A. Benwell, M. Checchin, J. Fuerst, D. Gonnella, T. Hiatt, S. Hoobler, B. Legg, J. Maniscalco, M. Martinello, J. Nelson, L. Zacarias
 SLAC National Accelerator Laboratory, Menlo Park, CA, USA
 L. Doolittle, S. Ferriera Paiagua, C. Serrano
 Lawrence Berkeley National Laboratory, Berkeley, CA, USA

Abstract

22 Linac Coherent Light Source II (LCLS-II) cryomodules were successfully tested at the Cryomodule Test Facility (CMTF) at Fermilab. Following the completion of the LCLS-II testing program, CMTF has shifted to testing cryomodules for the LCLS-II High Energy upgrade (LCLS-II-HE). The first LCLS-II-HE cryomodule, the verification cryomodule (vCM), was successfully tested and verified the readiness of LCLS-II-HE cryomodule testing at CMTF, and production cryomodule (CM) testing has begun. Presented here are the production CM test acceptance criteria, testing plan, and CM test results so far.

LCLS-II HIGH ENERGY UPGRADE

Having concluded the LCLS-II test program, Cryomodule Test Stand 1 at CMTF is now fully dedicated to LCLS-II-HE CM testing. The infrastructure of the test stand remains largely unchanged. Eight, 7 kW solid state amplifiers have replaced the 4 kW amplifiers used during the LCLS-II test program, which were installed and commissioned during the final LCLS-II CM test. An EPICS-based controls system has also been implemented to conform with a model like what is used for the accelerator controls at SLAC. CMTF houses a state-of-the-art cryogenic facility with a cryogenic capacity of 500 W at 2 K [1].

ACCEPTANCE CRITERIA

The acceptance criteria have been slightly modified to accommodate for the increase in nominal gradient but remains similar otherwise. The 1.3 GHz, 9-cell cavities for LCLS-II-HE now use a 2/0 nitrogen doping recipe, with a nominal gradient of 20.8 MV/m. Fig. 1 gives an overview of some of the acceptance criteria parameters and Table 1 shows some key differences with respect to LCLS-II.

* Work supported by the Department of Energy Contracts DE-AC02-76SF00515 (Fermilab), DE-AC02-76F00515 (SLAC), DE-AC02-05CH11231 (LBNL).

[†] cravatta@fnal.gov

Table 1: Key Parameter Differences

| Parameter | LCLS-II | LCLS-II-HE |
|--------------------------------|---------|------------|
| Nominal Cavity Gradient [MV/m] | 16 | 21 |
| Max. Cavity Gradient [MV/m] | 21 | 26 |
| Min. CM Voltage [MV] | 132 | 173 |
| Multipacting Processing [Days] | 1-2 | 4-5 |

| Parameter | Value | Minimum acceptable performance during test |
|----------------------------------------------------------------|-----------------------|---------------------------------------------------------------------------------------------------------------------------------------------------------------------------------------------------------------------------------------------------------------------------------------------------------------------------------------------------------------------------|
| Minimum usable gradient for an individual cavity | 16 MV/m | Usable gradient – the maximum gradient at which the following 3 conditions are met: <ul style="list-style-type: none"> radiation level is below 50 mR/hr, the cavity can run stably for one hour 0.5 MV/m below the quench field. |
| Nominal usable gradient | 20.8 MV/m | Individual cavities should reach a nominal usable gradient of 20.8 MV/m. |
| Minimum Usable CW voltage produced by an individual cryomodule | 173 MV | The total CW voltage produced by cryomodule with cavities running at their usable gradients shall be ≥ 173 MV with all cavities powered simultaneously in GDR/SELAP mode and with the magnet at nominal operating currents for at least one hour with the dark current <30 nA. Additionally, the individual cavity gradients during this run must be recorded. |
| Stable Operation | | For cavities that have a usable gradient above 20.8 MV/m, they must also be shown to be stable (no quenches or trips) at 20.8 MV/m for at least one hour. |
| Captured dark current | <30 nA | The dark current as measured by Faraday cups at each end of a cryomodule at the minimum CW voltage as defined above shall be ≤ 30 nA when the cavities are operated in GDR/SELAP mode with the relative phases set to accelerate speed of light electrons. This should be done in such a way to maximize the dark current measured at the Faraday cups. |
| Individual cavity Q_0 | | Individual cavity Q_0 's must be measured at the expected operating gradient (20.8 MV/m or the usable gradient whichever is lower) |
| Cryomodule operating duration with RF power during test | | Each cryomodule must operate at the minimum CW voltage or greater in GDR/SELAP and with the magnet at operating currents until the coupler temperatures achieve equilibrium or for a minimum of ten (10) hours with 90% operating time, whichever is less, to verify stable operation and confirm acceptable coupler heating. |
| 2 K Dynamic Load at 173 MV voltage | | The measured dynamic 2 K heat load of the cryomodule while operating at total voltage of 173 MV must be ≤ 137 W (equivalent to an average Q_0 of 2.7×10^{15}) |
| Static heat load at 2 K | | The static heat load at 2 K must be ≤ 7 W |
| Cryomodule thermometry | | All installed thermometry shall be verified functional by observing consistency in output with operational conditions. For sensors measuring identical locations on components within a cryomodule there shall be variation of no more than 0.2 Kelvin under the same conditions at each component and under static load with no power applied to the cavities or magnets |
| Cavity Microphonics | <10 Hz peak to peak | The microphonics for each cavity must be 10 Hz peak to peak or less, measured over a 1 hour period while at the operating gradient with the JT valve regulating the liquid level (not in a locked position). |
| Cryomodule liquid level sensors | | Liquid level sensors shall be verified functional by observing liquid levels and changes therein consistent with liquid supply rates and estimated boil-off rates |
| Cryomodule cryogenic valving | | JT valve, CoolDown/Warm up, Bypass valves shall all be verified functional during cryomodule operations by consistency with expectations for operational performance, in particular, no valve or actuator is to have ice form on the room temperature components. |
| Cavity tuning to resonance during test (coarse tuner) | | After cool-down to 2 K, each cavity must be able to be tuned to a resonant frequency of 1300.000 MHz. The tuner on the cavity #1 must be able to change the cavity's frequency from 1299.950 MHz to 1300.020 MHz. Tuners on cavities #2-#9 must be able to adjust cavity's frequency from 1299.535 MHz to 1300.020 MHz. |
| Fine tuner minimum range | 0-500 Hz | |

Figure 1: LCLS-II-HE acceptance criteria.

DISTRIBUTED COUPLING LINAC FOR EFFICIENT ACCELERATION OF HIGH CHARGE ELECTRON BUNCHES

A. Dhar*, M. A. K. Othman, G. White, Z. Li, S. G. Tantawi, M. Bai, E. A. Nanni,
 SLAC National Accelerator Laboratory, Menlo Park, USA

Abstract

Future colliders will require injector linacs to accelerate large electron bunches over a wide range of energies. For example the Electron Ion Collider requires a pre-injector linac from 4 MeV up to 400 MeV over 35 m. Currently this linac is being designed with 3 m long travelling wave structures, which provide a gradient of 16 MV/m. We propose the use of a 1 m distributed coupling design as a potential alternative and future upgrade path to this design. Distributed coupling allows power to be fed into each cavity directly via a waveguide manifold, avoiding on-axis coupling. A distributed coupling structure at S-band was designed to optimize for shunt impedance and large aperture size. This design provides greater efficiency, thereby lowering the number of klystrons required to power the full linac. In addition, particle tracking analysis shows that this linac maintains lower emittance as bunch charge increases to 14 nC and wake-fields become more prevalent. We present the design of this distributed coupling structure, as well as preliminary data from cold tests on the structure's real world performance.

INTRODUCTION

Future colliders, such as the Electron Ion Collider (EIC) will require injector linacs to accelerate large electron bunches over a wide range of energies [1]. Current designs are typically based around long travelling wave structures, where power is coupled on axis between cavities. We propose the use of a distributed coupling design as an efficient means of achieving high gradient acceleration. Distributed coupling uses unique waveguide and coupler design to power each cavity individually [2]. This in turn allows the cavity geometry to be optimized for shunt impedance, resulting in more efficient structures generating an equivalent gradient. Using the known parameters and specifications of the travelling wave design planned for EIC, we present here a potential alternative that leverages distributed coupling for better efficiency and higher bunch charge handling.

LINAC DESIGN

The re-entrant style cavity has become quite common amongst standing wave structures, featuring a nose cone to improve field enhancement while preventing surface magnetic fields from getting too large. As seen in Fig. 1, these designs exhibit the highest shunt impedance and efficiency with smaller beam apertures [2]. However in order to effectively handle large bunch charges, a large beam aperture would be needed. Based on this chart S-band (2.856 GHz) structures

represent the best balance between efficiency and beam aperture, and so an aperture radius of 14.12 mm in diameter was chosen, which corresponds to a ratio of $a/\lambda = 0.135$.

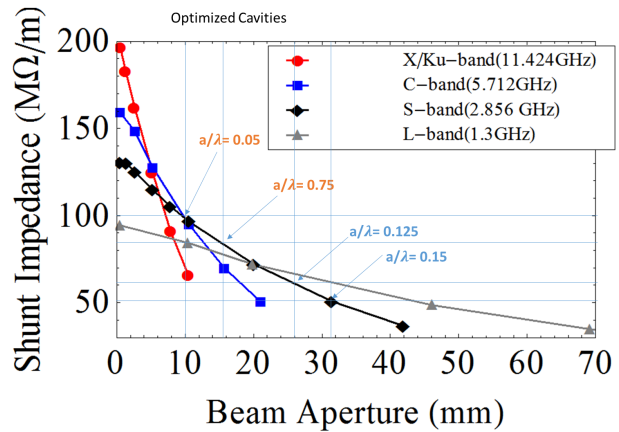


Figure 1: Plot of shunt impedance versus beam aperture for re-entrant cavities designed at various frequencies. When looking for a good balance between the two value, S-band cavities with a/λ ratios around 0.125. Reproduced from [2].

Implementing a distributed coupling manifold onto this choice of cavity results in a structure as shown in Fig. 2. The manifold incorporates a Y-coupler to split the power evenly between two halves. The lengths of the couplers to each cavity are design to provide π relative phase shift between cavities, to ensure the maximal power is coupled to the π mode. In order to reach the target gradient of 16 MV/m, this linac requires 4 MW of power. The relevant properties of interest for this mode of operation are summarized in Table 1. Further study in simulation revealed that cooling the structure down to liquid nitrogen temperatures ($\approx 80K$), would greatly improve performance within the same footprint [3].

Table 1: Distributed Coupling Linac Properties with 5 MW of Power.

| | | |
|-----------------------|---------|----------|
| Field Ratios | - | |
| E_{max}/E_{acc} | 2.63 | |
| E_{acc}/Z_0H_{max} | 0.995 | |
| Operation Temperature | 300K | 80K |
| Shunt Impedance | 60 MΩ/m | 210 MΩ/m |
| Acceleration Gradient | 16 MV/m | 30 MV/m |

* adhar@slac.stanford.edu

HIGH EFFICIENCY TRAVELING WAVE LINAC WITH TUNABLE ENERGY *

Valery Dolgashev[†], Agustin Romero, Anatoly Krasnykh, SLAC, Menlo Park, CA, USA
 Sergey Kuzikov, Roman Kostin, Euclid Techlabs LLC, Bolingbrook, IL, USA
 Philipp Borchard, Dymenso LLC, San Francisco, CA, USA

Abstract

We will present the physics design of a compact, highly efficient, energy-tunable 9.3 GHz linac to generate up to 500 W of 10 MeV electron beam power for medical and security applications. This linac will employ a patented travelling wave accelerating structure with outside power flow which combines the advantages of high efficiency with energy tunability of traveling wave cavities. Unlike standing wave structures, the proposed structure has little power reflected back to the RF source, eliminating the need for a heavy, lossy waveguide isolator. In contrast to the side-coupled cavity designs, the proposed structure is symmetrical and therefore it does not have deflecting axial fields that impair the beam transport. The high shunt impedance will allow the linac to achieve an output energy of up to 10 MeV when powered by a compact commercial 9.3 GHz 1.7 MW magnetron. For pulse-to-pulse tuning of the beam output energy we will change the beam-loaded gradient by varying the linac's triode gun current.

INTRODUCTION

The goal of this project is to design and high-power test a prototype of a linac which is based on a new highly efficient traveling wave accelerating structure [1, 2]. The structure offers high shunt impedance comparable to side-coupled standing wave structures, but without the disadvantage of RF power reflected back to the RF source. The goal is to meet or exceed most of the performance metrics required by Department of Energy funding opportunity announcement DE-FOA-0002463. The linac's accelerating cavity will be approximately 60 cm in length. The final linac will produce electron pulse bursts with tunable energy up to 10 MeV, an average beam power of at least 500 W and duty factor of about 0.08% driven by a commercial 9.3 GHz 1.7 MW magnetron [3]. These target requirements and the main design features are summarized in Table 1.

The physics design of the linac progressed in following steps: the first we performed an analytical study of the linac parameters in which we understood that the linac has to be of constant gradient type. To build the constant gradient linac, we need to tune group velocity, so we completed a parametric study of a unit cell to understand dependencies of the group velocity vs. cell shape. In the next step we performed beam dynamics simulations of a gridded gun to

show that it could achieve required currents, then we created a concept of the mechanical design of the cavity.

Table 1: Linac Target Requirements and Design Features.

| Metrics | Requirements |
|--------------------------------------------------------------------|-----------------|
| Energy Tuning Range | <5 MeV...10 MeV |
| Output average beam power at 10 MeV | >500 W |
| Maximum cavity size | 10x10x60cm |
| Target capital cost | < \$1M |
| Other Design Features | |
| Travelling wave structure with outside power flow No circulator | |
| Duty factor | 0.08% |
| Frequency | 9.3 GHz |

Table 2: Initial acc. structure and linac parameters [2].

| Metrics | Requirements |
|------------------------|---------------------------|
| Q _o | 6800 |
| Shunt Impedance | 144 MOhm/m |
| Phase Advance per Cell | 120 deg. |
| Cell length [mm] | 10.745 mm ($\beta = 1$) |
| Number of cavities | 56 (approximately) |

Table 3: Analytical linac parameters.

| Parameter | Value |
|-------------------------------|------------|
| Structure type | Const. Gr. |
| Linac length [cm] | 60 |
| Attenuation parameter, τ | 1.0 |
| Group Velocity, %c | 2 ... 0.3 |
| Beam current at 5 MeV | 200 mA |
| Beam current at 10 MeV | 70 mA |
| Average beam power at 5 MeV | 800 W |
| Average beam power at 10 MeV | 500 W |

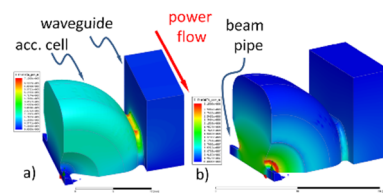


Figure 1: Quarter-cell finite element model of the $\beta = 1$, 9.3 GHz, 120 deg. phase advance per cell traveling wave accelerating

* This research is funded by the U.S. Department of Energy Office of High Energy Physics under Research Opportunities in Accelerator Stewardship, under funding opportunity announcement DE-FOA-0002463.

[†] dolgash@slac.stanford.edu

HIGHER ORDER MODES INVESTIGATION IN THE PERLE SUPERCONDUCTING RF CAVITY

C. Barbagallo^{*1}, P. Duchesne, W. Kaabi, G. Olry, F. Zomer¹

Laboratoire de Physique des 2 Infinis Irène Joliot-Curie (IJCLab), Orsay, France

R. A. Rimmer, H. Wang, Jefferson Lab, Newport News, VA 23606, USA

¹also at The Paris-Saclay University, Gif-sur-Yvette, France

Abstract

The regenerative Beam Break Up (BBU) excited by the dipole Higher Order Modes (HOMs) in superconducting RF (SRF) cavities is a crucial issue for continuous-wave high-current energy recovery linacs. Beam-induced monopole HOMs can increase the cryogenic losses of the linac also. One of the ways to limit these effects is to use HOM couplers on the beam tubes of cavities to absorb and untrap cavity eigenmodes. These couplers feature antennas designed to damp dangerous HOMs and adequately reject the fundamental mode. This study illustrates an investigation of the HOMs of a 5-cell 801.58 MHz elliptical SRF cavity designed for PERLE (Powerful Energy Recovery Linac for Experiments), a multi-turn energy recovery linac (ERL) currently under study and later to be hosted at IJCLab in Orsay. Time-domain wakefield and frequency-domain eigenmode simulations have been used to calculate the cavity broadband HOM impedance spectra and identify the dangerous BBU HOMs. The transmission characteristics of several coaxial HOM couplers have been studied. The efficiencies of several HOM-damping schemes have been compared to propose a HOM endgroup to be fabricated and added to the existing bare SRF cavity.

INTRODUCTION

PERLE [1] is a novel ERL focusing on the generation of high-current electron test beams in CW (continuous-wave) mode for a broad range of particle accelerator applications. For high-current ERL, a relevant effect is multi-pass BBU which emerges when the electron beam interacts with the Higher Order Modes of the accelerating cavity [2], giving rise to beam instabilities and increasing the cryogenic load. To mitigate this phenomenon, the next generation of ERLs, such as PERLE, calls for using SRF cavities with strong HOM-damping requirements [3].

This paper presents an HOMs investigation, carried out in CST Studio Suite [4], for the 5-cell 801.58 MHz bare-cavity design proposed for PERLE by Jefferson Lab (JLab) [1]. Several coaxial HOM couplers are optimized based on the HOM spectrum of the cavity to extract the energy of the most dangerous HOMs. In addition, HOM-damped cavities are compared in terms of beam impedance, and suitable HOM-damping schemes aimed to satisfy PERLE's BBU requirements are proposed.

* carmelo.barbagallo@ijclab.in2p3.fr

PERLE OVERVIEW

The PERLE accelerator complex, shown in Fig. 1, consists of a racetrack topology featuring two parallel superconducting linacs, each containing an 82 MeV cryomodule hosting four 801.58 MHz 5-cell elliptical Nb cavities. Three vertically stacked recirculating arcs on each side complete the accelerator configuration.

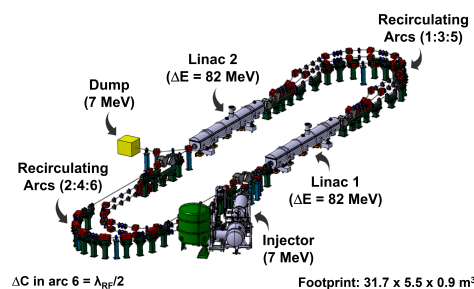


Figure 1: The PERLE accelerator complex layout.

Before entering the machine, a pre-accelerating unit following the source accelerates the electron beam up to the injection energy of 7 MeV. The 20 mA electron beam is boosted in energy by each of the two 82 MeV cryomodules. Hence, in three re-circulation passes, the target beam energy of approximately 500 MeV is achieved [5]. To allow operation in energy recovery mode, after the acceleration, the beam is phase shifted by 180° to be decelerated in three consecutive passes. Consequently, in the deceleration phase, the beam energy is transferred back to the SRF system, and the final beam is directed to a beam dump at its initial energy [1].

SRF CAVITY DESIGN

The first 5-cell 801.58 MHz Nb bare cavity suitable for PERLE has already been designed, fabricated, and successfully tested at JLab in 2018. The cavity design (Fig. 2) features a rather large cell-to-cell coupling ($k_{cc} = 2.93\%$) to cope with HOM-damping needs, while keeping the ratios of the surface peak electric field E_{pk} , and surface peak magnetic field, B_{pk} , to the accelerating field, E_{acc} , small to pursue a high accelerating gradient ($E_{pk}/E_{acc} = 2.38$, $B_{pk}/E_{acc} = 4.62$ mT/MV/m) [6]. The geometric shunt impedance of the cavity is $R/Q = 524.25 \Omega$.

Higher Order Modes

For high-current ERLs, identifying and damping potentially dangerous HOMs is crucial for the beam stability and

A GROUND EXPERIMENTAL APPROACH TOWARD UNDERSTANDING MYSTERIOUS ASTROPHYSICAL FAST RADIO BURSTS

Y. Sumitomo^{1*}, T. Asai¹, S. Kisaka², H. Koguchi³, K. Kusaka¹, R. Yanagi¹, Y. Onishi¹,
Y. Hayakawa¹, D. Kobayashi¹, S. Kumagai¹, T. Sakai¹, T. Seki¹

¹College of Science and Technology, Nihon University, Tokyo, Japan

²Hiroshima University, Hiroshima, Japan

³National Institute of Advanced Industrial Science and Technology (AIST), Tsukuba, Japan

Abstract

The Fast Radio Bursts are astrophysical events that get much more attentions that increases year by year, due to their mysterious properties of signals. The major properties of signals include a class of the brightest astrophysical events, short durations of emissions, and larger dispersion measures than the known short duration events observed so far. Interestingly, the large values of dispersion measures suggest the existence of abundant plasma around the parent bodies of emissions. To have a better understanding of basic mechanism of the Fast Radio Burst emissions, we initiated a ground-based research project at our 100 MeV electron LINAC facility, in combination with the high-beta plasma generation knowledge matured also at Nihon University, that mimics plasma fields in space. In this presentation, we overview our project and report on the status of the experiment for the induced enhanced emissions from integrated iterative interactions with plasma fields.

INTRODUCTION

Recently the astrophysical events named “Fast Radio Bursts” get much attention owing to their mysterious signals. The properties of the Fast Radio Bursts events include the milliseconds-scale short emissions and their brightness that is classified as a class of highest emissions ever observed. Therefore the Fast Radio Bursts are totally distinguished from the known astrophysical events. The signal was initially reported in 2007 [1], and more people started paying attentions after the report of four additional signals in 2013 [2]. Although the detection of signals accompanies difficulties due to their sudden occurrences and short emissions, the number of the observed events increases gradually year by year. It is worth mentioning that there appeared interesting papers in these years, including the signals from our Milky Way in 2020 [3, 4], over 500 events reported in 2021 [5], and also the detail analyses of signal time structures within milliseconds durations [6–8]. Although there have been significant progresses in observations regarding the Fast Radio Bursts, we still need much more information to understand their general features of emission mechanism that are still veiled in mystery (see e.g. this review article [9]).

One of the interesting progresses understanding the typical properties of Fast Radio Bursts is the implication of abundant plasma existence around the signal sources or par-

ent bodies. The dispersion measure of signals is one of the important measure classifying the parent bodies of emissions. When a radio signal penetrate through ionization regions, the signal suffers from a delay depending on its frequency. Hence a large dispersion measure suggests the existence of abundant plasma fields. For the Fast Radio Bursts, the observed dispersion measures are generically larger than those of the Galactic pulsars whose emission durations are the similar milliseconds-scales (see this review [10]). On the other hand, there are few known events emitting repeatedly, one of which was observed by the European Very Long Baseline Interferometry so that the position of the source was detected at a satisfactory accuracy [11]. After the observation, the other research group reported that the detail analysis of the polarization with the Faraday rotation measure for this event concluded the existence of an extreme and dynamic magneto-ionic environment around the source [12].

Once the high-energy charged particles enter into electromagnetic fields including plasma, the emissions occur as a result of interactions. Recently, there appeared the reports suggesting the existence of the high energy astrophysical bodies called “PeVatrons” where the accelerated particles reach the PeV scale, by observing the ultra-high energy γ -rays [13, 14]. Together with the fact that the synchrotron radiations are observed from many directions, we have no doubt that high-energy accelerated particles are ubiquitous in space.

To challenge the mystery of the Fast Radio Bursts, we have initiated a laboratory astrophysical project at the Nihon University, by reproducing the properties of the events on the ground. Especially, we pursue the possibility of ultra-bright emissions from the integrated iterative interactions between high-energy charged particles and plasma fields. We believe that the repeatable experiments on the ground provide the detail data enough to help understanding the basic mechanism of the mysterious events in space. In this paper, we first introduce the property of our accelerator system and the plasma generation method suitable for this project, and then illustrate our plan for the interaction experiment and also the current status of preparation.

EXPERIMENTAL BACKGROUND

We have the linear accelerator at Nihon University, where electrons are accelerated upto 100 MeV. We use three normal conducting tubes for the 2.856 GHz RF accelerations whose

* sumitomo.yoske@nihon-u.ac.jp

HOM DAMPING IN MULTI-CELL SUPERCONDUCTING CAVITIES FOR THE FUTURE ELECTRON SOURCE BriXSinO

S. Samsam*¹, M. Rossetti Conti, A.R. Rossi, A. Bacci, V. Petrillo², I. Drebot, D. Sertore, R. Paparella, A. Bosotti, L. Monaco, C. Curatolo, D. Giove and L. Serafini
INFN - Sezione di Milano, 20133 Milano and LASA, 20090 Segrate (MI), Italy

¹also at Università Sapienza, 00185 Roma, Italy

²also at Università degli Studi, 20133 Milano, Italy

A. Passarelli, M. R. Masullo, INFN - Sezione di Napoli, 80126 Napoli, Italy

Abstract

High order modes (HOMs) in multi-cell superconducting cavities are of particular concern in beam dynamics of linear accelerators, mainly those operating in CW mode with high current and high repetition rate. These undesired modes may invoke beam instabilities, beam breakup and increase the energy spread if not correctly pulled out and damped. The study reported in this paper is applied for damping the HOMs in the main Linac of BriXSinO, an ongoing project of an Energy Recovery Linac at LASA INFN laboratory. We developed a numerical model to study the interaction of monopole HOMs with the beam in long timescale. The presented model, named HOMEN (High Order Modes Evolution based on eNergy budget), allows the inclusion of loss factors k_{loss} , crucial for evaluating the effect of the perturbing modes. At the same time, electromagnetic simulations of the standing wave multicell cavity, highlighted the dangerous modes and revealed a tolerable beam energy spread induced by HOMs. This method allows us to distinguish all dangerous modes of our interest for implementing the necessary damping mechanisms.

INTRODUCTION

The LASA (Laboratory for Accelerators and Applied Superconductivity) INFN (National Institute for Nuclear Physics) laboratory is currently developing a test-facility, BriXSinO, which will address the challenges created by the Energy recovery Linac (ERL) generation. BriXSinO is dual high flux radiation Inverse Compton Source (ICS) of X-ray and Free-Electron Laser (FEL) in the THz range, devoted to medical applications and applied research [1–8]. The machine will allow studies of applications of electron accelerators, and eventually to demonstrate a high peak and high average brightness beam generation and acceleration. BriXSinO is following the same philosophy of other projects born on the MariX conception [9–11]. A key component of this project is the ERL as a driver of both FEL and ICS experiments, hosted by an arc compressor [12–14]. The proposed BriXSinO's ERL is designed to operate in CW at 1.3 GHz, 5 mA average current in each of the accelerating and decelerating beams with an energy ranging from 22 MeV up to 45 MeV. The recirculated beam in the arc will be later decelerated within the SW (Standing Wave) SC (

Superconducting) linac back to the injector beam energy. The beam will pass in two directions, first in the two-pass two-way acceleration mode, then in ERL mode with an opposite phase. This proposed scheme is intended to double the energy exchange in the Linac and promote the efficiency. In high current machines like BriXSinO, the excited HOMs need to be damped in an efficient way to bypass beam break up and avoid any additional cost regarding linac operation. In this paper, our investigations will mainly focus on cavity spectrum simulation, wakefields calculation and HOMs damping in the main linac cryomodule of BriXSinO's ERL.

SCOPE OF HOM INVESTIGATION

HOMs are always problematic in SC cavities and mainly those operating in CW regime. These parasitic modes are not only source of beam instabilities, but will also increase the cryogenic losses due to the power dissipated in the cavity walls [15]. In a previous work, we presented a new model called HOMEN, composed of a set of differential equations, solved numerically to study the consequence of HOMs on beam dynamics and stored energy inside SC cavities [16].

The main goal of the present paper is to underline which HOMs exactly are dangerous and need to be damped, instead of evaluating all the modes together.

WAKEFIELD SIMULATIONS IN 7-CELL CAVITY

The performance of any accelerator is related to wakefields, therefore, the evaluation of the loss factor k_{loss} is essential in order to study HOM damping. This factor is related to the amount of energy lost in modes when the beam traverses the resonator leaving behind a wakefield.

Usually HOMs whose frequencies are above the beam pipe cut-off are not of particular concern as they can be easily extracted or damped using couplers or absorbers once they propagate into the pipe. In case of coupled cavities, some of these propagating modes may still be problematic, as they can couple between the structures inducing trapped modes in the pipes. For a reliable beam dynamics study and for an effective HOM damping strategy, an electromagnetic study of the cavities is necessary to focus on the properties of the modes which are trapped in either the cavity or the beam-pipe region. With this aim, we used an eigen-mode study together with the wakefield simulations resorting to

* sanae.samsam@mi.infn.it

CONCEPTUAL DESIGN OF THE PERLE INJECTOR

B. Hounsell* ^{† 1, 2}, M. Klein, C.P. Welsch¹, University of Liverpool, Liverpool, United Kingdom
W. Kaabi, Université Paris-Saclay, CNRS/IN2P3, IJCLab, 91405 Orsay, France
B.L. Militsyn¹, STFC, Sci-Tech Daresbury, United Kingdom
¹also at Cockcroft Institute, Warrington, United Kingdom
²also at Université Paris-Saclay, CNRS/IN2P3, IJCLab, 91405 Orsay, France

Abstract

Energy Recovery Linacs such as PERLE require high average current high brightness beams. This sets particular requirements on the kind of injectors that they can use as the injectors must be capable of producing bunches at MHz repetition rates, compressing the bunches to the specified value and transporting those bunches while they are still in the space charge dominated regime into the main ERL all while keeping the emittance low. In particular, PERLE will require a 20 mA beam consisting of 500 pC bunches with a repetition rate of 40 MHz. These bunches will be required to have rms lengths of 3 mm, a total beam energy of 7 MeV, appropriate Twiss parameters to match them to the main loop and transverse emittances of < 6 mm-mrad. In this paper, a DC gun based injector capable of meeting this specification will be presented with beam dynamics simulation showing the behaviour of the beam from the photocathode to the exit of the first main linac pass. The beam dynamics challenges will be discussed in terms of both the transverse emittance growth and the sources of non-linearity in the longitudinal phase space.

INJECTOR DESIGN AND SPECIFICATION

PERLE (Powerful Energy Recovery Linac for Experiments) is a proposed three turn energy recovery linac (ERL) [1, 2]. The injector is the part of the machine where the electrons are generated and the initial beam manipulations are performed before the beam enters the main ERL loop. The design of the injector is important because it sets the lower bound on the achievable beam quality. The design needs to deliver bunches at MHz repetition rates, while preserving the beam quality from the cathode, compressing the bunches to the required length, matching the Twiss parameters of the bunch to the main ERL loop and physically transporting the beam into the main ERL. A number of different injector schemes were investigated before a baseline was chosen. The layout of the baseline scheme can be seen in Fig. 1.

The injector uses a 350 kV DC electron gun. PERLE will use the ALICE electron gun [3] with planned upgrades incorporated [4]. The shape of the electrode geometry was re-optimised for PERLE [5]. After the electron gun the beam is focused and emittance compensated [6] by a pair of solenoids. A buncher cavity to compress the bunch is installed between them. There is then an SRF booster linac

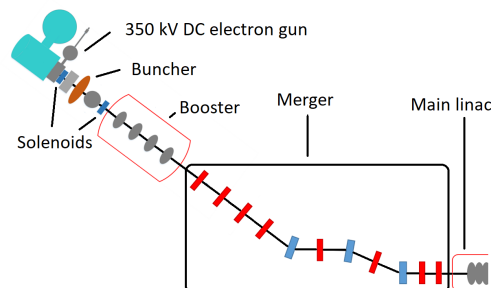


Figure 1: The layout of the PERLE injector. In the merger section quadrupoles are shown in red and dipoles in blue.

with four independently controllable single cell cavities which accelerates the beam to the injection energy of 7 MeV. The beam is then transported and matched into the main ERL loop by the merger. The merger presented here is a three dipole design which is an established design used and proposed by a number of ERL projects [7–10]. The example presented here uses four quadrupoles before the dipoles to match the beam, the quadrupoles between the dipoles to make the beamline achromatic (assuming no space charge) and two quadrupoles after the dipoles for the final matching. Only two quadrupoles are used after the dipoles due to the limited space between the final dipole and main linac.

The injector was optimised in three steps. First the electron gun electrode geometry was optimised [5] based on the beam dynamics performance using POISSON [11] to model the electrostatics, ASTRA [12] to model the beam dynamics and the many objective optimisation algorithm NSGAI [13] as the optimisation algorithm. The injector beamline from the cathode to the exit of the booster was optimised using OPAL [14] to model the beam dynamics and again using NSGAI as the optimisation algorithm. Then finally the merger from the exit of the booster to the exit of the first main linac pass was optimised. The matrix code Optim [15] was used to generate initial guesses for the magnet settings then the beam dynamics code OPAL and the optimisation algorithm NSGAI [14] were used for the final optimisation of the merger. At the end of this multistep optimisation procedure a solution was selected. The performance of that solution relative to the specification can be seen in Table 1.

The emittance values are within the specification. The final bunch length and Twiss parameters still require some fine tuning. The remainder of this paper will be a discussion of the beam dynamics of this chosen solution focusing on

* ben.hounsell@stfc.ac.uk

[†] Now at STFC, Sci-Tech Daresbury, United Kingdom

FLASH2020+ UPGRADE – MODIFICATION OF RF POWER WAVEGUIDE DISTRIBUTION FOR THE FREE-ELECTRON LASER FLASH AT DESY

B. Yildirim, S. Choroba, V. Katalev, P. Morozov, Y. Nachtigal, N. Vladimirov
Deutsches Elektronen-Synchrotron DESY, Notkestr. 85, 22607 Hamburg, Germany

Abstract

One goal of the FLASH2020+ upgrade is to increase the energy of the FLASH accelerator, which allows to generate even shorter wavelengths, which, in turn, will allow new fields of research. For this purpose, during the shutdown in 2022, two superconducting accelerator cryomodules for ACC2 and ACC3 will be replaced by new ones. To fully realize the potential of these cryomodules, European XFEL type optimized waveguide distributions will be installed on them. In addition, the existing ACC4 and ACC5 cryo-modules will also be equipped with new waveguide distributions, similar to the XFEL type. These waveguide distributions will be modified and improved so that the accelerator can operate with maximum energy due to individual power supply for each cavity. Furthermore, three RF stations will receive a new klystron waveguide distribution, which will improve the reliability of all systems. The new specific waveguide distributions have been developed, produced and tested at the Waveguide Assembly and Test Facility (WATF) at DESY. All together will lead to increasing the electron beam energy from 1.25 to 1.35 GeV.

This paper presents data on the production and tuning of waveguide distribution systems for the FLASH2020+ upgrade at DESY.

INTRODUCTION

The Free-Electron Laser FLASH consists of a 1.3 GHz RF gun and seven 12 m long TESLA type superconducting accelerating cryomodules (ACC) with eight cavities each. Five RF stations with 5 MW or 10 MW klystrons supply cryomodules through a specific waveguide distribution system with RF power [1].

One goal of FLASH2020+ upgrade is to achieve high energies of the accelerator with high reliability. Due to different cavity power requirements individual waveguide distribution systems for accelerator cryomodules were produced, tested and tuned. To create the entire waveguide distribution as reliable as possible all sub-systems such as klystron-, connecting- and cryomodule waveguide distributions have been customized to the module gradients and also to the space conditions in the tunnel.

An additional air flow system for each RF station will decrease the breakdown level in the waveguide distributions.

Figure 1 shows an overview of RF station 1 with its klystron-, connecting- and cryomodule waveguide distribution for ACC2 and ACC3. These cryomodules are European XFEL type modules with 0-degree phase advance between the cavities. This allows easier final measurements for the phase tuning.

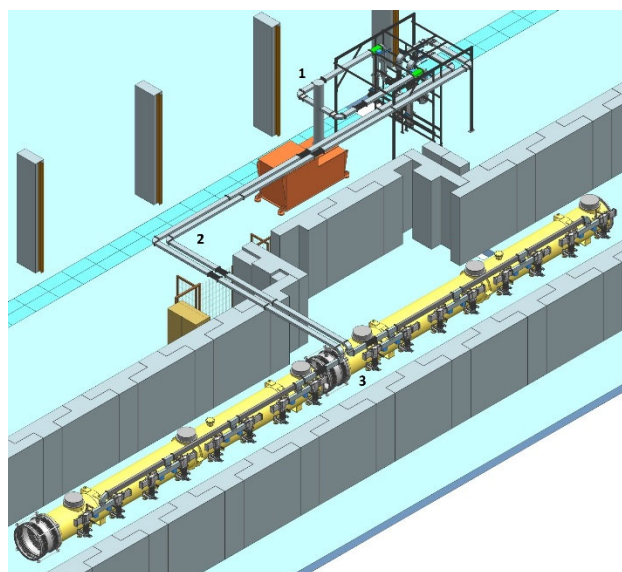


Figure 1: Overview of klystron- (1), connecting- (2) and cryomodule waveguide distribution (3) for ACC2 and ACC3.

The layout of RF station 5 is shown in Fig. 2. The cryomodule waveguide distributions for ACC4 and ACC5 are different to the ones of ACC2 and ACC3. The reason for that is both the module type and the insufficient space. Although these cryomodules have not been exchanged, new and optimized waveguide distributions were constructed and installed. The phase difference between the cavities of ACC4 and ACC5 has been compensated due to the final LLRF measurements [2].

In contrast to the previous modules the cryomodules as well as the waveguide distribution systems for ACC6 and ACC7 stay unchanged. The tuning for this station will be done within the final phase measurements of the complete accelerator.

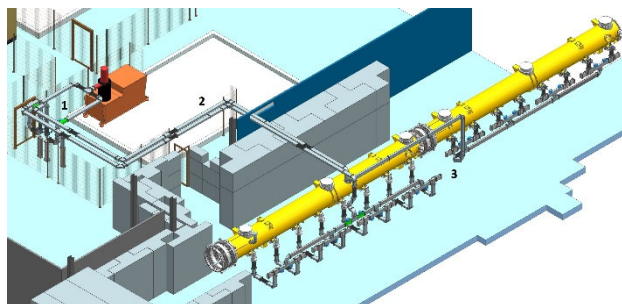


Figure 2: Overview of klystron- (1), connecting- (2) and cryomodule waveguide distribution (3) for ACC4 and ACC5.

UNFOLDING OF BREMSSTRAHLUNG PHOTONS ENERGY SPECTRA EMITTED FROM 28-GHz ECR ION SOURCE

M. J. Kumwenda*, University of Dar es Salaam, Dar es Salaam, Tanzania
J. K. Ahn, Korea University, Seoul, Republic of Korea

Abstract

The aim of present study is to determine end-point energies of the bremsstrahlung photons energy spectra emitted from 28-GHz Electron Cyclotron Resonance Ion Source (ECRIS) by using inverse-matrix unfolding method. Azimuthal angular distribution of the bremsstrahlung photons from 28-GHz ECR ion source were measured at Busan Center of Korean Basic Science Institute (KBSI). Gamma-ray detection system consists of three round type NaI(Tl) scintillation detectors positioned 62 cm radially from the beam axis and another detector placed at the extraction port for monitoring photon intensity along the beam axis. Bremsstrahlung photons energy spectra were measured at six azimuthal angles at RF power of 1 kW to extract ^{16}O beam with a dominant fraction of O^{3+} and O^{4+} . Monte Carlo simulation based on Geant4 simulation package was performed to take the geometrical acceptance and energy-dependent detection efficiency into account due to large non-uniformity in the material budget. We extracted true bremsstrahlung energy spectra using the inverse-matrix unfolding method. The unfolding method was based on a full geometry of the Geant4 model of the ECR ion source. The highest end-point energies after unfolding method were found at angles 90° and 330° which both reaches 1.690 ± 0.030 MeV. Therefore, the high end-point energies intensity at angles 90° and 330° were associated with the shape of the ECR plasma.

INTRODUCTION

Electron cyclotron resonance ion sources (ECRIS) are magnetized plasma ion source used to produce intense multiply charged ions taking advantage of accelerating electrons in the magnetic field with a GHz range radio frequency microwave [1]. The magnetic field of the modern ECRIS consists of mirror field (generated from 3 solenoid coils) combined with a hexapole field forming the so-called minimum-B structure. The magnetic field serves two purposes, it fulfills the condition for resonant interaction between plasma electrons and high frequency microwaves launched into the plasma chamber. Due to the resonant nature of the heating process electrons can gain energy beyond those required for efficient ionization which make ECRIS intense sources of bremsstrahlung. This is considered as an unfortunate consequence as it increases heat load of the cryostats of superconducting devices and poses a safety hazard [2].

In the ECRIS high energy bremsstrahlung photons are generated on the plasma chamber walls as a result of the interaction between the wall material and electrons escaping the magnetic confinement and, in the plasma, due to the deceleration and collision of the charged particle. The

generated bremsstrahlung photons deposits energy in the structure of ion sources and turns out to be substantial heat load to the cryostat in case of superconducting ECRIS [3]. The cryogenic system can remove only a limited amount of heat from the cryostat. If more heat is added to the system than can be removed, the temperature of the liquid helium rises and can cause the superconducting coils to quench [4].

Bremsstrahlung photons measurements produced in the ECRIS have been made since late 60s. However, many of these experiments used to measure the bremsstrahlung photons energy in only one direction (axially) using one or two detectors but under different conditions [5]. Therefore, this study aims at determining end-point energies of the bremsstrahlung photons energy spectra emitted from 28-GHz ECRIS using the three round type NaI(Tl) scintillation detectors positioned 62 cm radially from the beam axis.

EXPERIMENTAL SETUP

The experiment setup to measure bremsstrahlung photons energy intensity from 28 GHz superconducting ECRIS of the compact linear accelerator facility at the KBSI. ECRIS developed at the KBSI is composed of a six racetrack hexapole coils and three mirror solenoid magnets. The axial magnetic field is about 3.6 T at the beam injection area and 2.2 T at the extraction region, respectively. A radial magnetic field of 2.1 T can also be achieved on the plasma chamber wall. A higher current density NbTi wire was selected for winding of sextupole magnet. The inner face of the 0.05 m thick solenoid coil is placed at a distance of 0.44 m from the beam axis. The 0.10 m thick iron shielding structure is 1.20 cm wide, 1.22 cm high and 1.70 cm long [6].

Bremsstrahlung photons energy spectra were measured using three round type NaI(Tl) detection system as shown in Fig. 1 facing the edge of the ECRIS at the injection side. The detectors were labeled with letters D1, D2, D3 and D4, which were operated at +1300 V. The first three detectors were attached on supporting structure as shown in Fig. 1, while D4 was at the view port for monitoring the intensity of the ECR plasma. The photon energy intensity was measured at six angles in a 30° interval. The three detectors system were placed at the two sides of the ECRIS, on the top and left as depicted in Fig. 1.

Each NaI(Tl) detector was placed in a lead (Pb) collimator of a 0.5 cm hole. The Pb collimator covered a full dimension of the NaI(Tl) crystal. The 500 MHz FADC system was used for data acquisition as shown in Fig. 2. The detector signal was fed to splitting module and then to a NKFADC500 and recorded in a coincidence with a reference signal from the detector D4 placed at the view port. The 4-channel flash ADC module (Notice Co.) recorded full pulse information

* kmwingereza@yahoo.com

STATUS OF THE CLEAR USER FACILITY AT CERN AND ITS EXPERIMENTS

R. Corsini*, W. Farabolini, A. Malyzhenkov, CERN, Geneva, Switzerland

L.A. Dyks¹, P. Korysko¹, University of Oxford, Oxford, UK

K. N. Sjobak, V. Rieker¹, University of Oslo, Oslo, Norway

¹Also at CERN, Geneva, Switzerland

Abstract

The CERN Linear Accelerator for Research (CLEAR) at CERN is a versatile user facility providing a 200 MeV electron beam for accelerator R&D, irradiation studies for space, and medical applications. After successful operation in 2017-2020, CLEAR running was extended in 2021 for another 5-year period. In the paper we give a status of the facility, outlining recent progress in beam performance and hardware improvements. We report on beam operation over the last years and review the main results of experimental activities. Finally, we discuss the planned upgrades together with the proposed future experimental program.

INTRODUCTION

The CERN Linear Electron Accelerator for Research (CLEAR) user facility is composed of a 200 MeV electron linac followed by an experimental beamline, and it is operated at CERN as a multi-purpose facility with high availability, easy access and high-quality electron beams. Its main scientific goals are: a) perform R&D on accelerator components for existing and possible future machines at CERN, including beam instrumentation prototyping and high gradient RF technology; b) provide an irradiation facility with high-energy electrons, e.g. for testing electronic components or for medical studies on novel radiotherapy methods; c) conduct experiments on novel accelerating techniques, like electron-driven plasma and THz acceleration.

CLEAR also plays a role as a training infrastructure for the next generation of accelerator scientists and engineers.

The CLEAR facility provides an electron beam covering a large range of parameters [1–4] as shown in Table 1. A schematic layout of the beamline is shown in Fig. 1: the 200 MeV linac, composed by one RF photoinjector and three S-band accelerating structures, is followed by a 20m long experimental beam line which includes a diagnostics section and a first in-air spectrometer/test area (called VESPER, for Very energetic Electron facility for Space Planetary Exploration missions in harsh Radiative environments), a long section that can host several in-vacuum experiments and, just before the dump, a final in-air test stand with another spectrometer, where most of the experiments take place. The in-vacuum test areas are used for beam instrumentation R&D [5], high-gradient acceleration and linear collider related activities, and advanced accelerator technology studies like plasma lenses [6–8]. Both the in-air areas are inten-

sively used for studies on medical applications of Very High Energy Electrons (VHEE), like conventional and FLASH radiotherapy and sterilisation of personal protective equipment [9, 10]. The other main area of application for the in-air test stands is radiation hardness testing for electronics components for accelerator and space applications [11–14]. In particular the VESPER area has been initially developed in order to test components of the ESA's JUPITER ICy moons Explorer (JUICE) mission [15].

CLEAR re-uses equipment of the former CLIC Test Facility, CTF3, and began beam operation in September 2017. It is a fully independent installation and runs independently from other accelerators of the CERN Accelerator Complex. Therefore, the facility can function also during LHC's long shutdowns and periodic upgrades. An yearly run typically includes 35 to 40 weeks of beam time. At the beginning of 2021, CLEAR operation, initially approved for a period of four years, was formally extended until the end of 2025.

Table 1: Updated List of CLEAR Beam Parameters

| Parameter | Value |
|--------------------|---------------------------|
| Beam Energy | 30 – 220 MeV |
| Beam Energy Spread | < 0.2% rms (< 1 MeV FWHM) |
| Bunch length rms | 0.1 – 10 ps |
| Bunch frequency | 1.5 or 3.0 GHz |
| Bunch charge | 0.005 – 3 nC |
| Norm. emittance | 1 – 20 μm |
| Bunches per pulse | 1 – 150 |
| Max. pulse charge | 75 nC |
| Repetition rate | 0.8333 – 10 Hz |

BEAM PERFORMANCE AND UPGRADES

The CLEAR operation team gradually extended the range of available beam parameters during the last years, following the requests made by user groups. For instance, the beam energy range was extended from the initial range (100-200 MeV) first up to 200 MeV and down to 60 MeV, and very recently further down to 30 MeV, although at the cost of reduced beam quality.

The combination of improvements to the laser, the photoinjector and to the beam transport have increased the maximum charge per bunch to 3 nC. The implementation of a double-pulse setup, obtained by splitting the laser pulse and delaying one of the pulses through a tunable optical line, allowed to accelerate two bunches (or trains) with adjustable

* roberto.corsini@cern.ch

METHODS FOR VHEE/FLASH RADIOTHERAPY STUDIES AND HIGH DOSE RATE DOSIMETRY AT THE CLEAR USER FACILITY

P. Korysko^{1*}, J. Bateman¹, C. Robertson¹, University of Oxford, Oxford, United Kingdom
W. Farabolini, R. Corsini, L. Dyks, V. Rieker, CERN, Geneva, Switzerland
¹also at CERN, Geneva, Switzerland

Abstract

The CERN Linear Electron Accelerator for Research (CLEAR), operating since 2017, is a user facility providing electron beams for a varied and large range of experiments. The accelerator can generate a 60-220 MeV electron beam and it was recently selected to study the feasibility of using Very High Energy Electrons (VHEE) at Ultra High Dose Rate (UHDR) for cancer radiotherapy. One of the studies in CLEAR is to study the impact of sending the total dose in a short amount of time (also called UHDR) and study the FLASH biological effect in which deep-seated cancer cells are damaged while the healthy tissues are spared. The dosimetry in CLEAR is measured using both passive dosimetry with radiochromic films or radio-photo-luminescent dosimeters. In this paper different methods for dosimetry studies and experiments in which they are used will be presented.

INTRODUCTION

The CLEAR facility can offer an electron beam with a large range of parameters to its users [1–4]. They are shown in Table 1. A diagram of the beamline is shown in Figure 1. Two in-air test areas are available. The VESPER (Very energetic Electron facility for Space Planetary Exploration missions in harsh Radiative environments) and the In-Air Test Area. In practice, both areas can be used for medical applications studies like VHEE radiotherapy experiments.

Table 1: Updated List of CLEAR Beam Parameters

| Parameter | Value |
|--------------------|---------------------------|
| Beam Energy | 30 – 220 MeV |
| Beam Energy Spread | < 0.2% rms (< 1 MeV FWHM) |
| Bunch length rms | 0.1 – 10 ps |
| Bunch frequency | 1.5 or 3.0 GHz |
| Bunch charge | 0.005 – 3 nC |
| Norm. emittance | 1 – 20 μm |
| Bunches per pulse | 1 – 150 |
| Max. pulse charge | 75 nC |
| Repetition rate | 0.8333 – 10 Hz |

C-ROBOT

In order to increase the range of experiments done in CLEAR, four members of the CLEAR team designed, developed and built a robotic system called CLEAR-Robot (C-Robot) [5]. It was built to place samples in the beam line

* pierre.korysko@cern.ch

for irradiation for medical applications. The robot is made of 3 linear stages for X, Y and Z axis, 6 limit switches (2 for each axis), a 3D printed grabber, a mounted-camera system with a moving optical filter and two tanks (one storage tank and one tank in the electron beam). A rendered picture of the system is shown in Figure 2. The C-Robot is controlled using two custom Arduino circuits, and fully interface to the local computing network.

There are two separate areas on the C-Robot, the storage area where a laser-cut PMMA plate and PMMA water tank are installed and can accept 32 different 3D-printed holders. Each holder can be adapted for different experiments. Two dosimetric films can be installed on each holder, one before and one after the sample that needs to be irradiated. The position in the beam area where the transverse and longitudinal positions of the holder can be chosen with a 50 μm accuracy.

In order to measure the beam size and position where the samples will be irradiated, a dedicated holder with a YAG screen attached can be inserted in the beam area. The YAG screen is angled by 45° compared to the electron beam and thanks to camera mounted on the C-Robot, the beam position and the beam size of the electron pulses can be measured directly at any transverse and longitudinal positions in the beam area.

The C-Robot is fully open-source. Pictures, drawings, 3D renders and codes can be found on the C-Robot website [5] and on the C-Robot Gitlab Repository [6].

METHODS FOR DOSIMETRY STUDIES

Radiochromic Films

Radiochromic films change colour macroscopically due to polymerisation caused by ionising radiation. The change in colour is related to the accumulated dose. After being irradiated, the films are optically scanned and the resulting image is processed to determine the optical density (OD). The OD is then matched against a calibration curve, which must be obtained, for each irradiated batch, at a calibration facility. In CLEAR, various types of Gafchromic films are used: EBT3 (with a range from 0.1 to 10 Gy), MD-V3 (1 - 100 Gy) and HD-V2 (10 - 1000 Gy). They are calibrated at the eRT6 linac in the Centre Hospitalier Universitaire Vaudois (CHUV). The films are cut to the exact dimensions of the sample holder slots using a laser cutter. This method also avoids the issue of layer detachment frequently caused by other means of cutting.

To validate the scanning procedure, image processing methods and reproducibility of this method, a large number

HIGH STABILITY KLYSTRON MODULATOR FOR COMMERCIAL ACCELERATOR APPLICATION

Michael Kempkes, Merouane Benjane, Christopher Chipman, Marcel P.J. Gaudreau,
 Anthony Heindel, Ziliang Ruan, Rebecca Simpson, Henry von Kelsch IV
 Diversified Technologies, Inc., MA, USA

Abstract

Diversified Technologies, Inc. (DTI) designed and developed a high stability modulator system for a commercial linear accelerator application. The DTI modulator delivers significant advantages in klystron performance through highly reliable functionality as well as flicker- and droop-free operation from 50-500 μ s up to 400 Hz (duty limited). The main assemblies on the DTI system consist of a controls rack, high voltage power supply (HVPS), modulator, and cooling manifolds for the modulator, high voltage power supply and klystron tube. Two HVPS (upgradeable to four) provide stable and accurate DC voltage which is used to drive a CPI VKP-8352C UHF-band pulsed klystron for the linear accelerator. A solid state series switch, based on DTI's patented design, provides both pulse control and arc protection to the klystron. Operating with four HVPS, the DTI modulator is able to operate at a maximum average power of \sim 750 kW at 105 kV, 47 A nominal. At the end of the initial contract, DTI provided two systems and a total of four HVPS (two of which are used with each system).

INTRODUCTION

In 2021 Diversified Technologies, Inc. (DTI) completed the development and acceptance testing of two advanced, high voltage solid state klystron modulator systems for a commercial linear accelerator application. The modulators use a series-switch design that DTI has delivered to hundreds of clients over the last 25 years. Modulators based on this switch design are

operational at sites around the world for accelerators, radar transmitters, and industrial applications, and deliver extremely high-quality pulses for a wide range of klystrons, TWTs, and other high-power microwave tubes.

The modulator design provides significant advantages in klystron performance through highly reliable operation and significantly exceeded the contract requirements, as well as, flicker- and droop-free operation over a range of operating parameters. Each modulator system for this application includes two high voltage power supplies (upgradeable to up to four HVPS by a simple install of the additional HVPS), oil-filled modulator tank, controls cabinet, auxiliary electronics rack and cooling manifolds; the modulators connect to the klystron via high voltage output cables and other required interfaces (Fig. 1).

SPECIFICATIONS

DTI met the contractual pulse width and flatness requirements with a modulator design which included:

- Two switching power supplies (capable of operating with up to four), providing stable and accurate DC voltage.
- A solid state series switch, based on DTI's patented design and 25 years of refinement, providing both the pulse control and the arc protection to the klystron.

The major client-defined specifications are summarized in Table 1.

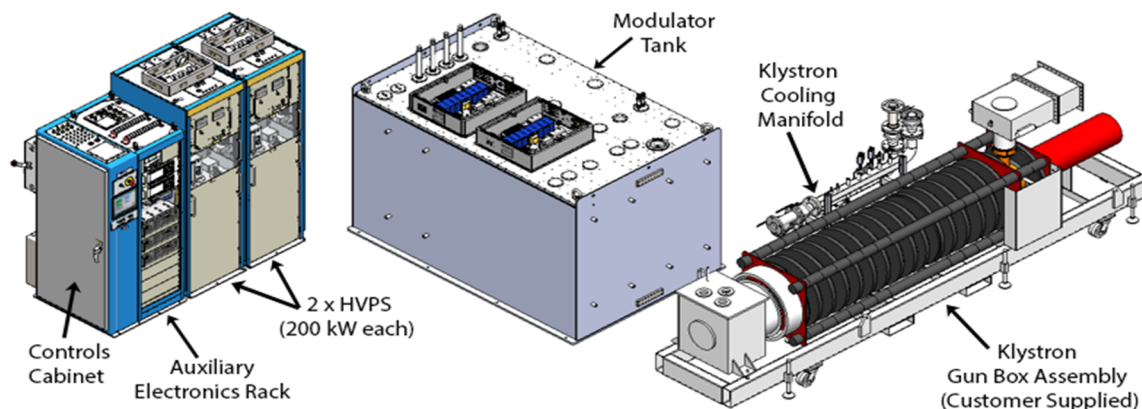


Figure 1. Modulator system major subassemblies.

DEVELOPMENT AND INTEGRATION OF A NEW LOW-LEVEL RF SYSTEM FOR MEDAUSTRON

M. Wolf*, M. Cerv, C. Kurfuerst, G. Muyan, S. Myalski, M. Repovz, C. Schmitzer
 EBG MedAustron GmbH, Wr. Neustadt, Austria
 A. Bardorfer, B. Baricevic, P. Paglovec, M. Skabar
 Instrumentation Technologies, Solkan, Slovenia

Abstract

The MedAustron Ion Therapy Centre is a synchrotron-based particle therapy facility, which delivers proton and carbon beams for clinical treatments. Currently, the facility treats 40 patients per day and is improving its systems and workflows to further increase this number. Although MedAustron is a young and modern center, the life-cycle of certain crucial control electronics is near end-of-life and needs to be addressed. This paper presents the 216MHz injector Low-Level Radio Frequency (iLLRF) system with option of use for the synchrotron Low-Level Radio Frequency (sLLRF - 0.4-10MHz). The developed system will unify the cavity regulation for both LLRFs and will also be used for beam diagnostics (injector/synchrotron) and RF knock-out slow extraction. The new LLRF system is based on a μ TCA platform which is controlled by the MedAustron Control System based on NI-PXIe. Currently, it supports fiber-optics links (SFP+), but other links (e.g. EPICS, DOOS) can be established. The modular implementation of this LLRF allows connections to other components, such as motors, amplifiers, or interlock systems, and will increase the robustness and maintainability of the accelerator.

INTRODUCTION

The MedAustron Therapy accelerator contains a linear accelerator [1] and a synchrotron to accelerate particles for medical treatment. The most important radio frequency components are the linear accelerator RF systems working at 216.816MHz and the synchrotron RF systems [2] working at 0.4-10MHz. Till now, both accelerator parts use different components to control the RF amplifiers and monitor the cavities and the beam. Unfortunately end of life notifications were received already for most of these components and updates will be necessary in the near future. A common solution for all replaced components is foreseen to reduce the needed implementation effort and user training. To develop this common solution, efforts of MedAustron and Instrumentation Technologies are bundled in a joint project.

SYSTEM ARCHITECTURE

Requirements

The analog conversion requirements are summed up in Table 1. To allow fast frequency changes for the synchrotron a direct sampling solution is required and the LLRF shall

* markus.wolf@medaustron.at

Table 1: Analog Conversion Requirements for the LLRF Systems

| | Injector | Synchrotron |
|-----------------|-----------------|--------------|
| Frequency Range | 216.816 ± 1 MHz | 0.4 – 10 MHz |
| Frequency Error | <10 kHz | <100 Hz |
| Sample Jitter | <1 ps | <27 ps |
| Channel Jitter | <6 ps | <125 ps |
| Amplitude Stab. | <0.2 %FS | <0.2 %FS |
| Phase Stab. | <0.1° | <0.1° |
| Group Delay | <500 ns | <500 ns |

provide CW and Pulsed operation modes. Furthermore, the LLRF shall allow connection to different supervising systems and subcomponents like plunger motors for cavity tuning or the RF amplifiers. If used as a beam diagnostic backend, only the analog input channels are used.

Hardware Architecture

Limited resources are available for hardware development and testing at MedAustron. Therefore only off-the-shelf (COTS) hardware was selected. For expected long term availability and easy replacement of single components, the μ TCA architecture was chosen. The most important components of the hardware are:

- Vadatech AMC560 [3]: Base board providing the computing power to connect to the supervision systems and to provide a local control interface. The FPGA is used for baseband conversion and cavity regulation.
- Vadatech FMC231 [4]: ADC/DAC extension board for the AMC560. Provides 4 channels of 16bit 1GSps ADC and 4 channels of 16bit 2.5GSps DAC.
- Vadatech FMC105 [5]: High speed connection to the MedAustron Control System (supervising system) via SFP+.
- Vadatech FMC155 [6]: GPIO for Interlocks and Modbus for plunger motor communication.
- Vadatech UTC004 [7]: μ TCA management and 10MHz reference clock distribution.

Firmware Architecture

The firmware architecture, seen in Fig. 1, was designed having reusability in mind. The goal was to have an unified firmware, which can support all applications planned in the future. All building blocks of the firmware can be configured

SUPERCONDUCTING CAVITY AND RF CONTROL LOOP MODEL FOR THE SPIRAL2 LINAC

F. Bouly*, LPSC, Université Grenoble-Alpes, CNRS/IN2P3, Grenoble, France
M. Di Giacomo, J.-F. Leyge, M. Tontayeva, GANIL, Caen, France

Abstract

The SPIRAL2 superconducting linac has been successfully commissioned with protons in 2020. During the commissioning, a model of the cavity and its LLRF control loop has been developed. The model enables to have a better understanding of the system and was used to tune the PI(D) correctors for beam loading compensation. Here we review the development of such a tool, computed with MATLAB/Simulink to model transfer functions of : the RF and mechanical behaviors (Lorentz detuning) of the cavity, as well as all the elements that compose the RF control loop (digital LLRF, amplifier, transmission lines, etc.). A benchmarking of the model with measurements is presented.

INTRODUCTION

A superconducting (SC) cavity model, with its associated control loops (Low level RF and Tuning system) have been developed, by using Matlab/Simulink [1]. The aim of this model was to assess the technological feasibility of fast (~ 100 ms) retuning of SC cavity for the operation of a CW (continuous wave) linac. This is a specific requirement for Accelerator Driven System (ADS) operation, where failure compensation is necessary to ensure a high reliability level of the machine [2, 3]. The model was also used to validate and adjust the incident coupling, as well as the performance requirements of the cold tuning system (CTS) actuators (motor, piezoelectric devices). It also enabled to carry out studies on ‘intelligent’ control of the CTS (Lorentz detuning compensation, microphonics damping, etc) [1, 4]. However, it had never been fully benchmarked on a cavity operating with beam. This has been achieved recently, during the commissioning and power ramp-up of the SPIRAL2 linac [5, 6]. We here give an overview of the model, present its benchmarking and the improvements : in particular for the digital LLRF model and the PI (proportional K_p , Integral K_i) controller.

MODEL

The block diagram of Fig. 1 describes the global principle of the model. It consists in two loops :

- the LLRF feedback loop to control the phase and the amplitude of the accelerating voltage (V_{cav}),
- the feedback loop of the tuning system. The transfer function of the controller and the actuator acting on the cavity frequency detuning can be adjusted depending the simulation needs.

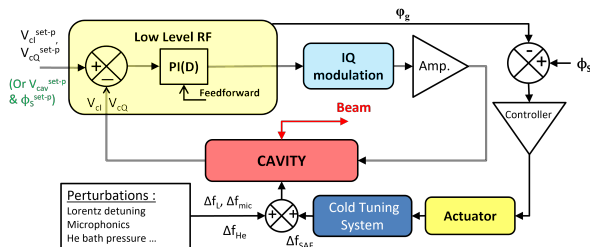


Figure 1: Model block diagram.

Computed in the Simulink environment, the main blocks of the RF feedback control loops are : the cavity, the LLRF, the IQ modulator and the RF power amplifier.

Cavity Model

The cavity accelerating voltage, V_{cav} , is deduced by modelling the cavity as an RLC resonating circuit (cf. Fig. 2 equivalent model).

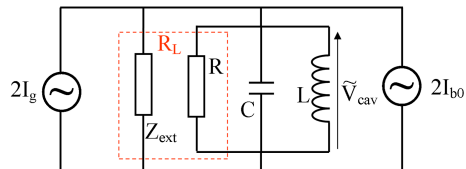


Figure 2: Equivalent circuit.

The RF power generator (I_g) and the beam (I_{b0}) are seen by the cavity as current generators [1, 7]. R_L is the loaded shunt impedance, which is the sum of two parallel resistances: the external impedance (coupling) Z_{ext} , and the cavity resistance R . The loaded coupling is classically defined as :

$$\frac{1}{Q_L} = \frac{1}{Q_0} + \frac{1}{Q_i} + \frac{1}{Q_t} \quad (1)$$

with Q_i the incident coupling from the power coupler, Q_t the coupling from the pick-up antenna and Q_0 is the cavity quality factor. The digital LLRF system is treating I/Q (In phase / Quadrature) parts of the signal. It was chosen to use the same formalism to derive equations that define V_{cav} evolution; and the associated Laplace transfer functions. As developed in [7], transient of the real part (V_{cI}) and imaginary part (V_{cQ}) of V_{cav} can be written¹ :

$$\begin{cases} \dot{V}_{cI} = \frac{\omega_0(r/Q)}{4} (2I_{gI} + I_{bI}) - \frac{\omega_0}{2Q_L} \left[V_{cI} + V_{cQ} 2Q_L \frac{\Delta\omega}{\omega_0} \right] \\ \dot{V}_{cQ} = \frac{\omega_0(r/Q)}{4} (2I_{gQ} + I_{bQ}) - \frac{\omega_0}{2Q_L} \left[V_{cQ} - V_{cI} 2Q_L \frac{\Delta\omega}{\omega_0} \right] \end{cases} \quad (2)$$

¹ with the ‘dot’ notation $\dot{f} = \frac{df}{dt}$

* frederic.bouly@lpsc.in2p3.fr

MTCA.4-BASED LLRF SYSTEM PROTOTYPE STATUS FOR MYRRHA

C. Joly^{p1}, S. Berthelot¹, N. Gandolfo¹, J. Rozé¹, J-F. Yaniche¹, IJCLab, CNRS/IN2P3 Orsay, France
 J-L. Bolli, I. Garcia, C. Gaudin, IOXOS Technologies, Gland, Switzerland
 O. Bourrion, D. Tourres, LPSC, CNRS/IN2P3 Grenoble, France
 S. Boussa, W. De Cock, P. Della Faille, F. Pompon, E. Verhagen, SCK CEN, Mol, Belgium
¹also at Université Paris-Saclay, Orsay, France

Abstract

Within the framework of MINERVA, the first Phase of MYRRHA (Multi-purpose hYbrid Research Reactor for High-tech Applications) project, IN2P3 labs are in charge of the development of several accelerator elements. Among those, a fully equipped Spoke cryomodule prototype was constructed. It integrates two superconducting single spoke cavities operating at 2K, the RF power couplers and the associated cold tuning systems. On the control side, a MTCA.4-based Low Level Radio Frequency (LLRF) system prototype has been implemented by IJCLab including FPGA specific firmware, a new μ RTM frequency downconverter module from the company IOXOS Technologies and EPICS developments in collaboration with the SCK CEN. The status of the LLRF system will be shown as well as its preliminary tests results.

INTRODUCTION

The MINERVA, is the first construction phase of the future MYRRHA facility (Fig. 1) [1]. It involves the realization of an accelerator up to 100MeV, composed of one injector operating at 176.1MHz [2] associated to a MEBT line including a fast switching magnet for a future parallel redundancy using a second injector, the first superconducting linac section (single Spoke cavities @352.2MHz) composed of fifteen cryomodules integrating 2 cavities each and a Proton target Facility.

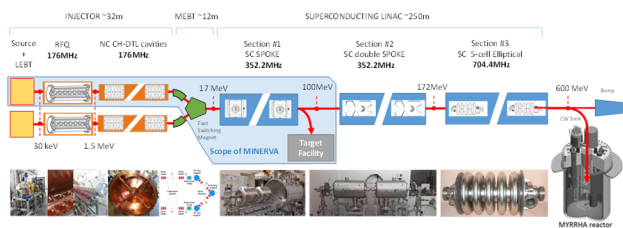


Figure 1: Conceptual layout of the MYRRHA Facility with in the cyan area, the MINERVA project (2019-2026).

A cooperation agreement on the ADS between the CNRS and the SCK CEN in 2017 has allowed to launch a specific prototyping contract, focusing on the realization and the tests of a fully equipped Spoke cryomodule at 2K and 20kW available by cavity for the accelerator field regulation [3]. Within this framework, a MTCA.4-based Low Level Radio Frequency system prototype has been developed and evolved with the a new flexible RF front-end μ RTM prototype developed by IOXOS and IJCLab, a complete overhaul of the firmware with new functions and

an optimized implementation for a maximal 250 MHz clock operation, allowing to use this LLRF system for the superconducting linac and the injector of MINERVA.

LLRF SYSTEM: HARDWARE

The MTCA.4-based LLRF system prototype is designed around a main digital board, called IFC1420, a NATIVE-R5 from NAT and a MRF Timing system (Fig. 2) [4].

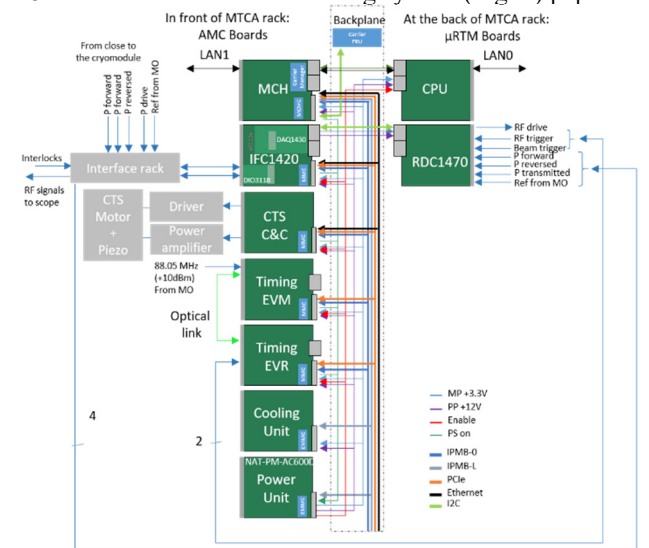


Figure 2: MTCA based LLRF prototype system scheme.

For more flexibility, the planned “Fast RF interlock” FMC mezzanine board prototype has been replaced by a FMC digital IO board called DIO3118 from IOXOS Technologies, associated to a specific 19” rack for the RF and interlocks signals conditioning and interfaces. Two boards have been also developed in collaboration, a μ RTM RF Front-end prototype called RDC1470 and a second Cold Tuning System AMC board prototype including Motor and piezo-actuators C&C.

The RDC140 board integrates four RF channels allowing a signal conditioning (variable gain, filtering and two operation modes: Direct sampling or down converter) for sampling up to 250 MS/s. A specific Accelerator reference channel associated to a PLL provides the synchronized clocks to ADC, DAC, mixers in particular. In addition, 3 DAC channels enable two output operation modes: vector modulator or direct sampling. The board operates with RF signals at 176.1 MHz or 352.2 MHz selected by soft configuration.

The RDC1470 μ RTM prototype (Fig. 3) has additional features including three triggers inputs (useable for RF, Beam and RF authorization triggers), two slow DAC and

ANOMALY DETECTION BASED QUENCH DETECTION SYSTEM FOR CW OPERATION OF SRF CAVITIES*

G. Martino^{†1,4}, A. Bellandi¹, A. Eichler¹, J. Branlard¹, H. Schlarb¹, L. Doolittle², S. Aderhold³, S. Hoobler³, J. Nelson³, R. D. Porter³, L. Zacarias³, A. Benwell³, D. Gonnella³, A. Ratti³, and G. Fey⁴

¹DESY, 22607 Hamburg, Germany

²LBNL, 94720 Berkley, CA, USA

³SLAC, 94025 Menlo Park, CA, USA

⁴TUHH, 21073 Hamburg, Germany

Abstract

Superconducting radio frequency (SRF) cavities are used in modern particle accelerators to take advantage of their very high quality factor (Q). A higher Q means that a higher RF field can be sustained, and a higher acceleration can be produced in the cavity for length unity. However, in certain situations, e.g., too high RF field, the SRF cavities can experience quenches that risk creating damage due to the rapid increase in the heat load. This is especially negative in continuous wave (CW) operation due to the impossibility of the system to recover during the off-load period. The design goal of a quench-detection system is to protect the system without being a limiting factor during the operation. In this paper, we compare two different classification approaches for improving a quench detection system. We perform tests using traces recorded from LCLS-II and show that the AR-SENAL classifier outperforms a CNN classifier in terms of accuracy.

INTRODUCTION

Modern linear accelerators use superconducting radio frequency (SRF) cavities as the main component for achieving high accelerating gradients. SRF cavities are used due to their superior energy efficiency for the same accelerating gradient and lower beam impedance. This means reaching higher particle energies than normally possible at a lower operating cost [1]. However, a lot of care needs to be posed to the control system of SRF cavities due to the high susceptibility to external factors, e.g., external microphonics and Lorentz force detuning [2]. One of the main limiting factors for SRF cavities is the disruption of the superconductivity in part or the entirety of the cavity. Such superconductivity disruption is also referred to as quench. Quenches are mainly caused by defects or contamination of the material [3]. They must be avoided since the disruption of the superconductivity leads to an increased heat load and subsequent lengthy disruptions in the cryogenic system.

The detection of quenches is usually performed by estimating the value of the unloaded quality factor Q_0 . However,

we can only measure the loaded quality factor Q_L , which relates to Q_0 and the external quality factor Q_{ext} as follows:

$$\frac{1}{Q_L} = \frac{1}{Q_{ext}} + \frac{1}{Q_0} \quad (1)$$

Typical values for Q_{ext} and Q_0 in normal conditions are approximately 3×10^6 and 2×10^{10} , respectively. In the case of a quench, Q_0 can reach values as low as 10^7 . With such values, from Eq. 1, it can be derived that it is necessary to detect minimal variations of the value of Q_L .

The decrease of Q_L , e.g., as a result of a quench, can be detected as an increase of the cavity half bandwidth $f_{(1/2)}$. In pulsed machines, the amplitude decay estimation can be used to calculate $f_{(1/2)}$ thanks to the following:

$$f_{(1/2)} = \frac{f_0}{2Q_L} = \frac{1}{2\pi\tau} \quad (2)$$

where f_0 is the cavity resonance frequency and τ is the exponential time constant of the cavity gradient decay. In CW machines, since no amplitude decay is available during normal operation, it is necessary to use the cavity signals expressed as in-phase and quadrature ($I&Q$) components. For the half bandwidth calculation, starting from the cavity dynamics model, the following is used:

$$f_{(1/2)} = \frac{I_p \left(KI_f + BI_B - \frac{\dot{I}_p}{2\pi} \right) + Q_p \left(KQ_f + BQ_B - \frac{\dot{Q}_p}{2\pi} \right)}{I_p^2 + Q_p^2} \quad (3)$$

where $K = \frac{f_0}{Q_{ext}}$, $B = \frac{f_0}{2} r/Q$, r/Q is the geometric shunt impedance, and the subscripts p , f and b refer to the probe, forward, and beam current signals, respectively. A possible different approach for the detection of a quench can be derived from the estimation of the cavity power dissipation:

$$P_{diss} = P_f - P_r - \dot{U} \quad (4)$$

where P_f is the forward power, P_r is the reflected power, and $U = \frac{V^2}{f_0(r/Q)}$ is the cavity stored energy equation. In this case, an increase in the cavity power dissipation above a certain threshold indicates a cavity quench.

The approaches presented for CW machines require a precise calibration of the cavity signals and suffer noisy signals.

* This work is supported by DASHH (Data Science in Hamburg — HELMHOLTZ Graduate School for the Structure of Matter) under Grant No.: HIDSS-0002.

† gianluca.martino@desy.de

DEVELOPMENT OF A TUNER CONTROL SYSTEM FOR LOW-ENERGY SUPERCONDUCTING LINAC AT RAON*

Hyunik Kim[†], Hyojae Jang, Youngkwon Kim, Moosang Kim, and Myung Ook Hyun¹
¹Institute for Basic Science, Daejeon, Republic of Korea

Abstract

We propose a tuner control system for low-energy superconducting linac at RAON. The frequency error of the superconducting cavities must be smaller than a few of Hz to operate in beam acceleration mode. To minimize the frequency error as much as possible, the error is calculated in the low-level RF(LLRF), and the proposed tuner control system changes the superconducting cavity frequency by using a mechanical tuner and a motor attached to the cavity directly. This control system deals with not only the initial frequency error of the cavity but also the frequency drift of the cavity induced by external disturbance such as the slow fluctuation helium pressure automatically. In addition, an automatic proportional gain calibration technique is also proposed. In this paper, the detailed operation and techniques will be described.

INTRODUCTION

The low-energy superconducting linac at RAON has been tested and installed in the SCL3 tunnel by the end of December 2021. In this low-energy section, there are two types of the superconducting RF cavities, a quarter-wave resonator (QWR) and a half-wave resonator (HWR) which target resonance frequencies are 81.25MHz and 162.5MHz respectively. The total number of QWR cavities and QWR cryomodules are 22(1 QWR cavity per a cryomodule). Also, there are two types of cryomodules for HWR cavities, HWRA type(2 HWR cavities per a cryomodule) and HWRB type(4 HWR cavities per a cryomodule), and the number of HWRA and HWRB cryomodules are 13 and 19 respectively.

Every cavity has a frequency tuning system, which consists of a mechanical tuner and a cryogenic stepping motor inside of the cryomodule. The stepping motor is driven by a power stage directly which exists in the SCL3 gallery.

The RF control bandwidths of QWR and HWR cavities are from 100Hz to 200Hz, therefore, the frequency error needs to be minimized as much as possible to excite cavities at target frequency during beam acceleration mode. Therefore, an automatic tuner control system to compensate the frequency error caused by external disturbances is required.

In this paper, a tuner control system for QWR and HWR cavities is proposed to compensate the frequency error of cavities by using this frequency tuning system automatically.

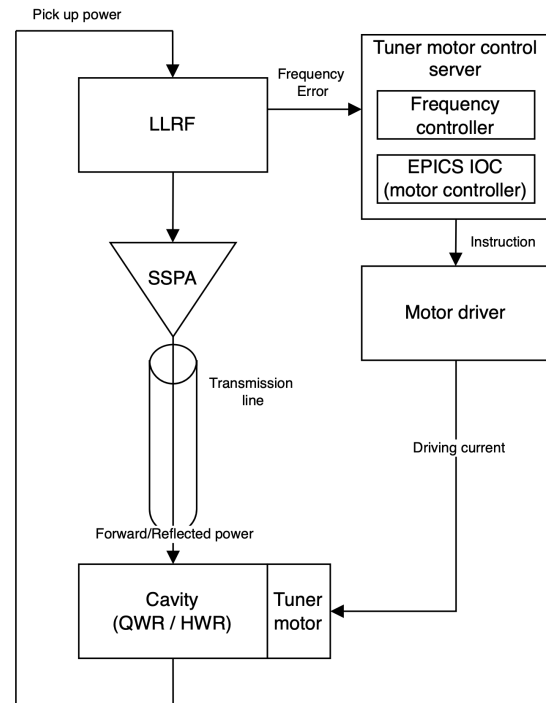


Figure 1: Tuner control system for SRF cavities.

CONTROL SYSTEM OVERVIEW

The tuner control system and RF system for one superconducting RF cavity are shown in the Fig. 1. There are a tuner motor control server, a motor driver, a cryogenic stepper motor, and a mechanical tuner for a cavity. The cryogenic stepper motor is attached to the mechanical tuner directly in the cryomodule. The motor driver generates driving current which makes the stepper motor rotated.

In the tuner motor control server, there are two programs running on it. The EPICS IOC [1] is for giving instruction to the motor driver via EPICS network. The frequency controller is a c++ program that controls tuner motor automatically when the feedback switch is on. The frequency controller acquires the frequency error of the cavity from LLRF via EPICS network.

In LLRF, the frequency error is calculated in two ways [2]. In self-excited loop(SEL) mode, the frequency error is obtained by differentiating measured phase. In generator-driven resonator(GDR) mode, the phase difference between the forward power and the pick-up power is used for the frequency error.

Eight tuner motors for cavities are controlled by one tuner motor control server. Therefore, there are a total of 16 tuner control servers for the low-energy section.

* This research was supported by the RISP of ibs funded by the Ministry of Science and the National Research Foundation (NRF) of the Republic of Korea under Contract 2013M7A1A1075764.

[†] email address : hifine@ibs.re.kr

INITIAL HIGH POWER RF DRIVING TEST USING DIGITAL LLRF FOR RF CONDITIONING OF 1 MeV/n RFQ AT KOMAC*

H. S. Jeong[†], K. H. Kim, S. G. Kim, W. H. Jung, J. H. Kim, H. S. Kim, Y. G. Song, H. J. Kwon, D. H. Kim, P. S. Lee

Korea Multi-purpose Accelerator Complex of KAERI, Gyeongju, Republic of Korea

Abstract

As a part of R&D toward the RFQ(Radio Frequency Quadrupole) based heavy ion irradiation system, the 1 MeV/n RFQ was designed, brazed, installed and commissioned by staff researchers and engineers at KOMAC (Korea Multi-purpose Accelerator Complex) of KAERI (Korea Atomic Energy Research Institute). This 1 MeV/n RFQ system includes the microwave ion source, EBIS, RFQ, quadrupole magnets, switching magnet and the target systems.

The digital based LLRF (Low-Level RF) was developed to provide the stable accelerating field to the RFQ. This LLRF has features such as direct RF detection/generation without mixer, non-IQ sampling, PI feedback control, iterative learning based feed-forward control, and the digital RF interlock.

In this paper, the characteristics of LLRF are described, as well as the processes and results of an initial RF driving test for the RFQ's RF conditioning.

INTRODUCTION

The 1 MeV/n RFQ was installed at KOMAC site as shown in Fig. 1.

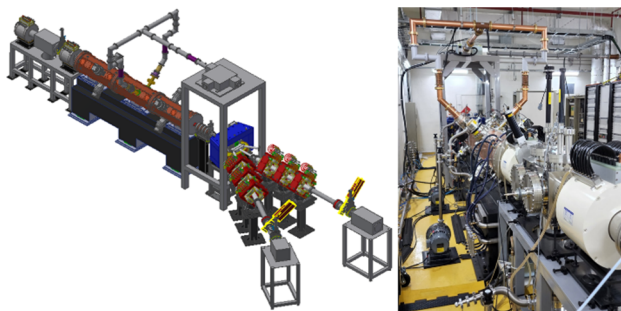


Figure 1: 1 MeV/n RFQ layout and installation.

The first beam acceleration experiment using 1 MeV/n RFQ was conducted successfully in August 2022. The LLRF commissioning and the high power RF driving test were completed before this beam experiment.

The digital LLRF was developed as shown in Refs. [1, 2]. Thanks to the configuration of the digital LLRF, we were able to achieve the simplification of analog parts such as eliminating analog mixer. As shown in Fig. 2, the sampling frequency of ADC(Analog to Digital Converter) is 320 MHz to detect the 200 MHz RF field using non-IQ sampling technic.

* Work supported by KOMAC operation fund of KAERI by MSIT

[†] jeonghs@kaeri.re.kr

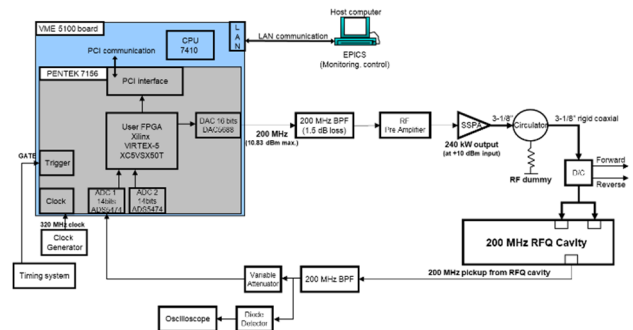


Figure 2: 1 MeV/n RFQ RF chain diagram.

A TOMCO 240 kW_{peak} SSA(Solid State Amplifier) is used as a high power RF source as shown in Fig. 3. The SSA's 240 kW_{peak} output was demonstrated using a dummy load. After that, the RFQ cavity's RF conditioning was successfully carried out up to 125 kW_{peak} until now.



Figure 3: High power RF source installation.

LLRF UPGRADE

To compensate the heavy beam loading effect, the feed-forward control logic is essential part in the LLRF algorithm [3-5]. The parallel type ILC(Iterative Learning Control) logic was implemented in the FPGA(Field Programmable Gate Array) of digital LLRF. As shown in Fig. 4, in case of an abnormal circumstance where the RF field in the cavity becomes unstable, this logic has a feature to bypass the learning data using 2x1 multiplexer. As described in Ref. [6], this was made possible via digital RF interlock logic using a cavity pickup signal.

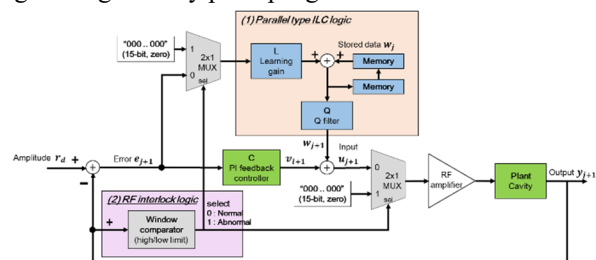


Figure 4: Implemented feed-forward control diagram.

NARROW BANDWIDTH ACTIVE NOISE CONTROL FOR MICROPHONICS REJECTION IN SUPERCONDUCTING CAVITIES AT LCLS-II*

A. Bellandi[†], J. Branlard

Deutsches Elektronen-Synchrotron DESY, Notkestr. 85, Hamburg, Germany

J. Diaz Cruz¹, S. Aderhold, A. Benwell, A. Brachmann, S. Hoobler, A. Ratti,

D. Gonnella, J. Nelson, R. D. Porter, L. Zacarias

SLAC, Menlo Park, CA, USA

¹also at University of New Mexico, Albuquerque, NM, USA

Abstract

LCLS-II is an X-Ray Free Electron Laser (XFEL) commissioned in 2022, being the first Continuous Wave (CW) hard XFEL in the world to come into operation. To accelerate the electron beam to an energy of 4 GeV, 280 TESLA type superconducting RF (SRF) cavities are used. A loaded quality factor (Q_L) of 4×10^7 is used to drive the cavities at a power level of a few kilowatts. For this Q_L , the RF cavity bandwidth is 32 Hz. Therefore, keeping the cavity resonance frequency within such bandwidth is imperative to avoid a significant increase in the required drive power. In superconducting accelerators, resonance frequency variations are produced by mechanical microphonic vibrations of the cavities. One source of microphonic noise is rotary machinery such as vacuum pumps or HVAC equipment. A possible method to reject these disturbances is to use Narrowband Active Noise Control (NANC) techniques. These techniques were already tested at DESY/CMTB [1] and Cornell/CBETA [2]. This proceeding presents the implementation of a NANC controller adapted to the LCLS-II Low Level RF (LLRF) control system. Tests showing the rejection of LCLS-II microphonic disturbances are also presented.

INTRODUCTION

The SRF cavity is the device responsible for storing energy in the form of electromagnetic field in a particle accelerator. When a particle beam passes through a cavity, it interacts with the field by exchanging energy with it. An SRF cavity can be modeled as a narrow band filter centered around its resonance frequency f_0 . Even though the nominal resonance frequency is specified at the cavity design stage, it can change due to unwanted mechanical deformations during operation. The difference between the nominal resonance frequency and the actual one is referred as *detuning*, Δf .

The relation between power consumption and detuning of a steady state cavity when driving it at its design resonance frequency is

$$P_f = \frac{V_c^2}{4 \left(\frac{R}{Q}\right) Q_L} \left[1 + \left(\frac{\Delta f}{f_{1/2}}\right)^2\right], \quad (1)$$

$$Q_L = \frac{f_0}{2f_{1/2}}, \quad (2)$$

where P_f is the required power to drive a cavity at the accelerating voltage V_c , $f_{1/2}$ is the cavity half bandwidth and $\frac{R}{Q}$ is the cavity shunt impedance. Therefore, even if decreasing $f_{1/2}$ can reduce the power consumption needed to reach a certain accelerating gradient, detuning signals that are comparable or higher than $f_{1/2}$ can negate such an advantage.

Resonance control systems then play a crucial role in modern SRF CW accelerators for FELs, by keeping the cavities close to the nominal resonance frequency. For LCLS-II the maximum peak detuning that can be withstand without lowering the gradient due to power constraints is equal to ± 10 Hz. A method to reduce the cavity detuning is to provide active compensation using the piezoelectric tuner actuators attached to the cavity. In LCLS-II, these tuners can steer the cavity frequency by up to 2 kHz.

TYPES OF MICROPHONICS DISTURBANCES

The cavity mechanical disturbances have different spectral and time characteristics. However, two kind of external mechanical perturbations are commonly found in every CW SRF system and are accountable for the major part of the cavity detuning.

- Drifts produced by the cooling system. Since SRF cavities are located in tanks filled with super-fluid cryogenic helium, every drift of the pressure results in a detuning variation. The typical timescale of this effect is usually higher than seconds.
- Vibrations produced by machinery located in the proximity of the accelerator. Due to the necessity of actively maintaining some physical characteristics in the accelerating system, like high vacuum and cryogenic temperatures, different kinds of pumps are required. This kind of noise has a narrow bandwidth and a sinusoidal-like shape.

* Work supported by the DOE and Helmholtz Institute

[†] andrea.bellandi@desy.de

C-BAND LOW LEVEL RF SYSTEM USING COTS COMPONENTS

J. P. Edelen, RadiaSoft LLC, Boulder, CO, USA

J. Krasna, COSYLAB, Ljubljana, Slovenia

R. D. Berry, A. Diego, D. Gavryushkin, A. Y. Smirnov, RadiaBeam, Santa Monica, CA, USA

Abstract

Low Level RF systems have historically fallen into two categories. Custom systems developed at national laboratories or industrial systems using custom hardware specifically designed for LLRF. Recently however advances in RF technology accompanied by demand from applications like quantum computing have led to commercially available systems that are viable for building a modular low-level RF system. Here we present an overview of a Keysight based digital LLRF system. Our system employs analog upconversion and downconversion with an intermediate frequency of 100MHz. We discuss our phase-reference system and provide initial results on the system performance.

INTRODUCTION AND HIGH LEVEL ARCHITECTURE

The Low-Level Radio Frequency (LLRF) control system is primarily responsible for delivering RF to amplifiers, receiving and processing signals for the various RF diagnostics, and control of the RF cavities to include phase, amplitude, and frequency. When building a LLRF system there are a number of design considerations that lead to the choice of frequency parameters, digital vs analog, and how to modulate the RF signals. One of the most common architectures utilizes an intermediate frequency that is used for digitization and an analog system to perform up and down conversion [1]. However, base-band modulation has also been used, for example the Swiss FEL utilized such an architecture [2]. Additionally, modern electronics are making systems that perform direct digital down-conversion more popular [3]. For C-Band there are limited commercial options for direct digital sampling that are also cost effective for a modest scale system. This is largely due to the development time required and operating in unusual modes such as the first Nyquist band. Moreover, the technical challenges associated with base-band modulation and noise mitigation makes a digital system operating at an intermediate frequency more attractive. As such we chose to build a COTS system based on digitization at a reasonable intermediate frequency with cost effective solutions. Figure 1 shows a functional block diagram of our COTS LLRF system. Here we highlight the notable interconnections and signals. For this system, we have a common local oscillator that is distributed to all of the analog electronics. The digital system generates a clean reference signal that is re-distributed to the LLRF system as a phase reference and also distributed to the timing system and the laser system for phase locking.

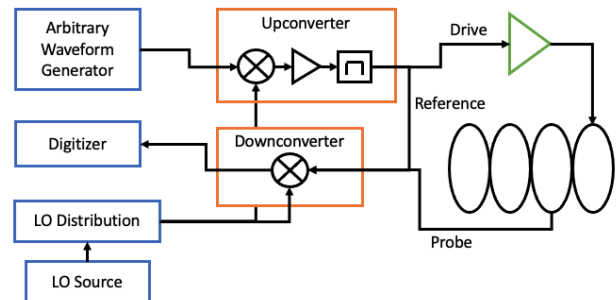


Figure 1: High level schematic of a generic LLRF control system.

In this paper we will provide an overview of our design choices and share some initial results of our phase and amplitude stability, noise levels, and linearity.

DIGITAL SYSTEM

The digital system is comprised of an M3102A PXIe Digitizer from Keysight and an M3201A PXIe Arbitrary Waveform Generator also from Keysight. Our AWG resolution is 16 bit at a 500 MS/s sample rate. The digitizer resolution is 14 bit at a 500 MS/s sample rate.

The choice of intermediate frequency is largely determined by the available digital components and the constraints on RF filtering. This typically is in the 10 – 100 MHz range. Our initial choice of the intermediate frequency is 100 MHz. This is to allow for good isolation between IF signals, RF signals, and baseband signals. When converting from RF to IF, the RF signal at 5712 MHz is mixed with the LO at 5810 MHz. This will generate a 100 MHz signal and a 11524 MHz signal. The 11.5GHz signal will be filtered out using analog components leaving the 100 MHz signal. The IF signals will be digitized at a rate of 500 MS/s which is readily available with modern digitizers. The choice of a digital system that is 2.5x Nyquist will provide higher signal quality while maintaining a reasonable cost. The digitizers have a bandwidth of up to 200MHz and we will show results of our system with an IF of up to 175MHz. To extract the RF waveforms the 100 MHz signal is mixed digitally with another 100MHz signal giving a baseband waveform and a 200MHz signal. In order to resolve the cavity dynamics, we need a minimum of 20 MHz bandwidth at baseband. Having 200MHz of space between the baseband signal and the secondary signal generated by the IF downmixing relaxes the constraints on the filter design and reduces the need for high order filters that cause ringing and other unwanted effects.

DIGITAL LLRF SYSTEM DEVELOPMENT AND IMPLEMENTATION AT THE APS LINAC *

Y. Yang[†], J. Byrd, G. Fystro, D. Meyer, A. Nassiri, A. Pietryla, T. Smith, Y. Sun,
 Advanced Photon Source, Argonne National Lab, Lemont, IL, USA
 B. Baricevic, Instrumentation Technologies, Solkan, Slovenia

Abstract

The current analog LLRF systems which have supported the APS linac operation for over 25 years, will be replaced with digital LLRF systems utilizing the latest commercially available electronics technology. A customized LLRF system has been developed as the next-generation APS linac controller. Two systems have been manufactured and delivered to the APS. On-site tests demonstrated they met the APS linac operation requirements with the first system expected to be integrated into APS linac operation this year.

INTRODUCTION

The linac at the Advanced Photon Source (APS) has been operating for over 25 years [1]. The current setup is shown in Fig. 1. It includes a number of S-band travelling-wave (TW) RF structures with two thermionic RF guns, RG1 and RG2. One provides beams for APS injection, while the other is used as backup [2]. Downstream of the RF guns, there are three linac sectors, L2, L4, and L5, each consisting of four TW RF accelerating structures. For each sector, it is powered by an S-band klystron with a SLED power compressor. The beams are accelerated to 425 MeV before injecting into the PAR and then the booster.

To prepare for the next decades of operation with APS-U, the APS linac is undergoing a major refurbishment. One of the main tasks is to develop new digital LLRF systems to replace the existing analog LLRF controllers which are getting obsolete.

RF CONTROL REQUIREMENT

There are five S-band klystrons in the APS linac. The linac operates at 30 Hz. Each klystron needs a new LLRF system. The main specifications are summarized in Table 1. There are three klystrons that are connected to a SLED to compress the RF pulse. As is required by the SLED, the RF pulse signal generated by the new LLRF system must have a phase reversal with a user-specified timing.

The new LLRF system needs to have enough RF monitor channels. The K2, K4, and K5 klystron stations, which power the linac sector downstream, need more RF monitor channels than the K1 and K3 stations. Each RF monitor channel needs to provide time-resolved amplitude and phase waveforms with around 10 ns resolution. Advanced features such as post-mortem buffer and RF stability analyzer should

be included. To support the interleaving operation required by the future advanced accelerator study such as the APS LEA [3], all the RF monitor values in the new LLRF system must have a corresponding timestamp with millisecond resolution.

Table 1: LLRF System Main Specifications

| Item | Parameter | Specification |
|--------------|----------------------|---------------|
| RF Drive Out | Amp. Jitter | 0.02 % |
| | Added Phase Noise | 10 fs |
| | Max Power Level | 20 dBm |
| RF Input | Data Rate | 119 MHz |
| | Repetition Rate | 30 Hz |
| | Channel Number | 10 and 20 |
| | Timestamp Resolution | 1 ms |
| | Amp. Resolution | 0.05 % |
| | Phase Resolution | 0.1 deg |

SYSTEM DEVELOPMENT

Over the past several years, the APS team has been collaborating with Instrumentation Technologies on the RF Beam Position Monitor (BPM) for the APS-upgrade [4]. The new digital LLRF system for the APS linac was developed in a similar way on the Libera platform [5]. Figure 2 shows the Libera LLRF system for the APS linac. It consists of two types of units. One is Libera TSRF, the other is the Libera digital processor.

Libera TSRF

Libera TSRF operates as the analog frontend of the LLRF system. It generates the Local Oscillator (LO) and clock (CLK) signals based on the reference 2856 MHz Master Oscillator (MO) signal. The unit converts up to fourteen 2856 MHz RF inputs including the MO signal to 44.6 MHz Intermediate Frequency (IF) signals.

Libera Digital Processor

The Digital Processor is based on MicroTCA.0 standard. There are six AMC slots available in the crate, shown in Fig. 2. Two single-width AMC cards, Vector Modulator (VM) and Timing Control Module (TCM) are installed in the middle. The VM in slot 1 operates as the up-converter to generate RF drive signals. Slot 2 is for the TCM, which distributes the CLK and trigger signals to other modules. It also has a built-in interlock protection function. Four double-width slots from slot 3 to slot 6 are reserved for the

* Work supported by U.S. Department of Energy, Office of Science, Office of Basic Energy Sciences, under Contract No. DE-AC02-06CH11357.

[†] yaweiyang@anl.gov

FIRST SELAP ALGORITHM OPERATIONAL EXPERIENCE OF THE NEW LLRF 3.0 RF CONTROL SYSTEM*

T. Plawski[†], R. Bachimanchi, S. Higgins, C. Hovater, J. Latshaw, C. Mounts
Jefferson Lab, Newport News, VA, USA

Abstract

The JLAB LLRF 3.0 system has been developed and is replacing the 30-year-old LLRF systems in the CEBAF accelerator. The LLRF system builds upon 25 years of design and operational RF control experience (digital and analog), and our recent collaboration in the design of the LCLSII LLRF system. The new system also incorporates a cavity control algorithm using a fully functional phase and amplitude locked Self Exciting Loop (SELAP). The first system (controlling 8 cavities) was installed and commissioned in August of 2021. Since then, the new LLRF system has been operating with cavity gradients up to 20 MV/m, and electron beam currents up to 400 μ A. This paper discusses the operational experience of the LLRF 3.0 SELAP algorithm along with other software and firmware tools like cavity and klystron characterization, quench detection and dynamic power allocation for beam current.

INTRODUCTION

The CEBAF Accelerator at Jefferson Lab provides electron beams to four different physics (experimental) halls at energies up to 12 GeV. This is accomplished using two linacs with over 400 superconducting cavities (SC) in 53 cryomodules. The linacs are connected with two recirculating arcs. Three of the experimental halls can receive up to five passes and a fourth can receive 5.5 passes [1]. The overall delivered dp/p rms energy spread is 5×10^{-5} at currents up to 400 μ A (cw).

As part of the CEBAF improvement plan, a new cryomodule, C75, has been developed by modifying an existing older cryomodule [2]. The modified cryomodule cavity's Q_{ext} is 1.5×10^7 and has a Q_0 of 8×10^9 . Average cavity gradient for C75 cavities is approximately 16 MV/m. In addition to the cryomodule upgrade, the plan calls for upgrading the RF zones with new LLRF systems (LLRF 3.0), which will replace the old analog LLRF (LLRF 1.0) designed in late 1980s. Every cavity is powered and controlled individually, similar to the older RF systems. The cavity amplitude and phase field stability remains unchanged and must be smaller than 0.04% and 0.5 deg rms. respectively, for measured frequencies > 1 Hz.

LLRF 3.0 HARDWARE

The new LLRF system design builds upon experience from the older CEBAF LLRF designs, and the recent participation in the LCLS-II LLRF design. The system utilizes

a modular architecture concept, where the RF receiver, RF transmitter, fast digitizer and the FPGA carrier are separate printed circuit boards.

RF Transceiver

There are three high frequency receiver channels (1497 MHz) and one high frequency transmitter channel (1497 MHz). The RF receiver and transmitter use heterodyning in a double balanced, level 13 frequency mixer. The RF receiver channels are designed to provide very high channel to channel isolation (>90 dB).

The RF receiver and transmitter are in the same chassis as the digitizer and FPGA carrier. This was done to keep the cost low and allow the new system to fit into the existing racks. The down side of this is an added crosstalk of 6 dB to the receivers from the transmitter, which is still within the LLRF requirement of 80 dB.

Fast Digitizer and FPGA Board

Digitizer has four inputs to the ADC, two DAC outputs and a clock generator. AD9653 is used for ADC to process the 70 MHz inputs from RF receivers, DAC9781 for the DAC to generate the 70 MHz for RF transmitter and LMK03328 for the clock generator. Input to the clock generator is 70 MHz master reference.

The FPGA board is designed based on Intel Cyclone 10GX 672 pin FPGA. This board uses a MAX10 FPGA for power sequencing and monitoring and is available in four different sizes for resources (85k Logic Elements, 105 k, 150 k and 220 k). It is flexible in this sense that the user can choose one of the options at the time of assembly without changing the design. The FPGA board can be connected to a server using the SFP module or RJ-45 for communication over Ethernet. QSFP modules are useful, if there is a need to exchange information between the boards at high speed (e.g., 2.5 Gbps).

The RF chassis communicates with an IOC using UDP protocol. RF chassis in a zone are connected to an IOC over a private network. All the chassis can transfer the data at 1 Gbps as the link between the server and the switch is 10 Gbps.

CONTROL ALGORITHM

The control algorithm is based on a digital Self Excited Loop concept [3-5] and extended by an amplitude and Phase Lock feature. This replaces the analog GDR (Generator Driven Resonator) based systems LLRF 1.0 and digital SEL/GDR LLRF 2.0 firmware. To distinguish this from of GDR topology we use name SELAP (SEL with amplitude and phase locked). Figure 1 shows a block diagram of this algorithm that was first developed for LCLS-II LLRF project [5]. At JLAB we developed a full (cavity +SELAP

[†] plawski@jlab.org

* Authored by JSA, LLC under U.S. DOE Contract DE-AC05-06OR23177 and DE-SC0005264. The U.S. Govt. retains a non-exclusive, paid-up, irrevocable, world-wide license to publish or reproduce this for U.S. Govt. purposes.

MACHINE LEARNING ASSISTED CAVITY QUENCH IDENTIFICATION AT THE EUROPEAN XFEL

J. Branlard[†], A. Eichler, J. Timm, N. Walker
DESY, Hamburg, Germany

Abstract

A server-based quench detection system is used since the beginning of operation at the European XFEL (2017) to stop driving superconducting cavities if they experience a quench. While this approach effectively detects quenches, it also generates false positives, tripping the accelerating station when failures other than quenches occur. Using the post-mortem data snapshots generated for every trip, an additional signal (referred to as residual) is systematically computed based on the standard cavity model. Following an initial training on a subset of such residuals previously tagged as “quench” / “non-quench”, two independent machine learning engines analyse routinely the trip snapshots and their residuals to identify if a trip was indeed triggered by a quench or has another root cause. The outcome of the analysis is automatically appended to the data snapshots and distributed to a team of experts. This constitutes a fully deployed example of machine-learning-assisted failure classification to identify quenches, supporting experts in their daily routine of monitoring and documenting the accelerator uptime and availability.

INTRODUCTION

The European X-ray free electron laser (EuXFEL) is a user facility delivering ultra-short hard and soft X-ray flashes with the highest brilliance worldwide, through three undulator lines and serving up to six experiments. It is based on a 10 Hz pulsed 17.5 GeV superconducting linac, commissioned since 2017. Large accelerators require a high level of automation, in particular for trip detection, classification and recovery. *XTLReport* is a tool developed over the last years [1] to track the linac uptime and categorize trips according to their root cause. In its current implementation, once an hour, the tool monitors for each RF station a total of 50 hardware interlock histories available in the control system, coming from the following subsystems: klystron, modulator, coupler, quadrupoles, cryogenics, vacuum and machine protection system. On top of these hardware interlock, software interlock properties (for example coming from the quench detection system or the finite state machine) are also being monitored. Often a trip fires several interlocks, requiring experts to look at the post-mortem time signals to reconstruct the chain of events that lead to the trip. However, the accelerator conditions at the time of the trip and the sequence of interlock often provide a unique signature allowing for trip classification, so that once identified, this process can be automated. *XTLReport* has gone through several iterations, each time assigning a newly found sequence of interlocks to a new root cause, hence providing live up/downtime accounting and

root cause analysis, or leaving the root cause unknown if it cannot (yet) be identified. The tool also fetches DAQ data of the tripped station, before (20 sec) and after (5 sec) the event, and bundles it into a data snapshot saved for post-mortem analysis. A classic example of such a trip is when the quench detection server (QDS) detects a quench and trips the station by stopping the RF to minimize the impact of the excessive cryo load induced by the quench on the cryogenic system. The QDS decision algorithm follows the standard approach of computing the cavity loaded quality factor (Q_L) for every pulse and comparing it to a running average [2]. Sudden drops in Q_L are interpreted as quench and the RF is stopped. While this approach proved extremely successful to minimize down time when quenches occur, false positives (i.e. “fake” quenches”) have also been observed. As a part of operations supervision, an expert routinely reviews the last trips, analyzes the RF waveforms and concludes if a quench was real or not. An example of a real and a fake quench, compared to a nominal pulse is given in Fig. 1. This plot illustrates the differences observed during the decay part of the RF pulse, where Q_L is computed by the QDS.

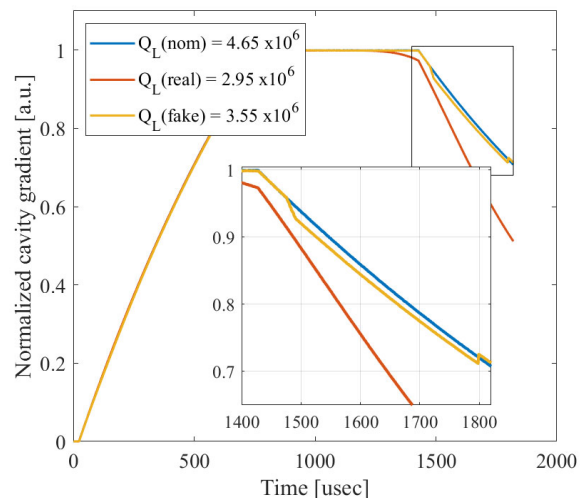


Figure 1: Normalized cavity gradient amplitude for a nominal, fake- and real-quenched pulse. The inset zooms on the decay section at the end of the pulse, when the RF is switched off.

As illustrated in Fig. 1, a real quench behavior corresponds to a steeper slope during the decay. However, other phenomena can occur during the pulse, interfering with the Q_L computation and fooling the QDS into detecting fake quenches. In the fake-quench example of Fig. 1, one can see a step-down in the decay around 1500 usec followed by a step-up around 1800 usec. This behavior (suspected to come from a failure in the digitization chain) is not a

[†]julien.branlard@desy.de

STUDY ON THE MULTIPACTOR BARRIERS OF THE SARAF-PHASE 2 LOW-BETA AND HIGH-BETA SUPERCONDUCTING CAVITIES*

Guillaume Ferrand[†], Matthieu Baudrier, Luc Maurice, Nicolas Pichoff

Commissariat à l’Energie Atomique et aux Energies Alternatives (CEA-Irfu) Institut de Recherche sur les lois Fondamentales de l’Univers, Gif-sur-Yvette, France

Abstract

CEA is committed to delivering a Medium Energy Beam Transfer line and a superconducting linac (SCL) for SARAF accelerator in order to accelerate 5 mA beam of either protons from 1.3 MeV to 35 MeV or deuterons from 2.6 MeV to 40 MeV. The SCL contains 13 half-wave resonator (HWR) low beta cavities ($\beta = 0.09$) at 176 MHz and 14 HWR high-beta cavities ($\beta = 0.18$) at 176 MHz. The low-beta and high-beta series were qualified in 2021 and 2022 respectively. This contribution will focus on the observation of the multipactor barriers for all cavities. It will present series of data obtained during the conditioning of these cavities.

INTRODUCTION

In 2014, CEA (Commissariat à l’Energie Atomique et aux Energies Alternatives, Saclay, France) was committed to delivering a Medium Energy Beam Transfer line and a superconducting linac (SCL) for SNRC (Soreq Nuclear Research Center, Soreq, Israel), on the SARAF (Soreq Applied Research Accelerator Facility) site [1].

This new accelerator, called Saraf-Phase II, was designed to accelerate 5 mA beam of either protons from 1.3 MeV to 35 MeV or deuterons from 2.6 MeV to 40 MeV. CEA planned the end of the commissioning of the last cryomodule for 2023.

The SARAF-Phase II accelerator contains 13 superconducting cavities with $\beta_{opt} = 0.09$, called low-beta (LB) cavities, and 14 superconducting cavities for $\beta = 0.18$, called high-beta (HB) cavities [2]. A detailed presentation of the results for LB series can be found in Ref. [3].

In 2022, the last HB series cavities were tested successfully. These 29 tests produced a lot of data concerning the multipactor (MP) conditioning. The purpose of this paper is to present some of these data and discuss them. It shows that the duration of the conditioning of these cavities is inversely proportional to the power accepted by the cavity.

DESIGN

The design of both cavity kinds began in 2016 and was described in Ref. [4]. The frequency for the superconducting LINAC is 176 MHz, in order to keep the RFQ [5]. Table 1 presents the performances for these accelerating fields as mentioned in Ref. [6].

* Work supported by the Commissariat à l’Energie Atomique et aux Energies Alternatives (CEA, France) and by Soreq Nuclear Research Center (SNRC, Israel)

[†] Guillaume.ferrand@cea.fr

Table 1: Performances According to Final RF Simulations

| Parameter | Low β cav. | High β cav. |
|----------------------------|------------------|-------------------|
| β_{opt} | 0.091 | 0.181 |
| $E_{acc}(MV/m)$ | 7 | 8.1 |
| $E_{pk}(MV/m)$ | 34.5 | 35.8 |
| $B_{pk}(mT)$ | 65.6 | 65.3 |
| $Q_{0,max}@4.45\text{ K}$ | $8 \cdot 10^8$ | $1.2 \cdot 10^9$ |
| $R/Q@ \beta_{opt}(\Omega)$ | 189 | 280 |
| Stored Energy (J) | 5.7 | 16.8 |
| RF losses @ Q_0 (W) | 7.9 | 15.5 |

Figure 1 (left) presents the final design of the LB cavity with its helium tank. Both inner and outer conductors are cylindrical. Figure 1 (right) presents the final design of the HB cavity with its helium tank. Contrary to the LB cavity, the inner conductor is conical. See Ref. [3] for more information.

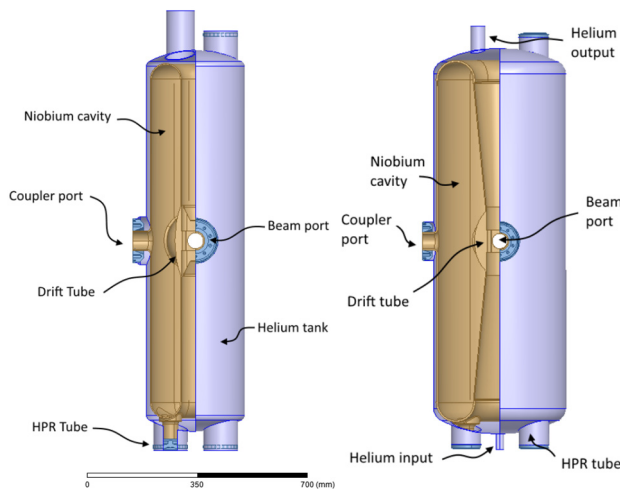


Figure 1: LB (left) HB (right) SARAF cavity.

SIMULATION OF MULTIPACTOR

Before launching the manufacturing of the cavities, we tried to simulate potential MP regions using the Music3D software [7]. A few MP regions were found at low field, from 30 kV/m to 100 kV/m as shown in Figure 2. We were not able to find MP barriers at higher field, even if the experience showed that they exist for both cavities.

INVESTIGATION OF HiPIMS-COATED S(I)S STRUCTURES FOR SRF CAVITIES

A.Ö. Sezgin, X. Jiang, M. Vogel

Institute of Materials Engineering, University of Siegen, Siegen, Germany

R. Ries, E. Seiler

Institute of Electrical Engineering SAS, Bratislava, Slovakia

D. Tikhonov, S. Keckert, J. Knobloch¹, O. Kugeler

Helmholtz-Zentrum Berlin für Materialien und Energie GmbH, Berlin, Germany

L. Smith, O. B. Malyshev

ASTeC, STFC Daresbury Laboratory, Warrington, United Kingdom

C. Z. Antoine

CEA Irfu, Centre d'Etudes de Saclay, Gif-sur Yvette Cedex, France

¹Also at Department of Physics, University of Siegen, Siegen, Germany

Abstract

The sustainable next generation particle accelerators require innovative solutions to overcome the current technological challenges set by existing bulk niobium superconducting radio-frequency (SRF) cavities. Thin film-based multilayer structures in the form of superconductor-insulator-superconductor (SIS) may be the long-sought-after breakthrough for higher performance SRF cavities by enhancing both accelerating gradients and quality factors. In order to understand better the underlying mechanisms of SIS structures to be coated onto (S)RF cavities, we study various material properties with the resultant superconducting properties of high-power impulse magnetron sputtering (HiPIMS)-coated S(I)S structures of Nb-(AlN)-NbN with different thicknesses which are designed to be coated mainly on OFHC copper (Cu) samples for more efficient SRF cavities. This contribution presents materials properties of the aforementioned HiPIMS-coated S(I)S structures as well as the superconducting and RF behaviours of these multilayers which are assessed comparatively via DC and AC magnetization techniques.

INTRODUCTION

The existing bulk niobium (Nb) superconducting radio-frequency (SRF) cavity technology, which has been the leading accelerator technology so far, is close to its theoretical field limit. Besides, field-dependent performance degradation along with local breakdown phenomena restrict not only achievable accelerating gradients, but also quality factors of bulk niobium SRF cavities [1]. Accordingly, innovative solutions need to be introduced to realize ever increasing high performances with reduced infrastructural and operational costs so as to build the next generation compact particle accelerators which would outperform the state-of-art particle accelerators based on bulk Nb, and surpass the expected accelerating gradients of 50 MV/m together with reduced RF losses.

In order to achieve these breakthroughs, one of the promising solutions is coating inner surface of (S)RF cavities with alternating thin film-based multilayers in the form of superconductor-insulator-superconductor (SIS) structure

given the fact that magnetic field penetration is a surface phenomenon (i.e., RF field penetration depth for bulk Nb is only about 40 nm.).

The theory, proposed by A. Gurevich, for *the alternating multilayer structures for SRF cavities* [2], especially for bulk niobium cavities, says that the simplest alternating multilayer structures (SIS), made of superconductive thin films with thicknesses less than the London penetration depth of the cavity wall material, enhances not only the quality factor (Q_0) with lower surface resistance (R_s), but also the vortex penetration field by means of the insulating layers.

Theoretically, the SIS structure is a stronger candidate to increase the theoretical field limit as well as the onset of the vortex penetration by means of the insulating layer, provided that the optimum layer thicknesses and material combinations are realised, as compared to the SS bilayer structure without any insulating layer. However, the SS bilayers are also worth studying as being a simpler structure with promising RF performance of the SRF cavities by enhancing the vortex penetration onset via SS boundary [3].

As being an emergent scalable sputtering technique, high-power impulse magnetron sputtering (HiPIMS) provides means to improve the quality of the deposited films by producing higher quality deposited films in the recent years thanks to its highly ionized denser plasmas, as compared to conventional physical vapor deposition techniques, yielding more effective control of the kinetic energy of the sputtered species with high ionization fractions, which arrive onto the substrate surface, so as to allow fine tuning of parameters of deposition processes [4].

In this paper, the assessment results of the HiPIMS-coated SS and SIS structures based on materials characterizations such as scanning electron microscopy (SEM) as well as superconducting and RF characterization techniques such as vibrating sample magnetometer (VSM), and quadrupole resonator (QPR), respectively are detailed.

EXPERIMENTAL METHODS

The multilayer SS and SIS structures in the form of Nb / NbN and Nb / AlN / NbN were coated mainly onto silicon

DESIGN & MULTIPHYSICS ANALYSIS OF THREE-CELL, 1.3 GHz SUPERCONDUCTING RF CAVITY FOR ELECTRON BEAM ACCELERATOR TO TREAT WASTEWATER

Pankaj Kumar,* Abhishek Pathak, Raghava Varma
 Indian Institute of Technology Bombay, Mumbai, India

Abstract

To treat industrial effluents including contaminants of emerging concern (CECs), Irradiation treatment by electron beam accelerator has shown promising results. Our aim is to design and develop a superconducting linear electron accelerator. A 1.3 GHz, three cell conduction cooled, TM class superconducting cavity has been proposed to accelerate a 100 mA electron beam from 100 keV to 4.5 MeV. The main aim of the design is to optimize the cavity for low heat loss and high accelerating gradient. The optimized ratio of peak surface electric and magnetic field to accelerating field for cavity are $E_{pk}/E_{acc} = 2.72$ and $H_{pk}/E_{acc} = 4.11$ mT/(MV/m). The optimized Geometry factor (G) and R/Q values for this cavity are 246.7 and 306.4 ohms respectively. Here we also addressed other multiphysics issues such as Lorentz force detuning (LFD), Higher order modes (HOMs) and Multipacting. The multiphysics analysis helps to estimate the degree of these challenges. The final Lorentz detuning factor of the cavity has been reduced to 0.12 Hz/(MV/m)², HOMs of 2.18 and 2.9 GHz modes are dominating except the main mode and Multipacting phenomena is not found at 15 MV/m of accelerating gradient.

INTRODUCTION

A 450 kW, 100 mA, 4.5 MeV High-Intensity Compact Superconducting Electron Accelerator (HICSEA) is proposed by IIT Bombay as a sustainable alternative to treat wastewater. Figure 1 shows the schematic and different components of the proposed accelerator.

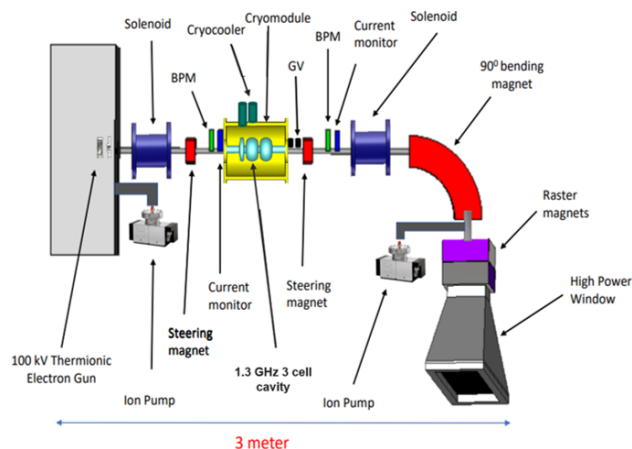


Figure 1: A Schematic figure of proposed accelerator structure.

* panku.r.k@gmail.com

This paper discusses the RF design, optimization, and multiphysics analysis of a 1.3 GHz, three-cell Superconducting RF cavity that will be used to accelerate the beam to a final energy of 4.5 MeV. The main aim is to optimize the cavity for low power loss and high energy gain while transmitting a high-intensity beam of 100 mA with minimum emittance growth and energy spread. To meet these requirements, the cavities must be tuned for low peak surface electric (E_{pk}) and magnetic (H_{pk}) fields, allowing us to raise the accelerating gradient and a high GR/Q value with a large beam pipe radius, allowing the beam to gain maximum energy and pass with minimal disruption. The simulation and optimization are done using the 3D electromagnetic simulating code CST Microwave Studio for high-frequency components.

This superconducting cavity also has certain technological hurdles that must be solved for efficient acceleration. These concerns include cavity deformation due to radiation pressure, beam instability induced by High order modes (HOMs), and multipacting of electrons through the cavity's surface. These faults are generated by the cavity's inadequate geometry optimization, resulting in increased power loss and beam instability.

Thus, a multiphysics analysis of this cavity is required to eliminate these kinds of cavity issues. The CST microwave studio is used to perform: (1) Lorentz Force Detuning (LFD), (2) HOMs analysis, and (3) Multipacting analysis. All of these simulations are performed for an accelerating gradient of 15 MV/m.

RF CAVITY DESIGN AND OPTIMIZATION

The designed cavity has three cells from which We have designed the inner and end cells individually to optimize the geometric parameters of the cavity due to the coupling of the beam tube pipe with the end cell. [1]. The second and third cells are tuned for minimum heat loss and a strong accelerating gradient which is constrained by the peak electric and magnetic fields. The power dissipation in the cavity is also influenced by the Geometry factor and the R/Q value. Therefore, both cells are tuned to reduce E_{pk}/E_{acc} and B_{pk}/E_{acc} while increasing the Geometry factor (G) and R/Q value for fundamental mode ($F = 1.3$ GHz). Both cells have a half-cell length of 5.77 cm ($L = \beta\lambda/4$), where ($\beta = 1$) is the ratio of electron velocity to light velocity, and λ is the wavelength of the fundamental mode. The iris radius of $R_i = 3.2$ cm is chosen to maximize the cell-to-cell coupling (K_{cc}) as well as R/Q. The cavity's initial cell design is critical because the electron entering the cavity has a low velocity ($v = 0.4c$ to $0.6c$). The synchronous electron must be able to see the cor-

Content from this work may be used under the terms of the CC BY 4.0 licence (© 2021). Any distribution of this work must maintain attribution to the author(s), title of the work, publisher, and DOI

SOME INTERESTING OBSERVATIONS DURING VERTICAL TEST ON ESS-HB-704 SRF CAVITIES*

K. Dumbell†, P. Smith, A. May, S. Pattalwar, A. Akintola, R. Buckley, J. Lewis, P. McIntosh, A. Wheelhouse, A. Moss, S. Hitchen, C. Jenkins, M. Ellis, M. Pendleton, S. Wilde, K. Middleman, M. Hancock, J. Hathaway, M. Lowe, D. Mason, C. Hodgkinson, P. Hornickel, G. Jones, G. Millar, J. Mutch, A. Oates and J. Wilson, STFC Daresbury Laboratory, Warrington, WA4 4AD, UK

Abstract

The vertical test stand in use at Daresbury has three cavities loaded horizontally at different heights. The jacketed cavities are supplied with liquid helium (LHe) from a header tank at the top of the configuration. A few cavities have been tested in different positions and the results have been analysed.

The pressure of the helium inside the jacketed cavities is affected by the height of the liquid helium column above the jacket. Using results from earlier analysis during cool-down enables the pressure of the cavity to be determined from the frequency of operation. Analysis of the effects may allow for corrections to the frequency to be made.

In addition, there have also been some challenges at higher power as the phase of the self-excited loop driving the system, has been seen to change.

This paper discusses some of the observations and challenges that are being addressed in the continuing use of this facility.

INTRODUCTION

High-β superconducting cavities for the European Spallation Source (ESS) are being tested in Daresbury Laboratory. The cryostat used [1] can be populated with up to three jacketed cavities that can be tested during the same run. The jacketed cavities are mounted horizontally but are stacked vertically on a Cavity Support Insert (CSI) (see Fig.1). For the accelerating gradient tests, the temperature of all cavities are assumed to be at the same superconducting temperature of 2.0 K. The pressure in the cavities will not however, be the same due to the different hydrostatic pressure as the height of liquid helium above each cavity will be different.

The separation of pairs of cavities is 0.62 m (h) and the height of the top cavity is 0.984 m below the height of the header. For the cavities the separation of 0.62 m can be used to calculate the change in the hydrostatic pressure. Assuming the density of LHe (ρ) is 146 kg/m³ at 2.0 K [2], this gives the increase in pressure (p) going down to a lower cavity:

$$p = \rho h g \tag{1}$$

where (g) is the gravitational potential.

Thus the increase in pressure going down to a lower cavity will be approximately 8.9 mbar.

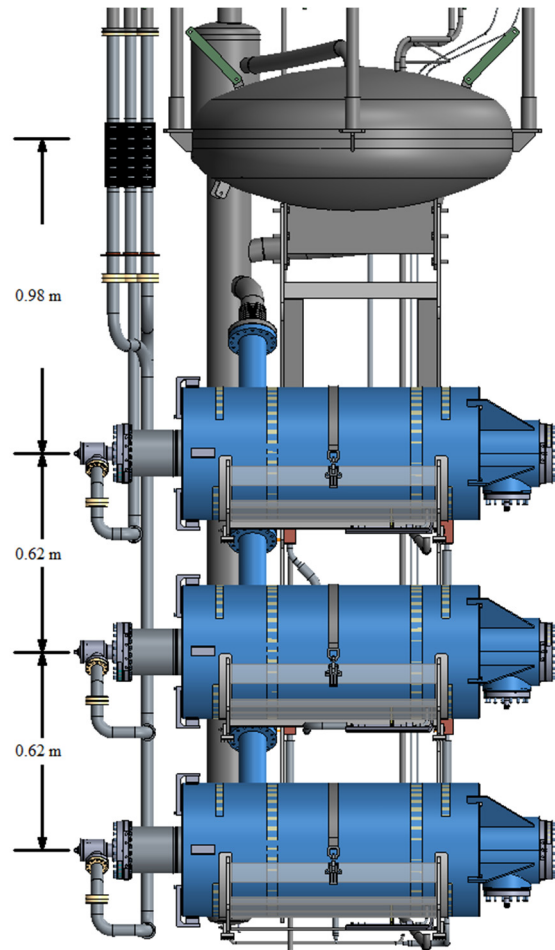


Figure 1: Arrangement of the cavities on the CSI.

During the commissioning phase of the test system there were a couple of opportunities to test the same cavity in different locations. This has yielded evidence of the effect of the pressure dependence: one cavity has been tested in all three possible locations.

As part of the specification tests the surface resistance of the cavities is measured at several temperatures between 2.0 K and 4.0 K: in practice the upper temperature is restricted by cryogenic operations depending on whether a top or bottom fill is used but the results presented here only show the results from after the LHe becomes superconducting. The resonant frequency of the fundamental mode of the cavity is measured at low power as the temperature decreases: this is achieved by pumping down on the LHe to bring the temperature down.

* Work supported by STFC
 † keith.dumbell@stfc.ac.uk

SPLIT THIN FILM SRF 6 GHz CAVITIES

T. Sian^{*1}, G. Burt¹, D. Seal¹ H. Marks, Lancaster University, Lancaster, UK
 R. Valizadeh¹, O.B. Malyshev¹, STFC Daresbury Laboratory, Warrington, UK
¹ also at Cockcroft Institute, Warrington, UK

Abstract

Radio-frequency cavities used in particle accelerators are usually manufactured from two half cells that are electron beam welded together. In this case, the weld is located across the peak surface current of the cavity. This weld can lead to large increases in surface resistance and limit the performance of thin film coated cavities. Many problems with the coating process for thin film Superconducting Radio Frequency (SRF) cavities are also due to this weld. Thin film SRF cavities can perform as well as bulk niobium cavities if the cavity is manufactured seamlessly, without any weld, as they have a more uniform surface, however, they are much more difficult and expensive to manufacture. A cavity with a longitudinal split, parallel to the direction of the electric field, would not need to be welded. These seamless cavities are easier to manufacture and coat. This opens the possibilities to coat with new materials and multilayer coatings. These cavities may allow SRF cavities to operate at significantly better parameters (higher quality factor and maximum accelerating field) than current state of the art cavities. This work discusses development and testing of longitudinally split seamless cavities at Daresbury Laboratory (DL).

INTRODUCTION

The advantages of SRF cavities are that they have a much lower surface resistance when superconducting (usually bulk niobium cavities have a surface resistance of 10^4 to 10^6 lower than bulk copper cavities [1]), which means that less heat is lost in the walls of the cavity. This leads to the fact that they can be run in continuous operation at high accelerating gradients [1–3], when the resistive losses in copper at high gradients can lead to melting of the cavity.

The main issue with using bulk super conducting cavities is that they have a lower thermal conductivity than copper cavities which can lead to localised heating and therefore, that can cause a small area of the superconductor to become normal conducting, when this happens the rest of the superconducting material quickly follows and becomes normal conducting, this is called a quench [2, 3]. The idea of coating the inside of a copper cavity with a thin film of a superconductor has been in development for many decades [2, 3]. The driving principle is that the copper cavity can provide better thermal conductivity than niobium spreading any localised heating on the superconductor to the rest of the cavity while the charge in the cavity is carried by the superconducting thin film [2, 3]. Another advantage of thin films is that materials that are too brittle to be formed into cavities, and have better superconducting properties than niobium,

can be coated onto a copper cavity and, perform just as well if not better than pure niobium. Some such materials include Nb₃Sn [4], MgB₂ [5] and V₃Si. Superconducting thin films have been used in several accelerators including PIAVE-ALPI at INFN [6] HIE-ISOLDE [7, 8], LEP [7, 9] and the LHC [7, 10].

A well known technique to manufacture RF cavities is to create two half cells and then use electron beam welding to join them. The main problem with this method of manufacture is that the weld, as it is around the area of highest magnetic field and highest surface current in the cavity which results in a higher resistance of the cavity. The weld also leads to problems with cavities coated with superconducting thin films. The cavities for HIE-ISOLDE for example found micro cracks around the weld, these cavities had a large decrease in quality factor as the accelerating gradient increased. Seamless cavities were then manufactured and coated and the Q-slope was reduced [11]. Longitudinally split SRF cavities are also currently in development at CERN, Slotted ELLiptical (SWELL) cavities are the baseline solution the Future Circular Collider (FCC). Because the welds will be in the Higher Order Mode (HOM) dampeners, they will be away from electric field of TM11 mode [12], however, SWELL cavities have not been manufactured or tested as of yet.

This work describes design, manufacture, coating and testing of seamless split niobium coated copper cavities at DL. The cavities were designed to be seamless so no weld was required and they were designed to be split so that they could be coated in an open geometry, this also allowed for easier access to the coated cavity for surface analysis.

CAVITY MANUFACTURE AND COATING

Three Oxygen Free High Conductivity (OFHC) copper cavities were designed using CST Microwave Studio. The cavities were designed to be TESLA shaped with a resonant frequency of 6 GHz. The peak electric field was simulated to be 150 MeV/m and the peak magnetic field was simulated to be 0.37 T with 1 J of stored energy. The body of the cavity was designed to be a cuboid shape to provide a simple geometry for attaching thermometers, heaters and heat links. The shape also provided a large thermal mass which aided temperature stability. At the small ends of the cavity four M6 holes were made to allow mechanically stable attachment of the antennas to the cavity to reduce microphonics from the pulsing of the cold head.

The cavities were manufactured in house at DL using a tungsten carbide milling tool. The milling tool for the initial manufacture had a 10 mm bore nose at a speed of 6000 RPM (the fastest speed it could be used). The first

^{*} taaj.sian@stfc.ac.uk

RF CHARACTERISATION OF BULK NIOBIUM AND THIN FILM COATED PLANAR SAMPLES AT 7.8 GHZ *

D. Seal^{1,2 †}, O.B. Malyshev^{2,3}, R. Valizadeh^{2,3}, T. Sian^{1,2}, H. Marks^{1,2}, O. Hryhorenko⁴,
D. Longuevergne⁴, C. Pira⁵, E. Chyhyrynets⁵, E. Marshall³, G. Burt^{1,2}

¹Engineering Department, Lancaster University, Lancaster, UK

²Cockcroft Institute, UKRI/STFC Daresbury Laboratory, Daresbury, Warrington, UK

³ASTeC, UKRI/STFC Daresbury Laboratory, Daresbury, Warrington, UK

⁴Université Paris-Saclay, CNRS/IN2P3, IJCLab, Orsay, France

⁵Legnaro National Laboratories INFN, Legnaro, Italy

Abstract

Research is ongoing into the use of superconducting thin films to replace bulk niobium for future radio frequency (RF) cavities. A key part of this research requires measuring the RF properties of candidate films. However, coating and testing thin films on full-sized cavities is both costly and time-consuming. Instead, films are typically deposited on small, flat samples and characterised using a test cavity. A cost-effective facility for testing such samples has recently been built and commissioned at Daresbury Laboratory. The facility allows for low power surface resistance measurements at a resonant frequency of 7.8 GHz, temperatures down to 4 K and sample surface magnetic fields up to 1 mT. A brief overview of this facility as well as recent results from measurements of both bulk Nb and thin film coated samples will be presented.

INTRODUCTION

For over 50 years, the overwhelming majority of superconducting radio frequency (SRF) cavities used in particle accelerators have been manufactured from bulk niobium. This material's extremely low surface resistance, R_S , means that cavities reach very high intrinsic quality factors ($Q_0 \approx 10^{10}$ - 10^{11}) at liquid helium temperatures. This also allows for continuous wave operation in order to create very stable beams with low energy spread.

However, Nb cavities are now pushing the theoretical limits in accelerating gradient, $E_{acc} \approx 55$ MV/m [1]. For example, 1.3 GHz TESLA shaped Nb cavities have recently reached $E_{acc} \geq 50$ MV/m [2]. As a result, there is a push to develop cavities using alternative superconducting materials to reach higher Q_0 and E_{acc} . These materials are typically deposited onto copper cavities as thin films tens of nanometers to a few micrometers thick. One of the main incentives for using bulk Cu instead of Nb as the substrate is the significant reduction in material and production costs. In addition, the much higher thermal conductivity of Cu allows for increased thermal stability of cavities during operation.

Ultimately, for these reasons, thin film cavities could lead to shorter, more sustainable accelerator structures.

The development of thin film SRF cavities requires 5 main areas of research: (1) substrate surface preparation, (2) thin film deposition, (3) film characterisation, (4) superconducting DC properties measurements, (5) superconducting RF evaluation. So far, the focus has been on studying the properties of thin films on small planar substrates mainly due to cost savings and ease of deposition and analysis. Results from all 5 areas of research will be used to determine which samples are most likely to perform well on a cavity-shaped geometry for further testing.

A facility for the superconducting RF evaluation has recently been commissioned [3]. The addition of this facility now allows for research and development in all 5 areas of the thin film development programme at Daresbury laboratory.

FACILITY OVERVIEW

The facility for RF testing of planar samples 90-130 mm in diameter is now in full operation [3, 4]. A diagram of the facility is shown in Fig. 1.

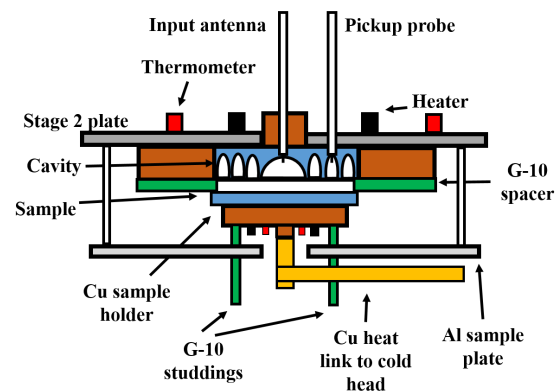


Figure 1: A schematic of the cavity and sample mounted to the stage 2 plate of the cryostat, previously reported at [3].

This facility utilises a bulk Nb half-cell cavity, first reported in [5], operating at a resonant frequency, $f_0 = 7.8$ GHz. The cavity itself is surrounded by three quarter wavelength chokes designed to contain the fundamental mode frequency within the cavity and minimise leakage. This means that no physical welding is required between the cavity and sample,

* This work has been supported by: the IFAST collaboration which has received funding from the European Union's Horizon 2020 Research and Innovation programme under Grant Agreement No 101004730.

† daniel.seal@cockcroft.ac.uk

DESIGN OF PRODUCTION PIP-II SSR1 CAVITIES *

C.Narug, M. Parise, D. Passarelli, J. Bernardini, FNAL, Batavia, IL, USA

Abstract

The testing and manufacturing process of the PIP-II Single Spoke Resonators Type 1 (SSR1) prototype jacketed cavity presented opportunities for refinement of the production series. Experience from the prototype cavity and the design of other cavities at Fermilab were used. The mechanical design of the production jacketed cavity has been modified from the prototype design to allow for improvements in overall performance, structural behavior, and manufacturability of the weld joints.

OVERVIEW

The PIP-II project has the scope to upgrade the existing Fermilab's accelerator complex to deliver the most intense high-energy beam of neutrinos for the international Deep Underground Neutrino Experiment at LBNF. It is based on a proton driver superconducting linac that composes of five different Superconducting Radio Frequency (SRF) cavity types: half wave resonator (HWR), 325 MHz single spoke resonators type 1 and type 2 (SSR1, SSR2), low-beta and high-beta 650 MHz elliptical 5-cell cavities (LB650, HB650). Significant contributions from international research institutions in India, United Kingdom, Italy, France and Poland are planned to provide expertise and capabilities in accelerator technologies to the project.

The current PIP-II beam optics design requires that each SSR1 cryomodule contains four superconducting focusing lenses (solenoids) and eight identical SSR1 cavities, where each cavity is equipped with one high-power RF coupler and one tuner. Positioned as the second cryomodule type in the linac, the two SSR1 cryomodules operate at a frequency of 325 MHz with continuous wave (CW) RF power and peak currents of 5 mA to accelerate H- beam from 10 MeV to 32 MeV.

CAVITY STRUCTURAL DESIGN

The SR1 resonator is made of two pressure vessel components, an SRF cavity and a liquid helium containment vessel. The cross sectional view of the assembly can be seen in Figure 1.

Cavity

The inner vessel of the SSR1 resonator is a superconducting cavity. This vessel is subject to external pressure exerted by the liquid helium while the inner surfaces see ultra-high vacuum. All cavity parts are formed and machined using bulk RRR (extra-pure) niobium and EB welded to each other. The system of stiffeners present on the cavities were investigated and optimized to maintain mechanical stability, acceptable response to microphonics and Helium pressure

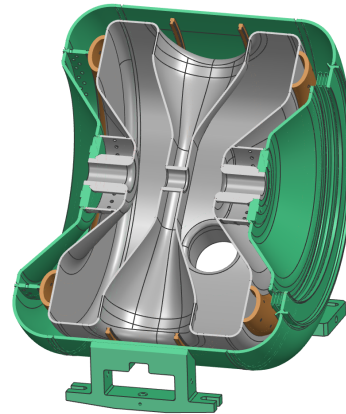


Figure 1: SSR1 Resonator Cross Sectional View

fluctuations and overall ease of tuning under operating conditions. To do this an internal niobium ring was EB welded to the cavity and flanges. The cavities are required to operate in CW regime in superfluid helium at a temperature within the range of 1.8 – 2.1K. The assembled cavity can be seen in Figure 2 and an explosion view with the components labeled can be seen in Figure 3.

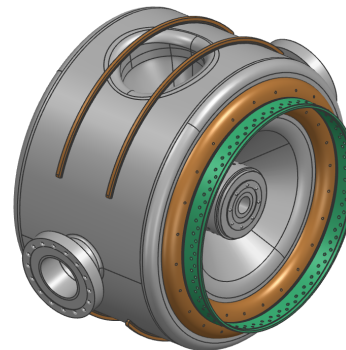


Figure 2: SSR1 Cavity

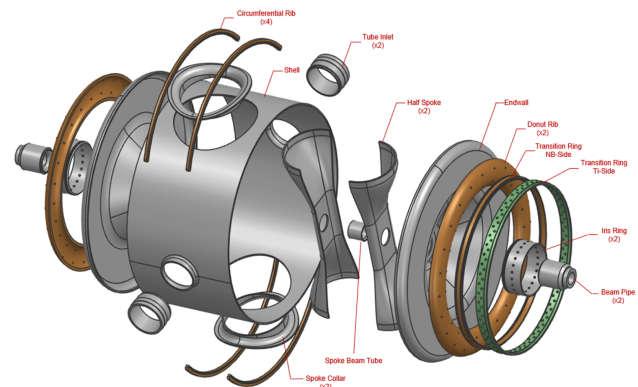


Figure 3: SSR1 Cavity Components

* Work supported by Fermi Research Alliance, CONF-22-633-PIP2-TD

MEASURING THE SEEBECK COEFFICIENT AT CRYOGENIC TEMPERATURES FOR LCLS-II-HE PROJECT

L. Shpani*, M. Ge, A. Holic, M. Liepe, J. Sears, N. Verboncoeur
Cornell Laboratory for Accelerator-Based ScienceS and Education (CLASSE),
Ithaca, NY, USA

Abstract

The Seebeck effect plays a crucial role during the cooldown procedure in SRF based accelerators, like LCLS-II at SLAC. The temperature-dependent Seebeck coefficient quantitatively measures the strength of electric potential induced by thermal gradients in metals. This effect is present in cryomodules and drives thermoelectric currents generating magnetic fields. These fields can get trapped in cavities and cause additional dissipation in RF fields. We have therefore designed and commissioned an experimental setup that does continuous measurements of the Seebeck coefficient for cryogenic temperatures ranging from 200K down to below 10K. We present results of the measurements of this coefficient for materials commonly used in cryomodules, such as niobium, titanium, niobium-titanium, silicon bronze, and stainless steel.

INTRODUCTION

LCLS-II will be the first XFEL based on 4GeV continuous-wave superconducting RF (CW-SRF) accelerator technology. The LCLS-II-HE will increase the energy of the CW-SRF to 8GeV, increasing the photon energy range from 5keV of LCLS-II to at least 13keV at 1MHz repetition rates [1].

Nitrogen-doped niobium SRF cavities with high quality factors of 2.7×10^{10} at 4K will be used. Because of the high sensitivity to RF dissipation from trapped magnetic vortices resulting from magnetic fields in cryomodules during cooldown, reducing thermoelectric currents and their resulting magnetic fields is crucial to maintain the high quality factor of the cavities [1, 2].

The Seebeck effect is a phenomenon in which a potential difference is induced between two ends of an electrical conductor when a temperature gradient is applied across it, as carriers diffuse from the hot end to the cold end of the sample [3–5]. The Seebeck coefficient is a temperature dependent material property, which is a crucial value needed to estimate these thermoelectric currents.

MEASUREMENT SETUP

The voltage difference induced induced in a metal due to a temperatre gradient can be described by

$$V = - \int_{T_1}^{T_2} S(T) dT, \quad (1)$$

where T_1 and T_2 are the temperatures of the two ends of the sample, and $S(T)$ is the temperature dependent Seebeck coefficient.

The value of the temperature-dependent Seebeck coefficient itself is the ratio of the potential difference and temperature gradient across the metal, namely

$$S_{ab}(T) = \lim_{\Delta T \rightarrow 0} \frac{\Delta V}{\Delta T}. \quad (2)$$

Measurement Method

Measurement was done using the differential method [3], using a small temperature gradient across the sample (between 1 to 5K). We simultaneously measure the temperature on each side of the sample and the induced potential difference. Figure 1 is an illustration of the Seebeck effect on two dissimilar metals with the interfaces at temperatures T_1 and T_2 ($T_1 \neq T_2$).



Figure 1: Seebeck effect for two dissimilar materials, namely the lead wires and the metal of interest, with the interfaces at temperatures T_1 and T_2 . A proportional voltage V is generated.

We can measure the potential difference across the metal of choice using lead wires shown in Fig. 1 as leads. The measured potential difference in this case is given by

$$V = - \int_{T_1}^{T_2} [S_b(T) - S_a(T)] dT, \quad (3)$$

where S_a is the Seebeck value of the metal of interest, and S_b is the Seebeck value of the Pb wires [5].

Using the known values of the Seebeck coefficient for Pb [6] we can add a correction as follows:

$$S_a(T_{ave}) = - \frac{\Delta V}{\Delta T} + S_b(T_{ave}), \quad (4)$$

where $T_{ave} = (T_1 + T_2)/2$ and $\Delta T = T_2 - T_1$.

* ls936@cornell.edu

EVALUATION OF SINGLE-CELL CAVITIES MADE OF FORGED INGOT NIOBIUM AT JEFFERSON LAB*

P. Dhakal^{1,†}, B. D. Khanal², G. Ciovati^{1,2}, G. R. Myneni^{1,3}

¹Thomas Jefferson National Accelerator Facility, Newport News, VA 23606, USA

²Department of Physics, Old Dominion University, Norfolk, VA 23529, USA

³BSCE Systems Inc., Yorktown, VA 23693, USA

Abstract

Currently, fine grain niobium (Nb) (grain size ~ 50 μm) and large grain Nb (grain size of a few cm) are being used for the fabrication of superconducting radio frequency (SRF) cavities. Medium grain forged ingot with grain size of a few hundred μm may be beneficial for cost-effectiveness as well as providing better performance for future SRF-based accelerators. Forged ingot Nb with medium grain size is a novel production method to obtain Nb discs used for the fabrication of superconducting radio frequency cavities. We have fabricated two 1.5 GHz single cell cavities made from forged Nb ingot with a residual resistivity ratio of ~ 100. The cavities were chemically and mechanically polished and heat-treated in the temperature range of 650-1000 °C before the rf test. One of the cavities reached an accelerating gradient of ~34 MV/m with a quality factor $Q_0 > 10^{10}$, while the second cavity was limited at 14 MV/m, likely due to a weld defect at the equator.

INTRODUCTION

Future accelerator projects have a high demand for high-performance and cost-effective superconducting radio frequency (SRF) cavities. SRF cavities made from fine grain (FG) (ASTM ~ 5-7) and large grain (LG) (grain size ~ cm) have been already installed in several accelerator facilities [1–3]. The production of FG niobium requires multiple steps and stringent quality assurance methods, whereas the LG niobium can be directly sliced from an ingot greatly simplifying and lowering the production cost of bulk Nb discs [4]. Even though the performance of cavities fabricated from LG Nb are comparable or better than that of cavities made from FG Nb, the accelerator community is reluctant to use LG Nb due to nonuniform mechanical properties arising from the large grains with different orientations. This feature complicates compliance with pressure vessel regulations in some countries. Twenty-four 1.5 GHz 5-cell cavities made of LG Nb have been recently built by Research Instruments GmbH, Germany, for the C75 cryomodule refurbishment program at Jefferson lab C75, with 16 of those cavities already operating in the CEBAF tunnel [3, 5].

To minimize the shape variation during the deep drawing process, while keeping the production cost low, medium grain (MG) Nb with the grain size of several mm was produced by forging and annealing a large grain billet [6]. The

process requires fewer steps than the manufacturing of FG Nb while producing more homogeneous grains with the mechanical properties required for deep drawing of half cell for SRF cavities [7]. Two 1.3 GHz single-cell cavities were fabricated at KEK using high-purity, residual resistivity ratio (RRR) > 300, MG Nb and one of them reached an accelerating gradient, E_{acc} , of 38 MV/m at 2 K [8]. Further material cost reduction could be realized with lower purity Nb, because of fewer ingot melting cycles. In this contribution we describe the fabrication, processing for two 1.5 GHz single cell cavities made of medium-purity MG Nb and present their cryogenic cryogenic rf test results for two 1.5 GHz single cell cavities made of medium-purity MG Nb. Measurements to characterize the flux expulsion as well as the rf performance with respect to annealing temperature and surface preparations were part of this study.

CAVITY FABRICATION AND SURFACE PREPARATIONS

The MG Nb cavity development at Jefferson Lab is being carried out as R&D related to the C75 CEBAF cryomodule refurbishment program [9]. Two single-cell cavities of the C75 inner cell shape and labeled C75-SC2 and C75-SC3, have been fabricated from 3 mm thick MG Nb discs of RRR ~ 100, produced by ATI Specialty Alloys, USA. The two discs used for the fabrication of C75-SC3 had been annealed by the Nb vendor at a higher temperature than those used for C75-SC2. The fabrication was done by using conventional methods of deep drawing of the Nb discs and electron beam welding of the half-cells and beam tubes. The shape deviation of the half-cells was inspected with a 3D laser scanner and ~ 63% of the points were within ±0.1 mm from the ideal shape, as shown in Fig.1. This value is consistent with what was achieved with a standard FG Nb discs, using the same dies, and it is better than those achieved using LG Nb.

After the fabrication, the cavities received ~120 μm of inner surface removal by electropolishing (EP) followed by vacuum annealing at 650 °C for 10 hours. The cavities again received 25 μm inner surface EP. Standard procedures were followed to clean the cavity surface in preparation for an rf test: degreasing in ultra-pure water with a detergent and ultrasonic agitation, high pressure rinsing with ultra-pure water, drying in the ISO 4/5 cleanroom, assembly of flanges with rf feedthroughs and pump out ports and evacuation.

After the first cryogenic rf test, the cavities were baked in-situ at 120 °C for 48 h and re-tested. Afterwards, the cav-

* This manuscript has been authored by Jefferson Science Associates, LLC under U.S. DOE Contract No. DE-AC05-06OR23177.

† dhakal@jlab.org

DESIGN OF A 1.3 GHz RF-DIPOLE CRABBING CAVITY FOR INTERNATIONAL LINEAR COLLIDER*

S. U. De Silva†, J. R. Delayen, Old Dominion University, Norfolk, VA, USA
R. Rimmer, Thomas Jefferson National Accelerator Facility, Newport News, VA, USA

Abstract

The International Liner Collider (ILC) requires crabbing systems to increase the luminosity of the colliding electron and positron bunches. There are several frequency options for the crabbing cavity. We have designed a 1.3 GHz compact 1-cell and 2-cell rf-dipole crabbing cavity to compensate for luminosity degradation due to large crossing angle. This paper presents the 1-cell and 2-cell cavities designed to meet the current specifications including the fundamental power coupler and higher order mode couplers.

INTRODUCTION

The International Liner Collider (ILC) is designed to collide electrons and positrons that are accelerated in two separate linacs spanning over 20 km as shown in Fig. 1 [1, 2]. The baseline design will operate at a center of mass (CoM) of 250 GeV colliding electrons and positrons at speed of light with an upgrade planned for CoM of 1 TeV. The expected luminosity goal is $\sim 10^{34}$ cm²sec⁻¹. The ILC requires crabbing cavities to compensate for the luminosity degradation due to the large crossing angle of 14 mrad [3]. Operation without crab cavities may lead to a luminosity reduction up to 80%.

The crabbing systems are installed on the electron beam line as shown in Fig. 2. The key specifications of the crabbing systems are following [4]:

- Total beam line space – 3.8 m
- Total transverse impedance specifications – $Z_x < 48.8$ M Ω /m and $Z_y < 61.7$ M Ω /m
- Minimum crab cavity beam aperture – 25 mm

The total transverse voltages are shown in Table 1.

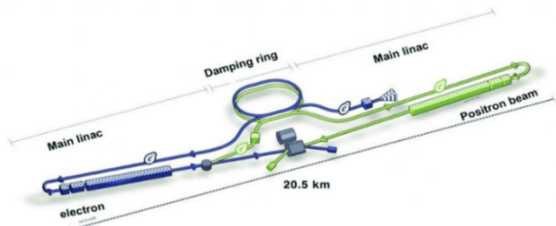


Figure 1: Layout of the Electron-Ion Collider.

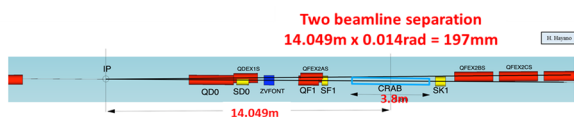


Figure 2: Beamline layout of the crabbing system.

* This research used resources of the National Energy Research Scientific Computing Center (NERSC), a U.S. Department of Energy Office of Science User Facility operated under Contract No. DE-AC02-05CH11231.

† sdesilva@jlab.org

Table 1: Total Transverse Voltages

| Beam Energy | 250 GeV | | | 1 TeV | | |
|--------------------|-----------------|-------|-------|-------|-----|-----|
| | Frequency [GHz] | 3.9 | 2.6 | 1.3 | 3.9 | 2.6 |
| Total Voltage [MV] | 0.615 | 0.923 | 1.845 | 2.5 | 3.7 | 7.4 |

The recent crabbing cavity system development for the ILC has several crabbing cavity options under study [4]. In this paper we study 1-cell and 2-cell cavity designs based on the rf-dipole design operating at 1.3 GHz [5, 6].

1.3 GHz CRABBING CAVITY DESIGNS

The 1.3 GHz rf-dipole crabbing cavity is a compact cavity design where both 1-cell and 2-cell options as shown in Fig. 3 that are viable solutions for the ILC. Both cavities are designed with a 25 mm pole separation and a 30 mm beam aperture for effective HOM extraction.

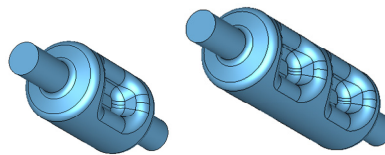


Figure 3: 1-cell (left) and 2-cell (right) 1.3 GHz rf-dipole crabbing cavities.

Table 2: RF Properties

| Property | 1-cell | 2-cell | Unit |
|----------------------------|--------------------|-------------------------------|------------|
| SOM | – | 1.198 | GHz |
| 1 st HOM | 2.142 | 2.039 | GHz |
| E_p^* | 3.83 | 3.85 | MV/m |
| B_p^* | 6.84 | 6.84 | mT |
| $[R/Q]_t (V^2/P)$ | 444.8 | 892.7 | Ω |
| G | 129.9 | 132.2 | Ω |
| $R_t R_s (V^2/P)$ | 5.78×10^5 | 1.18×10^4 | Ω^2 |
| V_t per cavity | 1.35 | 2.70 | MV |
| E_p | 44.8 | 45.0 | MV/m |
| B_p | 80.1 | 80.0 | mT |
| Cavity diameter | 100.3 | 103.4 | mm |
| Cavity length [#] | 310 | 450 | mm |
| At $E_t^* = 1.0$ MV/m | | [#] Flange to flange | |

FIELD SHIELDING OF NbTiN BASED MULTILAYER STRUCTURE FOR ACCELERATING CAVITIES*

I. H. Senevirathne[†], A. Gurevich, J. R. Delayen

Centre for Accelerator Science, Old Dominion University, Norfolk, VA 23529, USA

D. R. Beverstock¹, A.-M. Valente-Feliciano

Thomas Jefferson National Accelerator Facility, Newport News, VA 23606, USA

¹also at Applied Science Department, William & Mary, Williamsburg, VA 23185, USA

Abstract

Over the past few decades, bulk niobium (Nb) has been the material of choice for superconducting radio frequency (SRF) cavities used in particle accelerators to achieve higher accelerating gradients and lower RF losses. Multilayer (SIS) structures consisting of alternating thin layers of superconductor(S) and insulator(I) deposited on a bulk Nb have been proposed to enhance the sustained peak surface magnetic field and produce a higher accelerating gradient. In this study, multilayers based NbTiN and AlN deposited on bulk Nb are used to test the proposed enhancement using the DC magnetic Hall probe technique. The technique detects a penetrating magnetic field through the multilayer sample as it is placed under an external magnetic field produced by a magnetic coil. This work reports the characterization and measurements of the magnetic field of full flux penetration through single layers of NbTiN and bilayers of NbTiN/AlN on bulk Nb.

INTRODUCTION

Niobium (Nb) radio frequency cavities are widely used to accelerate a charged particle beam in particle accelerators. The performance of bulk Nb SRF cavities has significantly improved over the last decade and is approaching the peak magnetic field at the equatorial cavity surface close to the niobium dc superheating field $H_s \approx 240$ mT which gives the maximum accelerating field gradient to about 52 MV/m at 2 K for 1.3 GHz single cell cavities [1]. Since the best Nb cavities are already close to the fundamental limit of the material, new SRF materials with higher superheating magnetic fields than Nb are needed to reach accelerating gradients ~ 100 MV/m at 2 K or ~ 50 MV/m at 4.2 K.

The concept of multilayer structures comprised of alternating layers of superconductors and insulators fabricated on bulk Nb (Fig. 1) has been introduced as a feasible solution to overcome intrinsic material limitation in [2]. The type-II superconductor candidates with $T_c > T_c$ (Nb) and $B_{sh} > B_{sh}$ (Nb) such as Nb₃Sn [3], NbN [4], NbTiN [5], MgB₂ [6] and some Fe-based superconductors could potentially enhance the surface field at onset of vortex penetration, B_p above B_{c1} of Nb. The enhancement is achieved by depositing S layer films with thickness below its pene-

tration depth, λ to screen the bulk Nb from external magnetic field. B_{c1} of a thin film with thickness, $d \ll \lambda$, is given by

$$B_{c1} = \frac{2\phi_0}{\pi d^2} \left[\ln \frac{d}{\xi} - 0.07 \right], \quad (1)$$

where ϕ_0 is the flux quantum and ξ is the coherence length [7]. Eq. (1) shows that B_{c1} is greatly increased in the overlying superconducting layers. If a vortex penetrates at a defect in the first S layer, it can propagate into the next S layer and further in the bulk Nb triggering a thermomagnetic avalanche. An insulator layer between two superconductors provides a strong barrier for propagation of vortex to the bulk of the Nb cavity [7]. Materials such as MgO, Al₂O₃ and AlN are suitable candidates for I layers.

In this work, NbTiN and AlN based multilayers deposited on bulk Nb were studied for SRF accelerating cavity applications.

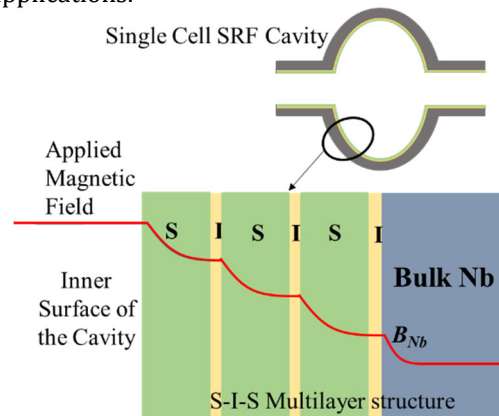


Figure 1: Superconductor (S)- Insulator (I)- Superconductor (S) multilayers to enhance the peak surface magnetic field of niobium RF cavities.

NbTiN is a suitable S layer material for SIS structures which is a B1-compound with a critical temperature of 17.8 K. It has a NaCl structure where Ti and Nb form a face centred cubic (fcc) lattice and N atoms occupy all the octahedral interstices. NbTiN adheres well with the substrate. AlN is the chosen insulator that can be grown with a wurtzite hexagonal close-packed or sphalerite B1 cubic structures. The deposition method was optimized to deposit the superconductor and insulator layers on bulk substrates and on top of each other maintaining the quality and properties of each layer and of the base substrate [8, 9]. In this work, the focus is on the magnetic field penetration measurements on NbTiN monolayers (SS' structure) and NbTiN/AlN multilayers (SIS' structure) on bulk Nb.

*Work supported by NSF Grants PHY-1734075 and PHY-1416051, and DOE Awards DE-SC0010081 and DE-SC0019399.

[†]isene001@odu.edu

MEDIUM TEMPERATURE TREATMENTS OF SUPERCONDUCTING RADIO FREQUENCY CAVITIES AT DESY*

L. Steder[†], C. Bate, H. Remde, D. Reschke, J. Schaffran, L. Trelle, H. Weise, M. Wiencek
Deutsches Elektronen-Synchrotron DESY, Germany
M. Wenskat, University of Hamburg, Germany

Abstract

Over the last years several different approaches to increase the performance of superconducting radio frequency (SRF) cavities by heat treatments have been developed and tested. At DESY, the R&D aims for cavities with enlarged quality factors while maintaining high accelerating gradients, since an envisaged upgrade of the European XFEL requires both. For this purpose, medium temperature (mid-T) treatments around 300 °C seem to be very promising. Lately, the furnace infrastructure at DESY was refurbished and now a niobium-retort furnace capable of carrying 1.3 GHz nine-cell cavities can be used for R&D studies. Vertical test results of single-cell cavities treated in this furnace at medium temperatures are presented and compared to four cavities treated similarly in a furnace at the company Zanon Research & Innovation Srl (Zanon). All mentioned cavities show enlarged quality factors but at the same time reduced gradients compared to their reference measurements before the mid-T treatment. The DESY treatments were accompanied by small niobium samples for surface analyses, which are also presented. Furthermore, the influence of post-treatment high pressure water rinsings is studied.

MEDIUM TEMPERATURE TREATMENT

Fundamental in-situ medium temperature (around 300 °C) bake studies [1] showed very high quality factors. Two studies [2, 3] applied then mid-T treatments using commercial UHV furnaces followed by subsequent cleaning and assembly steps under air. This modified process allows a possible future application for accelerator cavities. The typical cavity performance – described by quality factor Q_0 versus accelerating gradient E_{acc} ($Q(E)$) – is very similar to those of nitrogen doped cavities [4, 5], showing a rise of Q_0 culminating at an E_{acc} of about 16 MV/m, which is often called “anti-Q-slope”. It has to be investigated, whether the mid-T treatment results in similar gradient limitations like specific doping recipes [4, 6] or whether it is capable of high gradients above 30 MV/m.

TREATMENTS AT ZANON

Since the furnace infrastructure at DESY was under commissioning, in the year 2021 a cooperation with Zanon was established in order to study the effect of mid-T treatments of SRF cavities. Two sets of two 1.3 GHz single-cell cavities,

were treated for three hours at 300 °C. The first set of cavities was treated completely open in one furnace run, while the cavities of the second set were closed by DESY caps. One cavity per set was low temperature treated beforehand [7], while the other one came directly from an electropolishing (EP) procedure. All cavities were vertically tested before the furnace treatment in order to define a baseline performance.

Furnace Infrastructure at Zanon

The furnace chamber is made of stainless steel and actively water cooled, providing a usable space of $(0.6 \times 0.6 \times 1.3) \text{ m}^3$. Thermal shield layers are made of molybdenum, as well as the heaters. The temperature is controlled over three zones achieving a uniformity of $\pm 5 \text{ °C}$ using ten T-sensors, which are not placed directly on the treated cavities. A maximum operation temperature of 1250 °C is allowed and the furnace provides a starting pressure of $1 \times 10^{-8} \text{ mbar}$ at room temperature.

Results of Zanon Treatments

After the heat treatment at Zanon and a high pressure rinsing (HPR) at DESY, the vertical performance test took place. Compared to the baseline tests, all quality factors of the 2 K measurements are enhanced, while simultaneously the maximum accelerating gradient is decreased. For three of the four cavities relatively large (enhanced) residual resistances (R_{res}) in the range of 5 – 8 nΩ have been deduced, which mask the clear reduction of R_{BCS} . The only exception is cavity 1DE9, which shows by far the best result, not only in terms of R_{res} , and hence it will be discussed here in detail. The $Q(E)$ -curves before and after the mid-T treatment are shown in Fig. 1. This cavity underwent no low temperature treatment before and was closed by caps during the treatment. Some field emission was recorded in the test after the mid-T treatment. After an additional HPR, the cavity improved significantly to a $Q_{0,max}$ of 4.6×10^{10} measured at 2 K, the R_{res} is with 2 nΩ very low by DESY standards and the accelerating gradient reaches 24 MV/m.

For all of the curves shown in Fig. 1 – and elsewhere in this contribution – a test-to-test uncertainty of about 10% in E_{acc} and up to 20% in Q_0 can be assumed [8], even if it is for legible reasons not depicted. The uncertainty within curves of one single vertical test is about a factor of two lower.

Summarising the treatments at Zanon, it can be stated that relatively large R_{res} often mask the reduction of R_{BCS} . All 2 K-curves are also shown in the summary section in Fig. 4 marked by a “Z”. Caps are important for mid-T treatments in this furnace, since the two cavities treated without them, show the lowest gradients and higher R_{res} . Also, a prior

* This work was supported by the Helmholtz Association within the topic Accelerator R&D, the European XFEL R&D program, and partially by the BMBF under the research grant 05H21GURB2.

[†] lea.steder@desy.de

VERTICAL ELECTRO-POLISHING OF 704 MHz RESONATORS USING NINJA CATHODE: GRADIENT OVER 40 MV/m ACHIEVED ON SINGLE-CELL ESS CAVITY

F. Éozénou[†], M. Baudrier, E. Cenni, E. Fayette, G. Jullien, L. Maurice, C. Servouin
 Université Paris-Saclay, CEA, Département des Accélérateurs, de la Cryogénie et du Magnétisme,
 Gif-sur-Yvette, France
 Y. Ida, K. Nii, T. Yamaguchi, MGH, Hyogo-Ken, Japan
 H. Hayano, H. Ito, S. Kato, T. Kubo, H. Monjushiro, T. Saeki, KEK, Ibaraki, Japan

Abstract

CEA, KEK and Marui Galvanizing Company have been collaborating to apply the Vertical Electropolishing (VEP) process of elliptical SRF cavities to a 704.4 MHz single-cell $\beta=0.86$ ESS-type cavity, using a rotating so called and patented ‘Ninja’ cathode. First presented results were promising with a gradient of 27 MV/m achieved, without any heat treatment applied. The performance has been pushed further since. The cavity has undergone a heat treatment at 650 °C during 10 h, followed by a final VEP sequence and a baking at 120 °C during 48 hours. The achieved gradient at 2 K was 44 MV/m (power limitation), and the quality factor Q_0 exceeding 5E10 up to 10 MV/m. The superiority of VEP compared to standard ‘BCP’ chemical treatment is demonstrated and we intend now to scale the process to a 5-cell $\beta=0.86$ ESS cavity. We also intend to push further the performance by applying the “2-step baking” (75 °C and 120 °C) proposed by FNAL, which was successfully applied at CEA Saclay on 1300 MHz single-cell resonators with gradients above 50 MV/m achieved after VEP bulk treatment.

INTRODUCTION

In 2014, CEA Saclay has started studying vertical electropolishing of 704 MHz elliptical niobium cavities within Eucard project for Super Proton Linac (SPL) [1] $\beta=1$ cavity application. The involved 5-cell cavity was electropolished in a mixture made of hydrofluoric and sulphuric acids HF(40%)-H₂SO₄(96%) (volume ratio 1-9) with a fixed rod cathode and it appeared that efficient hydrogen removal was the key for a successful treatment. In fact, inefficient stirring of the acid generates topological features at the surface of the cavity, especially in upper cells, and results in a strong asymmetric removal between upper and lower half cells [2]. Furthermore, it is likely to generate so-called Q-disease [3] phenomenon, which can be efficiently cured by a heat treatment. The SPL cavity, which suffered from strong Q-disease reached 19 MV/m after heat treatment at 650 °C (test limited by field emission) [2].

In order to optimize the vertical electropolishing treatment, KEK, Marui Galvanizing Company Ltd and CEA Saclay have started a collaboration to improve the performance of 1300 MHz ILC type resonators, and more recently, 704.4 MHz ESS type elliptical resonators. The later goal is to improve the performance of ESS type cavities

routinely treated by standard ‘Buffer Chemical Polishing’ (BCP). The Marui technology involves a rotating cathode with wings nearing the surface of the cell. Extensive parameter investigation is presented in [4, 5]. A $\beta=0.86$ 704.4 MHz cavity has been purchased for the study (EH101 cavity). Bulk (200 μ m removal) VEP treatment was carried out and achieved performance was promising [6]. The experiments have been updated: the cavity was tested after heat treatments at 650 °C and 120 °C while 15 μ m were removed from the cavity (‘flash’ VEP) in between. The EH101 cavity on the VEP set-up is shown in Fig. 1.

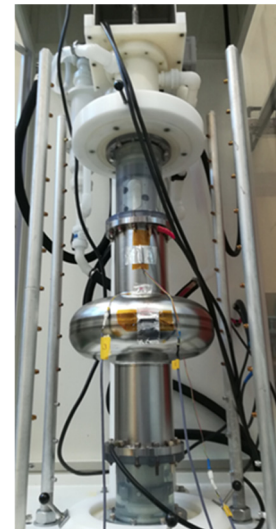


Figure 1: EH101 single-cell cavity installed on the VEP set-up.

BULK TREATMENT

The VEP set-up designed at Saclay is described in [7]. Experimental details (cavity, cathode, treatment parameters) used for the bulk treatment have been discussed in [6] and summarized in Table 1 below. The preliminary results were promising. First hints for a very efficient cavity treatment were achieved since no Q-disease was observed before any heat treatment. The corresponding RF test results are presented later in the graph in Fig. 3 which compiles all the tests carried out on the cavity. The performance achieved on the single-cell cavity before heat treatments matches ESS cavity performance specifications [8], with a gradient of 27 MV/m achieved at a Q_0 of 6E9.

MACHINE LEARNING FOR BEAM ORBIT CORRECTION AT KOMAC ACCELERATOR

Dong-Hwan Kim[†], Seung-Hyun Lee, Jeong-Jeung Dang, Hyeok-Jung Kwon, Sang-Phil Yoon, Han-Sung Kim, Korea Multi-Purpose Accelerator Complex-KAERI, Gyeongju, South Korea

Abstract

There are approaches to apply machine learning (ML) techniques to efficiently operate and optimize particle accelerators. Deep neural networks-based model is applied to experiments, correcting beam orbit through the low energy beam transport at the proton injector test stand. For more complex applications, time-series analysis model is studied to predict beam orbit in the 100-MeV beamline at KOMAC. This paper describes experimental data to train neural networks model, and presents the performance of the machine learning models.

INTRODUCTION

Korea Multi-purpose Accelerator Complex (KOMAC) has been providing 100-MeV proton beams to users since 2013 [1,2]. In order to make facility operation more stable and reduce the time required for beam tuning, an automatic scan program has been developed and utilized. However, it is not a systematic method due to lack of linkage between data and physics model. Advanced control techniques are applied only to specific areas such as feedback control to compensate for transient beam loading in low level RF systems [3].

Machine learning, which has recently been in the spotlight again with the rapid increase in computing power and the development of new algorithms, is showing various applications and good results in the field of accelerator control [4,5]. In the low energy beam transport (LEBT) section of high-power linear accelerator like KOMAC, beam orbit correction is important for beam matching with the subsequent RFQ to minimize beam loss. MYRHA and IPHI develops neural networks algorithm for LEBT tuning of proton injectors. The collimator position and vacuum pressure were set as input nodes, and the output nodes were trained on beam transmission data [6].

In KOMAC, there was a previous study verifying the practicality of a machine learning model trained with beam dynamics simulation data in LEBT. The model made with more than 700,000 computational data showed a similar level of accuracy while running more than 10 times faster than the traditional simplex algorithm [7]. Here, this study shows the results of developing a trained neural networks model which performs beam orbit correction based on beam measurement data so that beam control can be automated and advanced.

In addition, we present a preliminary study to develop an effective machine learning model in medium or high energy beam transport with more complexity. To overcome the finite number of beam diagnostics and beam correctors,

time series analysis is applied to the transverse dynamics of a bunched beam with time-sequence. It shows the results of applying the long short term memory (LSTM) model and a transformer model.

METHOD

Beam dynamics simulation and beam experiments are carried out to develop deep neural networks model for beam orbit correction at the proton injector test stand and time-series analysis model for beam orbit prediction at the KOMAC.

Deep Neural Networks Model for Beam Orbit Correction at the KOMAC Proton Injector Test Stand

Beam orbit correction has been studied in proton injector test stand at the KOMAC by developing deep neural network model. Proton injector has very simple structure to adapt machine learning model with just a few number of control variables and measured beam parameters as shown in Fig. 1.

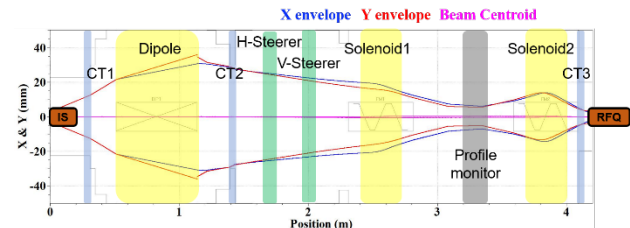


Figure 1: Layout and calculated beam dynamics of proton injector test stand at the KOMAC.

Low energy beamline consists of three focusing magnets including a dipole and two solenoids and two steering magnets. Transverse beam profiles are measured at the beam profile monitor installed at the diagnostics chamber located between two solenoids.

The initial beam properties change according to the operating parameters of the ion source, which affects the beam dynamics in the low energy beamline. As demonstrated in Fig. 2, we collect beam experimental data and train deep neural networks to make low energy beam orbit correction model for various operating variables.

Adjustable variables include absorbed power and ion source solenoid strength in microwave ion source part, and magnetic field strengths of dipole, solenoid#1, horizontal steerer, and vertical steerer magnets in the low energy beamline. As shown in Fig. 2(b), the neural networks

[†] one@kaeri.re.kr

DESIGN AND OPTIMIZATION OF A 1.3 GHZ GRIDDED THERMIONIC ELECTRON GUN FOR HIGH-INTENSITY COMPACT SUPERCONDUCTING ELECTRON ACCELERATOR (HICSEA) *

A. B. Kavar[†], A. Pathak, R. Varma Indian Institute of Technology Bombay, Mumbai, India

Abstract

The design and optimization of the proposed 1.3 GHz gridded thermionic electron gun aims to drive a conduction cooled superconducting electron accelerator that will be used to treat contaminants of emerging concern in water bodies. The gun geometry is Pierce-type and optimized for beam current of 1A with LaB_6 as cathode material at cathode potential of -100 kV. The final optimized cathode radius and angle of inclination of the focusing electrode are found to be 1.5 mm, and 77° respectively. For an emittance compensation electrode, the optimized values for thickness and potential are 2 mm and -50 kV respectively, and separation between cathode and compensator is 8 mm. Beam dynamics calculations have been performed with self-developed particle tracking code that assumes space charge interactions and imported fields. The beam dynamics simulations show that with an initial pulse length of 50 ps having a bunch charge of 5 pC, the pulse length of the bunch reduces to 33 ps. The diameter, transverse and longitudinal emittance obtained are 2.8 mm, 1 mm-mrad, and 5 mm-mrad respectively.

INTRODUCTION

Our aim (IIT Bombay in collaboration with Tohoku, KEK, Hiroshima, Waseda, Nihon, Osaka university, Japan) is to design and develop a compact, high intensity superconducting electron accelerator which will provide beam energy of 1 MeV and beam current of 100 mA for wastewater treatment. The preliminary stage of the project demands a start to end physics design that include, (a) design and optimization of a thermionic electron gun, (b) transport channel, and (c) a single cell, superconducting tesla cavity as shown in Fig. 1.

With an objective of delivering a high intensity electron beam, a thermionic electron gun is designed and optimized. In this gun, a gridded cathode [1] with RF and DC bias signals is used to produce electron bunches with high repetition rate. Such bunching mechanism makes the linac compact and portable. The major disadvantage of this method is the significant increase in beam emittance due to the presence of the grid. The design and optimization of such a gridded gun and the beam dynamics are the main emphasis of this paper. Our preliminary beam dynamics simulations with codes like CST demonstrate a significant dependence of beam parameters on mesh density and therefore we chose to develop our own beam dynamics code for reliable results with shorter computation time using PIC [2] algorithm. This paper thus also focuses on the discrepancies in the results obtained

* Work supported by Prime Minister's Fellowship by SERB-FICCI, Government of India.

[†] anjalikavar5454@gmail.com

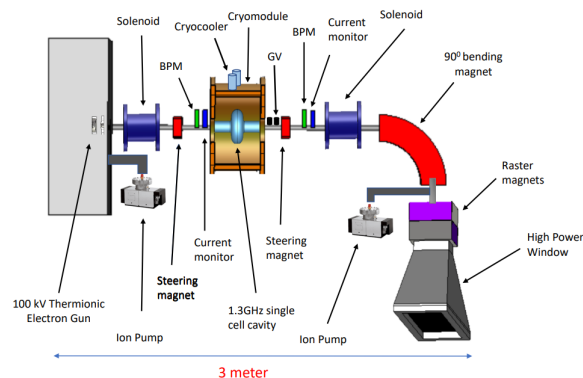


Figure 1: Schematic of proposed high-intensity, compact super-conducting linear electron accelerator.

using CST and compares it with our own particle tracking code.

GUN GEOMETRY

Thermionic electron gun designed here is configured by cathode, anode, Wehnelt and focusing electrode. The geometry of these electrodes is optimized for good beam quality and high beam current (1A) where the quality of the beam is assessed by measuring the RMS normalized emittance. Optimization to minimise the emittance is performed by varying: (a) Cathode radius, (b) angle of inclination of focusing electrode, (c) cathode-wehnelt gap, (d) Wehnelt thickness, and (e) Wehnelt voltage.

Cathode and Cathode Assembly

Our calculations suggests that the electron emission capacity of LaB_6 is better than tungsten and CeB_6 at same temperature as shown in Fig. 2.; therefore, LaB_6 is chosen as a cathode material for our electron gun. LaB_6 also has a low thermionic work function (2.66 eV) and a high melting point (2715°C), in addition to it's long life and lower sensitivity towards air exposure than typical dispenser cathodes [3].

Initially, the focusing electrode's angle is tuned for lower emittance. Figure 3 (a) depicts the results of simulations for angle of inclination of focusing electrode. It demonstrates that with the angle of inclination of 77° , emittance is reduced to 3.75 mm-mrad. The cathode radius was optimised with 77° of inclination angle as shown in Fig. 3(b). It has been observed that at 1.5 mm of cathode radius, the emittance is decreased to 2.52 mm-mrad. As a result, cathode radius of 1.5 mm and inclination angle of 77° was considered for further optimizations.

OPERATION OF THE CLARA LINEAR ACCELERATOR INJECTOR WITH 2.5 CELL 10 Hz PHOTOCATHODE GUN WITH INTERCHANGEABLE PHOTOCATHODES

B.L. Militsyn[†], D. Angal-Kalinin, A.R. Bainbridge, R.J. Cash, L.S. Cowie, B.D. Fell, A.J. Gilfellon¹, F. Jackson, T.J. Jones, N.Y. Joshi, K.J. Middleman, K.T. Morrow, M.D. Roper, T.C.Q. Noakes, R. Valizadeh, A.J. Vick, D.A. Walsh
 STFC Daresbury Laboratory, Warrington, UK
¹also at University of Lancaster, Lancaster, UK

Abstract

During the commissioning and operation run in 2021-2022 the photoinjector of the CLARA facility, a 2.5 cell cavity S-band photocathode gun originally developed for the ALPHA-X experiment [1] was used. The copper back wall of the cavity served as the gun photocathode during operation until 2019. In order to reduce the significant time required for replacement and/or reactivation of the photocathode, and to improve the flexibility of the injector the gun has been upgraded for operation with DESY/INFN style interchangeable photocathodes. This upgrade included a new design of the cavity back wall to accommodate the photocathode socket and equipping the gun with a load-lock system. Modification of the gun also required replacement of the bucking coil, which zeros field in the photocathode emission plane. After the upgrade, the gun was commissioned and then operated with a hybrid Cu/Mo photocathode during the last two years. During the winter 2021 - spring 2022 experimental run, the gun steadily operated with a cathode field of 60-70 MV/m (limited by the available RF power) and with an off-centre diamond turned photocathode which delivered stable bunches with a charge of 100 pC.

INTRODUCTION

Compact Linear Accelerator for Research and Application (CLARA) [2] is an S-band RF electron accelerator which is under development at STFC Daresbury Laboratory. Phase I of the machine is now in operation and delivers 35 MeV/c electron bunches with a charge of 100 pC at a repetition rate of 10 Hz. In 2019 the photoinjector of CLARA was upgraded for operation with interchangeable photocathodes with a final goal to improve beam quality, increase duty factor, reduce the dark current and eventually allow for operation with different type of photocathodes including high quantum efficiency Cs₂Te. This paper gives overview of the injector upgrade and its performance during the recent user run. The performance of the whole machine and achieved beam parameters are described in [3].

UPGRADE OF THE CLARA INJECTOR

The injector upgrade included three main tasks: the re-design of the cavity back wall to equip it with a photocathode socket, construction of a photocathode load-lock system and replacement of the bucking coil. In addition, de-

sign of the cavity cooling jacket was revised to improve thermal contact of the cavity with the jacket. Final scheme of the upgraded injector is shown in Fig. 1.

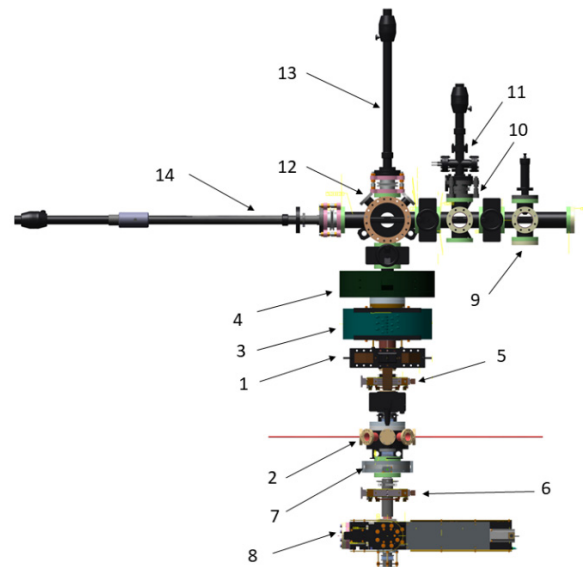


Figure 1: Layout of the CLARA photoinjector upgrade (top view). 1-photocathode gun, 2-light box, 3-main focusing solenoid, 4-bucking coil, 5, 6 H-V steering coils, 7-Wall Current Monitor, 8-YAG beam viewer-collimator, 9-photocathode transport vessel, 10- heating chamber, 11-heating stage, 12-interchange chamber, 13, 14-magnetic manipulators.

The original design of the gun, with a replaceable cavity back wall which also served as a photocathode, allowed the upgrade to be implemented without significant intervention into original construction. The cavity back wall, which was just bolted to the first cell, was redesigned and equipped with a photocathode socket. Special attention was paid to profile of the photocathode socket rim. Its elliptical profile was optimised to prevent surface field excess which may be potential source of field emission. RF contact between the photocathode and the socket is provided by a gold coated spring. The back wall has been diamond turned from oxygen free copper with final roughness of about 10 nm. A detailed description of the RF design and RF commissioning of the upgrade is described in [4].

[†] boris.militsyn@stfc.ac.uk

MACHINE LEARNING FOR RF BREAKDOWN DETECTION AT CLARA

A. E. Pollard*, A. J. Gilfellon¹, D. J. Dunning
 ASTeC, Cockcroft Institute, STFC Daresbury Laboratory, Warrington, UK
¹also at The University of Manchester, Manchester, UK

Abstract

Maximising the accelerating gradient of RF structures is fundamental to improving accelerator facility performance and cost-effectiveness. Structures must be subjected to a conditioning process before operational use, in which the gradient is gradually increased up to the operating value. A limiting effect during this process is breakdown or vacuum arcing, which can cause damage that limits the ultimate operating gradient. Techniques to efficiently condition the cavities while minimising the number of breakdowns are therefore important. In this paper, machine learning techniques are applied to detect breakdown events in RF pulse traces by approaching the problem as anomaly detection, using a variational autoencoder. This process detects deviations from normal operation and classifies them with near perfect accuracy. Offline data from various sources has been used to develop the techniques, which we aim to test at the CLARA facility at Daresbury Laboratory. Deployment of the machine learning system on the high repetition rate gun upgrade at CLARA has begun.

INTRODUCTION

There are two main aims with this project. Firstly, we aim to assemble a machine learning (ML) based system that could be used to replace the current mask method of radio frequency (RF) breakdown (BD) detection which is standard in the automated code used in the RF conditioning of accelerating cavities at CLARA[1]. Secondly, we aim to ensure that the mid-process features of the same mechanism could be used as inputs for an ML algorithm designed to predict whether or not the next RF pulse would lead to a BD.

To this end, we constructed a β convolutional variational autoencoder (β CVAE)[2] with RF conditioning data as inputs. After being trained as an anomaly detector this acted as a live BD detector, in conjunction with a dense neural network (NN), which would act with the capacity to replace the current non-ML based BD detection system. In addition to this, the β CVAE's latent space could act as a viable input for a long short-term memory (LSTM) recurrent neural network (RNN) that could be used to predict BDs, based on the methodology set out by Kates-Harbeck et al.[3] who had success in predicting disruptive instabilities in controlled fusion plasmas.

For this investigation, we used data from the CLARA accelerator (Compact Linear Accelerator for Research and Applications) based at Daresbury Laboratory. CLARA is a dedicated accelerator test facility with the capacity to deliver high quality electron beams for industry and research. In

addition to the CLARA data, a larger dataset was provided by the CLIC team at CERN covering a cavity test which took place in CERN's XBOX-2 test stand. The structure tested in this dataset was a T24 high-gradient prototype X-band cavity produced at the Paul Scherrer Institute; further details of this design have been reported previously [4, 5]. The CLARA data was collected as part of the routine RF breakdown detection system.

RELATED WORK

Solopova et al.'s [6] application of a decision tree model to assign both a fault type and cavity-specific location to a collected breakdown signal at CEBAF represents the first foray into using machine learning to classify RF cavity faults. This work was then continued in Tennant et al.[7] where the authors applied a random forest model to the classification of faults and cavity identity for a larger dataset of breakdown events.

Obermair et al. [8] took the first step towards machine learning based detection and prediction of breakdowns. The authors separately applied deep learning on two available data types (event and trend data) to predict breakdowns. In so doing, they were able to predict breakdowns 20 ms in advance with good accuracy. In addition, they utilised explainable AI on these models to elucidate the physics of a breakdown. This pointed them towards an increased pressure in the vacuum system before a breakdown, which they indicated as an option for an improved interlocking system. Their analysis of event data alone also reveals the possibility to predict breakdowns with good accuracy, if there has already been a breakdown in the previous minute, i.e. prediction of follow-up breakdowns.

Previous work within our organisation also informed the present studies. Another dataset from XBOX cavity testing was analysed for missed breakdowns using principal component analysis and neural networks [9]. Very high classification accuracy was reported, but there was suspected duplication of traces in the dataset.

METHODOLOGY

CLARA

Here we use data gathered during the RF conditioning of CLARA's 10 Hz photoinjector (Gun-10), which includes both the RF pulse traces themselves and other non-RF, such as the temperature and pressure inside Gun-10. The RF trace data was gathered before ML was taken into consideration and was therefore not ideal for our purposes, but it was deemed to be sufficient for progress to be made. The trace data was only recorded when the RF breakdown detector was

* amelia.pollard@stfc.ac.uk

HSMDIS PERFORMANCE ON THE ESS ION SOURCE

L. Neri[†], L. Celona, S. Gammino, O. Leonardi, G. Castro, A. Miraglia, INFN-LNS, Catania, Italy
F. Grespan, M. Comunian, L. Bellan, C. Baltador, INFN-LNL, Legnaro, Italy
B. Jones, E. Laface, A. Gacia Sosa, Ryoichi Miyamoto, ESS, Lund, Sweden

Abstract

The ESS ion source, developed at INFN-LNS and installed at the ESS facility, is fully working and in operation for the linac beam commissioning. The commissioning of the source was done in Catania and in Lund showing high reproducibility related to the beam diagnostic parameters that can be measured with the subset of equipment currently available in Lund. The analysis of the data collected during the commissioning in Catania discloses the possibility to use a new source configuration named High Stability Microwave Discharge Ion Source (HSMDIS), able to improve beam stability and lower beam emittance. This paper shows the capability to increase the beam current intensity, with preserving beam stability, by changing only the microwave power. Linearity was tested from 10 to 120 mA of the total extracted beam current. In addition to the nominal beam current, we can provide the lower values needed for the different phases of the accelerator commissioning and higher values for future accelerator development. The source stability is evaluated through intra-pulse stability and pulse-to-pulse stability.

INTRODUCTION

The project to build and commission the ESS accelerator to provide user beam in 2025 is progressing well. In particular, the Normal Conducting Linac (NCL) has been installed, RF conditioned and commissioned with full peak current beam up to the first DTL tank. A shutdown period has now started to allow the installation of three additional DTL tanks and a Faraday cup. RF conditioning activities of tanks 2, 3 and 4 will begin in early 2023 and further beam commissioning soon after. At the end of that phase, the temporary shielding wall in the tunnel will be removed to allow the installation of DTL5 and connection to the Super-Conducting Linac.

High Stability Microwave Discharge Ion Source

The commissioning of the high-intensity Proton Source [1, 2] developed by INFN-LNS, as an Italian In-kind contribution to the construction of the European Spallation Source, named PS-ESS [3], was accomplished at LNS in Catania [4-6]. Besides verifying the satisfaction of all ESS [7] accelerator beam requirements, a new magnetic field configuration [8] was discovered to be able to produce higher stability and lower beam emittance compared to the standard MDIS magnetic configuration. One of the key features that enabled the discovery was the development of a high-level control system [9] that make us able to test several thousands of source configurations. Our group is active in plasma and ECR ion source simulation since 2010

[†]neri@lns.infn.it

[10, 11]. Preliminary plasma simulations published in [8], and further ongoing simulations, show that the plasma heating schema and plasma dynamics change drastically between standard MDIS magnetic configuration and new one. For those reasons, we named this new mode of operation High Stability Microwave Discharge Ion Source (HSMDIS).

BEAM CURRENT CONTROL

Several sets of beam parameters, called beam modes, are defined to be used during the beam commissioning and general tuning of the ESS linac. These modes consist of various combination of beam current, pulse length and repetition rate to limit beam power for different stages of operation.

The probe mode is the lowest power beam, mainly for initial checks of the system and hardware and beam threading, the process to correct the trajectory and deliver the beam to the designated beam stop. In this mode, peak beam current must be reduced to 6 mA.

Six Blade Iris

After the first LEBT [12] solenoid, a six-blade movable collimator, named “iris”, was inserted to be able to reduce the amount of transmitted current. The mechanics and the control system enable the choice of the hole aperture diameter from 6 mm to 75 mm. It is also possible to change the relative position of the aperture with respect LEBT geometrical axis, in a few millimetres range, depending on the selected aperture size. The transmitted beam is measured by a Faraday cup located in the diagnostic tank. The beam intensity modulation measurement, done at ESS and shown in Fig. 1, revealed that the transmitted beam did not preserve the pulse shape of the beam coming out from the source. For the largest and the smallest diameters, the flatness of the flat-top beam pulse satisfies ESS accelerator requirements, while for most of the aperture sizes the beam pulse shows a decreasing trend. This can be ascribed to an accumulation of secondary electrons generated by the beam stopped by the iris blades. This additional space charge changes the beam space charge compensation configuration and produces a reduction of the transmitted beam proportional to the accumulated distortion. There can be a second hypothesis that can explain the observed behaviour, but the time-dependent emittance measurement performed during the LNS commissioning proves that cannot be ascribed to the observed phenomena. If the radial density distribution of the beam change during the pulse duration, we can have a non-flat time behaviour selecting only the beam inside a certain radius. Time-resolve emittance measurement showed that after one millisecond the

STATUS AND CHALLENGES AT TRIUMF ISAC FACILITY*

Z. Yao[†], Z. Ang, T. Au, K. Fong, X. Fu, J.J. Keir, P. Kolb, D. Lang, R.E. Laxdal, R. Leewe, Y. Ma, B. Matheson, R.S. Sekhon, B.S. Waraich, Q. Zheng, V. Zvyagintsev, TRIUMF, Vancouver, Canada

Abstract

The ISAC facility uses the ISOL technique to produce radioactive ions for experiments. The post-accelerator consists of a room temperature linac (ISAC-I) and a superconducting linac (ISAC-II). After more than two decades of beam delivery in ISAC, the RF systems have met various challenges regarding increased operation requirements, system stability issues and performance improvements. This paper discusses the detailed challenges in recent years in both ISAC-I and ISAC-II. The upgrade plan or mitigation solution to address each challenge is reported respectively. A hint of the long-term vision at ISAC is also briefly described at the end of the paper.

INTRODUCTION

The Isotope Separator and ACcelerator (ISAC) at TRIUMF (see Fig. 1) uses the Isotope Separation On-Line (ISOL) technique to produce rare-isotope beams (RIB) for studies in astrophysics, nuclear structure and reactions, electroweak interactions and material science [1]. RIB production consists of a 500 MeV cyclotron producing a proton driver beam of up to 100 μ A onto one of two thick production targets, an on-line ion source and a mass-separator. The radioactive ions are accelerated in a chain of linear accelerators (linac) consisting of a room temperature RFQ and DTL to an energy of 1.5 MeV/u and a superconducting linac that adds a further 40 MV to the beam for nuclear physics investigations near the Coulomb barrier.

The ARIEL project [1] is a new RIB production facility at TRIUMF under construction. An additional 100 μ A proton beam will be extracted from the main cyclotron and delivered to the 50 kW proton target of ARIEL. A new 1.3 GHz electron linac (e-Linac) will provide a 30 MeV electron beam with the average beam power up to 100 kW to the other electron converter target in the same target hall. The two ARIEL targets will add two RIBs and triple the RIB availability by delivering three simultaneous beams to ISAC. The e-Linac recently achieved 10 kW average beam power to a high power beam dump at the beam energy of 30 MeV during beam commissioning.

ISAC-I CHALLENGES

ISAC-I is the room temperature linac for RIB acceleration. It consists of 18 continuous-wave (CW) RF systems, with operating frequency ranges from 5.89 MHz to 106.08 MHz and RF power specified up to 90 kW. The first accelerator in ISAC-I is a 35.36 MHz split-ring, four-vane Radio Frequency Quadrupole (RFQ), designed without a gentle buncher or buncher section. The RFQ focusses and accelerates RIB from 2.04 keV/u ($\beta = 0.0021$) to 153 keV/u with a mass-to-charge ratio of $A/q \leq 30$ [2]. A post-stripper, 106.08 MHz variable energy drift tube linac (DTL) accelerates ions of $3 \leq A/q \leq 6$ to a final energy from 0.15 MeV/u to 1.53 MeV/u. The DTL structure has been configured as a separated function DTL [3]. Five independently phased IH tanks operating at $\phi_s = 0^\circ$ provide the main acceleration. Longitudinal focussing is provided by independently phased, triple gap, split-ring resonator structures positioned before the second, third and fourth IH tanks. Quadrupole triplets placed after each IH tank maintain transverse focussing. The ISAC-I linac has been accelerating RIBs and stable beams for experiments since 2000.

RF Amplifier

The demand of the accelerated RIBs at ISAC has been growing over the years. Manual re-phasing by operators is required to accommodate daily changes in energy and isotope species. Beam tuning is accomplished by turning off all RF systems and then setting up the amplitude and the phase of each RF system in the sequence from the upstream to the downstream. To minimize the re-phasing time, RF systems are required to ramp up from the 'OFF' state to the high-power state and to stabilize in the operating regime in a short time.

The tube amplifiers intrinsically require time for warmup and stabilization as the tube and RF circuits are heated by RF power. ISAC-I tube amplifiers have been in operation for over 20 years. The aged matching circuit in the tetrode tube amplifiers extends the warmup process, which challenges the beam delivery requirements. Blowing warm air was applied to pre-warm the matching circuit

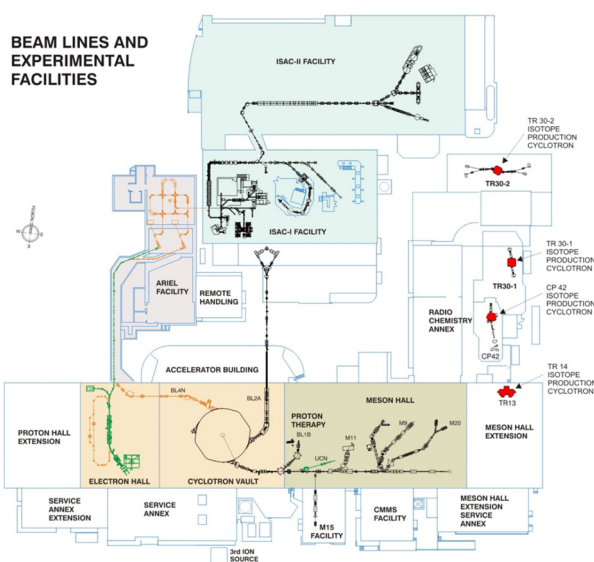


Figure 1: TRIUMF accelerator complex.

*TRIUMF receives funding via a contribution through the National Research Council Canada

[†]zyyao@triumf.ca

SARAF COMMISSIONING: INJECTOR, MEBT AND CHOPPER

A. Chance, D. Chirpaz, D. Darde, G. Desmarchelier, R. Duperrier, J. Dumas[†],
G. Ferrand, A. Gaget, F. Gohier, F. Gougnaud, T. Joannem, V. Nadot,
N. Pichoff, F. Senee, C. Simon, N. Solenne, D. Uriot, L. Zhao,

Commissariat à l'énergie atomique et aux énergies alternatives, Gif-Sur-Yvette, France
S. Cohen, I. Gertz, N. Goldberger, H. Isakov, B. Kaizer, A. Kreisel, Y. Luner, I. Mardor, H. Paami,
A. Perry, I. Polikarpov, E. Reinfeld, J. Rodnitsky, I. Shmueli, A. Shor, Y. Solomon, N. Tamim,
R. Weiss-Babai, L. Weissman, T. Zchut, Soreq Nuclear Research Center, Yavne, Israel

Abstract

IAEC/SNRC (Israel) is constructing an accelerator facility, SARAF, for neutron production. It is based on a linac accelerating 5 mA CW deuteron and proton beam up to 40 MeV. As a first phase, IAEC constructed and operated a linac (SARAF Phase I), from which remains an ECR ion source, a Low-Energy Beam Transport (LEBT) line and a 4-rod RFQ. Since 2015, IAEC and CEA (France) are collaborating in the second phase, consisting in manufacturing of the linac (Fig. 1). The injector control-system has been recently updated and the Medium Energy Beam Transport (MEBT) line has been installed and integrated to the infrastructure. It has been partially commissioned during the first semester of 2022. This paper presents the results of the integration, tests and commissioning of the injector and MEBT, before delivery of the cryomodules.

INTRODUCTION

The Medium Energy Beam Transport (MEBT) is about 5 m long and includes 3 rebunchers and 8 quadrupoles. Each quadrupole was equipped with a steerer for orbit correction. The main objectives of this MEBT are to:

- adapt the beam coming from the RFQ to the Linac,
- clean transverse halo if necessary: possibilities to add 3 sets of slits and a chopper,
- minimize the residual gas going to the Superconducting Linac (SCL), and
- measure the beam characteristics: current, position, phase, energy, transverse and longitudinal profiles and emittances.

The MEBT was first assembled and preliminary tests were conducted at CEA Saclay mostly during the first semester of 2020. A dedicated test stand was built for checking alignment, vacuum, cooling, power supplies and the associated control systems. The MEBT arrived in Israel in August of 2020, to be installed and integrated by SNRC teams in its final position between the RFQ and a D-plate already used during Phase I [1] for the purpose of the MEBT commissioning. Two periods of commissioning with beam at SNRC were scheduled in Dec. 2021, and from May-December 2022 in parallel with other activities.

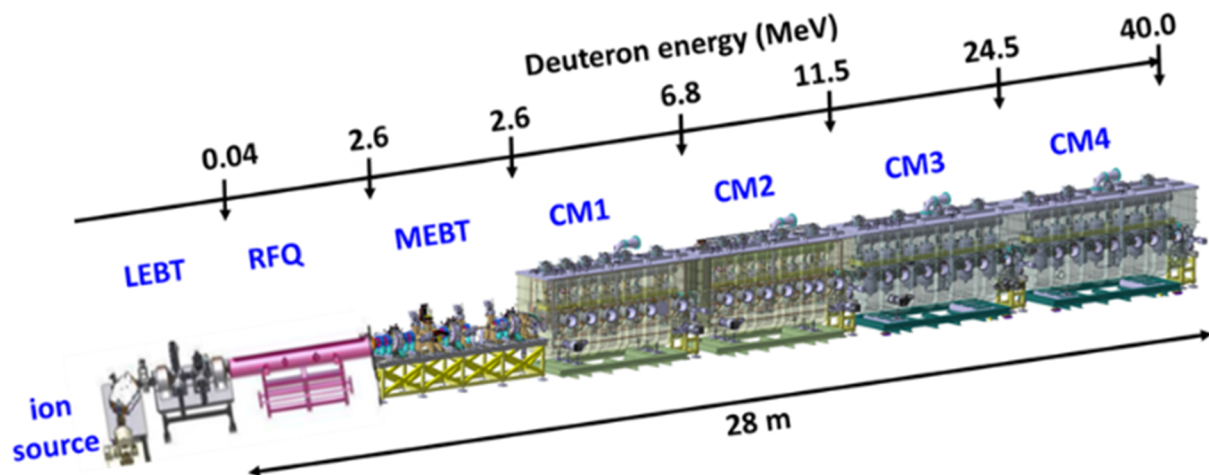


Figure 1: SARAF-LINAC.

[†] jonathan.dumas@cea.fr

DESIGN CONSIDERATIONS FOR A PROTON LINAC FOR A COMPACT ACCELERATOR BASED NEUTRON SOURCE

M. Abbaslou*, A. Gottberg, O. Kester, R.E. Laxdal†, D. Maharaj, M. Marchetto
 TRIUMF, Vancouver, BC Canada

S. Tabbassum, Purdue University, West Lafayette, Indiana, USA

D. Marquardt, University of Windsor, Windsor, ON Canada

Abstract

New neutron sources are needed both for Canada and internationally as access to reactor-based neutrons shrinks. Compact Accelerator-based Neutron Sources (CANS) offer the possibility of an intense source of pulsed neutrons with a capital cost significantly lower than spallation sources. In an effort to close the neutron gap in Canada, a prototype Canadian compact accelerator-based neutron source (PC-CANS) is proposed for installation at the University of Windsor. The PC-CANS is envisaged to serve two neutron science instruments, a boron neutron capture therapy (BNCT) station and a beamline for fluorine-18 radioisotope production for positron emission tomography (PET). To serve these diverse applications of neutron beams, a linear accelerator solution is selected, that will provide 10 MeV protons with a peak current of 20 mA within a 5% duty cycle. The accelerator is based on an RFQ and DTL with a post-DTL pulsed kicker system to simultaneously deliver macro-pulses to each end-station. Several choices of linac technology are being considered and a comparison of the choices will be presented.

INTRODUCTION

A Canadian consortium of neutron users, BNCT researchers and technical experts is proposing a compact accelerator-based neutron source (CANS) that would be hosted at the University of Windsor. The PC-CANS (prototype Canadian CANS) is a relatively low-cost facility that would serve the local community of neutron users, allow the development of BNCT in Canada and supply 18F for PET at the University of Windsor hospital. It is envisaged that the PC-CANS could serve as a model to set up other similar CANS facilities across Canada and serve as a technical development centre towards a more powerful facility, C-CANS (Canadian CANS) that would be a national-scale facility and could be located elsewhere. A schematic of PC-CANS is shown in Fig. 1. Briefly, it consists of a proton linear accelerator with a peak intensity of 10 mA at 5% duty factor (0.5 mA average current) to 10 MeV for a peak/average beam power of 100/5 kW. For neutron time-of-flight (TOF) considerations, repetition rates are in the range from 20 Hz to 200 Hz. For upgrade potential and engineering margin the linac is designed for a peak intensity of 20 mA. The beam intensity limitation is chiefly

due to present target technology that is foreseen to be developed in a staged way. In Stage 1, and assuming the addition of a pulsed switchyard, the 10 MeV beam is shared between three end-users delivering simultaneously 2 kW average power to the neutron Target-Moderator-Reflector (TMR) and BNCT stations with 1 kW to the 18F station. In Stage 2 the full current would be delivered in dedicated mode to the neutron or BNCT station at 5 kW average power. In Stage 3, after further target technology development, the full linac capability of 20 mA/1 mA would produce 10 kW average power on the neutron TMR.

A conceptual design study has been completed [1,2] that supports the funding proposal submitted to the Canada Foundation for Innovation (CFI). The conceptual design includes a study of accelerator options, design considerations of the TMR system, and studies towards a small angle neutron scattering (SANS) and multi-purpose neutron imaging end-station. This paper summarizes the work that has been done to characterize the linac system of PC-CANS.

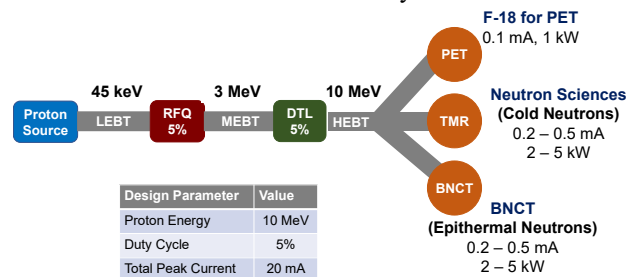


Figure 1: Schematic layout of PC-CANS [2].

LINAC CONSIDERATIONS

The pulsed low duty cycle high intensity scheme for the PC-CANS favours a normal conducting linac. Important optimization parameters are capital and operating cost, low losses for hands-on maintenance, footprint and ease of operation given the non-laboratory setting. The PC-CANS parameters allow some flexibility in the technical choice as the space charge forces are not extreme and the RF duty factor at ~7% (for 5% beam duty factor) reduces RF power density in the structures. Several facilities have been built or proposed in this regime with microwave frequencies ranging from 300-400 MHz, though lower frequency linacs [3] have been proposed for higher beam intensities (100 mA) requiring larger acceptances. The present PC-CANS studies consider 352 MHz as the baseline since this

*mabbaslou@triumf.ca
 †lax@triumf.ca

FULLY AUTOMATED TUNING AND RECOVER OF A HIGH POWER SCL

A. Shishlo†, C. Peters, Oak Ridge National Lab, Oak Ridge, TN 37831 USA

Abstract

Techniques have been developed for a fast (less than one hour), fully automated tune-up a high-power proton Superconducting Cavity Linac (SCL), as well as fully automated recovery from a cavity failure with no human intervention. These methods have been developed and demonstrated at the Spallation Neutron Source (SNS) SCL, but they are applicable to hadron SCL operation in general and will be especially relevant to future ADS applications.

INTRODUCTION

Any existing and future high-power hadron superconducting linacs have tens or hundreds of accelerating superconducting RF cavities. Therefore, the tuning process for these accelerators could take hours with high probability of human mistakes if it is performed by operators. For user facilities shortening the initial tuning setup time as well as the retuning (for different configurations) time is very important for good availability. In the first part of this paper, we describe the tuning process for the SNS superconducting cavity linac [1].

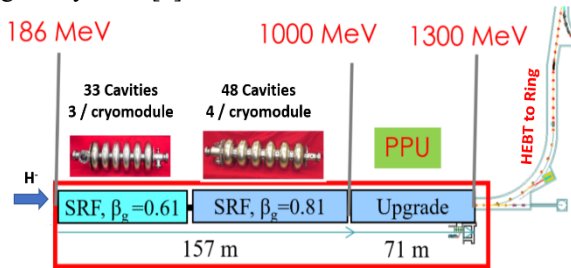


Figure 1: SNS superconducting linac. The last part of the SCL is an empty space holder for future cryomodules of the PPU project.

At this moment, the SCL accelerates H^- ions from 185.6 MeV to 1 GeV (after completion of the Proton Power Upgrade (PPU) project the final energy will be 1.3 GeV). The H^- ions are then injected into an accumulating ring to reduce the beam pulse width from ≈ 1 millisecond to ≈ 1 microsecond. The linac repetition rate is 60 Hz producing 1.44 MW of beam power at the exit of the linac.

The SCL configuration is shown in Fig. 1. The acceleration is provided by 81 RF cavities that are enclosed in 23 cryomodules. The RF resonant frequency of all cavities is 805.0 MHz. There are two types of superconducting cavities, one for medium relativistic beta parameter (0.61) and the other high beta (0.81). There is no difference between these types of cavities from the point of view of phase and field gradient control. The working temperature of the SCL cavities is 2 K.

† shishlo@ornl.gov.

The SNS SCL is operated with energy margin by leaving the final 1-2 RF cavities on but not accelerating. This is to be able to operate with one or two cavities offline (damaged couplers, mechanical tuner problems etc.). If one of the cavities is turned off during operation, the SCL can be immediately retuned by operators in a matter of minutes. This process also can be automated, and it was demonstrated during an experiment. The topic will be discussed in the second part of the paper.

SCL RF CAVITY SETUP PROCESS

A setup process for an RF cavity includes defining two parameters: field gradient (also called amplitude of the cavity in the control system) and phase. At SNS the amplitude of each cavity in the SCL is defined after initial RF conditioning after extended maintenance periods and before each production period. The amplitude should be as high as possible, but it should be low enough to avoid cavity trips caused by field emission and multipacting.

During the SCL tuning process, amplitudes of the cavities are not changed. If during a production run, particular cavity demonstrates increased trip rates, then the amplitude of this cavity is decreased, or it could be switched off completely. After that, the retuning procedure should follow. The distribution of cavity amplitudes for one of run periods in 2022 is shown in Fig. 2. This figure demonstrates that cavity gradients are not the same even inside each section, and we cannot consider the SCL as a periodic lattice.

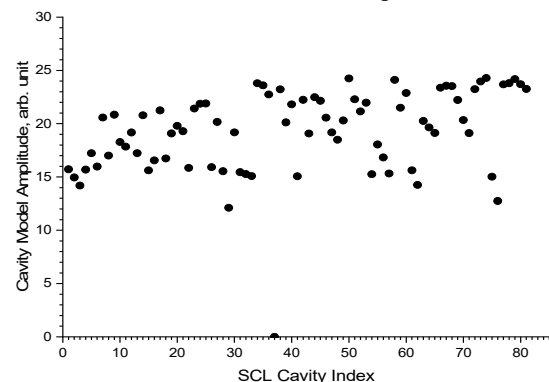


Figure 2: SCL cavity amplitudes on 03.15.2022.

Four Stages of SCL RF Phases Tuning

For the beam-based setup of SCL cavity phases we use a well-known Time-of-Flight (TOF) method. To measure the time-of-flight we have Beam Position Monitors (BPM) that are installed after each SCL cryomodule. In addition to the transverse deviation of the beam from the center, these BPMs can measure the beam bunch phase relative to the RF reference line and the amplitude of a signal generated by bunches passing through BPM.